NASA TT F-367

RADIO CONTROL OF ROCKETS

By M. V. Maksimov and G. I. Gorgonov

Translation of "Radioupravleniye Raketami,"
Izdatel'stvo "Sovetskoye Radio," Moscow, 1964.

NATIONAL AERONAUTICS AND SPACE ADMINISTRATION

For sale by the Clearinghouse for Federal Scientific and Technical Information
Springfield, Virginia 22151 – Price $7.25

UDC 623.451.8.054.93

ANNOTATION

This book presents the principles of design and elements of the theory of systems for the radio control of rockets and radio fuses. Emphasis is on the various aspects of electronic components of the control apparatus. The fact that these components are dynamic links of control systems is taken into account in the analysis. In addition, considerable attention is devoted to analysis of radio control systems as a whole, with different types of perturbations being considered.

The book is intended for radio engineers and students at advanced radio engineering technical schools and corresponding divisions at universities. It also can be useful for non-specialists in this field who are interested in methods of radio control of rockets.

CONTENTS

		Page
Foreword		ix
CHAPTER 1.	PRINCIPLES OF DESIGN OF ROCKET CONTROL SYSTEMS	1
1.1.	General Functional Diagram of Control Systems	1
1.2.	Classification of Control Systems	6
1.	Nonautonomous Control Systems	6
2.	Autonomous Control Systems	12
3.	Combined Control Systems	15
1.3.	Concise Description of Existing Rockets and Their Control Systems	18
1.4.	Principal Requirements Imposed on Control Systems	26
CHAPTER 2.	GENERAL INFORMATION ON CONTROL SYSTEM COORDINATORS. METHODS OF ROCKET GUIDANCE	36
2.1.	Introductory Comments	36
2.2.	Mismatch (Error) Equation	36
2.3.	Mismatch Equations for Rocket Guidance along Fixed Reference Trajectories	38
2.4.	Kinematic Equations for Rocket Guidance along Fixed Reference Trajectories	47
2.5.	Methods of Rocket Guidance along Unfixed Reference Trajectories	50
2.6.	Two-Point Guidance Methods	51
1.	Direct Guidance Method	51
2.	Vane Guidance Method and Pursuit Curve Method	53
3.	Parallel Approach Method	56
4.	Proportional Guidance Method	57
2.7.	Kinematic Equations for Two-Point Guidance Methods	59
2.8.	Three-Point Guidance Methods	68
1.	Matching Method	69
2.	Parallel Approach Method	71
2.9.	Kinematic Equations for Three-Point Guidance Methods	73
2.10.	Perturbations Affecting the Coordinators	78

Page

CHAPTER 3. ELECTRONIC COORDINATORS OF HOMING SYSTEMS 83

3.1. Functional Diagrams of Electronic Coordinators of Homing Systems 83
3.2. Coordinator Direction-Finding Apparatus 85
3.3. Functional Diagram of a Direction-Finding Apparatus with an Integral Equisignal Direction 86
3.4. Block Diagram of a Direction Finder with an Integral Equisignal Direction 92
3.5. Functional Diagram of a Direction Finder with an Instantaneous Equisignal Direction 109
3.6. Block Diagrams of Direction Finders with an Instantaneous Equisignal Direction 113
3.7. Target Selection 129
1. Range Target Selection 130
2. Velocity Target Selection 132
3.8. Block Diagram of a Fixed Coordinator 135
3.9. Block Diagram of a Coordinator with Mechanical Displacement of the Equisignal Direction 136
3.10. Block Diagram of a Coordinator with Electrical Displacement of the Equisignal Direction 155
3.11. Evaluation of the Accuracy of Coordinators of Homing Systems 158

CHAPTER 4. COORDINATORS OF RADIO ZONE (BEAM-RIDING) CONTROL SYSTEMS 172

4.1. Functional Diagram of the Coordinator of a Beam-Riding Control System 172
4.2. High-Frequency Channel of the Receiving Apparatus of the Rocket 173
4.3. Channel for Detection of Mismatch Signal 176
4.4. Reference Signal Channel 179
4.5. Block Diagram of the Coordinator of a Beam-Riding Control System 182
4.6. Characteristics of Operation of a Coordinator in the Launching Segment 186
4.7. Evaluation of the Accuracy of a Coordinator of a Beam-Riding Control System 189
4.8. General Information on Coordinators Using Radio Navigation Measurement Apparatus 192
4.9. Coordinators Based on the Use of Radio Navigation Angle-Measuring Apparatus 193
4.10. Coordinators Based on Use of Angle-Measuring– Range-Finding Radio Navigation Apparatus 197
4.11. Coordinators Based on the Use of Range-Finding Radio Navigation Apparatus 208
4.12. Coordinators Based on the Use of Add-Subtract– Range-Finding Radio Navigation Apparatus 212

		Page
CHAPTER 5.	COORDINATORS OF COMMAND CONTROL SYSTEMS. COMMAND FORMING APPARATUS	224
5.1.	Principles of Design and Principal Types of Coordinators of Command Control Systems	224
5.2.	General Functional Diagrams of Coordinators of Command Control Systems	227
5.3.	Sighting Apparatus of Coordinators	229
1.	Sighting Apparatus of Coordinators of the First Type	229
2.	Sighting Apparatus of Coordinators of the Second Type	233
5.4.	General Information on the Computers Used in Coordinators	234
5.5.	Functional and Block Diagrams of Coordinators of the First Kind for Different Rocket Guidance Methods	252
1.	Coordinators with Radar Sighting Apparatus	252
2.	Coordinators Based on Use of Radio Navigation Sighting Apparatus	259
5.6.	Errors of Coordinators of Command Control Systems	265
1.	Errors in Measurement of the Mismatch Parameter in Rocket Guidance by the Coincidence Method	267
2.	Errors in Measurement of the Mismatch Parameter when Guiding a Rocket by the Parallel Approach Method	274
3.	Errors in Determination of Flight Velocity of a Ballistic Rocket	277
5.7.	Principal Problems Solved by Apparatus for Forming Control Commands	280
5.8.	Apparatus for Forming Commands in Automatic Control Systems	281
5.9.	Apparatus for Forming Commands in Nonautomatic Control Systems	287
CHAPTER 6.	COORDINATORS OF AUTONOMOUS CONTROL SYSTEMS	294
6.1.	General Information	294
6.2.	Autonomous Electronic Coordinator Based on Use of the Doppler Effect	294
6.3.	Inertial Coordinator	300
6.4.	Celestial Navigation Coordinator	306
6.5.	Coordinators Based on Use of Terrestrial Features and Phenomena	307
6.6.	Complex Coordinators	309
CHAPTER 7.	COMMAND CONTROL RADIO LINKS	312
7.1.	Functional Diagram and Principal Characteristics of a Command Control Radio Link	312
7.2.	CCRL Coders and Decoders with Pulse-Width Modulation of Sinusoidal Subcarrier Oscillations	318

Page

7.3. CCRL Coders and Decoders with Pulse-Width Modulation of Pulse Subcarrier Oscillations 333
7.4. CCRL Coders and Decoders with Phase Modulation of the Subcarriers 344
1. CCRL with Sinusoidal Subcarrier Oscillations 344
2. CCRL with Pulse Subcarrier Oscillations 347
7.5. Principles of Design of CCRL with Pulse-Code Modulation 361
7.6. CCRL Coders and Decoders with Pulse-Code Modulation 368
7.7. Command Control Radio Links for Transmission of Single Commands 387
7.8. Selection and Computation of the Principal Parameters of CCRL Numerical Decoders 388
1. Rate of Transmission of Control Commands 389
2. Transmission Bands of Separation Filters 390
3. Frequency Separation of Subcarrier Oscillations 391
4. Minimum and Maximum Values of the Subcarrier Frequencies in CCRL with Pulse-Width Modulation 391
5. Capacity of Binary Codes in CCRL with Pulse-Code Modulation and Admissible Repetition Interval of Symbols in CCRL with Pulse-Counting and Pulse-Frequency Modulation 391
6. Capacity and Structure of Timing Codes 397
7.9. General Information on the Selection and Computation of the Principal Parameters of CCRL Receiving-Transmitting Apparatus 398
1. Required Directional Diagrams of CCRL Antennas 399
2. Wavelengths Used 402
3. Necessary Power of the CCRL Radio Transmitter 403
4. Required Passband and Amplification Factor of Radio Receiver 404

CHAPTER 8. NOISE IMMUNITY OF COMMAND CONTROL RADIO LINKS 407

8.1. Mathematical Description of Processes in Command Control Radio Links with Influence of Radio Interference Taken into Account 407
1. Qualitative Characteristics of Effect of Interference and of a Statistically Equivalent Filter 407
2. Conditions of Equivalence of CCRL and SEF 409
3. Linear SEF 411
4. Nonlinear Statistically Equivalent Filter. Principles of Statistical Linearization of CCRL 418
8.2. Quantitative Characteristics of Noise Immunity of CCRL 426
8.3. Effect of Low-Level Fluctuation Interference on a CCRL with Pulse-Width Modulation 429
1. Relationship between the Statistical Characteristics of the CCRL Output Signals and the Threshold Apparatus 430
2. Dependence of $G_f(0)$ and $G_{cf}(0)$ on the Signal-to-Noise Ratio at the Input of the CCRL Decoder and Radio Receiver 440

Page

8.4. Effect of High-Level Interference on a CCRL with Pulse-Width Modulation 448
8.5. Effect of Low-Level Fluctuation Interference on a CCRL with Pulse-Counting Modulation 467
8.6. Effect of High-Level Interference on a CCRL with Pulse-Counting Modulation 481
8.7. Effect of Low-Level Fluctuating Interference on a CCRL with Pulse-Phase Modulation 495
8.8. Effect of High-Level Interference on CCRL with Pulse-Phase Modulation 497
8.9. Influence of Fluctuating Low-Level Interference on CCRL with Pulse-Code Modulation 513
1. Qualitative Characteristics of Effect of Interference 513
2. Conditional Constant Components of Output Signals and Their Distortions 515
3. Conditional Spectral Densities of Fluctuations of Output Signals 519
8.10. Effect of High-Level Interference on a CCRL with Pulse-Code Modulation 522
1. Qualitative Characteristics of Influence of Interference 522
2. Conditional Constant Components of Output Commands and Their Distortions 527
3. Conditional Spectral Densities of Fluctuations of Output Signals 534

CHAPTER 9. THE ROCKET AS AN OBJECT OF AUTOMATIC CONTROL. ROCKET AUTOMATIC PILOTS 543

9.1. Rocket Equations of Motion 543
9.2. Rocket Block Diagrams 550
9.3. Functional Diagram of the Automatic Pilot 554
9.4. Sensing Elements of the Automatic Pilot 556
9.5. Automatic Pilot Control Apparatus 559
9.6. Actuating Apparatus of the Automatic Pilot
9.7. Rocket Banking Control Channel 566
9.8. Channels for Control of the Longitudinal and Lateral Motions of a Rocket 572
9.9. Self-Tuning of the Rocket Control System 576

CHAPTER 10. FUNCTIONAL AND BLOCK DIAGRAMS OF RADIO CONTROL SYSTEMS 578

10.1. Functional Diagrams of Radio Control Systems 578
1. Functional Diagrams of Homing Systems 578
2. Functional Diagrams of Radio Zone (Beam-Riding) Control Systems 579
3. Functional Diagrams of Command Control Systems 582
4. Functional Diagram of an Autonomous Control System 584

Page

10.2. General Description of the Equations and the Principal Problems in Investigation of Radio Control Systems 584
10.3. Block Diagrams of Electronic Homing Systems 586
10.4. Block Diagrams of Radio Zone (Beam-Riding) Control Systems 596
10.5. Block Diagrams of Command Control Systems 604
10.6. Block Diagrams of Autonomous Control Systems 612

CHAPTER 11. ACCURACY OF ROCKET GUIDANCE AND NOISE IMMUNITY OF RADIO CONTROL SYSTEMS 615

11.1. Principal Sources of Errors in Rocket Guidance 615
11.2. Dynamic Errors in Rocket Guidance 617
11.3. Quantitative Characteristics of Noise Immunity of a Radio Control System and Their Relationship to Fluctuation Errors of Rocket Guidance 626
11.4. Fluctuation Errors of Rocket Guidance in Command Control 633
11.5. Fluctuation Errors of Rocket Guidance in Radio Zone (Beam-Riding) Control 647
11.6. Gluctuation Errors of Rocket Guidance during Homing 652
11.7. Skewing of Coordinate Systems and Its Influence on the Quality of Rocket Guidance 660
11.8. Concise Information on Determination of Rocket Guidance Errors by the Modeling Method 668
11.9. General Characteristics of Methods for Increasing the Noise Immunity of Radio Control Systems 679

CHAPTER 12. RADIO FUSES 687

12.1. Principles of Design and Principal Types of Radio Fuses 687
12.2. General Information on the Matching of the Region of Damaging of the Target and the Region of Triggering of the Radio Fuse 688
12.3. Diagrams of Active Radio Fuses 695
12.4. Characteristics of the Operation of Radio Fuses and General Requirements Imposed on Them 700

References 705

FOREWORD

The radio control of rockets is one of the most important branches of rocket technology. Under present-day conditions, the intensive development of controlled rockets is undertaken not only for the purpose of their military application, but also for investigation of space and for interplanetary flights. A great number of different kinds of technical apparatus, making up the control system, are required for assuring flight of a rocket along a specified trajectory. /3

The complex of instruments used in the guidance of a rocket or any other pilotless object to a specified point in space, by use of radio apparatus, usually is called a radio control system.

Due to the broad development of rocket technology there has been a sharp increase in the radio control of rockets, and this gives rise to an acute need of technical literature on the methods of design and the theoretical principles of systems for the radio control of rockets.

In recent years a considerable number of books, brochures and individual articles on the automatic control of rockets and other air vehicles have appeared both in the USSR and abroad (refs. 1-29, 59, 60, 92, 93, 94, 103, 104, 106-112). In a number of these works and especially in the books (refs. 1 and 2) successful attempts have been made to generalize problems of planning and use of electronic apparatus in rocket technology and also the accumulating rich experience in the field of development of control systems.

At the same time, rocket technology is being continually perfected and as a result more and more new results of scientific investigations of radio control and related problems are appearing.

This book is a further attempt at systematization of available data. /4 In addition, the book presents a number of problems of a general theoretical character whose solutions have been obtained through the independent work of the authors.

As in all published books, brochures, reviews and articles, the problems involved in the radio control of rockets are treated in close relationship to military problems.

The presence of a considerable number of types of apparatus making up a control system and different kinds of interference (radio noise, atmospheric turbulence, etc.) causes errors in rocket guidance. Therefore, in some cases it becomes necessary to use proximity fuses. Radio fuses often are used for this purpose.

A radio fuse is an instrument ensuring the explosion of a warhead at a specified distance and when there is a fixed relative position of the rocket and the target.

Since the requirements imposed on radio control systems and radio fuses usually are interrelated, a special chapter of this book is devoted to radio fuses.

In writing this book, the authors attempted to expound the basic principles of design and the elements of the theory of radio control systems and radio fuses in such a way that the reader could prepare himself for a deeper study of the corresponding specialized materials. All examples pertaining to specific design, technical and tactical solutions are based on materials in the open literature, a list of which is presented at the end of the book. However, the quantitative data are fictitious and have a purely illustrative character.

The first chapter of the book, being essentially an introduction, is devoted to a description of the general functional diagrams and the principal types of control systems. In addition, this chapter gives the most important requirements imposed on control systems and gives a brief description of existing guided missiles.

The eight chapters which follow discuss the principal elements of radio control systems. In these chapters the emphasis is on coordinators, that is, apparatus for measuring the mismatch signals for control systems and control command radio links used in transmitting commands from the control point to the rocket (chapters 7 and 8). In addition, necessary information is given /5 on the automatic pilot and the rocket as objects of regulation (chapter 9).

Chapters 10 and 11 give the function and block diagrams of the principal types of radio control systems and present an analysis of errors of rocket guidance. Chapter 11 also contains materials devoted to problems involved in noise immunity of radio control systems and the general principles of modeling of guidance processes. Chapter 12 discusses radio fuses.

The authors hope that this organization of the book will make it possible for radio specialists to obtain a quite full idea concerning the place and role of electronic apparatus in radio control systems and also concerning the approaches followed in the planning of this apparatus and their connection to nonelectronic apparatus. This book can also be useful for specialists in related fields.

The authors express deep appreciation to Professor L. S. Gutkin and Engineer V. N. Yelizarov for their work in reviewing the book and extremely useful advice and their suggestions, which were taken into account during the writing of the book, and also to all those associates who participated in discussion of the manuscript.

CHAPTER 1. PRINCIPLES OF DESIGN OF ROCKET CONTROL SYSTEMS

1.1. General Functional Diagram of Control Systems

Among the infinite number of possible trajectories for approach of a rocket to a target in actual practice, are selected only those along which flight is accomplished using sufficiently simple technical means and which are the most desirable from the tactical point of view. For this reason the motion of a rocket should be definitely limited, or, as they say, "coherence" should be imposed on the motion of the rocket. Due to different kinds of external perturbations, imperfections of the apparatus used and also the imperfections of the engine and design of the rocket during guidance of the latter, there will be disruption of the coherence which must be eliminated. It therefore follows that for solution of its basic problem the control system should set the character of the coherence, determine the degree of disruption of this coherence and generate the control signals under whose influence the rocket moves along the necessary trajectory. /7

The coherence imposed upon the motion of the rocket assumes many aspects. For example, it can be required that the air velocity vector v of a rocket flying in the atmosphere be directed toward the target during the entire time of guidance. In this case, at the time of approach of the rocket to the target, such as in the vertical plane $o_r x_{er} y_{er}$ (fig. 1.1), where the point o_r characterizes the position of the center of mass of the rocket, and the axis $o_r y_{er}$ represents the extension of the Earth's radius, the control system primarily should determine whether the angles ϵ and θ, determining the inclination of the vectors r and v in relation to the axis $o_r x_{er}$, are equal. If $\theta \neq \epsilon$, appropriate instruments are used to measure the value and determine the sign of the difference $\Delta = \epsilon - \theta$, after which commands are produced which eliminate the disruption of coherence Δ. With the rigorous satisfaction of coherence, the rocket in the undisturbed atmosphere will follow a linear trajectory if the target is fixed. /8

It can be required also that the center of mass of the rocket in the course of its guidance will be at all times on a straight line connecting the control point with the target.

In the case of this type of coherence for rocket guidance, in the vertical plane $o_c y_{ec} x_{ec}$ (fig. 1.2), for example, from the control point o_c, the control system should measure either the angle $\Delta = \epsilon_t - \epsilon_r$ between the straight lines connecting the point o_c with the target T and the center of mass R of the rocket,

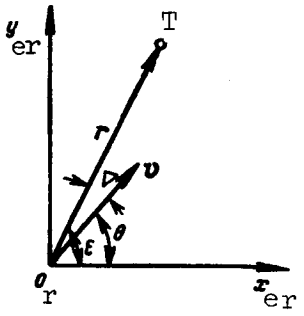

Figure 1.1

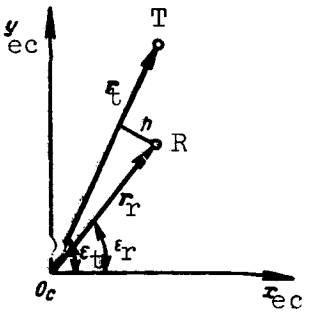

Figure 1.2

or the linear deflection h of the point R along the normal to the vector r_t and tend to make them equal to zero.

As a last example we will mention a coherence whose essential requirement is that it is necessary to assure the motion of the rocket in such a way that the vector r, coinciding with the "rocket-target" line, in the course of the guidance process moves parallel to itself. If the inclination of this vector, situated in the plane $o_r x_{er} y_{er}$ (fig. 1.1), in relation to the axis $o_r x_{er}$ is ϵ, a measure of the disruption of the coherence will be the value and sign of the angular velocity of rotation of the vector r, equal to $\dot{\epsilon} = \frac{d\epsilon}{dt}$.

The measure of disruption of coherence, which for one rocket guidance plane will be denoted Δ, is called the mismatch parameter (mismatch signal of the control system or the control parameter). When the mismatch parameter is recorded, as necessity dictates, a subscript is added to the symbol Δ characterizing the rocket guidance plane and the measured values.

If the rocket is guided along its course and is guided in altitude, the mismatch parameter is the vector Δ, whose components lie in two mutually perpendicular planes. It can be seen, from the examples cited above, that the angular deflections of the vectors v and r_r in relation to r and r_t (figs. 1.1 and 1.2), the linear displacement h of the center of mass of the rocket along the normal to the vector r_t (fig. 1.2) and the time derivative of the angle ϵ can be measures of the disruption of coherence. In a number of cases the mismatch parameter can be a complex function of a considerable number of parameters characterizing the motion of the rocket, target and control point. However, in the last analysis, in the control of the lateral and longitudinal motion of a rocket, coherence /9 is always imposed on the direction of the vector of its flight velocity, although very frequently this is indirect rather than direct.

On the basis of the foregoing it is possible to represent the general functional diagram of a control system for the course and altitudinal guidance of a rocket. This diagram is shown as figure 1.3a. Figure 1.3a shows that the

control system includes a coordinator, apparatus for forming and transmitting control commands, an automatic pilot and the rocket.

The coordinator is a complex of instruments and devices used in determining the measured value of the mismatch parameter Δ_m in accordance with the type of coherence imposed on the motion of the rocket. The difference between Δ_m and Δ, with the condition that both these parameters are expressed in the same measurement units, is determined by the errors of the coordinator and the interference affecting it. The shaping of the signal Δ_m in the coordinator is accomplished by the setting, measurement and functional conversion of those parameters which determine the selected form of coherence. In its structure, the coordinator can be either a relatively simple or an extremely complex apparatus. This is dependent on with what accuracy and what coordinates of the rocket and target, or what parameters of their relative motion must be measured for determination of the measure of disruption of the selected coherence. In a general case, the components of a coordinator are measuring instruments, a computer and a system for transmission of data.

Depending on the values Δ_m and the type of control system on the rocket or at the control point, the command forming apparatus produces control commands K_a. If the command forming apparatus is on the rocket, the K_a commands are fed to the automatic pilot (dashed line in figure 1.3a). When the commands are produced at a control point they are transmitted to the automatic pilot by a command transmission apparatus. The signal K forming at the output of the command transmission apparatus is related functionally to K_a and therefore to Δ_m. Sometimes in order to decrease the errors in rocket guidance the commands K and K_a are not only a function of Δ_m, but also are dependent on a number of additional parameters of motion of the target. The mentioned dependence is the result of the feeding of corresponding signals produced by the target coordinate measuring instruments from the coordinator to the command forming apparatus.

The automatic pilot is designed for stabilization of the rocket and control of its flight by direct action on the control components. If the rocket can rotate about its longitudinal axis, the automatic pilot, in addition to performing stabilization functions, solves the problem of conversion of commands in such a way that there will be proper deflection of the control surfaces during their turning together with the body of the rocket.

In a number of systems the automatic pilot and the command forming apparatus are combined in a single unit. This usually is the case when the parameter Δ_m is formed on the rocket. /10

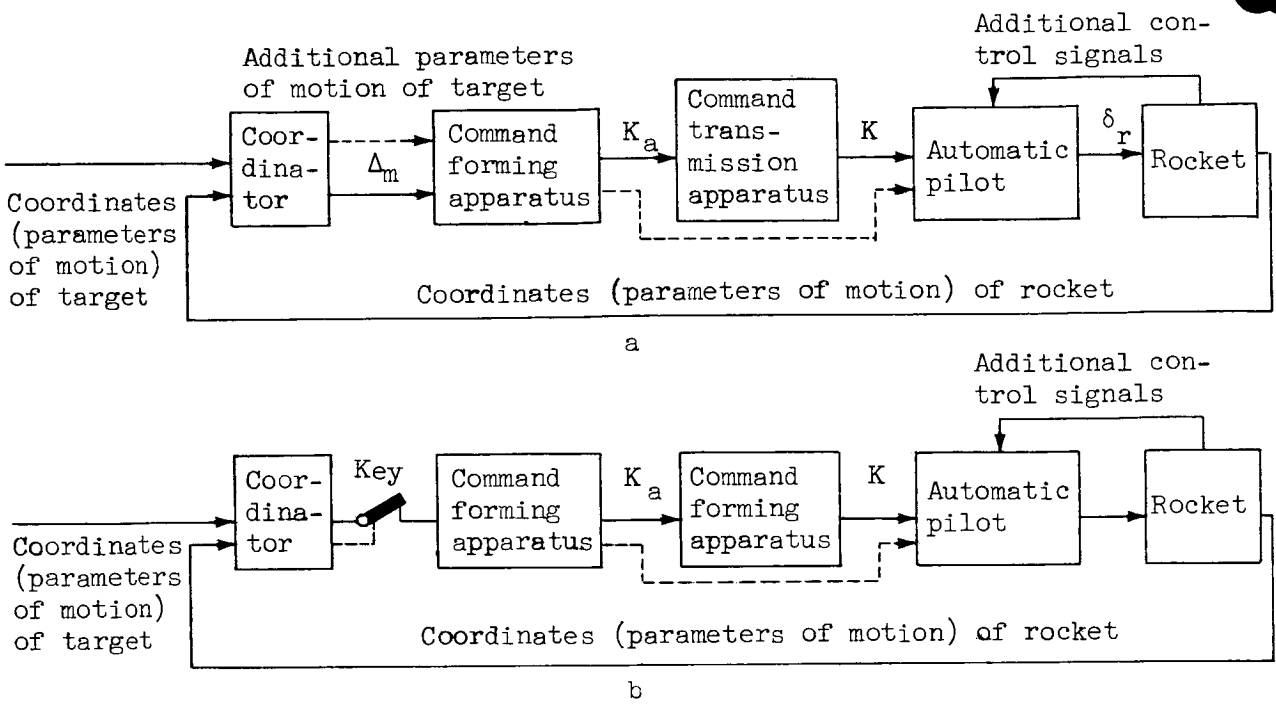

Figure 1.3

In addition to the commands K (or K_a) additional control signals are fed to the automatic pilot from the rocket. These signals, picked up by the sensing elements of the automatic pilot, characterize the values and the rates of change of the angles determining the direction of the axes of the rocket in space, the linear accelerations of the center of mass of the rocket, etc.

The additional control signals are used both for stabilization of the rocket and for improvement of the dynamic properties of the control system; this will be discussed in greater detail in chapters 9 and 10.

If corrective control commands are not fed to the automatic pilot, it performs the function of a stabilization apparatus and ensures the flight of the rocket along the previously specified trajectory. The commands K (or K_a) change the adjustment of the automatic pilot and as a result the rocket moves into another trajectory of motion.

As is well known, an automatic pilot contains sensing elements which pick up additional control signals, master controls for measurement of the /11 adjustment of the automatic pilot under the influence of control commands or in accordance with the program, amplification-conversion apparatus, and control surface mechanisms connected to the control surfaces of the rocket.

With the deflection of the rocket control surfaces by δ_r, where δ_r is a vector whose components are the movements of the elevator and rudder, depending

on their design, there is a change of the angles of attack, banking and slip, a disruption of the air flow or a displacement of the gas stream of the jet engine. As a result, there is a change of the direction and value of the total controlling force and the velocity vector of the rocket is turned.

A rocket in a control system is an object of regulation. The input actions of the rocket as an element of a control system are the movements of the control surfaces, and the output effect is a change of the angle of the velocity vector or lateral acceleration related to it.

As a result of change of the parameters of motion of the rocket there are changes of the mismatch parameter Δ and further conversions similar to those considered above. Thus, the system for control of the lateral and longitudinal motion of a rocket forms a closed control system sometimes called a guidance (control) circuit. The role of a regulator in this system is played by the coordinator, the command forming apparatus, the control command transmission apparatus and the automatic pilot.

Control systems also are known in which the commands are not produced for all values of the mismatch parameter, but only for definite values of this parameter. By means of such systems, whose general functional diagram is shown in figure 1.3b, it is possible, for example, to bring about the transition of a winged missile into a dive when it reaches to within a stipulated distance of the target and to cut off the engine of a ballistic missile at the end of the active part of the flight trajectory. It is assumed that all the switching apparatus is in the automatic pilot of the rocket. In the considered type of control systems the circuit for the transmission of the measured value of the mismatch parameter to the command forming apparatus is opened by the key Key. At the same time the coordinator measures and compares the parameters of motion of the target and rocket, much as is done in the systems whose functional diagram is shown in figure 1.3a.

When the mismatch parameter Δ reaches stipulated values Δ_{s1}, Δ_{s2}, ..., Δ_{sn}, the key Key is closed automatically or manually and the command forming apparatus produces the necessary control signals. The intervals of time T_k ($k = 1, 2, \ldots, n$) in which these signals should be fed to the automatic pilot after the conditions $\Delta = \Delta_{s1}$, $\Delta = \Delta_{s2}$, ..., $\Delta = \Delta_{sn}$ are satisfied are determined by the programming mechanism or the admissible deviations of Δ from Δ_{s1}, Δ_{s2}, ..., Δ_{sn}. Usually the intervals T_k are insignificant in comparison with the total time of rocket guidance T_g.

In a general case, the operation of the coordinators and the command /12
transmission apparatus can be based on different physical principles. However, in most cases this apparatus is electronic.

If the rocket is guided by radio apparatus in the coordinator, the command transmission apparatus or simultaneously in both, the entire complex of apparatus ensuring that the rocket will reach the target constitutes the radio control system.

The presence of electronic apparatus in control systems leads to the appearance of so-called open links. The receiving apparatus of these links is subject to the influence of interference, including artificial interference.

1.2. Classification of Control Systems

Existing rocket control systems are classified as nonautonomous and autonomous. In addition, combined systems can be classified in a separate group.

In the case of nonautonomous control systems there is a characteristic need for some signals which should arrive from the target or from the control point in the course of guidance of a rocket after its launching, for the forming of the measured value of the mismatch parameter Δ_m. These signals are not necessary for the functioning of autonomous systems. A combined control system is a combination of autonomous and nonautonomous systems, or only nonautonomous, or only autonomous control systems with different principles of operation.

1. Nonautonomous Control Systems

Nonautonomous systems include:

(1) homing systems;
(2) radio zone (beam-riding) control systems;
(3) command control systems.

a. Homing Systems. A homing system is characterized by the fact that the mismatch parameter and the control commands are formed aboard the rocket from signals arriving from the target. The coordinator carried on the rocket has a sensing element which picks up the radiations of the target which distinguish it from the surrounding medium. The target can be the source of primary or secondary (reflected) signals.

The energy of electromagnetic waves is used in electronic homing systems. The radio apparatus of the coordinators usually measures the angular deflection of the line o_rT connecting the center of mass o_r of the rocket with the target T from any direction o_rx_m (fig. 1.4) in space. In the simplest case this direction coincides with the longitudinal axis of the rocket.

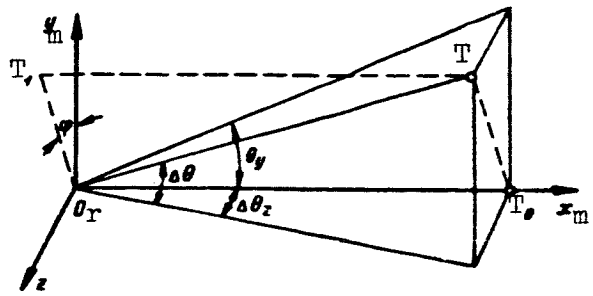

Figure 1.4

The position of the line o_rT relative to the straight line o_rx_m represents the x-axis of the measurement coordinate system; it can be determined by /13 the angles $\Delta\theta_z$ and $\Delta\theta_y$ or the angles $\Delta\theta$ and φ, where φ is the angle formed by the o_ry_m axis and the radius vector o_rT_1, drawn from point o_r to point T_1, corresponding to the projection of point T onto the plane $o_ry_mz_m$.

On the basis of the measured values of the mismatch parameter obtained as a result of corresponding conversions of the signals for the angular coordinates $\Delta\theta$, φ or $\Delta\theta_z$, $\Delta\theta_y$, control commands are formed on the rocket for each of the guidance planes; the developing disruptions of the coherence imposed on the motion of the rocket are eliminated by these control commands.

Depending on the location of the primary source of electromagnetic energy it is possible to distinguish active, semiactive and passive homing systems.

An active homing system is characterized by the fact that the energy source irradiating the target and the receiver of the signals reflected from it are on the rocket. In semiactive homing systems the source of electromagnetic energy for irradiation of the target is not on the rocket. A passive rocket homing system is based on signals produced directly by the target.

Homing systems have the following principal merits:

(1) the possibility of guidance of rockets to moving targets, which can be attributed to the continuity of control of the position of these moving targets;

(2) some autonomy of the systems, since all the apparatus necessary for shaping the signals for correction of the motion of the rockets are carried aboard the latter;

(3) improvement of conditions for control of the position of the target with approach of the rocket to it (to some limit) due to the continuous increase of the strength of the received signals and, at the same time, a decrease of the linear deflections of the rocket from the stipulated direction, assuming constant angular errors of the measuring instruments.

At the same time, electronic homing systems have a number of shortcomings. The most important of these are:

(1) a relatively short effective range, limited by the technical capa- /14
bilities of the means for control of the relative position of the rocket and target;

(2) relative complexity of the apparatus carried on the rocket, especially in the case of active guidance;

(3) they are subject to the effect of radio interference.

b. Radio Zone (Beam-Riding) Control Systems. In the case of radio zone control, whose form is dependent on the type of electronic apparatus used in the coordinator, the necessary flight trajectory for the rocket is fixed from a guidance point. When a radar set with conical scanning of the antenna directional diagram is a part of the coordinator, the term radio zone applies to the equisignal direction passing through the target or the future position. This type of radio zone also can be created by a radar set with different principles of automatic determination of the angular coordinates of targets.

Radio zones created by radio navigation apparatus can be classified as lines, planes and position surfaces. A plane (radio plane) and position surface (radio surface) are determined by the locus of points situated in a single plane or on a single surface in which at least one of the parameters of the radio signals (amplitude, phase, etc.) remains constant. A position line is defined as the locus of the points of intersection of two planes or position surfaces.

In radio control technology, systems which ensure the flight of a rocket along an equisignal direction created by a radar set are called beam-riding control systems, or as sometimes encountered in the technical literature, radio teleguidance systems. In well-known beam-riding control systems, the equisignal direction is created by a radar set with conical scanning of the antenna directional diagram.

The essence of the method of beam-riding control, under the condition that the equisignal direction giving the rocket flight trajectory at all times passes through the target, is essentially as follows.

By the time of the launching of the rocket, when the control point and the target are situated at points C_0 and T_0 (fig. 1.5), an equisignal direction is created which coincides with the straight line C_0T_0. With the approach of the rocket to the target, the equisignal direction changes its position in space and at times t_1 and t_2, when the target is at points T_1 and T_2 and the control point moves to points C_1 and C_2, the equisignal direction coincides with the straight lines C_1T_1 and C_2T_2, respectively.

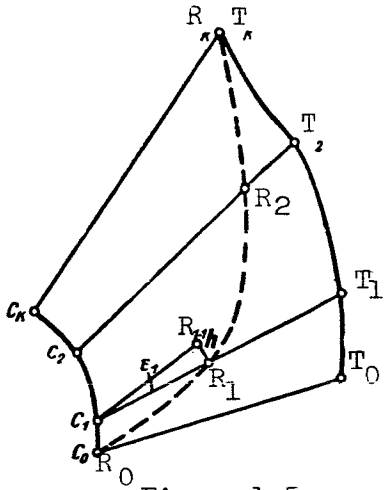

Figure 1.5

The rocket carries radio apparatus which measures the degree of disruption of coherence imposed on the motion of the rocket. For example, if at time t_1 the center of mass of the rocket should be at point R_1 on the straight line C_1T_1, but is situated at point $R_{1.1}$, the value and direction of the angle ϵ_1 are /15 fixed aboard the rocket, and the linear deflection h of point $R_{1.1}$ from the straight line C_1T_1 is determined. The measured value of the mismatch parameter obtained in this way is converted into commands under whose influence the rocket returns to an equisignal direction. As in homing systems, the commands, in most cases, are produced by apparatus which is integrated with the automatic pilot. At the same time, the apparatus for the forming of commands can be made in the form of an independent unit or placed in the rocket radio apparatus unit.

With the motion of the control point and the target along the curves $C_0C_1C_2C_k$ and $T_0T_1T_2T_k$, a rocket guided by a beam-riding control system will move along the trajectory $R_0R_1R_2R_k$; in this case points R_0 and R_k coincide with C_0 and T_k, respectively.

A distinguishing feature of this beam-riding control method is that only one radar set is required for its realization. If the center of mass of the rocket should be directed to a future point with a moving target, it is necessary to have two radar sets, one of which determines the coordinates of the target and the other forms an equisignal direction setting the rocket flight trajectory.

As a result of this consideration of the problem of the methods for creating beam-riding control systems, it can be concluded that the apparatus of the coordinators of these systems is situated both at the control point and on

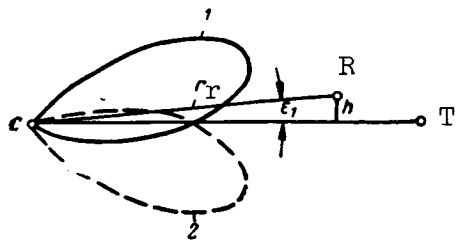

Figure 1.6

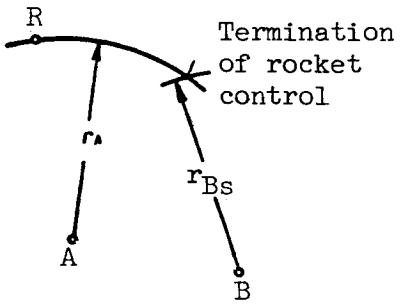

Figure 1.7

the rocket. The apparatus situated at the control point in the last analysis forms the reference line for the angles characterizing the required position of the center of mass of the rocket and is the source of the radio signals necessary for the operation of the rocket radio equipment. The latter determines the degree of disruption corresponding to the linear deflection h (fig. 1.5).

Various types of radio navigation apparatus can be used for creating a radio plane. The simplest radio plane is formed by use of a radio beacon for which the directional diagram of the transmitting antenna periodically is switched in relation to the selected direction in a horizontal plane (fig. 1.6). During the two halves of the switching period T, the diagram is in the positions 1 and 2, respectively. As a result, on the basis of the difference of strengths of the radio signals arriving at the input of the rocket receiver /16 it is possible to determine the deflection $h \approx \varepsilon_1 r_r$ of the center of mass of the rocket R from the vertical plane passing through the control point C and the target T.

The simplest form of a radio surface is a hemisphere which can be formed by a radio navigation range-finding system. In the case of a constant flight altitude and a stipulated range to a ground station A, the rocket R (fig. 1.7) will move automatically along the arc of a well-defined circle having the radius r_A.

In the case of deflection of the center of mass R from this circle by means of the apparatus carried on the rocket, it is possible to determine the value and the sign of the degree of disruption of coherence and eliminate the appearing guidance errors. The time of termination of rocket control can be determined by a comparison of the current distance from the rocket to the surface radio station B with the stipulated value r_{Bs}.

Other methods for formation of radio zones will be considered in detail in chapter 4.

Radio zone control systems are characterized by use of relatively simple radio equipment carried aboard the rocket. This can be attributed to the fact that it operates by reception of the direct signals of radar stations or powerful radio navigation systems on the ground. At the same time, it should

be remembered that with the approach of the rocket to the target and assuming constant errors in measurement of the angular coordinates of the target and rocket, the accuracy of determination of the parameter h deteriorates and there is an increase of guidance errors. The presence of several channels for the reception of radio signals in radio zone control systems, in some cases, makes it possible to create very effective radio interference in them.

c. Command Control Systems. Command control systems, also called telecontrol or remote control, are characterized by the fact that the control commands are not formed on the rocket but at the control point. The transmission of these commands to the rocket is accomplished by radio or by wire. Under modern conditions transmission usually is by electronic command trans-/17 mission apparatus, called control command radio links or radio guidance links.

The transmitting apparatus in the control command radio links, connected to the output of the coordinator by the operator and a command transducer or a computer, is at the control point and the receiver is aboard the rocket. The command transducer is a device which transforms the actions of the operator into signals convenient for feeding to the transmitting apparatus of the control command radio link. Sometimes the command transducer is considered an integral part of the control command radio link.

Direct participation of an operator in carrying out the entire process of rocket guidance is required only in nonautomatic and semiautomatic control systems. If the control system is automatic, the role of the operator is reduced to organization of the beginning of the guidance process and control of the correctness of operation of the apparatus used.

The command radio link, operator and command transducer form the apparatus for forming and transmitting commands in a nonautomatic system. In automatic systems this apparatus includes the control command radio link and a computer.

The coordinator apparatus is placed either completely at the control point (with the exception of the rocket responder) or in such a way that one part of it (the primary measuring instruments and the transmitting apparatus of the system for relaying the measurement results) is on the rocket and the other part (receiving apparatus of the relaying system and its indicators) is at the control point.

A considerable number of types of control command guidance systems now are known. However, the basic idea of their design for control of the longitudinal and lateral motion of a rocket is quite similar in all cases, and can be explained using the example of a system whose simplified block diagram is shown in figure 1.8.

The radar sets RS_1 and RS_2 are used to determine the coordinates of the target T and rocket R moving at the velocities v_t and v; in this case the effective range of RS_2 can be increased by the presence of a responder on the rocket.

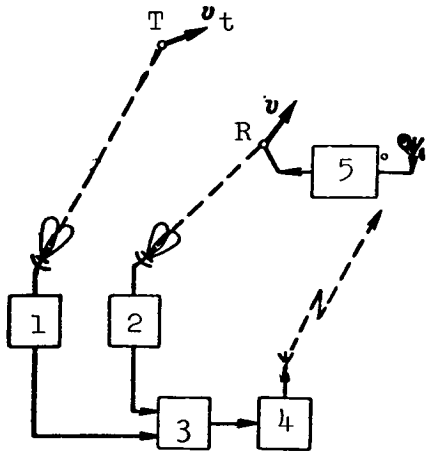

Figure 1.8

The output signals of RS_1 and RS_2 are fed to the computer Com which determines the measured value of the mismatch parameter and the control command. The latter is transmitted to the rocket by the transmitting apparatus of the control command radio link CCRLTr. The receiving apparatus of this same radio link /18 CCRLRec forms a signal which is sent to the rocket's automatic pilot. The considered system obviously is suitable for the guidance of rockets to moving targets. If the target is fixed, the system is simplified considerably. In some cases there can be other apparatus for coordinate measurement in addition to radar sets.

One of the important merits of control command guidance systems is the possibility of employing a very great variety of rocket flight trajectories in the process of approach to targets despite the relatively simple radio equipment carried aboard the rocket. It should be noted at the same time that these systems, like electronic homing systems and radio zone (beam-riding) control systems also are subject to the influence of radio interference in all the radio communication channels included in the system.

2. Autonomous Control Systems

Autonomous (programmed) control systems ensure the motion of a rocket along a previously specified (by the program) trajectory by means of apparatus carried on the rocket. In this case, during the rocket flight process, the rocket receives no signals from the target and none from a control point.

The programmed trajectory is determined by a combination of set parameters of motion of the rocket relative to the Earth or relative to some fixed coordinate system, such as an inertial coordinate system.

The parameters characterizing the current position of the rocket in space are determined by some complex of measuring instruments and are compared with

the programmed (set) values of these parameters. On the basis of this comparison control pulses are produced and as a result the current values of the parameters are set in accordance with the specified values.

Since the rocket flight program cannot be changed after launching, autonomous systems are used only for control of rockets designed for guidance to targets whose coordinates are known in advance with a high degree of accuracy. This is one of the shortcomings of autonomous control systems. The principal merit of such systems is their autonomous character, frequently making difficult, and sometimes completely excluding, the effect of radio interference by the enemy. In addition, it must be remembered that autonomous systems can be used for the control of rockets having a great flight range. This can be attributed to the fact that such systems are unhampered by the limiting factors inherent in radar and nonautonomous radionavigation apparatus used in determining the coordinates of objects situated beyond the range of geometric visibility.

Electronic and nonelectronic autonomous control systems can be distin- /19
guished.

Depending on the makeup of the measuring instruments carried on the rocket it is possible to list the following types of nonelectronic autonomous control systems:

(1) gyroscopic;
(2) inertial;
(3) celestial navigation;
(4) guidance systems using terrestrial features and properties.

Electronic autonomous control systems are divided into:

(1) systems based on the use of the Doppler effect;
(2) radio celestial navigation systems;
(3) control systems using terrestrial radar-observed features.

a. Gyroscopic Control Systems. Gyroscopic autonomous control systems are based on the use of the properties of gyroscopic instruments of maintaining their spatial position. Therefore, by placing on a rocket several position (three-power) and rate (two-power) gyroscopes it is possible to bring about stabilization of the specified angular position of a rocket in a fixed (inertial) coordinate system. Gyro systems are simple, but at the same time they have an important shortcoming--a relatively low accuracy. This can be attributed to the fact that gyroscopic instruments react only to angular movements of a rocket and do not take into account its lateral translational movements caused by such factors as the wind. As a result, gyro systems were used as independent systems only in early developments (ref. 4).

Under present-day conditions, gyro systems are used only as a means for the angular stabilization of a rocket, and the control of the position of its center of mass is accomplished by other apparatus (ref. 3).

b. Inertial Control Systems. Inertial control systems are based on continuous double time integration of the acceleration vector of rocket motion.

The inertial system includes instruments for measurement of accelerations (accelerograph) and integrating apparatus. After the first integration of acceleration the velocity of motion of the rocket is obtained and the integral of velocity characterizes the path travelled by the rocket. The coordinates of the center of mass of the rocket are determined from the integrator signals. Comparison of the current and specified values of the coordinates makes it possible to form the necessary control signals.

If the path is calculated in a terrestrial coordinate system, for a correct determination of the components of the acceleration vector it is necessary that the accelerometers measure acceleration in the plane of the horizon. Otherwise apparatus is needed to take the influence of acceleration of gravity into account. It therefore follows that the accelerometers should be /20
mounted on a platform which at all times will remain parallel to the plane of the horizon. This requires that the local vertical be determined on the rocket. This vertical can be determined by using gyro instruments corrected in a special way.

It is easy to see that an inertial system is considerably more complex than a gyroscopic system, but at the same time it also has a greater accuracy.

c. Celestial Navigation Control Systems. Celestial navigation control systems are based on known laws of the motion of celestial bodies which change little with time. One of the most important units in an astronavigation system is the so-called celestial navigation instrument for automatic tracking of selected celestial bodies in direction. In actual practice it is possible to determine the coordinates of celestial bodies of the first and second magnitude automatically. Information received from two celestial bodies is used simultaneously for rocket guidance. However, guidance is possible also by using the known coordinates of a single celestial body. By having on the rocket the vertical or the true horizon it is possible to determine the current angular coordinates of each of the selected celestial bodies. The signals produced by the celestial navigation system are compared with the specified values of the parameters of the celestial bodies and the control commands are formed on this basis.

A distinguishing characteristic of celestial navigation systems is that they are capable of operating only when the stars can be seen. This makes it necessary that the rocket flight be at a sufficiently great altitude. It should be noted further that modern celestial navigation instruments have a high accuracy of measurement.

For example, it is pointed out in the literature that in the case of rotation of the rocket-celestial body line at a rate up to 10°/sec the dynamic error in determination of the direction to the celestial body does not exceed 2'. However, the complex equipment which must be carried on the rocket and the meteorological limitations are important shortcomings of celestial navigation control systems.

d. Autonomous Control Systems Using Terrestrial Features and Properties. Autonomous control systems using terrestrial features and properties are based on the use of the Earth's magnetic field, the Earth's electrical field, the gravity field, atmospheric properties, geographic maps which are compared with the terrain observed from the rocket during its flight, etc. Among these, the only ones which have come into practical use are those systems whose principle of action is based on the properties of the atmosphere for the control of the flight altitude of a rocket using aneroid pressure sensors.

e. Systems Based on Use of the Doppler Effect. It is well known that there is electronic apparatus which makes use of the Doppler effect and thereby makes it possible to determine the vector of ground speed v_g of a rocket.

This means that such apparatus produces signals characterizing the module /21
of the vector $|v_g|$ and the drift angle α_{dr}. By knowing $|v_g|$ and α_{dr} it is

possible to find the deflection of the center of mass of the rocket from the stipulated flight direction and the path which it has followed.

An important merit of this system, in addition to its autonomous character, is the possibility of ensuring the guidance of the rocket over a great distance. However, as a result of the inaccuracy in taking into account the initial conditions and the fluctuations of the received signals, the errors of rocket guidance increase with an increase of their flight range.

f. Radio Celestial Navigation Control Systems. The coordinate measuring instruments in radio celestial navigation control systems make use of radio signals in the form of fluctuation noise emitted by celestial bodies. After processing, these signals later are used as in celestial navigation systems.

The received fluctuating signals are separated from the instrument noise of the radio receiver by the amplitude modulation of the former, for example, by scanning of the directional diagram of the antenna. It should be noted that for the normal operation of a radio celestial navigation system the antenna of the coordinate measuring instrument, frequently called a radio sextant, should be spatially stabilized.

g. Control Systems Using Terrestrial Radar-Observed Features. In electronic control systems based on the use of terrestrial radar-observed features the principle employed is comparison of an earlier prepared radar chart of the terrain over which the rocket is to pass with a continuously changing chart which is prepared by the radar set carried aboard the rocket. As a result of the comparison it is possible to determine the deviation of the rocket from the stipulated trajectory of motion and form the necessary corrective commands.

3. Combined Control Systems

One of the reasons for the use of combined control systems is the characteristics of the launching segment of the rocket trajectory. For example,

when using electronic rocket control systems the rocket enters the zone of normal operation of radio guidance apparatus only some time after the launching and this makes necessary an autonomous (programmed) control system in the launching segment.

A combination of different control systems can be desirable also when guiding a rocket on the main part of its flight trajectory, for example, when there are difficulties in the simultaneous satisfaction of the requirements of a great effective range and a high accuracy of guidance. In most cases control systems with a great effective range have a relatively low accuracy and accurate systems are limited in range. An attempt to reconcile these contradictions within the framework of any one control system results in an appre-/22 ciable increase of the complexity and size of the apparatus or it cannot be accomplished at all. Finally, in some cases for the forming of a master signal it is necessary to measure a variety of parameters (such as flight altitude, range to target, angular deflection from the stipulated direction, etc.). Here also, in many cases, it is more convenient to use measuring instruments of different systems.

Combined control systems usually are classified in three groups. The first type includes those systems in which rocket guidance is accomplished by different control systems in the course of the same stage of rocket flight. In the second type of combined systems the control system is replaced with transition from one stage of rocket guidance to another. Finally, in systems of the third type, which can be called mixed systems, the different control systems are combined both in the different guidance stages and within these stages.

As an example of a combined system of the first type we can mention the control system of a winged rocket (missile) of the "ground-to-ground" class during its guidance to a fixed target. For the accomplishment of horizontal flight of such a rocket and its transition into a dive at a stipulated distance from the target, it is necessary to measure the flight altitude and the lateral deflection of the center of mass from the stipulated direction of motion and also the remaining distance to the target. Each of the mentioned parameters is measured by a separate measuring instrument, sometimes unrelated to the other measuring instruments carried aboard the rocket. For example, in the considered example the altitudinal flight control is accomplished using an autonomous system (employing a barometric sensor) and lateral guidance is accomplished using a radio zone control system.

This example illustrates the simplest form of combined control of the first type, characterized by the fact that in this case each component part of the system operates independently. Therefore, the very fact of the use of different measuring instruments in a combined control system does not impose any additional requirements on their operation.

In more complex apparatus the individual measuring instruments are closely related to one another and form a unified complex. In these cases the specific characteristics of a combined control system become particularly obvious.

Combined control systems of the second type are used most frequently in those cases when it is necessary to ensure a high accuracy of guidance of a rocket having a great effective range.

The transition from one type of control system to another imposes a number of specific requirements on the components of the combined system: the necessity for a smooth coupling of the parts of the trajectories of the dif-/23 ferent guidance stages, stable cutting-in of different systems when the appropriate conditions arise for its use, etc.

A number of variants can be proposed for the formation of a combined control system of the second type. However, for many such systems it is characteristic that there is self-guidance (homing) of the rocket in the final flight stage. When developing such combined systems it is extremely important to determine the minimum computed range of transition to homing. This value, in many respects determining most of the parameters of the entire remaining system, should be selected in such a way that the following very important conditions are satisfied:

(1) A rocket moving in a maximum curvature trajectory should correct the errors accumulated during its earlier motion due to the inaccuracy of operation of the preliminary control system.

(2) The transient processes caused by switching of the system to a homing regime should attenuate by the time the rocket reaches its target.

(3) Prior to transition to homing there should be reliable reception of signals from the selected target.

The first condition presupposes the ideal operation of the homing system and determines the minimum distance at which the rocket is capable of eliminating the previously accumulated errors. Determination of the necessary range in this case is based on an analysis of the kinematics of motion of the rocket and target.

Determination of the transition range in accordance with the requirement that there be attenuation of transient processes makes it necessary to take into account the dynamic characteristics of the rocket. As an approximation it can be assumed that the sought-for range should not be less than the distance which the rocket travels in a time sufficient for attenuation of the transient process caused by a perturbation of the "single jump" type.

The third condition determines the necessary parameters of the electronic apparatus of the homing system, using as a point of departure the requirement of ensuring a reliable range detection and determination of the angular coordinates of the target by the time of the transition of the rocket into a homing regime. In some cases the conditions for pickup of the target can be limited to the necessary range of transition to homing. Sometimes they limit only some parameters of the radio apparatus of the rocket, such as the width of the antenna directional diagram.

In order to ensure the pickup of the target by the coordinator of the homing system it is most important that the target be situated in the "angle of view" of the coordinator antenna system. With the approach of the rocket to the target there is a decrease of the surface area scanned by a coordinator having a definitely set "solid angle of view," and therefore there is an increase of the probability that the target will not be picked up. If the transition range to a homing regime is determined from the first condition and the possible angles of deflection of the longitudinal axis of the rocket from the direction to the target at the time of transition of the rocket to homing are known, it is easy to determine the value of the "angle of view" at which the pickup of the target is ensured. However, in such an approach to solution of the problem the required value of the "angle of view" can be too great. Also, an increase of the "angle of view" of the coordinator is undesirable because in this case there is a decrease of its effective range and angular sensitivity. This contradiction is overcome by control of the adjustable angle of the coordinator antenna. /24

Combined systems of the third type are the most complex. However, the problems arising during their development are similar to those considered above.

1.3. Concise Description of Existing Rockets and Their Control Systems

A great number of guided rockets are known which vary in their tactical purpose, design, methods of use, type of control system, etc. Most frequently all types of rockets are classified on the basis of their site of launching and the position of the target. On the basis of this classification criterion guided rockets fall into the following classes: "air-to-air," "air-to-ground," "ground-to-air" and "ground-to-ground."

In recent years there has been considerable development of rockets which are put into an artificial earth-satellite orbit and spacecraft. For this reason it apparently is desirable to separately classify "earth-space" rockets.

It should be noted here that, in the mentioned classes, the term "ground" means the surface of our planet without distinction being made between continents, oceans, seas, etc.

Guided rockets of the "air-to-air" type are a means for damaging enemy aircraft in the air. The flight range r_∂ of such rockets falls in the range from less than ten kilometers to several tens of kilometers and is limited by the technical possibilities of airborne radar sets. The rocket weight G reaches several hundred kilograms. The greater part of the weight is accounted for by the engine, which in most cases uses solid fuel. Rockets of the "air-to-air" class move at supersonic velocity. The length l of these rockets usually is several meters and the diameter of their body d_r and length of the wings l_w usually does not exceed tenths of a meter.

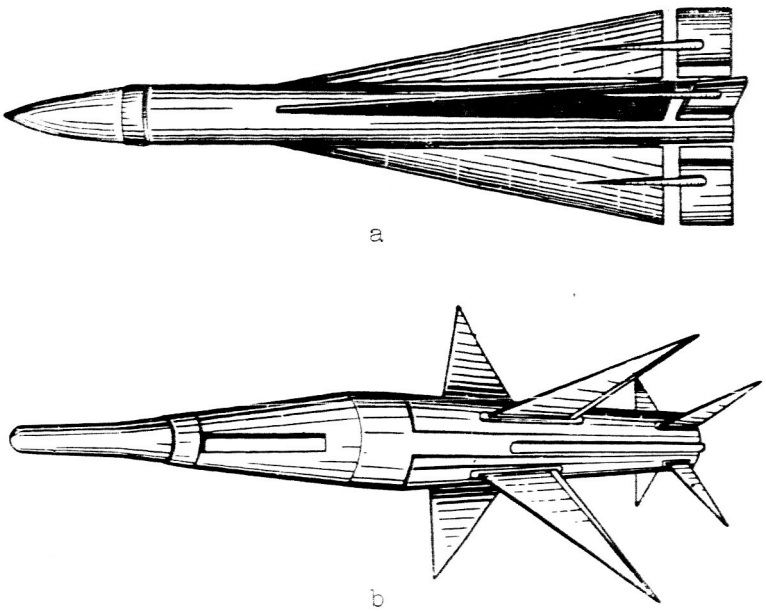

a

b

Figure 1.9

As an illustration of the above we note that American rockets of this class "Super Falcon" (GAR-3A) and "Sparrow 3" are characterized, respectively, by the following data: G = 54.9 and 172.4 kg; $l \approx 2$ and 3.66 m; $l_w = 0.61$ and 1 m; $d_r = 170$ and 220 mm; $r_\partial = 11$ and 18 km; v = 3600 km/hr; weight of warhead: 18 and 27 kg. Figure 1.9a and b shows the external appearance of the "Super Falcon" and "Sparrow 3" rockets. /25

Semiactive homing systems are used most frequently for guidance of rockets of the "air-to-air" class ("Falcon," "Sparrow 3"), although there are beam-riding rockets ("Sparrow 1").

Rockets of the "air-to-ground" class are designed for use from aircraft and other airborne vehicles against land, water surface and underwater targets. This class of guided weapons includes aircraft missiles, frequently called winged rockets, and aviation ballistic missiles.

Rockets of the "air-to-ground" type can be launched from rocket-carrying aircraft which fly at both great and small altitudes; they usually move at velocities of several hundreds of meters per second and can damage a target situated at a distance from ten to several hundreds or even thousands of kilometers from the launching point. As an example we can mention the American rockets "Hound Dog" (fig. 1.10) and "Bullpup" for which, respectively, $r_\partial \approx 800$ and 17 km; $G \approx 4350$ and 810 kg; $l \approx 13$ and 4 m; $l_w \approx 3.7$ and 1.2 m; $d_r \approx 0.71$ and 0.46 m; $v \approx 2000$ and 2500 km/hr. A wide variety of control systems are

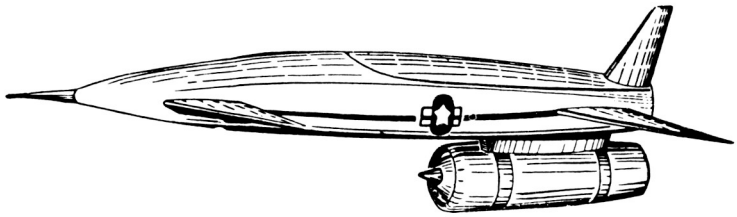

Figure 1.10

used for the guidance of winged rockets. For example, the guidance of the "Hound Dog" rocket is by means of an inertial system with correction by celestial navigation apparatus and the "Bullpup" is corrected by a radio control /26 command system. It should be noted that in recent years there has been a tendency to use autonomous systems for rockets guided to fixed targets.

Aviation ballistic missiles are a relatively new form of controlled airborne weapon. The use of a rocket-carrying aircraft as a launching platform makes it possible to ensure a considerable effective range, despite a relatively small fuel supply in comparison with ballistic missiles which are launched from the ground. This can be attributed to the fact that an aviation ballistic missile, released at a high altitude, does not have to overcome the dense layers of the atmosphere situated at ground level. However, as is well known, aviation ballistic missiles are controlled only in the initial part of their flight to the time when the required value and direction of the velocity vector of their motion is set, after which the rocket engine is shut down and it continues its flight by inertia, like any body ejected at some angle to the plane of the horizon. This gives rise to rigorous requirements on the movement of the rocket-carrying aircraft prior to the release of the aviation ballistic missile and on its control system.

The American "Skybolt" rocket can be cited as an example of an aviation ballistic missile of the "air-to-ground" type. This rocket is characterized by the following principal data: launching weight, 5150 kg; length, 11.6 m; diameter of fuselage, 0.9 m; flight range, 1600-2400 km (when released at an altitude of 11-13 km); maximum flight altitude, 320-480 km; flight velocity, approximately 11,000 km/hr. This rocket is designed for damaging fixed targets and has an inertial control system.

Rockets of the "ground-air" class, called antiaircraft guided missiles, are used for shooting down enemy aircraft and rockets and can be launched from the ground and the decks of surface vessels. The effective range of antiaircraft guided missiles is from several tens to several hundreds of kilometers and their flight velocity is hundreds and thousands of meters per second. The weight of rockets of this class is several tons. In order to ensure a rapid gain of altitude by the rocket there are additional booster engines which are automatically separated from the rocket after expenditure of the fuel. As an illustration of the average characteristics of antiaircraft guided missiles /27 cited here we can mention the principal tactical-technical data for rockets of the "Oerlikon," "Nike Hercules," "Nike Zeus" and "Hawk" types.

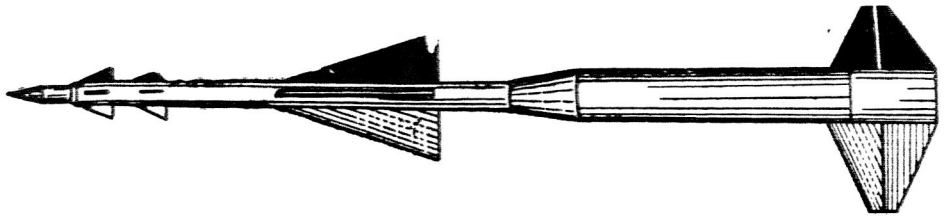

Figure 1.11

The "Oerlikon" missile was developed in Switzerland and is characterized by the following data: $G \approx 3700$ kg, weight of warhead: $G_{wh} \approx 40$ kg; $l \approx 6$ m; $l_w \approx 1.36$ m; $v \approx 2970$ km/hr; $r_\partial \approx 20$ km. The American rocket "Nike Hercules" and the antimissile missile "Nike Zeus" have the following characteristics, respectively: $G \approx 4500$ kg and 10 tons; $l \approx 12.2$ and 14.7 m; $l_w \approx 2.3$ and 2 m; $v \approx 3700$ and 5300 km/hr; $r_\partial \approx 137$ and 370 km. The "Hawk" missile is designed to damage low-flying targets. It has: $G \approx 600$ kg; $l \approx 5.1$ m; $l_w \approx 1.2$ m; $d_r \approx 0.36$ m; $v \approx 2500$ km/hr. We note that for the "Hawk" missile the values G and l are given without the booster taken into account.

Antiaircraft guided missiles use a beam-riding control systems ("Oerlikon"), a radio command control system ("Nike Hercules"), electronic homing systems ("Hawk") and combined nonautonomous radio control systems ("Nike Zeus" is guided by a radio command control system in the main flight stage and a homing system near the meeting with the target).

Figure 1.11 shows the typical appearance of an antiaircraft guided missile.

"Ground-to-ground" missiles are used for the damage of surface (usually fixed) targets. They usually are classified as winged (aircraft rockets) and ballistic missiles, among which, in turn, it is possible to distinguish tactical and strategic rockets (missiles). The latter can damage targets at a distance of 10,000 km or more from the launching point. Among the winged tactical rockets, which in essence are pilotless jet aircraft, we can mention the American rockets "Matador" and "Meuse 76." The "Matador" missile, which has an effective range of about 900 km, is guided by a radio zone control system which is based on the use of Shanicle radio navigation apparatus. The "Meuse 76" rocket (fig. 1.12a), which is 13.2 m in length and which has a flight velocity of about 1000 km/hr and an effective range of about 2000 km, is guided by a system based on the use of radar observation of the terrain features over which the flight path passes. /28

Among the ballistic missiles of the "ground-to-ground" class, the greatest attention has been given to the intercontinental ballistic missiles (ICBM)

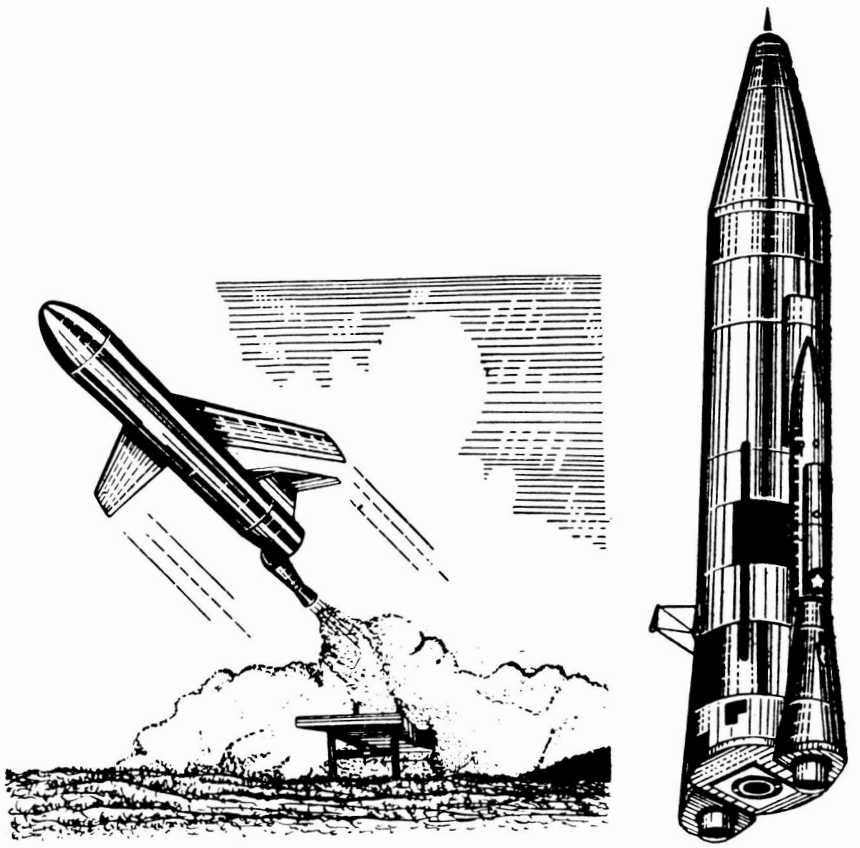

a b

Figure 1.12

which have an effective range of 10,000-20,000 km. To attain such ranges the ICBM, which also are used for putting artificial earth satellites and spacecraft into orbit, are supplied with powerful liquid- or solid-fuel jet engines.

Some additional information on the ICBMs can be given using the example of the American "Atlas" missile. This missile, whose external appearance is shown in figure 1.12b, has: $G \approx 118$ tons; $l \approx 25$ m; $d_r \approx 3$ m; $v \approx 30{,}000$ km/hr; $r_\partial \approx 16{,}000$ km.

In addition to ballistic missiles launched from the Earth's surface there are rockets which are launched by compressed air from the compartments of submarines. In particular, this applies to the American missile "Polaris" with an effective range of about 4500 km (model "Polaris A-3").

With the continuing development of ballistic rockets of the "ground-to-ground" class there has been a change in the system for controlling them. For example, whereas the first models of the "Atlas" were guided by radio command control, inertial systems superceded this. Inertial systems also are used for control of the "Polaris" missile, etc. /29

The flying qualities of a winged missile are influenced considerably by its aerodynamic form, determined by the type of body and wings, the placement of the wings relative to the body and the type of control components. In the selection of the aerodynamic configuration it is necessary to take into account the required value of the controlling force, the altitudinal and flight velocity ranges, etc.

Rockets with axial and plane aerodynamic symmetry are the most used. As is well known, the rotation of an axially symmetrical missile about its longitudinal axis does not change the vectors of total aerodynamic force and momentum if the control surfaces are in a neutral position. In the case of rockets with plane aerodynamic symmetry the mentioned vectors will turn in unison with the rocket.

For all practical purposes missiles with 3-4 wings, having an identical form and area and arranged symmetrically relative to the fuselage, are aerodynamically axially symmetrical.

Missiles with axial aerodynamic symmetry are used in those cases when the necessary controlling forces for the course and pitching planes should differ little from one another. Missiles of the "air-to-air" and "ground-to-air" classes therefore usually are aerodynamically axially symmetrical.

Winged missiles of the "air-to-ground" and "ground-to-ground" classes most frequently are designed in the form of an aircraft. There are also rockets of this class which have axial aerodynamic symmetry.

In the case of ballistic missiles which travel a large part of their controlled path outside the dense layers of the atmosphere where there are virtually no aerodynamic forces present, the wings are dispensed with.

The control of rockets with axial aerodynamic symmetry is accomplished in a rectangular (Cartesian) coordinate system.

The resultant lateral (normal) acceleration j_n of a rocket, in the case of Cartesian control, is formed by the creation, by the control components, of two independent forces acting in the plane normal to the flight trajectory. For example, if a rocket has four wings oriented at angles of 90° to one another, the acceleration characterized by the vector j_{nl} (fig. 1.13a) arises in a case when accelerations equal to j_{yl} and j_{zl} act in the direction of the axes $o_r y_l$ and $o_r z_l$, respectively. The vectors j_{yl} and j_{zl} are caused by the elevator and the rudder, and strictly speaking do not coincide with the vertical and horizontal transverse axes of the missile. However, in the first approximation, when explaining the principle of Cartesian control, this need not be taken into account.

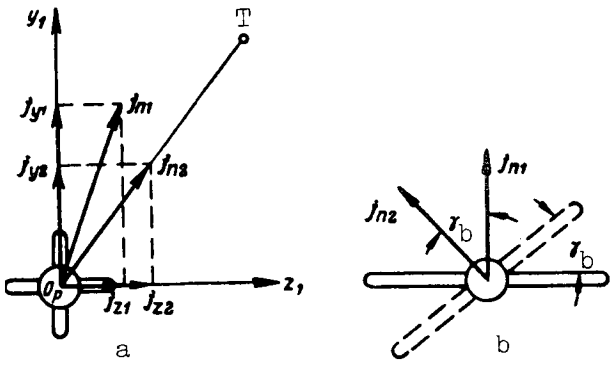

Figure 1.13

If at any time of the rocket flight the projection of the target onto the plane $o_r y_1, z_1$ is at point T, the creation of the required acceleration j_{n2} /30 requires such a deflection of the elevator and rudder that the component j_{y2} and j_{z2} are formed.

A distinguishing characteristic of Cartesian control is the absence of banking of the rocket (rotation around the longitudinal axis) during turns. In addition, arbitrary turnings of the body of the rocket about its longitudinal axis are inadmissible because, in this case, there would be a change of the direction of the acceleration vector.

Missiles having a plane aerodynamic symmetry are guided in a polar coordinate system. This can be attributed to the fact that the lift vector and, therefore, the lateral acceleration vector as well are always situated in the plane of symmetry. For example, when the rocket wings are situated in a plane normal to the vertical (fig. 1.13b) the acceleration vector j_{n1}, with an upward deflection of the elevator, will facilitate a climb. If the body of the rocket is turned by the angle γ_b about the longitudinal axis, the acceleration vector j_{n2} forming in the process is displaced by the same angle γ_b in relation to j_{n1}. The projection of the vector j_{n2} onto the horizontal plane causes acceleration and, under its influence, the rocket changes its flight course direction. Figure 1.13b shows that, with a constant value j_{n2}, an increase of γ_b leads to an increase of the intensity of turning on course and a decrease of the acceleration acting in the vertical plane. The necessary value of the module $|j_{n2}|$ can be attained by deflection of the elevator.

Thus, by changing the angle of banking, which usually is accomplished by use of ailerons and deflection of the elevator, it is possible to change the

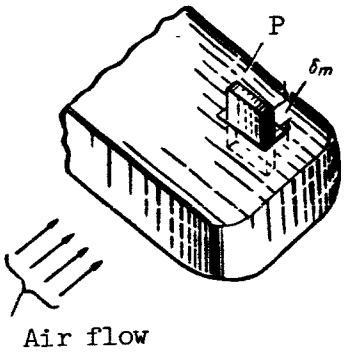

Figure 1.14

direction and value of the lateral acceleration of a rocket with plane aerodynamic symmetry. The existence of a relationship between the course and pitching control channels to a certain degree complicates the process of rocket control.

The control components of rockets bringing about changes of the controlling forces in both value and direction can be divided into aerodynamic and gas controls. A change of the controlling force acting on the rocket also can be attained by a deflection of the nozzle, the setting of the boosters and deflections of the principal lifting surfaces situated near the center of gravity. /31

Among the aerodynamic control surfaces used for rockets which travel only in the atmosphere there are smoothly moving control surfaces (control surfaces of the aircraft type) and spoilers (interceptors).

The action of smoothly moving control surfaces is based on a change of the angles of attack, banking and slip of the rocket. The spoiler is a small plate set perpendicular to the direction of the longitudinal axis of the rocket. This plate P (fig. 1.14) undergoes oscillatory motions caused by an electromagnetic drive; the plate periodically emerges the distance δ_m above the upper and lower surfaces of the wing or fin. When the plate P is in the upper position the disruption of the air flow gives rise to an aerodynamic force directed upward. This in turn causes a torque whose direction changes periodically due to the oscillations of the plate. However, by an appropriate selection of the frequency of vibrations of the plate it can be arranged so that the rocket will react only to the constant component M_c of the torque, equal to

$$M_c = M_M \frac{T_1 - T_2}{T},$$

where M_M is the maximum torque created by the plate P;

T_1 and T_2 are the times which the plate remains in the upper and lower positions;

$T = T_1 + T_2$ is the oscillation period of the plate.

It can be seen from this expression that the necessary curvature of the rocket flight trajectory can be attained by a change of the difference $T_1 - T_2$.

The principal merits of spoilers are their extremely small inertia and the smallness of the plates themselves and the apparatus causing their motion. At the same time, such control components increase the drag of the rocket and become ineffective when there are great flight velocities.

Gas-dynamical control systems are used for rockets flying at altitudes /32 exceeding several tens of kilometers. An example of a gas-dynamical system is the jet vane, which is a shaped plate made of a heat-resistant material and set within the jet of exhaust gases of the jet engine. When this plate is turned there is a change in the direction of the gas jet and the rocket therefore turns. The use of a gas vane decreases engine thrust. This can be avoided by replacing the gas vane by a booster placed at the center of mass of the rocket and ensuring a direct change of the lateral force acting on the rocket. In the latter case there no longer is a need for intermediate apparatus and links for changing the angular position of the rocket axes.

1.4. Principal Requirements Imposed on Control Systems

The requirements to be imposed on a planned control system usually are developed on the basis of an analysis of the problems which should be solved by the newly created rocket complex, taking into account the level of development of technology and also the accumulated experience in the field of production and operation of similar types of armament. For this reason, in this section, we will formulate a list of only those requirements which should be taken into consideration regardless of the type of rocket, control system, engine, etc.

The requirements imposed on control systems can be divided into three groups:

(1) requirements associated with the problems to be solved by the control system as a whole and its components (tactical requirements);

(2) operational requirements;

(3) requirements on the design of individual components and elements of the system.

In accordance with these groups of requirements it is possible to find an optimal, or close to optimal, type of system and determine its technical characteristics.

In the first group the most important requirements are assurance of:

(1) the necessary effective range and altitude of the control system;

(2) the stipulated probability of striking the target p_{st}, determined by the ratio of the number of strikes to the total number of launched missiles;

(3) a high flexibility of the tactical use of the guided missile, which is related to the mobility of the apparatus employed and the possibility of a rapid change of the direction of rocket launching.

The required effective range of radio control systems is attained by an appropriate selection of the type of electronic apparatus, wavelength range, strength of radio transmitters, etc. /33

The probability of striking the target p_{st} is influenced by a considerable number of factors, including:

(1) errors in rocket guidance caused by the maneuvering of the target and its properties, and also by errors in aiming, imperfection of individual elements of the control system, etc.;

(2) the weight, type and character of effect of the rocket warhead;

(3) the efficiency of operation and the principle of operation of the fuse;

(4) the reliability of operation of the control system in the rocket guidance process;

(5) influence of both natural and artificial radio interference;

(6) antiaircraft fire of the enemy.

We note that the term "striking of the target" usually means an event in which the object to which the rocket is guided ceases to perform its function (is knocked out).

The term guidance error (miss) of a rocket means the value of the deflection of the center of mass of the rocket from the target in the reference plane. This plane, frequently called the dispersion plane, should pass through the target if it is fixed or a set forward (computed) point. The problem of the orientation of the dispersion plane, which can be quite arbitrary, usually is solved using as a point of departure the convenience of investigation of the control systems.

When rockets are guided toward fixed surface and water targets it is desirable that the dispersion plane coincide with the plane which passes through the target and is perpendicular to the local vertical. Frequently it is convenient to pass the dispersion plane along the normal to the straight

line extending from the control point to the rocket or to the vector of the relative velocity of approach of the rocket to the target for that specific time when the control process ends. In the case of such orientation the reference plane will determine the minimum distance at which the rocket flies past the target.

An analysis of the factors characterizing p_{st} shows that the probability of striking the target is a function not only of the properties of the control system ensuring the flight of the rocket in accordance with the selected coherence, but also a number of other factors not dependent on the designer, or only slightly dependent. However, this does not mean that the development of a control system can be accomplished without the cooperation of those who design the entire complex of rocket control apparatus. As the basis of such cooperation there usually is a reasonable distribution of tolerances for the parameters of the elements of the control system complex and for the imposed requirements, working on the basis of the attained level of engineering development and the problem of attaining the stipulated probability of striking the target p_{st}.

Determination of the properties of the targets to be destroyed and the /34 required value p_{st} makes it possible to select the type of warhead and fuse and to impose corresponding requirements on them. This is followed by solution of the problem of the admissible errors of rocket guidance, the reliability of the operation of the control system, its noise immunity, etc.

It is customary to characterize the reliability of the control system by the probability p_r that this system will operate faultlessly during the entire time necessary for rocket guidance.

If no allowance is made for enemy countermeasures other than antiaircraft fire, as the probability of the target being struck by one missile we have the following expression

$$p_{st} = p_r p_\partial p_{st\,c}, \qquad (1.4.1)$$

where p_∂ is the probability of the rocket reaching the target; p_∂ is determined by the ratio of the number of rockets reaching the target without technical failures to the total number of launched rockets;

$p_{st\,c}$ is the conditional probability of striking the target, computed on the assumption that the control system operates reliably and that the rocket is not knocked out by the enemy.

Determination of the probability $p_{st\,c}$ requires a knowledge of the properties of the rocket warhead, fuse and control system and therefore this must be done in relation to a specifically formulated problem.

For example, if an impact-type fuse is used and it is probable that the target will be damaged only if there is a contact between it and the warhead of the rocket, then $p_{st\ c}$ will represent the probability that the center of mass of the rocket will fall in the contour of the target and its value with a sufficient degree of accuracy can be found using the following expression

$$p_{st\ c} = \iint_{(S)} W(y_r, z_r)\, dy_r dz_r \qquad (1.4.2)$$

Here $W(y_r, z_r)$ is the dispersion law of the rocket, characterizing the two-dimensional probability density for the coordinates of the point of the rocket in the reference plane; S is a region representing the projection of the contour of the target onto the reference plane.

The axes oy_r and oz_r of the coordinate system $oy_r z_r$, forming the dispersion plane, in the absence of a relationship between the errors of rocket course and banking guidance, should preferably be situated in the rocket control planes.

Then the coordinates y_r and z_r entering into expression (1.4.2) represent the components of the miss h of the rocket, read from the point o of the coordinate system $oy_r z_r$. Usually it can be assumed that z_r and y_r have a normal probability distribution law. This can be attributed to the fact that the errors of y_r and z_r are caused by a large number of approximately equal-valued and independent random effects. /35

In the absence of a dependence between the miss components y_r and z_r, distributed normally, for determination of $W(y_r, z_r)$ it is necessary, as is well known, to determine the mathematical expectations $\bar{y}_r$ and $\bar{z}_r$ and also the dispersions σ_y^2 and σ_z^2 for y_r and z_r. In those cases when the control channels are interconnected, in addition to knowing $\bar{y}_r$, $\bar{z}_r$, σ_y^2 and σ_z^2 in order to find $W(y_r, z_r)$ it is necessary to know the correlation coefficient for the random values y_r and z_r. We recall that the correlation coefficient of two random values represents the ratio of the covariance R_{yz} to the product $\sigma_y \sigma_z$.

Some groups of targets (such as ground targets) probably are not damaged only as a result of direct contact with the warhead of the rocket but also

through the actuation of a contact fuse in some plane region surrounding the target. Under these conditions S in (1.4.2) should be understood as the projection of the region of an unconditional impact onto the dispersion plane.

At the same time there can be a dependence of target damage on where the warhead explodes. In these cases the probability of target damage should be determined using the following expression

$$p_{st\ c} = \iint_{(S)} f(y_r, z_r)\, W(y_r, z_r)\, dy_r dz_r, \qquad (1.4.3)$$

where $f(y_r, z_r)$ is the conditional probability of striking of the target under the condition that the detonation of the warhead occurs at the point with the coordinates y_r, z_r.

When using proximity fuses which ensure the explosion of the charge both with a direct hit on the target and at some distance from it, depending on the work program of the fuse, the problem of computation of $p_{st\ c}$ of one rocket becomes more complex. However, with the approach of rockets with powerful demolition or nuclear warheads, it is possible to define a zone in which the hitting of the rocket by the time of ignition of the fuse leads to a virtually reliable damage of the target. Under this condition the value $p_{st\ c}$, in the case of the operation of the rocket against ground (water) and air targets, is equal to the probability of hitting of the rocket in a two- or three-dimensional area or space constituting part of the damage zone. If a proximity fuse and a fragmenting warhead are used, $p_{st\ c}$ can be found using expression (1.4.3) in which $f(y_r, z_r)$ is understood to be the conditional /36 probability of striking the target, determined on the assumptions that the errors of rocket guidance in the reference plane assume the values y_r and z_r.

Summarizing the above, it can be concluded that, when the rocket has a contact or proximity fuse, when computing the conditional probability of striking the target, it is sufficient to know the mathematical expectations, dispersions and correlation coefficients for the rocket miss components y_r and z_r and it is also sometimes required that these same statistical characteristics be known for range guidance errors.

When the rocket has a radio fuse and a directed action warhead, it is difficult to find $p_{st\ c}$ on a theoretical basis even in the case of quite simple conditions of rocket use. This can be attributed to the fact that the detonation of the rocket warhead as a result of the directed action of the antenna

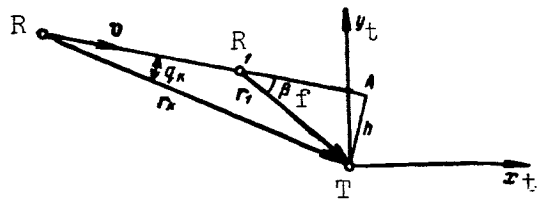

Figure 1.15

of the radio fuse is a function not only of the distance between the rocket and the target, but also the inclination of the vector v. In addition, it must be taken into consideration that the warhead does not act in different directions with the same efficiency. In this connection we will consider only one example which makes it possible to obtain some idea of the determination of those parameters of the control system whose knowledge makes it possible to compute the probability $p_{st\ c}$.

As an example we will analyze the flight process of a homing rocket in a vertical plane on the assumption that the target is fixed and is represented by point T (fig. 1.15). As a result of the presence of a blind zone in the coordinator measuring instruments and also of the inertia of the control system, it can be assumed that beginning with some specific time, when the center of mass of the rocket is at point R (fig. 1.15), the flight of the rocket becomes uncontrolled and the angle q_k of inclination of the velocity vector v to the straight line RT does not change. We will assume that, at this time, the distance between the rocket and the target is r_K and exceeds the effective range r_f of the fuse.

The detonation of the warhead of the rocket can occur at point R_1 when the distance r_1 between the target and the rocket is less than or equal to r_f, and the angle between the vectors v and r_1 is the value β_f, being one of the characteristics of the fuse used. From the triangles RAT and R_1AT, in which the side AT = h normal to the straight line RA represents the miss of the target, we have

$$h = r_K \sin q_k = r_1 \sin \beta_f. \qquad (1.4.4)$$

We note that the angle q_k in expression (1.4.4) characterizes the error in the position of the vector v, responsible for the miss h. /37

By solving (1.4.4) relative to r_1, we find the following condition for actuation of the radio fuse

$$r_1 = \frac{r_K \sin q_k}{\sin \beta_f} \leq r_f. \qquad (1.4.5)$$

It follows from this condition that for stipulated values r_K and r_f the error q_k should fall within specified limits. If $q_k < 30^\circ$, which is customary and which occurs in the absence of artificial interference, then

$$r_1 \approx r_K \frac{q_k}{\sin \beta_f}. \qquad (1.4.6)$$

By knowing the probability distribution law for the random value q_k it is possible to find the probability density $W(r_1)$ for the distance r_1 at which the warhead of the rocket is exploded.

Then it is possible to determine the conditional probability of striking the target $p_{st\ c}$

$$p_{st\ c} = \int_0^{r_f} f(r_1)\, W(r_1)\, dr_1.$$

Here $f(r_1)$ is the conditional probability of striking the target under the condition that the warhead of the rocket is exploded at the distance r_1 from the target.

Usually the random value q_k conforms to a normal probability distribution. Therefore

$$W(r_1) = \frac{1}{\sqrt{2\pi}\,\sigma_r} \exp\left[-\frac{(r_1 - \bar{r}_1)^2}{2\sigma_r^2}\right],$$

where, as follows from expression (1.4.6)

$$\bar{r}_1 = r_K \frac{\bar{q}_k}{\sin \beta_f},$$

$$\sigma_r^2 = \frac{r_K^2 \sigma_q^2}{\sin^2 \beta_f},$$

and $\bar{q}_k$ and σ_q^2 are the mathematical expectation and the dispersion of the random value q_k, respectively.

It follows from the derived relations that the admissible values $\bar{q}_k$ and σ_q^2 should be stipulated when developing the considered type of system. At the same time it also is possible to stipulate the admissible values of the mathematical expectation $\bar{h}$ and the dispersion σ_h^2 of the miss h, since

$$\bar{r}_1 = \frac{\bar{h}}{\sin \beta_f},$$

and

$$\sigma_r^2 = \frac{\sigma_h^2}{\sin^2 \beta_f}.$$

In conclusion we point out that computation of $p_{st\ c}$ for rockets supplied with radio fuses can be carried out using expression (1.4.3), if by $f(y_r, z_r)$ is understood a function characterizing the probability of striking of the target, under the condition that the center of mass of the rocket hits at a point with the coordinates y_r, z_r in the reference plane and when all necessary parameters of the radio fuse are taken into account. /38

It also is of very great importance to ensure the necessary resolution of the control system. We note that the resolution of the control system usually is characterized by the minimum distance between two targets at which they are sensed by the system separately, so that the rocket can be guided to one of the targets. In actual practice, the resolution of the control system is determined by the capabilities of the radar system used to separately determine the coordinates of two closely spaced targets.

In the case of insufficient resolution, the following cases are possible:

(1) guidance of the rocket to one of the targets, if the latter reflects considerably more energy than all the other targets simultaneously entering into the field of view of the control system;

(2) guidance toward a so-called center of reflection, provided that all the targets situated in the field of view of the control system have approximately identical reflective properties.

It therefore follows that when operating against grouped targets, the resolution exerts an influence on the accuracy of rocket guidance and therefore

on the probability of striking the selected target. This circumstance should be taken into account when developing the control system as a whole.

The mobility of control apparatus is related to a considerable degree to the applied principles of design of the coordinators and the apparatus for forming and transmitting the commands, the number of available fixed waves, the required accuracy of rocket guidance, etc.

Another requirement of extremely great importance is the possibility of rocket guidance when there is both unorganized (natural) and organized (artificial) radio interference. In a general case the interference leads to an increase of the miss of the rocket or a total disruption of the guidance process. The problem of the influence of interference is considered in sufficient detail in the following chapters of the book. In some cases the control system should be protected against the effect of the most probable and dangerous interference, even if this considerably complicates the apparatus and increases its cost.

The most important operational requirements are:

(1) faultless operation of all components of the control system under particular meteorological and climatic conditions and also despite possible dynamic overloads;

(2) assurance of a guaranteed service time, a stipulated time of continuous operation and a specified time for the reliable operation of all the apparatus making up the control system; /39

(3) speed, safety, objectivity and automation of technical maintenance, using as a point of departure the reduction of the system to combat readiness in a specified interval of time and with a high quality;

(4) the absence of any need for employing highly skilled specialists, which is particularly important in the case of large-scale use of rockets.

Among the principal design requirements are:

(1) simplicity of design and the possibility of its standard production by enterprises whose workers are not highly skilled;

(2) assurance of free access to individual units;

(3) assurance of convenient placement of the regulation and adjustment devices;

(4) minimum weight and size, especially of apparatus carried aboard rockets and rocket-carrying aircraft;

(5) minimum consumption of electrical and other forms of energy;

(6) assurance of high-quality airtightness and cooling of the units in accordance with the conditions of their operation.

When all the above-mentioned requirements are satisfied the control system can be considered to be planned with technical competence, provided its cost is relatively low. At the same time it must be remembered that in each specific case there can be some specific requirements which have not been considered here.

CHAPTER 2. GENERAL INFORMATION ON CONTROL SYSTEM COORDINATORS. METHODS OF ROCKET GUIDANCE

2.1. Introductory Comments

The coordinators of rocket control systems are devices which measure /40
the mismatch parameter, the form of which is determined to a considerable degree by the type of control system and the rocket guidance method used. For this reason, it is necessary to first derive mismatch equations for different types of control systems and different guidance methods. Analysis of these equations makes possible the determination of the makeup of the primary measuring instruments of the coordinator and to represent in general features the structure of its computer, which forms the mismatch parameter, on the basis of data received from the primary measuring instruments.

In the process of rocket guidance the components of the mismatch parameter which are to be measured change value continuously. This is caused by the relative motion of the rocket and the target, and in some cases also the movement of the control point. The formulation of the requirements imposed on the dynamic properties of the coordinator as a link in the automatic control system and computation of its dynamic errors are possible only when the law of change of the measured values is known. The character of the change of the values entering into the mismatch parameter for a particular guidance method is determined to a considerable degree by the kinematic equations relating the relative motions of the rocket, target and control point (if the latter is present in the investigated guidance system). Therefore, in this chapter we will discuss both the general principles of design of coordinators and the derivation of the principal kinematic relations for different guidance methods.

In addition to the controlling effects, the coordinator is subject to the influence of different kinds of perturbations whose presence also influ- /41
ences the accuracy of determination of the mismatch parameter. The perturbing factors for electronic coordinators are: instrument noise of the receivers in the coordinator, fluctuations of the signal reflected from the target, artificially created radio interference, etc. For this reason, in the final part of the chapter we will present some ideas on how perturbing effects are taken into account when evaluating the accuracy of measurement of the mismatch parameter.

2.2. Mismatch (Error) Equation

The mismatch equation establishes the dependence of the mismatch parameter on the parameters characterizing the relative motion of the rocket, target and control point. In general form it can be written as follows

$$\Delta = \Delta[x_1(t), x_2(t), x_3(t), \ldots], \qquad (2.2.1)$$

where Δ is the mismatch parameter and $x_1(t)$, $x_2(t)$, $x_3(t)$... are parameters characterizing the relative motion of the rocket, target and control point.

The specific value of $x_1(t)$, $x_2(t)$, $x_3(t)$... will be determined when discussing the special forms of the mismatch equation.

If the coherence imposed on the motion of the rocket by the control system is satisfied ideally, in the guidance process the mismatch parameter will be equal to zero, that is

$$\Delta = 0. \qquad (2.2.2)$$

Equation (2.2.2), being a special case of the mismatch equation, is called the ideal coherence equation.

Each specific form of the mismatch equation and of the ideal coherence equation following from it is applicable to a particular guidance method. If at all times the rocket flight proceeds exactly along the trajectory for which condition (2.2.2) is satisfied, this indicates that there is ideal rocket guidance and the trajectory being followed is the reference or theoretical trajectory. Each guidance method therefore has its own class of reference trajectories, and sometimes a guidance method is defined as a method of determining reference trajectories.

The actual or real rocket trajectory differs from the reference trajectory due to the presence of inertia and instrument errors in the control system and different kinds of perturbations acting on the control system.

In some cases the mismatch equation for a single control plane is con- /42
veniently represented in the form

$$\Delta = \varkappa_T - \varkappa_\partial, \qquad (2.2.3)$$

where $\varkappa_T$ is the given or theoretical value of the adjustable value characterizing the relative motion of the target and rocket or the control point, target and rocket during the flight of the latter along a reference trajectory, and $\varkappa_\partial$ is the actual value of the adjustable value.

The dependence $\varkappa_T = \varkappa_T(t)$ sometimes is called the control function because in a number of control systems it is the key effect for the guidance circuit.

The number of actually used mismatch equations and, therefore, the number of methods of guidance is limited for the most part by the possibilities of technical design of the required complex of measuring instruments making up the coordinator. The selection of a particular guidance method from among those technically possible is determined by tactical requirements imposed on the control system.

We will divide the possible reference trajectories into two groups for convenience in subsequent exposition. The first group includes fixed trajectories and the second group includes unfixed trajectories.

Guidance on fixed trajectories occurs when the target and the launching point of the rocket are fixed relative to the Earth's surface. It also is assumed that the coordinates of the target and launching point are known. In such a situation the reference trajectory can be computed in advance (before the launching of the rocket). It remains constant during the entire time of rocket guidance.

When a rocket is guided toward a moving and maneuvering target, it is virtually impossible to compute a fixed reference trajectory in advance because its character will be essentially dependent on the form of the maneuver of the target made after the launching of the rocket. Unfixed reference trajectories also are the rule when rockets are guided toward fixed targets from a moving control point.

2.3. Mismatch Equations for Rocket Guidance along Fixed Reference Trajectories

The conditions for applicability of the method of rocket guidance along fixed reference trajectories, noted above, indicate the feasibility of using this method in the guidance of winged and ballistic missiles of the "ground-to-ground" class.

When stipulating the reference trajectory and its principal elements it is most important to know precisely the coordinates of the target, the launching point and the control point, if the latter is part of the guidance system.

Since the form of fixed trajectories and therefore the mismatch equations will be different for winged and ballistic missiles, below we will discuss two examples, one of which illustrates the process of guidance of a winged missile of the "ground-to-ground" class and the second which illustrates the process of guidance of a ballistic missile of this same class. /43

Figure 2.1 shows one of the possible reference trajectories of a winged missile of the "ground-to-ground" class. Here points o_c, T and o_r denote the positions of the launching site, target and rocket, respectively. The origin of the ground coordinate system $o_c x_{ec} y_{ec} z_{ec}$ is related to point o_c. The axis

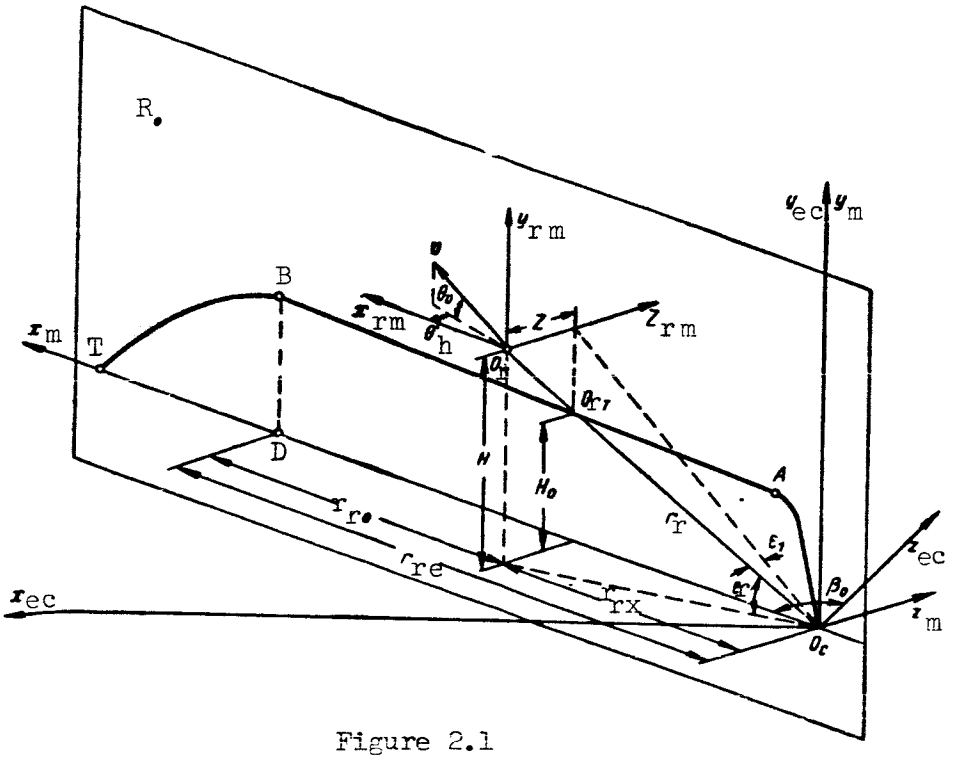

Figure 2.1

$o_c y_{ec}$ coincides with the local vertical and the axis $o_c z_{ec}$ is directed to the north.

The reference trajectory of the rocket lies in the plane R_0, normal to the Earth's surface and passing through the launching point o_c and the target T. The intersection of the plane R_0 at the Earth's surface is the arc of a great circle (orthodrome). The angle formed by the plane R_0 with the direction to north is denoted β_0. We have $\beta_0 = 360^\circ - \beta_{az}$, where β_{az} is the azimuth of the target. The trajectory can be broken down into three parts on the basis of altitude. The segment $o_c A$ is the climb, AB is the approach to the target /44 and BT is the dive. It is assumed that the principal part of the rocket trajectory AB lies at the constant altitude H_0, although this condition is not mandatory.

When a winged missile is guided along a fixed trajectory it is most common to use the method of coincidence of the center of mass of the missile and the reference trajectory. As a measurement coordinate system for measurement of the mismatch parameters when using the method of coincidence of the center of mass

of the rocket with the reference trajectory, it is convenient to introduce the orthodromic coordinate system $o_c x_m y_m z_m$ (fig. 2.1), whose origin coincides with the launching point of the rocket o_c. The $o_c y_m$ axis coincides with the $o_c y_{ec}$ axis of the ground coordinate system and the $o_c x_m$ axis lies in the plane R_0 along the tangent to the orthodrome. In this coordinate system the position of the rocket is given either by rectangular coordinates (altitude H, lateral deflection z and horizontal range r_{rx}) or the following are selected as such coordinates: flight altitude H, angle of lateral deflection ϵ_l and slant range r_r.

The use of spherical coordinates (slant range r_r, angle of lateral deflection ϵ_l and angle of elevation ϵ_r) in the case of a low flight altitude of the rocket is infeasible due to the difficulty in controlling the small angle ϵ_r. Theoretically it also is possible to use a geographical coordinate system for measurement of the mismatch parameter. In such a system the position of the rocket is determined by altitude H, longitude λ and latitude φ. However, the use of this coordinate system results in an appreciable complication of the coordinator computer.

The mismatch equations for the principal segment AB of rocket guidance along a fixed trajectory can be written in the form (2.2.3), assuming that the stipulated values of the adjustable values characterizing rocket flight along the reference trajectory are equal for the rectangular coordinates of the rocket $\nu_{TH} = H_0$, $\nu_{Tz} = 0$, $\nu_{Tr} = r_{re}$. The actual values of the mentioned parameters will be equal respectively to: $\nu_{\partial H} = H$, $\nu_{\partial z} = z$, $\nu_{\partial r} = r_{rx}$.

Then the mismatch equations assume the form

$$\left.\begin{aligned} \Delta_H &= H_0 - H, \\ \Delta_z &= -z, \\ \Delta_r &= r_{re} - r_{rx}. \end{aligned}\right\} \qquad (2.3.1)$$

If we select $\nu_{TH} = H_0$. $\nu_{T\epsilon} = 0$ and $\nu_{Tr} = r_{sr}$ as the stipulated values of the adjustable parameters, where r_{sr} is the slant range to the point B of transition of the rocket to a dive, and the actual values of these parameters are assumed equal to $\nu_{\partial H} = H$, $\nu_{\partial \epsilon} = \epsilon_l$ and $\nu_{\partial r} = r_r$, respectively, the mismatch equations are written in the form

$$\left.\begin{aligned}\Delta_H &= H_0 - H,\\ \Delta_{\varepsilon_1} &= -\varepsilon_1,\\ \Delta_{r_{sl}} &= r_{sr} - r_r.\end{aligned}\right\} \qquad (2.3.2)$$

Analysis of equations (2.3.1) and (2.3.2) shows that the controlling /45 functions for the principal part of the fixed trajectory are constant values (in a special case, zero). Equations similar to (2.3.1) and (2.3.2) can be written for the ascent and dive parts of the trajectory; in this case it is necessary to take into account only the change of the stipulated altitude of rocket flight with time.

The system of equations (2.3.1) can be considered as the combination of the projections of the mismatch parameter vector onto the axes of an orthodromic coordinate system.

Then

$$\Delta = \Delta_r i + \Delta_H j + \Delta_z k,$$

where i, j, k are the unit vectors of the coordinate system $o_c x_m y_m z_m$.

It follows from equations (2.3.1) and (2.3.2) that the coordinator should contain three measurement channels (altitude, lateral deflection and remaining range) for measurement of the components of the mismatch parameter Δ. We note that only the components of the mismatch parameter of the lateral deflection and altitude channels are used in forming the controlling signals fed to the control components of the rocket for maintaining it on its reference trajectory. However, the component of the mismatch parameter measured in the range channel is used for producing the command for the transition of the rocket into a dive or into a homing regime when it reaches point B of the trajectory, when the actual range to the rocket becomes equal to the stipulated range and the component of the mismatch parameter of the remaining range channel becomes equal to zero. This circumstance is due to the absence of effectively operating systems of control of the value of the velocity vector of winged missiles (ref. 22).

If only those components of the mismatch parameter on the basis of which signals are shaped for the control of a rocket in the horizontal and vertical planes are taken into account, the mismatch parameter can be represented in the form of a two-dimensional (complex) vector in the reference plane, that is, the plane passing through the center of mass of the rocket normal to its flight trajectory, assigning to the vertical component of the mismatch parameter the imaginary unit

$$j = \sqrt{-1}.$$

Then

$$\Delta = \Delta_z + j\Delta_H.$$

When a rocket is guided along a fixed trajectory each coordinator channel usually has its measuring instrument which operates independently of the measurement instruments of other channels. Therefore, the representation of the mismatch parameter in the form of a vector or complex value, to a considerable degree, has a formal character and is done exclusively for generality.

After establishing what values should be measured for determination /46
of the mismatch parameter during the guidance of a winged missile along a fixed trajectory we determine the apparatus which can be used for making these measurements.

Radio altimeters and barometric altitude sensors are used as altitude sensors during rocket flight. The latter have preference over radio altimeters due to the simplicity of design and their reliability of operation. In addition, the use of barometric altitude sensors makes it possible to have horizontal rocket flight, regardless of the character of the terrain over which the rocket is flying. For formation of the mismatch parameter of the altitude channel the signal from the output of the altitude sensor (in the form of a voltage or current) is compared with the signal of the altitude corrector, whose value is proportional to the stipulated flight altitude H_0. The altitude corrector is adjusted before the rocket launching. The difference of the signals received as a result of the comparison is used as the measured value of the mismatch parameter of the coordinator altitude channel.

Measuring instruments of different types are used for measurement of lateral deflection. They can be divided into three groups:

(1) nonautonomous electronic (angle-measuring, angle-measuring– range-finding, range-finding, add-subtract– range-finding);

(2) autonomous (autonomous electronic, inertial, celestial navigation measurement instruments, and those based on the use of ground features);

(3) combined.

A description of the principles of design of the mentioned measurement instruments and an analysis of their operation are given in the chapters which follow.

The formation of the mismatch parameter in the remaining range channel usually is accomplished using measurement instruments of the same types as used in the channel for measurement of lateral deflection.

The form of the reference trajectory of a ballistic rocket differs from the trajectory of a winged missile discussed earlier; this is due to the difference of the coordinators of missiles of the mentioned types.

Figure 2.2 shows the flight trajectory of a close-range ballistic missile. Here the origin of the ground coordinate system $o_c x_{ec} y_{ec} z_{ec}$ coincides with the

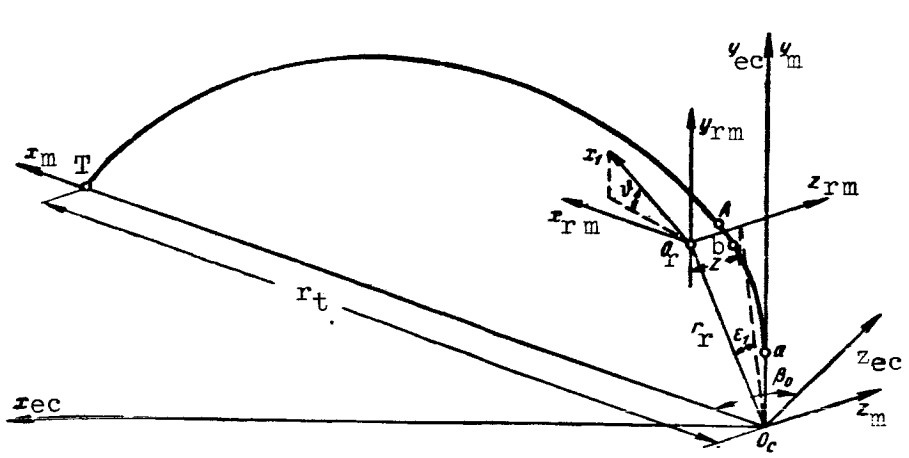

Figure 2.2

launching point o_c. The reference trajectory of the rocket lies in the plane $o_c x_m y_m$ of the measurement coordinate system $o_c x_m y_m z_m$, turned in the horizontal plane relative to the ground coordinate system in such a way that its axis $o_c x_m$ coincides with the launching point-target line. The position of the target in a ground coordinate system is given by the angle β_0 and the range r_t.

The rocket trajectory (curve $o_c AT$) consists of two parts: active $o_c A$ (a comparatively small part of the trajectory which the missile travels with engine operating), and passive AT (where the missile flies with the engine nonoperative).

The rocket flies a large part of the passive part of the trajectory /47 along a computed ballistic trajectory (the trajectory of a free projectile) under the influence of the initially applied force and the force of gravity. In the case of close-range missiles the ballistic trajectory is close to a parabola. Long-range missiles, including intercontinental missiles, fly along trajectories close to an elliptical curve representing part of an ellipse, one of whose foci is situated at the center of the Earth. This trajectory differs from a ballistic trajectory only at the end of the passive part as a result of deceleration of the rocket during its entry into the dense layers of the atmosphere.

The active part of the trajectory in turn can be divided into three parts: the launching segment $o_c a$, the control segment ab and the segment with engine inoperative bA.

In the launching segment the rocket moves vertically upwards, which decreases the time it moves in the dense layers of the atmosphere and therefore decreases the expenditure of energy in overcoming air resistance. Several seconds after launching, on commands received from the control system, the

longitudinal axis of the rocket begins to turn in the direction of the target and the trajectory becomes curved. When the parameters of rocket motion attain the computed values, a command is fed for cutting out the engine. Rocket flight in a ballistic curve begins after the engine becomes inoperative.

By establishing the character of the reference trajectory of the ballistic missile it is possible to obtain expressions for the mismatch parameter and determine the complex of apparatus making up the coordinator.

The flight distance of a close-range ballistic missile r_0, with some simplifying assumptions (absence of air resistance, replacement of the Earth's /48 surface by a plane, etc.), can be computed using the known formula

$$r_0 = \frac{v_{in}^2 \sin 2\theta_{in}}{g}. \qquad (2.3.3)$$

Here v_{in} and θ_{in} represent the velocity of the rocket and the angle formed by the velocity vector and the horizontal plane, respectively, at the time the engine becomes inoperative.

It follows from expression (2.3.3) that a change of the firing range is attained by variation of the values v_{in} and θ_{in}.

It follows from the above that the rocket hits the target if there is lateral pointing (the actual trajectory of the rocket will lie in the vertical plane $o_c x_m y_m$ passing through the launching point and the target) and the engine will become inoperative at the time when the values of the initial velocity v_{in} and angle θ_{in} attain those values at which the range of the striking point of the rocket will be equal to the range of the target r_t. We note that when stipulating the reference trajectory of a long-range rocket it is necessary to take into account the Earth's curvature and rotation.

For control of lateral pointing it is necessary to determine the lateral deflection of the rocket from its reference trajectory in the active part of the flight. This problem is solved by the coordinator lateral deflection channel.

The equation for the mismatch parameter of the lateral deflection channel, as in the case of guidance of winged missiles, can be represented in the form

or

$$\left.\begin{aligned} \Delta_z &= -z \\ \Delta_{\varepsilon_1} &= -\varepsilon_1, \end{aligned}\right\} \qquad (2.3.4)$$

where z is the linear deflection of the rocket from the plane in which the reference trajectory lies; ϵ_1 is the angular deflection of the rocket from this same plane.

Coordinators of the angle-measuring, add-subtract– range-finding and inertial types are in practical use for measurement of the lateral deflection of a ballistic missile, as well as measuring instruments based on use of the Doppler effect.

The functions of the range channels of the coordinators of ballistic and winged missiles differ from one another. Whereas in the control systems of winged rockets the role of a coordinator range channel is reduced essentially to the recording of the remaining range of the rocket, on the basis of the measurements made in the range channel of the coordinator of a ballistic rocket the initial flight range itself is set.

It follows from formula (2.3.3) that the stipulated range of striking of the target $r_0 = r_t$ is attained in a case if at the time of deactivation of the engine there is a rigorous correspondence between the value of the initial /49 velocity v_{in} and the angle of its inclination θ_{in}. It therefore would appear that the coordinator range channel should contain a unified system for measurement of the value and position of the velocity vector of the rocket. In practice, however, the range channel can consist of two different measurement systems, functionally unrelated to one another, which simplifies the design of the coordinator. The admissibility of such separate measurement of the value of the velocity vector and its angle of inclination can be justified by the following considerations. Formula (2.3.3) shows that the maximum value of the range of the point of striking of the rocket for a given initial velocity occurs when $\theta_{in} = 45^\circ$. The trajectory of a rocket with $\theta_{in} = 45^\circ$ sometimes is called an optimal trajectory, since moving along it the rocket covers the stipulated range with a minimum initial velocity, and therefore with a minimum possible expenditure of fuel. We note that when the curvature of the Earth's surface is taken into account the optimum angle of inclination of the velocity vector differs somewhat from 45° and is dependent on the velocity v_{in}.

The process of rocket guidance tends to be organized in such a way that rocket flight trajectories will be close to optimal. If the condition of the closeness of the trajectory to an optimal trajectory is satisfied, the influence of inaccurate setting of the angle θ_{in} on the error in range is insignificant. In actuality, by computing the differentials of both sides of equation (2.3.3) and converting to finite increments, we obtain

$$\frac{\Delta r_0}{r_0} = 2\frac{\Delta v_{in}}{v_{in}} + 2\frac{\Delta\theta_{in}}{\tan 2\theta_{in}}. \qquad (2.3.5)$$

In the case of an angle θ_{in} close to optimal, the value of the second term is increasingly small. Therefore, two functionally independent systems can be used for control of the flight range of a ballistic missile. One of these is used for the programmed change of the angle θ and the second for measurement of the current velocity value.

The program for the change of the angle θ is prepared on the basis of the approximately known law of the change of the velocity of the rocket with time. Therefore, by the time the engine becomes inoperative the angle θ attains a value close to optimal. Since the angle of attack for ballistic missiles does not exceed several degrees, the angle of inclination of the velocity vector can be considered approximately equal to the angle of inclination of the longitudinal axis of the rocket to the horizon, that is, to the angle of pitching ϑ (in figure 2.2 the longitudinal axis of the rocket is denoted $o_r x_1$). Then the system for change of the angular position of the rocket can be arranged in the following way. Several seconds after the launching (the time required for the rocket to pass through the launching part of the trajectory) the programming mechanism is cut in and produces the programmed value of the change of the angle of pitching ϑ_{pr}. The actual value of the angle of pitching ϑ is measured with a gyroscopic transducer. On the basis of a comparison of the actual and programmed values of the pitching angle a signal is shaped and fed to /50 the control components. By deflection of the control surfaces the longitudinal axis of the rocket changes its angular position. Therefore, the mismatch parameter of the apparatus for change of the angular position of the rocket of the coordinator range channel can be written in the form

$$\Delta_{\vartheta} = \vartheta_{pr} - \vartheta. \tag{2.3.6}$$

In addition to apparatus for the change of the angular position of the rocket, the coordinator range channel should contain apparatus designed for measurement of the current velocity v of the rocket and its comparison with the stipulated value of the initial velocity v_{in}. When the current velocity of the rocket becomes equal to the stipulated value, a command is produced for deactivation of the engine. The mismatch parameter of the system forming the command for deactivation of the engine has the form

$$\Delta_v = v_{in} - v. \tag{2.3.7}$$

The current velocity of the rocket is measured by inertial measurement systems and electronic apparatus based on use of the Doppler effect. In an inertial measurement system for velocity measurement, the signal received from the accelerometer, oriented properly in relation to the longitudinal axis of

the rocket, is fed to an integrator. A voltage appears at the output which is proportional to the velocity of rocket flight. In the comparison circuit this voltage is compared with the voltage from the master oscillator, whose value is set prior to the launching of the rocket, using the required flight range as a guide.

One of the variants of an electronic system for deactivation of the engine includes: a surface receiver-transmitter, a responder aboard the rocket and a control command radio link (ref. 4). The signals from the surface transmitter are received aboard the rocket and are reradiated by the responder. The response signal is received by the surface station receiver. Obviously, the frequency of the received signal differs from the frequency of the transmitted signal by the value of the Doppler frequency shift. By measuring the mentioned shift it is possible to determine the velocity of withdrawal of the rocket from the ground station. When this velocity becomes equal to the stipulated value, a command is transmitted through the control command radio link for deactivation of the engine.

2.4. Kinematic Equations for Rocket Guidance along Fixed Reference Trajectories

In order to impose requirements on the dynamic characteristics of any measuring instrument, including a coordinator, it is necessary to know the law of change of the measured values. With relation to the coordinator of a guided rocket this means that, even before beginning the planning of a /51 coordinator, it is desirable to have data on the character of the change of the mismatch parameter, at least for the most typical cases of rocket use.

Since the mismatch parameter represents the difference between the stipulated value of the adjustable value, which can be constant (in a special case equal to zero) or change in conformity to a known law, and its actual value, some idea of the character of its change can be obtained if the laws of change of these values are known. Since the character of change of the stipulated value of the adjustable value is known, it only remains to determine the laws of change of its actual value, which is dependent on the actual rocket flight trajectory.

The trajectory of a winged rocket during its flight in the unperturbed atmosphere can be determined if the law of change of the value and direction of the air velocity vector with time is established.

The position of the velocity vector in a moving coordinate system $o_r x_{rm} y_{rm} z_{rm}$ (fig. 2.1), whose axes are parallel to the corresponding axes of the measurement coordinate system $o_c x_m y_m z_m$, is given by the angles θ_v and θ_h, where θ_v is the angle between the direction of the velocity vector and its projection onto a horizontal plane (angle of inclination of the trajectory)

and θ_h is the angle between the projection of the velocity vector onto a horizontal plane and onto the axis $o_r x_{rm}$ (the turning angle of the trajectory).

The relationship between the parameters characterizing the rocket trajectory (v, θ_v, θ_h) and the above-mentioned adjustable value is set by a kinematic equation. Thus, if the law of change of the parameters v, θ_v, θ_h is found and the kinematic equation is determined, the character of change of the mismatch parameter also becomes known. However, here one apparent difficulty arises: it is impossible to obtain the real law of change of the values v, θ_v, θ_h without investigating the control system, as a whole, as a closed automatic control system. It therefore would appear impossible to formulate requirements on the dynamic properties of the coordinator until the rocket control system is fully planned. There is a solution of this problem because usually some limiting values of the parameters characterizing the actual rocket flight trajectory are known. For example, as such a parameter it is possible to use the maximum value of the projected overloads. By stipulating this value it is easy to determine the limiting value of change of the mismatch parameter, which is extremely important when evaluating the dynamic properties of the coordinator.

As an example we will consider the kinematic equations corresponding to guidance of a winged missile along a fixed trajectory. The kinematic equation for motion of a rocket in a vertical plane has the form /52

$$\frac{dH}{dt} = v \sin \theta_v, \tag{2.4.1}$$

where H is the flight altitude of the rocket.

If the angle of inclination of the trajectory θ_v is small, with a sufficient degree of accuracy it can be assumed that

$$\frac{dH}{dt} \approx v\theta_v. \tag{2.4.2}$$

The relation (2.4.2) is reflected in the block diagram by a kinematic link. The transfer function of such a link, written in symbolic form, will be equal to

$$W_{H/\theta}(D) = \frac{H(t)}{\theta_v(t)} = \frac{v}{D}. \tag{2.4.3}$$

Above and below the letter D is the symbol for differentiation of $\frac{d}{dt}$.

Expressions (2.3.1) and (2.4.3) were used in constructing the block diagram (fig. 2.3) illustrating the formation of the mismatch parameter of the altitude measurement channel. Figure 2.3 shows that the kinematic equation adds one integrating link to the control system block diagram.

Since the transverse load factor when a rocket moves in a vertical plane is expressed by the formula

$$n_y = \frac{v}{g}\dot{\theta}_v,$$

by differentiating (2.4.2) and assuming v = const, we will have

$$\frac{d^2H}{dt^2} \approx gn_y. \tag{2.4.4}$$

By substituting the maximum value of the projected load factor into equation (2.4.4) and using relation (2.3.1) it is easy to obtain the limiting value of the change of the mismatch parameter of the altitude measurement channel.

The kinematic equation for rocket motion in a horizontal plane has the/53 form

$$\frac{dz}{dt} = v \cos \theta_v \sin \theta_h, \tag{2.4.5}$$

where z is the lateral deflection of the rocket from the reference trajectory.

If the angles θ_v and θ_h are small, then

$$\frac{dz}{dt} \approx v\theta_h. \tag{2.4.6}$$

Introducing the load factor for lateral deflection, equation (2.4.6) can be represented in the form (2.4.4).

The transfer function of the kinematic link during motion of a rocket in a horizontal plane is expressed by the formula

$$W_{z/\theta}(D) = \frac{z(t)}{\theta_h(t)} = \frac{v}{D}.$$

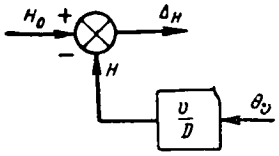

Figure 2.3

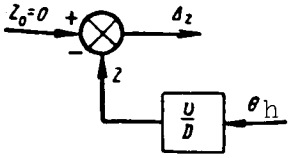

Figure 2.4

Figure 2.4 shows a block diagram clarifying the formation of the mismatch parameter of the lateral deflection channel.

In the same way it is possible to obtain a kinematic equation for the guidance of ballistic missiles.

2.5. Methods of Rocket Guidance along Unfixed Reference Trajectories

In the case of guidance of rockets along unfixed trajectories it is possible to speak only of a class of reference trajectories determined by the guidance method used, since the position of each of the reference trajectories of a particular class is dependent on a number of conditions which cannot be taken into account in advance (maneuvering of the target, initial launching range, etc.). The coordinator, therefore, checks the satisfaction of the coherence imposed on the motion of the rocket, not on the basis of the deflection of the rocket from its reference trajectory, but on the basis of the deviation of some parameter characterizing the relative position of the rocket and target from its stipulated value. The certain degree of freedom in selection of such parameters leads to an increase of the number of possible methods for guidance of rockets along unfixed trajectories.

As a convenience we divide methods of guidance along unfixed trajectories into two groups:

(a) two-point methods, determining the relative position of two points--rocket and target;

(b) three-point methods, determining the relative position of three points--rocket, target and control point.

Two-point guidance methods are used in homing and command control systems and three-point methods are used in command control and radio zone (beam-riding) guidance systems.

The most well-known methods in the first group are:

(1) the direct guidance method;
(2) the vane guidance method and the pursuit curve guidance method; /54
(3) the parallel approach method;
(4) the proportional guidance method.

Included in the second group are:

(1) coincidence with the target method;
(2) coincidence with a forward point method.

2.6. Two-Point Guidance Methods

In two-point guidance methods, coherence is imposed on the control system with respect to the position of the longitudinal axis of the rocket or its velocity vector in relation to a line connecting the rocket to the target or to some direction fixed in space. The specific form of coherence is established by the mismatch equation corresponding to the particular guidance method.

1. Direct Guidance Method

The direct guidance method requires that during the entire time of the rocket flight its longitudinal axis coincides with the rocket-target line. Therefore, in the direct guidance method, coherence is imposed on the position of the longitudinal axis of the rocket. We will obtain a mismatch equation for the considered guidance method. We will assume first that the guidance is accomplished in some single plane, such as a vertical plane. This case is illustrated in figure 2.5. In this figure the point o_r, situated at the center of mass of the rocket, coincides with the origin of the nonrotating coordinate system $o_r x_{er} y_{er}$ whose axes are parallel to the corresponding axes of a ground coordinate system. The axis $o_r x_1$ is directed along the longitudinal axis of the rocket. The position of the target (point T) in the coordinate system $o_r x_{er} y_{er}$ is given by the range vector $\mathbf{r}$ (its module r and the angle ϵ formed by the vector $\mathbf{r}$ and the axis $o_r x_{er}$). The angle between the longitudinal axis of the rocket and the range vector is denoted γ. The position of the velocity vector v of the rocket is characterized by the angle θ. The difference between the angles ϑ and θ is the angle of attack α. In accordance with the definition of the guidance method the mismatch equation is written in the form

$$\Delta_\gamma = \gamma. \tag{2.6.1}$$

Using the relationship between the angles ϵ, ϑ and γ it is possible to write the mismatch equation in the form (2.2.3) if it is assumed that $\varkappa_T = \epsilon$ and $\varkappa_\partial = \vartheta$, /55

$$\Delta_\gamma = \epsilon - \vartheta. \tag{2.6.2}$$

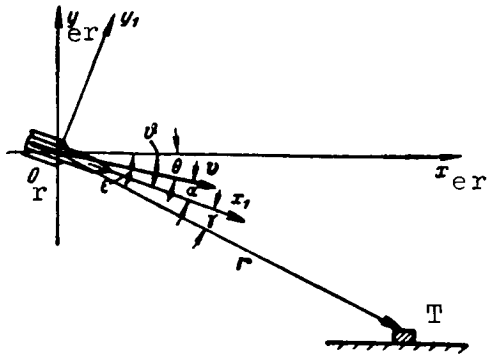

Figure 2.5

It follows from expressions (2.6.1) and (2.6.2) that the mismatch parameter can be determined either by the direct measurement of the angle γ or by the separate measurement of the angles ε and ϑ with subsequent subtraction of the measurement results.

The advantage of the first method for determination of the mismatch parameter is the relative simplicity of the design of the coordinator required for its realization. In this case it consists of an electronic angle-measuring apparatus whose antenna system is attached rigidly to the body of the rocket and which is oriented along its longitudinal axis. The signal at the output of such an apparatus will be proportional, in certain limits, to the angular deviation of the target from the longitudinal axis of the rocket and its sign will be dependent on the direction of deviation of the target.

The output signal of the coordinator is sent through the automatic pilot to the control mechanism of the rocket. Deflection of the control surfaces leads to a change of the angular position of the longitudinal axis of the rocket and, therefore, to a change of the position of the antenna system of the coordinator relative to the target. This change should be such that the mismatch parameter tends to zero. The latter is achieved by appropriate orientation of the axes of the measurement coordinate system $o_m x_m y_m z_m$, whose position is determined by the installation of the coordinator relative to the body of the rocket and its adjustment. The axis $o_m x_m$ of the measurement coordinate system is directed along the longitudinal axis of the rocket and the axes $o_m y_m$ and $o_m z_m$ should be situated in the control planes of the rocket R_z and R_y (fig. 2.6), which in turn coincide with the planes $o_r x_1 z_1$ and $o_r x_1 y_1$ of the related coordinate system.

If the mentioned conditions are satisfied, the coordinator will measure the two components of the mismatch parameter /56

$$\left.\begin{aligned}\Delta_{\gamma z} &= \gamma_z,\\ \Delta_{\gamma y} &= \gamma_y,\end{aligned}\right\} \qquad (2.6.3)$$

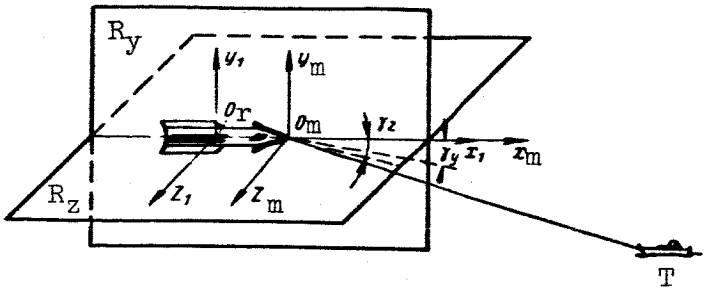

Figure 2.6

where γ_z and γ_y are the angles between the axis $o_m x_m$ and the projections of the rocket-target line in the planes R_z and R_y, respectively.

A signal proportional to $\Delta_{\gamma z}$ is used for control of the motion of the rocket in the plane R_z and a signal proportional to $\Delta_{\gamma y}$ for control of the motion of the rocket in the plane R_y. In the case of the small angles γ_z and γ_y, the two scalar equations (2.6.3) can be replaced by one complex equation, if the component of the mismatch parameter in the plane R_y is arbitrarily assigned the imaginary unit $j=\sqrt{-1}$. Then

$$\Delta_\gamma=\gamma_z+j\gamma_y=\gamma e^{j\varphi}, \qquad (2.6.4)$$

where $\gamma=\sqrt{\gamma_z^2+\gamma_y^2}$ is the module of the mismatch angle; φ is the phase angle of the target, read from the plane R_z.

Since the measurement coordinate system is rigorously related to the body of the rocket, the absence of automatic banking stabilization on the rocket does not lead to a disruption of control because, with the appearance of banking, there is a simultaneous turning of both the control planes and the axes of the measurement coordinate system. At the same time, the turning of the axes of the measurement coordinate system relative to the control planes (the so-called twisting of the coordinate system) causes the appearance of cross connections between the control channels which results in a disruption of the normal operation of the control system.

2. Vane Guidance Method and Pursuit Curve Method

In the vane guidance method and in guidance along a pursuit curve the coherence imposed on the rocket is as follows: during the entire time of

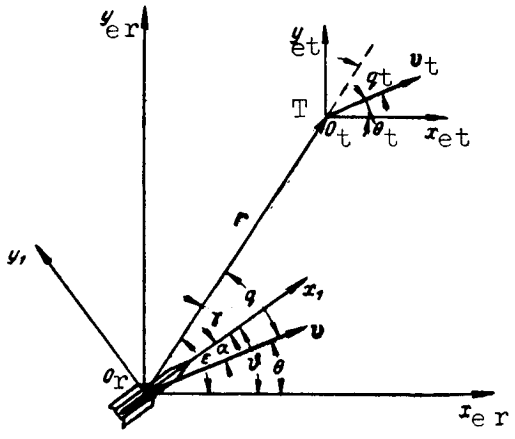

Figure 2.7

guidance the rocket-target line should coincide with the air velocity vector (in vane guidance) or the true velocity vector (in guidance along a pursuit curve). Both methods coincide when the rocket moves in an unperturbed atmosphere.

Figure 2.7 shows the principal geometrical relations in the case of rocket guidance in a vertical plane. The rocket velocity vector v is situated at the angle θ to the horizontal axis $o_r x_{er}$ of a nonrotating coordinate system whose origin coincides with the center of mass of the rocket and forms the angle q with the range vector r. The target moves with the velocity v_t. The position of the vector v_t in relation to a nonrotating coordinate system /57 $o_t x_{et} y_{et}$, whose origin is at the center of mass of the target, is given by the angle θ_t. The remaining notations are the same as in figure 2.5.

By definition the mismatch parameter is equal to

$$\Delta_q = q. \tag{2.6.5}$$

The mismatch equation (2.6.5) also can be written in the form (2.2.3) if the angle of inclination ϵ of the range vector and the angle of inclination θ of the trajectory are used as the stipulated and actual values of the adjustable parameters, respectively. Then

$$\Delta_q = \epsilon - \theta. \tag{2.6.6}$$

Finally, using the relationship of the angles q, γ and α it also is possible to obtain the following form of writing the mismatch equation for the vane guidance method

$$\Delta_q = \gamma + \alpha \tag{2.6.7}$$

Different variants of technical design of a coordinator are possible in the vane guidance method in accordance with the different forms of writing of the mismatch equation. In a coordinator with a power vane, the antenna of the electronic angle-measuring instrument is set on a platform which is movable relative to the body of the rocket. The angular position of the platform is changed by a servosystem whose transducer is the vane apparatus. The vane is a plate which is oriented freely in the oncoming flow (in the direction of the rocket air velocity vector). The turning angles of the plate are determined by a potentiometer. The voltage from the potentiometer is used as a controlling signal of the servosystem. Since the plate of the vane is set in the oncoming flow, the axis of the antenna of the angle-measuring instrument also will be set in the direction of the vector v. The signals from the output of the electronic angle-measuring apparatus, proportional to the deviation of the target from the axis of the antenna system, act through the automatic pilot on the control surfaces of the rocket. This coordinator forms the mismatch parameter in accordance with formula (2.6.5).

With transition of rocket control in a single plane to its control in space it is necessary, as in the direct guidance method, to have matching of the axes of the measurement coordinate system and the control planes. If /58 there is such matching, the controlling signals sent to the control surfaces will be proportional to the corresponding components of the mismatch parameter Δ_{qz} and Δ_{qy} and the mismatch parameter itself, in the case of small angles q_z and q_y, can be written in the form

$$\Delta_q = q_z + jq_y. \tag{2.6.8}$$

The coordinator measuring the mismatch parameter in two mutually perpendicular planes in accordance with formula (2.6.7) consists of an electronic angle-measuring apparatus whose antenna is fixed relative to the body of the rocket and is oriented along its longitudinal axis and transducers for the angles of attack and slip. Vane apparatus or accelerometers can be used as transducers for the angles of attack α and slip α_s. Since such a coordinator contains two types of measuring instruments, it is necessary that their coordinate measurement systems be matched with one another and with the control planes of the rocket. Satisfaction of the matching conditions makes it possible to represent the mismatch parameter in the complex form

$$\Delta_q = (\gamma_z + \alpha_s) + j(\gamma_y + \alpha). \tag{2.6.9}$$

The so-called method of guidance with a constant deflection angle is related closely to the vane method; in essence it is a further development of the vane method. In rocket guidance by the constant angle of deflection method it is necessary that some constant, earlier set angle q_0 be maintained between the vectors r and v. The mismatch equation for one control plane has the form

$$\Delta_{q_0} = q_0 - q. \tag{2.6.10}$$

The realization of the constant deflection angle guidance method is possible using the same apparatus as for the vane method. The deflection angle is set either by additional turning of the antenna by the value q_0 or by the introduction into the measured value of the mismatch parameter of an additional signal proportional to q_0.

3. Parallel Approach Method

In the parallel approach method in the guidance process, the rocket-target line remains parallel to its initial position. When this requirement is satisfied the relative velocity vector of the rocket, equal to $v_0 = v - v_t$, will be directed at the target.

The mismatch equation for the motion of the rocket and target in a single plane is written as the condition of plane-parallel movement of the range vector r, that is /59

$$\Delta_{\dot{\epsilon}} = \dot{\epsilon}, \tag{2.6.11}$$

where $\dot{\epsilon}$ is the angular velocity of rotation of the rocket-target line (range vector).

The parallel approach method is one of the deflection guidance methods. The required law of change of the angle of deflection can be obtained from the condition of equality of the projections of the velocity vector of the rocket and the velocity vector of the target onto the normal to the rocket-target line (fig. 2.7). Then

$$v \sin q_T = v_t \sin q_t. \tag{2.6.12}$$

Here q_T is the required deflection angle and q_t is the angle between the continuation of the rocket-target line and the velocity vector of the target.

By solving equation (2.6.12) relative to q_T we obtain

$$q_T = \text{arc sin } \left(\frac{v_t}{v} \sin q_t\right). \tag{2.6.13}$$

The mismatch equation is reduced to the form (2.2.3) if it is assumed that $\varkappa_T = \epsilon - q_T$ and $\varkappa_\vartheta = \theta$,

$$\Delta_\epsilon^{\cdot} = \epsilon - \text{arc sin } \left(\frac{v_t}{v} \sin q_t\right) - \theta. \tag{2.6.14}$$

In the practical realization of a coordinator for a rocket guided by the parallel approach method, it is preferable to use the mismatch equation (2.6.11). This means that the coordinator should measure the angular velocity of rotation of the range vector. As will be pointed out in chapter 3, the angular velocity of rotation of the rocket-target line can be measured with an electronic tracking angle-measuring instrument. Such a coordinator automatically tracks the target in direction, regardless of the motion of the body of the rocket.

When setting the necessary orientation of the axes of the measurement coordinate system the following complex form of writing the mismatch parameter is correct

$$\Delta_\epsilon^{\cdot} = \dot{\epsilon}_z + j\dot{\epsilon}_y, \tag{2.6.15}$$

where $\dot{\epsilon}_z$ and $\dot{\epsilon}_y$ are the components of angular velocity of the rocket-target line in the corresponding control planes.

4. Proportional Guidance Method

The proportional guidance method requires that the angular velocity of rotation of the velocity vector of the rocket be proportional to the angular velocity of rotation of the rocket-target line. During guidance of a rocket in a vertical plane the mismatch equation has the form /60

$$\Delta_\theta^{\cdot} = a\dot{\epsilon} - \dot{\theta}, \tag{2.6.16}$$

where a is the proportionality factor.

The first term on the right-hand side of equation (2.6.16) represents the required value of the adjusted value $\varkappa_T = a\dot{\varepsilon}$ and the second its real value $\varkappa_\partial = \dot{\theta}$.

Proportional homing, like parallel approach, is one of the group of control methods with a variable deflection angle. In the case of ideal guidance, the law of change of the required deflection angle q_T is determined from equation (2.6.16) if it is assumed in it that $\Delta_{\dot{\theta}} = 0$. Then

$$\dot{q}_T = (1 - a)\dot{\varepsilon}.$$

In contrast to the parallel approach method, whose ideal satisfaction requires of the control system an instantaneous elimination of the rotation of the rocket-target line, in proportional guidance the requirements on the control system are less rigorous because its role essentially involves only a decrease of the angular velocity of rotation of the line of sighting.

Measurement of the mismatch parameter in rocket guidance by the discussed method is accomplished by a coordinator which contains two types of measuring devices. One of these is an electronic scanning angle-measuring instrument which measures the angular velocity of the rocket-target line and the second measures the angular velocity of rotation of the velocity vector of the rocket. Such a measuring device can be designed on the basis of a normal acceleration sensor (accelerometer).

The mismatch parameter during the guidance of a rocket in space is written in the form

$$\Delta_{\dot{\theta}} = (a\dot{\varepsilon}_z - \dot{\theta}_z) + j(a\dot{\varepsilon}_y - \dot{\theta}_y). \qquad (2.6.17)$$

Formula (2.6.17) is correct provided there is matching of the measurement coordinate systems with the control planes.

We note in conclusion that equation (2.6.16) is the most general form of the mismatch equation for those two-point guidance methods in which coherence is imposed on the position of the velocity vector of the rocket.

In actuality, by integrating (2.6.16) we obtain

$$\Delta_\theta = a\varepsilon - \theta + q_0, \qquad (2.6.18)$$

where q_0 is the integration constant.

When a = 1 and q_0 = 0, the expression (2.6.18) represents the mismatch equation for the vane guidance method, and when q_0 = const and a = 1, for the method of guidance with a constant deflection angle. Finally, the ideal coherence equation for the parallel approach method $\dot{\varepsilon} = 0$ is obtained from the ideal coherence equation for the proportional guidance method if it is assumed in the latter that a = ∞. /61

2.7. Kinematic Equations for Two-Point Guidance Methods

The role of kinematic equations in the guidance of rockets along unfixed trajectories differs somewhat from their role in guidance systems for fixed trajectories. We recall that in the guidance of rockets along fixed trajectories the functions of the kinematic relations were reduced to the formation of the real value of the adjustable value on the basis of data characterizing the flight trajectory of the rocket, and the stipulated value of the adjustable value remained constant or was changed in accordance with the program. In the case of a moving target or a moving control point, which is characteristic of guidance methods for unfixed trajectories, the kinematic equations are used for forming both the real and the stipulated values of the adjustable value.

The relative movement of two points (rocket and target), moving in the same plane with the velocities v and v_t (fig. 2.7) is described by the following kinematic equations

$$\left.\begin{aligned} \dot{r} &= v_t \cos q_t - v \cos q, \\ r\dot{\varepsilon} &= v \sin q - v_t \sin q_t, \\ q &= \varepsilon - \theta, \\ q_t &= \varepsilon - \theta_t \end{aligned}\right\} \qquad (2.7.1)$$

or

$$\left.\begin{aligned} \dot{r} &= v_t \cos(\varepsilon - \theta_t) - v \cos(\varepsilon - \theta), \\ \dot{\varepsilon} &= \frac{v \sin(\varepsilon - \theta) - v_t \sin(\varepsilon - \theta_t)}{r}. \end{aligned}\right\} \qquad (2.7.2)$$

The first equation of system (2.7.2) establishes the dependence of the velocity of approach of the rocket to the target on the velocities of the rocket and target and their orientation relative to the range vector. The second equation defines the angular velocity of the rotation of the rocket-target line as a function of the values and orientation of the velocity vectors of the rocket and target and also the distance between them.

The qualitative aspect of the process of formation of the mismatch parameter for any guidance method can be traced by limiting ourselves to the case of

small angular deviations of the velocity vectors of the rocket and target relative to the range vector. Assuming that $\cos(\varepsilon - \theta) \approx 1$, $\cos(\varepsilon - \theta_t) \approx 1$, /62 $\sin(\varepsilon - \theta) \approx \varepsilon - \theta$ and $\sin(\varepsilon - \theta_t) \approx \varepsilon - \theta_t$, we obtain

$$\dot{r} = v_t - v, \tag{2.7.3}$$

$$r\dot{\varepsilon} = v(\varepsilon - \theta) - v_t(\varepsilon - \theta_t). \tag{2.7.4}$$

We transform (2.7.4) to the form

$$r\dot{\varepsilon} + (v_t - v)\varepsilon = v_t\theta_t - v\theta. \tag{2.7.5}$$

After replacing the difference $v_t - v$ by its value from (2.7.3) we find that

$$r\dot{\varepsilon} + \dot{r}\varepsilon = v_t\theta_t - v\theta. \tag{2.7.6}$$

But

$$r\dot{\varepsilon} + \dot{r}\varepsilon = \frac{d(r\varepsilon)}{dt}.$$

Then

$$\frac{d(r\varepsilon)}{dt} = v_t\theta_t - v\theta, \tag{2.7.7}$$

or, using the symbolic form of writing, we finally find

$$r\varepsilon = \frac{v_t}{D}\theta_t - \frac{v}{D}\theta. \tag{2.7.8}$$

On the basis of equations (2.7.8), (2.6.2) and (2.6.6), figure 2.8 shows block diagrams illustrating the process of determination of the mismatch parameters Δ_γ and Δ_q.

We will note some special features of these diagrams. As follows from figure 2.8, the kinematic relations for two-point guidance methods break down into three links. One of them, with the transfer function $W_{\theta t}(D) = \frac{v_t}{D}$, transforms the external control effect of the guidance system, which in the

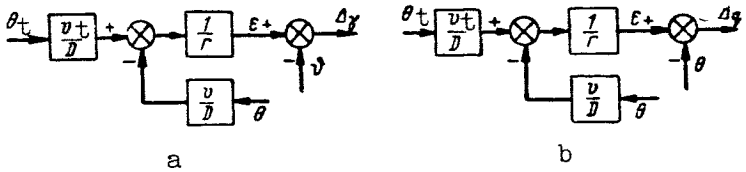

a b

Figure 2.8

considered case is the inclination of the trajectory of the target θ_t. The two others, with the transfer constant $k_r = \frac{1}{r}$ and the transfer function $W_\theta(D) = \frac{v}{D}$, enter the control circuit, changing its properties. A particularly strong influence is exerted by the link with a transfer constant inversely proportional to the rocket-target range. A sharp increase of this constant near the target can cause the control system to be incapable of processing the rapid increase of the value of the mismatch parameter and the guidance process will be disrupted until the rocket reaches the target. /63

Diagrams similar to figure 2.8 are easy to obtain for the parallel approach and proportional guidance methods as well. This requires differentiation of expression (2.7.6) for time and multiplication of the resulting equation by range r. Then we will have

$$\frac{d(r^2\dot{\varepsilon})}{dt} = v_t r\dot{\theta}_t - vr\dot{\theta}. \qquad (2.7.9)$$

In the derivation of (2.7.9) it was assumed that the velocities of the rocket and target are constant.

Figure 2.9 shows block diagrams of the formation of the mismatch parameters $\Delta_{\dot{\varepsilon}}$ and $\Delta_{\dot{\theta}}$. The mismatch equations (2.6.11) and (2.6.16) were used in constructing the diagrams, as well as expression (2.7.9). Here, as in the preceding case, the kinematic relations are represented by several links, part of which are external in relation to the control system, while others enter directly into the guidance circuit, determining its properties.

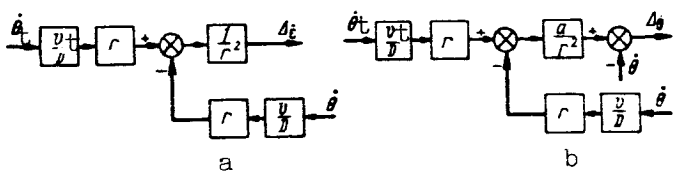

a b

Figure 2.9

As follows from figures 2.8 and 2.9, the pattern of change of the controlling effect in two-point guidance methods, that is, the dependence $\epsilon = \epsilon(t)$, can be determined if the law of change of the angle $\theta = \theta(t)$ is determined while using a specific hypothesis concerning the motion of the target. This law is found, in turn, by solution of a full system of equations describing the guidance process. The rocket flight trajectory is determined from their solution. On the basis of the known rocket trajectory it is easy to establish the character of the change of the controlling effect and, therefore, be able to formulate requirements on the dynamic properties of the coordinator.

The complexity of analysis of a full system of equations of motion of a rocket forces us to seek ways to simplify it. Such simplification is possible if a number of assumptions are made, related to idealization of the operation of the control system. These assumptions are essentially as follows.

First, the process of motion of the rocket to its target is broken down into the two components of motion: motion of the center of mass of the rocket and rotation of the rocket about its center of mass. This separation is based on the considerable difference in the duration of the transient processes of the mentioned types of motion.

In investigations of the motion of the center of mass, which is the /64
most interesting from the point of view of tactical use of a rocket, and the overloads acting upon it in flight, the transient processes of angular motions can be neglected. From the physical point of view this assumption is equivalent to the assumption of an instantaneous determination of the angles of attack and slip at the time of a sudden feeding of a control command.

In addition, the assumption is made frequently that there is a constancy of rocket velocity during the guidance process. This assumption is based on the fact that in a relatively short time of rocket flight the value v, computed in advance, changes insignificantly.

It is assumed further that the apparatus of the control system is inertialess and that the coherence imposed on the rocket motion is maintained absolutely precisely. Such an assumption leads to insignificant deviations of the trajectory of motion from that which would be obtained taking into account the real mismatch parameters because, in a properly constructed control system, the values Δ differ little from zero.

When these assumptions are taken into account it becomes possible for some (reference) guidance systems to compute purely kinematic trajectories, that is, trajectories computed solely on the basis of kinematic equations.

A knowledge of kinematic trajectories makes it possible to determine the required overloads for carrying out the maneuver associated with the guidance method used and, thereby, establish the applicability of a particular guidance method under specific tactical conditions.

The determination of kinematic trajectories is accomplished by solution of the system of equations (2.7.2). These equations contain six variables. Three

of them--rocket velocity v, target velocity v_t and the inclination of the target trajectory θ_t--can be considered stipulated, since the rocket velocity is known and the values v_t and θ_t are fixed by the hypothesis on motion of the target used.

Still another equation should be added for determination of the remaining three unknowns of system (2.7.2). With the assumptions made above this equation will be the equation of ideal coherence for the guidance method used. For example, in the vane guidance method system (2.7.2) is supplemented by the equation $q = \epsilon - \theta = 0$, for the parallel approach method $\dot{\epsilon} = 0$ and for the proportional guidance method $\dot{\theta} = a\dot{\epsilon}$. The situation is somewhat more complex in the solution of the kinematic equations for the direct guidance method because there, in the ideal coherence equation ($\gamma = 0$), there is a variable not present in system (2.7.2). Therefore, in this case still another equation is added which relates the variable γ to the used systems of equations (2.7.2).

After a closed system of equations has been derived for each guidance method it can be solved by some method relative to the unknowns r and ϵ, thereby determining the kinematic (reference) trajectory of the rocket. The reference trajectories will be different for different guidance methods and the assumed initial conditions. /65

Since the kinematic equations are nonlinear differential equations, their analytical solution can be obtained only for some special cases. However, even when such a solution is possible, the trajectory is given by the expression $r = f(\epsilon)$, which makes its determination difficult. Therefore, very frequently it is necessary to have recourse to a graphic method for determination of the kinematic trajectories. Such a method is simple and graphic.

We will begin with the vane guidance method. It is easy to demonstrate that if the target is fixed and there is no initial error in aiming, the kinematic trajectory is a straight line connecting the launching point of the rocket and the target. We will consider the case of a moving target. Assume the target trajectory is given by the curve T_0T_k (fig. 2.10). The points T_0 and R_0 correspond to the initial position of the target and rocket. The velocities of the rocket and target will be assumed constant and equal to v and v_t. We divide the curve T_0T_k into the segments T_0T_1, T_1T_2, T_2T_3, etc., travelled by the target in the equal intervals of time Δt.

If these intervals are quite small, it can be assumed that during each such interval the rocket moves linearly. The position of the linear segments of the trajectory are determined in the following way. The points of the initial position of the rocket and target T_0 and R_0 are connected by a straight

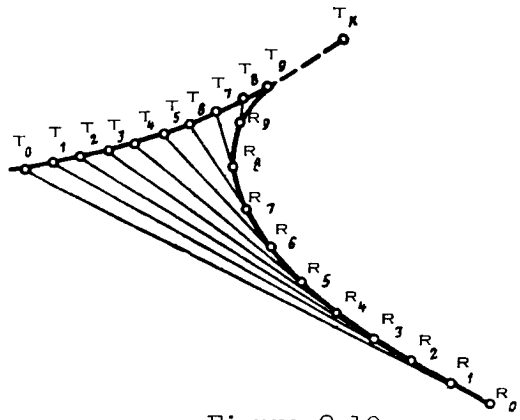

Figure 2.10

line on which the segment $R_0R_1 = v\Delta t$ is laid off. Since $\Delta t = \frac{T_0T_1}{v_t}$, then $R_0R_1 = \frac{v}{v_t} T_0T_1$.

When the rocket reaches point R_1, the target is in the position T_1. Therefore, the next segment of the rocket trajectory $R_1R_2 = \frac{v}{v_t} T_1T_2$ is laid off on the straight line R_1T_1. Continuing the construction further, we successively find points R_3, R_4, R_5, etc., and by connecting them by a smooth curve we obtain the kinematic trajectory of the rocket. The constructed trajectory makes it possible to draw a curve of the dependence of inclination ϵ and the values of the range vector r on time.

In an evaluation of the tactical possibilities which the vane guidance /66 method presents, we use some results of an analytical solution of kinematic equations obtained for the uniform and linear flight of a target given in reference 3. Under the mentioned conditions the value of the range vector r is related to the angle q_t (fig. 2.7) by the following expression

$$r = k_{va} \frac{(\sin q_t)^{k_q} - 1}{(1 + \cos q_t)^{k_q}}, \qquad (2.7.10)$$

where k_{va} is a constant coefficient determined by the initial values of the range r_0 and the angle q_{t0}, equal to

$$k_{va} = r_0 \frac{(1 + \cos q_{t0})^{k_q}}{(\sin q_{t0})^{k_q} - 1};$$

$k_q = \frac{v}{v_t}$ is the ratio of the velocities of the rocket and target.

Formula (2.7.10) is correct for angles q_{t0} differing from 0 and π.

Analysis of expression (2.7.10) shows that with approach of the rocket to the target ($r \to 0$) the angle q_t tends to zero. Therefore, whatever the initial values of the angle q_{t0} (except $q_{t0} = \pi$), at the end of rocket guidance the rocket will approach the target from the rear hemisphere.

The required value of normal acceleration during rocket flight along a kinematic trajectory is expressed by the formula

$$j_n = \left| \frac{vv_t}{r} \sin q_t \right|. \qquad (2.7.11)$$

Since upon reaching the target $r = 0$ and $q_t = 0$, in order to obtain the limiting values of acceleration it is necessary to remove uncertainty. This can be done by substituting into (2.7.11) the value r from (2.7.10) and tending q_t to zero. Then

$$\left.\begin{aligned} &\text{when } 1 < k_q < 2 \quad \lim_{q_t \to 0} j_n = 0, \\ &\text{when } k_q = 2 \quad \lim_{q_t \to 0} j_n = \frac{4vv_t}{k_{va}}, \\ &\text{when } k_q > 2 \quad \lim_{q_t \to 0} j_n = \infty. \end{aligned}\right\} \qquad (2.7.12)$$

It follows from an analysis of formula (2.7.11) and relations (2.7.12) that in the vane guidance method the law of change of the required accelerations in the process of approach of the rocket to the target is dependent on the value k_q. For example, if $1 < k_q < 2$, the required acceleration increases at first and then tends to zero; when $k_q = 2$ it increases monotonically but does not exceed the value $\frac{4vv_t}{k_{va}}$; finally, when $k_q > 2$ the required acceleration at the time of the approach of the rocket to the target tends to infinity. /67 However, it can happen that in all three cases the required acceleration, at some stage of the approach, will be greater than intended. Then the rocket will depart from the pursuit trajectory and will move in a circle with a radius equal to the minimum radius of curvature, determined by the available acceleration of the particular rocket. If the maneuver of the target becomes complicated, the trajectories become still less favorable from the point of view of the required accelerations.

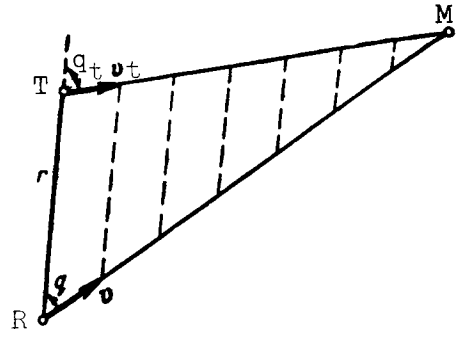

Figure 2.11

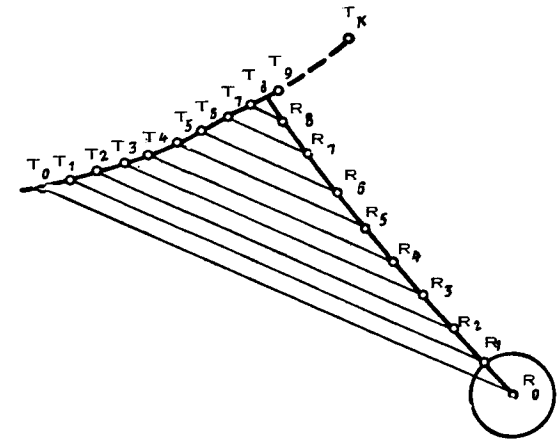

Figure 2.12

In summary it can be said that the vane method gives applicable results only when the rocket is guided toward slowly moving and fixed targets.

Expression (2.6.13) is used for determination of the kinematic trajectory of a rocket guided by the parallel approach method toward a uniformly and linearly moving target. Assuming v_t = const and q_t = const (conditions of uniform and linear motion of a target when $\dot{\epsilon} = 0$), and also v = const, we confirm that the required deflection angle is constant. Therefore, the rocket moves toward the target in a linear trajectory (fig. 2.11) and the necessary transverse acceleration is equal to zero. The rocket hits the target at point M.

In the case of arbitrary motion of the target the rocket trajectory is easily determined graphically. For this purpose, we will assume that the target moves along curve T_0T_k at the constant velocity v_t (fig. 2.12). We divide curve T_0T_k into segments T_0T_1, T_1T_2, etc., travelled by the target in quite short intervals of time Δt. The initial position of the rocket is denoted R_0. Since in the case of ideal guidance the line T_0R_0 moves parallel to itself, we draw rays from the points T_1, T_2, T_3, etc., which are parallel to T_0R_0. The rocket should be situated on these rays after the lapse of time intervals equal to Δt, $2\Delta t$, $3\Delta t$, etc.

In order to determine the position which the rocket occupies after the /68 time Δt, we draw a circle with the radius $R = v\Delta t$ with point R_0 as its center. The intersection of the circle with the ray emerging from point T_1 gives the position of the rocket (point R_1) occupied by it after the time lapse Δt.

Point R_2 of the trajectory will be determined in a similar way if point R_1 is used as the center of the circle. The remaining points of the trajectory are determined in a similar way.

By comparing figures 2.10 and 2.12 it is easy to confirm that, for the same form of target maneuver, the curvature of the trajectory of a rocket guided by the parallel approach method will be considerably less than when the vane method is used.

It can be demonstrated that for an arbitrary maneuver of the target the following equation applies

$$j_n = j_t \frac{\cos q_t}{\cos q_T}, \tag{2.7.13}$$

where j_n is the required normal acceleration of the rocket and j_t is the normal acceleration of the target.

According to expression (2.6.12), $v \sin q_T = v_t \sin q_t$. But $v > v_t$, and therefore $q_T < q_t$. We then find from (2.7.13) that $j_n < j_t$, that is, the normal accelerations required for guidance of a rocket by the parallel approach method do not exceed the normal accelerations of the target. The parallel approach method, therefore, can be used successfully for guiding rockets toward rapidly moving targets.

With respect to its kinematic properties, the proportional guidance method occupies an intermediate position between the vane and parallel approach guidance methods.

It is known (ref. 3) that in the case of a linear and uniform motion of a target, when the proportionality factor is $a = 2$ (2.6.16), the acceleration j_n will be a finite value if the following condition is satisfied

$$k_q \cos(q_0 + q_{t0}) \geq 1, \tag{2.7.14}$$

where q_0 and q_{t0} are the deflection angles of the rocket and target at launching time.

As follows from the inequality (2.7.14), the condition that there be a finite value of the required accelerations is less rigorous here than in the vane guidance method. With an increase of the proportionality factor a, the value of the required accelerations decreases. However, with an increase of a there is an increase of fluctuation errors and therefore the factor a usually

is assigned the value 2-5. The proportional guidance method is used when guiding rockets toward rapidly moving targets.

In the direct guidance method the adjustable value is the position of the longitudinal axis of the rocket and its trajectory is determined by the direction of the velocity vector, which in a general case does not coincide with the direction of the longitudinal axis. The reference trajectory of the rocket, even in the case of a fixed target, therefore is a rather complex /69 curve known as a hyperbolic spiral (ref. 1). The curvature of the hyperbolic spiral increases with the approach of the moving point of this curve to the target. When the radius of curvature of the reference trajectory becomes less than the minimum radius of turning of the rocket $\rho_{r\ min}$, a flight in a spiral is impossible and the rocket flies in a circle of the radius $\rho_{r\ min}$.

Thus, in the direct rocket guidance method, even for guidance to a fixed target with an ideally operating control system, a precise hit is impossible. The rocket miss is dependent on the initial aiming errors, the minimum turning radius of the rocket $\rho_{r\ min}$ and the initial launching range r_0. It decreases with an increase of r_0 and also with a decrease of aiming errors and $\rho_{r\ min}$. Computations show that, in the case of real values of the mentioned parameters, the miss does not exceed several tens of meters. The direct method therefore can be used for rocket guidance to fixed and slowly moving targets of relatively large size. An advantage of this method, encouraging its use, is the simplicity of the guidance apparatus aboard the rocket.

2.8. Three-Point Guidance Methods

Three-point methods are used when the guidance system includes a control point which is situated on Earth or on a moving object (rocket-carrying aircraft, surface vessel, etc.).

Three-point guidance methods, like two-point methods, can be divided into two groups. The first group includes guidance without deflection when the control system holds the rocket on a straight line passing through the control point and the target. The second group includes methods of guidance with deflection when the control system makes the center of mass of the rocket coincide with a line connecting the control point to some deflected point, selected in such a way that at the end of the guidance process the target is situated at this point. The laws which determine the deflection of the rocket can be very different. Below, as an example, we will consider two three-point guidance methods: the matching method and the parallel approach method, in which the deflection law is selected in such a way that the rocket moves toward the target in a parallel approach trajectory.

1. Matching Method

In the matching method it is required that the center of mass of the rocket remain on the line connecting the control point to the target during the guidance process. Figure 2.13 shows a nonrotating coordinate system $o_c x_{ec} y_{ec}$, situated in a vertical plane. Its origin o_c coincides with the /70 control point. The position of the target in the mentioned coordinate system is determined by the range r_t and the angle ϵ_t and the position of the rocket is determined by the range r_r and the angle ϵ_r. The angle ϵ_l represents the difference of the angles characterizing the direction to the target and to the rocket. The lateral deflection of the rocket from the target range vector is denoted h.

In accordance with the definition of the matching method the mismatch equation has the form

$$\Delta_{\epsilon_l} = \epsilon_l. \tag{2.8.1}$$

Writing the mismatch equation in the form (2.2.3) we will have

$$\Delta_{\epsilon_l} = \epsilon_t - \epsilon_r \tag{2.8.2}$$

Here the angle ϵ_t represents the theoretical value of the adjustable value $u_T = \epsilon_t$ and the angle ϵ_r is its real value ($u_\partial = \epsilon_r$).

Sometimes as a mismatch parameter it is desirable to have the linear rather than the angular deflection of the rocket from the control point-target line. Then the mismatch equation can be written as

$$\Delta_h = h. \tag{2.8.3}$$

The following approximate equation is correct for small angles ϵ_l

$$\Delta_h \approx \Delta_{\epsilon_l} r_r. \tag{2.8.4}$$

Proceeding on the basis of the mismatch equations (2.8.1) and (2.8.2) we can designate the makeup of the measuring devices entering into the coordinator of the rocket control system in the matching method. Two coordinator variants

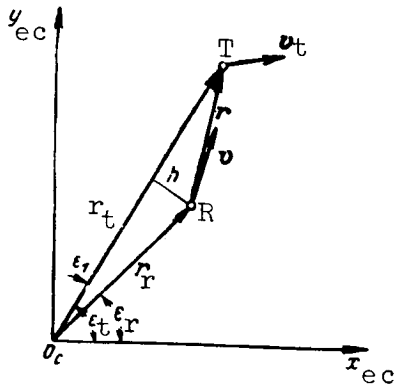

Figure 2.13

are possible when measuring the mismatch parameter at a control point. In the first variant the coordinator includes two angle-measuring devices. One of them is for automatic tracking of the target in direction and measures the angle ϵ_t; the other automatically tracks the rocket and measures the angle ϵ_r. The coordinator computer calculates the difference in the measured values. In the second variant the coordinator consists of one angle-measuring instrument which operates on the "groups" method (see section 5.3) and which directly measures the difference of the angles $\epsilon_t - \epsilon_r$.

When measuring the mismatch parameter for the rocket, one part of the apparatus is situated at the control point and the other on the rocket. The apparatus at the control point in this case consists of an automatic angle- /71 measuring instrument operating in a conical scanning regime and tracking the target in angular coordinates. In this operating regime of the angle-measuring instrument an equisignal direction is created in space, coinciding in the case of ideal operation of the angle-measuring instrument with the control point-target line. The departure of the rocket from the control point-target line, proportional to the angle ϵ_1, is measured aboard the rocket.

If it is necessary to measure the linear deviation of the rocket from the control point-target line, it is sufficient to multiply the measured value of the angle ϵ_1 by the distance between the control point and the rocket. This distance usually is introduced by a programming mechanism which is cut in at the time of the rocket launching.

For measurement of the mismatch parameter during the motion of the rocket in space it is convenient to introduce the measurement coordinate system $o_c x_m y_m z_m$, whose origin coincides with the control point, and the axis $o_c x_m$ is directed along the control point-target line. The axes $o_c y_m$ and $o_c z_m$ are situated in the vertical and horizontal (or inclined) planes, respectively.

If the mismatch parameter is measured on the rocket, measures should be taken to match the positions of the axes of the measurement coordinate system with the control planes. This usually is done by introducing gyrostabilization of the axes of the measurement coordinate system related to the control point in a case when the latter is moving and the banking of the rocket is stabilized.

When these measures are taken it is easy to write the mismatch equation in the complex form

$$\Delta\epsilon_1 = \epsilon_{1z} + j\epsilon_{1y},$$

where ϵ_{1z} and ϵ_{1y} are the components of the mismatch parameter in the corresponding deflection planes.

2. Parallel Approach Method

As in the case of two-point guidance, the parallel approach method requires that, in the process of rocket guidance, the rocket-target line moves parallel to the initial position of this line. Figure 2.14 shows the geometric relations when guiding a rocket in the vertical plane. Other than the angle ϵ between the rocket-target line and the axis $o_c x_{ec}$, and the angle ϵ_K determining the direction of the vector r_r in the case of ideal rocket guidance, the notations used here are the same as in figure 2.13.

Several variants of the mismatch equation can be derived for use in the parallel approach method. For example, the following form of the mismatch parameter was proposed in reference 2

$$\Delta\dot{\epsilon} = \frac{r}{v}\dot{\epsilon}. \qquad (2.8.5)$$

In accordance with expression (2.8.5), the coordinator apparatus should measure the distance between the rocket and the target, the velocity of the rocket and the angular velocity of the rocket-target line. Measurement of the value $\dot{\epsilon}$ at the control point is the most difficult problem. /72

A somewhat different approach to derivation of the mismatch equation for the parallel approach method in the case of three-point guidance also is possible. We will determine what law should be used to measure the angle ϵ_K in order for the rocket to move along a parallel approach trajectory.

From the triangle $o_c RT$ we find

$$\frac{r}{\sin\epsilon_1} + \frac{r_r}{\sin(\epsilon - \epsilon_t)}.$$

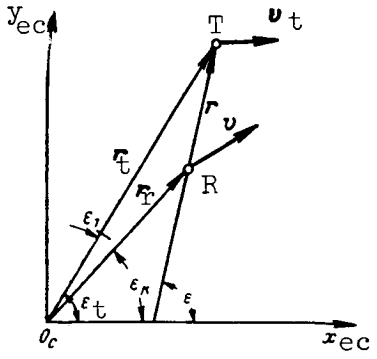

Figure 2.14

Hence

$$\varepsilon_1 = \arcsin\left[\frac{r}{r_r}\sin(\varepsilon - \varepsilon_t)\right] \tag{2.8.6}$$

If it is now required that the angle ε be constant during the entire time of guidance and equal to the value which it had at the time when the rocket was put into the parallel approach trajectory, that is, $\varepsilon = \varepsilon_0$, the expression (2.8.6) determines the theoretical value of the deflection angle ε_{1T}. Then the angle ε_K will be equal to

$$\varepsilon_K = \varepsilon_t - \arcsin\left[\frac{r}{r_r}\sin(\varepsilon_0 - \varepsilon_t)\right]. \tag{2.8.7}$$

When equation (2.8.7) is satisfied the rocket will be guided by the parallel approach method.

The mismatch parameter is determined as the difference between the theoretical value of the inclination of the vector r_r ($\varkappa_T = \varepsilon_K$) and its actual value $\varkappa_\partial = \varepsilon_r$. Then for the angular and linear deflections we will have

$$\left.\begin{aligned}\Delta_\varepsilon &= \varepsilon_K - \varepsilon_r = \varepsilon_t - \varepsilon_r - \arcsin\left[\frac{r}{r_r}\sin(\varepsilon_0 - \varepsilon_t)\right],\\ \Delta_h &= h \approx r_r \Delta_\varepsilon.\end{aligned}\right\} \tag{2.8.8}$$

The design of coordinators measuring the mismatch parameters determined by formulas (2.8.8) is a relatively complex problem. Expressions (2.8.8) can be simplified if the following approximations are made

$$\sin(\varepsilon_0 - \varepsilon_t) \approx \varepsilon_0 - \varepsilon_t, \quad \sin\varepsilon_{1T} \approx \varepsilon_{1T}$$

and

$$r \approx r_t - r_r.$$

It then is possible to obtain /73

$$\Delta_{\dot{\epsilon}} = \epsilon_t - \epsilon_r - \frac{r_t - r_r}{r_r}(\epsilon_0 - \epsilon_t). \qquad (2.8.9)$$

When forming the mismatch parameter on the basis of expression (2.8.9) the rocket flight trajectory will be the closer to a parallel approach trajectory the more precisely the approximations made above are satisfied.

Formula (2.8.9) makes it possible to judge the makeup of the measuring instruments included in the coordinator. It should contain angle-measuring instruments for measurement of the angles ϵ_t and ϵ_r, and range finders for measuring the distances r_t and r_r. The coordinator computer should perform relatively simple transformations of the measured values in accordance with formula (2.8.9).

If it is necessary to determine the mismatch parameter characterizing the linear deflection of the rocket from its reference trajectory it is sufficient to multiply $\Delta_{\dot{\epsilon}}$ by the range r_r. The latter usually is fixed by the programming mechanism $r_{pr} = r_r$. The mismatch equation in linear deflections has the form

$$\Delta_h = h = \Delta_{\dot{\epsilon}} r_{pr} = r_{pr}(\epsilon_t - \epsilon_r) - (r_t - r_r)(\epsilon_0 - \epsilon_t). \qquad (2.8.10)$$

If the motion of the rocket in space is considered, the mismatch equations for the parallel approach method, as in the preceding case, can be represented in the complex form.

2.9. Kinematic Equations for Three-Point Guidance Methods

The kinematic equations for three-point guidance methods characterize the motion of the target and rocket relative to the control point. By analyzing the kinematic equations, it is possible to trace the process of formation of the mismatch parameter and establish the applicability of a particular guidance method for specific tactical conditions.

If the control point (such as a rocket-carrying aircraft), rocket and target move in a single (vertical) plane, the kinematic equations have the following form

$$\left.\begin{aligned} \dot{r}_t &= v_t \cos q_t - v_c \cos q_c, \\ r_t \dot{\varepsilon}_t &= v_c \sin q_c - v_t \sin q_t, \\ \dot{r}_r &= v \cos q_r - v_c \cos q_{1c}, \\ r_r \dot{\varepsilon}_r &= v_c \sin q_{1c} - v \sin q_r, \end{aligned}\right\} \qquad (2.9.1)$$

where

/74

$$\left.\begin{aligned} q_r &= \varepsilon_r - \theta, \\ q_t &= \varepsilon_t - \theta_t, \\ q_c &= \varepsilon_t - \theta_c, \\ q_{1c} &= \varepsilon_r - \theta_c. \end{aligned}\right\} \qquad (2.9.2)$$

The notations used in equations (2.9.1) and (2.9.2) are explained by figure 2.15. Here $o_c x_{ec} y_{ec}$, $o_r x_{er} y_{er}$ and $o_t x_{et} y_{et}$ are nonrotating coordinate systems whose axes are parallel to the axes of a ground coordinate system and the origins of these coordinate systems coincide with the control point o_c and the centers of mass of the rocket R and the target T, respectively.

As an illustration of the formation of the mismatch parameters in the matching and parallel approach method, we will limit ourselves to the case of small angles q_r, q_t, q_c and q_{1c}, when the sines of these angles can be replaced by their arguments and the cosines by unity.

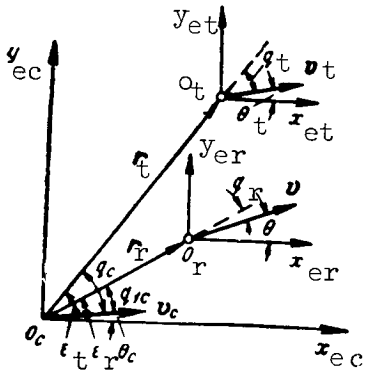

Figure 2.15

Then in place of equations (2.9.1) and (2.9.2) we obtain

$$\left.\begin{aligned} \dot{r}_t &= v_t - v_c, \\ \dot{r}_r &= v - v_c, \\ r_t\dot{\varepsilon}_t &= v_c(\varepsilon_t - \theta_c) - v_t(\varepsilon_t - \theta_t), \\ r_r\dot{\varepsilon}_r &= v_c(\varepsilon_r - \theta_c) - v(\varepsilon_r - \theta). \end{aligned}\right\} \tag{2.9.3}$$

Making transformations in (2.9.3) similar to those which were made in deriving formula (2.7.7), we will have

$$\left.\begin{aligned} \frac{d(r_t\varepsilon_t)}{dt} &= v_t\theta_t - v_c\theta_c, \\ \frac{d(r_r\varepsilon_r)}{dt} &= v\theta - v_c\theta_c. \end{aligned}\right\} \tag{2.9.4}$$

If the mismatch equation (2.8.2) is added to the expressions (2.9.4), the block diagram of the formation of the mismatch parameter for the matching method can be constructed (fig. 2.16). The controlling effects for the system of equations will be the changes of the angles θ_t and θ_c characterizing the motion of the target and the rocket-carrying aircraft. The angle θ, determining the trajectory of the rocket, appears as a feedback signal during the formation of the mismatch parameter Δ_{ε_1}. Changes of the ranges r_t and r_r lead to changes of the controlling effects and the parameters of the guidance circuits, respectively. In contrast to two-point guidance methods, where the link entering into the guidance circuit and having the transfer constant $1/r$ increases the amplification of the system as the rocket approaches the target, here the same link decreases the amplification of the system since with approach of the rocket to the target r_r increases. /75

The block diagram of the formation of the mismatch parameter in the parallel approach method can be obtained if the equations (2.9.4) are supplemented by the mismatch equation (2.8.9). This block diagram is shown as figure 2.17. In contrast to the preceding diagram there is an additional link here with a variable transfer constant dependent on the rocket-target range. The amplification of this link decreases to zero when $r_r = r_t$.

In order to determine the kinematic trajectories it is necessary to solve a full system of equations (2.9.1) with the addition to it of the ideal coherence equation for that guidance method for which the trajectory is determined. In a number of cases it is simpler and more graphic to have a graphic determination of the kinematic trajectories. We now will cite an example of such a construction for the matching method. The essence of the graphic method of

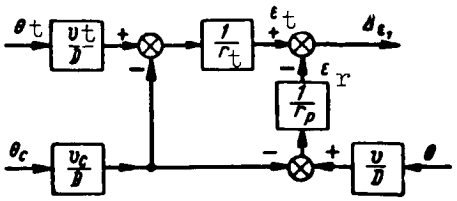

Figure 2.16

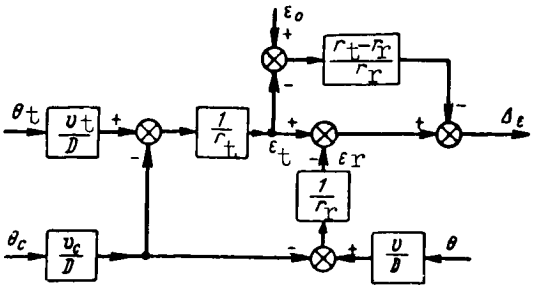

Figure 2.17

construction of a trajectory is as follows. The first step is to plot the trajectories of the proposed motion of the control point (curve C_0C_k in figure 2.18) and the possible motion of the target (curve T_0T_k). The entire interval C_0C_k and T_0T_k is broken down into sectors corresponding to the flight of the target and control point during the time Δt. The straight lines C_0T_0, C_1T_1, etc., thus constitute lines of sight.

At launching time ($t = 0$) the rocket is situated at point R_0 coinciding with C_0. When $t = \Delta t$ the rocket travels the distance $R = v\Delta t$ from point C_0. During this time the control point, moving with the velocity v_c, moves to the point C_1 and the target occupies the position T_1. Since $\Delta_{\varepsilon_1} = 0$ in guidance by the matching method, at the time $t = \Delta t$ the rocket should be situated on /76 the ray C_1T_1.

Thus, point R_1 (the position of the rocket on the line of sight C_1T_1) can be determined as the point of intersection of a circle of the radius $R = v\Delta t$ with its center at point C_0 and the straight line C_1T_1.

The positions of the rocket on the straight lines C_2T_2, C_3T_3, ... are determined in a similar way: successively, from the points R_1, R_2, ..., circles with the radii $v\Delta t$ are drawn to the intersection with the straight lines C_2T_2, C_3T_3, ...

The resulting curve R_0, R_1, R_2, ... T_k characterizes the kinematic trajectory of motion of the rocket when its guidance is by the matching method. By

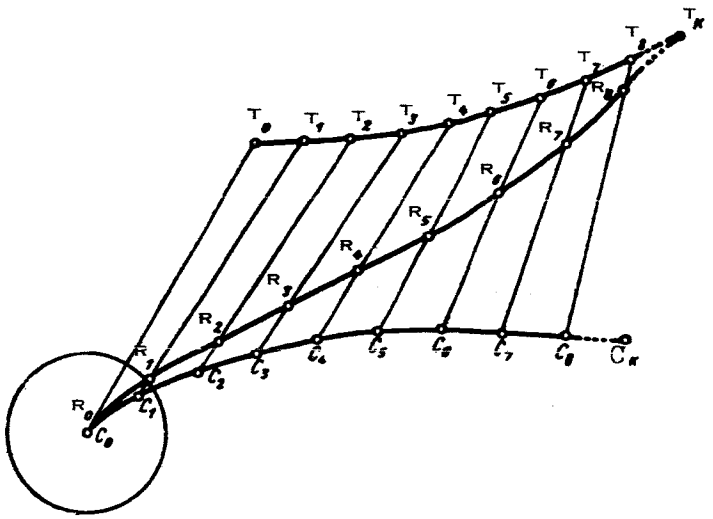

Figure 2.18

employing the curves shown in figure 2.18, it is easy to determine the required normal accelerations because, as is well known,

$$j_n = \frac{v^2}{R_{cu}}, \qquad (2.9.5)$$

where R_{cu} is the radius of curvature of the trajectory, determined using the curve in figure 2.18.

By using expression (2.9.5) it is possible to find the functional dependence of j_n on time for different characters of motion of the target and the control point.

After analyzing the trajectories of rocket motion for guidance by the matching method, it can be concluded that they are essentially dependent on /77 the character of flight not only of the target but also the motion of the control point. Usually the applicable value of the required accelerations is obtained only in a case when the attack of the moving target is made from the rear hemisphere. This fact limits the tactical possibilities of applying the matching method.

The graphic construction of the kinematic trajectory for the parallel approach method is accomplished using the same rules as in two-point guidance.

2.10. Perturbations Affecting the Coordinators

In evaluating the accuracy of measurement of the mismatch parameter by the control system coordinator, it is important to determine not only the errors caused by inexact reproduction of the controlling effect, but also the errors caused by various kinds of perturbations.

With respect to the coordinators, containing electronic devices, the perturbing effects are manifested in distortions of the signals carrying information on the mismatch parameter. These distortions are caused by various factors, the most important of which are:

(1) the instrument noise of the receiving apparatus of the coordinator;

(2) fluctuations of the amplitude of the signal reflected from the target;

(3) fluctuations of the apparent or effective center of reflection of the target;

(4) change of the conditions for passage of signals through space;

(5) artificial interference.

The signal distortions caused by the instrument noise of the receiver usually are insignificant and the errors caused by them during the measurement of the mismatch parameter are extremely small. We now will explain the foregoing in somewhat greater detail. When the coordinator is operating in an automatic control system it is necessary to ensure a stable (undisrupted) process of measurement of the mismatch parameter. The latter is attained by incorporating in the coordinator measuring instruments so-called automatic pickups, which cut in the measurement circuit only in a case when there is a specified excess of the received signal above the instrument noise of the receivers. Under these conditions, the distortions of the received signals by the instrument noise of the receivers usually are insignificant. The instrument noise of the receiver should be taken into account when determining the effective range of the measuring apparatus because the lower the instrument noise, the lower the triggering threshold of the automatic pickup can be set, and therefore the measurements will be made with the stipulated accuracy at a greater range.

All the principal targets have a relatively complex geometrical structure and as a result the reflected radio signal can be considered as the sum of /78 the oscillations arriving from a large number of surfaces of different configuration. These signals, having random amplitudes and phases, create intensifying or attenuating interference effects at the point of reception when there is an insignificant change of the relative position of the target, which leads to an appreciable change of the signal at the reception point.

The most important characteristic of a radar target is its effective reflection area S_{eff}. The value S_{eff}, characterizing the measure of energy

reflected from the target, determines for specified parameters of the system the maximum effective range of the coordinator.

Since the diagram of reflection from a target is multilobed, the effective reflecting surface of a target of complex configuration, in a general case, changes appreciably in dependence on the aspect of the target. The value S_{eff} also is dependent on wavelength. Therefore, the mean value S_{eff} usually is stipulated, as sometimes also will be the deviation from it in the form of the distribution law of the probabilities of the amplitudes of the reflected signal. The form of the distribution law can be used to judge the reliability of the effective range which will be determined from computations.

The mean value of the effective reflecting surface of a target and the deviations from this value characterize the target as an element in the control complex only from the point of view of the selection of the parameters of the coordinator ensuring a stipulated effective range of the control system. Also of considerable interest is the problem of fluctuations of the amplitudes of a reflected signal and the angular fluctuations of the apparent center of reflection of the target.

The fluctuations of the amplitudes of the reflected signal are caused by the multilobed character of the diagram of reflection from the target, the angular velocity of its motion relative to the rocket, and for air targets, the values of the frequencies and amplitudes of yawing and banking of the aircraft target and the rocket, their vibrations, etc.

Due to the mentioned fluctuations the strength of the signal arriving at the input of the measuring instrument receiver will vary randomly. The instantaneous value of the fluctuating signal is given by the noise modulation coefficient, representing the ratio of the increment of a random signal $\Delta E(t)$ to its mean value E_0, that is, $m_n(t) = \frac{\Delta E(t)}{E_0}$.

In many cases it is assumed that the random function $m_n(t)$ is stationary with a zero mean value and is evaluated by the correlation function $R_m(\tau)$ or the spectral density $G_m(\omega)$. The mentioned statistical characteristics are determined experimentally for each type of target. When used in analytical computations the experimental curves $R_m(\tau)$ and $G_m(\omega)$ are approximated by suitable functions.

The normalized correlation function $\rho_m(\tau) = \frac{R_m(\tau)}{R_m(0)}$ is described sufficiently accurately by the expression /79

$$\rho_m(\tau) = e^{-\alpha|\tau|}\cos\omega_1\tau, \qquad (2.10.1)$$

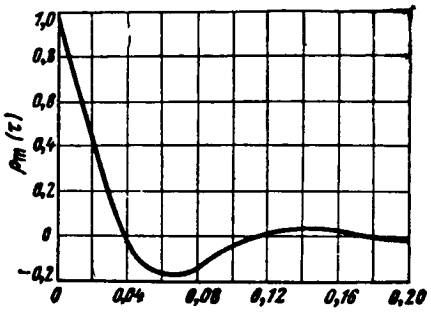

τ, sec

Figure 2.19

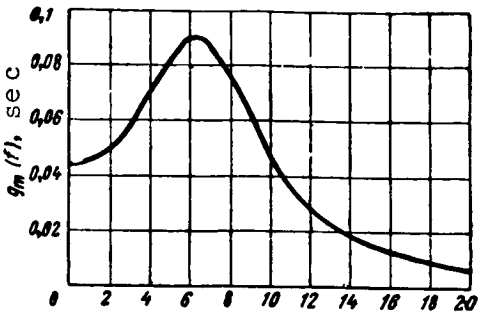

f, cps

Figure 2.20

where the values α and ω_1 are selected from the condition of approximation of the approximating function to the experimental curve.

If the correlation function of a random stationary process is determined, the spectral density of this process can be determined analytically as

$$G_m(\omega) = 4\int_0^\infty R_m(\tau)\cos\omega\tau d\tau. \qquad (2.10.2)$$

For the approximation of the correlation function used above the normalized spectral density $g_m(\omega) = \frac{G_m(\omega)}{R_m(0)}$ of the noise modulation coefficient is expressed using the formula

$$g_m(\omega) = 2\left[\frac{\alpha}{(\omega-\omega_1)^2+\alpha^2} + \frac{\alpha}{(\omega+\omega_1)^2+\alpha^2}\right]. \qquad (2.10.3)$$

As an example, figures 2.19 and 2.20 show the normalized correlation function and spectral density of the noise modulation coefficient $m_n(t)$ when α = 24 sec^{-1} and ω_1 = 40 sec^{-1}.

The measurement errors of the mismatch parameter in a number of cases are caused by the angular fluctuations of the apparent center of reflection of the target. The essence of these fluctuations can be clarified very roughly in the following simple example.

As pointed out, the diagram of reflection from the target has a clearly expressed multilobed character. There is a sharp change of the phases of reflected signals between adjacent lobes. For example, the phases of the signals of two adjacent lobes between which the gap attains zero, differ from one

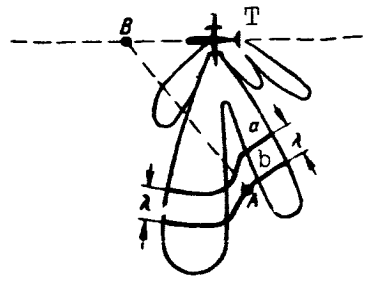

Figure 2.21

another by the angle π. As a result, the front of the reflected wave is distorted. Figure 2.21 shows part of the idealized diagram of reflection from an aircraft. Here the lines a and b conditionally represent the phase characteristics of the reflection diagram. If it is assumed that the direction to the effective center of reflection of the target is determined by the perpendicular to the wave front at the reception point, for the point A the apparent center of reflection is displaced to the position B. /80

Random angular oscillations of the target lead to disordered changes of the front of the reflected wave, and therefore to disordered fluctuations of the apparent center of reflection of the target. The fluctuations of the apparent center of reflection sometimes are called the angular noise of the target, in contrast to the fluctuations of the amplitude of the reflected signal, which are called amplitude noise.

Angular noise is given in the form of the angle $\varepsilon_n(t)$, whose value changes in conformity to the random law relative to the true direction to the target. It can be seen from figure 2.21 that when the movement of the center of reflection is given in linear measure the angular errors in determination of the actual direction to the target, caused by angular fluctuations, will increase approximately proportional to the decrease of range. This distinguishes angular noise from amplitude noise, whose parameters are insignificantly dependent on range, and makes difficult the determination of the statistical characteristics of the random function $\varepsilon_n(t)$.

For some constant range r between the measuring instrument and the target the spectral density $G_n(0)$ of the angle $\varepsilon_n(t)$, when $\omega = 0$, sometimes is given in the form

$$G_n(0) = k_{\varepsilon n}\left(\frac{L}{r}\right)^2, \qquad (2.10.4)$$

where L is the linear dimension of the target and $k_{\varepsilon n}$ is a coefficient dependent on the type of antenna of the measuring instrument.

A change in the conditions for transmission of signals in space leads to a change of the amplitude of the received signal. If these changes transpire slowly, they usually are eliminated by the automatic volume control system of the receiver. However, an allowance for rapid changes of transmission conditions, caused by the nonstationary absorption of radio waves in the rocket engine jet, is made using the same method as when taking into account the amplitude fluctuations of a signal reflected from a target.

CHAPTER 3. ELECTRONIC COORDINATORS OF HOMING SYSTEMS

3.1. Functional Diagrams of Electronic Coordinators of Homing Systems

The principal part of the electronic coordinator of homing systems is /81 an apparatus for the automatic tracking of the target on the basis of angular coordinates. Since the automatic tracking of an isolated target on the basis of angular coordinates usually can be accomplished only when using equisignal direction-finding methods, making it possible to establish not only the value but also the direction of deflection of the target from the equisignal line, the coordinators use antenna systems which make possible the creation of such an equisignal line. The signal received from the target is fed to an output apparatus after amplification in the receiver.

The antenna, radio receiver and output apparatus form a direction-finding apparatus (direction finder) in the coordinator. The mismatch signal at the output of the direction finder is a dc voltage in certain limits proportional to the angular deflection of the target from the equisignal line. If the target is situated on the equisignal direction the mismatch signal is equal to zero. With a change of the direction of deflection of the target the mismatch signal changes its sign.

In addition to the mentioned principal elements, the direction finder contains a number of additional devices which play an important role in the correct functioning of the direction-finding apparatus. In particular, these include an automatic selector (autoselector). It is known that the satisfactory operation of the mentioned system of automatic tracking of the target in direction is attained only in a case when there is tracking of only one target. Due to the low resolution possible when using angular coordinates inherent in systems having small antennas (and the latter are strictly limited by /82 the size of the rocket), it is possible for several targets to appear in the "angle of view" of the antenna of the direction-finding apparatus. It therefore is necessary to introduce an additional selection of signals so that only signals from a single target will be detected. The possibility of introducing additional selection in electronic coordinators of homing systems distinguishes them favorably from coordinators using the thermal radiation of a target.

The synchronization of the autoselector during active homing is accomplished using the signals of a transmitter carried aboard the rocket. In the semiactive homing method the autoselector is synchronized by signals received from an additional receiver which is connected to an antenna receiving signals of the radar set irradiating the target.

Thus, the direction-finding apparatus of the coordinator produces a mismatch signal characterizing the deflection of the target from the equisignal

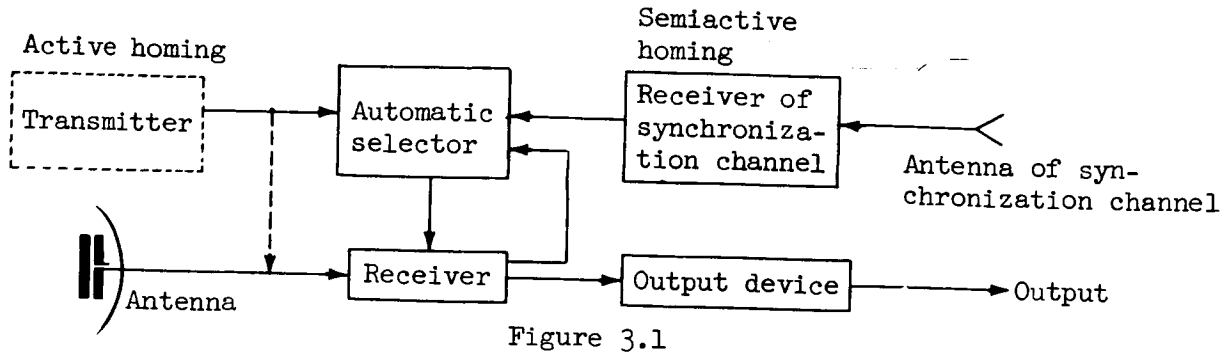

Figure 3.1

direction. The coordinator contains only one direction-finding apparatus if such a signal is adequate for homing, as in the direct guidance method, when the control command is proportional to the deflection of the target from the longitudinal axis of the rocket. In this case the antenna of the direction-finding apparatus is attached rigidly to the body of the rocket and its equi-signal direction is oriented along the longitudinal axis. Coordinators of this type will be called coordinators with fixed (relative to the body of the rocket) equisignal direction or simply fixed coordinators.

The term "fixed coordinator" is of an arbitrary character and is introduced for brevity in exposition. The term is arbitrary because such a coordinator is mounted on a moving object and moves together with it. The functional diagram of a fixed coordinator is shown in figure 3.1.

If it is necessary to move the equisignal direction relative to the body of the rocket independently of the motion of the latter, the coordinator must not only have a direction finder but also a final control mechanism. The final control mechanism is designed for movement of the equisignal direction in accordance with the change of the angular position of the rocket-target line. /83 Coordinators of this type will be called moving coordinators. Figure 3.2 shows the functional diagram of a moving coordinator.

When a moving coordinator is carried on a rocket the control system contains two automatic regulation series circuits. One of them is used for movement of the equisignal direction, performing automatic tracking of the target on the basis of angular coordinates, and the second is used for change of the position of the axis of the rocket in accordance with the signals received from the coordinator.

Displacement of the equisignal line can be accomplished either mechanically (by the turning of the antenna) or electrically. In the latter case the body of the antenna is attached rigidly to the body of the rocket and the movement of the equisignal line occurs as a result of the change of the electric state of individual components of the antenna system.

We note in conclusion that fixed coordinators usually are used in those cases when the guidance method employed does not require the fixing of large deflection angles and the introduction into the control law of the derivatives of the angle ϵ, characterizing the line of sight. Moving coordinators afford

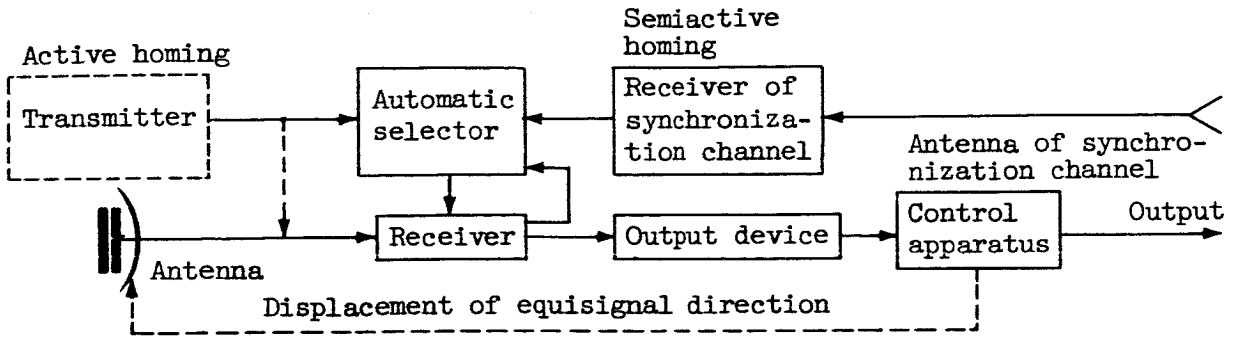

Figure 3.2

greater possibilities. They are used in guidance methods requiring both the fixing of considerable deflection angles and measurement of the derivatives of the angle ϵ.

3.2. Coordinator Direction-Finding Apparatus

The vigorous development of the technology of automatic determination of the coordinates of targets using electronic apparatus now being observed results in a great multiplicity in the principles of design and construction of the direction-finding apparatus of coordinators. Below we will consider only the most typical examples of the design of direction-finding apparatus which in essence are becoming classical.

We recall that the possibility of determination of the angular coordinates of a target by electronic apparatus is based on the use of the directional /84 properties of antenna, characterized by the directional diagram. In a general case the directional diagram of an antenna is described by a complex function of the angle of incidence of radio waves. The module and argument of this function are called the amplitude and phase directional diagrams, respectively.

Either an amplitude or phase directional diagram usually is used for direction finding, depending on which of the parameters of the high-frequency oscillation (amplitude or phase) arriving from the target is used for obtaining information on the angular position of the target in space, or in other words, for which of the mentioned parameters the antenna possesses spatial selectivity. The terms amplitude and phase direction-finding apparatus therefore are used. It should be remembered that it is not always technically possible to design a "purely" amplitude or "purely" phase direction finder because the phenomena of change of the amplitude and phase of the arriving signal at the time of angular deflection of a target accompany one another. The only difference is in the quantitative values of these changes. The basis for naming the type of direction finder is that parameter whose changes are predominant.

In the equisignal direction-finding method the angle of arrival of the incident wave is determined by a comparison of the signals received from two or

more noncoinciding directional diagrams. This comparison can be made either successively or simultaneously.

In the first case, the equisignal direction is created by a periodic change of the position of the directional diagram (amplitude or phase) of the direction-finding antenna. Data on the angular position of the target relative to the equisignal direction are obtained by successive comparison of the signals received with the directional diagram in different positions. Since an equisignal direction in the case of successive comparison is created only for a finite interval of time, direction-finding apparatus of this type are called direction-finding apparatus with an integral equisignal direction. We note that, with a periodic change of the position of the directional diagram, the parameter used in determining the angular position of the target experiences an additional periodic change--modulation. Either the amplitude or the phase of the received signal is modulated, depending on the design of the antenna used. This circumstance makes it possible to refer to direction finders with an integral equisignal direction as modulation-type apparatus. A direction finder with conical scanning of the directional diagram is an example of a direction-finding apparatus with an integral equisignal direction and amplitude modulation.

In the case of simultaneous comparison of signals, reception is by several spaced antennas. In this case, the equisignal direction is formed at each /85 specific moment and thereby there is "instantaneous" detection of the mismatch signal. An apparatus of this type is called a direction finder with an instantaneous equisignal direction. It is exemplified in so-called monopulse radar sets.

3.3. Functional Diagram of a Direction-Finding Apparatus with an Integral Equisignal Direction

Among the direction-finding apparatus with an integral equisignal direction for the automatic tracking of a target on the basis of angular coordinates, the most widely used are direction finders with the amplitude direction-finding method, especially direction finders with conical scanning. Phase-type direction finders with an integral equisignal direction are used for the time being only in some radio navigation systems (ref. 11) and will not be discussed here.

Figure 3.3 shows a simplified functional diagram of a direction-finding apparatus with conical scanning. It contains an antenna A, a receiver rec and an output apparatus which includes a mismatch signal detector D, a mismatch signal amplifier a, two phase detectors PD_1 and PD_2 and two dc amplifiers DCA_1 and DCA_2. In addition to the mismatch signal the phase detectors receive a reference signal produced by the reference voltage generator RVG, connected to the apparatus for rotation of the diagram ARD.

The antenna system, having a needle-shaped directional diagram, is constructed in such a way that the maximum of the diagram is displaced in relation

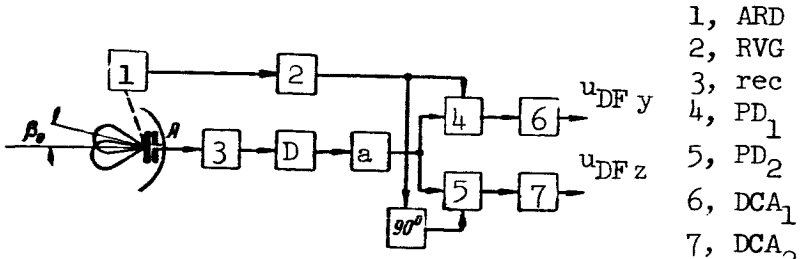

Figure 3.3

to the axis of symmetry of the antenna (equisignal direction) by the angle β_0.

If the target is not situated on the equisignal direction the signal received from the target receives additional amplitude modulation, and the depth of this modulation is dependent on the value of the angular displacement of the target in relation to the equisignal direction. The phase of the envelope, read from some fixed value, indicates the direction of displacement of the target. The conversions of the received signal after its passage through the receiver essentially involve detection of the envelope in the mismatch signal detector, amplification of the received mismatch signal and its conversion in the phase /86 detectors, and amplification by the dc amplifiers.

In direction finders with conical scanning it is most common to use parabolic antennas. An important characteristic of such an antenna is the rate of rotation of the directional diagram (scanning frequency). As will be demonstrated below, with an increase of the scanning frequency, there is an increase of the accuracy of tracking of the target when the signals received are of fluctuating amplitude. However, in the case of mechanical rotation of the reflector or exciter of the antenna, an increase of the scanning frequency requires a considerable increase of the power of the drive motor. In addition, in the case of rotation of the reflector with an increase of the rate of rotation, there is an increase of the difficulties in the mechanical balancing of the antenna system.

Below we give two examples of design of antenna systems in which the difficulties involved in obtaining high scanning frequency have been overcome. As the first example we will consider a system with mechanical rotation of the directional diagram (ref. 43). In contrast to ordinary antennas with conical scanning, where the diagram is rotated by rotation of the exciter, whose phase center is displaced relative to the axis of the antenna, a fixed exciter is used in this case and the phase center is displaced solely by rotation of a relatively light element of the exciter; in one revolution of this element there are three periods of movement of the phase center, that is, three revolutions of the directional diagram.

Figure 3.4 is a diagram of the antenna. It consists of a parabolic reflector, supply waveguide, exciter and a small electric motor which is situated in front of the reflector. The antenna exciter is a circular waveguide with a plane polarized wave H_{11}, at whose output there is a system of three radia- /87

tors which form angles of 120° with one another. Linear vibrators with a

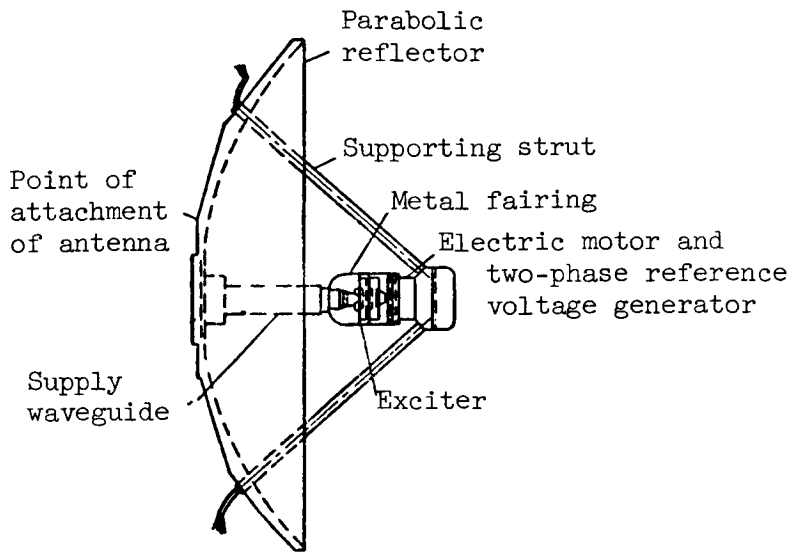

Figure 3.4

counter reflector or slotted plate can be used as the radiators. The system of radiators is driven by an electric motor.

The principle of operation of the primary radiating element is explained in figure 3.5. The relative amplitudes of excitation of the individual linear radiators are proportional to the projection of the electrical vector (and in the case of slots--the magnetic vector) onto the direction of radiation. For example, if the E vector is parallel to one of the vibrators (such as the vibrator A, fig. 3.5a) these projections are equal to 1 and cos 60° = 0.5 (fig. 3.5c). However, the components of the E fields radiated by them, parallel to the vibrator A, will be equal to 1 and $\cos^2 60^\circ$ = 0.25, respectively (fig. 3.5d). Thus, it is necessary to find the center of radiation of a system of three radiators with the amplitudes 1, 0.25 and 0.25, whose centers are situated as shown in figure 3.5b. This is equivalent to finding the center of gravity of a system of three material points. It is easy to confirm that, in this case, the phase center will be displaced along the vibrator A by a value equal to half the displacement of the center of the latter. Obviously, with rotation of the system of radiators the phase center will move along a circle.

Figure 3.6 shows that the frequency of its movement will exceed by a factor of 3 the frequency of rotation of the radiators. In figure 3.6 the diameters of the circles characterize the relative amplitude of the vertically polarized component of the field of each radiator. Horizontally oriented radiators are not excited because a vertically polarized wave is used.

Another possibility for obtaining a high scanning frequency is the use of antennas with a so-called electrically controlled beam (ref. 44). Such antennas consist of several exciting elements spaced relative to one another at distances ensuring the formation of a single composite directional diagram (one beam).

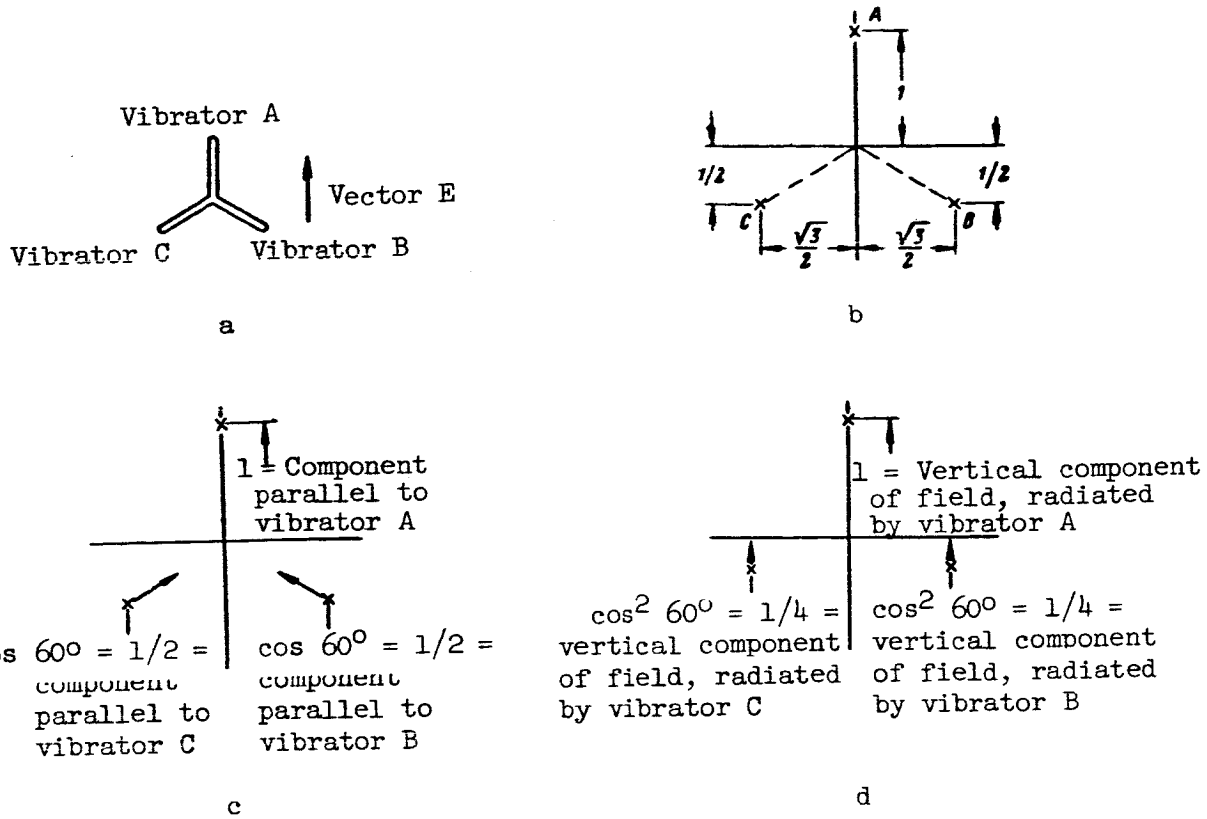

Figure 3.5

The position of this beam is determined by the phase shift of the currents of the supply elements. With a change of the phase shift of the currents there will be a change of the position of the beam in space. The phase is changed by a controlled phase inverter in the supply waveguide of each element.

The phase inverters are controlled by a distributor. If electrical /88
phase inverters are used, the distributor produces currents supplying the windings of the ferrites of the phase inverters, ensuring such a phase distribution that the beam moves in conformity to a specified law.

In the case of uniform rotations of the beam the distributor can be designed in the form of an ac multiphase generator, each voltage phase of which is used for control of one of the phase inverters. This same generator produces a reference voltage.

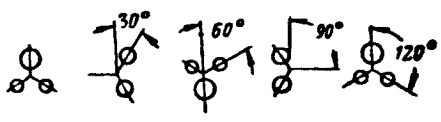

Figure 3.6

The radio receiving apparatus of the coordinator, with respect to both the functions which it performs and design of circuitry, is similar in many respects to the receiver of a standard radar set for automatic tracking of a target on the basis of angular coordinates (ref. 45). In most cases, a superheterodyne circuit is used for such a receiver.

It is known that in order to increase the sensitivity of a radar receiver, and therefore increase the effective range of the set, special measures must be taken for the elimination of instrument noise. The latter is achieved by designing the frequency converters in accordance with a balanced circuit, using low-noise amplifiers, etc. Similar measures can be taken in the receivers of coordinators, with the single reservation that they must not result in an increase of the size and weight of the apparatus above the admissible values, which in some cases are extremely limited.

All the processes associated with the tuning and adjustment of the receiver should be automated. For this reason the coordinator receiver is supplied with systems for automatic volume control (AVC), automatic frequency control (AFC) and automatic target selection.

The system for automatic volume control should have a relatively large dynamic range because in the homing process the rocket-target range changes in very broad limits. If the AVC is insufficiently effective the level of the output signal of the receiver also will vary, and as will be demonstrated below, this will lead to a change of the transfer coefficient of the direction finder, which is extremely undesirable.

The design of the AFC system can vary, depending on the homing method. For example, in the case of active homing, when a signal transmitter irradiating the target is carried aboard the rocket, the receiver heterodyne is tuned on the basis of the transmitter signal, much as is done in radar sets.

In the case of semiactive homing the receiver heterodyne is tuned on the basis of the frequency of the received signal (AFC on the basis of the received signal) or the heterodyne frequency is stabilized by means of a highly stable element (EFS). In the latter case the frequency of the signal of the transmitter "irradiating" the target also should be extremely stable and known in advance.

Finally, in the case of passive homing the receiver heterodyne is tuned solely on the basis of the arriving signal. Since a direct signal radiated by the target and which usually has a relatively high power is used in passive homing, in some cases it may be desirable to replace the superheterodyne receiver in the direction finder by a crystal receiver. Such a receiver has a quite broad-band input and therefore there is no need of AFC. /89

The system for automatic target selection will be discussed in greater detail in section 3.7.

As already mentioned, the output device consists of a mismatch signal detector, a mismatch signal amplifier, two phase detectors and a dc amplifier.

There are various designs for a mismatch signal detector. In selecting the parameters of any of them an effort must be made to reduce to a minimum the nonlinear distortions of the mismatch signal. Sometimes in addition to performing its direct role (detection of the video pulses envelope) the mismatch signal detector serves as an element of the "forward" AVC circuit.

The mismatch signal amplifier is a low-frequency electronic amplifier consisting of one or more stages, depending on the required value of the amplification factor. Since the mismatch signal in the case of small deflections of the target from the equisignal direction is a voltage of almost sinusoidal form of a frequency known in advance, the amplifier can contain a selective filter, tuned to the scanning frequency and having a relatively narrow pass band. The presence of such a selective filter improves the shape of the mismatch signal and facilitates an additional noise filtration. At the same time, extremely rigorous requirements are imposed on the constancy of the amplitude and especially the phase characteristic of this filter and also on the stability of the scanning frequency. Inadequate stability of the mentioned parameters leads to an additional uncontrolled phase shift of the signal, which in turn causes so-called dephasing of the system leading to a "skewing" or "twisting" of the axes of the coordinate measurement system. If there are difficulties in ensuring the admissible instability of these parameters, it is desirable to dispense with the narrow-band filter in the amplification channel.

The essential purpose of the phase detectors is scaling of the mismatch signal from a polar coordinate system to a rectangular coordinate system. In actuality, before reaching the phase detectors the mismatch signal was formed in a polar coordinate system, when its amplitude characterizes the module of angular deflection of the target from the equisignal direction, and the phase shift, read relative to the reference signal, determines the direction of /90 target deflection. However, at the output of the phase detectors there are two mismatch signals (in the form of slowly changing voltages) characterizing the angular movements of the target relative to the equisignal direction in two mutually perpendicular planes.

The direct-current amplifiers (DCA) are used for amplification of the signals and coupling the direction finder to the subsequent circuits. Depending on the character of these circuits the dc amplifiers can have anode or cathode outputs.

The phase detectors and dc amplifiers are the final stages of the direction finder, where the signal level is quite high. Their parameters therefore should be selected in such a way that the limiting of the mismatch signal sets in only when there is a definite value of the angular deflection of the target, set by the required width of the zone of linearity of the direction-finding characteristic. We note that the direction-finding characteristic expresses the dependence of the voltage at the output of the direction finder on the angle of deflection of the target relative to the equisignal direction. In addition, the phase detectors and the dc amplifiers should have a small zero drift (unbalance) because the latter leads to displacement of the zero of the direction-finding characteristic and therefore to errors in determination of the direction to the target.

In conclusion we will discuss the principal adjustments which are accomplished in the output device of the direction finder. These include setting of the balance in the output stages, phasing and setting of nominal amplification.

When the balance is set in the output stages it is possible to obtain zero signals at the output of the direction finder when there is no mismatch signal at the input of the phase detectors. The balance is regulated either in the phase detector circuits or in the dc amplifier circuits.

The phasing of the direction finder has the purpose of fixing the parallelism of the axes of the coordinate system, in which deflection of the target occurs, and the axes of the coordinate system in which the mismatch signal is measured. In a phased direction finder, with the deflection of the target relative to the equisignal direction in any one plane, such as in the vertical plane, the signal at the output of the dc amplifier of the horizontal deflection channel should be equal to zero and the signal at the output of the dc amplifier of the vertical deflection channel should be maximal.

Phasing is accomplished either by introduction of an additional phase shift of the mismatch signal prior to reaching the phase detectors or by change of the initial phase of the reference signal, depending on the convenience in designing the regulation system.

Finally, setting of the nominal amplification is necessary for obtaining the computed value of the direction finder transfer coefficient. This means that for a specific value of the angular displacement of the target relative to the equisignal line, the required value of the signal should be obtained at the direction finder output. Regulation is accomplished by a change of the amplification factor of the mismatch signal amplifier. /91

3.4. Block Diagram of a Direction Finder with an Integral Equisignal Direction

A coordinator with conical scanning, considered as an automatic control apparatus, belongs to the class of alternating current tracking systems in the subsonic range.

It is well known that alternating current tracking systems, or modulated systems, as they sometimes are called, contain a special part in the channel consisting of a modulator, an intermediate link and a demodulator. The role fo the special part of the channel in a coordinator with conical scanning is played by the direction finder. Therefore, in constructing a block diagram of the direction finder it is desirable to separate out the modulator, which includes the antenna system, receiver and mismatch signal detector, the intermediate link which is the mismatch signal amplifier, and the demodulator, which consists of two phase detectors. The dc amplifiers are used for coupling the demodulator to the subsequent circuits of the coordinator.

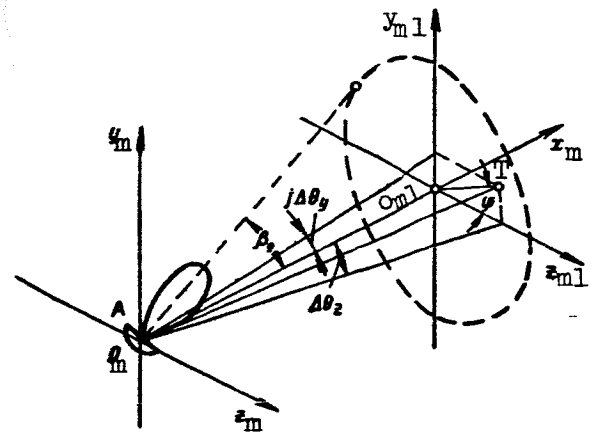

Figure 3.7

We introduce the measurement coordinate system $o_m x_m y_m z_m$ (fig. 3.7), whose origin is at the center of the antenna A, and whose axis $o_m x_m$ coincides with the equisignal direction. The plane $o_{m1} y_{m1} z_{m1}$ passes through the target point T normal to the straight line $o_m x_m$. The axes $o_{m1} y_{m1}$ and $o_{m1} z_{m1}$ are parallel to the corresponding axes of the measurement coordinate system. The circle /92 on the plane $o_{m1} y_{m1} z_{m1}$ indicates the trace of the point of the maximum of the directional diagram during its rotation. The displacement of the maximum of the directional diagram relative to the equisignal line is characterized by the angle β_0.

With a small displacement of the target from the equisignal direction its angular position is given conveniently in the form of the complex angle $\Delta\theta = \Delta\theta_z + j\Delta\theta_y = \Delta\theta e^{j\varphi}$, where $\Delta\theta_z$ and $\Delta\theta_y$ are the angles of deflection of the target in the planes $o_m x_m z_m$ and $o_m x_m y_m$, respectively; $\Delta\theta$ is the module of the angular mismatch; φ is the phase angle of the target.

The modulator transforms the angular coordinates of the target ($\Delta\theta_z$, $\Delta\theta_y$), representing a slowly changing function of time, into an ac mismatch signal. The process of modulation of the signal received from the target can be described by introducing the modulating function $F_M(\Delta\theta, t)$. As will be demonstrated below, this function can be obtained from the dynamic directional diagram of the antenna, that is, a directional diagram changing its position in space.

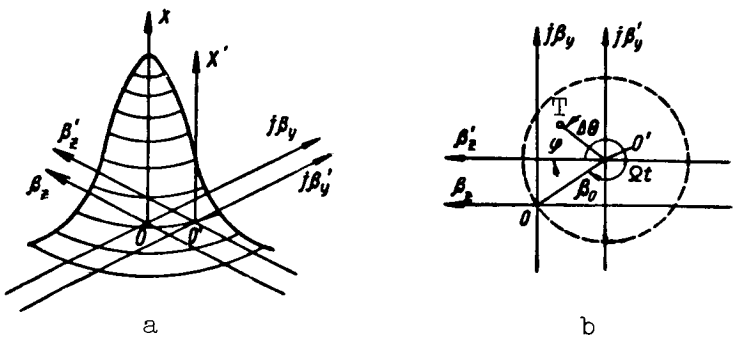

a b

Figure 3.8

Then for the emf acting in the circuit of the receiving antenna we can write

$$e = k_p E_0 G_0 F_м (\Delta\theta, t)\, e^{j\omega t}, \qquad (3.4.1)$$

where E_0 is the amplitude of the electrical component of the field at the reception point, caused by the signal arriving from the target; G_0 is the coefficient of directional effect of the antenna in the direction of the maximum; k_p is the proportionality factor; ω is the angular frequency of the received signal.

If the received signal has the character of a pulse this circumstance is taken into account by the introduction of a time factor into (3.4.1).

We now will explain the method for obtaining the modulating function. Assume

$$X = |F(\beta)| \qquad (3.4.2)$$

is the equation of a normalized spatial directional diagram of an antenna in a Cartesian coordinate system (fig. 3.8a). Here $\beta = \beta_z + j\beta_y$ is the complex /93 current angle, and β_z and β_y are the components of this angle along the $o\beta_z$ and $oj\beta_y$ axes, respectively. The selection of a Cartesian coordinate system in place of the spherical coordinate system usually used in writing the directional diagram equation is not of basic importance and was done exclusively for the sake of clarity.

Equation (3.4.2) describes in space some unclosed surface situated above the plane $o\beta_z j\beta_y$ in such a way that the point of the maximum of this surface is situated above the point o. Since hereafter we will consider only the amplitude directional diagram, the sign of the module in equation (3.4.2) will be omitted.

The reading of the target coordinates during the forming of the mismatch signal in a direction finder with conical scanning is accomplished relative to the equisignal direction, displaced from the axis of the maximum of the directional diagram by the angle β_0. In figure 3.8b the coordinate system relative to which the angular mismatch (displacement of the target from an equisignal line) is measured is denoted $o'\beta_z'j\beta_y'$. The point o' is the trace of the equisignal direction on the plane $o'\beta_z'j\beta_y'$.

The directional diagram equation in the frame of reference $o'\beta_z'j\beta_y'$ has the form

$$X = F(\beta' - \beta_0), \tag{3.4.3}$$

where $\beta' = \beta_z' + j\beta_y' = \beta' e^{j\psi}$ is the current value of the angle in a coordinate system related to the equisignal direction.

If the rotation of the directional diagram relative to the equisignal direction is taken into account, it is necessary to assume

$$\beta_0 = \beta_0 e^{-j\Omega t}, \tag{3.4.4}$$

where Ω is the angular frequency of scanning.

By substituting (3.4.4) into (3.4.3) we obtain the directional diagram equation for a scanning antenna

$$X = F(\beta' - \beta_0 e^{-j\Omega t}). \tag{3.4.5}$$

If the time t is set, equation (3.4.5) describes a static directional diagram whose position corresponds to the considered time. If the current value β' is set, assuming it to be equal to the angular coordinates of the target T (fig. 3.8b), the function $F_M(\Delta\theta - \beta_0 e^{-j\Omega t})$ shows the way in which the spatial information on energy distribution, characterizing the target position, is converted into a mismatch signal, that is, into temporal information, or, we would say, it gives the law of conversion of "target space" into "signal space."

The expression $F_M(\Delta\theta - \beta_0 e^{-j\Omega t})$ enters into formula (3.4.1) as a modulating function.

If the directional diagram is written in explicit form, in one approxi- /94
mation or another, and the receiver and mismatch signal detector transfer coefficients are taken into account, by using (3.4.1) it is possible to obtain the modulator transfer function. In actual practice, however, it is desirable to first simplify the expression for $F_M(\Delta\theta - \beta_0 e^{j\Omega t})$, making two assumptions: the target coordinates change slowly and the angular mismatch is small.

The angular mismatch $\Delta\theta$ is dependent on time, that is, $\Delta\theta = \Delta\theta(t)$. The character of its change is determined by the motion of the target and the movement of the equisignal direction. Assuming the changes of $\Delta\theta$ to be quite small and the scanning frequency to be constant, it can be assumed that $F_M(\Delta\theta - \beta_0 e^{j\Omega t})$ is almost a periodic function of time and it is represented in the form of a Fourier series

$$F_M(\Delta\theta - \beta_0 e^{-j\Omega t}) = \frac{1}{2} \sum_{k=-\infty}^{\infty} C_k e^{jk\Omega t}, \qquad (3.4.6)$$

where $C_k = \frac{2}{T} \int_0^T F_M(\Delta\theta - \beta_0 e^{-j\Omega t}) e^{-jk\Omega t} dt$ is the complex amplitude of the harmonic and $T = \frac{2\pi}{\Omega}$ is the period of the function $F_M(\Delta\theta - \beta_0 e^{-j\Omega t})$.

Each term of the series (3.4.6) contains information on the position of the target, but in actual practice only the information contained in the constant component and in the first harmonic of the expansion is used. The constant component is used in the automatic selector channel and in the AVC, while the first harmonic is used in the mismatch signal channel. Therefore, in order to obtain the transfer function of the modulator in the expansion (3.4.6) it is sufficient to retain the first two terms.

The derived expression can be simplified if the components C_0 and C_1, which are functions of the angular deflection $\Delta\theta$, are expanded into a power series of $\Delta\theta$. In the case of small mismatches it is sufficient to leave only the first terms of the expansion in the derived series. This gives a linear solution of the problem.

Now we will consider an example of computation of the modulating function, approximating the static directional diagram of the antenna by some function. In addition to being an illustration of the method of computing $F_M(\Delta\theta - \beta_0 e^{-j\Omega t})$, the example will make it possible to establish some of the

general properties of the modulator, characteristic both for other forms of approximation and for real diagrams.

If the antenna has axial symmetry, its spatial diagram can be approximated by a surface of revolution, the generatrix of which is a function describing the directional diagram in one plane. The equation for such a spatial diagram is obtained by replacement of the argument included in the expression for a "plane" diagram by the absolute value of the complex angle.

We will assume that the normalized directional diagram of the antenna /95 in a single plane is approximated by an exponential function. Then for passive (unidirectional) direction finding we will have

$$F(\beta) = \exp\left[-1{,}4\left(\frac{\beta}{\theta_0}\right)^2\right]. \tag{3.4.7}$$

where θ_0 is the width of the directional diagram for half-power.

The equation for a spatial diagram of a scanning antenna assumes the form

$$F\left(|\beta' - \beta_0 e^{j\Omega t}|\right) = \exp\left\{-\frac{1{,}4}{\theta_0^2}\left[(\beta')^2 + \beta_0^2 - 2\beta'\beta_0\cos(\Omega t + \psi)\right]\right\}. \tag{3.4.8}$$

In order to obtain the modulating function entering into expression (3.4.1) it is necessary to replace the current values of the coordinates β' and ψ in equation (3.4.8) by the target coordinates $\Delta\theta$ and φ. Then

$$F_M(\Delta\theta, \varphi, t) = \exp\left\{-\frac{1{,}4}{\theta_0^2}\left[\Delta\theta^2 + \beta_0^2 - 2\Delta\theta\beta_0\cos(\Omega t + \varphi)\right]\right\}. \tag{3.4.9}$$

The envelope of the signal at the receiver output is

$$U_{rec} = k_{rec} k_p E_0 G_0 \exp\left\{-\frac{1{,}4}{\theta_0^2}\left[\Delta\theta^2 + \beta_0^2 - 2\Delta\theta\beta_0\cos(\Omega t + \varphi)\right]\right\}. \tag{3.4.10}$$

Here k_{rec} is the transfer coefficient from the antenna output to the receiver output.

It follows from formula (3.4.10) that the signal at the output of the receiver is related by a nonlinear dependence to the angular mismatch of the target.

By expanding $F_M(\Delta\theta, \varphi, t)$ into a Fourier series we obtain an expression for the constant component and amplitude of the first harmonic of this function; these are proportional to the corresponding components of the mismatch signal

$$\frac{c_0}{2} = \exp\left(-1{,}4\frac{\beta_0^2 + \Delta\theta^2}{\theta_0^2}\right) I_0\left(\frac{2{,}8\beta_0}{\theta_0^2}\Delta\theta\right),$$

$$c_1 = 2\exp\left(-1{,}4\frac{\beta_0^2 + \Delta\theta^2}{\theta_0^2}\right) I_1\left(\frac{2.8\beta_0}{\theta_0^2}\Delta\theta\right). \qquad (3.4.11)$$

Here $I_0(x)$ and $I_1(x)$ are modified Bessel functions of the zero and first kind, respectively.

Figure 3.9 shows the dependence $\frac{c_0}{2} = f\left(\frac{\Delta\theta}{\theta_0}\right)$ for different values of the relative angle of displacement of the maximum of the directional diagram β_0/θ_0. In the case of small mismatch angles, the value $\frac{c}{2}$ changes insignificantly. With an increase of the mismatch angle to a value 25-30 percent of the width of the directional diagram the constant component does not change by more than 10 percent. In this range of angles, it can be assumed constant and equal to its value for a zero mismatch. With an increase of the ratio β_0/θ_0 the mean signal level decreases, which leads in the long run to a decrease of the effective range of the direction finder. It should be noted that if the receiver contains AVC operating on the basis of the mean signal level the dependence of this mean level at the output of the receiver on the mismatch angle will differ from the curves shown in figure 3.9. The difference is that there is a

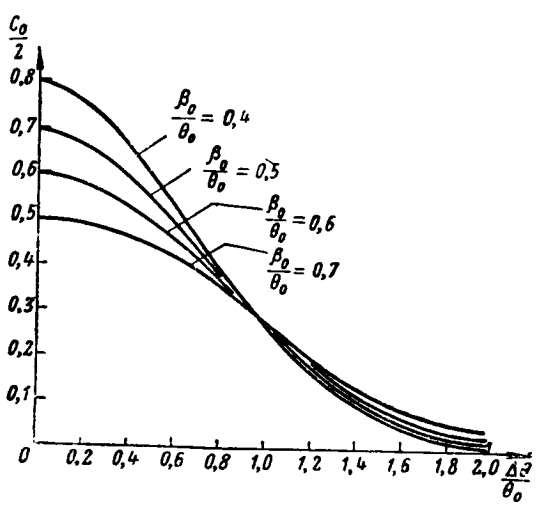

Figure 3.9

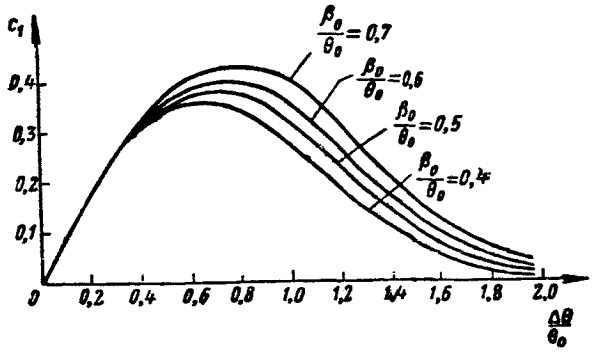

Figure 3.10

broadening of the zone of the characteristics where the mean level changes little with a change of the mismatch angle.

Figure 3.10 shows the dependence $c_1 = f\left(\frac{\Delta\theta}{\theta_0}\right)$, determining the character /96 of the change of the amplitude of the first harmonic of the mismatch signal, for different values of the ratio β_0/θ_0. In the case of mismatch angles which are 25-30 percent of the width of the directional diagram the function $c_1 = f\left(\frac{\Delta\theta}{\theta_0}\right)$ is close to linear. Then comes a zone of saturation which ends with a segment with negative steepness where the amplitude of the first harmonic decreases with an increase of the mismatch angle.

Analysis of the curves shown in figures 3.9 and 3.10 reveals that the modulator can be considered as a linear apparatus if the mismatch angle does not exceed 25-30 percent of the width of the directional diagram. Such a situation is correct both for different kinds of approximating functions and for real directional diagrams.

After expanding $\frac{c_0}{2}$ and c_1 into a power series and retaining the first /97 terms of the expansion we obtain

$$\frac{c_0}{2} \approx \exp\left(-1{,}4\frac{\beta_0^2}{\theta_0^2}\right),$$

$$c_1 \approx \exp\left(-1{,}4\frac{\beta_0^2}{\theta_0^2}\right)\frac{2{,}83_0}{\theta_0^2}\Delta\theta.$$

In the analysis of the modulation process in a linear approximation the envelope of the video pulses at the output of the receiver has the form

$$u_{rec} = U_p[1 + m\cos(\Omega t + \varphi)]. \qquad (3.4.12)$$

where $U_p = k_{rec} k_p E_0 G(\beta_0)$ is the mean amplitude of the pulses at the output of the receiver; $G(\beta_0)$ is the amplification factor of the antenna in the equisignal direction; $m = k_m \Delta\theta$ is the depth of modulation of the pulses at the output of the receiver.

The coefficient k_m characterizes the change of the depth of modulation with displacement of the target by a unit of angle measurement and is called the modulation transfer coefficient or the steepness of the modulation characteristic. It is measured either in percent per degree or in percent of a thousandth of the distance (a thousandth of a radian). As will be clear from the text which follows, the coefficient k_m plays an important role in the selection of some parameters of the direction finder, and therefore we will discuss its determination in somewhat greater detail. If the directional diagram of the antenna is described by the function $F(\beta)$, for the case of passive direction finding the coefficient k_m can be computed using the formula

$$k_m = \frac{\left|\frac{\partial F(\beta)}{\partial \beta}\right|_{\beta=\beta_0}}{F(\beta_0)}. \qquad (3.4.13)$$

The value k_m is doubled for active direction finding. In computations it is convenient to use the formulas

$$\left.\begin{aligned} k_m &\approx 4.25 \frac{\beta_0}{\theta_0} \frac{D_a}{\lambda} \frac{\%}{\text{degree}}, \\ k_m &\approx 0.24 \frac{\beta_0}{\theta_0} \frac{D_a}{\lambda} \frac{\%}{\text{distance} \times 10^3}, \end{aligned}\right\} \qquad (3.4.14)$$

where D_a is the diameter of the antenna; λ is wavelength.

Formulas (3.3.14) were derived for approximation of the directional diagram by the exponential function (3.4.7) and with the relation $\theta_0 \approx 66 \frac{\lambda}{D_a}$ taken into account. They give good agreement with the value k_m determined experimentally. The value β_0/θ_0 is selected in such a way as to obtain the /98 maximum angular sensitivity of the direction-finding apparatus with the instrument noise of the receiver taken into account and falls in the range 0.5-0.6.

Formulas (3.4.14) make it possible to select some parameters of the direction finder if the value k_m is known or to estimate the value k_m if the parameters of the direction finder are known. In particular, they indicate that by shortening the wavelength it is possible to decrease the size of the antenna while maintaining the former value k_m. The latter circumstance plays an important role for the coordinators of homing rockets whose size is small. However, a transition to shorter waves can lead to a decrease of the effective range of the direction finder as a result of an increase of absorption of electromagnetic energy.

By knowing the coefficient k_m it is easy to determine the static angular error $\Delta\theta_{err}$ of the direction finder by stipulating the minimum distinguishable modulation depth $m\%_{dist}$

$$\Delta\theta_{err} = \frac{m\%_{dist}}{k_m}. \qquad (3.4.15)$$

It has been established that in a real apparatus the presence of parasitic modulation, instrument (receiver)noise and instability of the circuits of the output stages of the direction finder make it impossible to detect the mismatch signal $m\% < 1$ percent.

Using formula (3.4.15) it is impossible to determine the accuracy of the coordinator under real operating conditions because a static regime (case of a fixed target and a fixed direction finder) is not encountered in actual practice. A knowledge of the coefficient k_m alone is inadequate for determination of the dynamic errors of the coordinator, even in the case of a known law of motion of the target. In addition, in the case of a real (not a point) target there will be errors in determination of the bearing due to fluctuations of the amplitude of the reflected signal and fluctuations of the apparent center of reflection, which considerably exceed the value of the static error. However, an effort always should be made to obtain the highest possible value of the coefficient k_m, since with its increase there is a decrease of the zone of insensitivity of the direction finder, which exerts a favorable influence on the character of transient processes in the coordinaotr, and as will be shown below, decreases the error caused by fluctuations of the signal reflected from the target.

Usually there is a linear mismatch signal detector at the output of the modulator. If the transfer coefficient of the detector is denoted k_D, the voltage of the mismatch signal at its output can be written as

$$u_м = k_D m U_p \cos(\Omega t + \varphi) = k_D k_m U_p \Delta\theta \cos(\Omega t + \varphi). \qquad (3.4.16)$$

Equation (3.4.16) will be written in a somewhat different form /99

$$u_м = k_м \Delta\theta \cos\varphi \cos \Omega t - k_м \Delta\theta \sin\varphi \sin \Omega t, \qquad (3.4.17)$$

where $k_M = k_D k_m U_p$ is the transfer coefficient of the modulator.

Using the obvious relations $\Delta\theta_z = \Delta\theta \cos \varphi$ and $\Delta\theta_y = \Delta\theta \sin \varphi$, we obtain

$$u_м = k_м \Delta\theta_z \cos \Omega t - k_м \Delta\theta_y \sin \Omega t. \qquad (3.4.18)$$

Figure 3.11 is the block diagram of a modulator constructed using formula (3.4.18). The operation of modulation of the input signals is reflected by links with variable transfer coefficients proportional to cos Ωt and sin Ωt, respectively.

The block diagram of the modulator can be shown differently by introducing the concept of complex amplitude of the mismatch signal. If the complex angular mismatch of the target $\Delta\theta = \Delta\theta_z + j\Delta\theta_y = \Delta\theta e^{j\varphi}$ is used as the input action of the modulator, the output signal of the modulator will be a complex temporal function

$$\dot{u}_м = \dot{U}_м e^{j\Omega t}. \qquad (3.4.19)$$

Here $\dot{U}_M$ is the complex amplitude of the mismatch signal, equal to

$$\dot{U}_м = U_м e^{j\varphi} = k_м \Delta\theta e^{j\varphi}. \qquad (3.4.20)$$

Figure 3.12a, b shows block diagrams of a modulator for the complex temporal function and for the complex amplitude of the mismatch signal.

The relative simplicity of the resulting block diagrams can be attributed to the fact that they were constructed for a linear approximation, when the value of the angular mismatch does not exceed 25-30 percent of the width of the

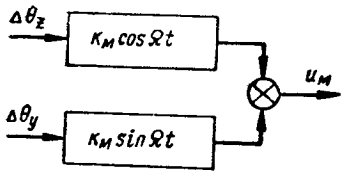

Figure 3.11

a b

Figure 3.12

directional diagram for half-power. This condition usually is satisfied in the absence of interference. However, when there is interference the peak values $\Delta\theta$ can exceed the indicated value and the represented mathematical model will not correspond to the real apparatus. It therefore is necessary to check the correctness of the assumptions made concerning the linearity of the modulator. It is assumed (ref. 48) that if the mean square value of the input signal /100 does not exceed one-third of the saturation value of a similar signal in the real system, the probability of saturation for such a signal falls in admissible limits. Otherwise, it is necessary to construct the block diagram of the modulator on the basis of more general relations (3.4.10) and (3.4.11), which naturally sharply increases the difficulties of analysis of the direction finder.

Another characteristic of the modulator is the dependence of its transfer coefficient k_M on the level of the received signal; this is expressed in the fact that the intensity E_0 of the received signal enters this coefficient as a factor. In actuality, it follows from (3.4.16) and (3.4.12) that

$$k_M = k_p E_0 G(\beta_0) k_{rec} k_D k_m. \qquad (3.4.21)$$

Such a dependence is characteristic of automatic control systems which contain electronic apparatus in their links.

Since it is desirable to have constant transfer coefficients for the adjustable parameter (in this example--angular mismatch) in automatic control systems, the mentioned dependence of k_M on E_0 should be eliminated. This is accomplished introducing automatic volume control into the receiving channel. In such apparatus automatic volume control usually is introduced both into the intermediate frequency amplification channel ("backward" AVC) and in the mismatch signal amplification channel ("forward" AVC). The necessity of a double AVC system dictates extremely rigorous requirements on the constancy of the modulator transfer coefficient and the entire direction finder.

The introduction of automatic volume control into the receiving channel makes the modulator stationary in relation to the adjustable parameter and nonstationary in relation to the electric signal, the carrier of this parameter. The latter should be taken into account during analysis of the passage of the signal through the receiver, especially when this signal contains noise.

The next element of the block diagram of the direction-finding apparatus is an ac amplifier. The amplification link of the single-channel part of the circuit in ac systems is described either by the transfer function for the instantaneous values of the signal or when using the method of complex amplitude, a transfer function for the envelope.

The process of finding the transfer function for the envelope is quite complex but it is simplified appreciably if the circuit has a two-channel very low-frequency component with identical channels in which the sinusoidal and the cosinusoidal components of the mismatch signal are used to an equal degree. In such systems the transfer function for the envelope is obtained by simple replacement of the instantaneous values of the operator D by $D + j\Omega$ in the transfer function (ref. 47).

If the instantaneous value of the voltage at the output of the amplifier can be written as /101

$$u_a = W_a(D)u_i, \tag{3.4.22}$$

where $W_a(D)$ is the transfer function of the amplifier, the complex amplitudes of the mismatch signal at the amplifier input and output are related by the equation

$$\dot{U}_a = W_a(D + j\Omega)\dot{U}_M.$$

The form of the transfer function $W_a(D)$ is determined for the most part by the type of filter used. However, frequently the inertia of the amplifier is such that it can be neglected in comparison with the inertia of the other elements of the coordinator. Hereafter it will be assumed that the amplifier is inertialess. At the same time it is assumed that it can introduce into the mismatch signal some constant phase shift which appears as a result of incorrect phasing of the system.

Therefore, in the block diagram the mismatch signal amplifier can be described by the complex transfer coefficient, whose amplitude and phase characteristics are not dependent on frequency.

The equation for complex amplitudes assumes the form

$$\dot{U}_a = k_a\dot{U}_M = k_a e^{j\mu}\dot{U}_M. \tag{3.4.23}$$

Here k_a is the absolute value of the amplifier transfer constant; μ is the phase shift introduced by the amplifier.

The amplifier is followed by a demodulator which consists of two phase detectors. It can be assumed that the phase detectors perform the operation of multiplication of the mismatch signal by the two reference signals which are periodic functions of time and are displaced relative to one another by a quarter period. If the reference signals constitute harmonic functions of time the mismatch signal is multiplied by a voltage proportional to cos $(-\Omega t)$ in the phase detector of the lateral deflection channel and by a voltage proportional to sin $(-\Omega t)$ in the phase detector of the longitudinal deflection channel. The minus sign assigned the arguments of the trigonometric functions formally reflects the fact that the demodulation process is the reverse of the modulation process for the mismatch signal. In addition, it is assumed that the phase detector filter transmits only the slowly changing part of the resultant signal.

If there is no additional phase shift in the mismatch signal amplification channel ($\mu = 0$), by performing the mentioned operations we obtain expressions for the signals at the output of the phase detectors of the course channel

$$u_{PD\ z} = k_{PD} U_a \cos \varphi \qquad (3.4.24)$$

and the pitching channel /102

$$u_{PD\ y} = k_{PD} U_a \sin \varphi. \qquad (3.4.25)$$

Here k_{PD} is the phase detector transfer coefficient.

The value k_{PD} is dependent on the type of phase detector used. In the case of ideal multiplication of signals $k_{PD} = 0.5$.

By multiplying both sides of equation (3.4.25) by $j = \sqrt{-1}$ and adding it to equation (3.4.24) we obtain a single complex equation

$$\dot{u}_{PD} = u_{PDz} + j u_{PDy} = k_{PD} U_a e^{j\psi} = k_{PD} \dot{U}_a. \qquad (3.4.26)$$

Equation (3.4.26) shows that the signal at the output of the demodulator is obtained as a result of multiplication of the complex signal from the amplifier by $e^{-j\Omega t}$ and its changes by k_{PD} times.

In actuality,

$$\dot{u}_{PD} = k_{PD} \dot{u}_a e^{j\Omega t} = k_{PD} \dot{U}_a e^{j\Omega t} e^{-j\Omega t} = k_{PD} \dot{U}_a. \qquad (3.4.27)$$

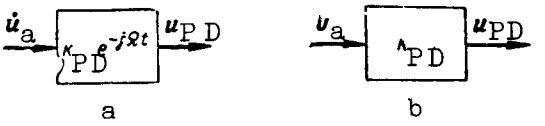

Figure 3.13

The block diagrams of the demodulator for a complex temporal function and for a complex amplitude are shown in figure 3.13a, b.

The construction of a block diagram of a demodulator for instantaneous values of the signals, taking into account the additional phase shift μ, are somewhat more complex. We obtain equations relating the voltages at the output of the phase detectors to the expressions for the instantaneous value of the mismatch signal at its input, which when $\mu \neq 0$ has the form

$$u_a = U_a \cos(\Omega t + \varphi + \mu). \tag{3.4.28}$$

By multiplying the mismatch signal by cos $(-\Omega t)$ and sin $(-\Omega t)$, and also taking into account the transfer coefficient of the phase detector, we will have

$$\left.\begin{aligned} u'_{PDz} &= k_{PD}U_a \cos\varphi\cos\mu - k_{PD}U_a \sin\varphi\sin\mu, \\ u'_{PDy} &= k_{PD}U_a \cos\varphi\sin\mu + k_{PD}U_a \sin\varphi\cos\mu. \end{aligned}\right\} \tag{3.4.29}$$

Since $u_{PD\,z} = k_{PD}U_a \cos\varphi$ and $u_{PD\,y} = k_{PD}U_a \sin\varphi$, we finally write

$$\left.\begin{aligned} u'_{PDz} &= u_{PDz}\cos\mu - u_{PDy}\sin\mu, \\ u'_{PDy} &= u_{PDz}\sin\mu + u_{PDy}\cos\mu. \end{aligned}\right\} \tag{3.4.30}$$

It is easy to see that when $\mu = 0$, $u'_{PD\,z} = u_{PD\,z}$ and $u'_{PD\,y} = u_{PD\,y}$. /103

Figure 3.14 is the block diagram of a demodulator designed on the basis of the derived equations.

Sometimes an allowance is made for the inertial properties of the demodulator which owe their origin to the presence of filters in the phase detectors. This requires only the replacement of the phase detector transfer coefficient k_{PD} in the earlier written equations by the transfer function

$$W_{PD}(D) = \frac{k_{PD}}{T_{PD}D + 1}, \tag{3.4.31}$$

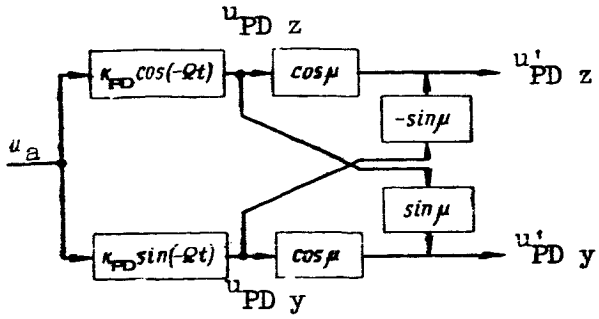

Figure 3.14

where T_{PD} is the time constant of the phase detector filter.

However, in the further analysis the inertial properties of the phase detector will not be taken into account because its inertia is negligibly small in comparison with the inertia of such elements of the coordinator as the control apparatus.

The output stages of the direction finder are dc amplifiers performing the role of elements coupling the phase detectors with the subsequent links of the coordinator.

These are characterized by the transfer coefficients $k_{DCA\ 1}$ and $k_{DCA\ 2}$.

In the case of identical values of the DCA transfer coefficients for both channels ($k_{DAC\ 1} = k_{DCA\ 2} = k_{DCA}$), as the output voltages of the direction finder we will have

$$\left.\begin{aligned} u_{DF\ z} &= k_{DCA}u'_{PD\ z}, \\ u_{DF\ y} &= k_{DCA}u'_{PD\ y}. \end{aligned}\right\} \qquad (3.4.32)$$

Converting to complex values, we obtain

$$u_{DF} = u_{DF\ z} + ju_{DF\ y} = k_{DCA}u'_{PD}.$$

Figure 3.15a is the block diagram of a direction finder for the real coordinates and instantaneous values of the mismatch signal in the amplification channel. Figure 3.15b is the same block diagram, but for the complex coordinates and the complex temporal functions in the mismatch signal amplifier channel. The block diagram (fig. 3.15c) was constructed for the complex amplitudes of the mismatch signal. /104

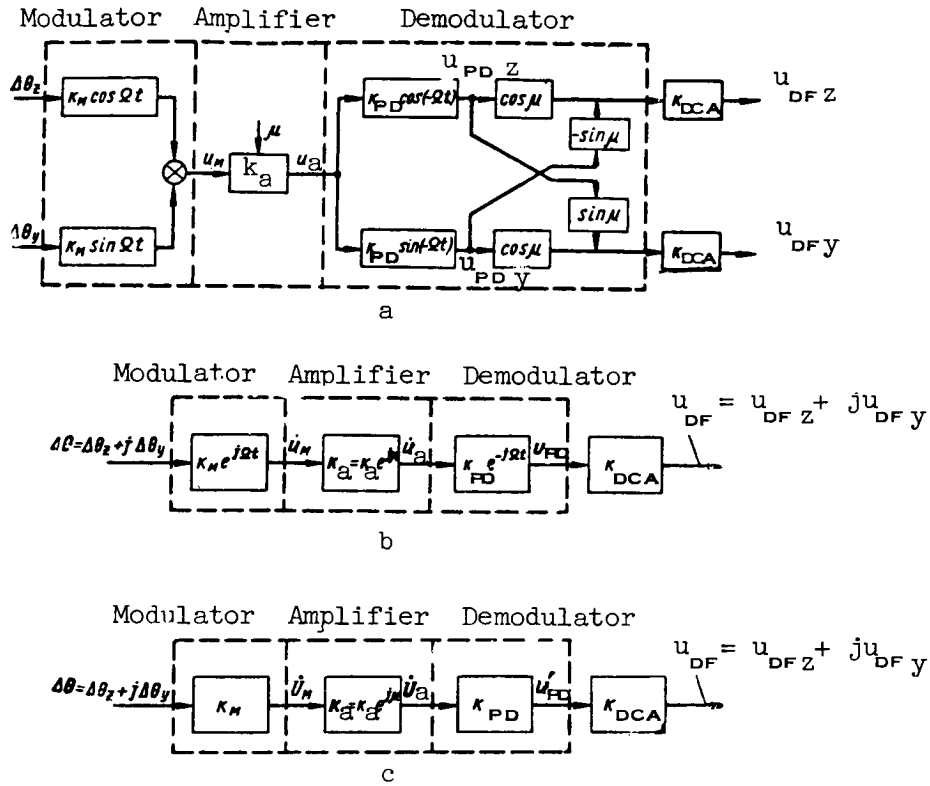

Figure 3.15

The direction finder as a link of the automatic control system is characterized by the complex transfer coefficient k_{DF}, relating the complex mismatch angle $\Delta\theta$ and the complex voltage u_{DF}, in accordance with the formula

$$u_{DF} = k_{DF}\Delta\theta. \qquad (3.4.33)$$

Here

$$k_{DF} = k_{DF}e^{j\mu} = E_0 G(\beta_0) k_p k_{rec} k_D k_m k_a k_{PD} k_{DCA} e^{j\mu}.$$

The block diagram of the direction finder as a link in the control system is shown in figure 3.16a for real coordinates and in figure 3.16b for complex coordinates.

It follows from figure 3.16a that when $\mu = 0$ the direction finder is broken down into two independent channels, one of which is used for measurement of the angle $\Delta\theta_z$ and the other for the angle $\Delta\theta_y$. However, if $\mu \neq 0$, such a breakdown becomes inadmissible due to the appearance of a cross connection between the channels.

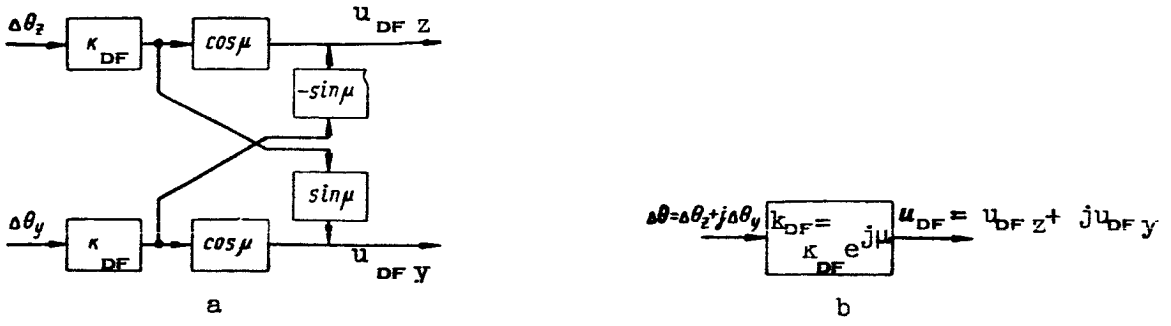

Figure 3.16

The module of the complex transfer coefficient of the direction finder/105 characterizes the value of the mismatch voltage (current) at the output of the direction finder when there is deflection of the target relative to the equisignal direction by a unit of angle. It can be computed or determined from experimental data as the steepness of the linear segment of the direction finding characteristic.

3.5. Functional Diagram of a Direction Finder with an Instantaneous Equisignal Direction

Direction finders with an instantaneous equisignal direction were developed, in particular, due to the need for increasing the accuracy of systems for automatic tracking of a target in direction. This can be attributed to the fact that direction finders with an equisignal direction are insensitive to amplitude fluctuations of a signal reflected from a target. Various variants of direction finders with an instantaneous equisignal direction now have been developed. Some of them form part of so-called monopulse radar stations (refs. 41 and 42).

One of the most typical and, in some respects, most modern is a direction finder in which an add-subtract method for determination of the mismatch angle is used.

Figure 3.17a is a simplified functional diagram of such an apparatus. The direction finder antenna system consists of four elements A_1, A_2, A_3 and A_4, whose relative positions are shown conventionally in figure 3.17b.

Depending on the position of the directional diagram of each element it is possible to have either amplitude or phase direction finding of the target. In the case of amplitude direction finding the phase centers of the individual elements of the antenna are situated quite close to one another and the maxima of their directional diagrams are displaced by a certain angle relative to the axis of the antenna (fig. 3.18a).

a

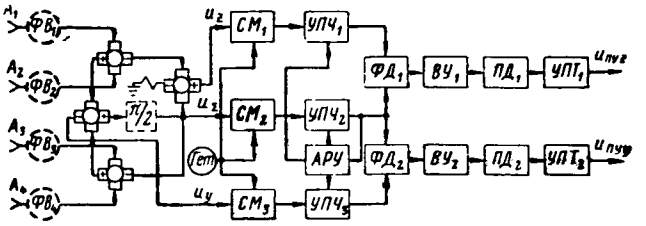

b

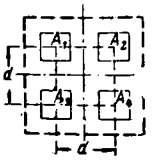

ФВ = PI Гем = Het СМ = Mix УПЧ = IFA АРУ = AVC
ФД = PD ВУ = SD ПД = PkD УПТ = DCA ПУ = DF

Figure 3.17

In the case of phase direction finding the phase centers of the individual elements of the system are spaced at the distance d and the maxima of their directional diagrams are oriented along the axis of the antenna (fig. 3.18b).

The antenna elements A_1, A_2, A_3 and A_4 are connected by a waveguide /106 to devices for summation and subtraction of high-frequency signals. The purpose of the phase inverters (PI_1-PI_4), situated between the antenna and the add-subtract devices, will be clarified below.

Three high-frequency signals are formed at the output of the add-subtract devices: the signal u_z, carrying information on the angle of deflection of the target in the plane $o_m x_m z_m$ (fig. 3.19), the signal u_y carrying information on the target in the plane $o_m x_m y_m$, and the reference signal u_Σ.

The mentioned signals are fed to three identical mixers Mix_1, Mix_2 and Mix_3, which also receive a voltage from the common heterodyne Het. After frequency conversion in the mixers, the signals are amplified in the intermediate frequency amplification channel which consists of three lines (IFA_1, IFA_2, IFA_3) and are fed to the phase detectors PD_1 and PD_2.

The signals at the output of the phase detectors have the form of dc pulses (when the direction finder has pulse operation), whose amplitude is

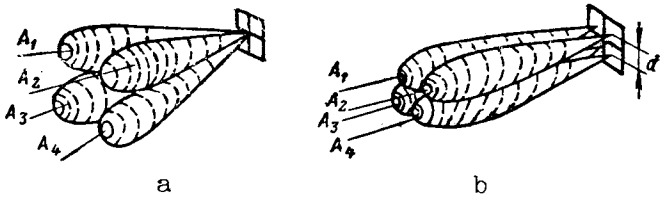

a b

Figure 3.18

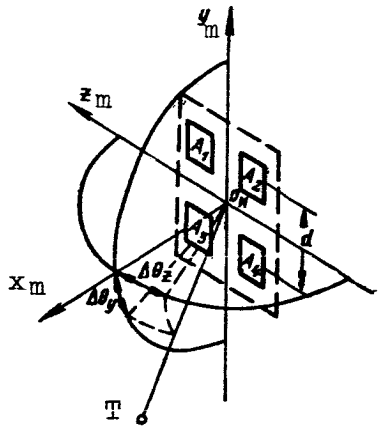

Figure 3.19

dependent on the value of the angular deflection of the target relative to the axis of the antenna, and the polarity is determined by the direction of this deflection. The pulses are amplified by the video amplifiers VA_1 and VA_2 and are widened in the peak detectors PkD_1 and PkD_2.

The constant components of the voltages of the widened pulses, which /107 are amplified by the dc amplifiers DCA_1 and DCA_2, are discriminated at the output of the peak detectors.

The design of the antenna system of a direction finder with an instantaneous equisignal direction is dependent on the form of direction finding used, the method for movement of the equisignal direction, the admissible size, etc. Usually the antenna has a clover-leaf primary radiating element with a common reflector or cloverleaf lens antennas. In the case of mechanical displacement of the equisignal direction it is desirable to avoid the use of rotating waveguide couplings in the design of the antenna system because they can cause errors in determination of the direction to the target.

The equisignal line can be moved electrically in direction-finding apparatus with an instantaneous equisignal direction (ref. 53). The electrical shifting of the equisignal direction is accomplished most easily in direction finders with a phase method of direction finding; in this case it is characterized by an equality of the phase shifts of the high-frequency oscillations in the different receiving channels.

Phase inverters PI_1-PI_4 are introduced into the waveguide transmission channel for the electrical shifting of the equisignal direction (fig. 3.17a); these phase inverters perform an additional shifting of the phase of the carrier of the received signal. Using phase inverters it is possible to equate the phase shifts of the carrier of the received signals caused by displacement of the target relative to the axis of the antenna, and the phase shifts introduced by the phase inverters in each of the receiving channels for a given value of the angle of deflection of the target. Therefore, the change of the value of the phase shifts introduced by the phase inverters is equivalent to

the change of the position of the equisignal line relative to the axis of the antenna.

The value of the phase shift is regulated either mechanically by introduction of a dielectric into the waveguide or electrically by the magnetization of a ferrite inserted in the waveguide. We note in passing that in some complicated circuits the electrical shifting of the equisignal direction is possible also when using the amplitude method of direction finding of a target.

An important element of the antenna-waveguide system in the add-subtract analysis of the received signals is an apparatus for forming the sums and the differences of the high-frequency oscillations. A classical example of the design of such an apparatus is a double waveguide triplet. However, in /108 actual practice it is more convenient to use hybrid ring connections and slotted bridges (refs. 41 and 49).

The elements of the antenna-waveguide channel should be designed in such a way that, in the working range of frequencies, the change of amplification of these elements and the phase changes introduced by them are in admissible limits.

A receiver of a direction finder with an instantaneous equisignal direction and add-subtract analysis of the signal contains three identical channels for the conversion of frequency and amplification.

It is supplied with a quite high-speed automatic volume control system which excludes the influence of a change in the intensity of the received signal on the steepness of the direction-finding characteristic, or, which is the same, on the value of the transfer constant of the direction finder.

The add signal is used for formation of the voltage of the automatic volume control system. In such a circuit for producing the voltage of the automatic volume control system there is a normalization of the amplitudes of the add and subtract signals relative to the amplitude of the add signal. In this case the amplitude of the output voltage of the add channel in an ideal case is constant in time, but the amplitude of the output voltage of each subtract channel becomes proportional to the ratio of the amplitudes of the subtract and add signals.

The remaining automatic regulations of the receiver--automatic frequency tuning and an automatic selection system--can be designed using the same circuits as in the receiver of a direction finder with conical scanning. These controls are not shown in figure 3.17.

The output apparatus of the direction finder includes phase detectors, video amplifiers, peak detectors and dc amplifiers.

The phase detectors receive signals directly from the intermediate frequency amplifiers. Therefore it is necessary to use those circuits of phase detectors which have relatively small input capacitances and a high input resistance.

The use of video pulses is dictated by the fact that the introduction of amplification at the video frequency makes it possible to avoid the use of multistage dc amplification circuits having a low stability of the zero. The circuits of the video amplifiers should be designed in such a way that both positive and negative pulses are amplified to an equal degree.

The output stages of the direction finder--the dc amplifiers--are used for coupling the direction finder to the succeeding elements of the coordinator. The principal requirements imposed on the dc amplifier circuit essentially involve the requirement for symmetry and linearity of its amplitude characteristic. In addition, the dc amplifier should have a small zero drift. /109

The most important regulations which must be accomplished in direction finders with an instantaneous equisignal direction are similar to the regulations of a direction finder with conical scanning. For example, the balance apparatus excludes the possibility of electrical asymmetry of the output stages of the direction finder. The mismatch signal at the output of the direction finder should be equal to zero if the target is situated precisely on the equisignal line.

A direction finder with an instantaneous equisignal direction is phased both for a high frequency (in the circuits of the antenna-waveguide channel to the add-subtract circuits), and for an intermediate frequency. As will be shown below, the absence of high-frequency phasing leads to a displacement of the zero of the direction-finding characteristic and in some cases to the appearance of a cross connection between channels, and a dephasing of the intermediate frequency causes changes of the steepness of the direction-finding characteristic.

A nominal amplification device is necessary to obtain a given value of the transfer constant of the direction finder. It usually constitutes part of the range finder output.

3.6. Block Diagrams of Direction Finders with an Instantaneous Equisignal Direction

In constructing the block diagram of a direction finder with an instantaneous equisignal direction for phase direction finding of a target we write equations which reflect the successive conversion of signals with their passage through the circuits of the direction finder.

We will assume that the target is deflected relative to the axis of the antenna $o_m x_m$ (fig. 3.19) by the angle $\Delta\theta_y$ in the plane $o_m x_m y_m$, and by the angle $\Delta\theta_z$ in the plane $o_m x_m z_m$. Then for the emf in the circuits of the antenna elements A_1, A_2, A_3 and A_4 we can write

$$\left.\begin{aligned} e_{A1} &= U_0 F(\Delta\theta)\sin\left(\omega t + \frac{\varphi_y}{2} + \frac{\varphi_z}{2}\right), \\ e_{A2} &= U_0 F(\Delta\theta)\sin\left(\omega t + \frac{\varphi_y}{2} - \frac{\varphi_z}{2}\right), \\ e_{A3} &= U_0 F(\Delta\theta)\sin\left(\omega t - \frac{\varphi_y}{2} + \frac{\varphi_z}{2}\right), \\ e_{A4} &= U_0 F(\Delta\theta)\sin\left(\omega t - \frac{\varphi_y}{2} - \frac{\varphi_z}{2}\right), \end{aligned}\right\} \qquad (3.6.1)$$

where $U_0 = E_0 G_0 k_p$ is the amplitude of the signal in the antenna in the direction of the maximum of the diagram; φ_y and φ_z are the phase shifts of the /110 carrier caused by movement of the target relative to the axis of the antenna of the system.

The values φ_y and φ_z are related to the angles of deflection of the target by the following expressions

$$\left.\begin{aligned} \varphi_y &= \frac{2\pi d}{\lambda}\sin\Delta\theta_y, \\ \varphi_z &= \frac{2\pi d}{\lambda}\sin\Delta\theta_z. \end{aligned}\right\} \qquad (3.6.2)$$

Here d is the distance between the phase centers of the antenna elements and λ is the wavelength.

In the derivation of formulas (3.6.1) it was assumed that the directional diagrams of the individual elements of the antenna are identical and have axial symmetry relative to the direction of their maximum. The latter circumstance makes it possible to write an expression for the spatial directional diagram as $F(\Delta\theta)$, where $\Delta\theta = \sqrt{\Delta\theta_z^2 + \Delta\theta_y^2}$. If the direction finder operates in a pulse regime, a time factor should be introduced into (3.6.1) or it should be assumed that formulas (3.6.1) are correct only for the time of the effect of the pulse.

We will assume that the waveguide system and the add-subtract devices do not introduce attenuation and additional phase shifts. In addition, we take into account that, in phase direction finding, the signal phase is turned by $\frac{\pi}{2}$ in the reference channel before the mixer. The device performing this phase shift is shown in figure 3.17 by a dashed line. Then for the voltages u_z, u_y and u_Σ at the input of the mixers Mix_1, Mix_2 and Mix_3, we obtain

$$\left.\begin{aligned} u_z &= \frac{1}{2}[(e_{A1}+e_{A3})-(e_{A2}+e_{A4})] = \\ &= 2U_0F(\Delta\theta)\sin\frac{\varphi_z}{2}\cos\frac{\varphi_y}{2}\cos\omega t, \\ u_y &= \frac{1}{2}[(e_{A1}+e_{A2})-(e_{A3}+e_{A4})] = \\ &= 2U_0F(\Delta\theta)\sin\frac{\varphi_y}{2}\cos\frac{\varphi_z}{2}\cos\omega t, \\ u_\Sigma &= \frac{1}{2}[(e_{A1}+e_{A2})+(e_{A3}+e_{A4})]_{\frac{\pi}{2}} = \\ &= 2U_0F(\Delta\theta)\cos\frac{\varphi_z}{2}\cos\frac{\varphi_y}{2}\cos\omega t. \end{aligned}\right\} \quad (3.6.3)$$

The factors 1/2 in front of the brackets of expressions (3.6.3) were introduced taking into account the balance of powers in the add-subtract devices. The subscript $\pi/2$ outside the bracket in the last formula means that after the operations indicated in the brackets are performed the phase of /111 the high-frequency signal should be turned by $\pi/2$.

It is useful to note that according to (3.6.3), in the add-subtract analysis of the signal, all four antenna elements are used in forming the mismatch signals in both measurement planes.

The signals at the output of the intermediate frequency amplifiers, on the assumption that the transfer constants of each channel are equivalent and that there are no additional phase shifts, have the form

$$\left.\begin{aligned} u_{in\,z} &= 2U_0F(\Delta\theta)k_1\sin\frac{\varphi_z}{2}\cos\frac{\varphi_y}{2}\cos\omega_{in}t, \\ u_{in\,y} &= 2U_0F(\Delta\theta)k_1\sin\frac{\varphi_y}{2}\cos\frac{\varphi_z}{2}\cos\omega_{in}t, \\ u_{in\,\Sigma} &= 2U_0F(\Delta\theta)k_1\cos\frac{\varphi_z}{2}\cos\frac{\varphi_y}{2}\cos\omega_{in}t, \end{aligned}\right\} \quad (3.6.4)$$

where ω_{in} is the intermediate frequency; $k_1 = k_{Mix}k_{IFA}$ is the transfer constant of the receiving channel, equal to the product of the transfer constant of the mixer (k_{Mix}) and the intermediate frequency channel amplification factor (k_{IFA}).

The voltages $u_{in\,z}$ and $u_{in\,y}$ are multiplied in the phase detectors PD_1 and PD_2 by the reference signal $u_{in\,\Sigma}$ and the phase detector filters pass only the slowly changing components of the resulting products.

The operations performed by the phase detectors can be written conventionally as follows

$$\left.\begin{aligned} u_{PD\ z} &= k_{PD}\overline{u_{in\ z}u_{in\ \Sigma}}, \\ u_{PD\ y} &= k_{PD}\overline{u_{in\ y}u_{in\ \Sigma}}, \end{aligned}\right\} \qquad (3.6.5)$$

where the line over the product denotes an averaging operation.

An ideal multiplier performs the multiplication of two harmonic oscillations with the coefficient 0.5. Since the phase detector is not such an ideal device, in the following formulas this circumstance will be taken into account by the phase detector transfer constant k_{PD}.

The voltages at the output of the direction finder are related to the voltages $u_{PD\ z}$ and $u_{PD\ y}$ by the expressions

$$\left.\begin{aligned} u_{DF\ z} &= k_2 u_{PD\ z}, \\ u_{DF\ y} &= k_2 u_{PD\ y}, \end{aligned}\right\} \qquad (3.6.6)$$

where $k_2 = k_{VA}k_{PkD}k_{DCA}$ is the transfer coefficient of the output device of the direction finder, and k_{VA}, k_{PkD}, k_{DCA} are the transfer coefficients of the video amplifier, peak detector and dc amplifier.

In the derivation of formulas (3.6.6) it was assumed that both channels have output devices of equal amplification. /112

Combining formulas (3.6.6), (3.6.5) and (3.6.4), we obtain

$$\left.\begin{aligned} u_{DFz} &= \frac{1}{2}U_0^2F^2(\Delta\theta)k_1^2k_{PD}k_2(1+\cos\varphi_y)\sin\varphi_z, \\ u_{DFy} &= \frac{1}{2}U_0^2F^2(\Delta\theta)k_1^2k_{PD}k_2(1+\cos\varphi_z)\sin\varphi_y. \end{aligned}\right\} \qquad (3.6.7)$$

After substituting the values φ_z and φ_y from (3.6.2) into (3.6.7) we finally will have

$$\left.\begin{aligned} u_{DFz} &= \frac{1}{2}U_0^2F^2(\Delta\theta)k_1^2k_{PD}k_2(1+\cos\varphi_y)\sin\left(\frac{2\pi d}{\lambda}\sin\Delta\theta_z\right), \\ u_{DFy} &= \frac{1}{2}U_0^2F^2(\Delta\theta)k_1^2k_{PD}k_2(1+\cos\varphi_z)\sin\left(\frac{2\pi d}{\lambda}\sin\Delta\theta_y\right). \end{aligned}\right\} \qquad (3.6.8)$$

It follows from (3.6.8) that the voltage at the direction finder output is related to the angle of deflection of the target by a nonlinear dependence. The equisignal direction, that is, the direction where $u_{DF\ z} = u_{DF\ y} = 0$, coincides with the direction of the axis of the antenna ($\Delta\theta_z = \Delta\theta_y = 0$).

The transfer constants of the direction finder for the lateral and longitudinal deflections, determined as the steepness of the direction-finding characteristics of the corresponding channel in an equisignal direction

$$k_{DF^z} = \left[\frac{\partial u_{DF^z}}{\partial \Delta\theta_z}\right]_{\Delta\theta_z = 0} \text{ and } k_{DF^y} = \left[\frac{\partial u_{DF^y}}{\partial \Delta\theta_y}\right]_{\Delta\theta_y = 0},$$

are equal to

$$\left.\begin{aligned} k_{DF\,z} &= U_0^2 F^2(\Delta\theta)\, k_1^2 k_{PD} k_2 (1 + \cos\varphi_y)\frac{\pi d}{\lambda}, \\ k_{DF\,y} &= U_0^2 F^2(\Delta\theta)\, k_1^2 k_{PD} k_2 (1 + \cos\varphi_z)\frac{\pi d}{\lambda}. \end{aligned}\right\} \qquad (3.6.9)$$

Formulas (3.6.9) show that the steepness of the direction-finding characteristic of each channel is dependent on the transfer constant of the individual links of the direction finder, the input signal level and the angle of deflection of the target in the plane normal to the deflection plane for the considered channel.

The instability of the steepness of the direction-finding characteristic with a change of the level of the received signal is eliminated to a considerable degree by automatic volume control.

The dependence of the steepness of the direction-finding characteristic on the angle of deflection of the target in the plane normal to the plane of deflection of the target for a particular channel indicates the presence of a singular cross connection between channels. This connection is such that the sensitivity of the direction finder for any one coordinate decreases with an increase of target deflection for the other coordinate.

Such a connection is characteristic of any type of direction-finding /113
apparatus in the case of large deflections of the target from an equisignal direction when the direction-finding characteristic becomes essentially nonlinear. It was not taken into account in the construction of the block diagram of the direction finder with conical scanning, since only the linear variant corresponding to small values of angular deflections of the target from an equisignal direction was considered.

Figure 3.20 shows the block diagram of a direction finder constructed using equations (3.6.8). The cross connection has been shown conventionally

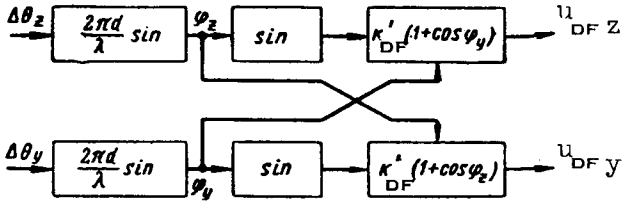

Figure 3.20

in order not to complicate the drawing. In addition, the following coefficient was introduced for shortening the expression

$$k'_{DF} = \frac{1}{2} U_0^2 F^2(\Delta\theta) k_1^2 k_{PD} k_2.$$

In the case of small deflections of the target, when the replacement $\cos \varphi_{z,y} \approx 1$, $\sin \varphi_{z,y} \approx \varphi_{z,y}$ is admissible, the block diagram breaks down into two independent channels with identical transfer constants

$$k_{DF} = U_0^2 F^2(\Delta\theta) k_1^2 k_{PD} k_2 \frac{2\pi d}{\lambda}. \qquad (3.6.10)$$

After introducing the complex coordinates $\Delta\theta = \Delta\theta_z + j\Delta\theta_y$ and $u_{DF} = u_{DF\ z} + ju_{DF\ y}$, we obtain

$$u_{DF} = k_{DF} \Delta\theta, \qquad (3.6.11)$$

where k_{DF} is determined using formula (3.6.10).

Thus, in the case of small mismatch angles the direction finder of the considered type can be represented in the form of a single link with a real transfer constant.

We now will discuss the selection of some parameters of the antenna system, characterizing it as a link of the automatic control system. From this point of view the antenna performs the function of conversion of the angular deflection of the target, from the equisignal direction into a change of phase of a high-frequency oscillation, in accordance with the equation

$$\varphi = \frac{2\pi d}{\lambda} \sin \Delta\theta.$$

The efficiency of this conversion is characterized by the coefficient /114

$$k_\varphi = \frac{2\pi d}{\lambda}. \qquad (3.6.12)$$

The larger the value k_φ, the greater is the sensitivity of the direction finder. However, an extreme increase of the coefficient k_φ can lead to ambiguity in reading of the angles and therefore to the appearance of false equisignal directions. The appearance of spurious equisignal directions can be avoided if it is required that, with a change of the angular position of the target within the limits of the width of the directional diagram, the phase shift of the high-frequency oscillation falls in the limits $\pm\pi$.

Mathematically this condition is written in the form

$$\frac{\theta_0}{2} \leqslant \arcsin \frac{\lambda}{2d}, \qquad (3.6.13)$$

where θ_0 is the width of the directional diagram of one of the antenna elements.

If the width of the antenna directional diagram does not exceed 20°, in place of (3.6.13) we can use the simplified expression

$$\theta_0 \leqslant \frac{\lambda}{d}.$$

Formula (3.6.13) makes it possible for a given width of the directional diagram to select the value of the conversion factor k_φ and vice versa, from the given value k_φ, select the width of the directional diagram.

We now will construct the block diagram of a direction finder with an instantaneous equisignal direction for amplitude direction finding. First, we will write relations describing the conversion of information on the angular position of the target relative to the equisignal direction into an electrical signal. This is done using the method employed for obtaining similar relations presented in section 3.4.

We will assume that all four antenna elements have directional diagrams of identical configuration.

Figure 3.21 shows in a Cartesian coordinate system the position of the maxima of the directional diagram of the antenna elements relative to one another and relative to the equisignal direction. Here the point o' denotes the trace of the equisignal direction on the plane of the drawing and /115 o_1, o_2, o_3, o_4 denote the traces of the maxima of the directional diagram.

We will assume that the angular deflections of the maxima of the directional diagram of the individual antenna elements β_{01}, β_{02}, β_{03} and β_{04} are identical

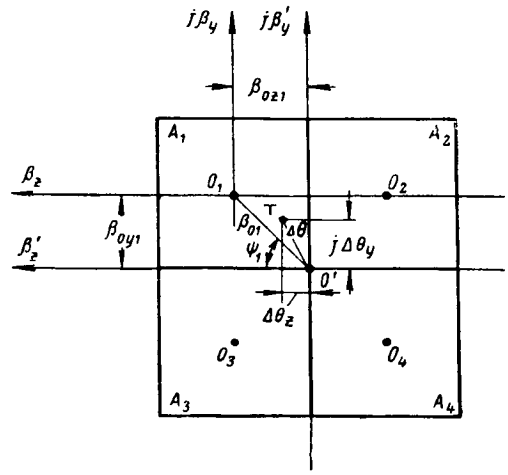

Figure 3.21

and equal to β_0. In addition, we will assume that the values of the angles of displacement of the maxima relative to the axes of the coordinate system related to the equisignal direction also are equal to one another, that is,

$$\beta_{0z1}=\beta_{0y1}=\beta_{0z2}=\beta_{0y2}=\beta_{0z3}=\beta_{0y3}=\beta_{0z4}=\beta_{0yi}=\beta_{0c}.$$

Under these conditions

$$\beta_{0c}=\frac{1}{\sqrt{2}}\beta_0. \tag{3.6.14}$$

Assume $X_i = F(\beta_i)$, where i assumes the values 1, 2, 3, 4, is the equation of the normalized spatial amplitude directional diagram of one of the antenna systems, written in a coordinate system related to the position of the maximum of the directional diagram of this element. Here $\beta_i = \beta_{zi} + j\beta_{yi}$ is the complex unfixed angle. Since the reading of the angular coordinates of the target is accomplished relative to the equisignal direction, the equation of the directional diagram should be written in the coordinate system $o'\beta'_z j\beta'_y$. After replacing $\beta_i = \beta' - \beta_{0i}$, we obtain

$$X_i=F(\beta'-\beta_{0i}). \tag{3.6.15}$$

If each of the diagrams has axial symmetry relative to the direction of the maximum, then

$$X_i = F(|\beta' - \beta_{0i}|). \qquad (3.6.16)$$

Since $\beta_{0i} = \beta_0 e^{j\psi_i}$, with the arrangement of the antenna elements shown in figure 3.21, we will have

$$\psi_1 = \frac{\pi}{4}, \quad \psi_2 = \frac{3}{4}\pi, \quad \psi_3 = \frac{7}{4}\pi, \quad \psi_4 = \frac{5}{4}\pi.$$

Replacing the unfixed value of the angle β' in (3.6.16) by the angle $\Delta\theta$ characterizing the deflection of the target relative to the equisignal direction, we obtain expressions describing the conversion of the angular coordinates of the target into electrical signals.

As the emf in the circuits of the antenna elements A_1, A_2, A_3, A_4, we can write

$$\left.\begin{aligned} e_{A1} &= U_0 F\left(\sqrt{(\Delta\theta_z - \beta_{0C})^2 + (\Delta\theta_y - \beta_{0C})^2}\right)\sin\omega t, \\ e_{A2} &= U_0 F\left(\sqrt{(\Delta\theta_z + \beta_{0C})^2 + (\Delta\theta_y - \beta_{0C})^2}\right)\sin\omega t, \\ e_{A3} &= U_0 F\left(\sqrt{(\Delta\theta_z - \beta_{0C})^2 + (\Delta\theta_y + \beta_{0C})^2}\right)\sin\omega t, \\ e_{A4} &= U_0 F\left(\sqrt{(\Delta\theta_z + \beta_{0C})^2 + (\Delta\theta_y + \beta_{0C})^2}\right)\sin\omega t. \end{aligned}\right\} \qquad (3.6.17)$$

It follows from (3.6.17) that there is a nonlinear dependence between /116 the angular deflections of the target and the amplitudes of the received signals. In the case of small deflections of the target relative to the equisignal direction, expression (3.6.17) can be linearized by expanding the function describing the directional diagram into a power series. Then

$$e_{A1} = U_0\left[F(\beta_0) + \left[\frac{\partial F(\beta_z, \beta_y)}{\partial\beta_z}\right]_{\substack{\beta_z=-\beta_{0C}\\ \beta_y=-\beta_{0C}}}\Delta\theta_z + \left[\frac{\partial F(\beta_z, \beta_y)}{\partial\beta_y}\right]_{\substack{\beta_z=-\beta_{0C}\\ \beta_y=-\beta_{0C}}}\Delta\theta_y\right]\sin\omega t,$$

$$e_{A2} = U_0\left[F(\beta_0) + \left[\frac{\partial F(\beta_z, \beta_y)}{\partial\beta_z}\right]_{\substack{\beta_z=+\beta_{0C}\\ \beta_y=-\beta_{0C}}}\Delta\theta_z + \left[\frac{\partial F(\beta_z, \beta_y)}{\partial\beta_y}\right]_{\substack{\beta_z=+\beta_{0C}\\ \beta_y=-\beta_{0C}}}\Delta\theta_y\right]\sin\omega t,$$

$$e_{A3} = U_0\left[F(\beta_0) + \left[\frac{\partial F(\beta_z, \beta_y)}{\partial\beta_z}\right]_{\substack{\beta_z=-\beta_{0C}\\ \beta_y=+\beta_{0C}}}\Delta\theta_z + \left[\frac{\partial F(\beta_z, \beta_y)}{\partial\beta_y}\right]_{\substack{\beta_z=-\beta_{0C}\\ \beta_y=+\beta_{0C}}}\Delta\theta_y\right]\sin\omega t,$$

$$e_{A4} = U_0 \left[F(\beta_0) + \left[\frac{\partial F(\beta_z, \beta_y)}{\partial \beta_z} \right]_{\substack{\beta_z = +\beta_{0C} \\ \beta_y = +\beta_{0C}}} \Delta\theta_z + \right.$$
$$\left. + \left[\frac{\partial F(\beta_z, \beta_y)}{\partial \beta_y} \right]_{\substack{\beta_z = +\beta_{0C} \\ \beta_y = +\beta_{0C}}} \Delta\theta_y \right] \sin \omega t.$$

Taking into account that the derivative $\frac{\partial F(\beta_z, \beta_y)}{\partial \beta_{z,y}} < 0$, we finally write

$$\left.\begin{aligned} e_{A1} &= U_0 F(\beta_0) [1 + k'_m \Delta\theta_z + k'_m \Delta\theta_y] \sin \omega t, \\ e_{A2} &= U_0 F(\beta_0) [1 - k'_m \Delta\theta_z + k'_m \Delta\theta_y] \sin \omega t, \\ e_{A3} &= U_0 F(\beta_0) [1 + k'_m \Delta\theta_z - k'_m \Delta\theta_y] \sin \omega t, \\ e_{A4} &= U_0 F(\beta_0) [1 - k'_m \Delta\theta_z - k'_m \Delta\theta_y] \sin \omega t. \end{aligned}\right\} \quad (3.6.18)$$

The following notation is used here

$$k'_m = \left| \frac{\left[\frac{\partial F(\beta_z, \beta_y)}{\partial \beta_{z,y}} \right]_{\substack{\beta_z = \pm\beta_{0C} \\ \beta_y = \pm\beta_{0C}}}}{F(\beta_0)} \right|.$$

If the directional diagram is approximated by an exponential function, /117 the following dependence exists between the coefficient k_m, determined by formula (3.4.14) and the coefficient k'_m

$$k'_m = \frac{1}{\sqrt{2}} k_m.$$

The relations (3.6.18) are basic for writing the following equations for signal conversion in a direction finder with amplitude direction finding, similar to the expressions (3.6.1) for a direction finder with phase direction finding.

The subsequent signal conversions are similar to those described earlier with the sole difference that in this particular type of direction finder there is no phase shift by $\pi/2$ in the add signal channel.

Now we will write the final expressions for the voltages at the output of the direction finder

$$\left.\begin{aligned} u_{DFz} &= 2U_0^2 F^2(\beta_0) k_1^2 k_{PD} k_2 k'_m \Delta\theta_z, \\ u_{DFy} &= 2U_0^2 F^2(\beta_0) k_1^2 k_{PD} k_2 k'_m \Delta\theta_y. \end{aligned}\right\} \quad (3.6.19)$$

Converting to complex coordinates, we obtain

$$u_{DF} = k_{DF}\Delta\theta, \qquad (3.6.20)$$

where $k_{DF} = 2U_0^2F^2(\beta_0)k_1^2k_{PD}k_2k_m'$ is the direction finder transfer constant.

Thus, in the last analysis the block diagram of a direction finder with amplitude direction finding consists of a single inertialess link with a real transfer constant.

In particular, the simplificty of the block diagram can be attributed to the fact that only the linear regime of operation of the direction finder, corresponding to small mismatch angles, was considered.

In the case of large angles of deflection of the target from the equisignal direction and in this particular type of direction finder it is necessary to expect the appearance of cross connections between the channels similar to those which occurred in the direction finder with phase direction finding.

The special characteristic of direction finders with an instantaneous equisignal direction is that each such apparatus includes several signal conversion channels which are similar in function. The relations presented above are correct for a case when all the conversion channels of the same type are identical, as occurs in an ideally adjusted direction finder. However, in actual practice, such an electrical symmetry can be disrupted for one reason or another. The nonidentity of the amplitude characteristics of the elements of the direction finder performing identical conversions in different channels leads to a relative change of the amplitudes of the signals passing through /118
these elements. The difference in the phase characteristics of the elements of the same type in the channels causes the appearance of a relative phase shift between the signals passing through them. Therefore, hereafter for brevity the difference of the amplitude characteristics will be called amplitude unbalance, and the difference of the phase characteristics will be called phase unbalance.

Amplitude and phase unbalance exert an unlike influence on the operation of the direction finder, depending on whether they occur before the formation of the add-subtract signals (so to speak, in the antenna system) or afterwards (in the receiver).

In phase direction finding the phase unbalance in the antenna system causes a displacement of the zero of the direction-finding characteristic, which is equivalent to displacement of the equisignal direction relative to the axis of the antenna. The value of the displacement of the equisignal direction in any one plane is expressed by the formula

$$\Delta\theta_{err} = \frac{\arcsin\varphi_1}{k_\varphi} \qquad (3.6.21)$$

or for small values φ_1

$$\Delta\theta_{err} = \frac{\varphi_1}{k_\varphi}.$$

Here φ_1 is the relative phase shift of signals passing through two similar channels of the antenna of the system.

An amplitude unbalance in the antenna system of a phase-type direction finder does not lead to displacement of the equisignal direction.

In a direction finder with amplitude direction finding the phase unbalance causes displacement of the equisignal direction by the value (ref. 108)

$$\Delta\theta_{err} = \frac{1}{k'_m} \cdot \frac{\sqrt{1 + \sin^2 \varphi_1 \tan^2 \varphi_2 - 1}}{\sin \varphi_1 \tan \varphi_2}, \qquad (3.6.22)$$

for small values of phase shifts φ_1 and φ_2, when the inequality $\sin^2 \varphi_1 \tan^2 \varphi_2 \ll 1$ is correct,

$$\Delta\theta_{err} = \frac{\sin \varphi_1 \tan \varphi_2}{2k'_m}, \qquad (3.6.23)$$

where φ_2 is the relative phase shift of the signals passing through two similar channels of the receiver.

It follows from (3.6.23) that the error in the position of the equisignal direction occurs only when there is simultaneously a phase unbalance in the antenna system and in the receiver.

The errors in the position of the equisignal direction in the case of an amplitude unbalance are determined by the relation

$$\Delta\theta_{err} \approx \frac{1}{2k'_m} \frac{q_1 - 1}{q_1 + 1}. \qquad (3.6.24)$$

Here $q_1 = \frac{k'_1}{k_1}$ characterizes the value of the unbalance of the amplitudes occurring in the antenna system. /119

Thus, for elimination of the systematic errors in the position of the equisignal direction in direction finders of the considered types, the antenna system must be regulated carefully.

If such a regulation is made, the amplitude and phase unbalance in the receiver no longer causes displacements of the equisignal direction and is reflected only in the steepness of the direction-finding characteristic, or, which is the same, on the value of the direction finder transfer constant.

It can be shown (ref. 41) that in the case of nonidentity of amplification of the different receiver channels, characterized by the value $q_2 = \frac{k_2'}{k_2}$, and with a relative phase shift φ_2 of the signals passing through two similar channels of the receiver, the transfer constant of the direction finder is determined by the relation

$$k^*_{DF} = k_{DF} q_2 \cos \varphi_2. \qquad (3.6.25)$$

Here k_{DF} is the transfer constant of a direction finder with ideal regulation. In the case of an amplitude-type direction finder it is expressed by formula (3.6.20), and for a phase type by formula (3.6.10). Formula (3.6.25) shows that the presence of phase unbalance in the receiver leads to a decrease of the sensitivity of the direction finder. When $\varphi_2 = \pi/2$ there is a total loss of sensitivity, and when $\frac{\pi}{2} < \varphi_2 < \frac{3}{2}\pi$ the sign of the mismatch signal becomes opposite, which leads to disruption of operation of the coordinator. However, such a case is possible only when the direction finder operates incorrectly.

The fact that the position of the equisignal direction does not change when there is an amplitude and phase unbalance in the receiver (if the antenna system is regulated) is an advantage of a direction finder with add-subtract signal analysis over other simpler direction finders.

In a direction finder with phase direction finding there is a relatively simple relationship between the displacement of the equisignal direction relative to the axis of the antenna and the relative phase shift of the received signals introduced by the antenna of the system. This relationship is expressed by formula (3.6.21). This circumstance is exploited for displacement of the equisignal direction electrically.

The principle of operation of direction finders with electrical displacement of the equisignal direction is as follows. High-frequency phase /120
inverters are introduced into the waveguide system connecting the antenna with the add-subtract devices (fig. 3.17); these phase inverters are used to change the phase shift of the received signals by a definite value, known in advance.

Shifting of the phase of the received signals by the phase inverters reduces the voltages at the output of the direction finder to zero, compensating the phase shift of the signal caused by displacement of the target from the axis of the antenna. By knowing the parameters of the antenna system and the values of the phase shifts introduced by the phase inverters and using formula (3.6.21) it is possible to determine the angle by which the target is deflected from the axis of the antenna. If the phase shifts are introduced automatically on the basis of the mismatch signals appearing at the output of the direction finder with displacement of the target from an equisignal direction, such an apparatus performs the automatic tracking of the target in direction with the antenna in a fixed position.

We will construct the block diagram of a direction finder with electrical displacement of the equisignal direction. The phase of the received signal in each supply waveguide is dependent on the deflection of the target both in the plane $o_m x_m z_m$ and in the plane $o_m x_m y_m$ (fig. 3.19). The phase inverter apparatus therefore should permit independent compensation of these phase shift components. With respect to an electrical phase inverter, this condition means that the ferrite in each of them should have two windings, the current in one of them being regulated in dependence on the value and sign of the mismatch signal $U_{DF\ z}$, while the current in the other is regulated in dependence on the value and sign of the mismatch signal $U_{DF\ y}$. The direction of the ampere turns of the windings is set in such a way that the phase shift introduced by the phase inverter is opposite in sign to the phase shift of the signal caused by displacement of the target relative to the axis of the antenna.

If all the phase inverters are identical and do not introduce additional attenuation, in place of (3.6.1) we will have

$$\left.\begin{aligned} e_{A1} &= U_0 F(\Delta\theta)\sin\left(\omega t + \frac{\varphi_y}{2} - \frac{\varphi_{py}}{2} + \frac{\varphi_z}{2} - \frac{\varphi_{pz}}{2}\right),\\ e_{A2} &= U_0 F(\Delta\theta)\sin\left(\omega t + \frac{\varphi_y}{2} - \frac{\varphi_{py}}{2} - \frac{\varphi_z}{2} + \frac{\varphi_{pz}}{2}\right),\\ e_{A3} &= U_0 F(\Delta\theta)\sin\left(\omega t - \frac{\varphi_y}{2} + \frac{\varphi_{py}}{2} + \frac{\varphi_z}{2} - \frac{\varphi_{pz}}{2}\right),\\ e_{A4} &= U_0 F(\Delta\theta)\sin\left(\omega t - \frac{\varphi_y}{2} + \frac{\varphi_{py}}{2} - \frac{\varphi_z}{2} + \frac{\varphi_{pz}}{2}\right). \end{aligned}\right\} \qquad (3.6.26)$$

where φ_{pz} is the phase shift introduced by the phase inverter for compensation of the phase shift of the signal caused by displacement of the target in the plane $o_m x_m z_m$, and φ_{py} is the phase shift introduced by the phase inverter for

compensation of the phase shift of the signal caused by displacement of the target in the plane $o_m x_m y_m$.

We use the notations /121

$$\Delta\varphi_z = \varphi_z - \varphi_{pz},$$
$$\Delta\varphi_y = \varphi_y - \varphi_{py}.$$

Then equations (3.6.26) assume the form

$$\left.\begin{aligned} e_{A1} &= U_0 F(\Delta\theta)\sin\left(\omega t + \frac{\Delta\varphi_y}{2} + \frac{\Delta\varphi_z}{2}\right),\\ e_{A2} &= U_0 F(\Delta\theta)\sin\left(\omega t + \frac{\Delta\varphi_y}{2} - \frac{\Delta\varphi_z}{2}\right),\\ e_{A3} &= U_0 F(\Delta\theta)\sin\left(\omega t - \frac{\Delta\varphi_y}{2} + \frac{\Delta\varphi_z}{2}\right),\\ e_{A4} &= U_0 F(\Delta\theta)\sin\left(\omega t - \frac{\Delta\varphi_y}{2} - \frac{\Delta\varphi_z}{2}\right), \end{aligned}\right\} \qquad (3.6.27)$$

Equations (3.6.1) are transformed into (3.6.27) if φ_y in each of them is replaced by $\Delta\varphi_y$ and φ_z by $\Delta\varphi_z$. Therefore, in place of (3.6 7) we immediately write

$$\left.\begin{aligned} u_{DFz} &= \frac{1}{2} U_0^2 F^2(\Delta\theta) k_1^2 k_{PD} k_2 (1 + \cos\Delta\varphi_y)\sin\Delta\varphi_z,\\ u_{DFy} &= \frac{1}{2} U_0^2 F^2(\Delta\theta) k_1^2 k_{PD} k_2 (1 + \cos\Delta\varphi_z)\sin\Delta\varphi_y. \end{aligned}\right\} \qquad (3.6.28)$$

Since in the process of automatic tracking of the target, $\Delta\varphi_z$ and $\Delta\varphi_y$ will be small, it can be assumed that $\cos\Delta\varphi_{z,y} \approx 1$, $\sin\Delta\varphi_{z,y} \approx \Delta\varphi_{z,y}$, and in addition, for small angles, $\varphi_{z,y} \approx \frac{2\pi d}{\lambda}\Delta\theta_{z,y}$.

Then

$$\left.\begin{aligned} u_{DFz} &= k'_{DF}(\varphi_z - \varphi_{pz}) = k'_{DF}\left(\frac{2\pi d}{\lambda}\Delta\theta_z - k_{P1} u_{pz}\right),\\ u_{DFy} &= k'_{DF}(\varphi_y - \varphi_{py}) = k'_{DF}\left(\frac{2\pi d}{\lambda}\Delta\theta_y - k_{P1} u_{py}\right), \end{aligned}\right\} \qquad (3.6.29)$$

where the following notation is used

$$k'_{DF}=\frac{1}{2}U_0^2F^2(\Delta\theta)k_1^2k_{PD}k_2,$$

where k_{PI} is the transfer constant of the phase inverter, and u_{pz} and u_{py} are the voltages fed to the windings of the phase inverter.

Converting to complex coordinates, we obtain

$$\mathbf{u}_{DF}=k'_{DF}\left(\frac{2\pi d}{\lambda}\Delta\theta-k_{PI}\mathbf{u}_p\right). \qquad (3.6.30)$$

Formulas (3.6.29) and (3.6.30) can be used for constructing the block diagram of a direction finder with electrical displacement of the equisignal direction. For real coordinates, the block diagram is shown in figure 3.22a, and for complex coordinates, in figure 3.22b. /122

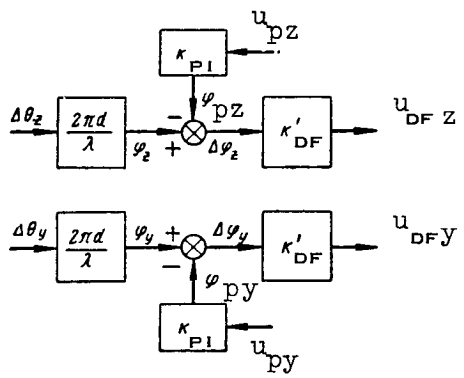

a

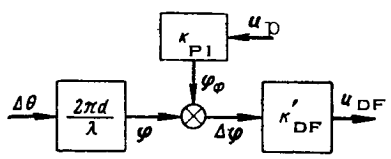

b

Figure 3.22

The block diagrams of the above-mentioned direction finders with an instantaneous equisignal direction, in the case of small deflections of the target from an equisignal direction, reduce essentially to a single inertialess link with a real transfer constant. In the case of large angles of deflection of the target a "crossover" feedback is formed between the channels, leading to a decrease of the transfer constant of the direction finder, but as before its value remains real.

However, it should not be supposed that, in contrast to a direction finder with conical scanning, the dynamic properties of a direction finder with an instantaneous equisignal direction always will be described by a real transfer constant. Departure from the classical model of such a direction finder, described above, can lead to direction finder circuits in which the transfer constant will be a complex value. For example, in a direction finder in which there are two amplification channels instead of three (ref. 41), additional phase shifts in the receiver lead to the appearance of direct antisymmetrical connections between the channels, and as a result its transfer constant becomes complex.

3.7. Target Selection

In an analysis of the operation of direction finders of different types in the preceding sections, it was assumed that a signal from a single target was received by the direction finder antenna. However, in actual practice such a situation can be encountered only in rare cases, which can be attributed, in particular, to the low spatial selection of the antenna systems of the coordinators of homing rockets, caused by the small size of the antennas. For example, when the "angle of view" of the direction finder is 20°, obtained using an antenna in the 3-cm wavelength range and a reflector approximately 20 cm in diameter, the direction finder at a range of 10 km will "view" a circle with a diameter greater than 3 km.

If there are several targets in the "angle of view" of the direction /123 finder, the operation of an automatic tracking system based on angular coordinates becomes unstable.

The selectivity of electronic homing systems is increased when additional selection is introduced, which makes it possible to detect the signals of only one target of those which are in the "angle of view" of the direction finder.

Range target selection usually is used as additional selection in pulsed direction finders. Target selection on the basis of the rate of change of range usually is introduced in continuous radiation systems.

The introduction of additional selection also solves a number of secondary but important problems: it protects the coordinator receiver from direct radiation in the case of semiactive homing, eliminates reflection from

the ground and increases the signal-to-noise ratio at the output of the receiver, which increases the limiting sensitivity of the direction finder, etc.

Finally, automatic selectors can serve as instruments for measuring the range coordinates or the velocity of approach in a case when it is necessary to measure such coordinates, for example, when controlling the time of detonation of the warhead.

1. Range Target Selection

The functional diagram of automatic range target selection, shown in figure 3.23, was constructed for use in the coordinator of a semiactive homing system.

The selection circuit includes a receiver and the antenna of the direction-finding channel, a system for automatic tracking of the target in range, a receiver and the synchronization channel antenna. The antenna of the synchronization channel is mounted in the rear part of the rocket, /124 and together with the receiver of the synchronization channel is used for reception of the sounding pulses of the radar station for "irradiation" of the target. These pulses are used for triggering the time delay stage of the system for automatic range tracking of the target.

In the coordinator of a system for active homing there is no synchronization channel in the form in which it has been described above. Its role is performed by a synchronizer producing pulses for triggering the transmitter.

The system for automatic range tracking of the target (automatic selector) includes: a time discriminator, a control device, a searcher, a time delay stage, a strobe pulse generator and a gate pulse generator.

Automatic range target selection is accomplished as follows. The video pulses of the target are fed from the output of the receiver of the direction-finding channel to the time discriminator. The latter is also fed two strobe pulses with a time difference. A mismatch signal is produced at the output of the time discriminator; the level is dependent on the value of the displacement of the center of the target pulse relative to the middle of the strobe pulses, or, in other words, on the value of the time mismatch between the target pulse and the strobe pulses. The polarity of the mismatch signal is determined by the sign of the time mismatch.

On the basis of the mismatch signal the control device forms a voltage causing a change of the duration of the time delay stage pulse. The search circuit is situated between the control device and the time delay stage. When the automatic selector operates in a regime of automatic target range tracking, the search circuit plays the role of an amplifier.

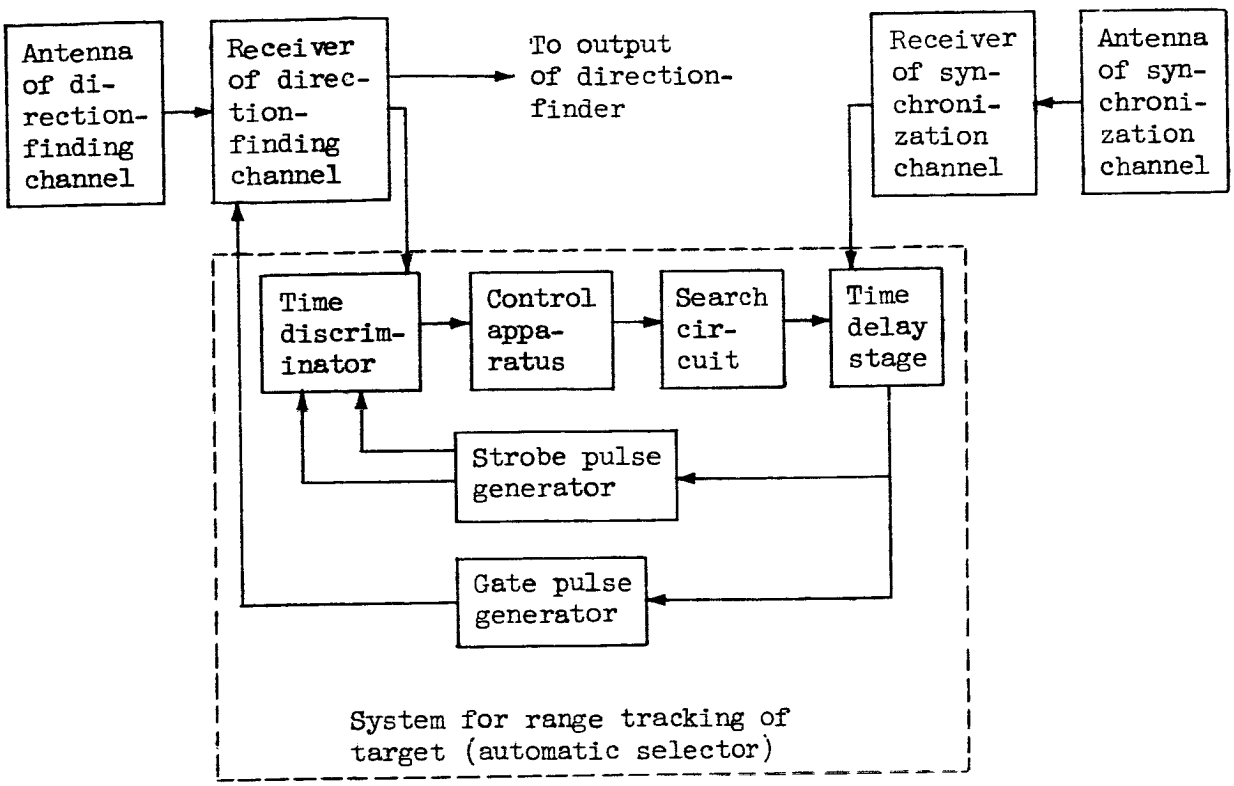

Figure 3.23

The time delay state is triggered by pulses fed from the synchronization channel and produces pulses whose duration is determined by the voltage fed from the control device. If the time mismatch between the target pulse and the strobe pulses is equal to zero, the duration of the pulses generated by the time delay stage is proportional to the rocket-target range.

The gate pulse generator and the strobe pulse generator form gate pulses and strobe pulses, respectively. The time position of these two types of pulses corresponds to the time position of the clipping of the time delay stage pulse.

The direction-finding channel receiver is blanked by a negative bias fed to the grids of the tubes of the intermediate frequency amplifier and this is removed only with receipt of a gate pulse. Since it is somewhat wider than the target pulses, the triggering of the receiver occurs at the time /125 directly preceding the time of arrival of the signal reflected from the selected target. Signals from other targets situated at different ranges within the limits of the "angle of view" of the direction finder do not pass to the output of the direction-finding channel receiver.

The selected pulses are fed from the output of the receiver of the direction-finding channel to the output device of the direction finder and to the automatic volume control system.

The regime of automatic range tracking of the target, described above, is preceded by a regime of search and pickup of the target. The target can be picked up manually or automatically.

The operator can pick up the target manually prior to the launching of the rocket. The operator, observing targets on the radar set scope, manually superposes the gate pulse on the mark of that target which is to be attacked. Further target range tracking is accomplished automatically by an automatic selector.

Automatic pickup of the target can be accomplished automatically either at the launching site or in trajectory, that is, after the launching of the rocket. In an automatic search regime the gate and strobe pulses are moved along the time scale, or, which is the same, along the range scale, in conformity to a periodic law determined by the form of the voltage produced by the search circuit. A target is picked up whose reflected signals possess sufficient strength.

An advantage of manual pickup is that it is possible to select the target to which the rocket should be guided, but in this case the range of rocket launching is decreased.

In the case of automatic target pickup in trajectory the launching range is increased considerably, but at the same time in some cases the possibility of selecting the target is lost.

2. Velocity Target Selection

Recently much attention has been devoted to radar systems with continuous radiation of radio waves. The coordinators of homing systems employing continuous radiation, in some cases, have a number of advantages over pulse coordinators. One of them is the possibility of target selection on the basis of velocity. The introduction of velocity target selection makes it possible not only to detect a signal from a single target when there are several, but also to distinguish it among sufficiently strong signals arriving from the fixed background surrounding the target. The latter circumstances increase the efficiency of homing systems with continuous radiation when used against low-flying aircraft and ships (ref. 51). Velocity target selection is based on the use of the Doppler effect in which, as is well known, with the relative movement of the transmitter and receiver, the frequency of the oscillations/126 picked up by the receiver differs from the frequency of the radiated oscillations by a greater value, the greater the velocity of their relative motion. The difference between the frequencies of the radiated and received oscillations is called the Doppler frequency increment F_D, or simply the Doppler frequency.

The Doppler frequency is related to the radial velocity component $v_r(t)$ of the relative movement of the receiver and transmitter by the following expression

$$F_D = f\frac{v_r(t)}{c} = \frac{v_r(t)}{\lambda}, \qquad (3.7.1)$$

where f is the radiation frequency, λ is the wavelength and c is the speed of light.

The basis for target selection on the basis of velocity is that the automatic selector contains a narrow-band filter tuned to the Doppler frequency corresponding to the velocity of approach of the rocket to the selected target. Angular tracking is accomplished on the basis of the signal passing through the mentioned filter. Therefore, the signals arriving from other targets, for which the approach velocity differs from the selected velocity, and signals arriving from the fixed background surrounding the target do not pass into the system for the tracking of the target on the basis of angular coordinates.

One of the possible circuits for the selection of a target on the basis of velocity for a semiactive homing system is shown in figure 3.24. It consists of a direction-finding channel, a synchronization channel and a system for automatic tracking of Doppler frequency (automatic selector). In the selected variant the automatic selector circuit includes: balancing /127 mixer BM_2, narrow-band amplifier, frequency discriminator, search circuit, reactance tube and tunable generator.

The operation of a system for automatic target selection on the basis of velocity involves the following. A signal reflected from the target arrives at the antenna of the direction-finding channel; its frequency is

$$f_{DFC} = f + F_{D1} + F_{D2},$$

where F_{D1} is the Doppler frequency increment caused by approach of the rocket to the target, and F_{D2} is the Doppler frequency increment caused by approach of the target and the transmitter of the "irradiating pulse."

The antenna of the synchronization channel, situated in the rear part of the rocket, receives a signal from the radar set used for "irradiation" of the target. The frequency of this signal is

$$f_{SC} = f - F_{D3},$$

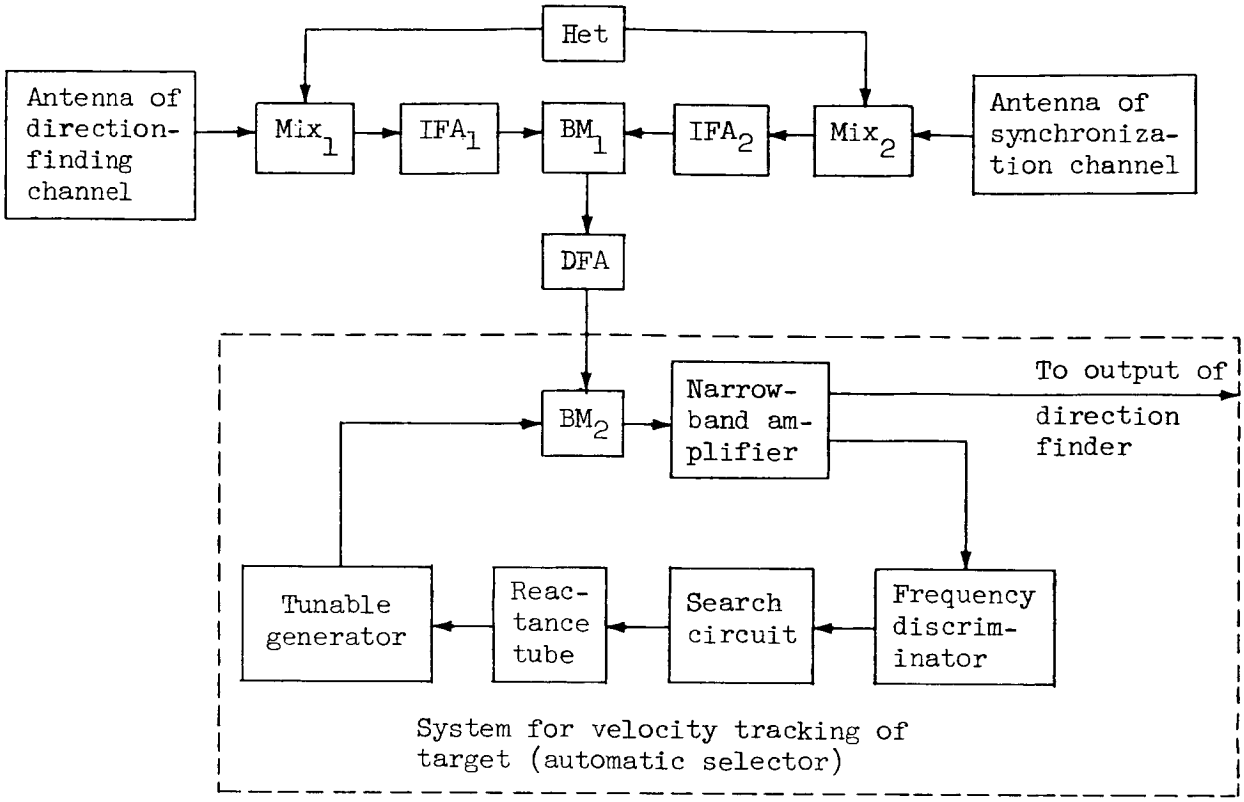

Figure 3.24

where F_{D3} is the Doppler frequency shift caused by withdrawal of the rocket from the transmitter of the "irradiating" pulses.

These signals are fed to the mixers Mix_1 and Mix_2. They also are fed oscillations with the frequency f_h from the common heterodyne Het.

After conversion in the mixers and amplification in the intermediate frequency amplifiers IFA_1 and IFA_2 of the direction-finding channel and the synchronization channel the signals are fed to the balancing mixer BM_1; the signal of the direction-finding channel has the frequency $f_{in} - F_{D1} - F_{D2}$ and the signal of the synchronization channel has the frequency $f_{in} + F$, where $f_{in} = f_h - f$ is the intermediate frequency.

The frequency of the signal forming at the output of the balancing mixer is equal to $F_D = F_{D1} + F_{D2} + F_{D3}$.

This signal is amplified in the Doppler frequency amplifier DFA to the level necessary for normal operation of the automatic selector. If the frequency F_D remained constant during the entire time of rocket guidance, it would be sufficient for target selection to narrow the DFA transmission band. However, due to the change of velocity of approach, the frequency F_D changes its value in a relatively broad range. The circuit therefore should be supplemented by an automatic selector, that is, by a narrow-band system for tracking the change of the Doppler frequency.

The target velocity automatic selector can be designed in various ways. It is most common to use circuits with a "track" filter and with automatic trimming of the low-frequency "track" heterodyne (ref. 50). The voltage from the output of the DFA and the voltage of the "track" heterodyne are fed to the balancing mixer BM_2. The signal at the output of BM_2 has a frequency equal to the sum of the frequencies of the fed oscillations: $F_\Sigma = F_D + F_h$. This signal is amplified by a narrow-band amplifier with constant tuning and is fed to a /128 frequency discriminator and to the output device of the direction finder, where it is used as the selected mismatch signal in the system for direction tracking of the target. If the frequency F_Σ changes its value relative to the nominal value, for example, due to the change of the Doppler frequency, at the output of the frequency discriminator there will be a mismatch voltage. By means of a reactance tube it changes the frequency of the oscillations generated by the "track" heterodyne by such a value that F_Σ again assumes its nominal value. The search circuit in the regime for tracking the Doppler frequency operates as an amplifier. The pickup of the target, as in the system for range tracking of a target, can be manual or automatic. In automatic target search, the search circuit generates a voltage which changes in amplitude in accordance with a periodic law. Accordingly, there is a periodic change of the frequency of the signal generated by the "track" heterodyne. The appearance in the search range of a signal with the frequency F_D leads to cessation of the search regime. The automatic selector then automatically tracks the frequency F_D.

3.8. Block Diagram of a Fixed Coordinator

A fixed coordinator consists only of a direction finder and therefore the processes in such a coordinator can be described by the equation

$$u_{DF} = \frac{k_{DF}}{T_{PD}D + 1}\gamma. \qquad (3.8.1)$$

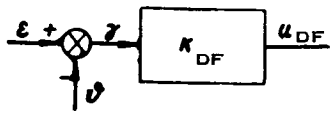

Figure 3.25

Here γ is the angular mismatch, u_{DF} is the voltage at the output of the coordinator, k_{DF} is the direction finder transfer coefficient, and T_{PD} is the time constant of the phase detector filter.

If it is admissible to neglect the time constant of the filter, the equation for a fixed coordinator assumes the form

$$u_{DF} = k_{DF}\,\gamma. \tag{3.8.2}$$

For the earlier discussed types of direction finders with an instantaneous equisignal direction, the transfer coefficient k_{DF} for the direction finder will be a real value. The same can be said with respect to direction finders with an integral equisignal direction in a case when there are no cross connections between channels in the direction finder. The equation for a direction finder with a real transfer coefficient is obtained from (3.8.2) as a special case.

The block diagram of a coordinator designed in accordance with equation (3.8.2) is shown in figure 3.25. Here the angle ε characterizes the position of the target relative to a fixed frame of reference and the angle ϑ determines the position of the longitudinal axis and the equisignal direction related to it, relative to this same frame of reference. /129

These coordinator equations are correct only in a relatively narrow part of the entire "angle of view" of the direction finder. In a broader range of change of the angles γ, the dependence between the measured value of the mismatch angle and the actual value of this angle has a nonlinear character. As mentioned, the form of this dependence gives the direction finder characteristic. It therefore follows that when a fixed coordinator is used it is impossible to employ guidance methods requiring the use of large deflection angles, since the difference in the measured and actual values of these angles exerts an appreciable effect on the quality of the operation of the homing system.

3.9. Block Diagram of a Coordinator with Mechanical Displacement of the Equisignal Direction

In addition to a direction finder, a moving coordinator contains a control device for moving the equisignal direction relative to the body of the rocket.

Extremely high requirements are imposed on the dynamic properties of the control devices of the coordinators of homing rockets; a number of circumstances account for these high requirements. In particular, the coordinator should be well "decoupled" relative to the angular motions of the body of the rocket. This means that it should not reproduce the rapid angular oscillations of the rocket which are inevitable during its flight. Insofar as possible the errors in target tracking should be minimal, even in the case of relatively short ranges to the target, when the angular velocity of the line of sight is high. In addition, an important requirement imposed on the coordinators of a number of homing rockets is the requirement of a precise and technically quite simple measurement of the angular velocity of the rocket-target line.

It can be shown that the mentioned requirements are satisfied most completely by a coordinator with a gyroscopic control device. In addition to its high dynamic qualities, an important property of such a coordinator is the absence of "hunting noise" in the control signal, which occurs in coordinators with other types of drives and which is caused by the need for controlling /130 the angular oscillations of the rocket. In addition, as pointed out in reference 53, an attempt to measure the angular velocity of the rocket-target line by means of a coordinator having a nongyroscopic drive causes the appearance of a positive feedback in the control circuit, which can lead to unstable operation of such coordinators.

As an example of a moving coordinator with mechanical displacement of the equisignal direction we will consider a one-gyroscope coordinator (ref. 107).

The functional diagram of the coordinator is shown in figure 3.26. This shows a three-power gyroscope which includes a rotor 1, an internal frame 2, an external frame 3 and two correcting motors 4 and 5. The axis $o_k x_k$ is the principal axis of the gyroscope. The axes $o_k y_k$ and $o_k z_k$ are equatorial axes. The gyroscope rotor is rotated relative to the axis $o_k x_k$ with the angular velocity Ω_g. An antenna system A is attached to the inner frame of the gyro unit. The form of the antenna system is determined by the type of direction finder.

The mismatch signal caused by the displacement of the target in relation to the equisignal direction, which coincides with the direction of the axis $o_k x_k$, is formed by the direction finder 6. It then is amplified in the power amplifiers 7 and 8, and is fed to the correcting motors 4 and 5 which are used in imparting momenta to the internal and external frames of the gyroscope. The axis of the gyroscope rotor will experience precession relative to the $o_k y_k$ axis of the external frame of the gyroscope under the influence of the momentum created by the motor 4, and relative to the axis $o_k z_k$ of the internal frame of the gyroscope under the influence of the momentum created by the motor 5. The system is phased in such a way that the precessional motion of the

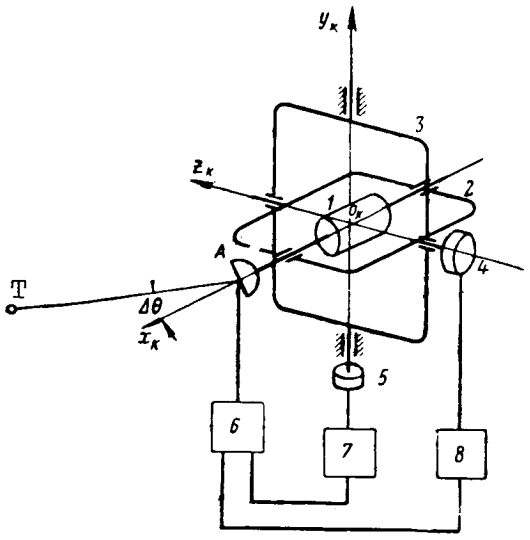

Figure 3.26

axis of the gyroscope rotor leads to elimination of the mismatch between the direction to the target and the equisignal line. When the equisignal direction coincides with the line of sight the mismatch signal becomes equal to zero, which causes disappearance of the correcting momenta, and precession of the gyroscope ceases.

In order to obtain the block diagram of the coordinator we will write /131 the equations defining the processes in its individual links.

The direction finder equation has the form

$$\mathbf{u}_{DF} = \mathbf{k}_{DF} \Delta\theta. \tag{3.9.1}$$

The power amplifier is represented in the form of an inertial link

$$\mathbf{u}_к = \frac{k_a}{T_a D + 1} \mathbf{u}_{DF}, \tag{3.9.2}$$

where u_K is the voltage at the output of the power amplifier, and k_a and T_a are the amplification factor and the time constant of the power amplifier, respectively.

The relationship between the correcting momentum developed by the correcting motor and the voltage fed to the motor is expressed by the equation

$$M = -jk_M u_K. \qquad (3.9.3)$$

Here k_M is the momentum transfer coefficient of the motor. The factor -j takes into account the cross distribution of the correction signals. Finally, the gyroscope transfer function can be obtained by using an equation relating the applied momentum to the complex angle of turning of the axis of the gyroscope rotor. The linearized gyroscope equation has the form

$$J_e \ddot{\varepsilon}_K - jH_g \dot{\varepsilon}_K = M, \qquad (3.9.4)$$

Here J_e is the equatorial moment of inertia of the gyroscope, $H_g = J\Omega_g$ is the kinetic moment of the gyroscope, and J is the moment of inertia of the gyroscope rotor relative to the principal axis.

In operational form equation (3.9.4) can be written as

$$\varepsilon_K = \frac{j}{H_g D(1 + jaD)} M. \qquad (3.9.5)$$

Here $a = \frac{J_e}{J\Omega_g}$.

Equations (3.9.1), (3.9.2), (3.9.3) and (3.9.5) were used to construct the block diagram of the coordinator shown in figure 3.27.

The input action ε is a complex angle characterizing the position of the target in a nonrotating coordinate system $o_m x_m y_m z_m$ (fig. 3.28). The out- /132 put value is the angle ε_K, determining the position of the equisignal direction.

The block diagram contains three links reflecting the dynamic properties of the direction finder, the power amplifier and the gyroscopic control apparatus. Since the equations which were used in the construction of the block diagram were written for complex coordinates the block diagram is for a single-channel apparatus. The presence of links with complex transfer functions in the single-channel circuit indicates that in a two-channel circuit, corresponding to the writing of equations for real coordinates, there are cross connections between

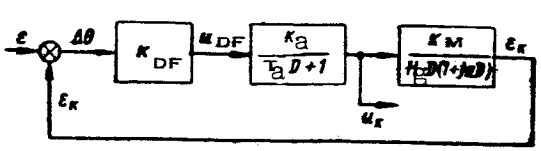

Figure 3.27

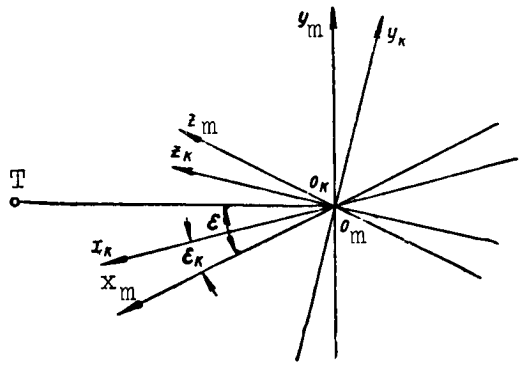

Figure 3.28

channels. This can be confirmed by converting from the writing of equations in complex form to their writing in real form. In actuality, assuming for small deflection angles in equations (3.9.1)-(3.9.5) $\epsilon = \epsilon_z + j\epsilon_y$, $\epsilon_K = \epsilon_{Kz} + l\epsilon_{Ky}$, $u_{DF} = u_{DF\,z} + ju_{DF\,y}$, $u_K = u_{Kz} + ju_{Ky}$ and assuming $k_{DF} = k_{DF}e^{j\mu}$, we obtain the system of equations

$$\left.\begin{aligned}
u_{DF\,z} &= k_{DF}\Delta\theta_z\cos\mu - k_{DF}\Delta\theta_y\sin\mu,\\
u_{DF\,y} &= k_{DF}\Delta\theta_y\sin\mu + k_{DF}\Delta\theta_z\cos\mu,\\
u_{кz} &= \frac{k_a}{T_aD+1}u_{DF\,z},\\
u_{кy} &= \frac{k_a}{T_aD+1}u_{DF\,y},\\
\varepsilon_{кz} &= \frac{k_M}{H_gD}u_{кz} + aD\varepsilon_{кy},\\
\varepsilon_{кy} &= \frac{k_M}{H_gD}u_{кy} - aD\varepsilon_{кz},\\
\Delta\theta_z &= \varepsilon_z - \varepsilon_{кz},\\
\Delta\theta_y &= \varepsilon_y - \varepsilon_{кy}.
\end{aligned}\right\} \qquad (3.9.6)$$

Figure 3.29 shows a block diagram constructed on the basis of equations (3.9.6). The circuit has two cross connections between channels. The first is due to the presence of an additional phase shift μ of the mismatch signal in the direction finder, and the second to the presence of an equatorial moment of inertia J_e of the gyroscope. Both connections are antisymmetrical: the /133

first is a direct link and the second is a feedback (ref. 54). If the phase shift μ is insignificant in absolute value and the equatorial moment of inertia of the gyroscope is small in comparison with its kinetic moment, the cross connections can be neglected. The channels become autonomous and the block diagram of the coordinator breaks down into two identical circuits. In this case the analysis of the spatial movement of the coordinator can be reduced to an analysis of both plane movements.

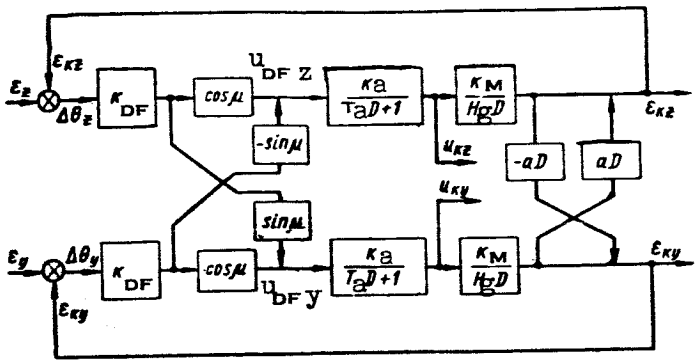

Figure 3.29

We will assume that the cross connections are negligibly small and we will establish the principal properties of the coordinator with a gyroscopic drive. It will be demonstrated below how important it is to take cross connections into account. Since the circuits of both channels are completely identical when there are no cross connections, in the subsequent computations the subscripts showing to which channel the variable apply will be omitted (fig. 3.30).

The transfer function of an open circuit of the coordinator is written as

$$W_k(D)=\frac{k_{DF}k_a k_M}{H_g D(T_a D+1)}=\frac{k_V}{D(T_a D+1)}. \qquad (3.9.7)$$

Here $k_V=\frac{k_{DF}k_a k_M}{H_g}$ is the amplification factor of the velocity coordinator.

We note that the transfer coefficient of the electronic part of the coordinator--the direction finder--is included as a factor in the velocity amplification factor.

The dependence between the angle ε, characterizing the direction to the target, and the angular position of the equisignal line ε_K is given by the relation /134

$$\varepsilon_k=\frac{W_k(D)}{1+W_k(D)}\varepsilon=\frac{k_V}{T_a D^2+D+k_V}\varepsilon. \qquad (3.9.8)$$

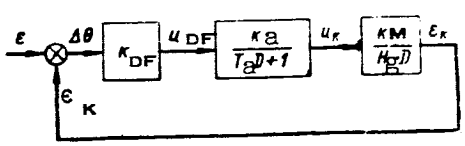

Figure 3.30

It therefore follows that a coordinator, as an apparatus for measurement of the angular position of the target on the basis of dynamic properties, is equivalent to an oscillatory link.

Since the correcting moment is proportional to the voltage fed to the correcting motor u_c, and the rate of precession in turn is proportional to the applied moment, by measuring u_c is is possible to determine the rate of precession. In the case of automatic tracking of the target the rate of movement of the coordinator axis will be equal (with an accuracy to transient processes) to the rate of movement of the rocket-target line. Therefore, the voltage u_c characterizes the angular velocity of movement of the line of sight.

In actuality, the connection between the angular movement of the target and the voltage u_c is determined by the relation

$$u_c = \frac{k_{DF}k_a}{T_aD^2 + D + k_V}\dot{\varepsilon}. \tag{3.9.9}$$

In steady-state movement, in the case of a constant angular velocity of the rocket-target line, we have

$$u_c = \frac{H_g}{k_M}\dot{\varepsilon}. \tag{3.9.10}$$

With respect to its dynamic properties, the coordinator as an apparatus for measuring angular velocity also is equivalent to an oscillatory link.

Formulas (3.9.8) and (3.9.9) can be simplified if the inertia of the power amplifier is small. When the condition $T_ak_V \ll 1$ is satisfied, in place of (3.9.8) and (3.9.9), we obtain

$$\varepsilon_к = \frac{1}{TD+1}\varepsilon, \tag{3.9.11}$$

$$u_c = \frac{H_g}{k_M(TD+1)}\dot{\varepsilon}, \tag{3.9.12}$$

where

$$T = \frac{1}{k_V}.$$

In this case the coordinator, on the basis of dynamic properties, both with respect to angle measurement and measurement of the angular velocity of the line of sight, is equivalent to an inertial link.

Using the coordinator described above it is possible to measure also the angle γ between the direction to the target and the longitudinal axis of the rocket. The coordinator is coupled to a potentiometer for measurement of the angle γ in any plane. The body of the potentiometric sensor is attached /135 to the axis of that frame of the gyroscope in whose deflection plane the angle γ is measured, and the sliding contact of the sensor is connected to the body of the rocket. In the case of automatic tracking of the target the voltage from such a sensor will be proportional to the angle γ between the direction of the target and the longitudinal axis of the rocket.

The relations obtained above, characterizing the dynamic properties of the coordinator for an ideal case when there are no cross connections between the channels, make it possible to judge both the stability of the system and the quality of the processes of control. In particular, it can be concluded that the coordinator maintains stability regardless of how large the amplification factor may be, since the characteristic equation of the system has the second order of magnitude. This assertion requires explanation. In the derivation of the formulas for the transfer functions of the coordinator a number of simplifying assumptions were made. For example, no allowance was made for the inertia of the direction finder, and the inevitable nonlinearities characteristic of actually constructed automatic control systems were not taken into account, etc. Allowance for the mentioned factors naturally modifies somewhat the conclusions drawn concerning the stability of the system.

Now we will clarify the effect of cross connections on the dynamic properties of the coordinator, retaining those simplifying assumptions which were made above. The results will make it possible to compare the properties of a system having cross connections with the properties of an idealized system.

When cross connections are taken into account the equation relating the output angle of the coordinator to the angle characterizing the position of the target is written as

$$\varepsilon_{\kappa} = \frac{k_V}{D(T_a D + 1)(1 + jaD) + k_V} \varepsilon. \qquad (3.9.13)$$

The influence of cross connections on the stability of the system can be represented most graphically by defining a region of stability in the plane of one complex parameter (ref. 30). As such a parameter it is convenient to use the complex coordinator velocity amplification factor k_V. In accordance with the D separation method, used in defining the region of stability, in the characteristic equation of the system, which for the considered coordinator has the form

$$D(T_a D + 1)(1 + jaD) + k_V = 0, \qquad (3.9.14)$$

it is necessary that D be replaced by $j\omega$.

In the derived expression the independent variable will be ω, which changes from $-\infty$ to ∞, and the function will be the complex coefficient $k_V = k_{V1} + jk_{V2}$. The dependences $k_{V1} = f_1(\omega)$ and $k_{V2} = f_2(\omega)$ represent the parametric equations of the boundary of the region of stability in a Cartesian coordinate system $ok_{V1}jk_{V2}$.

After replacing D by $j\omega$ in (3.9.14), we obtain

$$k_V = -j\omega(j\omega T_a + 1)(1 - a\omega) = -T_a a\omega^3 + T_a\omega^2 + j(-\omega - a\omega^2).$$

Hence

$$\left.\begin{aligned} k_{V1} &= T_a\omega^2 - T_a a\omega^3, \\ k_{V2} &= -\omega - a\omega^2. \end{aligned}\right\} \qquad (3.9.15)$$

We now transform equations (3.9.15), converting for convenience to the dimensionless parameters /136

$$k'_{V1} = k_{V1}T_a, \quad k'_{V2} = k_{V2}T_a, \quad k'_V = k_V T_a, \quad a_1 = \frac{a}{T_a} \quad \text{and} \quad \omega_1 = \omega T_a.$$

Then from (3.9.15) we obtain

$$\left.\begin{aligned} k'_{V1} &= \omega_1^2(1 - a_1\omega_1), \\ k'_{V2} &= -\omega_1(1 + a_1\omega_1). \end{aligned}\right\} \qquad (3.9.16)$$

Formulas (3.9.16) are used to determine the regions of stability of the coordinator in the plane of the complex transfer constant for different values of the parameter $a_1 = \frac{J_e}{J\Omega_g T_a}$, characterizing the value of the cross connection, caused by taking into account the equatorial moment of inertia of the gyroscope (fig. 3.31). The rays drawn from the origin of coordinates intersect the curves, being the boundaries of the region of stability, at points with identical values of the relative frequencies ω_1.

When taking into account only the one cross connection caused by the additional phase shift of the mismatch signal in the direction finder (case $a_1 = 0$), the region of stability is bounded by a parabola (curve $a_1 = 0$ in figure 3.31). The upper branch of the parabola corresponds to negative values ω_1, and the branch of the parabola situated below the x-axis corresponds to positive values ω_1.

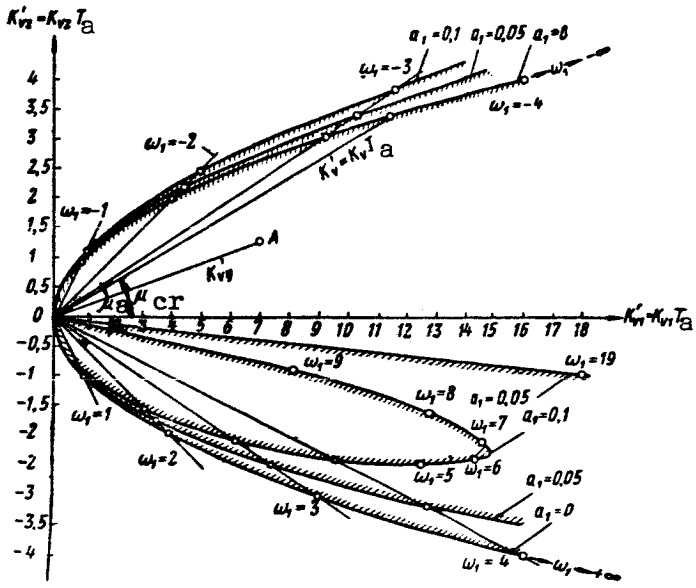

Figure 3.31

If the parameters of the coordinator are such that the so-called figurative point lies within the region bounded by the parabola, the coordinator is stable (in figure 3.31, the point A with the coordinates $k'_{Va}\mu_a$). Movement of the figurative point to the boundary of the region of stability (to one of the branches of the parabola) means that the particular solution of the equation of characteristic motions of the coordinator will have the form $\varepsilon_K = \varepsilon_{K0}e^{\pm j\omega t}$. /137

Therefore, the axis of the coordinator will experience circular motion and this is equivalent to a loss of stability. We note in passing that, whereas the concept of negative frequency for unidimensional systems in a certain sense has an arbitrary character, for two-dimensional systems it is completely specific. For example, the change of the sign of frequency in the solution of the considered example means a change of the direction of rotation of the axis of the coordinator.

Thus, using the diagram (fig. 3.31) it is possible to judge the stability of the coordinator if the values of its parameters (k_VT_a and μ) are given in advance, or such values of these parameters are selected which ensure the stable operation of the coordinator.

An important problem in the investigation of a coordinator is the admissible value of the phase shift μ, introduced by the direction finder, or, in other words, the admissible value of the skewing of the axes of the measurement coordinate system. Figure 3.31 shows that for each value of the product k_VT_a there is a corresponding minimum phase shift angle μ for which the coordinator

becomes unstable. The mentioned angle will be called the critical phase shift angle μ_{cr}.

It is easy to obtain a dependence establishing the relationship between the critical angle of the phase shift and the coordinator parameters. In actuality, from (3.9.16) when $a_1 = 0$ we have

$$\left.\begin{aligned} k'_{V1} &= \omega_1^2, \\ k'_{V2} &= -\omega_1. \end{aligned}\right\} \tag{3.9.17}$$

But at the same time

$$\left.\begin{aligned} k'_{V1} &= k'_V \cos \mu_{cr} \\ k'_{V2} &= k'_V \sin \mu_{cr} \end{aligned}\right\} \tag{3.9.18}$$

After excluding ω_1 from equations (3.9.17) and substituting the values k'_{V1} and k'_{V2}, determined by equations (3.9.18), we obtain

$$\tan \mu_{cr} \sin \mu_{cr} = \frac{1}{k_V T_a}. \tag{3.9.19}$$

By solving equation (3.9.19) for μ_{cr}, we obtain

$$\mu_{cr} = \pm \arccos\left(\sqrt{1 + \frac{1}{4k_V^2 T_a^2}} - \frac{1}{2k_V T_a}\right). \tag{3.9.20}$$

Figure 3.32 shows the dependence of the absolute value of the critical phase shift angle $|\mu_{cr}|$ on the product $k_V T_a$. In the case of large values of the product $k_V T_a$, expression (3.9.19) can be used to obtain an approximate expression for the critical phase shift angle

$$\mu_{cr} \approx \pm \frac{1}{\sqrt{k_V T_a}}. \tag{3.9.21}$$

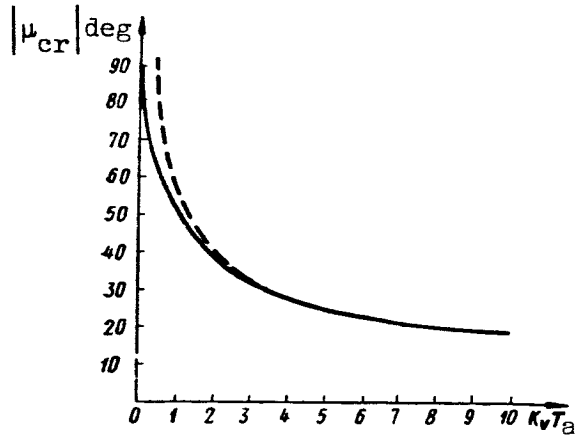

Figure 3.32

The dependence (3.9.21) has been shown in figure 3.32 by a dashed line. The admissible value of the phase shift angle should be less than the critical value by at least a factor of 5-10; this will be discussed in greater detail below.

Now we will take into account a second cross connection, caused by the presence of the equatorial moment of the gyroscope. When $a_1 \neq 0$, the region of stability becomes asymmetrical relative to the x-axis. For negative values of the cited frequency ω_1, the boundary of stability is situated somewhat above the curve $a_1 = 0$ and the farther from it the greater the value a_1. For positive frequencies the boundary of stability is represented by a closed curve situated within the region bounded by the parabola $a_1 = 0$. The /138 dimensions of the region of stability decrease with an increase of a_1. This configuration of the boundary of stability is due to the specific form of the frequency characteristic of a corrected gyroscope, which, as is well known, has two peaks, one of which is situated at a zero frequency, while the other is at the nutation frequency $\Omega_n = \frac{1}{a} = \frac{J\Omega_g}{J_e}$.

When constructing the limits of stability for the case $a_1 \neq 0$ we intentionally selected relatively large values of the parameter characterizing the degree of cross connection so as to reflect more graphically the decrease of the size of the region of stability with an increase of the equatorial moment of the gyroscope. In correctly planned systems the values a_1 are such that for the actually recorded values of the coordinator parameters (k_V, T_a) the boundaries of stability pass near the curves $a_1 = 0$.

The relationship between the critical phase shift angle μ_{cr} and the coordinator parameters is given by the equation

$$\tan \mu_{cr} \sin \mu_{cr} = \frac{1}{k_V T_a} + \frac{a_1}{k_V T_a \tan \mu_{cr}}, \qquad (3.9.22)$$

which differs from equation (3.9.19) only by the additional term on the right-hand side which becomes equal to zero when $a_1 = 0$. For small values a_1 the value of this term is small and conclusions on the admissible limits of change of the angle μ_{cr} can be drawn on the basis of the curve in figure 3.32.

Now we will clarify the influence of cross connections between channels on the quality of control processes. We recall that in the absence of cross connections the motion of the coordinate axes when the coordinator is tracking a target consists of two independent motions--lateral and longitudinal. Non-dependence of motions means that the displacement of the target in any one plane causes movement of the coordinator axes rigorously in this same plane. The character of the transient process in each channel is determined by equation (3.9.8), or in the case of small inertia of the power amplifier, by equation (3.9.11). In the first case the transient process with a jump-like change of the input action will be either aperiodic or will be oscillatory-attenuating, depending on the values of the coordinator parameters. In the second case it always will be aperiodic.

Taking into account cross connections, the transient process in a coordinator will be described by a third-degree linear differential equation with complex coefficients. Expression (3.9.13) represents the symbolic form of writing of this equation. The finding of the solution of such an equation for a given law of change of the input value presents no basic difficulties. However, the unwieldiness of the resulting solution does not make possible sufficiently simple clarification of the principal characteristics of the transient process and the influence exerted on it by change of individual coordinator parameters. Therefore, it is necessary to use the approach of maximum simplification of equation (3.9.13), at the same time retaining its specific character, necessitated by taking into account at least one cross connection. By solving such a simplified equation it is possible to establish the principal laws characterizing the transient process and then attempt /139 at least a qualitative tracing of the influence exerted on the transient process by parameters not taken into account earlier.

In the case of a small inertia of the power amplifier and a weak cross connection, caused by the equatorial moment of the gyroscope, equation (3.9.13) is transformed to the form

$$\dot{\varepsilon}_K + k_V \varepsilon_K = k_V \varepsilon. \qquad (3.9.23)$$

The characteristic equation

$$\lambda + k_V = 0$$

has one complex root

$$\lambda = -k_V = -k_V e^{j\mu} = -k_{V1} - jk_{V2}. \qquad (3.9.24)$$

Therefore, solution of equation (3.9.23) for zero initial conditions and with a change of the input action at the time t = 0 in a jump from to $\varepsilon_0 = \varepsilon_0 e^{j\varphi}$, where ε_0 is the module of angular deflection and φ is the phase angle of the target, has the form

$$\varepsilon_k = \left(1 - e^{-k_V t}\right)\varepsilon_0. \qquad (3.9.25)$$

We will assume for unambiguity that the deflection of the target occurred in the plane $o_m x_m z_m$ (fig. 3.28). As before, the angular deflections in the plane $o_m x_m z_m$ will be assigned the real values of the coordinates and the angular deflections in the plane $o_m x_m y_m$ will be assigned fictitious values of the coordinates. Then ε_0 in equation (3.9.25) should be replaced by ε_{0z}. By dividing both sides of equation (3.9.25) by ε_{0z} we obtain an expression for the conversion function in relation to a "real" input

$$H_{+1}(t) = \frac{\varepsilon_k(t)}{\varepsilon_{0z}} = 1 - e^{-k_V t}. \qquad (3.9.26)$$

Formula (3.9.26) shows that the conversion function for a two-channel system in relation to a "real" input is a complex function of the actual variable--time

$$H_{+1}(t) = H_{+1z}(t) + jH_{+1y}(t), \qquad (3.9.27)$$

the real part of which $H_{+1z}(t)$ expresses the reaction of the system to a unit jump applied to a "real" input, at the output of the lateral deflection channel

and the imaginary part $H_{+1y}(t)$ determines the reaction to this same action at the output of the longitudinal deflection channel.

The conversion function $H_{+1}(t)$ is a curve in a three-dimensional space $H_{+1z}H_{+1y}t$. Its projections onto the planes $oH_{+1z}t$ and $oH_{+1y}t$ are respectively equal to

$$\left.\begin{aligned} H_{+1z}(t) &= 1 - e^{-tk_V\cos\mu}\cos(tk_V\sin\mu),\\ H_{+1y}(t) &= e^{-tk_V\cos\mu}\sin(tk_V\sin\mu). \end{aligned}\right\} \qquad (3.9.28)$$

In addition, expressions (3.9.28) can be considered as the parametric equations of the trajectories of the axis of the coordinator when the "real" input is fed a unit jump. It is convenient to use the dimensionless value k_Vt as a parameter. Figure 3.33 shows some of the mentioned trajectories corresponding to different values of the phase shift angle μ, introduced by the direction finder.

Using formulas (3.9.28) and the curves in figure 3.33 it is possible to trace how changes of the value μ influence the character of motion of the coordinator axis. For example, when $\mu = 0$ the coordinator axis moves to the new position of the target (the point +1, j0 in figure 3.33) along a straight line. For values μ falling in the interval between 0 and 90°, the coordinator axis moves toward the target along a spiral. The greater the value μ, the greater is the number of loops of the spiral and the longer will be the duration of the transient process. When $\mu = 90°$ the coordinator axis experiences circular motion with the angular frequency $\Omega_0 = k_V$. If $90° < \mu < 180°$, the trajectories of the coordinator axis constitute diverging spirals. Finally, when $\mu = 180°$ the coordinator axis moves along a straight line in the direction away from the target. /140

If the target is deflected in the plane $o_mx_my_m$, the picture of the trajectories of the coordinator axis is turned by 90° relative to the axis oH_{+1z}. This can be concluded from the fact that the conversion function of the system for the "imaginary" channel is related to the conversion function of the system for the "real" channel by the relation

$$H_{+j}(t) = jH_{+1}(t).$$

In the case of an arbitrary direction of deflection of the target it is necessary to consider the generalized conversion function of the two-channel system $H_\varphi(t)$, characterizing a system with jump-like transfer of the action to

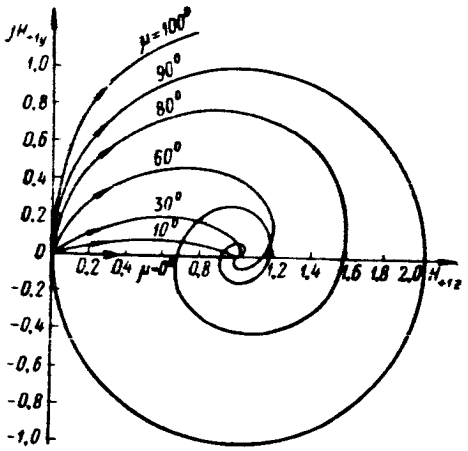

Figure 3.33

both channels simultaneously. If the conversion function $H_{+1}(t)$ is known, the generalized conversion function is determined as

$$\mathbf{H}_{\varphi}(t) = \mathbf{H}_{+1}(t)\, e^{j\varphi},$$

where φ is the phase angle of the target.

Analysis of the quality of control processes in a two-channel system of the simplest form shows that allowance for the cross connection between channels appreciably changes the dynamic properties of the coordinator. For example, the deflection of the target in any one plane causes motion of the axis of the coordinator both in the deflection plane and in the plane perpendicular to it.

The character of the the transient processes in each of the channels also changed. Whereas in the absence of cross connections, a jump-like change of the input action corresponded only to an aperiodic process for any values of the coordinator parameters, now in the same type of action the transient process can have an aperiodic, oscillatory-attenuating, oscillatory, and finally, diverging character, in dependence on μ, characterizing the relationship between the channels.

These results make it possible to evaluate the admissible value of the phase shift angle of the mismatch signal μ_{adm}. As the admissible value μ_{adm} we can use that value of it at which the maximum deflection of the coordinator axis in the plane normal to the plane of deflection of the target does not exceed a stipulated value. From (3.9.28) it is easy to obtain an expression for the maximum deflection of the coordinator axis along the axis oH_{+1y} as a function of the phase shift angle

$$H_{+1y\ max} = e^{-\mu \cot \mu} \sin \mu. \qquad (3.9.29)$$

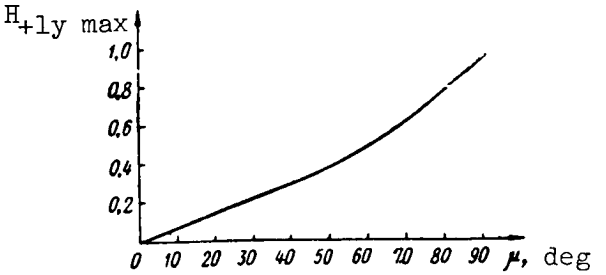

Figure 3.34

The curve of the dependence of (3.9.29) is shown in figure 3.34. In the case of small values μ formula (3.9.29) can be simplified. Assuming

$$\sin \mu \approx \mu \text{ and } \mu \cot \mu \approx 1,$$

we obtain

$$\left|\mu^{\circ}_{adm}\right| \leq 1.56\ H_{+1y\ adm}\%.$$

For example, if it is assumed that the maximum deflection of the coordinator axis in the plane normal to the plane of deflection of the target should not exceed 5 percent of the deflection of the coordinator in the direction of the target, the absolute value of the admissible phase shift angle μ_{adm} should be not more than 8°; when $H_{+1y\ adm} = 10$ percent, the admissible phase shift angle should be approximately 15°, etc. For the analyzed example, the critical angle of skewing $\mu_{cr} = \pm 90^{\circ}$ (the region of stability on the diagram in figure 3.31 occupies the entire right half-plane). Therefore, if $H_{+1y\ adm}$ falls in the limits 5-10 percent, $\frac{\mu_{cr}}{\mu_{adm}} \approx$ 6-11. /141

Allowance for inertia of the power amplifier, as well as for a second cross connection, somewhat complicates the picture of the transient processes. However, it has been demonstrated (ref. 97) that the qualitative side of the earlier considered phenomena still is retained. Cross connections lead to the appearance of spiral motion of the coordinator axis and therefore to its deflection in the plane normal to the plane of the mismatch angle. The relation between the admissible and critical phase shift angles also is maintained. However, now μ_{cr} should be selected using the diagram in figure 3.31 or using formulas (3.9.20) and (3.9.22).

If the coordinator is used for measurement of the angular velocity of the rocket-target line, the dynamic properties characteristic of it as an instrument for measuring angular velocity, under the conditions assumed above,

retain all the principal characteristics of the just considered case when the coordinator served as an angle-measuring instrument. In actuality, by comparing formulas (3.9.8), (3.9.9), (3.9.11) and (3.9.12) it is easy to confirm that the conversion function of the coordinator, as an instrument for measuring angular velocity $\dot{\epsilon}$, is equal with an accuracy to a constant real factor to its conversion function, as an instrument for measuring the angle ϵ.

The dynamic properties of the single-gyroscope coordinator described above deteriorate appreciably when it is combined with an antenna system of considerable size and weight, because this causes a significant decrease of the ratio of the polar moment of the gyroscope rotor J to the equatorial moment of inertia J_e of the gyroscope with the body. The latter, in turn, leads to a considerable influence of inertial moments, and therefore to a considerable manifestation of nutation. The operation of such coordinators will be influenced considerably by inertial forces in the axes of the suspension during oscillations of the rocket and also an inevitable residual unbalancing of the gyroscope.

However, an increase of the kinetic moment of the gyroscope for the purpose of attenuation of the mentioned factors is not always desirable because it causes an increase of the size and weight of the coordinator, and requires the use of correcting motors with a large torque.

When a relatively heavy antenna is coupled to a gyroscopic drive the best results are given when using gyroscopic stabilized platforms or stabilized platforms (ref. 1). Such apparatus consists of two-gyroscope platforms with power unloading of the gyroscopes (ref. 5). /142

The relations derived above for single-gyroscope coordinators can be applied to two-gyroscope tracking coordinators as instruments for measuring the angular position of the target and the angular velocity of the line of sight, at the same time taking into account that to a considerable degree such coordinators do not have the shortcomings inherent in single-gyroscope systems.

The gyrostabilized platform of a two-gyroscope power system is formed by two frames: an outer frame 1 and an inner frame 2 (fig. 3.35). The axes of the frames $o_K z_K$ and $o_K y_K$ are mutually perpendicular. The gyroscopes G_1 and G_2 are situated on the inner frame of the platform, made in the form of a housing. Each of them has two degrees of freedom relative to the gyrostabilized platform, including here the degree of freedom of the rotation of the rotor.

The angles of rotation of the gyroscope frames 3 and 4 relative to the platform are measured by the pickups P_1 and P_2, respectively. The voltages from the pickups directly or after amplification are fed to the unloading motors M_1 and M_2, creating moments around the axes $o_K z_K$ and $o_K y_K$. The gyroscopes, together with the pickups and the unloading motors, form a power unloading system for compensation of the external moments applied to the platform.

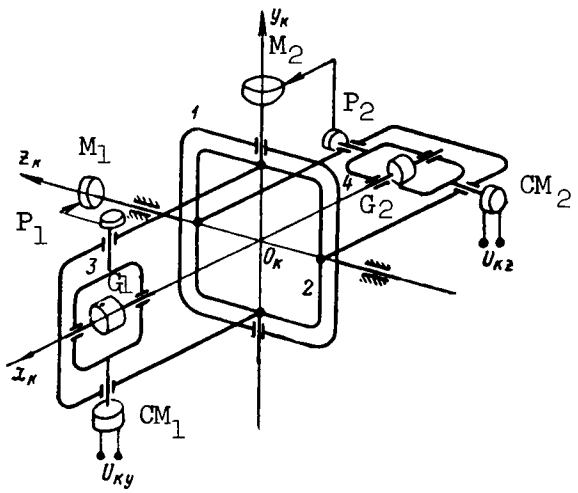

Figure 3.35

Now we will consider the behavior of a platform under the influence of the external moment which can arise, for example, during the oscillations of the rocket. We will assume that the moment is applied to the outer frame of the platform, that is, acts around the axis $o_K z_K$. Under the influence of the perturbing moment the gyroscope G_1 begins to experience precession, tending to bring the vector of its kinetic moment into coincidence with the vector /143 of the perturbing moment. With the rotation of the frame of the gyroscope G_1 relative to the platform, a voltage proportional to the angle of rotation of the gyroscope frame will be fed from the pickup P_1. In proportion to the voltage of the pickup the motor M_1 develops a moment around the axis of the outer frame of the platform, oriented in a direction opposite the direction of the external moment. Precession of the gyroscope will continue until the external moment equals the moment of the motor.

If the external moment is eliminated, the moment of the discharge motor, compensating it earlier, causes precession of the gyroscope G_1 to its former position. With the rotation of the gyroscope frame to the zero-signal position the value of the moment of the motor also will decrease. As soon as the gyroscope frame attains such a position the moment of the motor becomes equal to zero and the further precession of the gyroscope G_1 ceases.

Thus, in a power unload system the gyroscope G_1 performs the role of an external moment around the axis $o_K z_K$ of the platform and, jointly with the pickup P_1, produces a voltage necessary for compensation of the external moment.

The platform behaves similarly under the influence of the moments along the $o_K y_K$ axis. Only in this case will there be precession of the gyroscope G_2 and the motor M_2 will compensate the external moment.

Thus, the application of external moments to the axes of the platform frames does not lead to a rotation of the platform, but causes only precession of the corresponding gyroscopes. The suspension axes of the platform are unloaded from the action of the external moments.

The correcting moments, under whose influence the angular position of the axes of the platform should change, are created by the correcting motors CM_1 and CM_2, to which are fed the mismatch signals formed by the direction finder.

3.10. Block Diagram of a Coordinator with Electrical Displacement of the Equisignal Direction

A coordinator with electrical displacement of the equisignal direction consists of a phase-type direction finder and an actuating mechanism whose purpose is the forming of voltages which are fed to the windings of the phase inverters. The values and signs of these voltages are set in such a way that the phase inverters compensate the phase shift of the received signal caused by displacement of the target relative to the equisignal direction.

The actuating device used can be an electromechanical drive or the earlier discussed gyroscopic drive, coupled to potentiometric pickups. The body of each pickup is attached to the body of the rocket and the slide /144 is connected to the axis of the gyroscope or the output shaft of the reducer of the electric motor.

The principle of operation of the coordinator is as follows. We will assume that in the initial state the rocket-target line coincides with the direction of the axis of the antenna system (we recall that the antenna system in this type of direction finder is fixed rigidly to the body of the rocket, and its axis is oriented in the direction of the longitudinal axis of the rocket). The mismatch signal at the output of the direction finder will be equal to zero, and the gyroscope will occupy some initial position in which the voltage from the potentiometric pickups also will be equal to zero. There will be no additional phase shift from the phase inverters. Displacement of the target relative to the equisignal direction causes the appearance of a mismatch signal, precession of the gyroscope and appearance (as a result of movement of the slide of the potentiometric pickup from a zero position) of a voltage across the windings of the phase inverter ferrites. The phase inverters shift the phase of the received signal so as to compensate the phase shift caused by displacement of the target relative to the axis of the antenna.

When the phase shift of the signal caused by displacement of the target is completely compensated, the mismatch signal becomes equal to zero and precession of the gyroscope ceases. The target again will be on the equisignal direction, which no longer will coincide with the axis of the antenna. During movement of the target the equisignal direction automatically follows the position of the line of sight.

In constructing the block diagram of the coordinator it is necessary to use equations (3.6.30), (3.9.2), (3.9.3), (3.9.5) and equations relating the voltage at the output of the potentiometric pickups and the angle of rotation of their slides.

In complex form the equation for the pickups has the form

$$u_p = k_P \gamma_\partial, \tag{3.10.1}$$

where $k_P = k_{P1} = k_{P2}$ is the transfer constant of the pickup; $\gamma_\partial = \gamma_{\partial z} + j\gamma_{\partial y}$ is the angle of rotation of the pickup slides.

Since γ_∂ also is the angle of deflection of the gyroscope relative to the body of the rocket, then

$$\gamma_\partial = \epsilon_K - \vartheta. \tag{3.10.2}$$

Here ϑ is the angle characterizing the position of the longitudinal axis of the rocket relative to a fixed frame of reference.

Figure 3.36a, b shows block diagrams of a coordinator for complex and real coordinates. The block diagram of a coordinator with electrical displacement of the equisignal direction differs somewhat from a block diagram with mechanical displacement of the equisignal line (fig. 3.27). The most important difference is that, for the diagram shown in figure 3.27, the angle $\Delta\theta$ is the mismatch angle characterizing the deflection of the target from /145 the equisignal direction. Such a mismatch for the diagram in figure 3.36 will be the phase shift $\Delta\varphi = \varphi - \varphi_p$. However, the angle $\Delta\theta$ for a coordinator with electrical displacement of the equisignal line is the input action which characterizes the position of the target in the related coordinate system.

Using the block diagram in figure 3.36 it is possible to write an expression for the measured value of the angular position of the target

$$\varepsilon_K = \frac{k_V}{D(T_a D+1)(1+jaD)+k_V\frac{k_{PI}k_P}{k_\varphi}}\varepsilon + \frac{k_V\left(\frac{k_{PI}k_P}{k_\varphi}-1\right)}{D(T_a D+1)(1+jaD)+k_V\frac{k_{PI}k_P}{k_\varphi}}\vartheta. \qquad (3.10.3)$$

It follows from (3.10.3) that the angle ε_K is dependent not only on the actual angular position of the target ε, but also on the angular position of the longitudinal axis of the rocket ϑ. The latter dependence is extremely undesirable because the inevitable changes of ϑ in the process of motion of the target cause errors in determination of the coordinates of the target. /146 This dependence can be eliminated by the appropriate selection of the parameters of the coordinator and "decoupling" the coordinator from the angular oscillations of the rocket.

The "decoupling" condition is satisfaction of the equation

$$k_{PI}k_P = k_\varphi. \qquad (3.10.4)$$

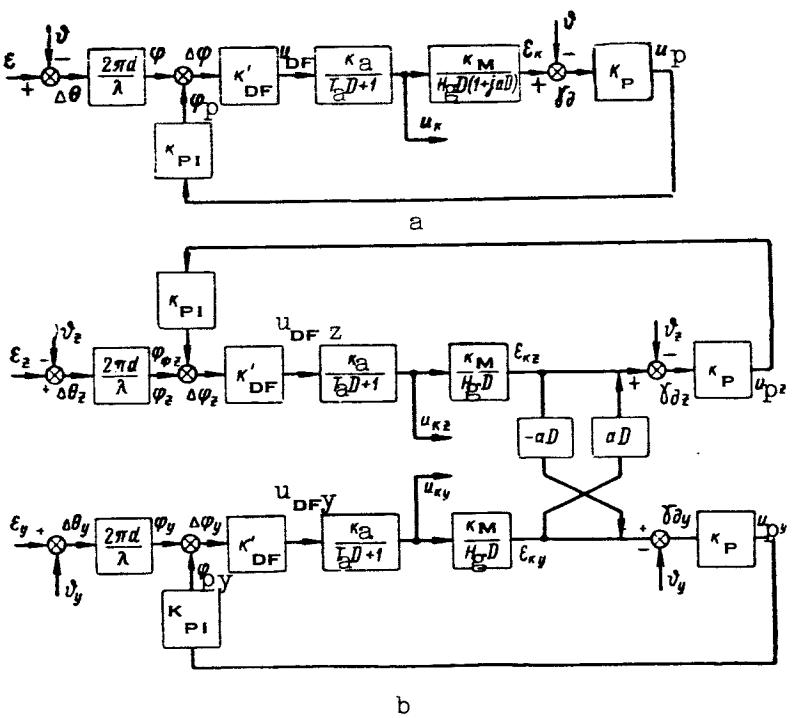

Figure 3.36

Then (3.10.3) assumes the form

$$\varepsilon_{\kappa} = \frac{k_V}{D(T_a D + 1)(1 + jaD) + k_V} \varepsilon. \qquad (3.10.5)$$

Equation (3.10.5) coincides in form with the equation of motion of the coordinator with mechanical displacement of the equisignal direction (3.9.13) if the velocity amplification factor of the latter is a real value.

In the case of satisfaction of condition (3.10.4) the voltage fed to the correcting motors of the gyroscope is expressed by the formula

$$u_c = \frac{k_{DF} k_a (1 + jaD)}{D(T_a D + 1)(1 + jaD) + k_V} \dot{\varepsilon}. \qquad (3.10.6)$$

Therefore, a coordinator of the considered type can be used as an instrument for measurement of the angular velocity of the line of sight.

3.11. Evaluation of the Accuracy of Coordinators of Homing Systems

The coordinator of a homing system is a measuring apparatus and, therefore, the most important index of its operation is the accuracy of measurement of the mismatch parameter.

The errors involved in use of the coordinator are reflected to a considerable degree in the value of the rocket miss. In actuality, if the coordinator measures the mismatch parameter with an error, this is equivalent to determination of the mismatch parameter for some fictitious target. Since the other elements of the homing system cannot compare the actual and measured values of the mismatch parameter, the rocket will be guided to a fictitious target whose position corresponds to the measured value of the mismatch parameter, which also leads in the last analysis to an increase of the rocket miss which cannot be eliminated.

Two types of actions are applied to the coordinator, as to any automatic control system: a controlling action and various kinds of perturbations. The coordinator errors are caused both by inexact reproduction of the controlling action and the influence of undesirable perturbations. Errors of the first kind sometimes are called dynamic errors, and errors of the second kind, fluctuation errors.

In the case of coordinators of homing systems the controlling action, that is, the action which should be performed with a high degree of accuracy, can be divided into two components: a component caused by the /147

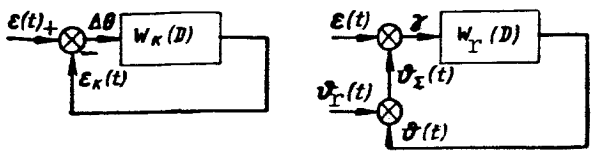

a b

Figure 3.37

relative motions of the rocket and target, which result in the angular motion of the line of sight, and a component caused by angular oscillations of the body of the rocket ("yawing" of the rocket). We note at once that the second component is characteristic only of systems for automatic tracking of a target using angular coordinates, carried on a moving object and having an electric motor control device and also coordinators with a fixed equisignal direction. In part, this component also will appear in the gyroscopic coordinator described in the preceding section, in which there is displacement of the equisignal direction with incomplete compensation of "yawing" error (3.10.3). A gyroscopic coordinator with mechanical displacement of the equisignal direction, as a result of the gyroscopic effect, has a good decoupling from the angular oscillations of the rocket, and therefore there will be virtually no "yawing" component in the controlling action.

Figure 3.37a shows the block diagram of a moving gyroscopic coordinator. Here $W_K(D)$ is the transfer function of the coordinator. The single controlling action--change of the angular position of the rocket-target line $\varepsilon(t)$--is applied to the input of the coordinator. The equisignal direction, characterized by the angle ε_K, is deflected from the line of sight by the angle $\Delta\theta$. Thus, $\Delta\theta = \varepsilon - \varepsilon_K$ represents the tracking error or the error in reproducing the controlling action.

Figure 3.37b is the block diagram of a homing rocket with a fixed coordinator. The transfer function $W_r(D)$ includes the transfer function of the coordinator, automatic pilot and rocket. The angle ϑ characterizes the angular position of the longitudinal axis of the rocket (it is assumed that the equisignal direction of the direction finder coincides with the longitudinal axis of the rocket). This diagram shows two controlling actions: the change of the angular position of the line of sight $\varepsilon(t)$ and the angular oscillation of the longitudinal axis of the rocket $\vartheta_r(t)$. The latter is combined with the angle ϑ and gives the angle ϑ_Σ, characterizing the angular position of the equisignal direction. Such a setting of the controlling action, necessitated by the oscillations of the axis of the rocket, is correct only in a case when "yawing" is not dependent on the angular position of the longitudinal axis of the rocket. /148

There are two approaches to setting of the controlling action, necessitated by the change of the angular position of the line of sight. According to the first of them $\epsilon(t)$ is given in the form of a determined function of time. In the second it is assumed that $\epsilon(t)$ is a random function and is given by its statistical characteristics.

In the first case, it is assumed that in the process of guidance of a rocket to a target, the angular position of the line of sight changes in conformity of a clearly defined law as a function of the velocity and maneuvering of the target, the guidance method used, velocity and the dynamic properties of the rocket, initial launching range, etc. The problem of determining the controlling action $\epsilon = \epsilon(t)$ for different methods of rocket guidance was considered in chapter 2. In computing the dynamic errors of the coordinator it is desirable to replace the dependence $\epsilon = \epsilon(t)$ by its approximate value. As such an approximation, it is convenient to use approximation of the function $\epsilon = \epsilon(t)$ by a polynomial of t

$$\epsilon(t) = \sum_{i=0}^{n} A_i t^i. \tag{3.11.1}$$

Since in actuality the $\epsilon = \epsilon(t)$ curves are quite smooth, the degree of the approximating polynomial cannot be very high.

In the second method for setting the controlling action it is assumed that as a result of the difference of target trajectories, and also the difference in the initial condition for each launching (aspect of attack, initial launching range, etc.), an individual kinematic trajectory, and therefore also its corresponding dependence $\epsilon = \epsilon(t)$, must be considered as one of the possible realizations of some random process. The controlling action in such an approach is given by the statistical characteristics of the mentioned random process. Reference 31 presents computations of the statistical characteristics of the controlling action for a radar set for automatic tracking of the target, on the basis of angular coordinates, which is used in an antiaircraft fire control system. The spectral density of the angular velocity of the line of sight is expressed by the formula

$$G_{\dot{\epsilon}}(\omega) = \frac{4\overline{A_1^2}\eta_1}{\omega^2 + \eta_1^2}, \tag{3.11.2}$$

where $\overline{A_1^2}$ is the mean value of the square of angular velocity of the target, and η_1 is a value inverse to the mean value of the interval within which the angular velocity remains constant.

However, a similar method can be used as the basis for computation of the statistical characteristics of the controlling action with respect to the coordinators of homing rockets. /149

The second method for setting the controlling action makes it possible to make a more general evaluation of the accuracy of the system for different variants of its use, whereas the first method makes it possible to evaluate the accuracy of the coordinator only for some special cases of its use. However, the expenditures involved in obtaining reliable statistical characteristics are very great, and therefore in actual practice preference frequently is given to the first method for setting the controlling action.

Chapter 2 discussed the principal types of perturbations acting on the coordinators. In computing the accuracy of measurement of the mismatch parameter in the tracking coordinators of the angle-measuring type, it is necessary to take into account the fluctuations of the signal reflected from the target and also artificially created interference.

The instantaneous value of the fluctuations of the amplitude of the reflected signal is characterized, as already pointed out, by the relative change of the amplitude or the coefficient of noise modulation $m_n(t)$. As the averaged characteristics of amplitude noise, it is possible to use the correlation coefficient of noise modulation $R_m(\tau)$ or its spectral density $G_m(\omega)$.

Fluctuations of the amplitude of the reflected signal lead to the appearance of distortions of the output voltage of the direction finder, which in the long run cause errors in determination of the target coordinates. Therefore, for introducing into the block diagram of the coordinator the perturbing action caused by amplitude noise, it is first necessary to make an investigation of the direction finder outside a closed control system. Such an investigation essentially involves an analysis of the passage of a useful signal together with fluctuations through the direction finder, in accordance with the signal conversion equations for a direction finder of a particular type. We note that intentionally created interference can be taken into account in a similar way if the transmitter of the interference is situated at the target.

As a result of such an investigation we find the voltage at the output of the direction finder as a function of the mismatch angle, the parameters of the direction finder and the values characterizing the amplitude noise. The output voltage of the direction finder consists of the useful component u_{DF} and low-frequency noise $u_{lfn}(t)$. Therefore, the perturbation caused by the fluctuations of the reflected signal can be introduced into the block diagram of the coordinator in the form of low-frequency noise at the output of the direction finder.

If the noise voltage $u_{lfn}(t)$ is not dependent on the mismatch angle $\Delta\theta$, it is possible to compute the errors caused by the fluctuations, leaving the block diagram of the direction finder in the same form it had in the absence of fluctuations. The dependence of the voltage $u_{lfn}(t)$ on the mismatch

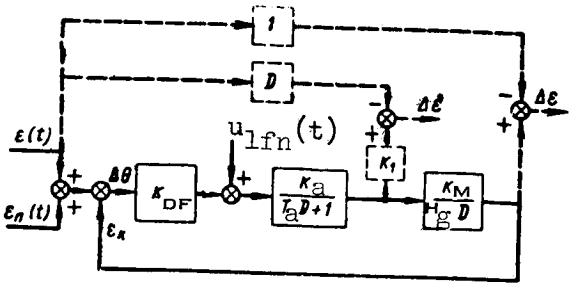

Figure 3.38

angle $\Delta\theta$, which occurs in the case of a high level of fluctuations of the reflected signal or when there is artificial interference, makes necessary changes of the block diagram of the direction finder as a link in the automatic control system. /150

Fluctuations of the apparent center of reflection (angular noise) are given in the form of the angle $\varepsilon_n(t)$, whose value changes randomly relative to the true direction to the target, determined by the angular position of the line of sight ε.

Figure 3.38 is the block diagram of one of the channels of a tracking gyroscopic coordinator, with the fluctuations of the signal reflected from the target taken into account. The dashed line in this figure denotes ideal systems of reproduction of the angular position of the line of sight and the angular velocity of the rocket-target line. The first system has a transfer coefficient equal to unity and the second is characterized by the transfer function $W_m(D) = D$.

The error in determination of the angular position of the line of sight will be characterized by the measurement error or by the distortions of the measured parameter $\Delta\varepsilon$, representing the difference between the measured value of the angle ε, equal to ε_K, and its actual value ε, that is

$$\Delta\varepsilon = \varepsilon_K - \varepsilon. \tag{3.11.3}$$

The concept of reproduction error, defined as $\Delta\varepsilon_{0\,r} = \varepsilon - \varepsilon_K$, sometimes is used in evaluation of the accuracy of the tracking system. By comparing this expression with formula (3.11.3), it is easy to establish that $\Delta\varepsilon = -\Delta\varepsilon_{0\,r}$.

By using the block diagram shown in figure 3.38, we write an expression for the measurement error

$$\Delta\varepsilon = -\frac{1}{1+W_к(D)}\varepsilon + \frac{W'(D)}{1+W_к(D)}u_{lfn} + \frac{W_к(D)}{1+W_к(D)}\varepsilon_n. \tag{3.11.4}$$

Here $W_K(D)$ is the transfer function of the closed coordinator, equal to

$$W_к(D)=\frac{k_V}{D(T_a D+1)}, \tag{3.11.5}$$

and $W'(D)=\frac{W_K(D)}{k_{DF}}$ is the transfer function of the power apparatus and the /151 power amplifier.

Formula (3.11.4) shows that the error $\Delta\varepsilon$ consists of two components: the dynamic error $\Delta\varepsilon_\partial$, determined by the difference $\varepsilon - \varepsilon_K$ when $u_{lfn} = 0$ and $\varepsilon_n = 0$, and also the fluctuation error $\Delta\varepsilon_f$, representing $\Delta\varepsilon$ when $\varepsilon = 0$. The following formulas are derived for computation of $\Delta\varepsilon_\partial$ and $\Delta\varepsilon_f$

$$\Delta\varepsilon_\partial=\frac{1}{1+W_к(D)}\varepsilon, \tag{3.11.6}$$

$$\Delta\varepsilon_f=\frac{W'(D)}{1+W_к(D)}u_{lfn}+\frac{W_к(D)}{1+W_к(D)}\varepsilon_n. \tag{3.11.7}$$

If the controlling action is given in the form of a determined function of time, the dynamic error in a steady-state regime is represented conveniently in the form of a series

$$\Delta\varepsilon_\partial=c_0\varepsilon(t)+c_1\dot{\varepsilon}(t)+\frac{c_2}{2!}\ddot{\varepsilon}(t)+\ldots+\frac{c_к}{k!}\varepsilon^{(k)}(t)+\ldots, \tag{3.11.8}$$

where the coefficients for the input action and its derivatives represent the so-called error coefficients, computed using the formula

$$c_к=\left\{\frac{d^k}{dD^k}\left[\frac{1}{1+W_к(D)}\right]\right\}_{D=0}. \tag{3.11.9}$$

After substituting (3.11.5) into (3.11.9) and after computation, we obtain

$$c_0=0,\quad c_1=\frac{1}{k_V},\quad c_2=\frac{T_y}{k_V}-\frac{1}{k_V^2},\ \text{etc.} \tag{3.11.10}$$

Computation of the dynamic error requires stipulation of the specific law of change of the controlling action. We will assume that the angular position of the line of sight changes in conformity to the law

$$\varepsilon(t) = A_0 + A_1 t + \frac{1}{2} A_2 t^2, \tag{3.11.11}$$

where A_0 is the initial angular position of the line of sight, A_1 is the angular velocity of the line of sight, and A_2 is the angular acceleration of the line of sight.

Then

$$\Delta\varepsilon_\partial = \frac{A_1}{k_V} + \frac{A_2(k_V T_a - 1)}{2k_V^2} + \frac{A_2}{k_V} t. \tag{3.11.12}$$

It follows from formula (3.11.12) that in the case of a fixed line of sight ($A_1 = A_2 = 0$) the dynamic error is equal to zero. If the line of sight moves with a constant angular velocity, the dynamic error in a steady-state regime (after attenuation of the characteristic motions of the system) is equal to the constant value /152

$$\Delta\varepsilon_\partial = \frac{A_1}{k_V}.$$

Finally, with movement of the line of sight with a constant angular acceleration, the dynamic error increases linearly.

When the controlling action is stipulated in the form of a random function of time the dynamic error usually is characterized by a mean square value which is computed in the following way. From (3.11.6) and (3.11.5) we have

$$\Delta\varepsilon_\partial = \frac{D(T_a D + 1)}{D(T_a D + 1) + k_V} \varepsilon = \frac{T_a D + 1}{D(T_a D + 1) + k_V} \varepsilon. \tag{3.11.13}$$

In the example cited above an expression was obtained for the spectral density of the angular velocity of the line of sight (3.11.2). If it is assumed that such an expression can be obtained also for the controlling signal of the coordinator of a homing rocket, the dispersion of error of determination of the position of the line of sight is expressed by the formula

$$\sigma^2_{\Delta\varepsilon_\partial} = \frac{1}{2\pi} \int_0^\infty \left| \frac{j\omega T_a + 1}{j\omega(j\omega T_a + 1) + k_V} \right|^2 \frac{4\overline{A_1^2}\gamma_1}{\omega^2 + \gamma_1^2} d\omega. \tag{3.11.14}$$

The integral in (3.11.14) can be computed easily if the tables compiled for this purpose in reference 31 are used. Making the computations and assuming that $\eta T_a \ll 1$ and $\frac{\eta}{k_V} \ll 1$, we determine the mean square value of the dynamic error

$$\sigma_{\Delta\varepsilon\partial} \approx \frac{\sqrt{\overline{A_1^2}}}{k_V} \sqrt{1 + k_V T_a \eta}. \qquad (3.11.15)$$

It follows from (3.11.15) that the dynamic error increases with an increase of the mean square value of angular velocity of the line of sight and with a decrease of the duration of the segments of flight of a target with a constant angular velocity.

The fluctuation errors in determination of the position of the line of sight will be characterized by the dispersions or the mean square values.

If the noise component of voltage at the output of the direction finder is not dependent on the mismatch angle and is given by the spectral density $G_{lfn}(\omega)$, the dispersions of errors of determination of the position of the line of sight, caused by amplitude and angular noise, are equal respectively to /153

$$\sigma_a^2 = \frac{1}{2\pi} \int_0^\infty \left| \frac{W'(j\omega)}{1 + W_K(j\omega)} \right|^2 G_{lfn}(\omega)\, d\omega, \qquad (3.11.16)$$

$$\sigma_y^2 = \frac{1}{2\pi} \int_0^\infty \left| \frac{W_K(j\omega)}{1 + W_K(j\omega)} \right|^2 G_n(\omega)\, d\omega. \qquad (3.11.17)$$

It frequently is found that the spectral densities $G_{lfn}(\omega)$ and $G_n(\omega)$ within the limits of the pass band of the coordinator approximately retain a constant value, equal to their value at the zero frequency. We recall that the spectral density $G_n(\omega)$ is computed for some fixed range to the target.

Then, formulas (3.11.16) and (3.11.17) can be represented in the form

$$\sigma_a^2 = \frac{G_{lfn}(0)}{2\pi} \int_0^\infty \left| \frac{W'(j\omega)}{1 + W_K(j\omega)} \right|^2 d\omega, \qquad (3.11.18)$$

$$\sigma_y^2 = \frac{G_n(0)}{2\pi} \int_0^\infty \left| \frac{W_K(j\omega)}{1 + W_K(j\omega)} \right|^2 d\omega. \qquad (3.11.19)$$

Since amplitude noise is given by the spectral density of the coefficient of noise modulation $G_m(\omega)$, $G_{lfn}(\omega)$ in formula (3.11.18) must be expressed through $G_m(\omega)$. We will show the relationship between these spectral densities using the example of a direction finder with conical scanning, since in direction finders with an instantaneous equisignal direction the influence of amplitude noise is reflected only when there is a nonidentity of the reception channels. In a well-adjusted direction finder of such a type, the error caused by amplitude noise will be increasingly small.

The voltage at the output of a direction finder with conical scanning, with amplitude noise taken into account, is equal to (ref. 1)

$$u^*_{DF} = k_{DF}\Delta\theta + k_{DF} m_n(t)\,\Delta\theta + \frac{2k_{DF}}{k_m} m_n(t)\cos\Omega t. \qquad (3.11.20)$$

The last two terms in expression (3.11.20) represent the fluctuating part of the output voltage; the first of these terms is dependent on the mismatch angle $\Delta\theta$. The presence of such a dependence indicates that the amplitude noise caused a change of the properties of the direction finder. The block diagram of the direction finder, constructed on the basis of (3.11.20), is shown in figure 3.39. It follows from figure 3.39 that the direction finder as a link in the automatic control system possesses a variable amplification factor which changes randomly. The change in the properties of the direction finder is reflected not only in the character of the fluctuation error, but also in the value of the dynamic error. This example illustrates one of the possible manifestations of the mutual relationship and mutual dependence of fluctuation and dynamic errors mentioned earlier. /154

The coefficient of noise modulation $m_n(t)$, caused by fluctuations of the reflecting surface of the target, is considerably smaller than unity and therefore for simplification of the problem the variability of the transfer coefficient of the direction finder, in most cases, is neglected. In the analysis of the effect of artificial interference on a coordinator such a simplification can prove to be unsound.

Hereafter in formula (3.11.20) we will take into account only the last term, assuming that the low-frequency noise at the output of the direction finder is expressed by the formula

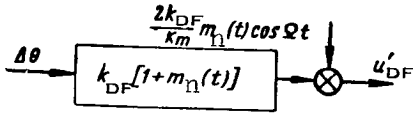

Figure 3.39

$$u_{1fn}(t) = \frac{2k_{DF}}{k_m} m_n(t) \cos \Omega t. \qquad (3.11.21)$$

Then it is necessary to express the spectral density of noise voltage through the direction finder parameters and the spectral density of the coefficient of noise modulation. It can be shown that

$$G_{1fn}(0) = \frac{2k^2_{DF}}{k^2_m} G_m(\Omega). \qquad (3.11.22)$$

Then expression (3.11.18) assumes the form

$$\sigma^2_a = \frac{2G_m(\Omega)}{k^2_m} \cdot \frac{1}{2\pi} \int_0^\infty \left| \frac{W_K(j\omega)}{1 + W_K(j\omega)} \right|^2 d\omega. \qquad (3.11.23)$$

The effective passband of the coordinator is equal to

$$\Delta F_e = \frac{1}{2\pi} \int_0^\infty \left| \frac{W_K(j\omega)}{1 + W_K(j\omega)} \right|^2 d\omega. \qquad (3.11.24)$$

With (3.11.24) taken into account, expressions (3.11.23) and (3.11.19) are transformed to the form

$$\sigma^2_a = \frac{2G_m(\Omega)}{k^2_m} \Delta F_e. \qquad (3.11.25)$$

$$\sigma^2_y = G_n(0) \Delta F_e. \qquad (3.11.26)$$

Formulas (3.11.25) and (3.11.26) make possible a sound selection of some parameters of the direction finder for the purpose of decreasing the tracking error. For example, the error due to amplifier noise can be decreased by increasing the size of the antenna (at the same time, the coefficient k_m /155 increases), decreasing the equivalent pass band of the coordinator and increasing the scanning frequency, thus leading to a decrease of the spectral density $G_m(\Omega)$. The latter approach apparently is the most rational.

By computing the integral (3.11.24) we obtain

$$\Delta F_e = \frac{k_V}{4}. \qquad (3.11.27)$$

Then

$$\sigma_a^2 = \frac{G_m(\Omega)\, k_V}{2k_m^2}, \tag{3.11.28}$$

$$\sigma_y^2 = \frac{G_n(0)\, k_V}{4}. \tag{3.11.29}$$

Formulas (3.11.28) and (3.11.29) make it possible to determine the measurement errors in any one channel of the coordinator in the absence of cross connections between channels. In order to compute tracking errors when there is a cross connection between channels, it is necessary when computing the integral (3.11.24) to assume that the amplification factor for the velocity coordinator is a complex value $k_V = k_V e^{j\mu}$. If such computations are made, the following coefficient appears in formulas (3.11.28) and (3.11.29)

$$k_\mu = \frac{1}{\cos\mu - k_V T_a \sin^2\mu}. \tag{3.11.30}$$

With an increase of μ from zero to the value at which the following condition is satisfied

$$\tan\mu_{cr} \sin\mu_{cr} = \frac{1}{k_V T_a}, \tag{3.11.31}$$

the coefficient k_μ increases from unity to infinity. We recall that the equality (3.11.31) applies at the limit of coordinator stability. Therefore, the fluctuation errors of the coordinator increase with an increase of the cross connection between channels.

The mean square total error of determination of the direction of the line of sight, on the assumption that the line of sight moves at a constant velocity, is expressed by the formula

$$\overline{\Delta\varepsilon^2} = \frac{A_1^2}{k_V^2} + \frac{G_m(\Omega)\, k_V}{2k_m^2} + \frac{G_n(0)\, k_V}{4}. \tag{3.11.32}$$

Formula (3.11.32) shows that the first term (dynamic error) decreases with an increase of the amplification factor of the velocity coordinator and the two others (fluctuation errors) increase with an increase of k_V. It is possible to determine the value of the amplification factor k_V which is optimal from the point of view of the minimum of the mean square total error. It is equal to /156

$$k_{V\ opt} = \sqrt[3]{\frac{8A_1^2 k_m^2}{2G_m(\Omega) + k_m^2 G_n(0)}}. \qquad (3.11.33)$$

The minimum value of the total error can be found by substituting (3.11.33) into (3.11.32).

The error in measurement of the angular velocity of the line of sight can be determined by using the block diagram in figure 3.38.

Assuming $k_1 = \frac{k_M}{H_G}$, we obtain

$$\dot{\Delta\varepsilon} = -\frac{D}{1 + W_K(D)}\varepsilon + \frac{DW'(D)}{1 + W_K(D)}u_{1fn} + \frac{DW_K(D)}{1 + W_K(D)}\varepsilon_n. \qquad (3.11.34)$$

The steady-state dynamic error, on the assumption that the controlling action changes in conformity to the law $\varepsilon(t) = A_0 + A_1 t + \frac{1}{2}A_2 t^2$, will be equal to

$$\dot{\Delta\varepsilon}_\partial = \frac{A_2}{k_V}. \qquad (3.11.35)$$

The dispersions of the fluctuation errors caused by amplitude and angular noise are expressed by the formulas

$$\sigma^2_{\dot{\varepsilon}a} = \frac{2G_m(\Omega)}{k_m^2} \cdot \frac{1}{2\pi}\int_0^\infty \left|\frac{j\omega W_K(j\omega)}{1 + W_K(j\omega)}\right|^2 d\omega, \qquad (3.11.36)$$

$$\sigma^2_{\dot{\varepsilon}y} = G_n(0) \cdot \frac{1}{2\pi}\int_0^\infty \left|\frac{j\omega W_K(j\omega)}{1 + W_K(j\omega)}\right|^2 d\omega. \qquad (3.11.37)$$

Computing the values of the integrals in (3.11.36) and (3.11.37), we will have

$$\sigma^2_{\dot{\varepsilon}a} = \frac{G_m(\Omega)k_V^2}{2T_a k_m^2}, \qquad (3.11.38)$$

$$\sigma^2_{\dot{\varepsilon}y} = \frac{G_n(0)k_V^2}{4T_a}. \qquad (3.11.39)$$

The mean square total error in determination of the angular velocity of the line of sight, on the assumption that the controlling action changes in conformity to the law $\varepsilon(t) = A_0 + A_1 t + \frac{1}{2}A_2 t^2$, is expressed by the formula

$$\overline{\Delta\varepsilon^2} = \frac{A_2^2}{k_V^2} + \frac{G_m(\Omega)\,k_V^2}{2T_a k_m^2} + \frac{G_n(0)\,k_V^2}{4T_a}. \qquad (3.11.40)$$

The value of the velocity amplification factor for which the mean square total error has a minimum value is equal to /157

$$k_{V\ opt} = \sqrt[4]{\frac{4A_2^2 k_m^2 T_a}{2G_m(\Omega) + k_m^2 G_n(0)}}. \qquad (3.11.41)$$

Comparing formulas (3.11.33) and (3.11.41) we note that the optimal value of the velocity amplification factor will be different, depending on whether the position of the line of sight or its angular velocity is determined with a minimum error.

The computation of the coordinator errors under the influence of artificial interference has some features in common with the computations cited above, because the principles for creating artificial interference in part are based on the complication of the natural factors responsible for measurement errors. Here it is important only to clarify those specific properties of interference which are the basic cause for the appearance of errors to be able to correctly introduce the interference signal into the coordinator circuit.

It is also useful to know the methods that make it possible to attenuate the effect of intentionally created interference of some type. The following table, taken for reference 109, gives a list of some of the possible types of interference and measures available to overcome them. This list was compiled for use with radar sets with automatic tracking of the target and employing the equisignal direction method.

Interference	Methods for overcoming interference
Noise interference	Closed velocity memory circuit for determining correlation Range selection with narrow strobe pulses for improving the signal-to-noise ratio Instantaneous automatic volume control
Rotation of antenna with reverse modulation	Direction finder with instantaneous equisignal direction

Interference	Methods for overcoming interference
Random radar interference	Modulation of pulse repetition frequency Velocity selection Range selection with narrow gate pulses Narrow pass band Acceleration selection
Air-dropped chaff	Acceleration selection Tie-in of pulse edges, clipping and range selection Velocity differentiation
Chaff fired into rocket path	Automatic frequency tracking Velocity selection Range selection with narrow strobe pulses Acceleration selection
Spurious targets	Acceleration selection Investigation of trajectory
Remote interference (disrupting range selection)	Velocity selection Range selection with narrow strobe pulses Automatic frequency tracking Acceleration selection

/158

CHAPTER 4. COORDINATORS OF RADIO ZONE (BEAM-RIDING) CONTROL SYSTEMS

4.1. Functional Diagram of the Coordinator of a Beam-Riding Control System

The coordinator of a beam-riding control system consists of two separated parts, one of which is situated at the control point and the other on the rocket. The apparatus of the coordinator carried on the rocket consists of an antenna, placed in the rear part of the rocket, a radio receiver and an output device which is designed for functional conversions of the received signal. /159

If the rocket is situated precisely on the equisignal direction, the pulses received by the radio apparatus aboard the rocket from the radar set will have a constant amplitude. Deflection of the rocket from the equisignal line causes the appearance of amplitude modulation of the received pulses with the frequency of rotation of the directional diagram of the antenna of the radar set.

The conversion of the signal in the output device of the apparatus carried aboard the rocket essentially involves the detection of the envelope of the received pulses, amplification of the mismatch signal and its breakdown into two components characterizing the deflection of the rocket from an equisignal line in two mutually perpendicular planes. These components are used in forming the controlling effects which cause the rocket to return to an equisignal direction.

In order to detect the two mentioned components on the rocket, it is necessary to have a reference signal which fixes the beginning of reading of the phase of the envelope of the received pulses. This reference signal is transmitted from the radar set by the additional modulation of the radiated pulses.

What has been said above makes it possible to construct the functional diagram of the coordinator of a beam-riding control system. Figure 4.1 shows such a diagram. The position of the antenna A_1 is set by the antenna control unit ACU, which is controlled by target designation signals. The diagram rotation motor DRM is connected to a reference voltage generator RVG. The voltage produced by it is fed to the unit for shaping the reference signal RSS which forms the signal used for additional modulation of the pulses received by the radar set. /160

Aboard the rocket the signals received by the antenna A_2 are amplified by the receiver rec and are fed to two channels: a mismatch signal channel MSC

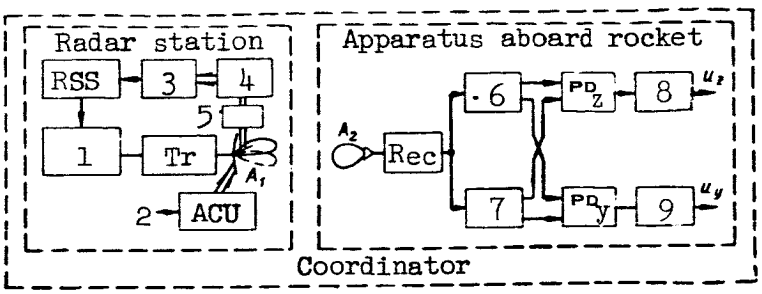

KEY:
1, Synchronizer
2, Target designation signals
3, RVG
4, DRM
5, Red
6, MSC
7, RSC
8, DCA_z
9, DCA_y

Figure 4.1

and a reference signal channel RSC. The signals from the outputs of these channels are fed to phase detectors PD_z and PD_y for measurement of the lateral and longitudinal deflection of the rocket, and then to the dc amplifiers DCA_z and DCA_y.

The output voltages u_z and u_y of the coordinator are dependent on the displacement of the rocket relative to the radar beam in the corresponding control planes.

Figure 4.1 shows that the functional diagram of the apparatus aboard the rocket partially coincides with the diagram of the direction-finding apparatus of the homing system coordinator. For this reason, we will consider only the specific features of its operation in a beam-riding control system.

4.2. High-Frequency Channel of the Receiving Apparatus of the Rocket

One of the characteristics of the operation of the high-frequency channel of the receiving apparatus is the fact that the rocket antenna usually is situated at its rear, and therefore is in the jet of gases of the jet engine containing a large quantity of ionized molecules. As a result, the antenna is surrounded by ion plasma which influences the received signal. Also, there is reflection of electromagnetic waves from the "gas jet-air" discontinuity and absorption of energy on the path of propagation of the radio waves to the /161 antenna. Both factors lead to an additional attenuation of the strength of the signal fed to the antenna. The degree of attenuation of the signal during its passage through the jet is dependent on the frequency of the received electromagnetic oscillations, the type of jet engine, the characteristics of the fuel, etc. In the case of waves in the centimeter range, the decrease of signal strength can attain one or two orders of magnitude (ref. 3).

The degree of absorption of radio waves in the jet during the operation of the jet engine does not remain constant but varies continuously and these variations are as great as 50 percent. This leads to amplitude modulation of the

signal by the jet with a quite high frequency. This parasitic modulation causes the appearance of a false mismatch signal if the frequency of scanning is close to the frequency of fluctuations of the jet.

A considerable drop of the strength of the received signal due to a change of range between the radar set and the rocket in the course of its flight to the target also is characteristic of the operation of the receiving channel. In this case, when the launching site is situated in the immediate vicinity of the radar station, such as when launching a rocket from a rocket-carrying aircraft, the signal strength arriving at the receiver antenna immediately after the launching can have an inadmissibly high value. If the necessary measures ar not taken, this will result in the disruption of operation of the input elements of the radio receiving apparatus and even total malfunctioning. One of the measures for protecting the receiver is the introduction of a special signal attenuator into the waveguide channel. The attenuation which it causes is changed in accordance with the program from a maximum value at the time of rocket launching to zero by the time of arrival in the target area. The introduction of an attenuator operating in accordance with a program also lowers the requirement on the dynamic range of the receiver.

The electromagnetic oscillations radiated by the radar set forming the radar beam usually have plane polarization. If there is conical scanning in the radar by rotation of the primary radiating element, the polarization plane is rotated with the scanning frequency. When rotation of the reflector is used for scanning, the turning of the polarization plane of the arriving wave relative to the orientation of the waveguide of the high-frequency channel of the receiver occurs due to the transverse oscillations of the rocket. In both cases, there is a so-called polarization effect leading to a change of the amplitude of the received signal during the turning of the polarization plane of the arriving wave.

If the polarization effect is caused by rotation of the polarization plane with the frequency of scanning, there will be polarization errors in the mismatch signal whose presence leads to a change of the amplitude of the actual value of the mismatch signal and to a distortion of its phase(ref. 1). The first is equivalent to a change of the transfer coefficient of the mismatch signal channel and the second to a twisting of the axes of the measurement coordinate system. Therefore, it is necessary to take special measures for exclusion of the polarization effect. /162

One of the methods for elimination of polarization errors is the use in the apparatus carried aboard the rocket of an antenna with circular polarization. An example of such an antenna is a horn antenna with a dielectric plate (ref. 49). It consists of a horn 1 (fig. 4.2a), excited by a standard waveguide 2 with a wave H_{10}. A phasing section 3 is placed between the horn and waveguide and is used in turning the horn relative to the axis of the waveguide by 45°. A longitudinal dielectric plate 4 is inserted in the phasing section.

The conversion of the incident wave with plane polarization into a field with circular polarization in such an antenna occurs because the vector E of

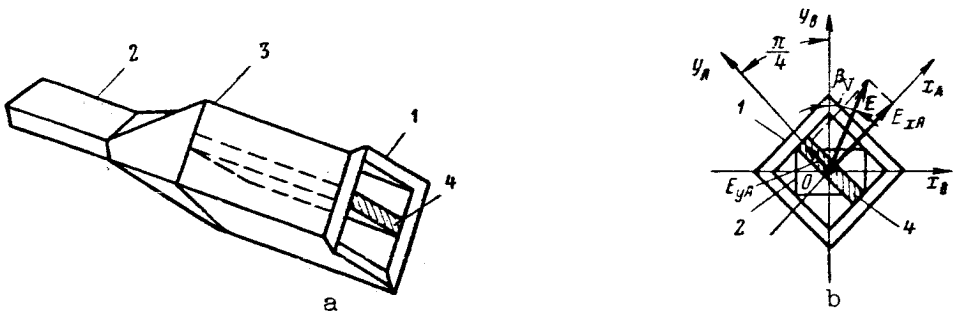

Figure 4.2

the arriving electromagnetic oscillation breaks down into two mutually perpendicular components with a time phase shift of 90° relative to one another. This shift is the result of use of a dielectric plate in the phasing section.

It is easy to show that by use of such a device the amplitude of the high-frequency oscillations at the output of the phasing section is not dependent on the angle β_v at which the vector E of the incident wave is oriented (fig. 4.2b). It can be seen from figure 4.2b that the components of the vector E along the narrow and broad edges of the dielectric plate are

$$\left.\begin{aligned} E_{xA} &= E\cos\left(\frac{\pi}{4}-\beta_V\right), \\ E_{yA} &= E\sin\left(\frac{\pi}{4}-\beta_V\right). \end{aligned}\right\} \qquad (4.2.1)$$

For the instantaneous values of the electrical field at the output of the phasing section (without allowance for the attenuation created by it) we obtain /163

$$\left.\begin{aligned} e_1 &= E\cos\left(\frac{\pi}{4}-\beta_V\right)\sin\omega t, \\ e_2 &= E\sin\left(\frac{\pi}{4}-\beta_V\right)\cos\omega t. \end{aligned}\right\} \qquad (4.2.2)$$

By projecting the oscillations (4.2.2) onto the axis y_B, parallel to the narrow wall of the waveguide, for the resultant field e_y we find

$$e_y = e_1\cos\frac{\pi}{4} + e_2\cos\frac{\pi}{4} = \frac{1}{\sqrt{2}}(e_1+e_2)$$

or

$$e_y = \frac{E}{\sqrt{2}}\sin\left(\omega t+\frac{\pi}{4}-\frac{\beta_V}{2}\right). \qquad (4.2.3)$$

The latter equation shows that the amplitude of the oscillations at the input of the receiver is not dependent on the orientation of the vector E. Therefore the turning of the polarization plane of the arriving wave has no influence on the operation of the coordinator apparatus aboard the rocket.

The described method for exclusion of the polarization error leads to a decrease of the signal strength at the input of the receiver by a factor of 2 in relation to the maximum possible value. However, this circumstance is no limitation on the use of such an antenna because the receiving apparatus is under the influence of direct (sounding pulses) of the radar set. We note that the operation of the radar apparatus carried aboard the rocket using the direct signals of the radar set makes it possible to use receiving apparatus having a low sensitivity, if the effective range of the beam-riding control system is low.

4.3. Channel for Detection of Mismatch Signal

The channel for detection of the mismatch signal includes a peak detector, an amplifier and a range potentiometer.

We recall that in the case of a small deflection of a rocket from an equisignal direction, the envelope of the video pulses at the output of the receiver has the form (3.4.12)

$$u_{rec} = U_p[1 + m \cos(\Omega t + \varphi)]. \tag{4.3.1}$$

The mean amplitude of the pulses U_p is expressed by the formula

$$U_p = \sqrt{\frac{k_{jc} P_R G_{RO}(\beta_O) G_r \lambda^2}{g_{mix}(4\pi r_r)^2}}\, k_{rec}. \tag{4.3.2}$$

Here k_{jc} is the absorption coefficient for the jet, P_R is the radar pulse power, $G_{RO}(\beta_O)$ is the coefficient of directional effect of the antenna of the radar on the equisignal direction, G_r is the coefficient of directional /164 effect of the rocket antenna, λ is the wavelength, g_{mix} is the conductivity of the mixer of the rocket receiver, r_r is the distance between the radar and the rocket, and k_{rec} is the amplification factor of the receiver from the mixer to the output of the video amplifier.

The depth of modulation m of the signal is proportional to the angular deflection of the rocket from the equisignal direction ϵ_{lR}, that is

$$m = k_m \epsilon_{lR}, \tag{4.3.3}$$

where the coefficient k_m is determined by formula (3.4.13). The peak detector and the amplifier in the channel for detection of the mismatch single are similar in their purpose and diagrams to the same apparatus in a direction finder with an integral equisignal line. The voltage amplitude at the output, therefore, is expressed by the formula

$$U_a = U_p k_m k_D k_a \epsilon_{lR}. \tag{4.3.4}$$

It follows from the cited expression that the amplitude of the mismatch signal when U_p = const is proportional to the angular deflection of the rocket from an equisignal direction. The constancy of the mean value of the amplitude of the pulses U_p is ensured by the use of an automatic volume control system.

In some cases it is desirable that the mismatch signal be proportional to the linear deflection of the rocket from the axis of the radar beam h, rather than to the angular deflection.

In the case of small mismatches

$$h \approx \epsilon_{lR} r_r. \tag{4.3.5}$$

By comparing expressions (4.3.4) and (4.3.5), it is easy to see that in order to obtain a proportional dependence between the amplitude of the mismatch signal and the linear deflection of the rocket the voltage at the output of the amplifier should be multiplied by a factor changing proportional to the distance r_r. This is achieved by introduction into the channel for detection of the mismatch signal of an element whose transfer coefficient increases proportional to the range r_r. In connection with this element, the apparatus carried aboard the rocket should contain an instrument for measurement of the "radar set-rocket" range.

Since the signal proportional to the range r_r is used only for change of the transfer coefficient of the amplification channel, it is not necessary /165 to measure it with a high accuracy. For practical purposes, an element with

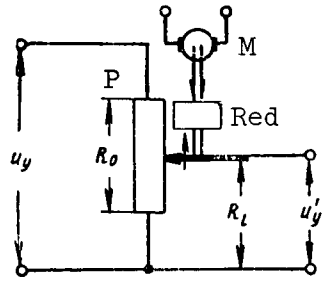

Figure 4.3

a variable amplification factor is constructed in the form of a programming mechanism called a range potentiometer whose diagram is shown in figure 4.3. A ring potentiometer P is fed a voltage u_y proportional to the angular deflection of the rocket from the axis of the radio beam. The slide of the potentiometer is moved by the motor M of the reducer Red. The motor is cut in at the time of the rocket launching. If it is assumed that the velocity v_0 of the rocket relative to the radar set is constant and the potentiometer has a uniform winding, the resistance R_t of part of the potentiometer changes in conformity to the law

$$R_t = R^o \frac{n\omega_m}{v_0} r_r, \tag{4.3.6}$$

where R^o is the change of the resistance of the potentiometer with a turning of the slide by one degree, ω_m is the speed of rotation of the rotor of the motor, and n is the gear ratio of the reducer.

Then for the amplitude of the voltage from the potentiometer we obtain

$$U'_a = \frac{R_t}{R_0} U_a = k_{pot\partial} r_r U_a. \tag{4.3.7}$$

Here $k_{pot\partial} = \frac{R^o}{R_0} \frac{n\omega_m}{v_0}$ is the transfer coefficient of the range potentiometer and R_0 is the total resistance of the potentiometer.

The coefficient $k_{pot\partial}$ has the dimensionality $\left[\frac{1}{m}\right]$ and shows to what extent there is an increase of the relative voltage at the output of the potentiometer with a change of range by one meter.

The value $k_{pot\partial}$ should be selected in such a way that the potentiometer still is not fully cut in when the rocket flies a distance equal to its effective range $r_{r\ max}$. If the mentioned reserve is 10-20 percent, the maximum value $k_{pot\partial}$ is determined as

$$k_{pot\partial\ max} = \frac{0.8\text{-}0.9}{r_{r\ max}}.$$

In designing the range potentiometer, it is desirable that the value $k_{pot\partial}$ be selected close to the maximum.

4.4. Reference Signal Channel

The signal produced by the reference voltage generator of the radar set (fig. 4.1) has the form of a sinusoidal oscillation rigidly in phase with the scanning of the directional diagram of the antenna. The transmission of /166 the reference signal to the rocket is accomplished by additional modulation of the pulses radiated by the radar set.

The reference signal channel of the radar apparatus aboard the rocket is used for detection of the reference signal from the received sequence of pulses.

Two methods are used for transmission of the reference signal: in the first the sinusoidal reference voltage is transmitted completely, whereas in the second only individual values of this voltage related to the characteristic points of the position of the maximum of the directional diagram are transmitted, such as "up-down" and "right-left."

The following types of modulation now are used widely for the transmission of a continuous communication by pulsed signals (which in the considered case is a sinusoidal oscillation with a phase unknown to the recipient): pulse-amplitude (PAM), pulse-width (PWM), pulse-phase (PPM), pulse-frequency (PFM) and pulse-code (PCM) modulation. Briefly we will evaluate the possibility of using the mentioned types of modulation for the purposes of transmission of a reference signal. The unsuitability of PAM is due to the impossibility of detecting the reference signal and the mismatch signal at the receiving end, because the latter is formed from pulses modulated in amplitude by an oscillation of the same frequency as the reference signal. The use of PWM makes it necessary to increase the mean power of the transmitter, which frequently is undesirable. In the case of transmission of a sinusoidal oscillation, phase and frequency modulation are almost similar in their properties, though PFM continues to have some advantages because its use does not require forming of synchronizing pulses. Finally, PCM in theory can be used for transmission

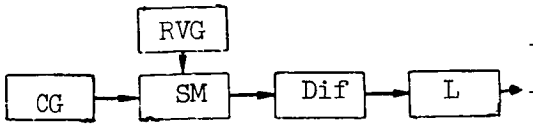

Figure 4.4

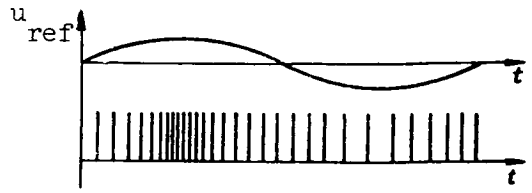

Figure 4.5

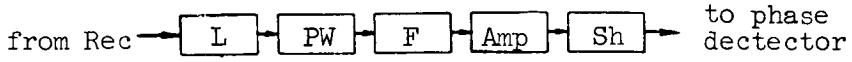

Figure 4.6

of a reference signal but quite complex systems of coding and decoding are necessary for its use.

The brief analysis made above shows that PFM is the most convenient form of modulation for transmission of a reference signal. For example, such modulation is used in the control system of the "Oerlikon" rocket (ref. 14).

On the transmitting end the PFM modulator is designed most simply using the conversion of PWM into PFM. The functional diagram of such a modulator is shown in figure 4.4. The video pulses from the cadence generator CG, which serves as a radar set synchronizer, are fed to the slave multivibrator SM and periodically trigger it. At the same time a sinusoidal reference voltage from the RVG is fed to the grid circuit of the multivibrator. Square pulses are formed at the output of the mutlivibrator. The pulse duration is proportional to the voltage fed to a differentiator Dif and then to a limiter L. The limiter suppresses the pulses corresponding to the times of trig- /167
gering of the multivibrator. Therefore, a sequence of pulses is formed at its output. The position of each of these pulses will be determined by the value of the modulating voltage (fig. 4.5). The resulting sequence is used for triggering the radar set transmitter.

The channel for detection of the reference signal in the considered type of modulation contains a limiter and demodulator. The limiter is designed to eliminate the amplitude modulation caused by the deflection of the rocket from an equisignal direction. The circuitry of the demodulator can be designed in different ways. The detection of the component of the reference signal contained in the received sequence of pulses can be accomplished by use of a band filter tuned to this frequency. The mentioned component is increased by placing a pulse widener in front of the filter. As an example, figure 4.6 shows the functional diagram of the reference signal channel when the signal is transmitted by PFM. It consists of a limiter L, a pulse widener PW, a filter F, an amplifier Amp and a shaper Sh. In the shaper the reference signal assumes the necessary shape and is brought to the required strength.

In the second method for transmission of the reference signal, when the maximum of the directional diagram of the radar set antenna intersects certain characteristic points, the radar radiates special cadence pulses which differ

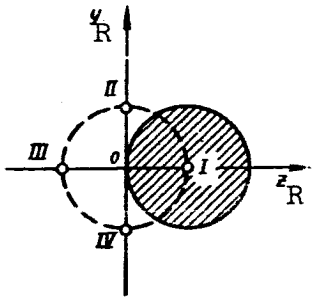

Figure 4.7

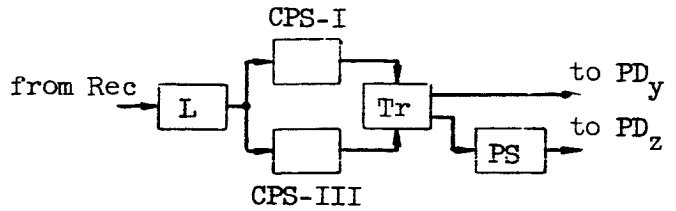

Figure 4.8

from the main sequence with respect to some qualitative criterion, such as duration, timing code, additional modulation, etc. (ref. 2).

In figure 4.7, the crosshatched circle represents the cross section of the directional diagram of the radar set antenna, and the dashed line denotes the path covered by its maximum during rotation about the equisignal line. /168 The point o denotes the trace of this line on the sectional plane. The figures I, II, III and IV denote the right, upper, left and lower positions of the directional diagram, respectively. The reference signal can be transmitted either by two cadence pulses radiated at times corresponding to the passage of the diagram through the points I, III or II, IV, or four cadence pulses corresponding to the passage of the diagram through the points I, II, III and IV.

Figure 4.8 shows the functional diagram of the reference signal channel in the case of signal transmission by two cadence pulses radiated at points I and III. The received sequence of pulses is fed from the output of the receiver to the limiter L, eliminating the amplitude modulation of the signal. This is followed by two cadence pulse selectors CPS-I and CPS-III. The circuits of the selectors are selected on the basis of what qualitative criteria are imposed on the cadence pulses. The selector CPS-I separates out from the entire sequence only the cadence pulses radiated at point I and the selector CPS-III, only those radiated at point III. The selected pulses activate the trigger Tr, whose output voltage serves as the reference signal for the longitudinal deflection channel (deflection along the oy_R axis). The lateral deflection signal (for deflection along the oz_R axis) is formed by shifting the rotation of the diagram by a quarter period in the phase shifter PS. If the cadence pulses are radiated at points II and IV, the voltage from the trigger is fed to the phase detector of the lateral deflection channel and from the phase shifter to the phase detector of the longitudinal deflection channel.

The functional diagram of the reference signal changes somewhat during the transmission of four cadence pulses (fig. 4.9). After passing through the /169 limiter L, the received sequence of pulses is fed to four cadence pulse selectors CPS-I, CPS-III, CPS-II and CPS-IV. The selected pulses activate the two triggers Tr_1 and Tr_2. The trigger Tr_1 produces the reference voltage of

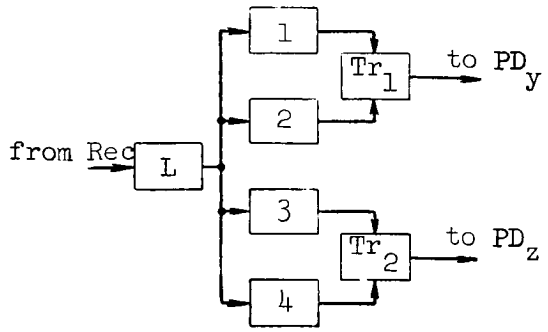

Figure 4.9

the longitudinal deflection channel and Tr_2 the reference voltage for the lateral deflection channel.

4.5. Block Diagram of the Coordinator of a Beam-Riding Control System

Now we will discuss the block diagram of a beam-riding control system for a case when the radar set forming the beam automatically tracks the direction of the target, that is, when the rocket is guided by the coincidence method.

Figure 4.10 shows the relative position of the target, rocket and radar beam for some moment of time. Here $o_c x_{ec} y_{ec} z_{ec}$ is a ground coordinate system whose origin is at the site of the radar station. The directions to the target and rocket are given by the angles ϵ_{tv}, ϵ_{th}, ϵ_{rv} and ϵ_{rh}, respectively. The position of the radar beam is characterized by the angles ϵ_{Rv} and ϵ_{Rh}.

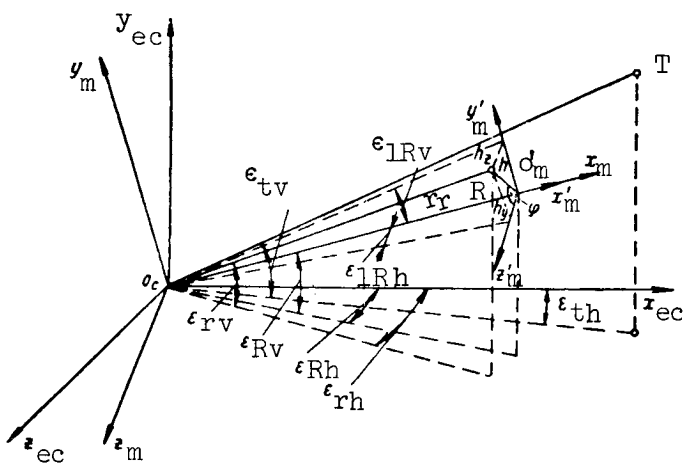

Figure 4.10

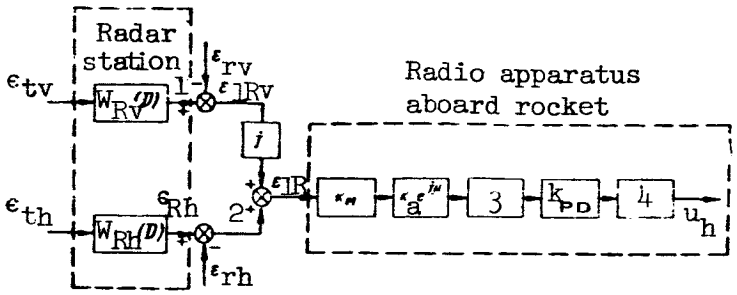

Figure 4.11

Due to the errors of the system for automatic tracking of the target by angular coordinates, which occur under real conditions, the direction of the beam does not coincide with the radar set-target line. Since the apparatus aboard the rocket measures the mismatch signal characterizing the displacement of the rocket in relation to the radar beam, it is convenient to introduce a measurement coordinate system $o_c x_m y_m z_m$, whose axis $o_c x_m$ is directed along the axis of the beam and whose axes $o_c y_m$ and $o_c z_m$ are situated in the vertical and horizontal planes, respectively. The position of the rocket in the measurement coordinate system can be given by different methods, especially by the/170 range r_r and the two linear deflections h_y and h_z, or the range r_r and the two angular deflections ϵ_{lRv} and ϵ_{lRh}.

In addition, the linear displacement of the rocket relative to the beam is given by the coordinates h and φ, where $h = \sqrt{(h_y)^2 + (h_z)^2}$ and $\varphi = \text{arc tan } \frac{h_y}{h_z}$.

The controlling effects for the coordinator of the beam-riding control system will be the angular movements of the target $\epsilon_{tv} = \epsilon_{tv}(t)$ and $\epsilon_{th} = \epsilon_{th}(t)$. These movements are measured by the radar and this establishes the necessary direction of the equisignal line ϵ_{Rv} and ϵ_{Rh}. Here

$$\left.\begin{aligned} \epsilon_{Rv} &= W_{Rv}(D)\ \epsilon_{tv}, \\ \epsilon_{Rh} &= W_{Rh}(D)\ \epsilon_{th}. \end{aligned}\right\} \qquad (4.5.1)$$

In the block diagram figure 4.11, the mentioned conversions are shown to occur in links with the transfer functions $W_{Rv}(D)$ and $W_{Rh}(D)$. In the case of guidance by the coincidence method they represent the transfer functions of

the vertical and horizontal deflection channels of the closed system for automatic tracking of the target in direction.

If the rocket is guided to a future position, the mentioned links reflect the dynamic properties of the radar set tracking the target, of the computer calculating the future position and of the radar set creating the radar beam.

In the case of small deflections of the rocket from an equisignal direction and in the case of a small angle of elevation of the latter ϵ_{Rv}, the angular mismatches ϵ_{lRv} and ϵ_{lRh} can be determined as

$$\left.\begin{aligned}\epsilon_{lRv} &= \epsilon_{Rv} - \epsilon_{rv},\\ \epsilon_{lRh} &= \epsilon_{Rh} - \epsilon_{rh}.\end{aligned}\right\} \qquad (4.5.2)$$

In the case of small mismatch angles, it is convenient to introduce the complex angle $\epsilon_{lR} = \epsilon_{lRh} + j\epsilon_{lRv}$. Then the considered block diagram is represented by the links of a single-channel system.

The first link (modulator) relates the angular mismatch of the rocket /171 ϵ_{lR} to the complex amplitude of the mismatch signal at the output of the peak detector.

The transfer coefficient of the link k_M is equal to

$$k_M = U_p k_m k_D.$$

The next link is the mismatch signal amplifier. The amplifier transfer coefficient can be used to take into account the presence of an additional phase shift between the reference voltage and the mismatch signal if it is assumed that this coefficient has the complex value $k_a = k_a e^{j\mu}$. The additional phase shift μ is caused by various factors: a signal delay in the mismatch signal channel, inaccuracy of transmission of the reference voltage from the radar set, etc. The mentioned shift causes a twisting of the axes of the measurement and command coordinate systems.

The range potentiometer, following the amplifier, has a variable amplification factor k_{potr_r}. Its value increases with an increase of the range r_r between the radar set and the rocket.

The last two links--the phase detector and the dc amplifier--are characterized by the transfer coefficients k_{PD} and k_{DCA}. If it is necessary to

take into account the inertia of the phase detector, the coefficient k_{PD} should be replaced by the transfer function $W_{PD}(D) = \frac{k_{PD}}{T_{PD}D+1}$, where T_{PD} is the time constant of the phase detector filter.

The electronic apparatus carried aboard the rocket as a component part of the beam-riding control system is characterized by the transfer coefficient k_{DF}, representing the product of the above-mentioned coefficients, that is

$$k_{DF} = U_p k_m k_D k_a k_{pot} \partial^r r k_{PD} k_{DCA} e^{j\mu}. \tag{4.5.3}$$

It establishes the relationship between the angular value of the mismatch u_{1R} and the measured value of this mismatch ϵ_h

$$u_h = k_{DF}\epsilon_{1R}. \tag{4.5.4}$$

If $\mu = 0$, the transfer coefficient of the apparatus carried aboard the rocket will be a real value and both measurement channels will become independent. Then

$$\left.\begin{aligned} u_y &= k_{DF}\epsilon_{1Rv}, \\ u_z &= k_{DF}\epsilon_{1Rh}. \end{aligned}\right\} \tag{4.5.5}$$

We note that k_{DF} increases with an increase of the range between the rocket and the radar set. The latter means that the angular sensitivity of the coordinator of the beam-riding control system increases with an increase of r_r.

In the case of small angles ϵ_{1Rv} and ϵ_{1Rh} it can be assumed that /172

$$\left.\begin{aligned} \varepsilon_{1Rh} &\approx \frac{h_z}{r_r}, \\ \varepsilon_{1Rv} &\approx \frac{h_y}{r_r}. \end{aligned}\right\} \tag{4.5.6}$$

After substituting the values ϵ_{1Rv} and ϵ_{1Rh} from (4.5.6) into (4.5.5), we obtain

$$\left.\begin{aligned} u_z &\approx k'_{DF} h_z, \\ u_y &\approx k'_{DF} h_y, \end{aligned}\right\} \qquad (4.5.7)$$

where $k'_{DF} = \frac{k_{DF}}{r_r}$ is the transfer constant of the apparatus aboard the rocket used for determination of linear deflection.

Thus, due to the introduction of a range potentiometer, the sensitivity of the coordinator for linear deflection becomes a constant value. In this connection, it sometimes is said that the range potentiometer performs a scaling of a conical coordinate system into a cylindrical coordinate system.

The principal regulations which are performed in the output apparatus of a coordinator for a beam-riding control system are similar to the regulations of the output apparatus of a direction finder with an integral equisignal direction. These include: establishing a balance in the output stages, phasing and establishing nominal amplification.

4.6. Characteristics of Operation of a Coordinator in the Launching Segment

The initial or launching segment of the trajectory continues from the time of launching of the rocket to its entry on the radio beam. In the first stage of the launching segment the rocket is controlled by an autonomous (programmed) guidance system.

A stable transition from autonomous flight to radio beam control, that is, stable entry of the rocket into the beam, is possible only when a number of conditions are met. For example, it is of great importance to select the value of the angle at which the rocket approaches the radio beam. If this angle is sufficiently great, the rocket rapidly enters an equisignal zone, but there is danger of "jumping" of the radio beam and therefore a disruption of guidance. In the case of a small angle of approach, the process of entry into the beam is prolonged and can be disrupted due to distortion of the mismatch signal, when the rocket passes through the zone of the side lobes of the directional diagram of the radar set antenna, and disruption of the phase relations between the reference signal and the mismatch signal.

The value of the admissible angle of entry of the rocket into the beam is determined by a number of factors: width of the directional diagram of the radar set antenna, amplification factor of the system, properties of the rocket, etc. The computed value of this angle is assured by proper orientation of the launching apparatus relative to the axis of the radio beam at the time of rocket launching. For rockets with a small effective range it also is of considerable importance to take into account the time required for the attenuation of transient processes after the rocket has entered the beam. /173

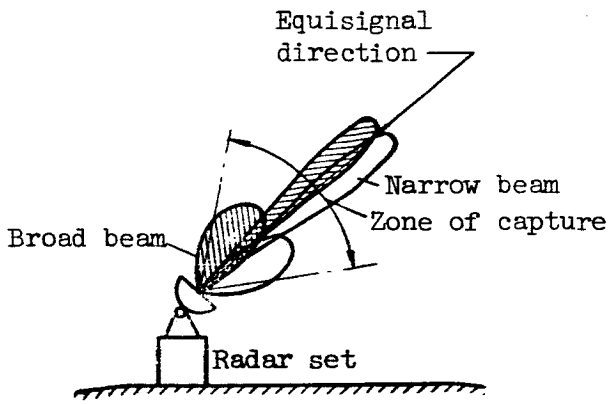

Figure 4.12

The process for entry of the rocket into the radio beam is facilitated by using a radar set with two beams--broad and narrow (ref. 14). Such a set contains two transmitters operating at spaced frequencies and feeding two antennas, one of which forms a beam with a width of 20°, and the other with a width of 3° (fig. 4.12). The rocket is controlled initially by the signals of the broad-beam transmitter. After the intensity of modulation of the broad-beam signals becomes less than a stipulated value, there is automatic switching aboard the rocket to control by narrow-beam signals. In such a system, in addition to retention of accuracy associated with guidance by a narrow beam, the conditions are superior for entry of the rocket into the radio beam due to the use of a broad beam.

A number of specific peculiarities arise in the coordinator of a beam-riding control system in the process of passage of a rocket through the zone of the side lobes and discontinuous irradiation.

One of these peculiarities can be attributed to the presence of a considerable level of the side lobes in the directional diagram of the radar system which can cause the formation of spurious equisignal directions. If the slope of the direction-finding chraracteristic in the spurious equisignal zone has the same sign as in the principal control zone, there is a danger of the rocket being caught in the spurious equisignal direction. If the signs of the slope of the mentioned characteristics are opposite, the rocket will be repulsed from the radio beam instead of being drawn into it.

Disruption of operation of a beam-riding control system in the launching segment of the trajectory also can occur when there is a low level of the side lobes due to the presence of a so-called zone of discontinuous radiation. Figure 4.13 shows the envelopes of video pulses at the output of the receiver with a change of the angle ϵ_{1R} between the rocket and the equisignal /174

direction. The envelopes were constructed without taking into account the effect of the automatic volume control of the radio receiver. Curve 1 corresponds to small angular deflection. Curves 2, 3 and 4 were constructed for increasing angles of deflection.

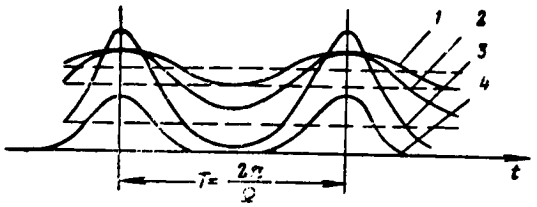

Figure 4.13

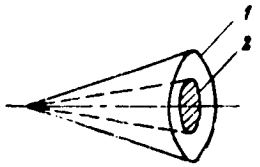

Figure 4.14

The figure shows that the amplitude of the mismatch signal first increases together with an increase of the angle ϵ_{1R}, and then begins to decrease. In the case of large angular deflections the signal at the output of the receiver constitutes individual groups of video pulses repeated with the frequency of rotation of the diagram. The amplitude and duration of the groups decrease with an increase of the angle ϵ_{1R}. The space around the axis of rotation of the directional diagram of the radar set can be broken down into three zones with conical surfaces, whose intersections with the planes perpendicular to the axis of rotation of the diagram form concentric circles 1 and 2 with centers on this axis. (fig. 4.14). The zone of continuous radiation or the zone of normal operation is the part of the space in which the intensity of the signals reaching the input of the radio receiver of the rocket is always greater than the response threshold. The section of the zone of continuous radiation in figure 4.14 is crosshatched. In the zone of discontinuous radiation, the intensity of the signals reaching the input of the radio receiver of the rocket, during some part of the period of rotation of the radar set antenna diagram, becomes less than the response threshold of the receiver. In figure 4.14, the section of this zone is represented by the ring between the outer circle and the crosshatched circle. Finally, the zone where there is no radiation is the remaining part of the space. When the effect of automatic volume control of the radio receiver is taken into account, these zones remain but change their size.

In the zone of discontinuous radiation, the received signal has the form of a group of pulses repeated with the frequency of rotation of the diagram. This character of the received signal is reflected both on the operation of the mismatch signal channel and on the operation of the reference signal channel.

In the first channel, this is expressed in a rather sharp decrease of the transfer constant k_{DF}. However, in some cases the operation of the second channel is disrupted completely. For example, in the transmission of a reference signal using additional pulse-frequency modulation, the voltage formed at the output of the reference signal channel will contain a rather considerable component of the mismatch signal in addition to the reference signal. The presence of this component in the reference voltage disrupts the regularity of breakdown of the mismatch signal in the phase detectors, and the output signal of the coordinator will not correspond to the actual deflection of the rocket

from the equisignal direction. In the case of transmission of voltage by cadence pulses, disruption of the operation of the reference signal channel in the zone of discontinuous irradiation is caused by the absence of individual cadence pulses when there is no radiation. /175

In each specific case, computation of the zone of the side lobes and discontinuous radiation makes it possible to determine the time of transition of the rocket from autonomous flight to beam-riding control. This transition should occur only after the rocket overcomes this zone.

4.7. Evaluation of the Accuracy of a Coordinator of a Beam-Riding Control System

The method for evaluating the accuracy of a coordinator in a beam-riding control system will be considered using the example of rocket guidance by the coincidence method. It will be assumed that there are no cross connections between measurement channels, and therefore the errors of only one measurement channel need be taken into account. For unambiguity, we will consider the case of measurement of the mismatch parameter for guidance in a vertical plane.

We recall that in the coincidence method the mismatch parameter is the angular or linear displacement of the rocket relative to the control point-target line, that is, $\Delta_{\varepsilon_1} = \varepsilon_1 = \varepsilon_t - \varepsilon_r$, or $\Delta_h = h \approx r_r \varepsilon_1$ (fig. 4.15). On the basis of the measured value of this parameter, a control or command signal is formed which causes the rocket to hold to the line o_cT. Errors in measurement of Δ_{ε_1} or Δ_h therefore will lead to inexact guidance of the rocket.

Different factors give rise to errors in measurement of the mismatch parameter. In particular, they arise due to inexact tracking of a target by the radar set forming the radio beam. This inaccuracy is caused by dynamic and fluctuation errors of the radar set. In addition, it can be caused by artificial noise created by the radar set.

Another group of errors in measurement of the mismatch parameter is caused by distortions of the signals in the apparatus carried aboard the rocket. These distortions arise due to the noise in the receiver, nonstationary absorption of radio waves in the jet and the effect of artificial interference on the radio apparatus carried aboard.

In theory all the mentioned errors can be taken into account and the total error in measurement of the mismatch parameter can be determined. /176 However, hereafter we will limit ourselves, in the computations, to a number of perturbing effects which should be taken into account when determining the accuracy of a coordinator of the considered type. We will compute only the measurement errors caused by fluctuation and dynamic errors of radar tracking of the target. We also will assume that the fluctuation errors of tracking are caused by fluctuations of the amplitude of the signal reflected from the target

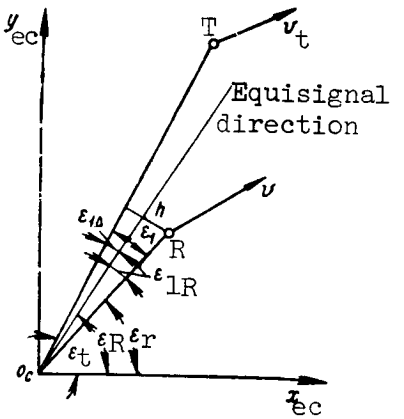

Figure 4.15

(amplitude noise) and noise interference created by the target. As was demonstrated earlier, the nature of its effect on a system for automatic tracking of a target based on measurement of angular coordinates and using conical scanning is identical. The angular noise caused by the disordered movement of the effective center of reflection of the target can be neglected due to the considerable distance between the radar tracking set and the target.

As a result of allowance for the errors in tracking of a target by a radar set in an analysis of the motion of the rocket and target in the plane $o_c x_{ec} y_{ec}$ (fig. 4.15) an additional component Δu_y, caused by the mentioned errors, appears in the output voltage of the channel for measurement of longitudinal deflection. Then the voltage at the output of the coordinator can be represented in the form

$$u'_y = u_y + \Delta u_y. \tag{4.7.1}$$

The voltage $u'_y = k_{DF}\varepsilon_{1R}$ characterizes the deflection of the rocket from the equisignal direction and the signal $u_y = k_{DF}\varepsilon_1 = k'_{DF}h$ is the measured value of the mismatch between the control point-target line and the direction to the rocket.

The additional voltage component Δu_y is equal to

$$\Delta u_y = k_{DF}\varepsilon_{1\Delta}. \tag{4.7.2}$$

The angle $\varepsilon_{1\Delta}$ between the line of sight and the direction of the radio beam is caused by the inaccuracy of tracking of the target by the radar set. It consists of two parts

$$\varepsilon_{1\Delta} = \varepsilon_{1\Delta\partial} + \varepsilon_{1\Delta f}, \qquad (4.7.3)$$

where $\epsilon_{1\Delta\partial}$ is the dynamic tracking error and $\epsilon_{1\Delta f}$ is the fluctuation error.

As was pointed out in section 3.11, the dynamic error of the system for automatic tracking of the target using angular coordinates is expressed by the formula

$$\varepsilon_{1\Delta\partial} = \frac{1}{1 + W_R(D)} \varepsilon_t, \qquad (4.7.4)$$

where $W_R(D)$ is the radar set transfer function.

By stipulating the specific law of change of the angle $\epsilon_t(t)$ it is /177

possible to determine the component of the dynamic error in the voltage measured by the coordinator

$$u_{\partial C} = k_{DF} \varepsilon_{1\Delta\partial}. \qquad (4.7.5)$$

The fluctuation error in measurement of the mismatch parameter, representing the voltage of low-frequency noise at the output of the coordinator, is

$$u_{nc} = k_{DF} \epsilon_{1\Delta f},$$

and is characterized by the spectral density $G_{nc}(\omega)$ or the dispersion σ^2_{nc} (it is assumed that the mathematical expectation of the random function $u_{nc}(t)$ is equal to zero).

The spectral density $G_{nc}(\omega)$ is determined using the formula

$$G_{nc}(\omega) = k^2_{DF} \left| F_R(j\omega) \right|^2 \cdot \frac{2G_m(\Omega)}{k^2_m R}, \qquad (4.7.6)$$

where $F_R(j\omega)$ is the frequency characteristic of the closed radar system, $G_m(\Omega)$ is the spectral density of the coefficient of noise modulation caused by fluctuations of the amplitude of the signals received by the radar set, and k_{mR} is the modulation transfer constant for the radar set used in tracking the target.

By using (4.7.6) it is easy to obtain the dispersion of the fluctuations of the measured voltage

$$\sigma^2_{nc} = \frac{1}{2\pi}\int_0^\infty G_{nc}(\omega)\, d\omega. \qquad (4.7.7)$$

The statistical characteristics of the fluctuation error of the coordinator usually are computed for some constant range between the rocket and the control point.

4.8. General Information on Coordinators Using Radio Navigation Measurement Apparatus

Coordinators of radio zone (beam-riding) control systems which employ radio navigation measurement apparatus can be used on rockets guided along fixed trajectories. As already mentioned, the guidance of rockets along fixed trajectories is the practice in those cases when the launching point, control point and target are fixed relative to the Earth's surface. Under these conditions the function of the coordinator is reduced essentially to determination of the deflection of the rocket from the stipulated reference trajectory. It was noted earlier that the coordinators of systems for the guidance of winged rockets along fixed trajectories should contain three measurement channels: altitude, lateral deflection and remaining range.

The coordinators of systems for the control of ballistic rockets /178
include channels for measurement of lateral deflection, velocity and inclination of the trajectory. Navigation measurement apparatus is used most frequently for measurement of the mismatch parameters for lateral deflection, remaining range and velocity. Hereafter emphasis will be on the design of coordinators for winged rockets, although for some measurement apparatus it will be noted that they can be used for measurement of the mismatch parameters in systems for guidance of ballistic missiles. For the sake of unambiguity, in the classification of coordinators with navigation measurement apparatus given below the basis used is the type of measuring instrument used for the lateral deflection channel. On the basis of this criterion, the mentioned coordinators can be grouped as angle-measuring, angle-measuring – range-finding, range-finding and add-subtract – range finding. In the sections which follow, we will give the diagrams of coordinators employing the mentioned types of measuring instruments and we will clarify the functional changes which the measured values must experience for formation of the mismatch parameters. The basic considerations involved in evaluation of the accuracy of coordinators of the mentioned types also will be given.

Since hereafter we will consider the possibilities of measuring the mismatch parameter only for the lateral deflection and remaining range channels, all the graphic constructions associated with the rocket trajectories will be made in a horizontal plane without taking into account the curvature of the

Earth's surface. In case of necessity the curvature of the Earth's surface can be taken into account without special difficulty, but this somewhat complicates the final formulas, depriving them of their graphic character.

4.9. Coordinators Based on the Use of Radio Navigation Angle-Measuring Apparatus

The apparatus of a coordinator based on use of radio navigation angle-measuring apparatus consists of two parts: one on the ground and the other carried aboard the rocket. The ground part of the coordinator is situated at the control point, in the immediate vicinity of the rocket launching point. A vertical equisignal plane oriented along the rocket launching point-target line is formed by the ground apparatus, which consists of a transmitter and antenna system.

Figure 4.16 shows the position of the launching point of the rocket o_c, the rocket itself R and the target T. The notations used in figure 4.16 correspond to the notations used in figure 2.1.

The equisignal plane formed by the ground apparatus of the coordinator is oriented along the axis $o_c x_m$ by means of a positioning apparatus for an angle β_0 determined from the map.

In principle the operation coordinators of the angle-measuring type differ little from the coordinators of beam-riding control systems considered above. In this case the formation of the equisignal plane is accomplished/179 either by rotation of the narrow directional diagram of the antenna, whose maximum is displaced relative to the axis of rotation, or by oscillation of the diagram in a small range. In addition, the ground apparatus forms and transmits to the rocket a reference signal which carries information on the change of the position of the maximum of the directional diagram.

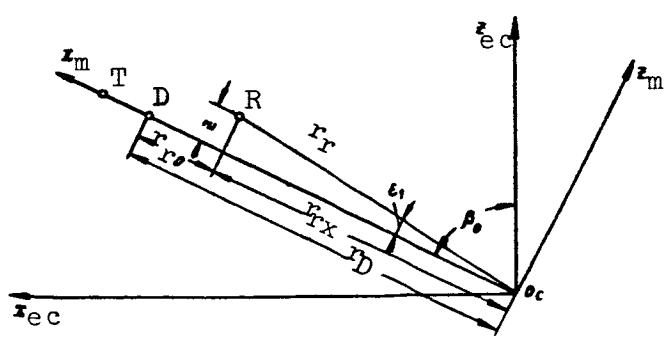

Figure 4.16

The electronic apparatus carried aboard the rocket includes an antenna, a receiver and an output. In turn, the latter includes: a mismatch signal channel, a reference signal channel, a phase detector and a dc amplifier. A range potentiometer is included in the mismatch signal channel so that the output voltage of the coordinator will be proportional to the linear deflection of the rocket from the equisignal plane. Since such a coordinator should measure rocket deflection only in the course plane, the output contains only one phase detector.

The output voltage u_z of the coordinator in the case of small deflections of the rocket from the reference trajectory is

$$u_z = k'_{DF} z, \tag{4.9.1}$$

where $k'_{DF} = \frac{k_{DF}}{r_r}$, and k_{DF} is determined using formula (4.5.3).

In the case of guidance of winged rockets, the control point or the rocket must have data on the remaining range r_{ro}, that is, the distance between the rocket and the point where it begins its dive. On the basis of these data, a command is formed for diving. Such data cannot be obtained using the coordinator described above and it therefore is supplemented by a range-finding system. An interrogator is included in the ground apparatus and a responder is carried on the rocket for measurement of the range from the control point to the rocket r_r. Using such a system the range r_r is measured at the control point on the basis of the delay of the response pulse relative to the interrogation pulse. Since with a sufficient degree of accuracy $r_r \approx r_{rx}$, /180

the mismatch parameter of the remaining range channel is expressed as

$$\Delta_{ro} = r_D - r_{rx}. \tag{4.9.2}$$

The command for the rocket to begin its dive is produced at the time when the mismatch Δ_{ro} becomes equal to zero.

In the case of guidance of ballistic missiles there usually is no need of a range channel and the angle-measuring coordinator is used only for the purpose of lateral correction of the rocket in the active part of the trajectory.

As an example of the use of such a coordinator we will examine the lateral correction apparatus of the V2 rocket (ref. 4).

The functional diagram of the coordinator is shown in figure 4.17. The equisignal plane is created by an antenna system consisting of two half-wave vibrators V_1 and V_2, spaced at the distance $d_a \gg \lambda$, where λ is the wavelength.

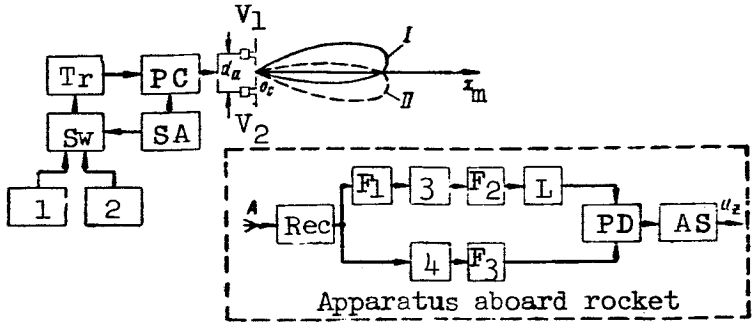

Figure 4.17

The form of the interference pattern created by the lobes of the diagrams is dependent on the phase shift of the currents in the vibrators. With a change of the current phase in the antennas by $\pm \frac{\pi}{2}$, the diagrams are displaced by a small angle (about 1°), that is, the major lobes of the diagram occupy the position I or II. The diagrams are switched by the phase commutator PC, controlled by a synchronizing apparatus SA with the frequency F_{com} = 50 cps. At the same time, the synchronizing apparatus controls the switch of the subcarrier oscillations generators SOG_1 and SOG_2, which form sinusoidal voltages with the frequencies F_1 = 5000 cps and F_2 = 8000 cps. These voltages are fed through the switch Sw to the transmitter modulator. The switching of SOG_1 and SOG_2 is with the same frequency commutation F_{com} = 50 cps. Therefore, when the directional diagram of the antenna is in the position I, it radiates an amplitude-modulated voltage of the frequency F_1; with movement of the diagram into position II, the carrier is modulated by a voltage of the frequency F_2.

The apparatus carried on the rocket consists of an antenna, receiver and output device. The form of the received signal is dependent on the orientation of the rocket relative to the axis $o_c x_m$.

Figure 4.18 shows the temporal diagrams of the signal at the reception point for cases when the rocket is situated precisely on the axis $o_c x_m$ (fig. 4.18a), to the left of it (fig. 4.18b) and to the right of it (fig. 4.18c).

The signal is amplified and rectified in the receiver Rec. The temporal diagrams of the voltage at the receiver output, when the rocket is to the left and to the right of the line $o_c x_m$, are shown in figure 4.18d and e, respectively. The output device for the radio receiving

/181

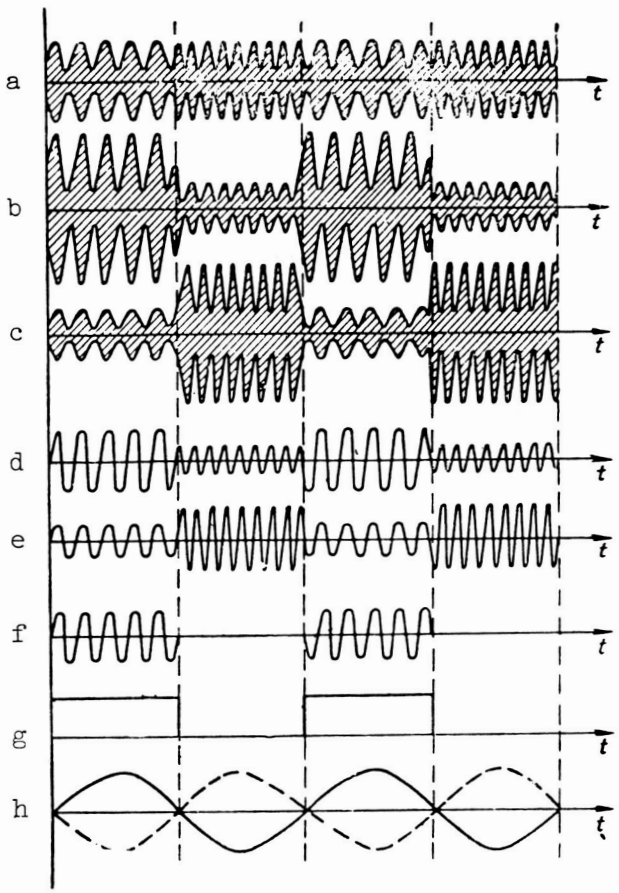

Figure 4.18

apparatus aboard the rocket includes a reference signal channel and a mismatch signal channel. The reference signal channel contains a filter F_1 which is tuned to a frequency F_1 = 5000 cps, a peak detector PkD_1, a filter F_2 tuned to a frequency F_{com} = 50 cps and a limiter L. The voltage curves for the output of the filter F_1 and the limiter are shown in figure 4.18f, g. We note that the initial phase of the reference voltage u_{ref} is not dependent on the direction of deflection of the rocket. This voltage is fed to the phase detector PD.

The mismatch signal channel contains a peak detector PkD_2 and a filter F_3 tuned to the frequency F_{com} = 50 cps. The voltage curves for the output of the channel are shown in figure 4.18h, where the solid curve represents

the mismatch voltage for deflection of the rocket to the left of the equisignal plane, while the dashed curve represents deflection to the right. The amplitude of this signal within the limits of the direction-finding characteristic will be proportional to the angle ϵ_1 (fig. 4.16) and the phase changes by 180° with a change of the direction of deflection. The mismatch signal also is fed to the phase detector. The value and sign of the rectified voltage at the output of the phase detector are dependent on the value and direction of deflection of the rocket from the equisignal plane. /182

In the amplification stage AS, which follows the phase detector, there is a range potentiometer which is controlled by a programming mechanism. As a result, the mismatch voltage at the output of a coordinator of the considered type will be proportional to the linear deflection of the rocket from the equisignal plane.

The sources of errors of coordinators of the angle-measuring type are: inaccuracy of setting of the equisignal plane, distortions of the plane due to reflections from the Earth and local features, instrument noise of the receiver and external interference.

In order to decrease the errors caused by instrument noise of the receiver, the power of the transmitter of the ground station is selected in such a way that, at the maximum computed range, the power of the received signal will be an order of magnitude greater than the instrument noise.

4.10. Coordinators Based on Use of Angle-Measuring–Range-Finding Radio Navigation Apparatus

By use of a navigational angle-measuring–range-finding system aboard a rocket or aircraft, it is possible to measure its polar coordinates (range and azimuth) relative to some navigation point. When a computer is included in the apparatus aboard, such a system makes it possible to determine (using the measured values of range and azimuth) the deviation of the craft from the stipulated course and the path it has covered. Such a system, therefore, can be used as the basic system for designing the coordinator of a rocket to be guided along a linear fixed trajectory.

A coordinator of such a type consists of two parts: one on the ground and the other on the rocket. The ground apparatus of the coordinator is installed at the control point, which can be some distance from the point of the rocket launching.

Different designs of an angle-measuring–range-finding coordinator are possible. In order to be specific, we will assume that it is designed on the basis of the "Tacan" navigation system (ref. 11).

The simplified functional diagram of the coordinator is shown in figure 4.19. The ground part of the coordinator is an omnidirectional /183

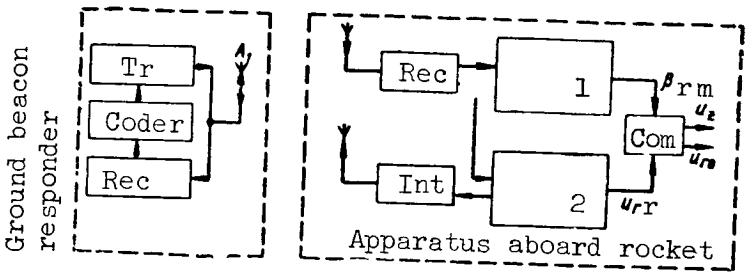

KEY:
1, Angle-measuring channel
2, Range-measuring channel

Figure 4.19

phase transponder. It consists of a receiver of interrogation pulses Rec, a coder, designed for coding of response signals, a transmitter Tr and an antenna system A_1. The directional diagram of the antenna, constituting a nine-lobe cardioid, is rotated in a horizontal plane with a constant angular velocity Ω_M. As a result, the radio beacon signals at the reception point are amplitude-modulated with the frequency Ω_M. The phase of the envelope of the received pulses is dependent on the azimuth of the reception point. The reference signal required for determination of the azimuth is transmitted in the form of coded pulses radiated when the maximum of the cardioid passes through north.

The apparatus carried aboard the rocket includes: a pulse interrogator Int, a receiver of response pulses Rec, an angle measurement channel, a range measurement channel and a computer Com.

The range between the beacon and the rocket r_{br} is measured from the time which elapses from the time of radiation of the interrogation pulse to the time of reception of the response pulse. The synchronization of the interrogator and the triggering of the range phantastron of the circuit for measurement of r_{br} is accomplished using a single synchro-generator placed in the range measurement channel. The position of the response pulses is compared in the time discriminator with the position of a pair of strobe pulses formed from clipping of the pulse of the range phantastron. In the case of a mismatch between the mentioned pulses, an error signal is produced which acts on the control apparatus, the latter being an electric motor to which a potentiometer is connected. The voltage of this potentiometer controls the pulse duration of the range phantastron. Under the influence of the error signal, the pulse duration of the range phantastron will vary until the strobe pulses coincide with the responder pulses. Obviously, in this case the voltage across the potentiometer of the control apparatus will be proportional to the distance r_{br} between the beacon and the rocket, that is, it will represent the instrument analog of the mentioned range.

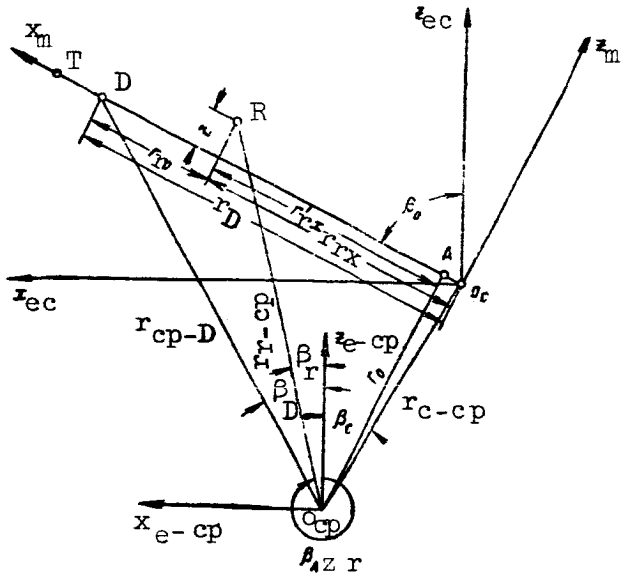

Figure 4.20

The principle of measurement is measurement of the phase of the envelope of the received pulses in relation to the phase of the reference signal. The angle-measurement channel, therefore, in many respects is similar to the channel for measurement of angular mismatch of the coordinator of the angle-measuring type considered in the preceding section.

Since the geographical coordinates of the launching point o_c, of the control point o_{cp} and the point of transition of the rocket into a dive D are known, the initial data for guidance can be obtained from a map or by computations. These include: the angular coordinates of the target, launching point and point of transition of the rocket into a dive β_0, β_c and β_D, and also the ranges r_D, r_{c-cp} and r_{cp-D} (fig. 4.20).

In addition, the minimum distance r_0 from the control point to the /184 axis $o_c x_m$ is considered known. This distance is determined from a map or is computed using the formula

$$r_0 = r_{cp-D} \sin (\beta_0 - \beta_D). \qquad (4.10.1)$$

The rocket measures the range r_{r-cp} between the rocket and control point and the angle β_r, equal to $\beta_r = 360^\circ - \beta_{az\ r}$, where $\beta_{az\ r}$ is the azimuth of

the rocket in a coordinate system related to the control point. Figure 4.20 shows that the lateral deflection of the rocket from the reference trajectory can be determined using the formula

$$z = r_{r\text{-}cp} \sin (\beta_0 - \beta_r) - r_0. \qquad (4.10.2)$$

The remaining range to the point of diving r_{ro} is determined from the expression

$$r_{ro} = r_D - r_{rx} = r_{cp\text{-}D} \cos (\beta_0 - \beta_D) - r_{r\text{-}cp} \sin (\beta_0 - \beta_r). \qquad (4.10.3)$$

Formulas (4.10.2) and (4.10.3) determine the work program of the computer used for computation of the mismatch parameters of the coordinator for the lateral deflection, and of the remaining range channels for rocket guidance by the method of coincidence with the reference trajectory.

At the output of the coordinator we obtain instrument analogs u_z and /185 u_{ro} of the mismatch parameters $\Delta_z = -z$ and $\Delta_{ro} = r_D - r_{rx}$

$$u_z = u_{rr} \sin (\beta_{0m} - \beta_{rm}) - u_0, \qquad (4.10.4)$$

$$u_{ro} = u_{r\text{-}cp} - u_{rr} \cos (\beta_{0m} - \beta_{rm}), \qquad (4.10.5)$$

where u_{rr}, u_0, $u_{r\text{-}cp}$ are the instrument analogs of the ranges $r_{r\text{-}cp}$, r_0, $r_{cp\text{-}D} \cos (\beta_0 - \beta_D)$, and β_{0m}, β_{rm} are the instrument analogs of the angles β_0 and β_r.

The functional diagram of one of the possible designs of the computer for the lateral deflection channel is shown in figure 4.21.

The voltage u_{rr}, proportional to the range between the rocket and the control point, is fed to the sine-cosine potentiometer SCP. This potentiometer is designed in the form of a rectangular plate of insulating material covered by a semiconducting layer. The voltage u_{rr} is applied to the opposite ends of the plate. Two pairs of brushes I, I' and II, II', oriented perpendicular to one another, are attached to the o-axis of the potentiometer.

The signal from the brushes I, I' is proportional to the sine of the angle $\beta_{0m} - \beta_{rm}$, and the voltage between the brushes II, II' is proportional to

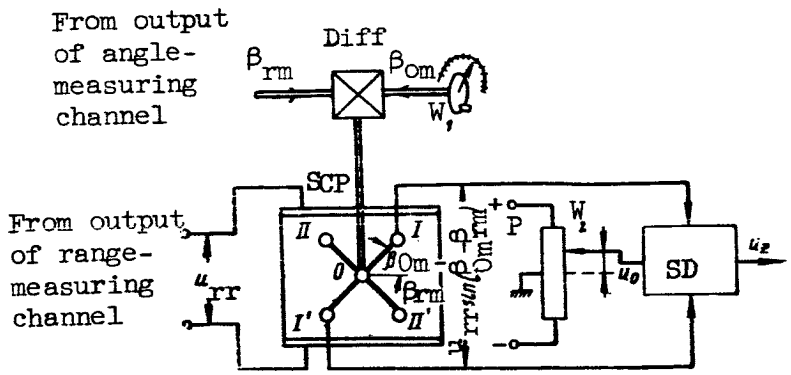

Figure 4.21

the cosine of this angle. The brushes are turned about the o-axis by a shaft connected to the differential Diff. The differential is used in forming the difference of the angles β_{0m} and β_{rm}. The angle β_{0m} is set by the wheel W_1 before launching of the rocket and β_{rm} is introduced from the angle-measuring channel.

The voltage $u_{rr} \sin (\beta_{0m} - \beta_{rm})$ from the brushes I, I' of the sine-cosine potentiometer is fed to the subtracting device SD. The latter also is fed the voltage u_0, set by the wheel W_2, connected to the slide of the potentiometer P. The setting of the required value u_0 also is accomplished before the rocket launching. The instrument analog of the mismatch parameter Δ_z of /186 the lateral deflection channel is formed at the output of SD. A computer of this type can be used also for measurement of the mismatch parameter of the remaining range channel.

Study of the principle of operation of an angle-measuring – range-finding coordinator shows that its use gives a certain tactical flexibility of the control system because by the use of a single ground complex of equipment, it is possible to guide simultaneously several rockets launched from different launching sites. This requires only the introduction of appropriate initial data into the coordinator apparatus aboard the rocket.

The accuracy of operation of the coordinator is dependent on a whole series of factors. It is determined, in particular, by the accuracy of computation and the introduction of initial data. In addition, the accuracy of operation of the coordinator is influenced by instrument errors of the apparatus forming the current values of the mismatch parameter. Finally, the accuracy is dependent on the errors in measurement of range and azimuth caused by the presence of fluctuation components in the received signal caused either by noise in the receivers or interference acting on the radio apparatus carried aboard the rocket.

Now we will describe the method for evaluating the accuracy of a coordinator, taking into account only the fluctuation components, although the final formulas will make it possible to draw more general conclusions on the accuracy of the investigated coordinator.

In the analysis it will be assumed that interference does not change the transfer properties of the measuring instruments and its effect leads only to the appearance of additional fluctuation components in the measured angle and range values. Then the signal at the output of the range measurement channel can be written in the form: $u_{rr} + \Delta u_{rr}$, where u_{rr} is the undistorted value of the measured range between the rocket and the control point and Δu_{rr} is the random component of the measured range caused by noise in the receiver or interference. The output signal of the angle-measuring channel under these same conditions is written as $\beta_{rm} = \beta_r + \Delta\beta_r$.

Due to the mentioned random components, the measured values of the mismatch parameters of the lateral deflection and remaining range channels of the coordinator also receive additional fluctuation components, and therefore can be written in the form $u_z + \Delta u_z$ and $u_{ro} + \Delta u_{ro}$.

The components Δu_z and Δu_{ro} are determined as

$$\Delta u_z = \frac{\partial u_z}{\partial u_{rr}} \Delta u_{rr} + \frac{\partial u_z}{\partial \beta_r} \Delta \beta_r, \tag{4.10.6}$$

$$\Delta u_{ro} = \frac{\partial u_{ro}}{\partial u_{rr}} \Delta u_{rr} + \frac{\partial u_{ro}}{\partial \beta_r} \Delta \beta_r. \tag{4.10.7}$$

After substituting the values u_z and u_{ro} from (4.10.4) and (4.10.5) into equations (4.10.6) and (4.10.7) and performing the mentioned operations, we obtain /187

$$\Delta u_z = \sin(\beta_0 - \beta_r)\,\Delta u_{rr} - u_{rr}\cos(\beta_0 - \beta_r)\,\Delta\beta_r, \tag{4.10.8}$$

$$\Delta u_{ro} = -\cos(\beta_0 - \beta_r)\,\Delta u_{rr} - u_{rr}\sin(\beta_0 - \beta_r)\,\Delta\beta_r. \tag{4.10.9}$$

We will assume that Δu_{rr} and $\Delta\beta_r$ are stationary functions of time with mathematical expectations equal to zero. The latter can be attributed to the fact that when there is a low level of interference, the electrical symmetry of the circuits of the measurement channels usually is not disrupted. In addition, in the subsequent analysis we will apply the principle of "freezing" of range. This means that the determination of the statistical characteristics of the random functions Δu_z and Δu_{ro} will be made for determined constant

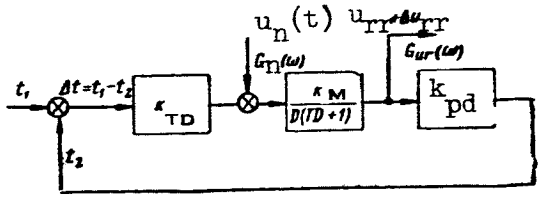

Figure 4.22

values of the range between the control point and the rocket. Under the mentioned conditions Δu_z and Δu_{ro} are stationary random functions with a zero mathematical expectation.

Assuming that the channels for measurement of range and angle are independent, for the spectral densities $G_{u_z}(\omega)$ and $G_{u_{ro}}(\omega)$ of the boosting noise voltages Δu_z and Δu_{ro} we obtain

$$G_{u_z}(\omega) = \sin^2(\beta_0 - \beta_r)\, G_{ur}(\omega) + u_{rr}^2 \cos^2(\beta_0 - \beta_r)\, G_\beta(\omega), \qquad (4.10.10)$$

$$G_{u_{ro}}(\omega) = \cos^2(\beta_0 - \beta_r)\, G_{ur}(\omega) + u_{rr}^2 \sin^2(\beta_0 - \beta_r)\, G_\beta(\omega). \qquad (4.10.11)$$

Here $G_{ur}(\omega)$ and $G_\beta(\omega)$ are the spectral densities of the random functions Δu_{rr} and $\Delta\beta_r$.

Formulas (4.10.10) and (4.10.11) show that for determination of $G_{u_z}(\omega)$ and $G_{u_{ro}}(\omega)$, it is necessary to know the spectral densities of the random components at the output of the angle-measuring and range-finding channels.

Since the method for determination of the spectral density of the noise component of the angle-measuring instrument has been presented in detail in chapter 3, here we will discuss only the method for computation of the spectral density $G_{ur}(\omega)$ of the fluctuation part of the voltage at the output of the automatic range finder.

The block diagram of the earlier considered channel for measurement of range is shown in figure 4.22. It includes three dynamic links. The link /188 with the transfer constant k_{TD} is for the time discriminator. The motor together with the reducer and recording potentiometer are represented by a link

with the transfer function $W_M(D) = \frac{k_M}{D(TD + 1)}$. The third link, with the transfer constant k_{pd}, reflects the properties of the pulse delay apparatus.

The input value to be measured is the time t_1 elapsing from the time of radiation of a sounding pulse to the time of reception of a response pulse. This time is proportional to the range $r_{r\text{-}cp}$. The value t_2 corresponds to the delay time of the strobe pulses. It is proportional to the voltage u_{rr}, determining the measured range value. The difference $\Delta t = t_1 - t_2$ serves as a mismatch measured by the time discriminator. Therefore, the voltage at its output will be proportional within certain limits of the mentioned difference.

If noise is superposed on the received signal, a random component of the mismatch signal $u_n(t)$ appears at the output of the time discriminator. In order to find $u_n(t)$, it is necessary to consider the problem of the passage of the signal and noise through the receiving channel and the time discriminator. In the solution of such a problem, it is most common to find not the random function $u_n(t)$ itself but its spectral density $G_n(\omega)$.

In a case when the time discriminator is subjected to wide-band noise passing through the dc amplifier, linear rectifier and video amplifier, the value $G_n(\omega)$ is equal to (ref. 36)

$$G_n(\omega) = (0.2\text{-}0.12)\,\frac{k_{TD}^2 t_{sp}^2 \sigma_{nv}^2}{T_{sp} U_{ap}^2 \omega^2}, \qquad (4.10.12)$$

where t_{sp} is the duration of the strobe pulses; σ_{nv}^2 is the dispersion of the noise voltage at the input of the time discriminator; T_{sp} is the repetition interval of the strobe pulses, and U_{ap} is the amplitude of the pulses at the input of the time discriminator.

The desired spectral density $G_{ur}(\omega)$ can be determined as

$$G_{ur}(\omega) = |F(j\omega)|^2 G_n(\omega). \qquad (4.10.13)$$

Here $F(j\omega)$ is the frequency characteristic of the closed control system if the point of application of u_n is considered the input and u_{rr} is considered the output.

The frequency characteristic $F(j\omega)$ corresponds to the transfer function

$$F(D)=\frac{W_M(D)}{1+W(D)}, \qquad (4.10.14)$$

where $W(D) = \frac{k_{TD}k_M k_{pd}}{D(TD+1)}$ is the transfer function of the open system for the automatic range-measuring instrument.

After the initial spectral densities of distortions of signals at the output of the channels for measuring angle and range $G_{ur}(\omega)$ and $G_{\beta}(\omega)$ have been determined, formulas (4.10.10) and (4.10.11) can be used to compute the spectral densities of the random components of the measured values of the mismatch parameters at the coordinator output. /189

It should be noted that if an analysis of operation of the coordinator, taking into account the fluctuations of the received signals, is used hereafter for evaluation of the accuracy of the entire system for guidance of the rocket to the target, a knowledge of the mentioned spectral densities is adequate for solution of such a problem. The method for computing the rocket miss, in the case of known statistical characteristics of distortions of the mismatch parameters, is presented in chapter 11.

In addition, formulas (4.10.10) and (4.10.11) can be used for computation of the accuracy of only one coordinator, as an element of a control system. A knowledge of the errors of measurement of the mismatch parameter makes possible an intercomparison of coordinators of different types with respect to accuracy and noiseproofing.

Now we will discuss the errors in measurement of the mismatch parameters of the lateral deflection and remaining range channels, characterized by the dispersions $\sigma^2_{u_z}$ and $\sigma^2_{u_{ro}}$.

Using the known relation between spectral density $G_x(\omega)$ of the random function $x(t)$ and its dispersion σ^2_x

$$\sigma_x^2=\frac{1}{2\pi}\int_0^{\infty} G_x(\omega)\,d\omega,$$

from (4.10.10) and (4.10.11) we find

$$\sigma^2_{u_z}=\sin^2(\beta_0-\beta_r)\,\sigma^2_{ur}+u^2_{rr}\cos^2(\beta_0-\beta_r)\,\sigma^2_{\beta}, \qquad (4.10.15)$$

$$\sigma^2_{u_{ro}}=\cos^2(\beta_0-\beta_r)\,\sigma^2_{ur}+u^2_{rr}\sin^2(\beta_0-\beta_r)\,\sigma^2_{\beta}, \qquad (4.10.16)$$

where σ_{ur}^2 is the dispersion of the error of the measured range value, and σ_β^2 is the dispersion of the error of the measured angle value.

For convenience it is possible to convert from voltages characterizing linear deflections to linear deflections themselves. Assuming that the instrument range value u_{rr} is related to its actual value $r_{r\text{-}cp}$ by the scale factor k_{act} (that is, when $r_{r\text{-}cp} = \text{const}$ $u_{rr} = k_{act} r_{r\text{-}cp}$), and assuming that the computer does not change the scale of range measurement, we obtain

$$\sigma_z^2 = \sin^2 (\beta_0 - \beta_r)\, \sigma_r^2 + r_{r\text{-}cp}^2 \cos^2 (\beta_0 - \beta_r)\, \sigma_\beta^2, \qquad (4.10.17)$$

$$\sigma_{ro}^2 = \cos^2 (\beta_0 - \beta_r)\, \sigma_r^2 + r_{r\text{-}cp}^2 \sin^2 (\beta_0 - \beta_r)\, \sigma_\beta^2. \qquad (4.10.18)$$

Here σ_z^2, σ_{ro}^2 and σ_r^2 are the dispersions of the errors of measurement of lateral deflection, remaining range and distance between the rocket and control point, respectively, expressed in linear units. /190

Formulas (4.10.17) and (4.10.18) show that for given errors in measurement of range and azimuth, characterized by the dispersions σ_r^2 and σ_β^2, the accuracy of determination of the mismatch parameters Δ_z and Δ_{ro} is dependent on the withdrawal of the rocket from the launching point and the control point.

We will characterize the position of the current point on the reference trajectory by the range r'_{rx} (fig. 4.20), that is, the withdrawal of the mentioned point from the intersection of the perpendicular dropped from o_{cp} on the axis $o_c x_m$ and this axis. Figure 4.20 shows that

$$r'_{rx} = r_{r\text{-}cp} \cos (\beta_0 - \beta_r).$$

Therefore,

$$\cos^2 (\beta_0 - \beta_r) = \frac{(r'_{rx})^2}{r_{r\text{-}cp}^2}, \qquad (4.10.19)$$

$$\sin^2 (\beta_0 - \beta_r) = \frac{r_{r\text{-}cp}^2 - (r'_{rx})^2}{r_{r\text{-}cp}^2}. \qquad (4.10.20)$$

Substituting (4.10.19) and (4.10.20) into (4.10.17) and (4.10.18), and also taking into account that for points of the reference trajectory $r^2_{r-cp} = (r'_{rx})^2 + r^2_0$, we obtain

$$\sigma_z^2 = \frac{r_0^2}{r_0^2 + (r'_{rx})^2}\sigma_r^2 + (r'_{rx})^2\sigma_\beta^2, \tag{4.10.21}$$

$$\sigma_{ro}^2 = \frac{(r'_{rx})^2}{r_0^2 + (r'_{rx})^2}\sigma_r^2 + r_0^2\sigma_\beta^2. \tag{4.10.22}$$

We introduce the relative range $a = \frac{r'_{rx}}{r_0}$ and we will characterize the dispersion of errors of the angle-measuring channel by the value

$$(\sigma'_\beta)^2 = r_0^2\sigma_\beta^2. \tag{4.10.23}$$

Then, for the mean square errors of measurement of lateral deflection and remaining range we will have

$$\sigma_z = \sqrt{\frac{1}{1+a^2}\sigma_r^2 + a^2(\sigma'_\beta)^2}, \tag{4.10.24}$$

$$\sigma_{ro} = \sqrt{\frac{a^2}{1+a^2}\sigma_r^2 + (\sigma'_\beta)^2}. \tag{4.10.25}$$

Analysis of formulas (4.10.24) and (4.10.25) shows that the errors in /191 measurement of the mismatch parameters will be minimal and equal to

$$\sigma_{z\ min} = \sigma_r,$$

$$\sigma_{ro\ min} = \sigma'_\beta.$$

at the point A of the reference trajectory, when a = 0.

With withdrawal from this point the errors of measurement of Δ_z and Δ_{ro} increase, and the error in measurement of lateral deflection increases most.

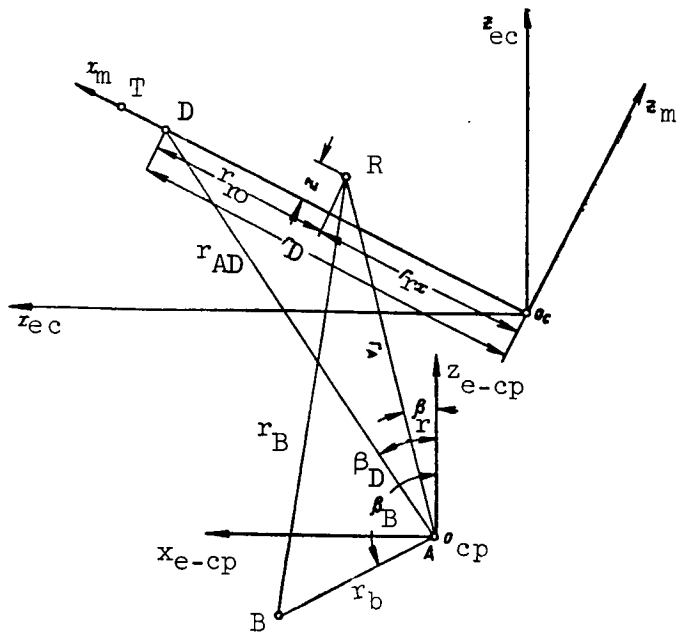

Figure 4.23

4.11. Coordinators Based on the Use of Range-Finding Radio Navigation Apparatus

When a range-finding navigation system is used, the position of the rocket is determined by measurement of the distances between it and two ground points whose coordinates are determined with a high accuracy. On the basis of such a system, it is possible to design a coordinator for measurement of the mismatch parameter for rocket guidance along a fixed trajectory.

The ground complex for such a coordinator consists of two stations situated at points A and B (fig. 4.23), each of which contains an antenna system, an interrogation signal receiver and a responder. /192

The apparatus carried aboard the rocket (fig. 4.24) usually includes an interrogation signal transmitter Tr, controlled by a synchronizer, a receiver Rec, two range measurement channels and a computer Com.

In pulse range-finding systems, the distances r_A and r_B are measured from the delay of the response signals received by the rocket from the stations A and B in relation to the time of radiation of the interrogation pulse.

We will assume that the mismatch parameters (lateral deflection and remaining range) are measured in the coordinate system $o_c x_m z_m$, whose axis $o_c x_m$ coincides with the launching point-target line (fig. 4.23).

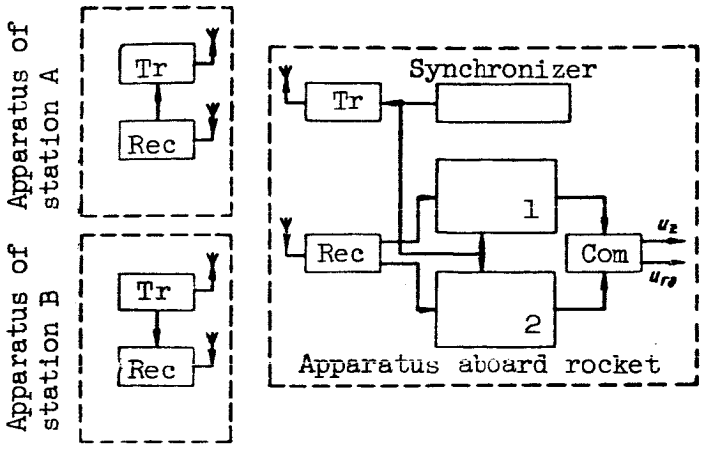

Figure 4.24

The values which are known before the launching of the rocket are: distance between stations r_b (system base), distances from each of the stations to the launching point o_c and the point of transition of the rocket into a dive D, and also the angles characterizing the relative position of the ground station, launching point and the point of transition of the rocket into a dive. The ranges r_A and r_B are measured during the guidance.

The problem of determining the mismatch parameters for the lateral deflection and remaining range channels, in the case of a coordinator of the range-finding type, is solved ambiguously, that is, several varieties of the formulas relating Δ_z and Δ_{ro} with the known and measured values can be proposed.

For this reason we will cite only one of the possible variants of the mismatch equations, when they are essentially the same as the equations for a coordinator of the angle-measuring—range-finding type.

If the angle β_r is expressed through known and measured values, it is /193 possible to write expressions for lateral deflection and remaining range in the form (4.10.2) and (4.10.3).

From figure 4.23 we find

$$\beta_r = \beta_B - \angle RAB, \qquad (4.11.1)$$

where β_B is the angle characterizing the position of station B. Since one side of the triangle RAB is known and the other two are measured during the guidance process, it is possible to determine any of its angles. In particular,

$$\angle \text{RAB} = 2 \arctan \frac{r}{p - r_b}, \tag{4.11.2}$$

where

$$p = \frac{1}{2}(r_A + r_B + r_b); \tag{4.11.3}$$

$$r = \sqrt{\frac{(p - r_A)(p - r_B)(p - r_b)}{p}}. \tag{4.11.4}$$

In accordance with (4.10.2) and (4.10.3) the mismatch parameters of the lateral deflection and remaining range channels Δ_z and Δ_{ro} of a range-finding coordinator can be written in the form

$$\Delta_z = r_A \sin(\beta_0 - \beta_r) - r_{AD} \sin(\beta_0 - \beta_D), \tag{4.11.5}$$

$$\Delta_{ro} = r_D - r_{rx} = r_{AD} \cos(\beta_0 - \beta_D) - r_A \cos(\beta_0 - \beta_r). \tag{4.11.6}$$

When a computer is used for performing operations in accordance with formulas (4.11.1)-(4.11.6), a coordinator of the range-finding type makes possible simultaneous guidance of several rockets, from different launching apparatus, along orthodromic trajectories situated arbitrarily relative to the base line AB. However, the structure of such a computer is extremely complex.

It is possible to simplify the structure of the computer of a coordinator of the range-finding type only by a restriction of the tactical possibilities of using the rockets. For example, the structure of the computer is quite simple when a rocket is guided along an orthodromic trajectory passing through the center of the base, along the normal to it or along a circular trajectory.

Figure 4.25 shows the location of the ground stations A and B, the rocket R and the point of transition of the rocket into a dive D, corresponding to the condition of rocket flight along the straight line $o_c x_m$. The trajectory line divides the segment AB in half. The launching apparatus is situated at the point of intersection of the trajectory line with the segment AB, although in some cases it can be displaced forward or backward along the trajectory line relative to the point of intersection.

If $r_b \ll r_r$, which frequently is actually the case, and the deflec- /194 tions of the rocket from the reference trajectory are small, the angle ε_1 is determined using the following approximate equation

$$\varepsilon_1 \approx \frac{r_A - r_B}{r_b}. \tag{4.11.7}$$

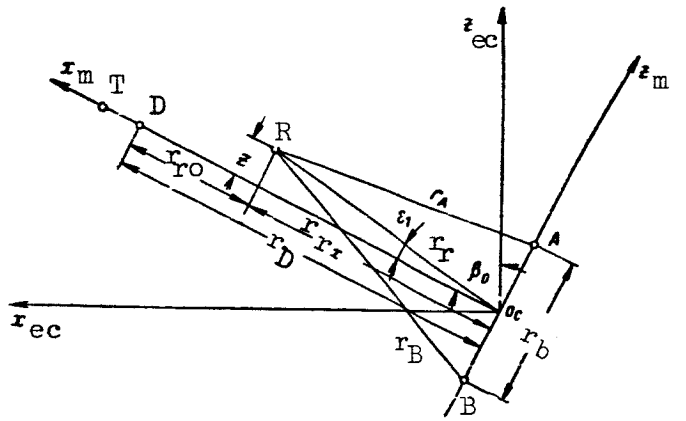

Figure 4.25

Since in the case of small mismatch angles

$$z \approx r_r \varepsilon_1,$$

on the rocket, it is easy to obtain the instrument analog of the mismatch parameter of the lateral deflection channel. We will have

$$\Delta_z = -z \approx \frac{r_B - r_A}{r_b} r_r. \qquad (4.11.8)$$

The values of the ranges r_A and r_B are measured by the coordinator apparatus carried aboard the rocket, the value r_b is given and r_r usually is stipulated by a programming mechanism. In the case of small z, it can be assumed that $r_r \approx r_{rx}$. Then the mismatch parameter of the remaining range channel can be expressed by the formula

$$\Delta_{r0} = r_D - r_{rz} \approx r_D \sqrt{r_A^2 - \frac{r_b^2}{4}}. \qquad (4.11.9)$$

Analysis of formulas (4.11.8) and (4.11.9) shows that for the considered case of use of a range-finding coordinator the structure of the computer is relatively simple. However, such a method for the use of a coordinator /195 of the range-finding type limits the tactical flexibility of the guidance system, since it requires changes of the position of the ground stations for each new target.

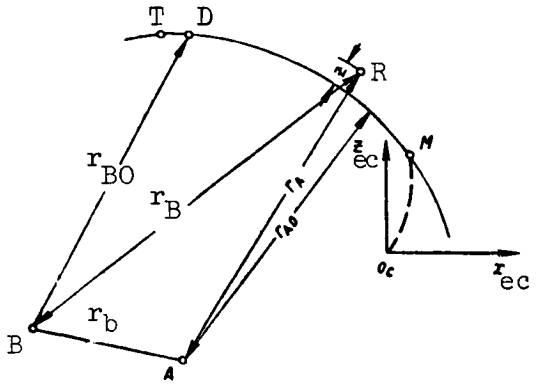

Figure 4.26

Figure 4.26 shows the location of the ground stations A and B, the rocket R and the point of transition of the rocket into a dive D, for rocket guidance along a circular trajectory. After launching at the point o_c, the rocket goes into a reference trajectory (point M), passing through the target and constituting the arc of a circle whose center is one of the surface stations (in the considered example, the station A). The lateral deflection of the rocket from a reference trajectory (or, in the language of navigation, drift of the rocket from orbit) is determined by a comparison of the given range value r_{AO} with the distance r_A measured on the rocket. The approach of the rocket to the target is determined from the signals of the second ground station (station B). When the distance r_B becomes equal to the stipulated range r_{BO}, a signal should be formed on the rocket for its transition into a dive.

Thus, it is easy to obtain on the rocket instrument analogs of the mismatch parameters, expressed by the formulas

$$\Delta_z = r_{AO} - r_A, \tag{4.11.10}$$

$$\Delta_{ro} = r_{BO} - r_B. \tag{4.11.11}$$

The structure of the computer forming the mismatch parameters on the basis of formulas (4.11.10) and (4.11.11) is extremely simple.

4.12. Coordinators Based on the Use of Add-Subtract–Range-Finding Radio Navigation Apparatus

A coordinator of the add-subtract–range-finding type can be designed on the basis of an add-subtract–range-finding or hyperbolic navigation system.

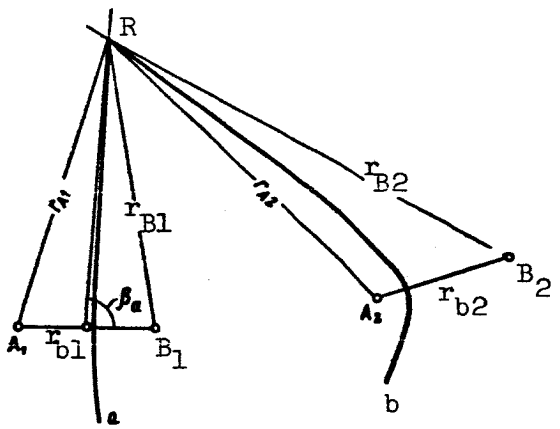

Figure 4.27

As is well known, such a system consists of two pairs of ground stations A_1B_1 and A_2B_2 (fig. 4.27) and apparatus carried on the moving object R, whose position is determined.

Each pair of ground stations, operating synchronously, radiates pulses /196 with a stable repetition frequency. By use of apparatus carried on the moving object and consisting of a receiver and a computer, these pulses are received and the time difference between the arrival of the pulses from one pair of stations $\Delta\tau_1$ and the other $\Delta\tau_2$ is measured. The time difference of receipt of the pulses obviously will be proportional to the corresponding distance differences $\Delta r_1 = r_{A1} - r_{B1}$ and $\Delta r_2 = r_{A2} - r_{B2}$.

Since the lines of constant distance differences to the two points on the plane represent a family of hyperbolas, the position of the object in an add-subtract—range-finding radio navigation system is determined as the point of intersection of two hyperbolas a and b, each of which corresponds to the measured value of the difference of distances.

The functional diagram of the coordinator designed on the basis of an add-subtract—range-finding radio navigation system is shown in figure 4.28. Each of the ground stations contains a synchronizer, transmitter, receiver and antenna system. The matching of the operation of the two stations forming the pair is possible by having one of them, called the master station, control the operation of the other, the controlled station. The transmitter of the master station radiates pulses whose pulse frequency is stabilized rigorously by a synchronizer. These pulses are received by the receiver aboard the rocket and by the receiver of the controlled station. The transmitter of the controlled station reradiates the received signals, and they are also sent to the receiver aboard the rocket. Since each of the stations of one pair can be both a master and a controlled station, their apparatus is completely identical.

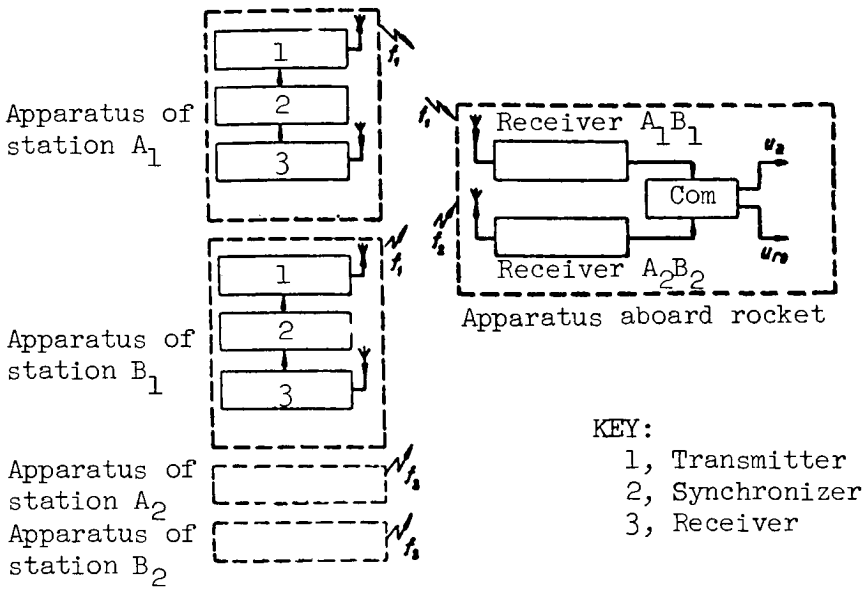

Figure 4.28

In the coordinator, there should be provision for the separation of the signals of the master and controlled stations aboard the rocket. This is done by introducing an additional delay of the pulses radiated by the master station, or the signals of each station are marked with their time code.

The second pair of stations A_2, B_2 operates in the same way. The carrier frequency f_2 of these stations differs from the carrier frequency f_1 of the first pair of stations, which makes it possible to discriminate their signals at the receiving end.

The apparatus aboard the rocket contains two receivers, one of which /197 (the receiver A_1B_1) receives the signals of the stations A_1 and B_1, while the other (the receiver A_2B_2) receives the signals of the stations A_2 and B_2 and the computer Com makes the required conversions of the received signals.

The form of the mismatch parameter which should be produced when using a coordinator of the add-subtract – range-finding type and therefore the structure of the computer are determined by the form of the stipulated reference trajectory. It can be shown that, if an orthodrome oriented arbitrarily relative to the ground stations is used as a reference trajectory, the structure of the computer in the rocket apparatus is extremely complex. The computer will be relatively simple in a case when the reference trajectory is one of the hyperbolas. In actuality, using for example one of the hyperbolas of the stations A_1 and B_1 as the reference trajectory, with sufficient withdrawal

of the rocket from the base A_1B_1, we obtain the following expression for the mismatch parameter of the lateral deflection channel (ref. 11)

$$\Delta_z = \frac{r_{pr}}{r_{bl}\sin\beta_a}\left[(r_{A1} - r_{B1})_0 - (r_{A1} - r_{B1})\right]. \qquad (4.12.1)$$

Here r_{pr} is the distance from the center of the base to the rocket, stipulated by the program, r_{bl} is the base length, β_a is the angle between the asymptote of the selected hyperbola and the base line, $(r_{A1} - r_{B1})_0$ is the difference in distances determining the selected hyperbola, and $(r_{A1} - r_{B1})$ is the current difference in distances measured on the rocket. /198

When a rocket is guided along a so-called "zero" hyperbola (a straight line perpendicular to the base and intersecting the base at its center), for which $(r_{A1} - r_{B1})_0 = 0$ and $\sin\beta_a = 1$, formula (4.12.1) coincides with (4.11.8).

The signals of the second pair of stations are used in forming the mismatch parameter of the remaining range channel. The mismatch parameter of the remaining range channel in this case is written in the form

$$\Delta_{r0} = (r_{A2} - r_{B2})_0 - (r_{A2} - r_{B2}). \qquad (4.12.2)$$

where $(r_{A2} - r_{B2})_0$ is the difference of distances corresponding to a hyperbola passing through the point of transition of the rocket into a dive.

Consequently, the command for transition of the rocket into a dive will be formed when the rocket intersects a particular hyperbola.

The inevitable curvature of the trajectory is a shortcoming of rocket guidance along a hyperbolic trajectory. However, by the use of a relatively simple computer, it is possible to ensure rocket guidance by using a coordinator of the add-subtract—range-finding type along a trajectory close to orthodromic. This requires selection of a definite law in conformity to which the rocket will intersect both families of hyperbolas. For example, as such a law it is possible to use the law of equal increments, whose essence is as follows (ref. 3). Assume the distance difference at the initial guidance point for the first pair of stations will be $\Delta r_{i1} = (r_{A1} - r_{B1})_i$, and for the second pair of stations $\Delta r_{i2} = (r_{A2} - r_{B2})_i$. At the target, these differences will be equal to $\Delta r_{t1} = (r_{A1} - r_{B1})_t$ and $\Delta r_{t2} = (r_{A2} - r_{B2})_t$, respectively.

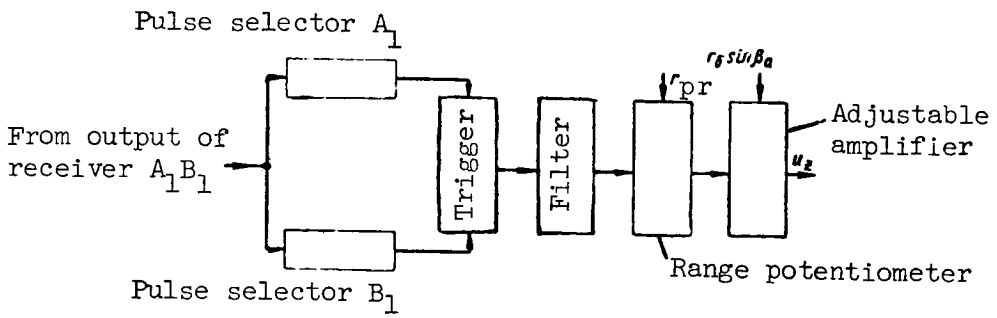

Figure 4.29

We write the ratio

$$\frac{\Delta r_{t_1} - \Delta r_{i_1}}{\Delta r_{t_2} - \Delta r_{i_2}} = b. \qquad (4.12.3)$$

It is obvious that b will be a constant, dependent on the relative position of the initial guidance point, target and ground stations.

Using the law of equal ratios, the reference trajectory is stipulated in such a way that a ratio similar to (4.12.3), written for the current values of the distance differences Δr_1 and Δr_2 in the case of rocket motion along a reference trajectory, will remain constant and equal to b. The reference trajectory stipulated in this way will be close to an orthodrome and sometimes is called a hyperbolodrome.

With such a stipulation of the reference trajectory the mismatch parameter characterizing lateral deflection can be represented in the form /199

$$\Delta_\delta = (\Delta r_1 - \Delta r_{i1}) - b(\Delta r_2 - \Delta r_{i2}), \qquad (4.12.4)$$

where Δr_1 and Δr_2 are the current values of the distance differences measured on the rocket.

The signals of any one pair of stations can be used for determination of the time of transition of the rocket into a dive. The mismatch parameter of the remaining range channel will be represented by a formula similar to (4.12.2).

As an example of the design of a computer for the coordinator of the add-subtract–range-finding type, we will describe one of the possible variants of the computer of the lateral deflection channel for rocket guidance along one of the hyperbolas when its structure is determined by equation (4.12.1). The functional diagram of such a computer is shown in figure 4.29.

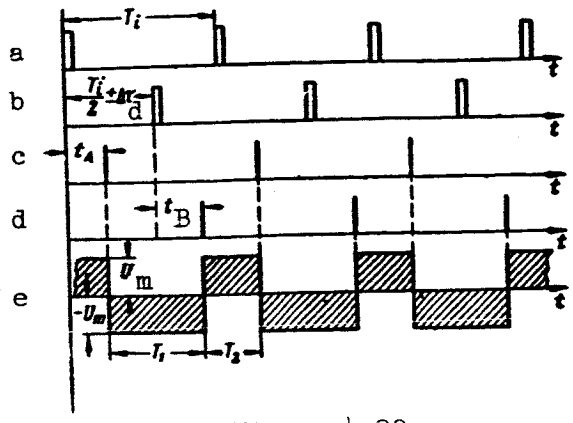

Figure 4.30

The master station A radiates a pulse signal with a repetition interval T_i (fig. 4.30a). The time of radiation of the signal of the master station B is delayed by the time $\frac{T_i}{2} \pm \Delta\tau_d$ relative to the time of appearance of the /200 pulses of station A (fig. 4.30b). Here $\Delta\tau_d$ is the time difference in the receipt of the pulses of stations A and B on the rocket during its flight along an earlier stipulated hyperbola, used as the reference trajectory. This difference is determined using the formula

$$\Delta\tau_d = \frac{(r_{A1} - r_{B1})_0}{c}, \qquad (4.12.5)$$

where $(r_{A1} - r_{B1})_0$ is the distance difference, determining the selected hyperbola, and c is the velocity of radio wave propagation.

The sign of $\Delta\tau_d$ will be positive if the reference hyperbola is situated to the right of the zero hyperbola and negative if it is situated to the left.

For satisfaction of the mentioned relations between the times of radiation of the stations A and B, the signal received from station A at the master station is delayed by the value

$$t_d = \frac{T_i}{2} - t_b \pm \Delta\tau_d. \qquad (4.12.6)$$

Here t_b is the time required for propagation of the radio waves the distance r_{b1}.

The signals received from the output of the receiver A_1B_1 are fed to the pulse selectors A_1 and B_1. The pulse selector A_1 passes only the signals of station A_1, and the pulse selector B_1 the signals of station B_1. The circuits of the selectors are determined by those qualitative criteria of the signals which are used as the basis for their discrimination.

The times of appearance of the signals relative to the times of their radiation are dependent on the position of the rocket and are equal to $t_A = \frac{r_{A1}}{c}$, $t_B = \frac{r_{B1}}{c}$ (fig. 4.30c, d), respectively.

The output pulses of the selectors activate a trigger. The temporal voltage diagram at the trigger output is shown in figure 4.30e. The low-frequency filter following the trigger separates the constant voltage from the bipolar pulses. The constant voltage is

$$u_f = U_m \frac{T_1 - T_2}{T_1 + T_2}, \tag{4.12.7}$$

where U_m is the voltage amplitude at the output of the trigger, and T_1 and T_2 are the durations of the negative and positive voltage drops of the trigger.

In the derivation of formula (4.12.7) it was assumed that the transfer coefficient of the filter for the constant component is equal to unity.

It is easy to determine the values T_1 and T_2 by using the temporal diagrams in figure 4.30. We have /201

$$\left.\begin{aligned} T_1 &= \frac{T_i}{2} \pm \Delta\tau_d - t_A + t_B, \\ T_2 &= \frac{T_i}{2} \mp \Delta\tau_d + t_A - t_B. \end{aligned}\right\} \tag{4.12.8}$$

Then for the constant component of voltage at the output of the filter, we obtain

$$u_f = 2U_m \frac{\pm \Delta\tau_d - \Delta\tau_1}{T_i}, \tag{4.12.9}$$

where $\Delta\tau_1 = t_A - t_B$ is the actual value of the difference in the time of arrival of the pulses of the stations A and B. The $\pm$ sign in front of $\Delta\tau_d$ in formula (4.12.9) is of an arbitrary character, indicating whether the

particular hyperbola is to the right or left of the zero hyperbola; therefore, hereafter it will be omitted and as the voltage u_f, we will have

$$u_f = 2U_m \frac{\Delta\tau_\partial - \Delta\tau_1}{T_l}. \qquad (4.12.10)$$

The next component in the functional diagram of the computer will be a range potentiometer, which is used for introducing the programmed range value r_{pr} entering into formula (4.12.1).

The signal at the range potentiometer output will be

$$u_{pot\partial} = k_{pot\partial} r_{pr} u_f. \qquad (4.12.11)$$

Due to the introduction of the range potentiometer, the coordinator acquires a constant sensitivity in relation to the linear deflection of the rocket for the entire range of its flight. If there is no range potentiometer, the sensitivity of the coordinator with respect to linear deflection decreases with an increase of range.

The output stage of the computer is an amplifier with an adjustable amplification factor k_{aa}. This coefficient changes inversely proportional to the product of the base r_{bl} and the sine of the angle β_a, that is

$$k_{aa} = \frac{k'_{aa}}{r_{bl} \sin \beta_a}, \qquad (4.12.12)$$

where k'_{aa} is the value of the amplification factor for a base of one kilometer and an angle $\beta_a = \frac{\pi}{2}$.

The introduction of an amplifier with an adjustable amplification makes it possible to maintain constant sensitivity of the coordinator with a change of the value of the base of the system and with a change of reference hyperbolas. The required amplification is set manually when preparing the /202
rocket for launching. The the voltage u_z at the output of the computer is expressed by the formula

$$u_z = k_{aa} u_{pot\partial}. \qquad (4.12.13)$$

By combining formulas (4.12.9)-(4.12.13), we obtain

$$u_z = \frac{2U_m k_{pot} \partial k'_{aa} r_{pr}}{T_i r_{bl} \sin \beta_a} (\Delta\tau_d - \Delta\tau_1). \qquad (4.12.14)$$

It follows from (4.12.14) that when $\Delta\tau_1 = \Delta\tau_d$, the voltage at the output of the computer will be equal to zero. With an increase or decrease in the difference of the arrival time of the pulses from stations A_1 and B_1 in comparison with the value $\Delta\tau_d$, the output voltage u_z will change both in value and sign.

Since

$$\Delta\tau_d = \frac{(r_{A1} - r_{B1})_0}{c},$$

and

$$\Delta\tau_1 = \frac{r_{A1} - r_{B1}}{c},$$

expression (4.12.14) is reduced to the form

$$u_z = \frac{2U_m k_{pot} \partial k'_{aa} r_{pr}}{T_i c r_{bl} \sin \beta_a} [(r_{A1} - r_{B1})_0 - (r_{A1} - r_{B1})]. \qquad (4.12.15)$$

If relation (4.12.1) is used, we obtain

$$u_z = \frac{2U_m k_{pot} \partial k'_{aa}}{T_i c} \Delta_z. \qquad (4.12.16)$$

Formula (4.12.16) establishes the relationship between the actual value of the mismatch parameter Δ_z of the lateral deflection channel and its measured value u_z.

After introducing the concept of the transfer coefficient of the coordinator for lateral deflection, which is equal to

$$k_z = \frac{2U_m k_{pot} \partial k'_{aa}}{T_i c}, \qquad (4.12.17)$$

we obtain from (4.12.16)

$$u_z = k_z \Delta_z. \qquad (4.12.18)$$

In completing the description of the functional diagram of the computer for a coordinator of the add-subtract– range-finding type, we note that in addition to the mentioned regulation of amplification of the channel for measurement of lateral deflection, there should be provision for at least one other regulation involving a setting of the balance of the output stages of the computer. This regulation makes it possible to obtain a zero voltage at the computer output, if the time difference in the arrival of pulses from the /203 stations A_1 and B_1 is equal to zero.

The computer for the remaining range channel has much in common with the computer discussed above for the lateral deflection channel and it therefore will not be described here.

Now we will discuss the method used for evaluation of the accuracy of a coordinator of the add-subtract– range-finding type. As before, we will determine the statistical characteristics of the distortions of the measured value of the mismatch parameter caused by the instrument noise of the receiving apparatus of the rocket or noise interference.

We will assume that the level of noise interference is quite low and does not cause a change in the transfer properties of the coordinator. Then an allowance for the fluctuation components in the received signal leads to the appearance of an additional random component in the output voltage of the coordinator which, in this case, can be represented in the form $u_z + \Delta u_z$. The appearance of Δu_z in the output voltage can be attributed to the fact that, under the influence of the noise, there is fluctuation of the times of formation of the received pulses and their durations. Therefore, the arrival times of the pulses from stations A_1 and B_1 will be equal to $t_{A1} + \Delta t_A$ and $t_{B1} + \Delta t_B$. We will assume that Δt_A and Δt_B represent stationary random functions with mathematical expectations equal to zero. The latter assertion is based on the fact that, in the case of small levels of fluctuations, positive and negative displacements of the times of formation of the pulses will be equiprobable. Since the mathematical expectations of the functions Δt_A and Δt_B are equal to zero, the mathematical expectation of the random component of the output voltage of the coordinator also will be equal to zero, that is, $\overline{\Delta u_z} = 0$.

In the further analysis, it will be assumed that the distance between the rocket and stations A_1 and B_1 does not change and $r_{pr} = \text{const}$, that is, the principle of "freezing" of the coefficients is applicable.

The spectral density of the random component of the output voltage at the output of the coordinator $G_{\Delta u_z}(\omega)$ will be equal to

$$G_{\Delta u_z}(\omega) = G_b(\omega) |W_l(j\omega)|^2, \qquad (4.12.19)$$

where $G_b(\omega)$ is the spectral density of the bipolar pulses at the output of the trigger, caused by fluctuations of the times of formation of the received pulses; $W_l(j\omega)$ is the frequency characteristic of the linear part of the coordinator from the filter to its output.

Since hereafter we will be concerned only with the components of the spectrum of fluctuations of the output voltage close to the zero frequency, in place of (4.12.19) we write

$$G_{\Delta u_z}(0) = k_l^2 G_b(0). \tag{4.12.20}$$

Here k_l is the transfer coefficient of the linear part of the coordinator /204 equal to

$$k_l = \frac{k_{pot} \partial^{k'}_{aa} r_{pr}}{r_{bl} \sin \beta_a}. \tag{4.12.21}$$

The spectral density $G_b(0)$ was determined in section 8.3. It is expressed by the formula

$$G_b(0) = \frac{8U_m^2}{T_i}(\sigma^2_{t_A} + \sigma^2_{t_B}), \tag{4.12.22}$$

where $\sigma^2_{t_A}$ and $\sigma^2_{t_B}$ are the dispersions of the fluctuations of the times of appearance of the received pulses Δt_A and Δt_B.

We will assume that $\sigma^2_{t_A} = \sigma^2_{t_B}$. The value $\sigma^2_{t_A}$, whose method of determination was given in section 8.5, is

$$\sigma^2_{t_A} = \frac{1}{q^2_p \Delta f^2_{ew}}, \tag{4.12.23}$$

where q_p is the ratio of the pulse power of the signal to the effective strength of the noise, recalculated to the input of the receiver; Δf_{ew} is the effective width of the passband of the intermediate frequency amplifier.

After combining formulas (4.12.20)-(4.12.23), we obtain

$$G_{\Delta u_z}(0) = \frac{16k_i^2 U_m^2}{T_i q_p^2 \Delta f_{ew}^2}. \qquad (4.12.24)$$

A knowledge of the spectral density of fluctuations at the output of the coordinator makes it possible later, during analysis of the entire control circuit, to determine the errors in rocket guidance.

In addition, using formula (4.12.24), it is possible to compute the errors of the coordinator itself, caused by the noise effect. We will estimate the coordinator error caused by dispersion of the fluctuation component of the output voltage $\sigma^2_{\Delta u_z}$ equal to

$$\sigma^2_{\Delta u_z} = \frac{16k_i^2 U_m^2 \Delta F_e}{T_i q_p^2 \Delta f_{ew}^2}. \qquad (4.12.25)$$

Here ΔF_e is the effective passband of the coordinator filter.

The error in measurement of lateral deflection also can be expressed in linear values, much as was done for the coordinators of the angle-measuring–range-finding type. This requires use of relation (4.12.18), establishing a relationship between the measured and actual values of the mismatch parameter.

CHAPTER 5. COORDINATORS OF COMMAND CONTROL SYSTEMS. COMMAND FORMING APPARATUS

5.1. Principles of Design and Principal Types of Coordinators of Command Control Systems

In the process of rocket guidance using command control systems, the control point should have data making it possible to determine the degree of disruption of the coherence imposed on the rocket motion. These data, used in producing the mismatch parameter Δ_m, are obtained using the measurement /205

instruments in the coordinator. On the basis of the Δ_m signals forming at the output of the coordinator, the operator (in nonautomatic or semiautomatic control systems) or a computer (in automatic control systems) produces commands which are transmitted to the rocket for its return to the reference (kinematic) trajectory.

In a general case, the coordinator of the command control system consists of one or more angle-measuring and range-finding instruments and instruments for measuring the velocities of motion of the rocket and target. In addition, the coordinator has a computer and sometimes electronic instruments for the radio transmission of the measurement results (relay system) of the rocket coordinates to the control point.

Two types of coordinators can be distinguished. In coordinators of the first type, all the measurements are made relative to the control point or points situated near it; however, in the case of coordinators of the second type, the origin of the measurement coordinate system is situated on the rocket.

Coordinators of the first type can be both automatic and nonautomatic. In automatic coordinators, the output signals of the measurement instruments represent a voltage or a current in a form convenient for producing the mismatch parameter Δ_m in the computer and its conversion into a control command /206

without human participation. In nonautomatic coordinators, the parameter Δ_m is produced in a form which is unsuitable for the conversion of Δ_m into a command without human participation. Nonautomatic coordinators are constructed using optical or radar sights.

Coordinators of the second type are nonautomatic because otherwise it is possible to construct an automatic homing system. They determine the position of a target relative to the rocket in a related or moving coordinate system,

and can be used in those cases when the targets to be attacked stand out inadequately against the surrounding background so that automatic apparatus cannot operate reliably. Such targets usually are on the Earth's surface.

In coordinators of the first type, the measurement instruments usually produce signals characterizing the distances r_t and r_r from the control point C to the target T and also the angles ϵ_t and ϵ_r in an earlier selected coordinate system. Sometimes it is also necessary to know the velocities of motion of the target and rocket in relation to the control point.

Measurement coordinate systems coinciding with a ground system or forming certain angles with it (so-called oblique coordinate systems $o_{ob}x_{ob}y_{ob}z_{ob}$) are selected for the operation of measurement instruments on the ground. The latter type of coordinate systems often is used in radar sighting, making possible measurement of slant ranges to the target and rocket and also their azimuths and angles of inclination (places). Since rockets usually have a small reflecting surface, in order to obtain a sufficient radar contrast they carry a radar responder (a receiving-transmitting apparatus) or an autonomously operating radio transmitter.

The data obtained from the measurement apparatus are fed to a computer where the measured value of the mismatch parameter for the selected guidance method is produced. In accordance with the possible values subject to measurement, coordinators of the first type make it possible to employ different three-point methods of rocket guidance.

It follows from the mismatch equations cited in chapter 2 for three-point guidance methods that the output signal of a coordinator of the first type should characterize the linear or angular deflection of the center of mass of a rocket from the reference trajectory.

Measurement apparatus of coordinators of the first type can be placed at the control point or away from it. In all cases, this apparatus is at the control point in the case of guidance of rockets from aircraft, ships and other types of rocket carriers. In the case of rocket guidance from the ground, the measurement apparatus frequently is situated away from the control point. Under these conditions, the coordinators include not only measurement instruments and computers, but also one or a large number of systems for transmission of data (relay systems). /207

The principle of design of coordinators of the second type is as follows. The measurement apparatus carried aboard the rocket produces a signal reflecting the angular position of the vector **r**, connecting the target T with the center of mass of the rocket o_r, in relation to the longitudinal axis of the rocket $o_r x_1$, the vector of its air velocity v or some fixed direction $o_r x_{er}$ in space (fig. 5.1a).

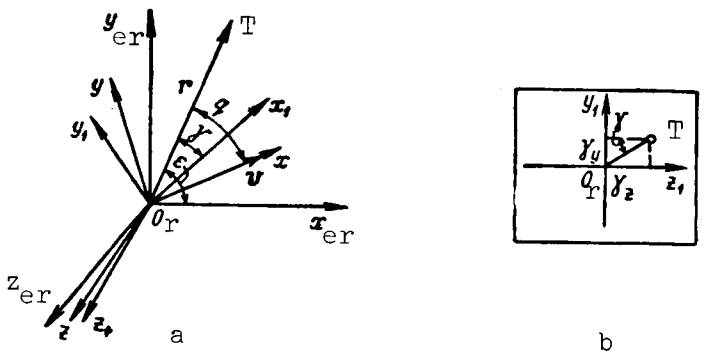

Figure 5.1

To obtain the measured value of the mismatch parameter Δ_m at the control point, it is necessary that the control point receive both the signals arriving at the measuring instrument from the target and the signals characterizing the direction of the axes of the measurement coordinate system. The coordinator therefore should include a relay system.

The directions of the straight lines $o_r x_1$, $o_r x$ and $o_r x_{er}$, in relation to which the angles γ, q and ϵ are measured, are transmitted most easily by radio signals characterizing the position of the axes $o_r y_1$, $o_r z_1$; $o_r y$, $o_r z$ or $o_r y_{er}$, $o_r z_{er}$. The decoding of the signals of the relay system makes it possible to obtain on the indicator (a cathode-ray tube or optical system) the image of the target and an intersection. With appropriate calibration of the indicator, the operator in charge of the rocket guidance is able to measure the angles of deflection of the target in two mutually perpendicular control planes. As an example, figure 5.1b shows a simplified image of the target T and an intersection characterizing the position of the related axes of the rocket $o_r y_1$ and $o_r z_1$. Using the projections of the point T onto the axes $o_r y_1$ and $o_r z_1$, it is possible to find the components γ_y and γ_z of the vector γ corresponding to the angle γ in figure 5.1a and guide the rocket by the direct method.

Since the measurement apparatus of coordinators of the second type /208
makes it possible to measure the mismatch parameter characterizing the degree of disruption of coherence imposed on the position of the rocket axis $o_r x_1$ or the vector v, command control systems with such coordinators make it possible to employ two-point guidance methods.

Using coordinators of the second type, an operator can make a high-quality selection of targets at the control point. This can be attributed to the fact that a man is capable of distinguishing an image on radar set scopes, television sets, etc., more precisely and can react better to various peculiarities of the target than any of the modern automatic apparatus devised. It also must be remembered that the conditions for observation of a target with coordinators of the second type improve with approach of the target to it, and it is possible to guide a rocket beyond the limits of radar visibility of the target from the control point (as long as radio communication with the rocket is maintained). However, the absence of automation in coordinators of the second type sets a considerable limitation on the area of their applicability during the guidance of rockets toward rapidly moving targets.

It follows from the considered principles of design of coordinators of the first and second types that, in the first, the conditions for control of the position of the center of mass of the rocket deteriorate during its withdrawal from the control point. However, the relative simplicity of automation of these coordinators and the need for only relatively simple radio apparatus aboard the rocket make them extremely desirable for command control systems.

5.2. General Functional Diagrams of Coordinators of Command Control Systems

A coordinator of the first type, whose general functional diagram is shown in figure 5.2, consists of instruments for measurement of the coordinates of the target and rocket, forming a sighting apparatus, and systems for the transmission of data (in some cases these systems can be absent). In addition, a coordinator includes a computer and a radar responder (or an autonomously operating transmitter) on the rocket, which in figure 5.2 has been arbitrarily grouped with the sighting apparatus.

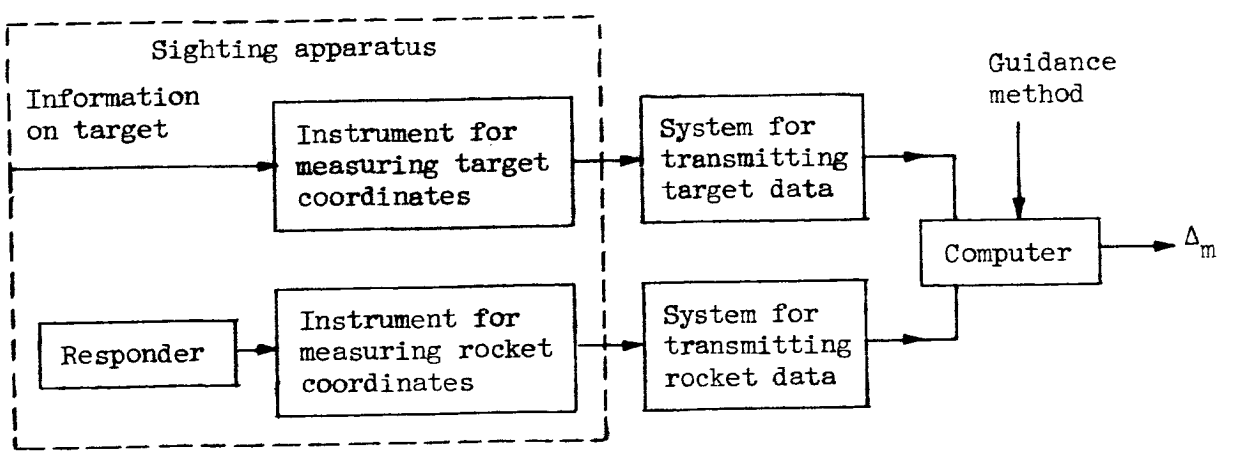

Figure 5.2

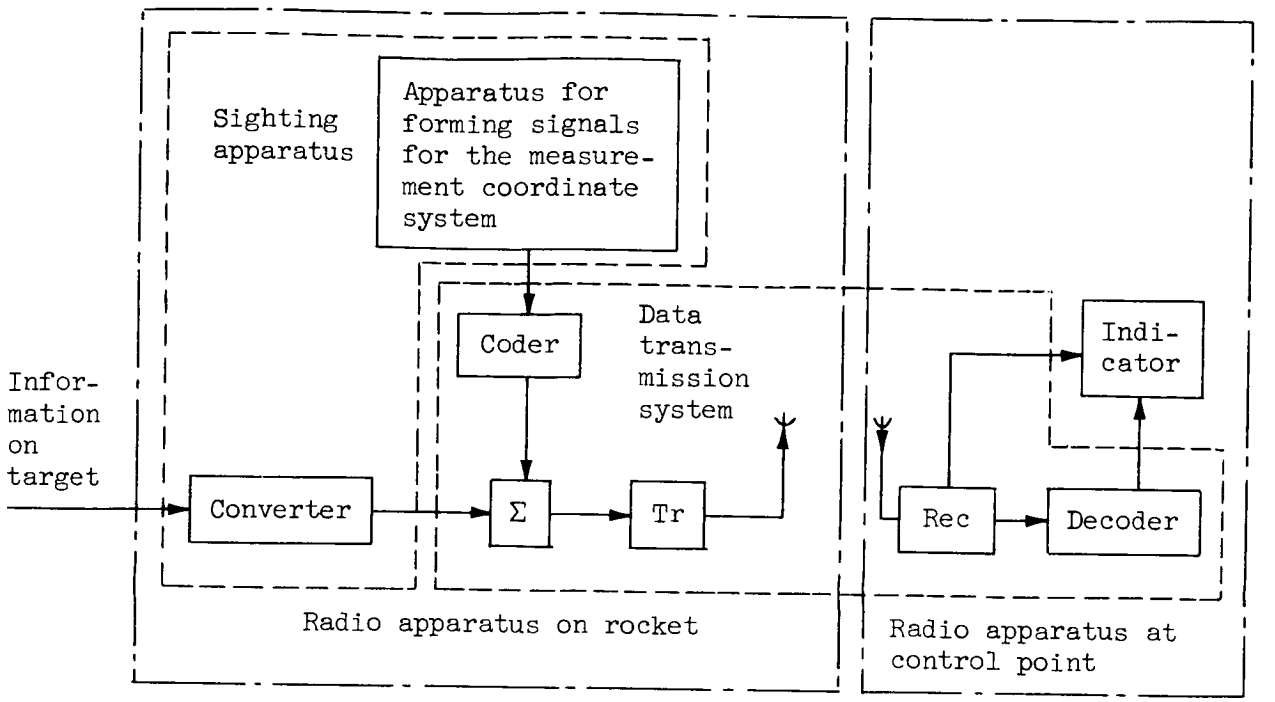

Figure 5.3

The computer calculates the mismatch parameter in accordance with the selected guidance method; in figure 5.2 this has been represented conventionally by the notation "guidance method."

The specific form of the functional diagram of the coordinator is determined by the rocket guidance method used and the type of measuring apparatus employed.

We note that in coordinators of the first type the apparatus for measurement of the coordinates of the target will be absent if the rocket is guided to a fixed target. In this case the coordinates are introduced into the computer in advance.

Figure 5.3 shows the general functional diagram of a coordinator of the second type. Information on the target can be fed to the sighting apparatus in the form of light, thermal or radar signals characterizing the region in which the target is situated. /209

The sighting apparatus of the coordinator includes a converter which has a sensing element and a scanning system and also an apparatus for shaping signals for representing the measurement coordinate system.

The sensing element (camera tube with an optic, radar receiver with an antenna, etc.) senses the energy incident upon it and the scanning system makes a component-by-component study of the target region. The electrical voltage or current at the output of the converter is fed to a summation apparatus Σ, which

also receives signals from a coder connected to the apparatus for producing the measurement coordinate system signals. The latter, in the case of rocket guidance by the vane or direct methods, produces voltage pulses representing the axes $o_r y_1$, $o_r z_1$ or $o_r x$, $o_r z$ (fig. 5.1). For example, if a radar /210

sighting device is used in a coordinator, these pulses are produced at those times when the antenna directional diagram passes along the corresponding coordinate axes. In order to detect the signals characterizing the coordinate measurement system at the control point, the signals are coded in a coder.

The resultant signal is fed to the radio transmitter Tr, relayed to the control point and then received by the receiver Rec. From there, the decoder, on the basis of the given code criteria, detects the signals of the measurement coordinate system. They are used to control the indicator so that the scanning in the converter on the rocket and the scanning of the light or electron beam in the indicator will be synchronized. The coder, decoder, adder, transmitter and receiver make up the data transmission system.

The image of the region of the target and the intersection characterizing the transmitted axes of the coordinate system, produced on the indicator (either of the cathode ray or optical type), make it possible for the operator to determine the mismatch parameter Δ_m.

5.3. Sighting Apparatus of Coordinators

1. Sighting Apparatus of Coordinators of the First Type

Coordinators of the first type use optical, radar and radio navigation sighting apparatus.

An optical sighting apparatus, located at a control point without any additional apparatus, makes it possible to measure the angles ϵ_{1y} and ϵ_{1z} (see chapter 2).

When the necessary visibility is present, optical sighting apparatus is characterized by a high resolving power, absolute concealment and maximum simpliticity of design. Together with the mentioned merits, the optical sighting method has the following shortcomings:

(1) a short sighting range, due to conditions of geometrical visibility;

(2) dependence of the operation of the sighting system on meteorological conditions and time of day;

(3) low noise immunity (sighting becomes impossible, for example, when smoke screens are used).

Radar sighting apparatus can be automatic and nonautomatic. Automatic apparatus is used in most cases. Automatic and nonautomatic sighting apparatus

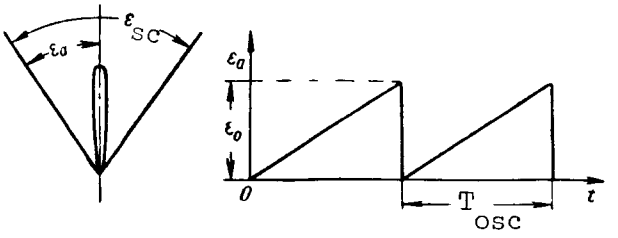

a b

Figure 5.4

in turn can be divided into two classes. Sighting apparatus of the first class is characterized by the fact that one radar set can determine the coordinates of only one rocket or target. The radar set of a sighting apparatus of the second type can measure simultaneously the coordinates of several rockets and several targets in specific sectors of inclination angle and azimuth. /211

Radar sets both with an integral equisignal direction (with conical scanning) and with an instantaneous equisignal direction can be used as sighting apparatus of the first type. The equations characterizing the operation of the angle-measuring channels of such sets were discussed in chapter 3.

A shortcoming of radar sighting apparatus of the first type is that despite relatively complex equipment (two radars), it is possible to guide only one rocket to one target.

Measurement of coordinates by sighting apparatus of the second type is based on the so-called group method. Radar sets operating by the group method usually have two antennas for use in progressive scanning of space in oblique and azimuthal planes. The beams of these antennas, narrow in the planes of motion, oscillate within the limits of set sectors in a sawtooth regime (fig. 5.4). As a result, the angle ϵ_a of deflection of the maximum of the directional diagram from its initial (zero) position changes as shown in figure 5.4b (for one of the target observation planes). We note that the angle ϵ_{sc} in figure 5.4 represents the sector scanned.

Since the channels for measurement of azimuth and inclination angle are identical, hereafter we will discuss only one channel. During the time of irradiation of the target (rocket), a group of pulses reaches the radar set receiver from the target (rocket); the number of pulses is

$$N_p = \frac{\theta_0}{\Omega_{osc}} F_p,$$

where θ_0 is the width of the directional diagram of the antenna at half-power, Ω_{osc} is the angular velocity of oscillation of the antenna beam, and F_p is the frequency of the sounding pulses.

In a case when there is one target in the scanned sector (later for unambiguity, we will discuss the method of determination of the coordinates of the target), the signals forming at the output of the radio receiver, in the "voltage-time" and "voltage-angle of deflection of the antenna ϵ_a" coordinate systems in one scanning period, have the form shown in figure 5.5a and figure 5.5b. /212

We note that, as the origin of the coordinate systems, we use the range to the target corresponding to the time of radiation of the sounding pulse and the initial position of the antenna beam. The form of the group in figure 5.5b and the difference in the amplitudes of the pulses shown in figure 5.5a are determined by the form of the directional diagram of the antenna and the plane of movement of the beam.

It follows directly from an inspection of the character of the signals forming at the output of the radar set that they contain data necessary for determination of the range r_t to the target and its angular coordinate ϵ_t.

The distance to the target can be found by measurement of the time t_t (fig. 5.5a) characterizing the position of the reflected pulses in relation to the sounding pulse, and the angular coordinates can be determined from the position of the center of the group on the angles scale (fig. 5.5b) relative to the origin of the scanning sector.

Automatic determination of the mentioned coordinates can be accomplished using closed systems of automatic control. In the system determining range, as in an ordinary automatic range finder, there is production of gating pulses automatically tracking the center of the video pulses forming at the output of the receiver. Automatic systems for determination of the angular coordinate produce gating pulses tracking the energy center of the group of received pulses. It follows that, when using the group method, systems essentially for

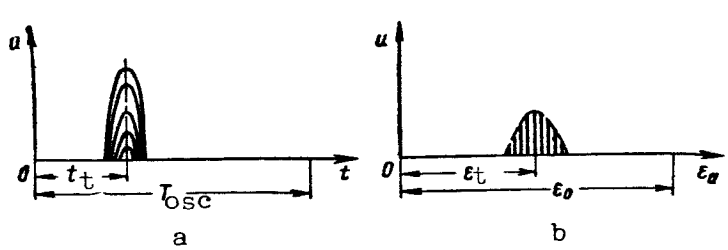

Figure 5.5

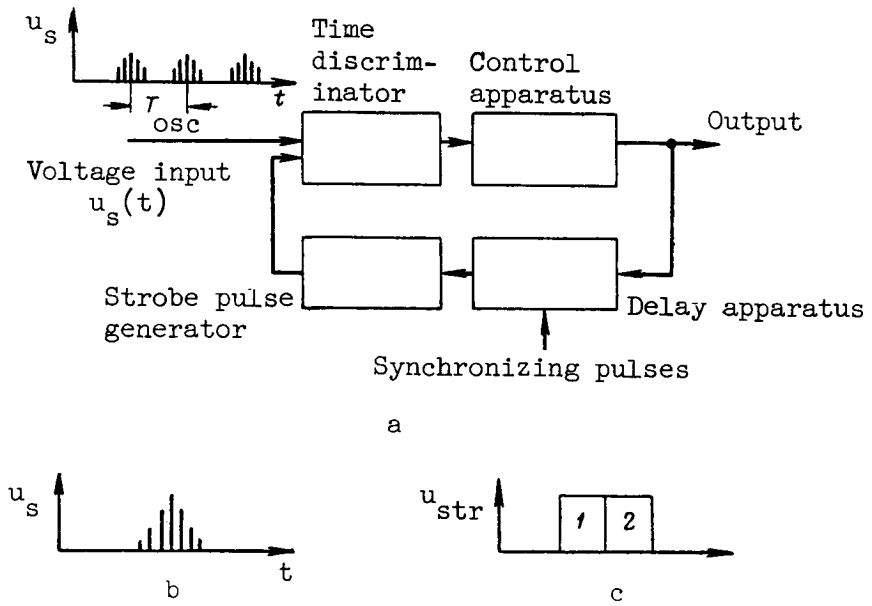

Figure 5.6

automatic determination of angular coordinates are close to the automatic range finders considered earlier.

The functional diagram of one of the possible automatic instruments for measurement of the angular coordinate is shown in figure 5.6a (ref. 62).

The voltage $u_s(t)$ is fed from the output of the radio receiver in the form of groups (fig. 5.6b) to a time discriminator which also receives strobe pulses u_{str} (fig. 5.6c). The time discriminator operates in such a way that the /213 increment of its output voltage is equal to zero if each of two selector pulses overlaps an identical area of the group. In such cases when the pulse 1 (fig. 5.6c) coincides with a lesser area of the group (fig. 5.6b), the mismatch voltage formed by the time discriminator becomes negative. If the axis of the selector pulses is displaced to the right in relation to the center of the group, the mismatch voltage will be positive.

The time discriminator signals act on the control apparatus which regulates the time lag of the master pulses fed to it.

We note that the master pulses are produced at times corresponding to the initial position of the antenna.

Selector pulses are formed under the influence of the delayed master pulse. As a result of the interaction of all the signals appearing in the servosystem shown in figure 5.6a, the tracking of the selector pulses of the center of the group is ensured. As the output of the considered system, it is

possible to use the voltage of the control apparatus or the position of the delayed master pulse.

The described method for automatic determination of the angular coordinate has been called in technical literature the method of division of a group of video signals in half.

A distinguishing feature of the operation of this system for determination of coordinates is the discreteness of receipt of information from the target and the high accuracy of measurement of the angle ε_t.

Radio navigation sighting apparatus can be used in those cases when a /214 rocket is to be guided along a fixed trajectory. In principle, the coordinates of a rocket can be measured satisfactorily by all the types of navigation measurement instruments discussed in the preceding chapter and also by Doppler systems for measuring ground velocity. However, the apparatus carried aboard the rocket for recording its coordinates in relation to ground stations, in radio zone control systems and in the case of command guidance of a rocket, should be situated at the control point; in this case, only a radar responder should be aboard the rocket. It follows that the principle of command radio guidance appreciably simplifies the apparatus of the rocket.

2. Sighting Apparatus of Coordinators of the Second Type

In coordinators of the second type for command guidance systems for rockets, the sighting apparatus can be based on the television, thermal and radar principles. One of the principal components of a television sighting apparatus is a camera tube with optic. Coordinators with television sighting apparatus provide the simplest means of determining the mismatch parameter for guidance of the rocket by the direct and vane methods. For this purpose, the longitudinal axis of the tube should coincide with the $o_r x_1$ axis or the velocity vector v of the rocket, respectively. In the latter case, the tube is attached to a base oriented by means of the vane in the direction of the air flow. A grid is plotted on the photoelectronic mosaic of the tube for characterizing the transverse axes of the rocket or the direction of the vector v.

In the vane method, the sighting apparatus can be made in such a way that the television tube with the optic is fixed relative to the body of the rocket and the grid is related to the vane.

The signals from the camera tube, together with the signals from the grid and scanning of the image are transmitted to the control point where a picture tube is used as the output apparatus.

Television sighting apparatus makes it possible to have a very graphic image, provide for quite high concealment of the work (radiation is in a direction opposite the direction of motion of the rocket) and makes it possible to guide a rocket to targets having neither radar nor thermal contrast. At the same time, such apparatus has a number of shortcomings, the most important

of which are dependence of the operability of the sighting apparatus and quality of the received image on meteorological conditions and time of day. In addition, the insufficiently high noise immunity of systems for the transmission of television images must be borne in mind.

Using a sighting apparatus designed on the thermal principle, it is possible to determine the thermal "relief" of the terrain over which the rocket is flying. The sensing element of a thermal sighting apparatus is mounted /215 in exactly the same way as the camera tube. The signals received from the thermal sighting apparatus, together with the signals characterizing the measurement coordinate system, are transmitted to the control point by electronic means. Appropriate converters are carried on the rocket for this purpose.

Thermal sighting apparatus makes it possible to determine the position of a target having thermal contrast, regardless of time of day, and since they constitute passive systems, there is a quite high secretiveness of their operation. However, the effective range of such sighting apparatus is low because of the considerable absorption of thermal radiation during its propagation in the atmosphere.

Radar sighting apparatus is used in forming the radar "relief" of the area in the neighborhood of the target. Radar sighting apparatus can be passive, active and semiactive. The operation of passive sighting apparatus is based on the presence of radio emission from terrain which is not subject to prior irradiation. If a rocket carries a radar transmitter and receiver, the sighting apparatus becomes active. When the radar transmitter is away from the rocket, the sighting apparatus becomes semiactive. Obviously, from the point of view of weight and size of rocket equipment, it is more desirable to have passive and semiactive radar sighting apparatus. Semiactive radar sighting apparatus ensures the producing of mismatch signals with an appropriate scanning of the terrain by the receiving antenna, the same as in ordinary nonautomatic radar sets. The only difference between them is that, in the coordinator of a command control system, the cathode-ray indicator is connected to the search antenna and the receiver output by a data transmission system.

Radar sighting apparatus makes it possible to guide rockets to targets having a radar contrast ensuring a relatively great effective range during active and semiactive sighting. However, such sighting apparatus has a relatively low noise immunity. In some cases, guided rockets should move at a constant altitude. Since the signals characterizing flight altitude of the rocket are not produced by the mentioned sighting apparatus, it is necessary for the rocket to have altimeters whose information is used for flight stabilization or which is transmitted to the control panel by a relay system.

5.4. General Information on the Computers Used in Coordinators

The computers used in the coordinators of systems for the command control of rockets are classified as analog and digital. In each specific case, the

types of computers and the problems solved by them are determined by the mismatch equation and the shape of the input and output signals.

If radar sighting apparatus ensuring the automatic determination of /216
the coordinates of the target and rocket is used, coordinators can be created which make possible guidance of the center of mass of a rocket without deflection (by the coincidence method) and with deflection (for example, by the parallel approach method). The equations which should be solved by the computers in this case are given in chapter 2. For example, for guidance of a rocket in the vertical plane, it is necessary to solve equations (2.8.2), (2.8.3), (2.8.4), (2.8.8) and (2.8.10), which have the following form:

(a) for the coincidence method

$$h = r_{pr}(\epsilon_t - \epsilon_r); \tag{5.4.1}$$

(b) for the approximate method of parallel approach

$$h = r_{pr}\left[\epsilon_t - \epsilon_r - \frac{r_t - r_r}{r_{pr}}(\epsilon_0 - \epsilon_t)\right] \tag{5.4.2}$$

and when $r_{pr} = r_r$

$$h = r_t(\epsilon_t - \epsilon_0) - r_r(\epsilon_r - \epsilon_0); \tag{5.4.2a}$$

(c) for the precise parallel approach method

$$h = r_{pr}\left\{\epsilon_t - \epsilon_r - \arcsin\left[\frac{r_t - r_r}{r_{pr}}\sin(\epsilon_0 - \epsilon_t)\right]\right\}. \tag{5.4.3}$$

We recall that in the cited equations the value $r_{pr} \approx r_r$ produced by the programming mechanism characterizes the range from the control point to the rocket. The signal reflecting the angle ϵ_0 also is shaped by the programming mechanism.

When radio navigation apparatus for measurement of coordinates is used, it is possible to create coordinators ensuring the guidance of rockets along fixed trajectories. In this case, the mismatch parameter for the vertical and horizontal guidance planes is a signal characterizing the linear deflection of the center of mass of the rocket from the stipulated fixed trajectory.

Different types of mismatch equations are obtained, depending on the type of radio navigation apparatus used. For example, if an angle-measuring radio navigation apparatus is used in the control system (a ground direction finder), the computer solves equations of type (5.4.1), taking into account that ϵ_t is a given value.

The same mismatch equations are obtained when the coordinator is designed on the basis of angle-measuring – range-finding and range-finding radio navigation apparatus as for fixed radio zone control systems.

In addition to control of rockets in planes perpendicular to the vector v, in some cases the problem arises of guiding a rocket in range and velocity. In most cases, the essence of the process of guidance in range involves transition of the rocket (usually winged) into a dive at a stipulated distance from the target. The formation of the mismatch parameter on the basis of which /217 the command for diving is produced occurs in the coordinator by a comparison of the stipulated and remaining distances r_{st} and r between the rocket and the target. Depending on what types of sighting apparatus are used in the coordinators, the determination of $r \approx r_t - r_r$ is accomplished by the computer on the basis of signals directly or indirectly characterizing r_r and r_t.

In the formation of the mismatch parameter determining the time of transition of the rocket into a dive the computer will be simplest in those cases when the coordinator includes range-finding apparatus; the computer will be more complex when it is necessary to compute r using signals received from instruments measuring velocity, angles, etc.

As already noted in chapter 2, in the case of guidance of ballistic missiles it is necessary to cut out the engine at the time when the value $|v|$ of velocity v attains a stipulated value v_{st}. If the engine is cut out by a command control system, the signal should be formed at the computer output when the condition $|v| = v_{st}$ is satisfied.

There is now a considerable number of textbooks and a considerable quantity of specialized technical literature on problems involved in the design and analysis of apparatus which performs mathematical operations with electrical signals, both in the form of a dc voltage and in the form of pulses representing digits in some (most frequently in a binary) numbering system. These problems are discussed in the greatest detail in the books cited as references 64 and 65.

The book cited as reference 63, intended for engineers and technicians, discusses the principles of design, circuits and construction of various devices for conversion of analog signals into digital signals and back. Information on conjugation and conversion devices also can be found in journal articles. For this reason, in this section for the purpose of giving a

fuller idea of the problems arising in the development of radio control systems, we will give only the necessary general information on the methods and devices for connection of the computer to the measuring instruments and the apparatus for producing the commands.

Information on the coordinates of the rocket or on the differences of the coordinates of these objects most frequently is fed to computers in the form of a dc voltage, a time interval whose limits are set by video pulses and the turning angle of an antenna, electric motor or other device.

If an analog computer is used, in a case when it is fed dc voltages, the only problem involved is matching the input and output resistances. Such a problem is solved quite easily by use of cathode followers. When the coordinates or their differences are given by time intervals which can represent the range from the control point to the rocket and target, the difference in distance between the rocket and target, the angular coordinates of the /218
rocket and target (for example, using the group method for their measurement), etc., the analog computer should include a converter making possible the use of dc voltages.

The interval determined by two video pulses is converted into a voltage by means of triggers and low-frequency filters. The trigger in such an apparatus converts the input pulses, one of which can be considered a reference pulse and the other a phase-modulated pulse, into width-modulated pulses. The low-frequency filter separates out the constant component of the voltage u_{mean} from these pulses which usually follow one another periodically; the constant component is equal to

$$u_{mean} = U_m \frac{t_i}{T_i},$$

where t_i and T_i are the duration of the time interval and the repetition interval, respectively, and U_m is the amplitude of the pulses produced by the trigger.

It is most desirable to use a potentiometer whose slide is connected to the rotating component for conversion of the angle of rotation into a voltage.

The output signal of an analog computer is a dc voltage. Therefore it is simplest to couple it to apparatus for forming commands suitable for conversion of such signals.

The operation of a digital computer requires that the voltage, time interval or angles of rotation first be converted into a code (digit). In most cases, digital computers employ a binary numbering system in which, as is well known, the digits are formed by columns of units, pairs, sets of four, etc., and each column is represented by a pulse. In this case, the

presence of a pulse characterizes the presence of a particular digit in the number, and the absence of this pulse indicates that there should be a zero in the place of the considered digit in the number. Therefore, the output signal of the converter of the digital computer should represent a so-called binary code formed of video pulses or pulses with a sinusoidal duty factor.

However, it should be noted that, in those cases when the information received by electronic measuring instruments is analyzed by digital computers, there is no need of special converters for digital computers.

The output signals of digital computers are code groups of pulses characterizing the numbers in a selected numbering system. For this reason, it is most desirable to couple such computers to apparatus for formation and transmission of commands based on the use of digital communication methods. At the same time, in some cases it can be desirable to convert the numbers into /219 analog values. Then the output apparatus of a digital computer is a converter of the "number-voltage" type.

Converters of the latter type are of basic importance for rocket equipment and are discussed adequately in chapter 7. Here, however, we describe the principles of operation and give diagrams of converters of the "time interval-number" type, "voltage-number" type and "angle-number" type.

For conversion of the time interval t_i, which is repeated periodically, into a number it is customary to use apparatus ensuring the counting of the number of pulses created during t_i by a so-called cadence generator.

The functional diagram of one of the possible variants of apparatus for conversion of the interval t_i into a binary number is represented in figure 5.7a.

The pulses u_{start} and u_{stop} (fig. 5.7c, d), denoting the beginning and end of the converted interval and usually called start and stop pulses respectively, control the operation of a trigger Tr. The latter produces a voltage which is fed to the coincidence stage CS ("I"-type circuit), which at the same time is fed u_{PG} signals (fig. 5.7b) of the pulse generator PG. During the time t_i, u_{CS} pulses are formed at the output of the CS (fig. 5.7e), the number of which is determined by the interval t_i.

It follows from the above that, by use of the trigger Tr, the pulse generator PG and the coincidence stage CS, the time interval t_i is transformed into the number of pulses n_i. Sometimes this type of conversion is called counter-pulse modulation.

The voltage u_{CS} acts on a binary counter containing N triggers Tr_1 - Tr_N; N characterizes the significance (number of digits) of the binary code used.

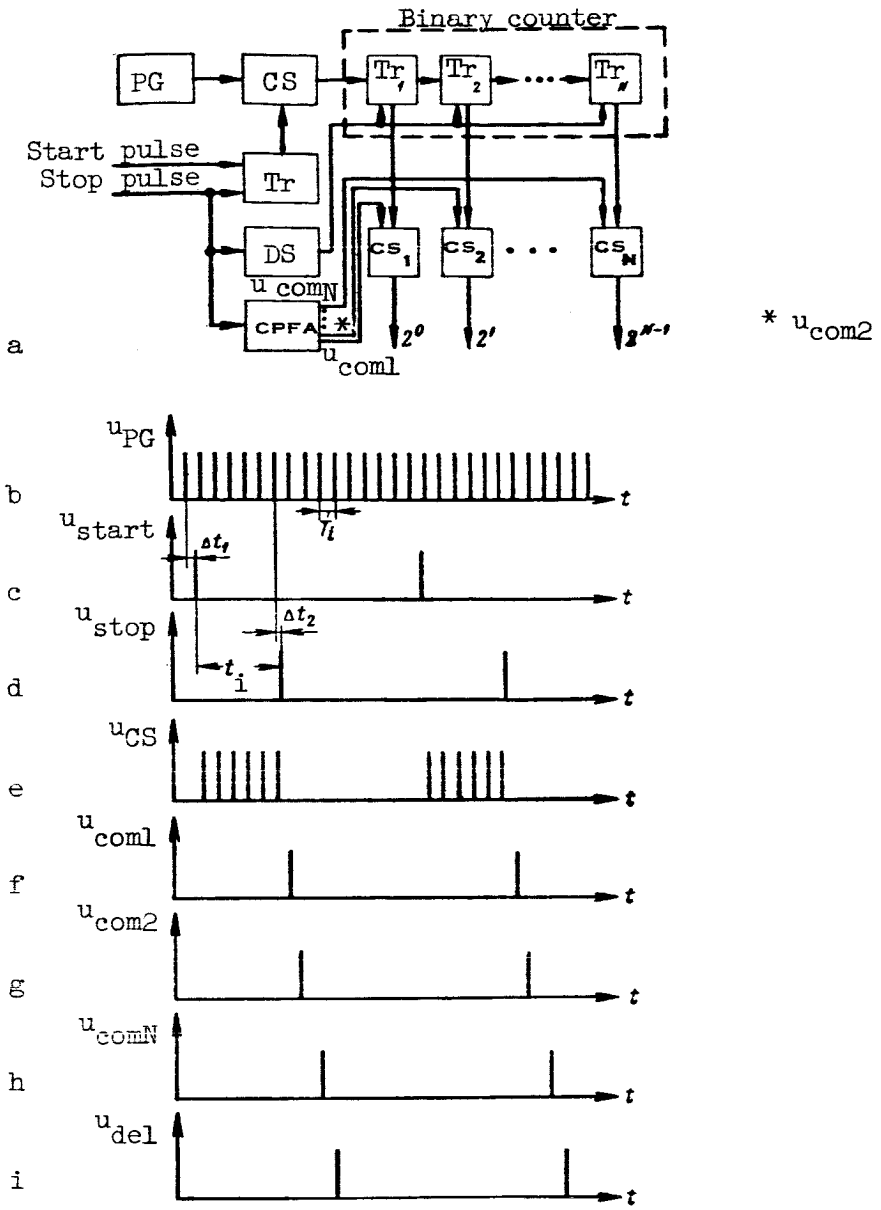

Figure 5.7

We recall that the i-th digit of the binary code (i = 1, 2, ..., N) corresponds to the number 2^{i-1} in a decimal numbering system.

The triggers in the binary counter are interconnected in such a way that two flippings of the preceding trigger cause one triggering of the next. This means that each trigger unit is a 1:2 scaler.

After all the pulses pass through the CS, the left tubes of the triggers Tr_1-Tr_N assume positions corresponding to the record of the number n_i of u_{CS}

pulses in a binary numbering system. Thus, when $n_i = 6$, as is shown in figure 5.7e, the following processes occur in the binary counter. The trigger Tr_1 "flips" 6 times and after arrival of the last pulse occupies the initial position when the left tube is "open" and the right is "closed." During this time, Tr_2 is triggered three times and at the end its right tube is "open" (unblocked). The next counting trigger flips only once, and all the other elements of the binary counter remain in position.

The signals of the binary counter are fed from the left tubes of each trigger by means of coincidence stages ("I"-type circuits) CS_1, CS_2, ..., CS_N, to which are also fed time-shifted pulses u_{com1}, u_{com2}, ..., u_{comN} (fig. 5.7f, g, h) from the output of the apparatus for forming commutating pulses CPFA. The distances at which the CPFA pulses are separated from one another correspond on the time axis to the intervals between the pulses denoting individual digits in a binary code. The stop pulse controls the operation of the CPFA. /220 /221

Under the influence of the signals u_{com1}, u_{com2}, ..., u_{comN}, at the outputs of the coincidence stages to which positive voltage drops are fed from the binary counter, pulses are formed which reflect the digits 2^0, 2^1, ..., 2^{N-1} of the binary number. In addition to the successive feeding of data from the binary counter, parallel feeding also is possible in which the commutating pulse acts simultaneously on all the CS_1, CS_2, ..., CS_N.

For preparation of the binary counter for conversion of a new time interval, prior to the arrival of each succeeding start pulse, all the triggers Tr_1, Tr_2, ..., Tr_N are returned to the initial position. This is accomplished by the voltage u_{del} (fig. 5.7i), formed by the delay stage DS under the influence of a stop pulse. The delay stage DS parameters should be selected in such a way that the u_{del} signals appear only upon termination of the action of the pulses u_N (fig. 5.7h).

In the described method, the feeding of data from the binary counter and the restoration of the triggers Tr_1, Tr_2, ..., Tr_N, the times of formation of the pulses u_{com1}, u_{com2}, ..., u_{comN} and u_{del} will change relative to the sectors of time during which the start pulses act. This can be attributed to the change of the value t_i. Elimination of this effect requires that the CS and CPFA be triggered by u_{start} pulses (fig. 5.7c).

Errors arise in the conversion of the time interval into a binary code with the apparatus whose functional diagram is shown in figure 5.7a. The principal causes of the appearance of conversion errors are: instability of the pulse generator PG, level and time quantization of the time interval and also ambiguity in the position of the start and stop pulses relative to the PG signals.

Errors in level quantization are caused by the fact that binary numbers cannot be used to reflect all the possible values of the time interval t_i. The maximum error in conversion Δt_{lev}, arising due to level quantization, is determined by a value equal to the repetition interval T_i of the PG pulses (fig. 5.7b).

If the values of the maximum possible interval $t_i = t_{i\,max}$ and the interval T_i are known, the required number N of triggers of the binary counter can be found using the following expression

$$2^N - 1 = \frac{t_{i\,max}}{T_i}.$$

It can be seen from this expression, determining the number of intervals into which the time interval $t_{i\,max}$ is divided, that with a decrease of T_i the value N increases.

In some cases, in place of the maximum error $\Delta t_{lev} = T_i$, it is pos- /222
sible to use the concept of mean square error, which can be computed using the known probability distribution law characterizing the difference between the length of the real time interval and the interval corresponding to the whole number $n_i + 1$ of intervals T_i appearing at the CS output (fig. 5.7a).

The time quantization errors are determined by the fact that the converted function is sensed by the converter only at individual moments of time. It is easy to see that with an increase of the repetition frequency F_{rep} of the start and stop pulses, this form of errors can be reduced to a stipulated value. The selection of F_{rep} should be accomplished on the basis of the properties of those elements which, on the basis of discrete data, restore the initial continuous time function.

Due to the uncertainty in the position of the start and stop pulses in relation to the PG pulses, there will be errors Δt_1 and Δt_2 (fig. 5.7c, d), one of which (Δt_1) is positive and the other negative, since by definition the

error is characterized by the difference between the interval which is received and the actual value t_i. It must be remembered that the interval T_i, situated before the first pulse, which is formed at the output of the coincidence stage CS, is included in the length of the determined (measured value) interval.

If the start pulses and the PG signals are fed synchronously, the error Δt_1 does not occur. For synchronization of the mentioned signals, it is possible to form start pulses by the division of the repetition frequency of the PG pulses or creation of PG pulses under the influence of start pulses after corresponding multiplication of their repetition frequency.

It is impossible to eliminate the error Δt_2 completely. However, by a decrease of the period T_i, it can be made as small as desired. At the same time, there always is a limit of increase of the frequency $F_i = \frac{1}{T_i}$, determined by the attained speed of response of the first stages of the binary counter.

Therefore, when the required frequency F_i becomes inadmissibly large, to ensure the decrease of Δt_2 additional devices are used which operate under the influence of pulses shifted relative to the PG signals by a time determining the admissible value of the error Δt_2.

The functional diagram of one of the possible variants of the converter, making it possible to decrease Δt_2 without a change of T_i, is shown in figure 5.8. In this converter, the pulse generator PG, trigger Tr, coincidence stage CS, delay stage DS, apparatus for forming commutating pulses CPFA, binary counter BC and data feeding apparatus DFA, which contains a type "I" circuit, perform the same functions as in the converter discussed earlier. Additional elements of the converter are the delay lines DL_1-DL_n, coincidence stages /223 CS_1-CS_n and triggers Tr_1-Tr_n; n defines the number of intervals by which the interval T_i is divided in order for the maximum value of the error $\Delta t_2 = \frac{T_i}{n}$ not to exceed the stipulated value. The coincidence stages are fed pulses from the Tr and series of pulses with the cadence period T_i, with the time shift $\frac{T_i}{n}, \frac{2T_i}{n}, \ldots, \frac{(n-1)T_i}{n}$. The necessary shift is given by the delay lines. Each of the coincidence stages CS_1-CS_n transmits to the output pulses whose number is dependent on the length of the converted interval. Under the influence of the pulses fed from CS_1-CS_n, there is flipping of the triggers Tr_1-Tr_n.

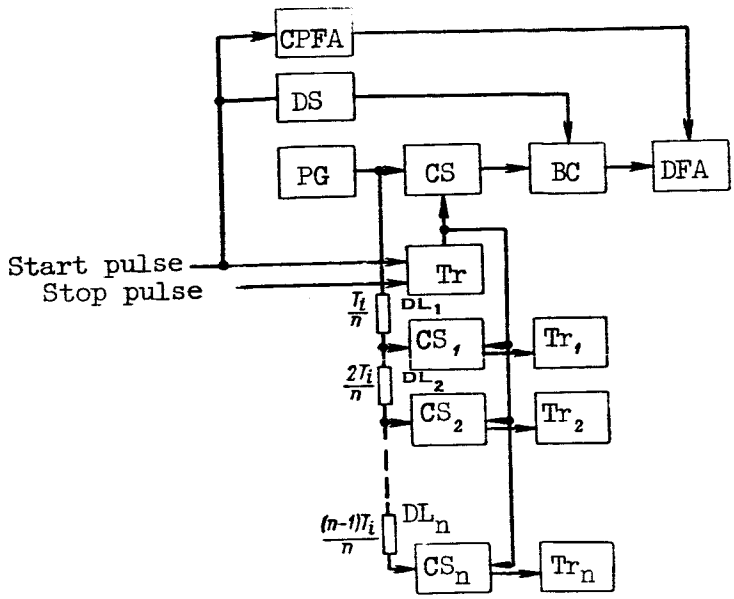

Figure 5.8

For example, if the interval t_{pi} between the last pulse passing through the coincidence stage CS and the stop pulse exceeds $\frac{T_i}{n}$, the trigger Tr_1 is fed the same number of pulses as are fed to the principal binary counter BC. Therefore, the trigger Tr_1 and the first unit of the binary counter at the end of counting are in an identical position. Similar processes also will occur in the triggers Tr_2, ..., Tr_n, if the interval t_{pi} is greater than the value

$$\frac{2T_i}{n}, \ldots, \frac{(n-1)\,T_i}{n}.$$

The fixed positions of the triggers Tr_1-Tr_n after termination of operation of the coincidence stages CS can be used for more precise determination of the value t_i of the converted time interval.

The principal shortcomings of the considered method for decreasing the error Δt_2 can be attributed to the extremely rigid requirements imposed on the duration and shape of the pulses produced by the delay lines. It is easy to see that the duration of these pulses should be less than the interval $\frac{T_i}{n}$.

Due to the instability of the repetition frequency of the pulses of /224 the generator PG, the same interval t_i can be reflected by a different number of PG pulses. The maximum error is obtained in the conversion of the

maximum time interval $t_{i\ max}$. If the repetition frequency F_i of the PG pulses remains constant, the maximum number of pulses n_{max} will be formed at the CS output and will be equal to

$$n_{max} = \frac{t_{i\ max}}{T_i}. \tag{5.4.4}$$

When the repetition frequency of PG pulses is $F_{il} = F_i(1 + \alpha_{in})$, where α_{in} is the frequency instability coefficient, the binary counter will be fed n_1 pulses; then

$$n_1 = \frac{t_{i\ max}(1 + \alpha_{in})}{T_i}. \tag{5.4.5}$$

On the basis of expressions (5.4.4) and (5.4.5) we find

$$n_1 = n_{max} + \alpha_{in} n_{max}. \tag{5.4.6}$$

If the admissible value of the error $n_1 - n_{max}$ is stipulated, it is easy to use formula (5.4.6) to compute the necessary stability of the pulse generator PG. For example, when $|n_1 - n_{max}| = 1$, the following condition should be satisfied.

$$|\alpha_{in}| \leq \frac{1}{n_{max}}.$$

The derived expression in essence characterizes the admissible instability of the frequency F_i under the condition that the conversion errors associated with α_{in} and the level quantization of the interval t_i have identical values.

In conversions of intervals of short duration the principle of change of the time scale is applied, which in essence is equivalent to the multiplication of t_i by some factor greater than unity. This problem is solved by the preliminary conversion of t_i into a voltage and the amplification of the latter. The voltage u_t obtained in this way then is converted in a time interval.

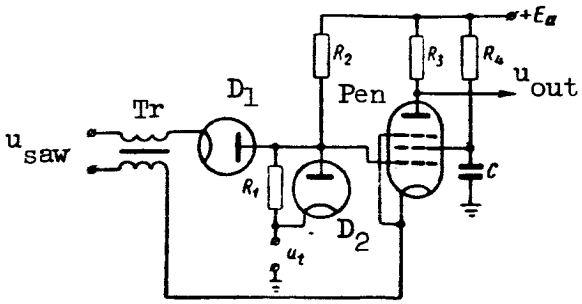

Figure 5.9

This usually is done using a saw-toothed wave generator and an amplitude discriminator, which give a pulse when there is equality of u_t and the sawtooth voltage u_{saw}. The interval between the times characterizing the beginning of the saw and the appearance of a pulse at the output of the amplitude discriminator reflects the interval t_i at some scale.

The most widely used amplitude discriminators are so-called diode-regenerative comparators, one of whose diagrams is shown in figure 5.9.

The linearly decreasing sawtooth voltage u_{saw} is applied to the transformer Tr, whose primary winding is connected to the cathode circuit of the pentode Pen and thereby ensures a positive connection with the pentode grid, and the positive voltage u_t is connected to the cathode of the diode D_2 /225 and the anode of the diode D_1.

If the value u_{saw} exceeds u_t, the diode D_1 is blocked out and as a result the positive feedback circuit is unblocked, despite the fact that a current flows through the primary winding of the transformer. When $u_{saw} = u_t$, the diode D_1 is unblocked and due to the closing of the positive feedback circuit the pentode Pen is blocked out. Then the pentode Pen remains blocked out because $u_{saw} < u_t$. At the time of blocking out of the pentode Pen a voltage pulse u_{out} is formed at its output. In the considered diagram, the diode D_2 is used for compensation of the shift of the characteristic of the diode D_1 (for example, due to a change of the filament voltage), which leads to the appearance of conversion errors.

The methods used for conversion of a voltage into a number are based on timing and frequency coding and also on the preliminary conversion of a voltage

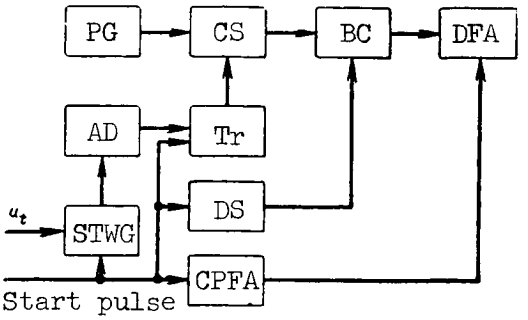

Figure 5.10

into amplitude-modulated pulses. The essence of the first method, which is one of the most feasible, is a preliminary conversion of a voltage in a time interval. Accordingly, the functional diagram of the apparatus for conversion of a voltage into a number will have the form shown in figure 5.10. The voltage u_t is converted in a time interval by the saw-toothed wave generator STWG and the amplitude discriminator AD. All the remaining elements of the converter are the same as in figures 5.7a and 5.8.

The errors in conversion of the voltage u_t into a binary code are determined primarily by the properties of the saw-toothed wave generator and the amplitude discriminator because the time interval, if appropriate measures are taken, can be converted into a number with whatever accuracy is desired. It is necessary, therefore, to ensure corresponding stability of the beginning of the saw-toothed wave and its steepness, and also to determine correctly the /226 time of the equality of the u_t and u_{saw} voltages.

The principle of frequency coding is based on the preliminary conversion of a voltage into a sinusoidal signal of the corresponding frequency. This mission is performed in the converter whose functional diagram is shown in figure 5.11 by the FM generator FMG. The signals from the output of the FMG and the special generator Gen_2 of the standard frequency f_2 are fed to the converter Con which produces a sinusoidal voltage of the difference frequency $f_{dif} = f_1 - f_2$, where f_1 is the frequency of the oscillations formed in the FMG. The pulse generator PG forms pulses at those times when the voltage u_{con} of the converter Con becomes equal to zero, with its transition, for example, from negative to positive values.

The PG also is fed a pulse u_∂ from the output of the time interval pickup. The voltage u_∂ determines the time during which the PG pulses can act on the binary counter BC. The signals of the binary counter are fed to a data feeding

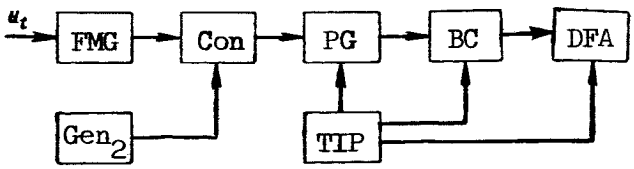

Figure 5.11

apparatus DFA of the type described above. The restoration of the counter BC and control of the operation of the data feeding apparatus DFA is by signals from the TIP.

It follows from a study of figure 5.11 that the output signal of such a converter will represent a number reflecting the value of the voltage for some time interval t_i and that the generator Gen_2 is necessary for obtaining a zero number when $u_t = 0$. The accuracy of conversion of the described apparatus is determined primarily by the characteristics of the generator FMG and usually is relatively low.

The principle of conversion of the voltage u_t into a binary number by pulse-amplitude modulation will be illustrated using the example of the apparatus whose functional diagram is shown in figure 5.12. The converted voltage u_t and the periodically repeated pulses u_p are fed to the pulse-amplitude modulation stages where pulse-amplitude modulation occurs.

Each video pulse, whose amplitude is proportional to u_t, after passing through the mixer Mix is fed to the delay line DL, fixing the intervals between the pulses for digits in a binary code.

The pulses are fed from the output of the delay line to the amplitude analyzer AA and the subtracting device SD. It will be assumed hereafter that the mixer and the subtracting device SD have amplification factors equal to unity. In the amplitude analyzer the amplitude of the arriving pulse is compared with the standard voltage $u_{st} = 1/2\ U_m$, where U_m is the maximum possible amplitude of a modulated pulse. /227

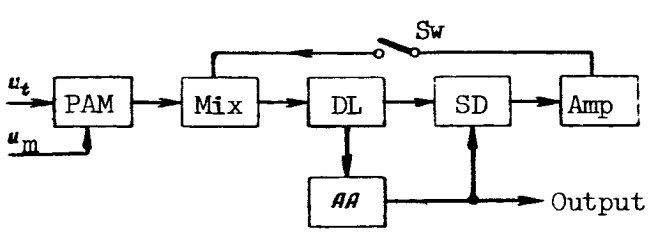

Figure 5.12

If the amplitude of the arriving pulse is greater than u_{st}, at the output of the amplitude analyzer there will be a standard pulse with the stipulated duration τ_p and the amplitude $1/2\ U_m$. When the amplitude of the arriving pulse is less than u_{st}, there will be no signal at the AA output.

The subtracting device forms the difference between the voltages fed to the SD from the delay line DL and the amplitude analyzer AA. If there are no pulses at the AA output, the delay line (DL) signal passes to the amplifier Amp, having the transfer constant 2, without changes. The switch Sw which operates automatically breaks the feedback circuit after final formation of the binary code.

The described circuit can be changed by elimination of the amplifier Amp. However, in this case in the amplitude analyzer AA, it is necessary to compare the amplitudes of the pulses produced by the delay lines DL with the voltage, which decreases by a factor of 2 after each cycle of passage of the signal through the amplitude analyzer.

A distinguishing characteristic of converters based on the use of pulse-amplitude modulation is the dependence of errors on changes of the amplitude characteristics of a considerable number of elements. For this reason such converters can be used only when there is a small number of digits in the binary code.

The conversion of an angular value into a code can be based on preliminary conversion of the angle into a dc voltage or the phase of a sinusoidal voltage and also by the use of magnetic drums and converters of the so-called storage type.

The preliminary conversion of an angle into a voltage is accomplished most easily using a potentiometer. However, the errors of standard-produced potentiometers usually are not less than 0.1 percent. Therefore, taking into account the errors of conversion of voltage into a number, it can be concluded that it is possible to use the above-described method in those cases when a high accuracy is not required.

The preliminary conversion of an angle into the phase of a sinusoidal voltage is rather commonplace in actual practice. The functional diagram of one of the possible "angle-phase-number" conversion apparatuses is shown in figure 5.13a.

The sinusoidal oscillations generator SOG produces a voltage u_0 (fig. 5.13b) called a reference voltage. This voltage is fed to the phase inverter PI and the pulse shaper Sh-2. In the phase inverter, as a result of the rotation of its axis under the influence of the converted angle β_m, a voltage u_p is formed (fig. 5.13b). The difference of the phases $\Delta\varphi$ of the voltages u_0 and

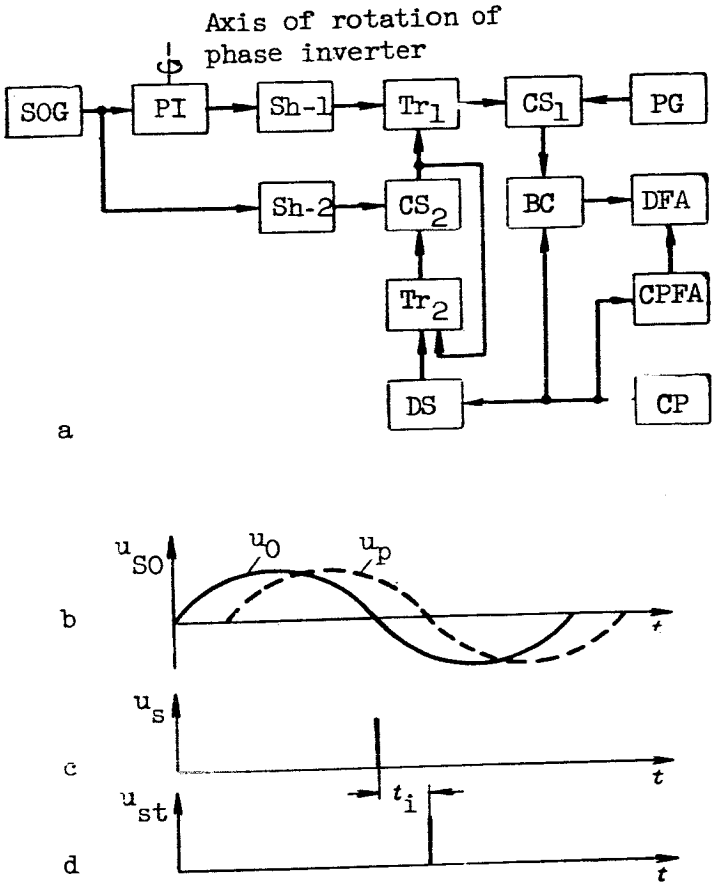

Figure 5.13

u_p characterizes the angle θ_m. Accordingly, in the shaper Sh-1, to which is fed the u_p signal, and in Sh-2, stop and start pulses are formed (fig. 5.13d, c) determining the limits of the interval t_i by means of which $\Delta\varphi$ is re- /228 flected. The start pulse is fed to the coincidence stage CS_2, whose second input signal is the output pulse of the trigger Tr_2. The latter is triggered by a pulse of the delay stage DS at whose input signals arrive from the cycle pickup CP. In addition, the cycle pickup ensures restoration of the initial position of all the trigger units of the binary counter BC.

In the case of simultaneous effect of the Sh-2 and Tr_2 voltages, a pulse is formed at the CS_2 output which triggers both Tr_1 and Tr_2. The next triggering of Tr_2 leads to cutting out of Sh-2 from Tr_1 until the arrival of the

next pulse from the delay stage DS. The end of the effect of the positive voltage drop from Tr_1 is caused by a stop pulse. All the other elements, the coincidence stage CS_1, the pulse generator PG, the binary counter BG, the data /229 feeding apparatus DFA and the apparatus for forming commutating pulses CPFA perform the same functions as in the earlier considered types of converters.

In the process of conversion of "angle-number," errors arise whose principal sources are the phase inverter and the apparatus for forming stop and start pulses. In addition, errors are caused by the frequency instability of the oscillations created by the PG and SOG generators.

If the entire range β_{max} of the converted angle β_m should be reflected by n intervals and the minimum length of an interval corresponds to $\Delta\beta$ degrees, the required relation between the frequencies f_0 and F_i of the signals fed from the SOG and PG can be determined on the basis of the following expression

$$n = \frac{\beta_{max}}{\Delta\beta} = \frac{T_0}{T_i} = \frac{F_i}{f_0},$$

where $T_0 = \frac{1}{f_0}$.

For example, if $\beta_{max} = 360^\circ$, $\Delta\beta = 1'$ and $f_0 = 400$ cps, the required frequency is $F_i = 8.6$ Mc/s. It therefore follows that performance of a converter with an error $\Delta\beta = 1'$ encounters virtually insuperable difficulties.

In order to obtain sufficiently small errors at relatively low frequencies f_0, it is desirable to use a two-channel converter similar to the method used in selsyn transfer systems.

The principle of design of converters based on the use of magnetic drums is illustrated in figure 5.14. The magnetic drum D, rotating with the constant angular velocity ω_D, has two magnetic tracks T_1 and T_2. On the magnetic track T_1 which together with the counting head CH_1 plays the role of a pulse generator PG in the apparatus considered earlier, marks are plotted at equal intervals in the form of magnetized sectors of a small width. At the same time, there are no such marks on the track T_2.

The recording head RH magnetizes a short part of the track T_2 at the time when the cycle pickup CP forms a voltage pulse which is fed to RH through the

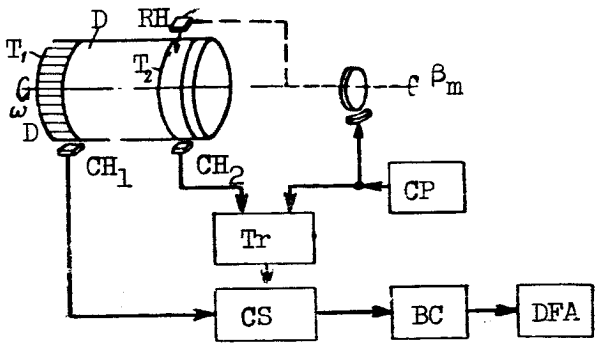

Figure 5.14

axis of rotation, whose angle of rotation β_m is to be converted into a digit. At the same time, the CP signals flop the trigger Tr, which opens the way for the pulses of the T_1 track to travel to the binary counter BC through the coincidence stage CS. The time of the "flopped" trigger Tr is dependent on the angular distance between the fixed counting head CH_2 and the moving recording head RH. The signals from the BC are fed to the data feeding apparatus DFA. At the end of each cycle, the mark on the track T_2 is erased. The elements restoring the SD elements and commutating the DFA have not been shown in figure 5.14. /230

The maximum error in quantization is

$$\Delta\beta = \frac{360^\circ}{m\pi d_d},$$

where m and d_d are the number of pulses from one millimeter of the track T_1 and the drum diameter, respectively.

All the types of apparatus considered here are converters of the cyclic type. A distinguishing characteristic of such converters is that in each new cycle the total value of the measured parameter is determined again. Converters of the storage type react only to increments of the input value. Thus, during the conversion of an angle into the number of rotations of the input axis by one unit angle, that is, an angle corresponding to the level quantization interval, the binary number produced by the counter increases (decreases) by one binary unit. In order to be able to determine what operation (addition or subtraction) should be accomplished in the counter, the converter must include a device which reacts to the direction of change of the angle.

The simplest method for designing a converter of the storage type is based on creation of a contact system around a shaft which rotates by the converted angle β_m.

5.5. Functional and Block Diagrams of Coordinators of the First Kind for Different Rocket Guidance Methods

A coordinator for the measurement of the mismatch parameter in two mutually perpendicular planes usually consists of two identical parts. Therefore, hereafter we will determine the makeup of the coordinators and the functional relationship of their individual elements only with respect to the determination of the mismatch parameters for the vertical plane alone. The target coordinates measuring instrument (TCI) can be placed together with the rocket coordinates measuring instrument (RCI) or in any other point in space.

The simplest coordinator is obtained in those cases when the TCI, RCI and control point are situated in the same place. This can be attributed to the fact that with such a placement of the instruments for measuring coordinates and forming commands, it is not necessary to have data transmission systems and the TCI and RCI coordinate systems coincide with one another. The same conclusion can be drawn when there is an insignificant distance between /231 the RCI and the TCI, since the resulting parallax in such cases is insignificant.

In those cases when the control point, RCI and TCI are situated at relatively great distances from one another, the coordinator will be more complex. This is because data transmission systems will be needed and also an additional computer for scaling the signals of the measurement instruments from one coordinate system to another.

Hereafter in order to obtain simpler and more graphic diagrams and equations which will be analyzed, it is assumed that the RCI and the TCI, for determination of the target and rocket coordinates for rocket guidance by the coincidence method and the parallel approach method, and also the control point are situated in the same place. In addition, for unambiguity it will be assumed that the output signals of the RCI, TCI and computer are dc voltages.

The latter assumption does not essentially limit the number of types of measuring instruments which can be used in the coordinators considered here. This is because when the signals formed by the measuring instruments are not in the form of voltages, the computer will include appropriate converters. Since hereafter only the vertical guidance plane will be considered, for the sake of brevity the subscript "y" on the symbols characterizing target and rocket coordinates will be omitted.

1. Coordinators with Radar Sighting Apparatus

As follows from equation (5.4.1), when a rocket is guided by the coincidence method, it is necessary to measure the angles ε_r and ε_t, and the

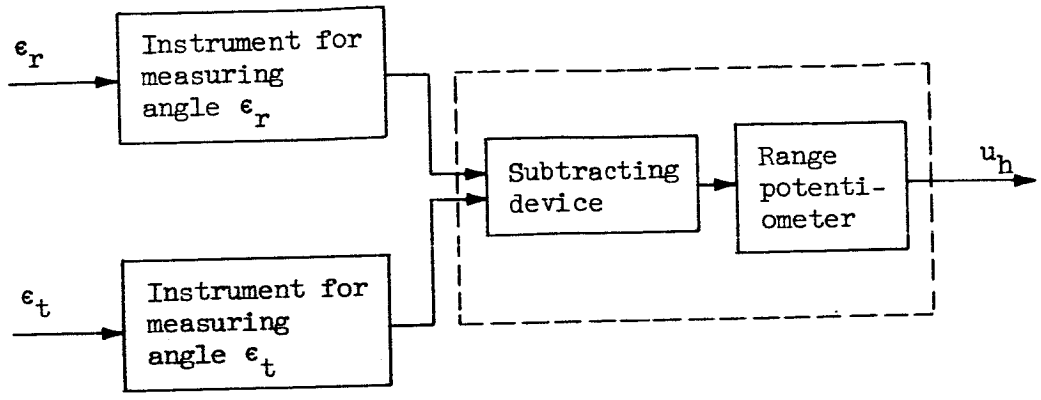

Figure 5.15

programming apparatus should produce a signal characterizing the distance $r_{pr} \approx r_r$.

Electronic apparatus for measurement of the angles ϵ_r and ϵ_t create voltages $u_r(t)$ and $u_t(t)$ which are unambiguously related to ϵ_r and ϵ_t if random errors are not taken into account. The voltage $\Delta u = u_t - u_r$ is formed in the computer; this voltage is fed to the range potentiometer, increasing Δu by $k_{pot\partial} r_{pr} \approx k_{pot\partial} r_r$ times, where $k_{pot\partial}$ is the transfer coefficient of the range potentiometer. In accordance with the above, we can write the following equation for the coordinator producing the voltage $u_h(t)$ which is necessary for rocket guidance in a vertical plane by the coincidence method

$$u_h(t) = k_{pot\partial} r_{pr} [u_t(t) - u_r(t)]. \qquad (5.5.1)$$

On the basis of this equation we obtain the functional diagram of the coordinator shown in figure 5.15 (without the radio transmitter carried on the rocket).

The signals formed by the rocket and target coordinates measuring instruments can be represented as functions of time, expressed in degrees, if $u_r(t)$ and $u_t(t)$ are separated into the coefficients k_{rc} and k_{tc}. These coefficients characterize the values u_r and u_t in a steady-state regime when the angles ϵ_r and ϵ_t of a unit value act at the inputs of the RCI and TCI. We note that this approach for conversion fron u_r and u_t to ϵ_r and ϵ_t is admissible only in linear systems. /232

Under real conditions, as a result of the presence of inertial elements, the changes of the supply voltages, etc., the voltages $u_r(t)$ and $u_t(t)$ reflect the angular coordinates of the rocket and target with an error. Therefore, it is possible to write that

$$u_t = k_{tc}\epsilon_{tm}, \quad u_r = k_{rc}\epsilon_{rm},$$

where ϵ_{tm} and ϵ_{rm} are the measured values of the angles $\epsilon_t(t)$ and $\epsilon_r(t)$, differing from ϵ_t and ϵ_r by the values of the errors dependent on the dynamic properties TCI and RCI and also on the stability of the characteristics of the elements forming these apparatuses.

The voltage u_h at some scale represents the so-called measured value h_m of the mismatch parameter h; h_m differs from h by the value of the error caused by the conversion properties of the coordinator as a whole. Then we will have

$$u_h = k_h h_m,$$

where k_h is the value of the voltage forming at the output of the coordinator in a steady-state regime with a unit linear deflection of the center of mass of the rocket from the control point-target line.

By substituting the determined values u_t, u_r and u_h into expression (5.5.1) we obtain

$$u_h = k_h h_m = r_r k_{pot\partial} k_{rc}\left(\frac{k_{tc}}{k_{rc}}\epsilon_{tm} - \epsilon_{rm}\right). \qquad (5.5.2)$$

It therefore follows that in order to ensure a zero voltage u_h when $\epsilon_t = \epsilon_r$ and identical errors of determination of these angles, the measuring instruments ϵ_t and ϵ_r should have equivalent transfer functions k_{tc} and k_{rc}. /233

In addition, when $k_{tc} = k_{rc}$, the condition $k_h = k_{pot\partial} k_{rc}$ should be satisfied, since the linear deflection of the center of mass of the rocket from a reference trajectory with a high degree of accuracy is determined by the product of the distance r_r and the difference of the angular coordinates of the target and rocket.

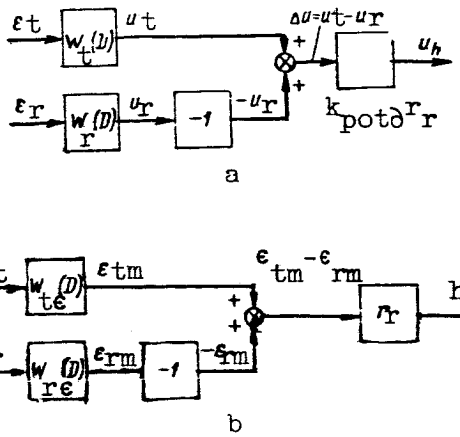

Figure 5.16

Then the second form of the coordinator equation assumes the form

$$h_m = r_r\,(\varepsilon_{tm} - \varepsilon_{rm}). \qquad (5.5.3)$$

The derivation of the second form of the coordinator equation is of importance in computing the errors in measurement of the mismatch parameter, expressed in linear units, for cases when the measuring instruments can be considered linear systems. However, this equation is not necessary in an analysis of errors in rocket guidance dependent on the parameters of the control system as a whole. On the other hand, in the solution of the mentioned problem, it is more desirable to have an equation written in the form (5.5.1).

Equations (5.5.1) and (5.5.3) show that the coordinator is a system with variable parameters. This also follows from the fact that $r_r \approx r_{pr}$ is a function of time. However, in actual practice, the value $r_r(t)$ changes considerably more slowly than all the other components entering into the coordinator equation and the equations for the control system as a whole. This gives basis for using the principle of "freezing" of the variable coefficient $r_r \approx r_{pr}$.

If the transfer functions of the RCI and TCI measuring instruments, whose output signals are $u_r(t)$, $u_t(t)$, $\varepsilon_{rm}(t)$ and $\varepsilon_{tm}(t)$, are denoted respectively by $W_r(D) = \dfrac{u_r(t)}{\varepsilon_r(t)}$, $W_t(D) = \dfrac{u_t(t)}{\varepsilon_t(t)}$, $W_{r\varepsilon}(D) = \dfrac{\varepsilon_{rm}(t)}{\varepsilon_r(t)}$ and $W_{t\varepsilon}(D) = \dfrac{\varepsilon_{tm}(t)}{\varepsilon_t(t)}$, on the basis of equations (5.5.1) and (5.5.3) we obtain

$$u_h(t) = k_{pot\partial}\, r_r\,[W_t(D)\varepsilon_t(t) - W_r(D)\varepsilon_r(t)], \qquad (5.5.4)$$

$$h_m(t) = r_r [W_{t\epsilon}(D)\epsilon_t(t) - W_{r\epsilon}(D)\epsilon_r(t)]. \quad (5.5.5)$$

It should be noted that in these equations /234

$$W_{t\epsilon}(D) = \frac{1}{k_{tc}} W_t(D)$$

and

$$W_{r\epsilon}(D) = \frac{1}{k_{rc}} W_r(D).$$

The block diagrams corresponding to equations (5.5.4) and (5.5.5) are shown in figures 5.16a and 5.16b, respectively.

On the basis of expression (5.4.2), it is possible to obtain the following coordinator equation ensuring the formation of the voltage u_h, corresponding to the approximate method of parallel approach which technically is most easily feasible

$$u_h(t) = k_{pot\partial} r_r \left\{ u_t(t) - u_r(t) - \frac{u_{\partial t}(t) - u_{\partial r}(t)}{u_{pr}(t)} [u_\epsilon(t) - u_t(t)] \right\}, \quad (5.5.6)$$

where $u_{pr}(t)$ is the voltage characterizing the distance r_{pr} between the rocket and control point; $u_\epsilon(t)$, $u_{\partial t}$ and $u_{\partial r}(t)$ are the voltages reflecting the angles ϵ_0 and the distances r_t and r_r.

In the writing of the equation (5.5.6) it was assumed that the voltage

$$u_{res} = u_t(t) - u_r(t) - \frac{u_{\partial t}(t) - u_{\partial r}(t)}{u_{pr}(t)} [u_\epsilon(t) - u_t(t)],$$

produced in the computer in the long run is converted by the range potentiometer.

If the output signal of the coordinator is expressed in linear units defining the deflection of the center of mass of the rocket from the reference trajectory, it is possible to find the second form of the coordinator equation

$$h_m(t) = r_r (\epsilon_{tm} - \epsilon_{rm}) - (r_{tm} - r_{rm}) (\epsilon_{0m} - \epsilon_{tm}), \quad (5.5.7)$$

where r_{tm}, r_{rm} and ϵ_{0m} are the measured values of the distances r_t and r_r and also the angle ϵ_0.

In this case, r_{tm} and r_{rm} differ from r_t and r_r by the value of the measurement error, and $\epsilon_{0m} - \epsilon_0$ characterizes the accuracy of the apparatus used in setting the angle ϵ_0.

We note that the second form of the coordinator equation in the parallel approach method is obtained the same as for the coordinator which is used in rocket guidance by the coincidence method.

It also should be emphasized that in determining the equation (5.5.7), the scale factors for the instruments for measuring the angles ϵ_t, ϵ_r and the pick-up for the angle ϵ_0 were assumed to equal one another. The scale factors for the distance measuring instruments and pickup r_t, r_r and $r_{pr} \approx r_r$ also were considered identical.

Expression (5.5.6) can be used in constructing the block diagram for /235 the coordinator shown in figure 5.17. In such a coordinator the master controls serve for conversion of the angle ϵ_0 and the distance r_{pr} into voltages. We recall that equations (5.5.6) and (5.5.7), as well as the diagram shown in figure 5.17, are correct only if the TCI and RCI are in the same place.

Figures 5.18a and 5.18b show the block diagrams corresponding to equations (5.5.6) and (5.5.7), respectively. In the representation of these block diagrams, it was assumed that the transfer functions $N_t(D)$, $N_{tr}(D)$ and $N_{rr}(D)$ are equal to

$$N_t(D) = \frac{u_{\partial t}(t)}{r_t(t)}, \quad N_{tr}(D) = \frac{r_{tm}(t)}{r_t(t)},$$

$$N_r(D) = \frac{u_{\partial r}(t)}{r_r(t)}, \quad N_{rr}(D) = \frac{r_{rm}(t)}{r_r(t)}.$$

In case it is necessary to use the approximate method of parallel approach corresponding to equation (5.4.2a), or the precise method of parallel approach, the functional and block diagrams of the coordinator should be developed in accordance with equations (5.4.2a) and (5.4.3), the same as in the preceding case.

If the rocket and target sighting apparatus are not situated at the same place, it is necessary to introduce into all the cited equations and diagrams

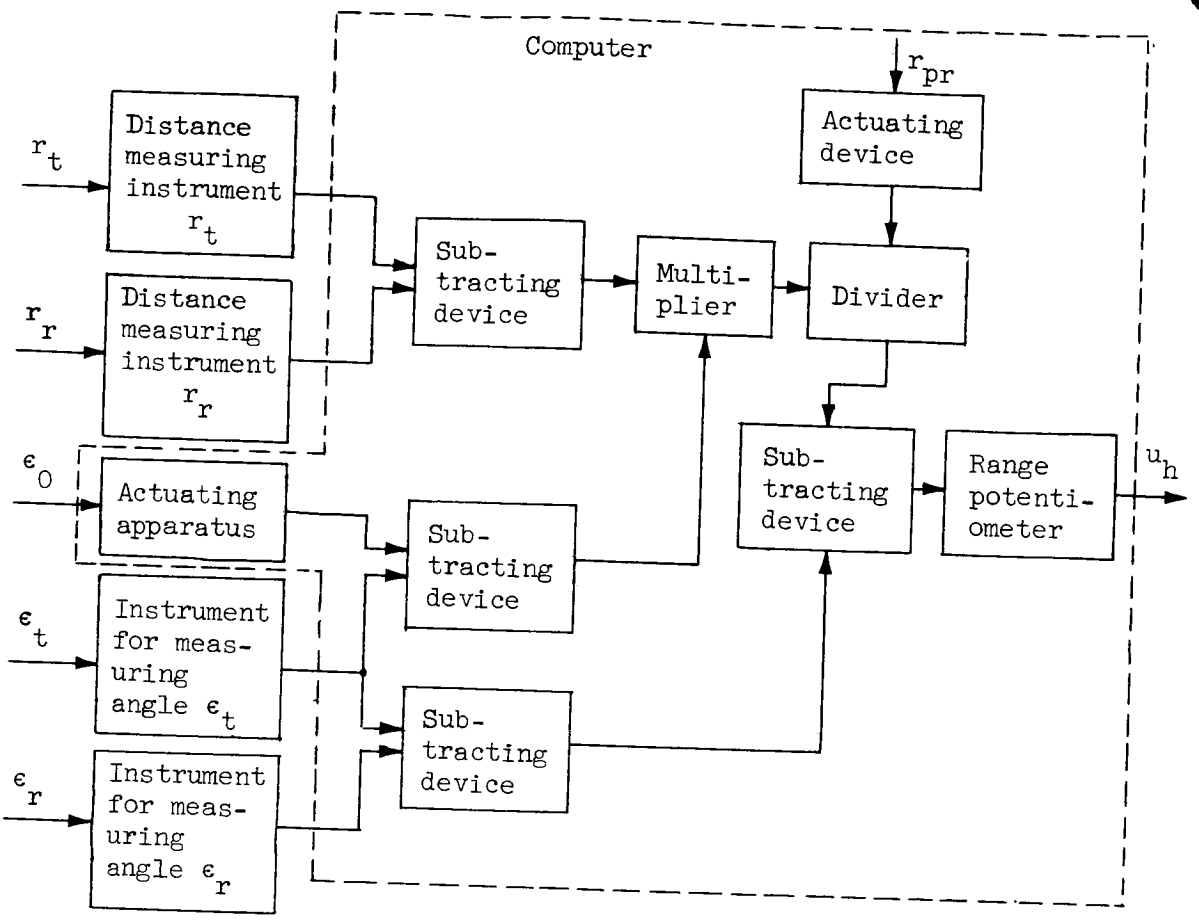

Figure 5.17

appropriate changes because of the presence in the computer of instruments for the scaling of ϵ_t, ϵ_r, r_t and r_r from one coordinate system to another. /236

In addition to regulating the position of the center of mass of the rocket in accordance with the signals characterizing the linear deflection h, it is possible to construct a coordinator for guidance by the parallel approach method in such a way that during the control process there will be formation of commands determining the value of the deflection of the vector v from the stipulated direction. In this case, the coordinator should be constructed on the basis of equation (2.8.5).

In order to ensure the transition of a winged rocket into a dive or cut-off of the engine of a ballistic rocket, the signals of radar measuring instruments are used for the computation of the remaining range from the rocket to the target or the value of the velocity vector tangent to the trajectory, respectively.

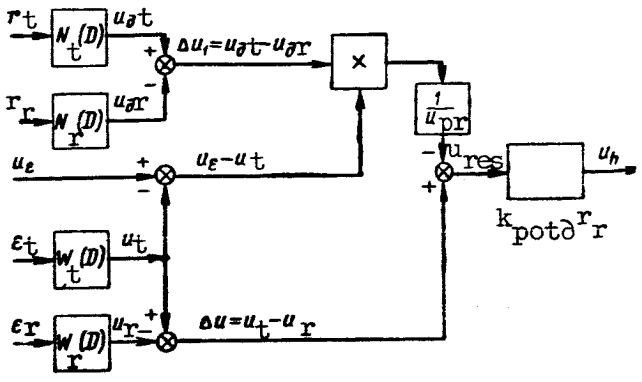

a

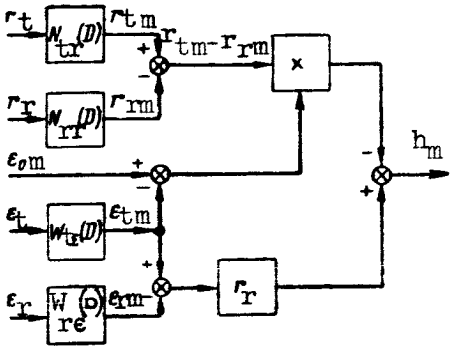

b

Figure 5.18

2. Coordinators Based on Use of Radio Navigation Sighting Apparatus

Radio navigation apparatus only makes it possible to measure rocket coordinates. Therefore, as already noted, command control systems based on radio navigation sighting apparatus can be used only for guidance of rockets along fixed trajectories. The simplest coordinator is obtained in those cases when a winged rocket moves on the main segment of the trajectory with a constant course at a constant altitude, and goes into a dive at a stipulated distance from the target on commands transmitted from the control point. In such a flight regime, the coordinator of the command control system is constructed for the determination of the linear deflection of the center of mass of the rocket from the reference trajectory in the horizontal plane only and the difference between the remaining and stipulated ranges between the rocket and the target. In this case, the stabilization of rocket flight altitude is accomplished by an autonomous control system. /237

In command control of ballistic rockets the coordinator should produce signals characterizing the deflection of the center of mass of the rocket from

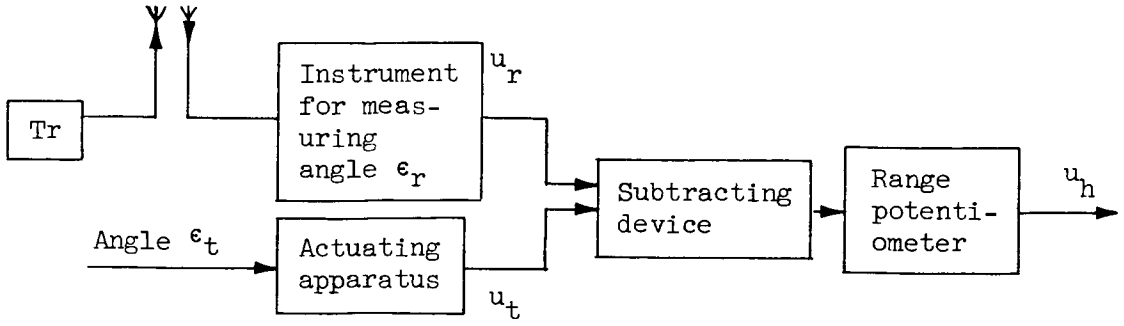

Figure 5.19

a reference (fixed) trajectory in the horizontal plane and the signal determining the time of the equality of the values of the stipulated and current velocities v_{st} and v.

Radio navigation sighting apparatus for coordinators of command control systems can include Doppler instruments for measuring velocity and angle-measuring, range-finding, angle-measuring – range-finding and add-subtract – range-finding apparatus.

When using an angle-measuring radio navigation apparatus, the functional diagram of the coordinator has the form shown in figure 5.19. This diagram differs from the diagram shown in figure 5.15 due to the absence of an instrument for measuring the angle ϵ_t and the presence of a radio transmitter Tr aboard the rocket. The instrument for measuring the angle ϵ_t is replaced by master controls which convert the stipulated angle ϵ_t into an electrical signal u_t.

The equations and the block diagrams for this coordinator can be obtained from equations (5.5.4) and (5.5.5) under the condition that in them

$$u_t = W_t(D)\epsilon_t = \text{const}$$

and

$$W_{te}(D) = 1.$$

It should be noted that with the separate placement of the control point and the instrument for measuring the angle ϵ_r, the coordinator should be supplemented by a system for the transmission of the voltage u_r. /238

If the coordinator is based on the use of an angle-measuring – range-finding radio navigation apparatus, its makeup remains the same as in a control system based on a fixed radio zone. However, the coordinator apparatus which

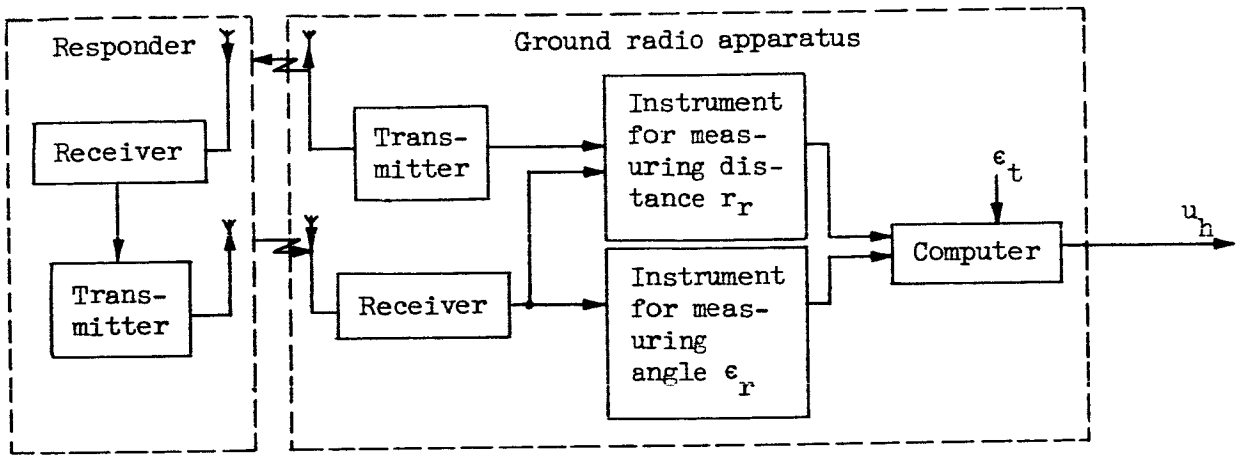

Figure 5.20

is carried on the rocket in radio zone control systems should be located on the ground in command control systems, and may or may not coincide with the control point. Figure 5.20 shows one of the possible functional diagrams of a coordinator under the condition that the control point and the ground radio apparatus of the coordinator are situated at the same place. The angular coordinates of the rocket and the range to it are measured by apparatus located on the ground. The signals necessary for the operation of this apparatus are received from a radio responder carried on the rocket and ground radio apparatus. The latter includes a computer, a transmitter (an interrogator), a receiver, an instrument for measuring the angular coordinate of the rocket and an apparatus for measuring the distance between the rocket and the control point. In those cases when the ground apparatus of the radio navigation sighting apparatus is situated away from the control point, the coordinator is supplemented by a system for the relaying of the signals characterizing the mismatch parameters.

It can be shown that the equations solved by the computer and the block diagram of the coordinator for command control systems and systems of radio zone control with angle-measuring—range-finding radio navigation apparatus are similar. This follows from the common character of the signals determined by the radio navigation sighting apparatus of the coordinators.

The functional diagram of one of the possible variants of coordinators based on the use of range-finding radio navigation apparatus is shown in figure 5.21.

The rocket carries extremely simple equipment--a radar responder designed for reradiation by the transmitter Tr of the radio signals to the ground stations A and B, in response to the signals arriving from them to the receiver Rec. If the transitters Tr A and Tr B of stations A and B operate at the same wavelength, they should form coded signals so that the transmitter Tr of /239 the radio responder can answer separately for both station A and station B. When the transmitters Tr A and Tr B operate at different frequencies, two radio receivers should be carried on the rocket.

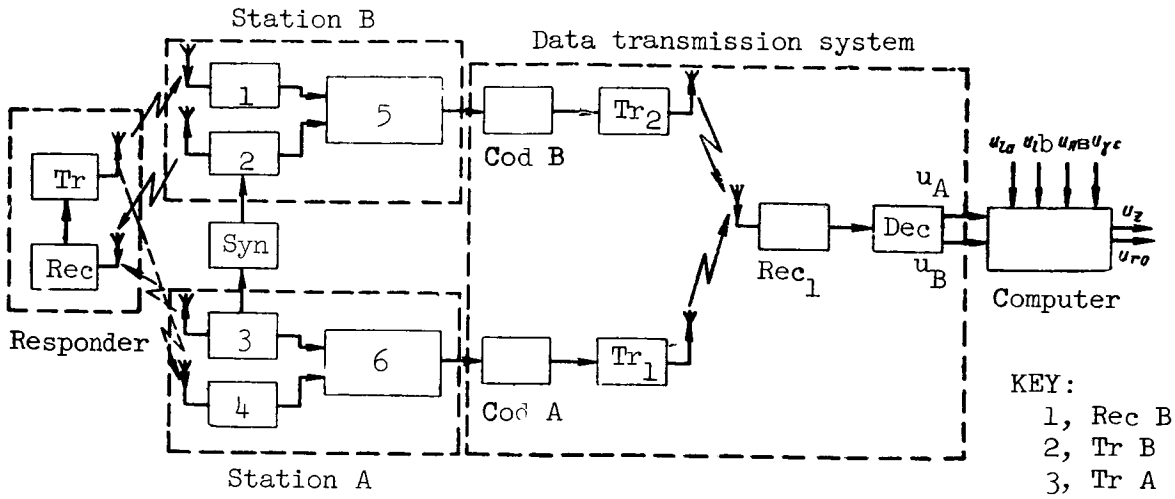

Figure 5.21

For the normal operation of the entire complex of radio apparatus of the sighting apparatus, the operation of the transmitter Tr B of the station B is synchronized by the synchronizer Syn of the transmitter Tr A of station A.

The receivers Rec A and Rec B receive the signals of the responder and feed them to the apparatus for automatic measurement of distances r_A and r_B from the stations A and B to the rocket. This apparatus also is fed synchronization signals from the transmitters Tr A and Tr B, setting the zero for reading of r_A and r_B.

Since in this case it is assumed that the control point coincides neither with station A nor station B, the coordinator includes data transmission systems. These systems consist of coders Cod_A and Cod_B, transmitters Tr_1 and Tr_2 for the transmission of information on the distances r_A and r_B, a receiver Rec_1 and a decoder Dec. The Dec output is connected to a computer which is fed the u_A, u_B, u_{la}, u_{lb}, u_{AB} and $u_{\gamma c}$, characterizing the distances r_A and r_B from stations A and B to the rocket, the distances l_a and l_b from stations A and B to the target, the distance r_{AB} between stations A and B and also the angle γ_c between the directions "target-station A" and "target-launching point."

On the basis of information on r_A, r_B, l_A, l_B, r_{AB} and γ_c, the computer produces signals u_z and u_{ro}, determining the linear deflection of the center of

mass of the rocket from the reference trajectory in a horizontal plane. In this type of coordinator and the coordinator of a radio zone control system with range-finding radio navigation apparatus, the very same parameters of motion of a rocket are measured. Therefore, the equations solved by the computers of these coordinators will be identical. The same can be said of the structural diagrams if all the apparatus for measurement and transmission of data on the distances r_A and r_B is assumed to be included in the corresponding measurement instruments.

This discussion of the coordinators of command control systems with radio navigation instruments for measurement of coordinates reveals that, in their functions and in the structure of their computers, they are similar in many ways to the coordinators of fixed radio zone control systems. However, there is one important difference between them: in command control systems, all the most unwieldy coordinator apparatus is on the ground. As a rule, the rocket should carry only a relatively small responder.

The computer at the control point, when there is a change of the initial data introduced into it, makes it possible to determine the form of the reference trajectory, which in some cases can be desirable from the tactial point of view. /241

When Doppler instruments are used for measuring velocity for course and range control of rockets, the coordinator must include several (not less than 3-4) ground stations ensuring determination of the radial velocities of motion of the rocket in different directions and a corresponding computer. The simplest such coordinator is obtained for systems producing commands for control of the cutoff of the engine of a ballistic rocket.

Figure 5.22 is the functional diagram of one of the possible variants of such a coordinator.

A radio transmitter Tr_1 and a radio receiver Rec_1 are set up at the point of intersection of the Earth's surface with the tangent to the trajectory of motion of the rocket for the presumed time of cutoff of the engine. The receiver and transmitter are interconnected by a frequency multiplier FM_1 which increases the frequency f_0 of oscillations radiated by the transmitter Tr_1 by n_1 times, where n_1 is any whole or fractional number.

With withdrawal of the rocket, the input of its receiver Rec_2 receives signals with the frequency /242

$$f_1 = f_0 - \frac{v_r}{c} f_0,$$

where $F_D = \frac{v_r}{c} f_0$ is the Doppler frequency and v_r is the radial component of rocket velocity.

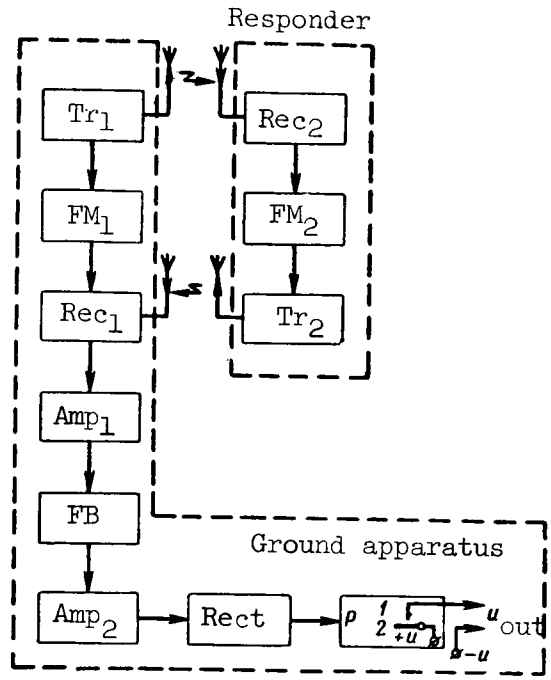

Figure 5.22

The frequency multiplier FM_2 increases the frequency f_1 by n_1 times. As a result, the transmitter Tr_2 produces a voltage with the frequency

$$f_2 = n_1(f_0 - F_D).$$

At the output of Rec_1, the responder signals formed by the tramsmitter Tr_2 will have the frequency

$$f_3 = f_2 - \frac{v_r}{c} f_2.$$

The signals having the frequency f_3 are mixed with the voltage received from the output of FM_1.

In the mixer of the receiver Rec_1, there will be a difference frequency voltage

$$F_d = n_1 f_0 - f_3 \approx 2n_1 \frac{v_r}{c} f_0. \qquad (5.5.8)$$

We note that expression (5.5.8) was derived neglecting the extremely small term $n_1 F_D \frac{v_r}{c}$. Formula (5.5.8) shows that F_d and v_r are related by an unambiguous dependence and when the rocket attains a specific velocity of motion, the frequency F_d becomes equal to F_{st}. At the time when $F_d = F_{st}$, a signal should appear at the output of the coordinator. For this reason, in the considered coordinator, the difference frequency voltage F_d, after passing through the amplifier Amp_1, is fed to the frequency bridge FB. At the output of this bridge, to one of whose diagonals the amplifier Amp_1 is connected and to whose other diagonal the amplifier Amp_2 is connected, a non-zero voltage is formed when $F_d \neq F_{st}$ and a zero voltage when $F_d = F_{st}$.

The rectifier Rect creates a dc voltage which is fed to the winding of the electromechanical relay Relay. The contacts 1 and 2 of the relay Relay to which the dc voltage +U is fed are open when $F_d \neq F_{st}$. When F_d becomes equal to F_{st}, the contacts 1 and 2 close, creating the output voltage u_{out} which is used for forming commands for cutoff of the rocket engine.

5.6. Errors of Coordinators of Command Control Systems

In many cases, in coordinators of command control systems, the errors /243 arising due to amplitude and angular fluctuations of signals arriving from the target and interference created by the enemy are of basic importance. In addition, dynamic errors occur--errors caused by the instrument noise of the receivers; instrument errors; errors caused by yawing of the rocket carrier, if the entire coordinator or part of it is carried aboard the rocket carrier, etc.

An analysis of the errors of coordinators with add-subtract—range-finding, angle-measuring, range-finding and angle-measuring—range-finding radio navigation measurement instruments can be made the same as described in chapter 4. This is because the equations are the same for both types of coordinators if it is assumed that the data transmission systems are inertialess, and their errors are taken into account when determining the errors in measurement of the angular coordinates of the rocket and the distances from it to the corresponding ground radio apparatus.

Therefore, in this section we will consider only coordinators which include radar sighting apparatus and Doppler instruments for measurement of velocity; errors of coordinators of the second type will not be analyzed here. In the case of coordinators of the first kind, we will take into account the dynamic errors and also the fluctuation errors whose sources are various kinds of radio interference. The dynamic errors for each particular type of rocket

guidance for a given hypothesis on the motion of the target are determined functions of time, although under some conditions which were discussed in chapter 3 they also can be considered random functions of time. Instrument errors are not taken into account because they are different for different models of coordinators and, in most cases, are negligibly small. The principal problem in an analysis of fluctuation errors is determination of the mathematical expectation and spectral density of the distortion of the mismatch parameter, expressed in linear units. We will assume here that effective interference does not lead to the appearance of nonlinear relationships between the output and input signals of the measuring instruments making up the coordinator.

Conversion from errors expressed in linear units to errors in the form of a voltage (current), which is necessary for determination of the miss of the rocket as a result of analysis of the guidance circuit as a whole, is accomplished as was described in the preceding section using a scale factor $k_h = k_{pot\partial}k_{rc}$ under the condition that $k_{tc} = k_{rc} = k_\epsilon$ and $k_{pr} = k_{\partial t} = k_{\partial r}$. We note that here k_ϵ, k_{pr}, $k_{\partial t}$ and $k_{\partial r}$ are scale factors relating the voltages /244 u_ϵ, u_{pr}, $u_{\partial t}$ and $u_{\partial r}$ to the angle ϵ_0 and the distances r_{pr}, r_t and r_r. The need for data on the distortions of the parameter h and not its individual components is due, if for no other reasons, to the fact that in such a formulation of the problem:

- the random input signal arriving at the apparatus for forming and transmission of control commands is determined;

- it becomes possible to make an approximate estimate (without taking the guidance circuit as a whole into account) of the deflection of the center of mass of the rocket from the reference trajectory;

- conditions for comparison of methods of rocket guidance on the basis of the values of the distortion of the mismatch parameter are ensured;

- in the interpretation of the equations of the control system by means of computers, regardless of the number of measuring instruments in the coordinator, only one apparatus is required for producing signals which simulate random perturbations at the input of the apparatus for forming and transmitting control commands.

The essence of the method for evaluating coordinator errors is as follows. The first step is computation of the distortions of the mismatch parameter in dependence on the errors of the individual measuring instruments making up the coordinator. Then the errors of the measuring instruments are determined as functions of the input interference, the parameters of the motion of the target and the internal properties of the measuring instruments.

1. Errors in Measurement of the Mismatch Parameter in Rocket Guidance by the Coincidence Method

It follows from equation (5.5.5) that the output signal of the coordinator for the vertical rocket guidance plane is the difference between two components. One of them is determined by the law of the change of the angle ε_t and the other by ε_r. This circumstance and also allowance for the properties of linearity of the coordinator in the case of a "frozen" distance r_r make it possible to represent the dynamic error $h_{\partial c}$ of the coordinator, considered as a determined function of time, in the form of the difference of the components $h_{\partial c1}$ and $h_{\partial c2}$. The errors $h_{\partial c1}$ and $h_{\partial c2}$ arise due to the dynamic properties of the measuring instruments with the transfer functions $W_{t\varepsilon}(D)$ and $W_{r\varepsilon}(D)$, respectively, and are dependent on the character of the change of ε_t and ε_r with time.

Then it is possible to write

$$h_{\partial c} = h_{\partial c1} - h_{\partial c2} = r_r(\varepsilon_{t\partial} - \varepsilon_{r\partial}), \tag{5.6.1}$$

where $\varepsilon_{t\partial}$ and $\varepsilon_{r\partial}$ are the dynamic errors in determination of the angular coordinates of the target and rocket.

In accordance with the method described in chapter 3, the components $\varepsilon_{t\partial}$ and $\varepsilon_{r\partial}$ can be found from the following expressions /245

$$\varepsilon_{t\partial} = c_0\varepsilon_t(t) + c_1\dot{\varepsilon}_t(t) + \frac{1}{2}c_2\ddot{\varepsilon}_t(t) + \ldots, \tag{5.6.2}$$

$$\varepsilon_{r\partial} = e_0\varepsilon_r(t) + e_1\dot{\varepsilon}_r(t) + \frac{1}{2}e_2\ddot{\varepsilon}_r(t) + \ldots, \tag{5.6.3}$$

where

$$c_n = \frac{d^n}{dD^n}\left[\frac{1}{1 + W_{tr}(D)}\right]_{D=0}, \tag{5.6.4}$$

$$e_n = \frac{d^n}{dD^n}\left[\frac{1}{1 + W_{rr}(D)}\right]_{D=0}, \tag{5.6.5}$$

$W_{tr}(D) = \dfrac{W_{t\varepsilon}(D)}{1 - W_{t\varepsilon}(D)}$ is the transfer function of the open circuit of the tracking system determining the angle ε_t, and $W_{rr}(D) = \dfrac{W_{r\varepsilon}(D)}{1 - W_{r\varepsilon}(D)}$ is the

transfer function of the open circuit of the tracking system determining the angle ε_r.

It follows from expressions (5.6.1)-(5.6.5) that the value $h_{\partial c}$ is easy to determine if the functions $\varepsilon_t(t)$, $\varepsilon_r(t)$, $W_{tr}(D)$ and $W_{rr}(D)$ are known and also the value of the coefficient $r_{pr} \approx r_r$ for the selected time.

We note that for a given law of change $\varepsilon_t(t)$, the function $\varepsilon_r(t)$ can be determined with a sufficiently high degree of accuracy by the graphic construction of reference (kinematic) trajectories.

Computation of the dynamic errors of the coordinator is simplified considerably in those cases when $W_{t\varepsilon}(D) = W_{r\varepsilon}(D)$ and (5.5.5)

$$h_m(t) = W_{t\varepsilon}(D)\, r_{pr}\, [\varepsilon_t(t) - \varepsilon_r(t)] = W_{t\varepsilon}(D)\, h(t). \qquad (5.6.6)$$

This expression shows that it is sufficient to know the law of change of h(t) with time and the function $W_{t\varepsilon}(D)$ in order to be able to compute $h_{\partial c}$. The function h(t), being the controlling function, can be found approximately for given parameters of motion of the target and when taking into account the ideal coherence equation for the coincidence method.

For example, if

$$W_{t\varepsilon}(D) = \frac{2k_1 D + \omega_0^2}{D^2}, \qquad (5.6.7)$$

then when

$$h(t) = v_{0l}\left(t + \frac{1}{2}a_1 t^2 + \frac{1}{3}a_2 t^3\right),$$

where v_{0l} is the velocity of motion of the rocket along the line between /246 the control point and the rocket; a_1 and a_2 are coefficients of the polynomial, v_{0l} = 70 m/sec, $a_1 = 3.66 \cdot 10^{-2}$ sec, $a_2 = 2.73 \cdot 10^{-4}$ sec^2 and t = 50 sec and the dynamic error is $h_{\partial c}$ = 26.2 m.

The fluctuation error of the coordinator, expressed in linear measure and caused by different kinds of interference, can be determined on the basis of equation (5.5.3). As before, the range r_{pr} is assumed to be a constant value and equal to r_r.

We will assume that the input of tracking systems reacting to the angles ϵ_t and ϵ_r, in addition to the signals $\epsilon_t(t)$ and $\epsilon_r(t)$, are acted upon by "noise" angles $\epsilon_{tn}(t)$ and $\epsilon_{rn}(t)$, representing stationary random functions of time. The functions $\epsilon_{tn}(t)$ and $\epsilon_{rn}(t)$ are determined by scaling of the fluctuation components of the voltages forming at the output of the discriminators of the corresponding measuring instruments (at the output of the phase detectors in systems with conical scanning). Scaling of the voltages into the values of the angles can be accomplished using the direction-finding characteristic or by using the coefficient k_{tc}, if the direction-finding characteristic is linear.

The statistical characteristics (mathematical expectation and spectral density or correlation function) of the "noise" angles are determined during an investigation of measuring instruments, taking into account the effect on them of some form of interference. In solution of the problem of the random errors of coordinators, these characteristics are considered known.

Taking into account the presence of the "noise" angles $\epsilon_{rn}(t)$ and $\epsilon_{tn}(t)$, we obtain the following expression determining the instantaneous value of the mismatch paramcter $h_c(t)$

$$h_c(t) = h_m(t) + h_{mn}(t) = r_{pr}\,[\epsilon_{tm}(t) - \epsilon_{rm}(t) + \epsilon_{tnm}(t) - \epsilon_{rnm}(t)], \quad (5.6.8)$$

where h_{mn} is a component of the mismatch parameter caused by the "noise" angles $\epsilon_{tnm}(t)$ and $\epsilon_{rnm}(t)$, which act at the output of tracking systems with the transfer functions $W_{t\epsilon}(D)$ and $W_{r\epsilon}(D)$.

We find from equation (5.6.8) that

$$h_{mn}(t) = r_{pr}\,[\epsilon_{tnm}(t) - \epsilon_{rnm}(t)], \quad (5.6.9)$$

where

$$\epsilon_{tnm}(t) = W_{t\epsilon}(D)\ \epsilon_{tn}(t) \text{ and } \epsilon_{rnm}(t) = W_{r\epsilon}(D)\ \epsilon_{rn}(t).$$

Averaging for the ensemble or time (which is dimensionless for ergodic stationary processes) the right- and left-hand sides of expression (5.6.9),

for the mathematical expectation $h_{mn}(t)$ of the distortion of the mismatch parameter $h_{mn}(t)$ we obtain /247

$$\overline{h_{mn}(t)} = r_{pr}\,[\overline{\epsilon_{tnm}(t)} = \overline{\epsilon_{rnm}(t)}].$$

In practice, most frequently, $\overline{\epsilon_{tnm}(t)} = \overline{\epsilon_{rnm}(t)} = 0$. Since the functions $\epsilon_{tnm}(t)$ and $\epsilon_{rnm}(t)$ usually are mutually independent (as a result of the considerable difference in the arrival time of radio waves from the rocket and target), then

$$G_h(\omega) = r_{pr}^2\,[G_{tnm}(\omega) + G_{rnm}(\omega)], \tag{5.6.10}$$

where $G_h(\omega)$ is the spectral density of the distortion $h_{mn}(t)$ of the mismatch parameter; $G_{tnm}(\omega)$ and $G_{rnm}(\omega)$ are the spectral densities of the random functions $\epsilon_{tnm}(t)$ and $\epsilon_{rnm}(t)$.

But

$$G_{tnm}(\omega) = \left|W_{t\epsilon}(j\omega)\right|^2 G_{tn}(\omega) \tag{5.6.11}$$

and

$$G_{rnm}(\omega) = \left|W_{r\epsilon}(j\omega)\right|^2 G_{rn}(\omega). \tag{5.6.12}$$

Here

$$W_{t_\epsilon}(j\omega) = W_{t_\epsilon}(D)\,|_{D=j\omega},$$
$$W_{r_\epsilon}(j\omega) = W_{r_\epsilon}(D)\,|_{D=j\omega},$$

$G_{tn}(\omega)$ and $G_{rn}(\omega)$ are the spectral densities of the random functions $\epsilon_{tn}(t)$ and $\epsilon_{rn}(t)$.

Substituting the determined values $G_{tnm}(\omega)$ and $G_{rnm}(\omega)$ into expression (5.6.10), we obtain

$$G_h(\omega) = r_{pr}^2\,[\left|W_{t\epsilon}(j\omega)\right|^2 G_{tn}(\omega) + \left|W_{r\epsilon}(j\omega)\right|^2 G_{rn}(\omega)]. \tag{5.6.13}$$

If it becomes necessary to compute the dispersion σ_h^2 of the random function $h_{mn}(t)$, expression (5.6.13) should be integrated for all frequencies ω.

As a result of integration we find

$$\sigma_h^2 = r_{pr}^2 (\sigma_{tnm}^2 + \sigma_{rnm}^2), \tag{5.6.14}$$

where

$$\sigma_{tnm}^2 = \frac{1}{2\pi}\int_0^\infty |W_{t.}(j\omega)|^2 G_{tn}(\omega)\, d\omega, \tag{5.6.15}$$

$$\sigma_{rnm}^2 = \frac{1}{2\pi}\int_0^\infty |W_{r.}(j\omega)|^2 G_{rn}(\omega)\, d\omega. \tag{5.6.16}$$

Since the passbands of the tracking systems of the measuring instruments usually are considerably smaller than is the passband of the apparatus for measuring the mismatch voltage, it can be assumed that in the integrals (5.6.15) and (5.6.16) /248

$$G_{tn}(\omega) \approx G_{tn}(0) = \frac{\sigma_{tn}^2}{\Delta F_{c1}} \text{ and } G_{rn}(\omega) \approx G_{rn}(0) = \frac{\sigma_{rn}^2}{\Delta F_{e2}}.$$

Here σ_{tn}^2 and σ_{rn}^2 are the dispersions of the "noise" angles ε_{tn} and ε_{rn}; ΔF_{e1} and ΔF_{e2} are the effective passbands of the instruments for measuring the mismatch voltage (for example, phase detectors in systems with conical scanning) on the basis of angular coordinates.

If we introduce the effective passbands of the tracking systems of measuring instruments

$$\Delta F_{et} = \frac{1}{2\pi}\int_0^\infty |W_{t.}(j\omega)|^2 d\omega,$$

$$\Delta F_{er} = \frac{1}{2\pi}\int_0^\infty |W_{r.}(j\omega)|^2 d\omega,$$

in accordance with expressions (5.6.13) and (5.6.14) we obtain

$$G_h(\omega) = r_{pr}^2 \left[|W_{t.}(j\omega)|^2 \frac{\sigma_{tn}^2}{\Delta F_{e1}} + |W_{r.}(j\omega)|^2 \frac{\sigma_{rn}^2}{\Delta F_{e2}} \right], \tag{5.6.17}$$

$$\sigma_h^2 = r_{pr}^2 \left(\sigma_{tn}^2 \frac{\Delta F_{et}}{\Delta F_{e1}} + \sigma_{rn}^2 \frac{\Delta F_{er}}{\Delta F_{e2}} \right). \tag{5.6.18}$$

When

$$W_{t_h}(j\omega) = W_{r_h}(j\omega),$$

$$G_h(\omega) = r_{pr}^2 |W_{t_h}(j\omega)|^2 \left(\frac{\sigma_{tn}^2}{\Delta F_{e1}} + \frac{\sigma_{rn}^2}{\Delta F_{e2}}\right), \tag{5.6.19}$$

and

$$\sigma_h^2 = r_{pr}^2 \Delta F_{et} \left(\frac{\sigma_{tn}^2}{\Delta F_{e1}} + \frac{\sigma_{rn}^2}{\Delta F_{e2}}\right). \tag{5.6.20}$$

The derived expressions (5.6.17), (5.6.18), (5.6.19) and (5.6.20) make it possible to compute $G_h(\omega)$ and σ_h^2, provided r_{pr}, σ_{tn}^2, σ_{rn}^2, ΔF_{e1}, ΔF_{e2}, $W_t(j\omega)$ and $W_r(j\omega)$ are known. As an example, we point out that when $\frac{\Delta F_{et}}{\Delta F_{e1}} = \frac{\Delta F_{er}}{\Delta F_{e2}} = 0.5$, $\sigma_{tn} = \sigma_{rn} = 0.2^\circ$ and $r_{pr} = 10$ km, the value σ_h is approximately 30 m. In practice, if the effect of artificially created interference is not taken into account, the error of the measuring instrument ϵ_t is of basic importance, /249 since it is fed signals from the target, which fluctuate in amplitude and phase.

At the same time, the errors $\overline{\epsilon}_{rnm}$ and σ_{rn}^2 need not be taken into account because the instrument measuring the angle ϵ_r usually is fed virtually nonfluctuating signals from the rocket responder.

The errors of the coordinator, expressed in the form of a voltage, are determined on the basis of expression (5.6.9), after multiplication of the scale factor $k_h = k_{pot\partial} k_{rc}$ under the condition that $k_{rc} = k_{tc}$. We recall that the problem of conversion from a voltage to signals in linear and angular units was discussed in detail in the preceding section.

Denoting the voltages corresponding to $h_{mn}(t)$, $\epsilon_{tnm}(t)$ and $\epsilon_{rnm}(t)$ through $u_{nc}(t)$, $u_{nt}(t)$ and $u_{nr}(t)$ we will have

$$\overline{u}_{nc} = k_{pot\partial} r_{pr} [\overline{u_{nt}(t)}\, W_t(0) - \overline{u_{nr}(t)}\, W_r(0)], \tag{5.6.21}$$

$$G_{nc}(\omega) = k_{pot\partial}^2 r_{pr}^2 [|W_t(j\omega)|^2 G_{nt}(\omega) + |W_r(j\omega)|^2 G_{nr}(\omega)], \tag{5.6.22}$$

$$\sigma_{nc}^2 = k_{pot\partial}^2 r_{pr}^2 \left(\sigma_{nt}^2 \frac{\Delta F_{et}}{\Delta F_{e1}} + \sigma_{nr}^2 \frac{\Delta F_{er}}{\Delta F_{e2}}\right), \qquad (5.6.23)$$

where $W_t(0)$ and $W_r(0)$ are the transfer constants of the instruments for measuring ε_t and ε_r; $G_{nc}(\omega)$, $G_{nt}(\omega)$ and $G_{nr}(\omega)$ are the spectral densities of the random components of the voltages $u_{nc}(t)$, $u_{nt}(t)$ and $u_{nr}(t)$; σ_{nc}^2, σ_{nt}^2 and σ_{nr}^2 are the dispersions of the voltages $u_{nc}(t)$, $u_{nt}(t)$ and $u_{nr}(t)$.

If $W_t(j\omega) = W_r(j\omega)$, and $G_{nt}(\omega) \approx G_{nt}(0) = \dfrac{\sigma_{nt}^2}{\Delta F_{e1}}$ and $G_{nr}(\omega) \approx G_{nr}(0) = \dfrac{\sigma_{nr}^2}{\Delta F_{e2}}$

for frequencies lying within the limits of the passbands of the tracking systems, we obtain

$$G_{nc}(\omega) = k_{pot\partial}^2 r_{pr}^2 \left|W_t(j\omega)\right|^2 \left(\frac{\sigma_{nt}^2}{\Delta F_{e1}} + \frac{\sigma_{nr}^2}{\Delta F_{e2}}\right);$$

$$\sigma_{nc}^2 = k_{pot\partial}^2 r_{pr}^2 \Delta F_{et} \left(\frac{\sigma_{nt}^2}{\Delta F_{e1}} + \frac{\sigma_{nr}^2}{\Delta F_{e2}}\right).$$

The values $\bar{u}_{nt}$, $\bar{u}_{nr}$, $G_{nt}(\omega)$ and $G_{nr}(\omega)$ and also the parameters related to them through scale factors, $\bar{\varepsilon}_{tnm} = W_{t\varepsilon}(0)\,\bar{\varepsilon}_{tn}$, $\bar{\varepsilon}_{rnm} = W_{r\varepsilon}(0)\,\bar{\varepsilon}_{rn}$, $G_{tn}(\omega)$ and $G_{rn}(\omega)$ are determined, as already noted, on the basis of an analysis of the influence of the noise in the radio receivers and in the discriminators of the measuring instruments. It should be recalled here that in the absence of artificial interference, the errors $\bar{u}_{nr}$ usually are absent and $G_{nr}(\omega)$ is negligibly small in comparison with $G_{nt}(\omega)$.

For example, if a radar set with conical scanning is used as the instrument for measuring ε_t, the fluctuations of the amplitudes and the center of the received signals lead to errors ε_{tn}, whose mathematical expectation is equal to zero. The dispersions are determined by formulas (3.11.25) and (3.11.26). /250

When using radar sets determining the angular coordinates by the "groups" method, the measurement errors ε_t caused by fluctuations of the received signals and the instrument noise of the radio receivers can be determined using the formulas presented in reference 62.

Since $\bar{h}_{mn}$ characterizes the systematic error of guidance of a winged rocket situated at a distance $r_r = r_{pr}$ from the control point, and σ_h is the maximum possible mean square deviation of the center of mass of the rocket from the reference trajectory, in accordance with the formulas derived earlier, it is possible to impose requirements on the accuracy of determination of the angular coordinates by the rocket and target measuring instruments.

If a coordinator of the considered type is used for guidance of a ballistic rocket, the values $\bar{h}_{mn}$ and $G_h(0)$, determined for the horizontal control plane, are the initial data for computation of the rocket miss at the end of its flight.

2. Errors in Measurement of the Mismatch Parameter when Guiding a Rocket by the Parallel Approach Method

Since the quality of rocket guidance in the last stage of its flight, when $\frac{r_t - r_r}{r_{pr}} \ll 1$ is of basic importance, in an analysis of errors of a coordinator of this type, it is possible to limit ourselves to a consideration of the approximate method of parallel convergence, characterized by equation (5.4.2).

The dynamic errors of the coordinator are determined by the same method as used for a coordinator of the preceding type.

The coordinator equation (5.5.7), where h_m is dependent on the measured values ϵ_{tm}, ϵ_{rm}, r_{tm} and r_{rm}, and also on ϵ_{0m} and r_r, is nonlinear. However, in those cases when the most probable distortions of the distances r_t and r_r are small in comparison with the values r_t and r_r themselves, which always is the case if artificial interference is not taken into account, the function $h_m(t)$ can be linearized. Then the instantaneous value of the error $h_{mn}(t)$ caused by the "noise" angles $\epsilon_{tnm}(t)$ and $\epsilon_{rnm}(t)$ and the "noise" ranges $r_{tnm}(t)$ and $r_{rnm}(t)$, acting at the outputs of the corresponding tracking systems, is determined as the full differential equation (5.5.7). In this case, the partial derivatives of $h_m(t)$ for different parameters should be sought for /251 those values of angles and ranges which are obtained in the absence of interference.

Then, on the basis of equation (5.5.7) when $r_r = r_{pr}$ we find

$$h_{mn}(t) = r_{pr}\,[\epsilon_{tnm}(t) - \epsilon_{rnm}(t)] - [r_{tnm}(t) - r_{rnm}(t)]\,[\epsilon_{0m} - \epsilon_{tm}(t)]$$

$$+ [r_{tm}(t) - r_{rm}(t)]\,\epsilon_{tnm}(t). \qquad (5.6.24)$$

Usually r_{tm}, r_{rm} and ϵ_{tm} change considerably more slowly than r_{tnm}, r_{rnm} and ϵ_{tnm}, and the error in stipulation of the angle ϵ_0 and the dynamic errors in measurement of range and angles r_t, r_r, ϵ_t and ϵ_r are negligibly small in comparison with the ranges and angles themselves. The last condition means that $r_{tm} \approx r_t$, $r_{rm} \approx r_r$, $\epsilon_{tm} \approx \epsilon_t$, $\epsilon_{rm} \approx \epsilon_r$ and $\epsilon_{0m} \approx \epsilon_0$. Then, taking into account the nondependence of the functions ϵ_t, ϵ_r, r_t and r_r, we obtain

$$\overline{h_{mn}(t)} = r_{pr}\,[\overline{\epsilon_{tnm}(t)} - \overline{\epsilon_{rnm}(t)}] + (r_t - r_r)\,\overline{\epsilon_{tnm}(t)}$$

$$- (\epsilon_0 - \epsilon_t)\,[\overline{r_{tnm}(t)} - \overline{r_{rnm}(t)}], \qquad (5.6.25)$$

$$G_h(\omega) = r_{пр}^2 \left\{ \left(1 + \frac{r_ц - r_р}{r_{пр}}\right)^2 |W_{цε}(j\omega)|^2 G_{цп}(\omega) + \right.$$

$$+ |W_{рε}(j\omega)|^2 G_{рп}(\omega) + \frac{(\epsilon_0 - \epsilon_п)^2}{r_{пр}^2} [\,|N_{цr}(j\omega)|^2 G_{цr}(\omega) +$$

(see key below)

$$\left. + |N_{рr}(j\omega)|^2 G_{рr}(\omega)] \right\}, \qquad (5.6.26)$$

where $G_{tr}(\omega)$ and $G_{rr}(\omega)$ are the spectral densities of the fluctuations $r_{tnm}(t)$ and $r_{rnm}(t)$. Taking into account the earlier comments on the width of the pass-bands of the tracking systems and the frequency range occupied by the spectral densities $G_{tn}(\omega)$, $G_{rn}(\omega)$, $G_{tr}(\omega)$ and $G_{rr}(\omega)$, we obtain

пр = pr
ц = t
р = r
цп = tn
рп = rn
э = e

$$G_h(\omega) \approx r_{пр}^2 \left\{ \left(1 + \frac{r_ц - r_р}{r_{пр}}\right)^2 |W_{цε}(j\omega)|^2 \frac{\sigma_{цп}^2}{\Delta F_{э1}} + |W_{рε}(\omega)|^2 \frac{\sigma_{рп}^2}{\Delta F_{э2}} + \right.$$

$$\left. + \frac{(\epsilon_0 - \epsilon_п)^2}{r_{пр}^2} \left[|N_{цr}(j\omega)|^2 \frac{\sigma_{цr}^2}{\Delta F_{э3}} + |N_{рr}(j\omega)|^2 \frac{\sigma_{рr}^2}{\Delta F_{э4}} \right] \right\}, \qquad (5.6.27)$$

$$\sigma_h^2 \approx r_{пр}^2 \left[\left(1 + \frac{r_ц - r_р}{r_{пр}}\right)^2 \sigma_{цп}^2 \frac{\Delta F_{эц}}{\Delta F_{э1}} + \sigma_{рп}^2 \frac{\Delta F_{эр}}{\Delta F_{э2}} + \right.$$

$$\left. + \frac{(\epsilon_0 - \epsilon_п)^2}{r_{пр}^2} \left(\sigma_{цr}^2 \frac{\Delta F_{цр}}{\Delta F_{э3}} + \sigma_{рr}^2 \frac{\Delta F_{рr}}{\Delta F_{э4}} \right) \right], \qquad (5.6.28)$$

where σ^2_{tr} and σ^2_{rr} are the dispersions of the random functions $r_{tnm}(t)$ and $r_{rnm}(t)$; ΔF_{e3} and ΔF_{e4} are the effective passbands of the discriminators in the voltage-measuring instruments, characterizing r_t and r_r; ΔF_{tr} and ΔF_{rr} are the effective passbands of the tracking systems of the instruments for measuring r_t and r_r.

The formulas (5.6.26), (5.6.27) and (5.6.28) make it possible to compute $G_h(\omega)$ and σ^2_h for stipulated parameters of the coordinate measuring instruments and stipulated dispersions σ^2_{tn}, σ^2_{rn}, σ^2_{tr} and σ^2_{rr}, and also to formulate requirements as to the necessary accuracy of operation of the measuring instruments, using as a point of departure the admissible errors of rocket guidance. Here, as in the preceding cases, the errors ϵ_{tn} and r_{tn} are most important. /252

By knowing $\overline{h_{mn}(t)}$ and $\overline{G_h(\omega)}$, it is possible to determine easily the mathematical expectation $u_{nc}(t)$ and the spectral density $G_{nc}(\omega)$ of the voltage $u_{nc}(t)$, characterizing the coordinator error. This is done by multiplying $\overline{h_{mn}(t)}$ and $G_h(\omega)$ by the scale factor $k_h = k_{pot\partial}k_{rc}$ and its square, respectively, assuming that the coefficients relating the angles ϵ_t, ϵ_r and ϵ_0 with the voltages u_t, u_r and u_ϵ are equal to one another. In addition, it also is necessary to consider identical the coefficients by means of which r_t, r_r and r_{pr} are converted into voltages reflecting the distances r_t, r_r and $r_{pr} \approx r_r$.

In actual practice, when taking into account fluctuations of natural origin, the mathematical expectation of the distortions $\overline{h}_{mn}(t)$ usually are equal to zero. Therefore, we will compare the dispersion of errors arising during rocket guidance by the coincidence method and the approximate method of parallel approach. In the comparison, we will assume that the coordinate measuring instruments have identical parameters in both types of coordinators.

Comparison of expressions (5.6.18) and (5.6.28) makes it possible to draw the following conclusions:

(1) in the coincidence method, the distortions of the mismatch parameter are smaller than in the parallel approach method;

(2) in the parallel approach method, the dispersion of error decreases with approach of the rocket to the target and essentially is dependent on the value $\epsilon_0 - \epsilon_t$;

(3) with an increase of the rocket guidance range, the errors decrease in the parallel approach method, approaching the errors of the coincidence method.

In addition, it should be noted that the minimum errors in the parallel approach method in the region where the rocket meets the target, coinciding with the errors in the coincidence method, occur when $\epsilon_0 - \epsilon_t = 0$. Satisfaction of the condition $\epsilon_0 - \epsilon_t = 0$ corresponds to guidance by the parallel approach method of both the rocket and the control point under the condition that, at each moment of time, the center of mass of the rocket is on the straight line connecting the control point to the target. In essence, the latter means rocket guidance by the coincidence method in relation to the control point, which itself is guided to the target by the parallel approach method.

On the basis of the first conclusion, it can be affirmed that in the /253
parallel approach method, it is necessary to expend a greater quantity of the available rocket overload on the elimination of fluctuation errors than in the coincidence method.

However, as already pointed out, the coincidence method has worse dynamic properties than any of the rocket guidance methods based on a future position. The guidance method and therefore the type of coordinator must be selected in accordance with the application of the principle of the minimum of the rocket error in rocket guidance.

3. Errors in Determination of Flight Velocity of a Ballistic Rocket

In coordinators for determination of the time when a ballistic rocket attains a specified flight velocity, there usually are no elements with significant inertia. Fluctuation errors, therefore, play the most important role.

It follows from an analysis of the operation of the apparatus whose diagram is shown in figure 5.22 that the voltage u_{rect} forming at the output of the rectifier Rect, as a result of the influence of various kinds of interference and the inaccuracy of operation of individual elements of the circuit (especially the frequency bridge) will not reflect the frequency F_d, but some other frequency F_{dm}. Therefore

$$F_{dm} = F_d + \Delta F_d,$$

where ΔF_d is the error in frequency measurement.

Since F_d is a function of v_r and f_0, by using the method of finding the total differential, on the basis of expression (5.5.8), we obtain

$$\frac{\Delta v_r}{v_r} = \frac{\Delta F_d}{F_d} - \frac{\Delta f_0}{f_0}, \qquad (5.6.29)$$

where Δv_r is the error in determination of the radial flight velocity of the rocket; Δf_0 are the fluctuations of the carrier frequency f_0 in the radio transmitter Tr_1 (fig. 5.22).

The relation (5.6.29) characterizes the instantaneous value of the error Δv_r. Therefore, carrying out statistical averaging and taking into account that ΔF_d and Δf_0 change independently of one another and also independently of F_d and f_0, for the mathematical expectation $\overline{\Delta v_r}$ and the spectral density $G_v(\omega)$ we find

$$\overline{\Delta v}_r = v_r\left(\frac{\overline{\Delta F_d}}{F_d} - \frac{\overline{\Delta f_0}}{f_0}\right), \qquad (5.6.30)$$

$$G_v(\omega) = v_r^2\left[\frac{1}{F_d^2} G_F(\omega) + \frac{1}{f_0^2} G_f(\omega)\right], \qquad (5.6.31)$$

where $G_F(\omega)$ and $G_f(\omega)$ are the spectral densities of the random functions /254 ΔF_d and Δf_0.

The relations (5.6.30) and (5.6.31), making possible computation of $\overline{\Delta v_r}$ and $G_v(\omega)$, show that in order to decrease the errors it is desirable to select the largest possible values f_0 and F_d, where F_d for a specified velocity v_r changes directly proportional to f_0.

In accordance with expression (5.6.31), for the dispersion σ_v^2 of error in determination of velocity v_r we will have

$$\sigma_v^2 = v_r^2\left(\frac{\sigma_F^2}{F_d^2} + \frac{\sigma_f^2}{f_0^2}\right) \qquad (5.6.32)$$

Here σ_F^2 and σ_f^2 are the dispersions of the random functions ΔF_d and Δf_0.

If a frequency bridge (fig. 5.22) is used as the frequency discriminator in the coordinator, $\frac{\sigma_F}{F_d} \approx (1\text{-}2)\cdot 10^{-3}$ (ref. 2), and therefore for a case when $\sigma_f = 0$ the mean square error σ_v is

$$\sigma_v = (1\text{-}2)\cdot 10^{-3} v_r.$$

When $v_r = 8000$ m/sec, the value $\sigma_v = (8\text{-}16)\ \frac{m}{sec}$.

At the same time, the admissible errors in measurement of velocity for a specific effective range r_0 of a rocket and the mean square error σ_r should be determined using formula (2.3.5). It follows from this formula that the values $\frac{\sigma_v}{v_{in}}$, where $v_{in} = v_r$ at the time of cutoff of the engine should be determined from the condition

$$\frac{\sigma_v}{v_{in}} \leq \frac{1}{2}\frac{\sigma_r}{r_0}.$$

For example, if $\frac{\sigma_r}{r_0} = 1\cdot 10^{-4}$, the admissible value $\frac{\sigma_v}{v_{in}}$ should be

$$\frac{\sigma_v}{v_{in}} = 0.5\cdot 10^{-4}.$$

It is noted in the foreign literature that for putting artificial Earth satellites into orbit and guidance of intercontinental missiles with a high accuracy, the error σ_v should not exceed (0.5-1) m/sec. This means that the use of a frequency bridge does not always ensure the necessary quality of the radio control system.

More precise results are obtained when counters of the periods of oscillations having the frequency F_d are used. These counters determine the /255 number of mentioned periods in the course of some time interval Δt.

It can be shown (ref. 2) that when counters are used and $\sigma_f = 0$,

$$\frac{\sigma_v}{v_r} \approx \frac{1}{F_d \Delta t}$$

and for $n_1 = 2$, $f_0 = 3\cdot 10^{10}$ cps and $\Delta t = 0.01$ sec, the error σ_v is only 0.75 m/sec.

However, it should be remembered that an increase of the frequency F_d for an increase of the accuracy of the coordinator is limited by the possibilities

of amplification of the oscillations of superhigh frequency (equal approximately to $n_1 f_0$) aboard the rocket. In order to decrease the influence of fluctuations of frequency f_0 on the accuracy of measurement of v_r, it is necessary to create a master oscillator for the radio transmitter Tr_1 with a quartz frequency stabilizer.

5.7. Principal Problems Solved by Apparatus for Forming Control Commands

Command forming apparatus (CFA) is one of the links of the system for forming and transmitting control commands. It is designed for producing signals (commands) which are related functionally to the mismatch parameters and additionally, in some cases, are dependent on the characteristics of motion of the target. The signals forming at the output of the command forming apparatus are fed to the command control radio link (CCRL) or directly to the automatic pilot of the rocket. The relationship between the control commands and the mismatch parameters and the target coordinates is selected in such a way as to obtain the required dynamic properties of the control system and ensure that there will not be excessive errors in rocket guidance.

In addition to solving the main problem (forming of commands), the command forming apparatus also is used for coupling the coordinator to the subsequent links of the control system. For this reason, the use of input and output converters which perform no other useful functions other than coupling should be avoided in the command forming apparatus insofar as possible. In homing, radio zone control and in autonomous control systems, the command forming apparatus usually is used for coupling the coordinator to the automatic pilot, whereas in command control systems it is used for coupling the coordinator to the command transmission apparatus (CCRL).

In order for the coupling of the command forming apparatus to the succeeding apparatus of the control system to be of a high quality, which is necessary to ensure stable rocket guidance to the target with the required accuracy, the selection of the structure and the principal parameters of the command forming apparatus also is tied-in to the structure and parameters of the automatic pilot of the rocket or the command control radio link.

In control systems for ballistic and winged rockets, the command forming apparatus most frequently produces course and pitching control commands which represent continuous or discrete functions of the input signals. Accordingly, it is possible to distinguish analog (continuous) and digital (discrete) commands. In addition to the mentioned level discreteness of commands, when the commands do not reflect all the possible values of the mismatch parameters or target coordinates, there is time discreteness characterized by the fact that the information on the mismatch parameters is not produced continuously but at some constant or variable time intervals. /256

If the commands formed in the command forming apparatus are fed directly to the automatic pilot of the rocket, they usually should represent continuous functions of time. When commands are transmitted by the CCRL, the output signals of the command forming apparatus can be either continuous or discrete.

In the case of guidance of antiaircraft guided missiles, in addition to course and pitching control commands, it is frequently necessary to form commands for the triggering of the radio fuse, while in the case of guidance of winged rockets along fixed trajectories commands are produced for transition of the rocket into a dive. At the end of the active segment of their flight, ballistic rockets should receive commands from the control point for cutoff of the engine or these commands should be produced aboard the rocket. Commands of this type usually are called single or individual commands.

Therefore, in a general case, the command forming apparatus produces commands which appear both continuously or at some interval and also once during the entire guidance process. Continuous, discrete and individual commands are produced during the motion of the rocket after its launching. At the same time, the command forming apparatus also frequently solves the problem of creating commands for the control of the direction of the launcher in a horizontal (oblique) and a vertical plane, and also some special commands while the rocket is being put into a reference trajectory.

In essence, the command forming apparatus is a computer which operates automatically under the influence of coordinator signals or semiautomatically, when the initial data are fed into the command forming apparatus by an operator.

In its design, the command forming apparatus has the form of an individual unit or is combined with the automatic pilot of the rocket, as in radio zone control systems, homing systems and autonomous control systems. In command control systems, the command forming apparatus frequently is a continuation of the coordinator computer.

In accordance with the problems which are solved by the command forming apparatus, it must meet a number of technical requirements. One of these is ensuring the formation of a given number and form of control commands and also the required accuracy of conversion of the input signals into commands.

5.8. Apparatus for Forming Commands in Automatic Control Systems

In a general case, the command forming apparatus in automatic control /257 systems performs the following operations after the rocket is put into a reference trajectory:

(1) it produces signals characterizing the change of the mismatch parameter with time;

(2) it computes the derivatives and the integrals of the mismatch parameters for those planes in which the rocket is controlled;

(3) it forms additional compensating signals in dependence on the character of the motion of the target;

(4) it produces individual commands in the form of dc voltage pulses or closings (openings) of the contacts of electromechanical relays which regulate the feeding of signals to the automatic pilot or the CCRL.

Differentiators, which are used in forming a signal proportional to the derivative of the mismatch parameters, are employed in the command forming apparatus (CFA) for ensuring the necessary stability of the guidance process and the rapid and smooth putting of the rocket into a reference trajectory. The appearing dynamic errors are compensated by introducing into the command a component which is proportional to the angular velocity of rotation of the control point-target line or other parameters associated with motion of the target. If it is necessary to obtain small dynamic guidance errors, apparatus is used which ensures producing of commands when there are minimum deflections of the rocket from the reference trajectory. One of these apparatuses can serve as an integrator for which the input action is the mismatch parameter. The output signal, produced by the integrator and transmitted eventually to the automatic pilot of the rocket, will increase until its value becomes sufficient for deflection of the control surfaces and return of the rocket to a reference trajectory.

It should be noted that the use of an integrator in the command forming apparatus increases the degree of astaticism of the guidance circuit and, thereby, makes it possible to exclude systematic error in rocket guidance occurring due to the zero drift in the command forming apparatus and in the automatic pilot, and also due to the asymmetry of the rocket, etc.

In some cases, the command forming apparatus includes corrective filters ensuring acceptable reserves of stability of the control system and improvement of its principal characteristics.

The output signals of the command forming apparatus in automatic control systems can be either dc voltages or pulses characterizing digits in binary form, determined by the corresponding state of the electron tubes or other elements of the memory units.

Command forming apparatus of the analog type usually is linear with /258 respect to the mismatch parameters and the compensating signals in the course and pitching control planes and in a general case is described by the following equation

$$K_a = L_1(D)\,\Delta_m + L_2(D)\,S_{com}, \qquad (5.8.1)$$

where $K_a = K_{ay} + jK_{az}$ is the output signal of the CFA; K_{ay} and K_{az} are components of the output signal of the CFA for two mutually perpendicular planes, and especially for the vertical and horizontal control planes of the rocket;

$S_{com} = S_{cy} + jS_{cz}$ is the compensation signal fed to the CFA; S_{cy} and S_{cz} are the components of the compensation signal in planes for which the commands K_{ay} and K_{az} are formed; $L_1(D) = \frac{K_a}{\Delta_m}$ is the transfer function of the CFA in symbolic form in relation to the measured values of the mismatch parameter; $L_2(D) = \frac{K_a}{S_{com}}$ is the transfer function of the CFA in symbolic form in relation to the compensating signal.

In expression (5.8.1), the presence of the first term is mandatory, whereas the second term in some cases can be lacking.

In addition to the simplest command forming apparatus performing only the function of coupling the corresponding inputs and outputs, and also amplification of the mismatch parameter, there are CFA with a differentiator, integrator, integrating-differentiating apparatus, dynamic error compensation apparatus, etc. Since in most cases control commands for both control planes, regardless of their orientation, are produced by identical apparatus, henceforth we will consider CFA only for one vertical plane. Moreover, for the input and output signals of the CFA, which will be considered the voltages u_a and K_a, the subscripts "a" will be omitted. If the CFA is connected to the automatic pilot of the rocket, in place of K_a it is necessary to write K.

It should be emphasized that the voltage u_a characterizes the measured value of the mismatch parameter and in dependence on the type of coordinator can be denoted u_c, u_h, etc.

The functional diagram of a CFA with a differentiating link is shown in figure 5.23. The voltage u_a characterizing the mismatch parameter, passes through the coupling device CD_1, the differentiating link DL, the amplifier Amp and a coupling device CD_2. In order for the output voltage K_a to be dependent not only on the derivative $\dot{u}_a$, but also on the signal u_a itself, the differentiating link should contain an ohmic voltage divider. The CD_1 and CD_2 ensure the matching of the input and output of the CFA with the output of the coordinator and the input of the automatic pilot of the rocket or command control radio link (CCRL). /259

As differentiators it is possible to use R-C circuits, mechanical differentiators, velocity gyroscopes, etc.

Operation of a CFA of the analog type with a differentiating link DL (fig. 5.23) is described by the following equation

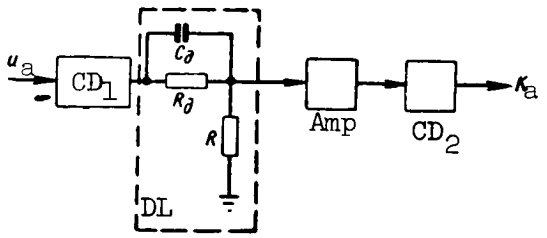

Figure 5.23

$$K_a = k_1 k_\partial \frac{1 + T_\partial D}{1 + k_\partial T_\partial D} u_a,$$

where k_1 is the transfer constant of the amplifier and the coupling device; $k_\partial = \frac{R}{R + R_\partial}$ is the transfer constant of the differentiator; $T_\partial = R_\partial C_\partial$ is the time constant of the differentiator.

Usually in order to obtain a high quality of differentiation, the values R and R_∂ are selected in such a way that the value k_∂ is considerably less than unity. In this case, the conditions are

$$K_a = k_1 k_\partial \times (1 + T_\partial D) u_a. \qquad (5.8.2)$$

As is well known, one of the characteristics of differentiators is "emphasis" of the high frequency components in comparison with the low-frequency components of the input voltages. This leads to an increase of the role of CFA fluctuation errors. However, the use of special correction filters in the CFA can lead to a considerable decrease of fluctuation errors. In performing their function, the correcting filters can transmit the derivatives of useful signals and attenuate high-frequency components. The mentioned condition is satisfied quite precisely by a filter whose transfer function corresponds to an inertial dynamic link.

If an increase of astaticism of the control system and elimination of the influence of the drift of the zero and asymmetry of the rocket are of basic importance, the command forming apparatus usually is a combination of amplifiers, coupling apparatus and integrator. The connection of an integrator into the CFA also makes it possible to eliminate the influence of systematic errors in rocket guidance caused, for example, by the influence of interference /260 on the constant component of the output signal of the command control radio link. This problem will be considered in greater detail in chapter 11.

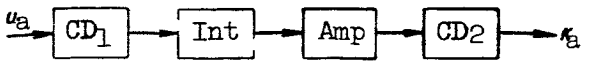

Figure 5.24

The functional diagram for such an apparatus is shown in figure 5.24. The coupling devices CD_1 and CD_2 ensure the matching of the input and output of the CFA with the preceding and following links of the system, the integrator Int performs the operation of integration and the amplifier Amp amplifies the produced voltage to some necessary value.

The role of integrators can be performed by electric motors, R-C and R-L elements without electronic amplifiers and with amplifiers, integrating gyroscopes, etc.

If a CFA with an integrator operates on direct current it creates a voltage (current) K_a equal to

$$K_a = k_1 \frac{k_m}{D} u_a, \qquad (5.8.3)$$

where k_m is the transfer constant of the integrator.

Expression (5.8.3), representing the equation of the CFA apparatus with an integrator, makes it possible to construct the structural diagram of a CFA and compute its dynamic and fluctuation errors.

In solution of the problem of the desirability of using CFA with an integrator, it is necessary to remember that the introduction of an integrator into the circuit, in a general case, reduces the reserve of stability of the control system.

In those cases when the automatic pilot must suppress signals reflecting the mismatch parameter, its integral and its rate of change with time, it is necessary to use CFA with integrating-differentiating devices. The functional diagram of such a CFA is shown in figure 5.25.

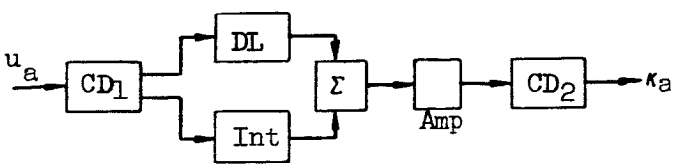

Figure 5.25

As in the preceding diagrams, the CD_1 and CD_2 elements perform coupling functions. The signals forming at the output of the differentiating link DL and the integrator Int characterize the value of the voltage u_a, its derivative and the time integral of u_a. These signals are added in the summer Σ and /261 pass through the amplifier Amp. Taking into account all the earlier introduced coefficients, we obtain the following expression relating u_a and K_a when $k_\partial \ll 1$

$$K_a = k_1\left[k_\partial (T_\partial D + 1) + \frac{k_m}{D}\right] u_a. \qquad (5.8.4)$$

In the three considered types of command forming apparatus, the transfer function $L_2(D)$ entering into equation (5.8.1) is equal to zero. The construction of a CFA with $L_2(D) = 0$ is introduced most frequently in systems whose characteristic criterion is the formation of the mismatch parameter aboard the rocket. This can be attributed to the difficulties in the placement of complex and unwieldy apparatus aboard small rockets guided to rapidly moving targets or the absence of requirements for formation of the function $L_2(D)$ in the system in rockets designed for damage of fixed and slowly moving targets.

In command control systems, the CFA is placed at the control point (land, ship, aircraft) where the weight and the size of the individual apparatus do not have particular importance. The CFA of systems which are used for the guidance of a rocket to rapidly moving targets, therefore, can contain elements forming the transfer functions $L_1(D)$ and $L_2(D)$.

In those cases when the input of the CFA receives signals reflecting the mismatch parameter and the compensating signals in digital form, the coupling elements, amplifiers and other stages of the CFA should be pulse signals.

An apparatus for forming single commands usually includes an electromechanical or electronic relay triggering when there is a zero value of the difference between the signals characterizing the stipulated and actual states of the controlled object.

Depending on the specific tactical problems involved in rocket guidance, it is possible to devise CFA which have different circuitry from the CFA shown in figures 5.22 to 5.25. To a considerable degree, this can be attributed to the requirements which are imposed on the control system and the characteristics of the sighting apparatus, automatic pilots and computers which are available to the designer during the design and planning stage.

5.9. Apparatus for Forming Commands in Nonautomatic Control Systems

As pointed out in chapter 1, command control systems only can be nonautomatic. In nonautomatic systems, there is direct participation by man (an operator), in addition to the use of electronic and electromechanical instruments. All the electronic, electromechanical and other types of apparatus included in a nonautomatic command forming apparatus customarily are referred to as a command pickup or a command instrument. In essence, a command /262 pickup is an apparatus designed for the initial conversion of the actions of an operator into electrical or some other signals of convenient form for feeding to the modulator of the transmitter of the CCRL. In addition, these signals should reflect the mismatch parameter.

The input device of the command pickup is a control lever which can be turned in one or two mutually perpendicular planes (for forming smooth and discrete commands), or a push-button mechanism used in forming single commands.

In most cases, the output signals of the command pickups are dc voltages, changes of the values of resistance, capacitance and inductance, closing and opening of the contacts of electromechanical relays, etc.

The forming of smooth commands is accomplished in most cases using potentiometric, capacitance and inductance pickups. At the same time, command pickups are known which produce signals in the form of periodic closings of contacts during a time proportional to the angle of rotation of the control lever. Pickups of the latter type will be called commutator pickups.

In the simplest potentiometric pickup (fig. 5.26) the control lever is connected to the potentiometer slide. The output value K_a of such a pickup can be the resistance R or the dc voltage $u_=$ between the points a and b.

The principal equation of a potentiometric pickup has the following form .

$$K_a = R = k_R \Delta_{lev} + \frac{R_{pot}}{2}, \qquad (5.9.1)$$

where Δ_{lev} is the angle of rotation (linear movement) of the control lever: R_{pot} is the total resistance of the potentiometer; k_R is the transfer coefficient of the pickup, characterizing the value of the increment of the resistance $R - \frac{R_{pot}}{2}$ for a unit value of the angle Δ_{lev}.

If the potentiometer is fed by a dc voltage, the output signal of the pickup is

$$K_a = u_= = k_u \Delta_{lev} + \frac{u}{2}. \qquad (5.9.2)$$

Here u is the dc voltage fed to the potentiometer, and k_u is the transfer /263 constant of the voltage command pickup measured relative to $\frac{u}{2}$.

In expressions (5.9.1) and (5.9.2) with the transfer of the zero value of the mismatch parameter $\Delta_m = u_a$, when $\Delta_{lev} = 0$, the values R and $u_=$ are $\frac{R_{pot}}{2}$ and $\frac{u}{2}$. When maximum positive or negative commands are produced, $R = R_{pot}$ and $R = 0$, and $u_= = u$ and $u_= = 0$, respectively.

The coefficients k_R and k_u can be computed in the following way. If $\Delta_{lev} = \Delta_{lev\ max}$, where $\Delta_{lev\ max}$ is the maximum angle of deflection of the control lever from a neutral position, $R = R_{pot}$ and $u_= = u$. Therefore, from equations (5.9.1) and (5.9.2)

$$k_R = \frac{R_{pot}}{2\Delta_{lev\ max}},$$

$$k_u = \frac{u}{2\Delta_{lev\ max}}.$$

Strictly speaking, equation (5.9.2) characterizes not only the command pickup itself, but the primary converter of the angle Δ_{lev}. This equation also reflects the operation of modulation of the dc voltage by movement of the potentiometer slide, which from the systematic point of view is more convenient to assign to one of the functions performed by the command control radio link.

Sometimes a single potentiometer is replaced by two with slides connected by a control lever (fig. 5.27). During the transmission of the zero command

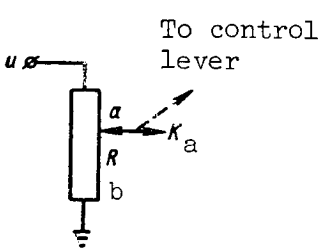

Figure 5.26

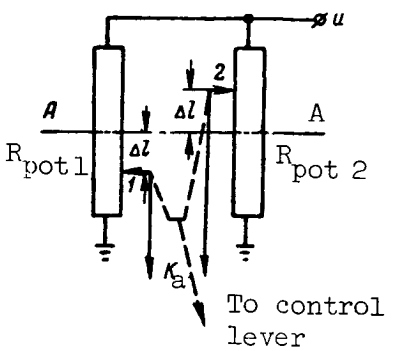

Figure 5.27

the control lever sets the slides 1 and 2 on the line AA which passes through the midpoints of the potentiometers $R_{pot\ 1}$ and $R_{pot\ 2}$. During transmission of the positive and negative values of the mismatch parameter, the slides 1 and 2 are deflected in different directions by the same value.

Accordingly, the equations for such command pickups can have the following form (when $R_{pot\ 1} = R_{pot\ 2} = R_{pot}$)

$$K_a = \Delta R = 2k_R\Delta_{lev}, \tag{5.9.3}$$

$$K_a = \Delta u = 2\,k_u\Delta_{lev}, \tag{5.9.4}$$

where ΔR and Δu are the difference of the resistances and the drops of the dc or sinusoidal voltage across the potentiometers $R_{pot\ 2}$ and $R_{pot\ 1}$.

The apparatus shown in figure 5.27 essentially is a pickup of the differential type. It is easy to see that the transfer constants for such a sensor are equal to $2k_R$ and $2k_u$, respectively.

In pickups of the capacitance and inductance types, a movement of the /264 control lever is accompanied by a change of the value of the capacitance Cap (due to the movement of the movable capacitor plate) or the inductance L (for example, due to introduction of a ferrite core). For these command pickups we find that

$$K_a = Cap = k_{cap}\Delta_{lev} + \frac{Cap_{max}}{2}, \tag{5.9.5}$$

$$K_a = L = k_L\Delta_{lev} + \frac{L_{max}}{2}, \tag{5.9.6}$$

where k_{cap} and k_L are the transfer constants of the capacitance and inductance pickups, and Cap_{max} and L_{max} are the maximum possible ranges of change of capacitance and inductance.

By analogy with potentiometric pickups, it is possible to create capacitance and inductance pickups of a differential type.

Commutator pickups usually are electromechanical devices.

Figure 5.28a shows the simple diagram of a sensor which produces a signal in the form of a periodic closing of the contacts at a time proportional to Δ_{lev}. The shaped shaft SS, one of whose sections is shown in figure 5.28b, is rotated with a constant angular velocity. A contact system moves along the

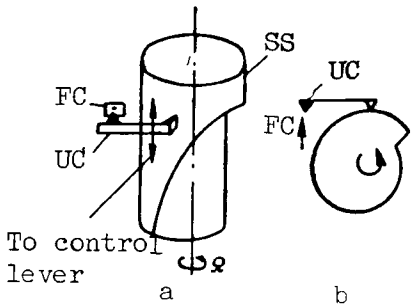

Figure 5.28

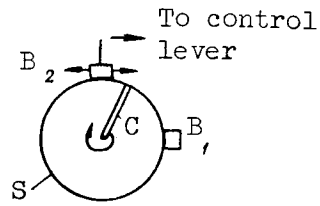

Figure 5.29

generatrices of this shaft, accompanying the movement of the control lever. This contact system consists of the unfixed and fixed contacts UC and FC. The unfixed contact comes into contact with the shaft SS, and as a result one part of the period of rotation of FC and UC is closed and the other is open. The times T_1 and T_2 of the closed and open states of FC and UC are dependent on what distance the entire contact system is situated from the SS base. A pickup of the considered type is constructed in such a way that when $\Delta_{lev} = 0$, the contact system is set on the midsection of the shaft SS. Under this condition $T_1 = T_2$. If $\Delta_{lev} > 0$, the contact system moves upward, but when $\Delta_{lev} < 0$ it moves downward. This means that the angular deflection of the control lever from a neutral position causes a proportional change of the difference $T_1 - T_2$. Therefore, the relationship between Δ_{lev} and $T_1 - T_2$, determining the equation for such a command pickup, has the following form

$$K_a = T_1 - T_2 = k_{\partial c}\Delta_{lev}, \qquad (5.9.7)$$

where $k_{\partial c}$ is the transfer constant of the command pickup.

Since $T_1 + T_2 = T = \text{const}$, where T is the period of formation of the /265 commands, then

$$T_1 = \frac{k_{\partial c}\Delta_{lev}}{2} + \frac{T}{2}. \qquad (5.9.8)$$

This indicates the proportionality between Δ_{lev} and T_1.

A pickup producing signals in the form of two brief closures of the contacts with an interval T_1 proportional to Δ_{lev} in one period T can be represented schematically as shown in figure 5.29. This figure shows that there are

two brushes (B_1 and B_2) connected to the rotating shaft S. One of them (B_1) is fixed and the other (B_2) can move under the influence of the control lever in the directions shown by arrows.

If $\Delta_{lev} = 0$, both brushes are situated within the same diameter and during the time T of one revolution of the shaft S the collector C closes with the brushes B_1 and B_2 each $\frac{T}{2}$. When $\Delta_{lev} > 0$, the brush B_2 moves clockwise and when $\Delta_{lev} < 0$, it moves counterclockwise relative to its position corresponding to $\frac{\Delta_{lev}}{2}$. Therefore, it is possible to derive a command pickup equation coinciding in form with expressions (5.9.7) and (5.9.8). The difference will be only in the physical essence of the values T_1 and T_2. If it is necessary to decrease the time T_1, in place of an increase of the rate of revolution of the shaft S, it is possible to select a large number of fixed brushes, appropriately limiting the range of movement of the moving brush B_2.

Commutator pickups also include devices producing video pulses which are width- or phase- (position-) modulated. Applicable to the two considered types of pickups, this means that the pickup also includes a dc voltage source. In addition, in order to obtain such electrical signals, it is possible to use potentiometers; the dc voltage from the latter is fed to a delay multivibrator or a delay phantastron. The triggering of the multivibrator and the phantastron is accomplished by a special generator of periodically repeated video pulses. In addition to multivibrators and phantastrons, it is possible to use saw-toothed wave generators with external triggering and circuits for comparison of the instantaneous voltage of the "sawtooth" with the dc voltage from the potentiometer. The latter types of pickups in essence are time-interval voltage converters.

In such apparatus, there is not only primary conversion of Δ_{lev} into /266 the movement of the potentiometer slide, but also modulation of the dc and video pulse voltages.

Taking into account the concept of a command pickup used here as a primary converter of the angle Δ_{lev} into an electrical or some other signal, these apparatuses should be broken down into two parts. The first part (potentiometer) is the pickup and the second is the modulator, which in accordance with the functions performed by the CCRL is a component part of the CCRL (see chapter 7).

Discrete commands can be formed by pickups whose principle of operation is based on the conversion of the value and sign of the angle Δ_{lev} into a stipulated number. This problem was discussed in section 5.4.

The operation of the sensor ensuring conversion of the angle Δ_{lev} into a binary number is characterized by the following equation

$$K_a = \sum_{l=1}^{N} 2^{l-1}\delta_l = k_{\partial c}\Delta_{lev}, \qquad (5.9.9)$$

where N is the number of used binary digits, δ_l is a function assuming the values 0 and 1, depending on the value Δ_{lev}, and $k_{\partial c}$ is the transfer constant of the command pickup.

In the transmission of single commands, pickups are used which are contacts closed or opened by a control button mechanism.

In conclusion, we point out that the principles of design and circuitry of command pickups considered here do not exhaust all the possible variants.

In an analysis of nonautomatic control systems, it frequently is convenient to replace the action of an operator by an equivalent dynamic link. The mathematical description of the action of an operator is based on the fact that, with a certain amount of practice, there are definite patterns in the operator's reaction to changes of the mismatch parameter. For example, the deflection Δ_{lev} of the control lever by the operator in the rocket guidance process can be described as follows

$$\Delta_{lev} = k_o(1 + T_o D)\,\Delta_m\,(t - \tau_o), \qquad (5.9.10)$$

where τ_o is the time characterizing the lag of the reaction of the operator, equal on the average to 0.2-0.4 sec; k_o is a transfer constant which, in a general case, is a function of time and which changes for different operators in rather broad limits; T_o is the time constant of the operator.

Equation (5.9.10) shows that the operator exerts control in accordance with the measured value of the mismatch parameter Δ_m and its derivative. The latter is an extremely important factor in ensuring the stability of the guidance process. /267

If expression (5.9.10) is taken into account and also the earlier derived relations for command pickups of different types, it is possible to obtain equations for the command forming apparatus in nonautomatic control systems.

In general form, this equation can be written in the following form

$$K_a(t) = L_1(D)\ \Delta_m\ (t - \tau_{lag}), \tag{5.9.11}$$

where $L_1(D)$ is the transfer function of the CCRL, whose specific form can be determined on the basis of equations (5.9.1)-(5.9.10); $K_a(t)$ is the signal acting at the output of the command pickup; τ_{lag} is the time characterizing the lag in producing the command.

In accordance with equation (5.9.11), it is possible to find the CCRL errors if the errors in determination of Δ_m are known, and also the specific form of the transfer function $L_1(D)$.

CHAPTER 6. COORDINATORS OF AUTONOMOUS CONTROL SYSTEMS

6.1. General Information

It is a characteristic of the coordinators of autonomous control systems, or autonomous coordinators, to use a briefer term, that the mismatch /268
parameter is formed using only the apparatus carried aboard the rocket. For this reason, the rocket does not receive signals from a control point or from the target to which the rocket is guided. Because of this the creation of artificial interference is extremely difficult for such coordinators, and in some cases is simply impossible. At the same time, the property of autonomy limits the range of problems which can be solved by a rocket with an autonomous coordinator. Such rockets can be used only for damaging fixed surface targets whose coordinates are known in advance with a high accuracy.

The following forms of autonomous coordinators can be distinguished:

(a) autonomous electronic coordinators based on the use of the Doppler effect;

(b) inertial coordinators;

(c) celestial navigation and radio celestial navigation coordinators;

(d) coordinators based on use of terrestrial features and phenomena;

(e) complex coordinators.

In the discussion of different coordinators in the sections of this chapter which follow, information on nonelectronic coordinators will be given only to the degree that it is required for clarifying the principles serving as a basis for the creation of complex systems containing instruments for measuring different physical values.

6.2. Autonomous Electronic Coordinator Based on Use of the Doppler Effect

The principal sensing element of an autonomous electronic coordinator /269
is a Doppler instrument for measuring the ground velocity and drift angle. Its principle of operation is based on the dependence of the frequency shift of a signal reflected from the Earth's surface (in relation to the frequency of the sounding signal sent from the rocket) on the velocity of its motion relative to the Earth's surface.

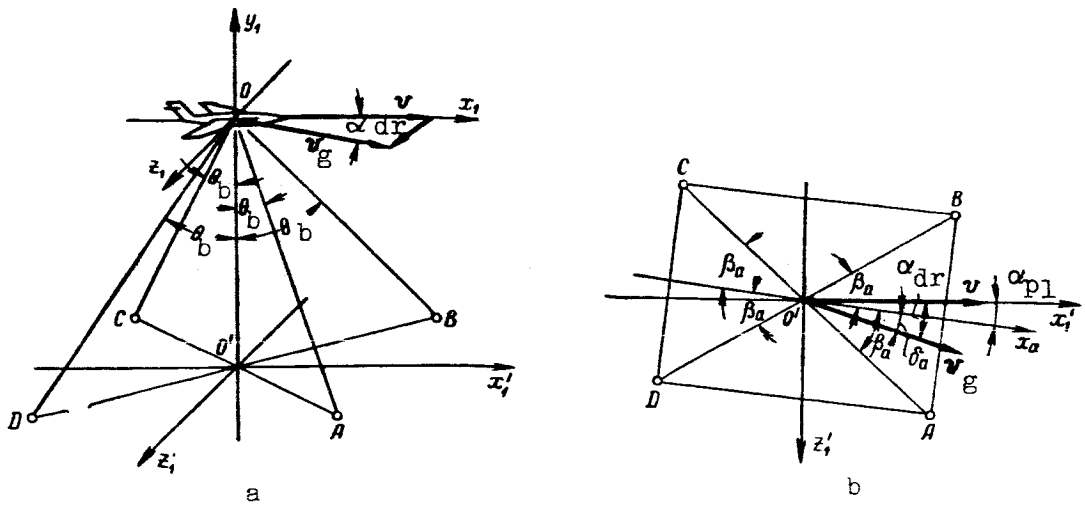

Figure 6.1

A Doppler instrument for measuring the ground velocity and the drift angle, DIGVA, includes a transmitter, antenna system, receiver, instrument for measuring Doppler frequency, drift velocity computer and drift angle. In addition to the Doppler instrument, the autonomous electronic coordinator includes: a gyro-vertical, a course system of some kind and a computer.

There is a great variety of technical variants of a Doppler system. Below, as an example, we present a brief description of a Doppler system with a cloverleaf antenna stabilized in a horizontal plane. The antenna is stabilized by a servosystem whose mismatch signal sensor is a gyro-vertical. As a result of the introduction of stabilization, there is elimination of errors caused by change of the angular position of the rocket relative to its longitudinal and transverse axes, that is, change of the angles of banking and pitching. At the same time, such a system makes it possible to measure the horizontal projection of the velocity vector of the rocket relative to the Earth, that is, the ground velocity v_g and the drift angle α_{dr}. A knowledge of these parameters is sufficient for guidance of a rocket along a fixed trajectory when its flight altitude is controlled by an autonomous sensor (altimeter). /270

The geometric relations characterizing the operation of a cloverleaf antenna system are shown in figure 6.1a. Figure 6.1b shows the projection of the spatial pattern onto the Earth's surface. It is assumed that the rocket flies in a horizontal plane with the ox_1 and oz_1 axes of the related coordinate system parallel to the Earth's surface. It also will be assumed that the angle of slip is small and that the horizontal component of air velocity v virtually coincides with the longitudinal axis ox_1 of the rocket.

The position of the beams oA, oB, oC and oD of the antenna system is characterized by the adjusting angles θ_b and β_a. The first of these represents the angle between the vertical oo' and each of the beams, and the second the angle between the axis of the gyrostabilized platform $o'x_a$ and the projections of the straight lines oA, oB, oC and oD onto a horizontal plane. The position of the gyrostabilized platform relative to the longitudinal axis of the rocket is determined by the angle α_{pl}. The drift angle is denoted by α_{dr}. Finally, the angle between the ground velocity vector and the axis of the platform is $\delta_a = \alpha_{dr} - \alpha_{pl}$. The frequencies of the signals received on the four beams differ from the frequencies of the signals emanating from the transmitter by the values of the Doppler shifts. These shifts are determined by the formulas

$$\left.\begin{aligned} F_{DA} &= \frac{2v_{plA}}{\lambda}, \\ F_{DB} &= \frac{2v_{plB}}{\lambda}, \\ F_{DC} &= \frac{2v_{plC}}{\lambda}, \\ F_{DD} &= \frac{2v_{plD}}{\lambda}, \end{aligned}\right\} \qquad (6.2.1)$$

where F_{DA}, F_{DB}, F_{DC}, F_{DD} are the Doppler frequencies of the signals received along the beams oA, oB, oC and oD; v_{plA}, v_{plB}, v_{plC}, v_{plD} are the projections of the ground velocity vector onto the direction of the beams oA, oB, oC and oD.

Using figure 6.1 it is easy to express the projections of the ground velocity vector through its value and the corresponding angles. Then we obtain

$$\left.\begin{aligned} F_{DA} &= \frac{2v_g}{\lambda}\sin\theta_b\cos(\beta_a - \delta_a), \\ F_{DB} &= \frac{2v_g}{\lambda}\sin\theta_b\cos(\beta_a + \delta_a), \\ F_{DC} &= -\frac{2v_g}{\lambda}\sin\theta_b\cos(\beta_a - \delta_a), \\ F_{DD} &= -\frac{2v_g}{\lambda}\sin\theta_b\cos(\beta_a + \delta_a). \end{aligned}\right\} \qquad (6.2.2)$$

In cloverleaf systems, the radiation and reception usually are through/271 two elements of the antenna simultaneously along two diagonal beams. Each pair of antenna elements operates alternately, making it possible to use only one receiving-transmitting channel.

After rectification of the received signals, voltages are discriminated which have the following difference frequencies

$$\left.\begin{aligned} F_{DAC} &= \frac{4v_g}{\lambda}\sin\theta_b\cos(\beta_a - \delta_a), \\ F_{DBD} &= \frac{4v_g}{\lambda}\sin\theta_b\cos(\beta_a + \delta_a). \end{aligned}\right\} \qquad (6.2.3)$$

At the output of the instruments measuring the frequencies F_{DAC} and F_{DBD}, the voltages will be proportional to these frequencies. The signals from the output of the measuring instruments are fed to a comparing device in which a voltage is formed which is proportional to the voltage difference of the mentioned signals. It is easy to show that it will be equal to

$$u_{com} = k_{com}k_F \frac{8v_g}{\lambda} \sin\theta_b \sin\beta_a \sin\delta_a, \qquad (6.2.4)$$

where k_{com} is the transfer constant of the comparing device, and k_F is the transfer constant of the frequency measuring instrument.

All the values in expression (6.2.4), except v_g and δ_a, are given. Using the notation $k_1 = \frac{8k_{com}k_F}{\lambda} \sin\theta_b \sin\beta_a$ and taking into account that $\delta_a = \alpha_{dr} - \alpha_{pl}$, we obtain

$$u_{com} = k_1 v_g \sin(\alpha_{dr} - \alpha_{pl}).$$

The voltage u_{com} is fed to the motor for final adjustment of the position of the platform and as a result the platform will be set in a direction in which $\alpha_{dr} = \alpha_{pl}$. By measuring the angle of rotation of the platform relative to the longitudinal axis of the rocket it is possible to determine the drift angle α_{dr}.

The value of the ground velocity vector v_g in such a system can be determined by measuring one of the frequencies F_{DAC} or F_{DBD} when $\delta_a = 0$ (in this case they are equal to one another). Then

$$v_g = \frac{\lambda F_{DAC}}{4\sin\theta_b\cos\beta_a}.$$

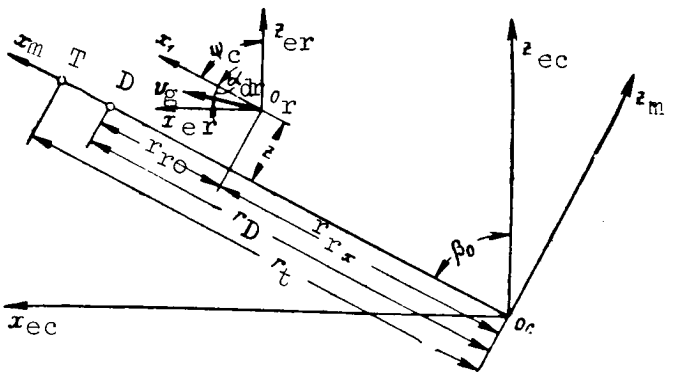

Figure 6.2

A rocket coordinator for determination of the mismatch parameters of the lateral deflection and remaining range channels, in the case of guidance along a fixed trajectory, should contain a course system for measuring the course angle of the rocket ψ_c, in addition to the Doppler system for measuring the ground velocity and drift angle.

Figure 6.2 shows the geometric relations illustrating the guidance of a rocket along a fixed trajectory. The position of the target T in a ground /272 system of coordinates $o_c x_{ec} z_{ec}$, whose origin is at the point where the autonomous electronic coordinator begins to operate, is given by the angle β_0 and the range r_t. D denotes the point where the rocket begins its dive. The mismatch parameters of the lateral deflection channel and the remaining range channel are measured in an orthodromic coordinate system $o_c x_m z_m$. The moving coordinate system $o_r x_{er} z_{er}$ has its origin at the center of mass of the rocket o_r, and its axes are parallel to the axes of the system $o_c x_{ec} z_{ec}$. The position of the longitudinal axis of the rocket in a moving coordinate system is characterized by the angle ψ_c.

As the components of the ground velocity vector along the axes $o_c z_m$ and $o_c x_m$ of an orthodromic coordinate system, we can write

$$\left.\begin{aligned} v_{gz} &= v_g \sin(\psi_c + \alpha_{dr} - \beta_0), \\ v_{gx} &= v_g \cos(\psi_c + \alpha_{dr} - \beta_0). \end{aligned}\right\} \qquad (6.2.5)$$

On the basis of equations (6.2.5) we write expressions for the mismatch parameters of the lateral deflection and remaining range channels

$$\Delta_z = \int_0^t v_g \sin(\psi_c + \alpha_{dr} - \beta_0)\, dt, \tag{6.2.6}$$

$$\Delta_{ro} = r_D - \int_0^t v_g \cos(\psi_c + \alpha_{dr} - \beta_0)\, dt. \tag{6.2.7}$$

By using formulas (6.2.6) and (6.2.7) it is easy to construct the functional diagram of an autonomous electronic coordinator (fig. 6.3). The signals of the transmitter Tr are radiated by the cloverleaf antenna of system A. The signals reflected from the Earth's surface are fed to the antenna A and then to the receiver Rec where they are amplified. The Doppler frequency voltages are fed to the instruments measuring the drift angle α_{dr} and ground velocity v_g. /273

A voltage is produced in the instrument measuring α_{dr} for control of the motor M for turning the gyrostabilized platform on which the antenna system is mounted. The angle of rotation of the platform relative to the body of the rocket determines the drift angle α_{dr}.

A signal is produced in the instrument for measuring v_g which is proportional to the ground velocity of the rocket. This signal is fed to a sine-cosine generator. The sine-cosine potentiometer described in section 4.10 can be used as such an apparatus. In this case, the brushes of the potentiometer are turned by the angle $\alpha_{pot} = \psi_c + \alpha_{dr} - \beta_0$. The angles ψ_c, α_{dr} and β_0 are summed in the differentials DF_1 and DF_2. The angle β_0 is introduced into the computer prior to the launching of the rocket.

A signal from one of the outputs of the sine-cosine generator is fed to an integrator for measurement of the lateral deflection Δ_z. The remaining range Δ_{ro} is measured by a subtracting device SD; one input of the latter is fed a voltage proportional to the travelled distance, and the other a voltage u_{rD} proportional to the range r_D to the point of transition of the rocket into a dive. The voltage u_{rD} is introduced into the computer before launching of the rocket.

The measured values Δ_{zm} and Δ_{rom} of the mismatch parameters Δ_z and Δ_{ro} are used for control of the rocket course and the producing of a command for its transition into a dive.

The errors of an autonomous electronic coordinator include the errors of the Doppler system for measuring ground velocity and drift angle, the course system and the computer. /274

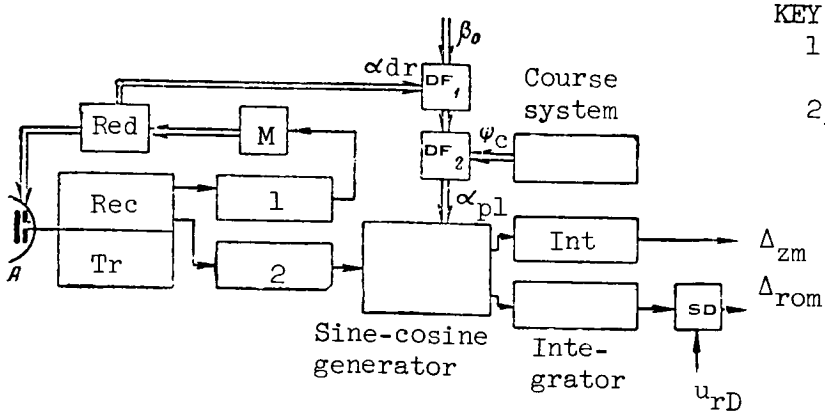

Figure 6.3

The Doppler system errors can be attributed to the fact that the received signal is not reflected from a single point, but from some surface which can be replaced by a large number of elementary reflectors situated within the limits of the irradiated area. The signals from all the elementary reflectors are summed with random phases. The resultant signal, therefore, has a random character and has a finite spectrum of frequencies grouped around the actual value of the Doppler frequency. The accuracy of measurement of Δ_z and Δ_{ro} can be determined if the statistical characteristics of the random values entering into formulas (6.2.6) and (6.2.7) are known.

6.3. Inertial Coordinator

The principal element of a coordinator of the inertial type is a measuring instrument which is used for determination of the distance covered by double time integration of the absolute accelerations measured by the linear acceleration sensors (accelerometers).

When the path of a rocket relative to the Earth's surface is calculated using an inertial measuring instrument, it is necessary to place the accelerometers on a movable platform which during the entire time of the flight should be set normal to the local vertical. This placement of the accelerometers eliminates the errors caused by accelerations of gravity.

Two methods for design of such a platform are used most frequently. In the first method, the platform with the accelerometers is set in a fixed position on a gyrostabilizer whose position is corrected in accordance with the change of the position of the local vertical (system with a horizontal stabilizer). In the second method, the gyrostabilizer remains fixed in relation to an inertial coordinate system and the position of the platform with the accelerometer is changed in relation to it in accordance with the change of the position of the local vertical (system with a gyrostabilizer fixed in relation to an inertial coordinate system). In both the first and second cases,

the local vertical is obtained using the signals of the accelerometers of the inertial measuring system itself. Such a vertical is called an inertial vertical.

In addition to the above, when calculating the path in a ground coordinate system, it is also necessary to take into account the Earth's rotation on its axis. In systems with a gyrostabilizer fixed relative to an inertial coordinate system, the Earth's rotation can be taken into account by an additional turning of the platform with the accelerometers in relation to the gyrostabilizer, with an angular velocity equal to the angular velocity of the Earth's rotation. In a system with a horizontal gyrostabilizer, the Earth's rotation is taken into account by the introduction of compensating signals into the measured acceleration values. /275

An inertial measuring instrument, an apparatus for determining the vertical, a system for introducing corrections for the Earth's rotation and a computer form an inertial coordinator which can be used for formation of the mismatch parameters used in guidance of rockets along fixed trajectories.

Now we will obtain expressions for the mismatch parameters of the lateral deflection and remaining range channels for rocket guidance along an orthodromic reference trajectory.

At the initial point of the trajectory, the gyroplatform is set in such a way that the measurement axes of the accelerometers are in a horizontal plane; the measurement axis of one of the accelerometers coincides with the direction of the reference trajectory, and the measurement axis of the other is oriented normal to it. Then double integration of the signal of the first accelerometer (with a correction for the Earth's rotation taken into account) gives a value proportional to the path travelled by the rocket, and double integration of the signal of the second accelerometer (also with the correction for the Earth's rotation taken into account) determines a value proportional to the lateral deflection of the rocket from the reference trajectory.

If the initial setting of the platform is made, the expressions for the mismatch parameters of the lateral deflection and remaining range channels will have the following form

$$\Delta_z = \int_0^t \left[\int_0^t j_z dt - v_{cz} \right] dt, \tag{6.3.1}$$

$$\Delta_{ro} = r_D - \int_0^t \left[\int_0^t j_x dt - v_{cx} \right] dt. \tag{6.3.2}$$

Here j_z, j_x are the acceleration components along the axes of the orthodromic coordinate system $o_c x_m z_m$; v_{cz}, v_{cx} are the compensating signals taking into account the migratory motion associated with the Earth's rotation, and r_D is the

distance between the initial point of the trajectory and the point of transition of the rocket into a dive.

The values of the compensating signals v_{cz} and v_{cx} can be computed using the formulas (ref. 6)

$$v_{cz} = R\omega_e \sin \epsilon \cos u, \tag{6.3.3}$$

$$v_{cx} = R\omega_e \cos \epsilon, \tag{6.3.4}$$

where R is the distance from the center of the Earth to the rocket, for all practical purposes equal to the Earth's radius, ω_e is the angular velocity of the Earth's rotation, ϵ is the angle of inclination of the orthodrome to the equator, $u = u_0 + \frac{r_r}{R}$ is the angle between the local vertical and the line /276 of intersection of the planes of the equator and the orthodrome, called the argument of latitude, u_0 is the initial argument of latitude and r_r is the distance travelled by the rocket along the orthodrome from the time of activation of the system.

The compensating signals are shaped by the computer in accordance with formulas (6.3.3) and (6.3.4). The values R, ω_e, ϵ and u_0, introduced into the computer as initial data, are constants for a particular orthodrome.

During a long period of the rocket flight perceptible azimuthal departures of the platform in relation to its initial position can be observed.

For the control system of a rocket, this is equivalent to the stipulation of a new orthodromic trajectory not coinciding with the reference trajectory. Elimination of the departure of the platform in azimuth is attained by the introduction of a course system into the coordinator. The signals of the course system, correcting the position of the platform, are shaped on the basis of a comparison of the actual and stipulated target (course) angle.

Figure 6.4 shows the functional diagram of the mentioned coordinator. The range and lateral deflection accelerometers are mounted on a corrected gyroplatform. The correction signals are shaped by the first integrators of the coordinator. The accelerometers, first integrators and corrected gyroplatform form the circuit of the apparatus for determination of the inertial vertical.

The signal from the output of the first integrator of the range channel is fed to the subtracting device SD_1, which also is fed a compensating signal taking into account the migratory motion caused by the Earth's rotation. /277 The latter is formed in the computer of the range channel on the basis of the stipulated values R_m, ω_{em} and ϵ_m characterizing the measured values R, ω_e

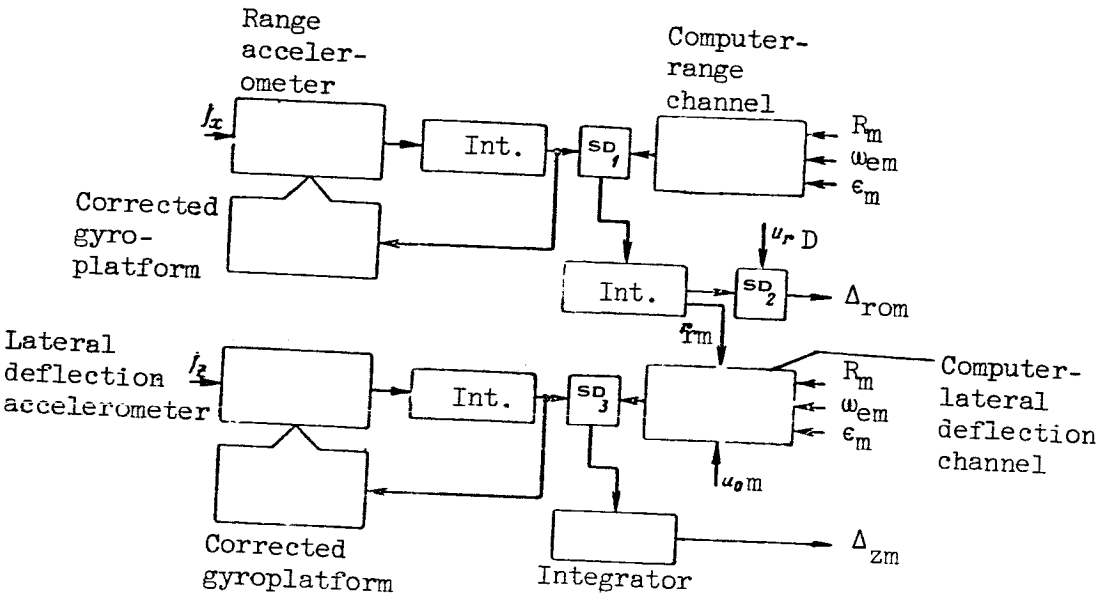

Figure 6.4

and ϵ_m. A difference voltage from the output of the subtracting device SD_1 is fed to the second integrator and then to the subtracting device SD_2, where this voltage is compared with a voltage proportional to the range to the point of transition of the rocket into a dive.

The lateral deflection channel is devised in a similar way. The only difference is that the computer of this channel is fed not only the values R_m, ω_{em} and ϵ_m, but also the measured values r_{rm} and u_{om} of the travelled range r_r and the initial argument of latitude u_0. The mismatch parameter of the lateral deflection channel is formed at the output of the second integrator.

An inertial coordinator is a completely autonomous apparatus and its operation is not dependent on external conditions. In addition, it is not subject to the influence of artificial interference.

The principal shortcoming of an inertial coordinator is the increase of measurement errors with an increase of the time of rocket flight as a result of the imperfection of the components. The most significant errors are due to the characteristics of operation of the apparatus for determining the inertial vertical. We will assume that the accelerometer Ac is mounted on the gyroplatform GP, which at the initial time is oriented horizontal to the Earth's surface (fig. 6.5). With motion of the rocket from position I to position II, the signal from the accelerometer is integrated and fed to the correcting motors of

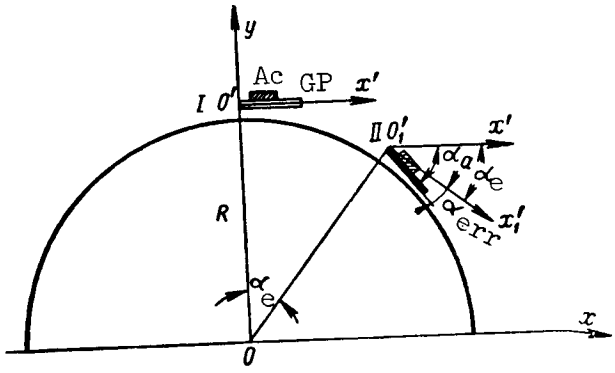

Figure 6.5

the gyroplatform. Under the influence of this signal, the gyroplatform is turned relative to its initial position. In the case of ideal operation of the system, the platform should maintain a horizontal position relative to the Earth's surface. However, due to the errors of the correction system it turns by the angle α_{err} relative to the true horizon (the axis $o'_1x'_1$).

Obviously, the acceleration measured by the accelerometer will be /278 equal to

$$j = \dot{v}\cos\alpha_{err} - g\sin\alpha_{err} \approx \dot{v} - g\alpha_{err}, \qquad (6.3.5$$

where $\dot{v}$ is the tangential acceleration caused by the effective forces.

Taking into account that the corrected gyroplatform plays the role of an integrator relative to the correction signal, we find the angle of deflection of the platform in relation to its initial position

$$\alpha_a = k_{ver}\int_0^t\int_0^t (\dot{v} - g\alpha_{err})\,dtdt. \qquad (6.3.$$

Here k_{ver} is the general transfer constant of the accelerometer, integrator an gyroplatform.

It follows from figure 6.5 that

$$\alpha_a = \alpha_{err} + \alpha_e = \alpha_{err} + \frac{1}{R}\int_0^t v\,dt. \qquad (6.3$$

After substituting expression (6.3.7) into (6.3.6), we obtain

$$\alpha_{err} + \frac{1}{R}\int_0^t v\,dt = k_{ver}\int_0^t\int_0^t (\dot{v} - g\alpha_{err})\,dt\,dt. \qquad (6.3.8)$$

Differentiating the latter equation twice, we find

$$\ddot{\alpha}_{err} + \frac{1}{R}\dot{v} = k_{ver}\dot{v} - k_{ver}g\alpha_{err}$$

or

$$\ddot{\alpha}_{err} + k_{ver}g\alpha_{err} = \dot{v}\left(k_{ver} - \frac{1}{R}\right). \qquad (6.3.9)$$

In order for the vertical to be invariant to accelerations, that is, maintain its position despite the influence of external perturbations, it is necessary to satisfy the condition

$$k_{ver} = \frac{1}{R}. \qquad (6.3.10)$$

The selection of the transfer constant k_{ver} of the apparatus for determining the vertical, equal to $\frac{1}{R}$, is a necessary condition for maintaining the platform in a horizontal position in the case of zero initial conditions. In actuality, with the satisfaction of (6.3.10), equation (6.3.9) assumes the form

$$\ddot{\alpha}_{err} + \frac{g}{R}\alpha_{err} = 0. \qquad (6.3.11)$$

If $\alpha_{err\ 0} = \dot{\alpha}_{err\ 0} = 0$ when $t = 0$, the angle α_{err} will be equal to zero during the entire time of the flight, that is, a gyroplatform with an accelerometer maintains its horizontal position in relation to the Earth's surface. /279 In the case of nonzero initial conditions, the motion of the gyroplatform relative to the horizon is represented by harmonic oscillations

$$\alpha_{err} = \alpha_{err\ 0}\cos\Omega_{Sch}t + \frac{\dot{\alpha}_{err\ 0}}{\Omega_{Sch}}\sin\Omega_{Sch}t, \qquad (6.3.12)$$

where $\Omega_{Sch} = \sqrt{\frac{g}{R}}$ is the angular frequency of the oscillations.

The period of the oscillations $T = \frac{2\pi}{\Omega_{Sch}} = 2\pi\sqrt{\frac{R}{g}} = 84.4$ min is called the M. Schuler period. It is equal to the period of oscillations of a mathematical pendulum with a length of suspension equal to the Earth's radius.

The oscillations of the platform lead to errors in the measurement of the mismatch parameter. Thus, in the case of initial deflection of the platform $\alpha_{err\ 0} = 1'$, the error in determination of distance will change periodically from zero to 1.85 km. Since these changes transpire very slowly, a rocket with an inertial coordinator will change its trajectory in accordance with the measured distances.

In some cases, the errors in guidance of a rocket with an inertial coordinator are inadmissibly large. For this reason, in many cases, it is desirable to combine an inertial measuring instrument with a measuring instrument of a different type not having the mentioned shortcoming. In such a complex coordinator, the inertial system, which is operating continuously during the entire time of the flight, plays the role of a singular "memory" while the apparatus of the second measuring instrument, which cuts in periodically, is used for "transcribing" the accumulated errors.

6.4. Celestial Navigation Coordinator

The principal measurement component in a celestial navigation coordinator is a so-called automatic sextant. This is an apparatus for automatic tracking of a selected celestial body on the basis of angular coordinates. This tracking is possible using the light or radio emission of the celestial body and accordingly optical or radio sextants are used.

In astronomical orientation for determination of a position of a point on the Earth's surface in a horizontal coordinate system, it is most common to measure the altitudes of two celestial bodies (the altitude of a celestial body is the angle between the direction to the celestial body and the projection of this direction onto the horizontal plane passing through the observation point). Therefore, the coordinator should include either two automatic sextants, each of which tracks a single celestial body, or one sextant which is used for tracking two celestial bodies alternately. After the altitudes of the celestial bodies have been measured, they should be converted by a computer into coordinates characterizing the current position of the rocket relative to the Earth's surface. Such conversions can be made if the computer is fed the declinations and Greenwich hour angles of the celestial bodies, as well as their altitudes. If the current coordinates of the rocket are determined in an orthodromic coordinate system, they represent the mismatch parameters of the lateral deflection and remaining range channels. It should be noted, however, that the analytical relationships between the mismatch parameters and the measured values (altitudes of the celestial bodies) are very unwieldy. If the coordinates of the celestial bodies are measured

/280

in an equatorial coordinate system, with stipulation of an orthodromic reference trajectory, the mismatch parameters of the lateral deflection and remaining range channels are obtained directly from the measuring instrument used in determination of the coordinates of celestial bodies without conversion. The shortcoming of such coordinators is the complexity of the kinematics of their mechanisms.

The book listed as reference 22 describes an apparatus designed for measurement of the mismatch parameters for guidance of rockets having a celestial navigation coordinator. Data on the position of the celestial body (its azimuth and altitude) relative to each point of a set trajectory are registered on the tape of the programming mechanism. During rocket flight, this tape is drawn through a tape decoder at whose output a voltage is produced controlling the position of the telescope of the automatic sextant in azimuth and angle of elevation. If the actual position of the rocket does not coincide with the stipulated position, the automatic sextant produces a signal which later is used for control of the position of the rocket.

In addition to the considered cases of the use of celestial navigation measuring instruments, very frequently they are used for correction of an inertial coordinator, together with the latter forming a celestial navigation–inertial coordinator.

6.5. Coordinators Based on Use of Terrestrial Features and Phenomena

As examples of coordinators based on use of features and phenomena rigidly related to the Earth, we will consider briefly coordinators based on magnetic orientation and orientation on the basis of terrain images.

The possibility of using magnetic orientation for the guidance of rockets along fixed trajectories is based on the nonuniformity of the Earth's magnetic field, its relative constancy and the rigidity of its relationship to the Earth. This possibility was exploited in one of the early developments of /281 winged rockets of the "ground-to-ground" class, guided along fixed trajectories, specifically the German V-1 rocket. The rocket was guided along its course by a course system with a magnetic sensor. In the event that the actual course of the rocket did not correspond to the specified course set in the magnetic corrector before launching, a mismatch signal was produced which was used for guiding the rocket along its course. In the case of ideal guidance, the rocket flew along a loxodrome (a line intersecting all meridians at the same angle); in the case of short ranges, a loxodrome is close to an orthodrome. The mismatch parameter of the range channel was formed by an aerolog. When the rocket attained a range equal to the specified range, a command was produced for the rocket to dive.

The control system of the V-1 rocket had a relatively low accuracy of guidance. This was due for the most part to the absence of measuring instruments reacting to the lateral deflection of the rocket.

This control system made use of only one component of the Earth's magnetic field--the horizontal component of the field strength vector. However, this does not exhaust the possibilities of magnetic orientation.

Let us recall some definitions. The Earth's magnetic field at each point around the Earth is characterized by the value and direction of the total vector of field strength T. The T vector can be broken down into two components which are perpendicular to one another--horizontal and vertical. The angle between the T vector and its horizontal component is called magnetic inclination and the angle between a meridian and the horizontal component of the Earth's magnetic field is called magnetic declination.

The distribution of the magnetic field over the Earth's surface is represented by isomagnetic lines. These are curves on a map connecting points with an identical value of the same element. The isomagnetic lines of the value of the T vector and its components are called isodynamic lines. Isolines of declination are called isogonic lines; isolines of inclination are called isoclinic lines.

These elements of the Earth's magnetic field can be measured by magnetometers forming part of a magnetometric coordinator.

Theoretically, it is possible to have different variants of design of such a coordinator. For example, a coordinator has been described in reference 22, which is designed for formation of the mismatch parameter of the lateral deflection channel during the flight of a rocket along a reference trajectory coinciding with the isomagnetic line passing through the target. Formation of the mismatch parameter of the range channel is possible making use of the circumstance that, in a general case, isolines of different kinds intersect one another. Obviously, in magnetic orientation, those elements of the Earth's magnetic field should be selected whose isolines intersect at large angles in the region of the proposed use of the rocket, and whose horizontal gradients /282 (isoline density) are maximal for the selected elements. The merit of a magnetometric coordinator is its complete autonomy and relatively high noise immunity.

The difficulties associated with the use of magnetometric coordinators are caused by the temporal instability of the Earth's magnetic field and the inevitable influence of the magnetic fields of the rocket--which often attain an inadmissibly large value--on the accuracy.

The use of a coordinator of the second type, using features and phenomena related to the Earth, is based on the identification of characteristic features on the Earth's surface and guidance of the rocket in reference to them. The essence of the operation of such a coordinator, which for brevity will be called cartometric, is as follows. The image of the terrain zone over which the rocket is to fly is registered in advance on a photographic film. The concept "terrain image" in this case has a generalized character. It includes the aerial photographic image of the terrain and also the image of the radar or thermal relief of the natural radio emission of parts of the terrain. The selection of the particular type of image is determined by the type of sensing

element of the coordinator used for identification of the features. The film produced in this way plays the role of a singular relief map.

In the guidance process, the image received from the sensing element of the coordinator is compared with the image registered on the photographic film; the latter is moved by a special film-moving mechanism at a rate approximately equal to the ground velocity of the rocket.

In most cases, the comparison is made by superposing one image on the other. When they fail to coincide, a mismatch signal is formed which is used both for control of the rocket and for a change of the rate of movement of the film moving mechanism. A mark is plotted on this same film and its appearance serves as a command for the rocket to dive.

Thus, a cartometric coordinator carried aboard a rocket should contain a sensing element for the continuous scanning of the terrain, a system for comparison of images and a computer which converts the results of the comparison into a mismatch parameter.

When cartometric coordinators are used, the problem arises of obtaining relief maps of the area of military hostilities. There are two ways to solve this problem:

(1) reconnaissance flights by aircraft with appropriate apparatus along the proposed paths of rocket launching;

(2) obtaining the necessary relief maps by some artificial method.

Thus, if a rocket uses a sensing element of the radar type for scanning the terrain it is possible to create an artificial map of the radar relief by use of an ultrasonic radar trainer. The initial data on the proposed region of launching of rockets, obtained from ordinary geographic maps, aerial photographic surveys and reconnaissance are introduced into the trainer. It is noted in reference 22 that the artificial map of radar relief created in this way is virtually identical to the natural relief. /283

6.6. Complex Coordinators

Recently, there has been a tendency to create complex systems for measurement of the coordinates of aircraft and rockets. Such systems include measuring instruments employing navigational information of different physical nature. As a result, it is possible to organize the results of the measurements, which in the long run increases appreciably the reliability of the information obtained.

The quality of the operation of a complex coordinator is determined to a considerable degree by the successful selection of the set of measuring instruments and the algorithm of the matching apparatus.

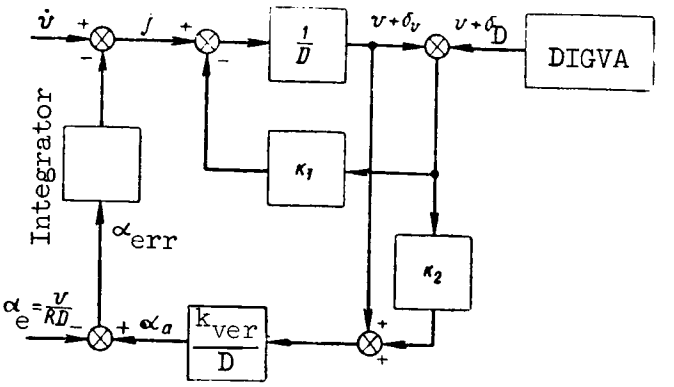

Figure 6.6

As an example, below we will discuss a complex inertial–Doppler coordinator containing an inertial measuring instrument and an autonomous electronic instrument for measuring the ground velocity (ref. 11). The role of the latter in such a coordinator is essentially correction of the apparatus for determining the inertial vertical. Change of the properties of the latter under the influence of the correcting signals considerably increases the accuracy of calculation of the path by the inertial system.

Figure 6.6 shows the block diagram of the apparatus for determining the vertical with the introduction into it of correcting signals from the Doppler measuring instrument. The block diagram was constructed on the basis of equations (6.3.5)-(6.3.9). The correction signals are introduced in the following way. The velocity of the rocket relative to the Earth, measured by the inertial system, is compared with the velocity indicated by the Doppler measuring instrument. It is assumed that the inertial measuring instrument measures velocity with the error δ_v and the Doppler instrument with the error δ_D. The difference signal is fed through a feedback link with the transfer constant k_1 to the input of the integrator. Then the difference signal, passing through the amplification link k_2 is added to the output signal of the integrator and is fed to the correcting motor of the gyroplatform.

It is easy to show that the process of determining the inertial vertical is described by the following operational equation

$$[D^2 + k_1 D + (1 + k_2)k_{ver}g]\alpha_{err} = k_{ver}(D + k_1)v - \\ - \frac{D + k_1}{R} v + k_{ver}k_1 - k_2 D)\delta_D. \qquad (6.6.1)$$

With the selection of the transfer constant of the apparatus for determining the vertical from the condition of its imperturbability $k_{ver} = \frac{1}{R}$, equation (6.6.1) assumes the form /284

$$\left[D^2 + k_1 D + (1 + k_2)\frac{g}{R}\right] \alpha_{err} = \frac{k_1 - k_2 D}{R} \delta_D. \qquad (6.6.2)$$

Comparison of expression (6.3.11) with (6.6.2) shows that the introduction of a correcting signal changes the form of the process for determination of the vertical with retention of its invariance to a change of rocket velocity. This process now has an oscillatory-attenuating character.

By changing the parameters of the correction circuits (the transfer constants k_1 and k_2), it is possible to change the attenuation factor for the apparatus for determining the vertical and its natural frequency in broad limits.

In the example considered above, one of the measuring instruments of the complex system is used for correction of the other measuring instrument. However, it is possible to design systems in which there is mutual correction of a number of measuring instruments.

CHAPTER 7. COMMAND CONTROL RADIO LINKS

7.1. Functional Diagram and Principal Characteristics of a Command Control Radio Link

The input device of a command control radio link whose functional diagram for one channel is shown in figure 7.1 is a coder Cod. The coder /285
forms special voltages (continuous or in the form of pulses) which are called subcarrier oscillations, there is modulation of the signals produced by the command forming apparatus and the subcarrier is given those qualitative criteria which ensure separation of commands in individual circuits (channels) at the receiving end and increase of noise immunity of the command control radio link (CCRL). The modulation parameters of the subcarrier oscillations reflect the quantitative values of the control commands. If the CCRL has a single channel, only a single command K_a is fed to the coder input.

In order to perform the necessary functions, the coders usually contain generators of electrical oscillations, modulators, commutators, summation devices, etc. The coder signals are used for modulation of the carrier in the radio transmitter Tr. The coder and transmitter form the transmitting apparatus of the CCRL, which is situated at the control point.

The need for using sinusoidal or pulse subcarrier oscillations in the coder usually is due to the multichannel character of the CCRL or to specific characteristics of the method for transmission of commands in a single-channel CCRL.

The radio signals produced by the radio transmitter are radiated by the CCRL transmitting apparatus in the direction of the rocket. /286

At the output of the radio receiver Rec, voltages are formed which are similar to those fed to the radio transmitter. These signals are fed to the decoder Decod. The decoder accomplishes both separation for the individual circuits of commands having different purposes (corresponding qualitative criteria of subcarrier oscillations are used for this purpose) and for demodulation and conversion of the subcarrier oscillations into signals convenient for transmission to the automatic pilot. In addition, the decoder accomplishes a separation of useful signals from interference on the basis of those

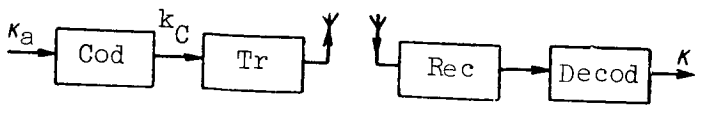

Figure 7.1

additional criteria which were imparted to the subcarrier oscillations in the coder.

In a single-channel CCRL, only one command K is formed at the output of the decoder. This command is a function of time. The number of signals produced by the decoder of a multichannel CCRL is dependent on the number of objects to be controlled (control surfaces, motor, etc.). The decoder includes filters, demodulators, commutators, decoding devices, etc.

The radio receiver and decoder form the receiving apparatus of the CCRL carried on the rocket.

In most cases, the output signals (commands) of the CCRL should be a dc voltage. If control is accomplished by smoothly moving control surfaces, the CCRL commands should be continuous functions of time. When it is necessary to bring the rocket into a dive, cut out the engine, etc., the CCRL should produce commands in the form of dc pulses (video pulses) which act upon the corresponding relay in the automatic pilot. As already mentioned, commands of this type are called single commands. One of the distinguishing characteristics of these commands is that the definite effect produced by them on the controlled object subsequently usually cannot be reversed.

When the rocket has spoilers or oscillating control surfaces, the CCRL decoder includes apparatus for producing periodic bipolar square pulses with the durations T_1 and T_2, depending on the value K_a. Commands in the form of bipolar pulses also are called continuous commands.

The concept of a "continuous command," in essence, means that there is a functional relationship between K and K_a which can exist at each particular moment or only at individual (discrete) times. In the latter case, the continuous function $K_a(t)$ is transmitted discretely in time and a continuous CCRL output signal is obtained as a result of processing pulses reflecting the value and sign $K_a(t)$ when $t = t_1, t_2, \ldots, t_{i-1}, t_i, \ldots, t_n$, where the intervals $\Delta t_i = t_i - t_{i-1}$ when $i = 1, 2, \ldots$ can be identical or different. If the pulses are transmitted sufficiently frequently, the command produced /287
by the CCRL virtually precisely characterizes $K_a(t)$.

In addition to time quantization of the function $K_a(t)$, there can be also level quantization. In this case, the CCRL is constructed so that not all values $K_a(t)$ are transmitted, but only earlier stipulated values. If in the case of level quantization of $K_a(t)$ the process of control of a rocket or other object remains virtually constant, it is assumed that the CCRL ensures the transmission of continuous commands.

Since the rocket course and pitching control signals should be bipolar, the transmission of the command K_a usually is accomplished using two subcarrier oscillations. One of them is a sort of reference and at the receiving end serves as a comparison voltage; the other is a working signal. The working subcarriers always are modulated by the transmitted command, whereas the reference oscillation can be modulated or unmodulated. If the command K_a acts upon both subcarrier oscillations, the coder modulator is constructed in such a way that the increment of the modulated parameter of one subcarrier oscillation increases and that of the other decreases.

Due to the use of two subcarrier oscillations for transmission of the command of one control channel, good conditions are ensured for obtaining a high stability of the zero of the amplitude characteristic of the CCRL, which determines the dependence of K on K_a.

At the same time, CCRL can be created in which the command modulates only one subcarrier oscillation. The sign of the command in such CCRL is determined by the formation of a signal difference at the output of the CCRL, obtained from the subcarrier oscillation and a standard comparison voltage (current) created by a special source on the rocket. However, CCRL constructed on such a principle, although they are the simplest from the technical point of view, do not ensure the stability of transmission of the zero command and possess low noise immunity.

For transmission of continuous smooth and level-quantized commands, the CCRL coders can employ various kinds of modulation of sinusoidal or pulse subcarrier oscillations by commands fed from the command forming apparatus and especially pulse-width, phase, frequency and pulse-code modulation of the subcarriers. We note that phase and frequency modulation of video pulses (pulse subcarriers) frequently are called pulse-phase (pulse-time) and pulse-frequency modulation. The transmission of single commands is accomplished using code groups of video pulses or pulses of sinusoidal oscillations.

The CCRL transmitter can produce both continuous and pulse signals. The times characterizing the beginning of signal formation by it can be given in the course of rocket guidance by coder pulses or by special commands. The /288 latter method is used in those cases when the transmitter should not generate oscillations between the times characterizing the change of the values of the transmitted commands. The carrier produced by the transmitter is modulated by coder signals, either in amplitude or frequency.

In order to ensure the possibility of commands for different purposes in separate circuits (channels) at the receiving end, the principles of frequency, time and code selection are used, as in multichannel systems of radiotelephonic communication. Whereas in the frequency and time methods of separation of channels each subcarrier oscillation is characterized by corresponding frequency and time criteria, the code selection method is based on the use of combinations of pulse subcarriers, forming for each channel a group of pulses with a preset interval between them.

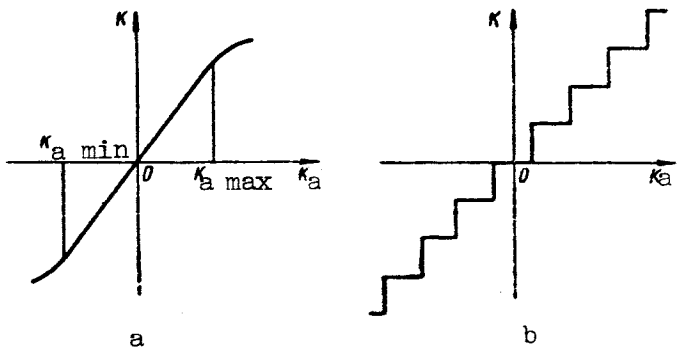

Figure 7.2

The considered functions of the individual components of the CCRL and the character of its output signals show that CCRL differ from one another in types of subcarriers, kinds of modulation in the coder, methods of separation of channels, operating regimes and types of modulation of the transmitter carrier, types of CCRL output signals, types of comparison signals, etc. This means that in practice it is possible to encounter a great variety of types of command radio links.

A command control radio link used for signal transmission for actuating the control surfaces of a rocket is one of the links (radio links) of the control system and is characterized by corresponding equations relating the CCRL input and output signals. In the study of the characteristics of a multichannel CCRL as a link of the control system, it must be remembered that the CCRL is an apparatus with several inputs and outputs. However, the CCRL apparatus used for transmission of several commands usually can be divided into a number (depending on the number of channels) of identical and independently operating parts. Therefore, in all cases when the effect of radio interference is not taken into account, when such interference causes appearance of a reciprocal effect on the channels, one CCRL channel alone need be considered. /289

If inertial properties are not taken into account, the processes occurring in a single-channel CCRL, as in a link of a closed control system, the first step is to determine the amplitude characteristic of the CCRL. When K_a and K represent continuous functions of time, the CCRL amplitude characteristic has the form shown in figure 7.2a. Usually, the curve $K = f(K_a)$ is symmetrical relative to the K and K_a axes.

The value

$$k_{CCRL} = \frac{dK}{dK_a}\Big|K_a = 0 \qquad (7.1.1)$$

is called the transfer constant of the CCRL. This constant can be either dimensionless or dimensional. In most cases, the CCRL is constructed in such

a way that its amplitude characteristic is not only symmetrical, but within certain limits is linear.

If the CCRL is used for transmission of level-quantized commands, the approximate form of its amplitude characteristic can be represented as shown in figure 7.2b. The transfer constant of a CCRL of this type can be determined using formula (7.1.1) if it is assumed that the dependence $K = f(K_a)$ is characterized by a curve passing through the middle of the "steps."

These types of amplitude characteristics can be obtained in CCRL with both direct and variable comparison voltage (current) if K_a assumes positive and negative values.

When $K_a \geq 0$, which usually is the case when using command forming apparatus of the discrete type or when using nondifferential command pickups in nonautomatic control systems, the amplitude characteristics of the CCRL can be represented as shown in figure 7.2a and b, provided K_a is understood to be the value of the signal at the output of the command forming apparatus or the command pickup, decreased by the value $\frac{K_{a\ max}}{2}$, where $K_{a\ max}$ is the maximum value of the transmitted command.

In the planning of CCRL, one of the principal requirements is that there be linearity of its amplitude characteristic for the working range of changes of K_a from $K_{a\ min}$ to $K_{a\ max}$ (fig. 7.2a). This requirement essentially can be reduced to the problem of ensuring the constancy of k_{CCRL} for all values K_a in the range $K_{a\ min} \leq K_a \leq K_{a\ max}$. The need for satisfaction of the condition $k_{CCRL} = \text{const}$ can be attributed to the fact that k_{CCRL} enters as one of the cofactors into the expression determining the general amplification factor of the control system. Considerable changes of k_{CCRL} can be a cause of worsening of the quality and stability of the guidance process, especially if K_a contains components intended for the compensation of dynamic errors in guidance of a rocket to the target. In addition, the nonlinearity of the amplitude characteristic when various fluctuations are present leads to an increase of distortions of transmitted commands. In actual practice, the range of linearity of the dynamic characteristic usually is limited by the technical possibilities of electronic instruments. /290

Taking into account the inertia of a CCRL with a linear amplitude characteristic, the CCRL transfer function can be represented in operator form most frequently as

$$L(D) = \frac{K(t)}{K_a(t)} = \frac{k_{CCRL}}{1 + T_{CCRL}D}, \qquad (7.1.2)$$

where T_{CCRL} is the time constant of the CCRL (output filters of the decoder).

In comparative evaluations of different types of CCRL, it is convenient to deal not with the commands K, but with the dimensionless coefficient K_c, determined by the relation

$$K_c = \frac{K}{K_{max}}, \qquad (7.1.3)$$

where K is the current value of the CCRL output command, and K_{max} is the maximum value K.

The value K_c usually is called the command coefficient or the relative command. In CCRL with a symmetrical amplitude characteristic, the coefficient K_c varies in the range ±1. If the CCRL has an amplitude characteristic which is asymmetrical relative to the K-axis, the negative value K_c can be both greater than and less than unity.

Expression (7.1.3) shows that the value of the output command is

$$K = K_{max}K_c.$$

The command coefficient can be found not only for the CCRL output signal, but also for signals forming at different points in the coder and decoder, including the CCRL input.

In addition to the mentioned requirements on the high stability of transmission of a zero command and the constancy of k_{CCRL}, it is necessary that the errors in transmission of commands (recalculated to rocket miss) be at least an order of magnitude less than the total mean square error of guidance and that the CCRL have high noise immunity and reliability.

We note in conclusion that the functions performed by the CCRL coders and decoders, and also by the instruments for conversion of analog values into a number and vice versa coincide to a considerable degree. Therefore, all the material which follows will be based on extensive data on problems involved in the design of CCRL, multichannel radio communication systems and instruments for conversion of certain values into others (refs. 2, 4, 14, 16, 20, 63, 109, 110 and others). /291

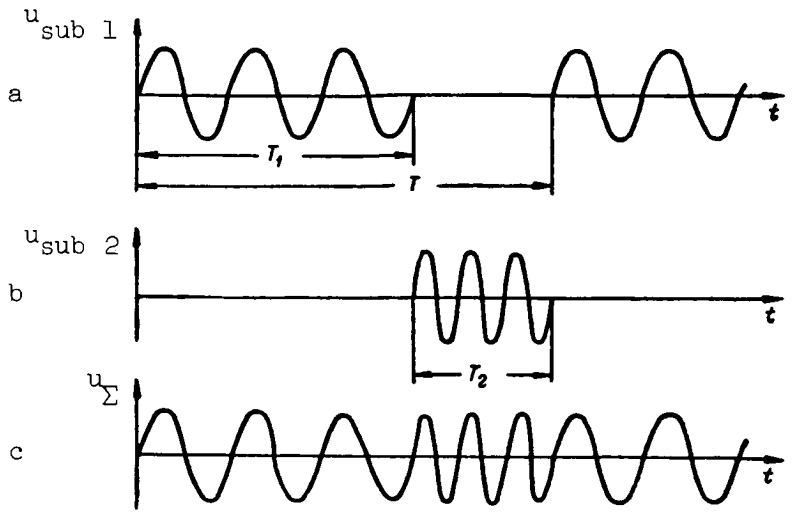

Figure 7.3

7.2. CCRL Coders and Decoders with Pulse-Width Modulation of Sinusoidal Subcarrier Oscillations

In a single-channel CCRL with sinusoidal subcarriers and variable comparison voltage, the durations T_1 and T_2 of effect of the subcarriers $u_{sub\ 1}$ and $u_{sub\ 2}$ (fig. 7.3a, b), transmitted periodically, vary in dependence on the value of the transmitted command. With an increase of K_a, the value T_1 increases and T_2 decreases, but in such a way that the sum $T_1 + T_2$ remains constant and equal to the repetition interval T of the voltages $u_{sub\ 1}$ and $u_{sub\ 2}$. In order for the subcarriers to be separated at the receiving end, they should have the different frequencies $f_{sub\ 1}$ and $f_{sub\ 2}$.

The value of the command K_c at the output of the coder in such CCRL is determined by the difference of T_1 and T_2, that is

$$K_c = T_1 - T_2.$$

The value K_c coincides with the value of the command produced by the command commutator pickups or is related by the following relation to K_a if the command forming apparatus produces K_a in the form of a dc voltage

$$K_C = T_1 - T_2 = k_C K_a. \qquad (7.2.1)$$

Here k_C is the transfer constant of the coder, characterizing the value K_C for a unit value K_a.

The coder should be constructed in such a way that when $K_a = 0$, the condition $T_1 = T_2$ is satisfied. Since the maximum value of the command at /292 the coder output can be equal to T, for the coder command coefficient K_{Cc}, we find

$$K_{Cc} = \frac{T_1 - T_2}{T}. \qquad (7.2.2)$$

As a result of summation of the subcarriers $u_{sub\ 1}$ and $u_{sub\ 2}$, modulated by commands, we obtain the total signal u_Σ (fig. 7.3c), which is fed to the CCRL radio transmitter for modulation of the carrier.

The discussed method for modulation of subcarriers sometimes is called the time method for formation of the quantitative values of commands with an active pause or the time relations method.

Command radio links with a passive pause also are possible. They are /293 characterized by the fact that the value and sign of the control command are transmitted by only one subcarrier oscillation. However, the use of CCRL with a passive pause, despite its relative simplicity, is less desirable. This can be attributed to the fact, in particular, that they afford more favorable conditions for disruption by interference in those intervals of time when useful signals are not present.

If the CCRL with an active pause should be an N_k-channel apparatus, the coder should contain $2N_k$ individual generators of subcarrier oscillations, each pair of which is used for formation of the command for a single control channel, or N_k generators, the frequency of each of which can be manipulated.

The form of the functional and circuit diagrams of coders of CCRL with pulse-width modulation of sinusoidal subcarrier oscillations is determined to a considerable degree by the type of the initial signals of the command forming apparatus. However, in any case, the coder should include generators of sinusoidal subcarriers and modulators ensuring the formation of groups of sinusoidal oscillations of the corresponding durations and also a summer.

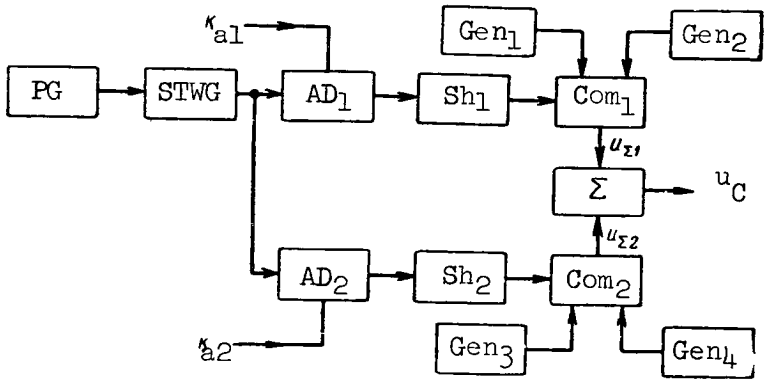

a

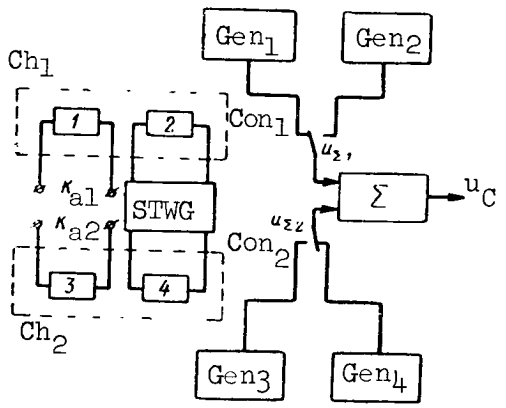

b

Figure 7.4

If the output signals of the command forming apparatus are dc voltages, the functional diagrams of the coders can be represented as shown in figures 7.4a and b, depending on whether only electronic devices are used or both electronic and electromechanical apparatus are employed. These figures show diagrams of coders for a two-channel CCRL. Coders for CCRL with $N_k > 2$ can be designed in a similar way.

The input signals K_{a1} and K_{a2} of the first and second control channels in the coder, whose functional diagram is shown in figure 7.4a, are fed to the amplitude discriminators AD_1 and AD_2. These same components are fed a /294 sawtooth voltage u_{saw} (fig. 7.5b) from the constant-potential generator CPG. The CPG is synchronized by u_{PG} pulses (fig. 7.5a) from the pulse generator PG. In the range $0 \leq t \leq T_1$ (fig. 7.5b), when $K_{a1} > u_{saw}$, the tube of the amplitude discriminator AD_1 is blocked out. At the time $t = T_1$, the tube AD_1 is

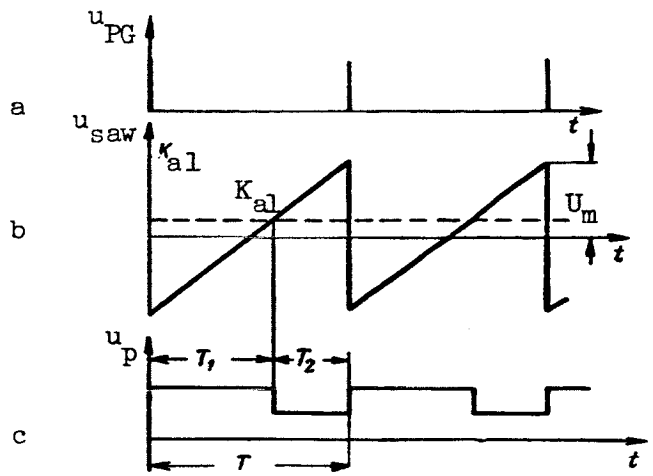

Figure 7.5

unblocked, and as a result a negative voltage jump is formed on its load resistance. The amplitude discriminator AD_1 remains operative to the time t = T, when the condition $K_a > u_{saw}$ again begins to be satisfied. It is easy to see that the time during which AD_1 remains unblocked and blocked out within the limits of the period T is dependent on K_{al}. The amplitude discriminators, pulse generator and saw-toothed wave generator are used for conversion of voltages into time intervals.

By means of the shaper Sh_1, the AD_1 output signals are converted into square pulses (fig. 7.5c). The duration of the pulses corresponding to the condition $K_{al} > u_{saw}$ is equal to

$$T_1 = \frac{T}{2}\left(1 + \frac{K_{al}}{U_m}\right),$$

where U_m is the amplitude of the voltage u_{saw}.

This expression shows that T_1 is determined by the value of the command K_{al}.

The signals u_p (fig. 7.5c) cause operation of the commutator Com_1, ensuring the passage of the subcarrier oscillations of the generators Gen_1 and Gen_2 to the summer Σ. Since

$$T_2 = T - T_1 = \frac{T}{2}\left(1 - \frac{K_{al}}{U_m}\right),$$

the command K_{C1} and the command coefficient K_{Cc1} for the first channel at the coder output are equal to

$$K_{C1} = T_1 - T_2 = \frac{T}{U_m} K_{a1} = k_{C1} K_{a1}, \tag{7.2.3}$$

$$K_{Cc1} = \frac{T_1 - T_2}{T} = \frac{1}{U_m} K_{a1} = \frac{k_{C1}}{T} K_{a1}, \tag{7.2.4}$$

where k_{C1} is the transfer constant of the K_{a1} command coder.

Figure 7.5 and expression (7.2.3) show that the value K_{a1} can assume any values in the range from $-U_m$ to $+U_m$. This makes it possible to obtain a command coefficient K_{Cc1} which varies in the closed interval ± 1.

Since the input command coefficient K_{ic1} is

$$K_{ic1} = \frac{K_{a1}}{K_{a1\ max}},$$

where $K_{a1\ max}$ is the maximum value of the transmitted command K_{a1}, on the /295 basis of expression (7.2.4), we obtain the following formula determining the relationship between K_{Cc1} and K_{ic1}

$$K_{Cc1} = k_{C1} \frac{K_{a1\ max}}{T} K_{ic1}.$$

The value $\frac{k_{C1} K_{a1\ max}}{T} K_{ic1}$, which can be equal to or less than unity, characterizes the transfer constant of the command coefficient K_{ic1} of the coder.

In addition to the saw-toothed wave generator and the amplitude discriminators, it is possible to use delay multivibrators and phantastrons in the coders. However, their use is undesirable because, in actual practice, it is not possible to obtain the values $|K_{Cc}| \geq 0.6\text{-}0.7$.

Formation of the voltage $u_{\Sigma 2}$, representing groups of sinusoidal oscillations with the durations T_3 and T_4, determined by the command K_{a2}, is

accomplished as in the first control channel. For this purpose, it is possible to use the pulse generator PG, the saw-toothed wave generator STWG, the amplitude discriminator AD_2, a pulse shaper Sh_2, a commutator Com_2 and the generators Gen_3 and Gen_4 (fig. 7.4a).

The expressions for the command K_{C2} and the command coefficient K_{Cc2} formed in the second channel are determined by relations (7.2.3) and (7.2.4), if K_{C1} and K_{Cc1} in them are replaced by K_{C2} and K_{Cc2}, and K_{a1} by K_{a2}.

The coder output signal is the voltage u_C forming at the output of the summer Σ.

Figure 7.4a shows that the coder includes elements common for all channels (pulse generator, saw-toothed wave generator and summer) and also elements for only one (specific) channel. Elements of the first type form a synchronizer and control apparatus, and elements of the second type form modulators in which width-modulated video pulses are produced under the influence of the arriving commands. It should be noted that such a makeup of coders is characteristic of most CCRL.

In the coder whose functional diagram is shown in figure 7.4b, the formation of the voltage $u_{\Sigma 1}$ occurs in the following way. The command voltage K_{a1} (fig. 7.6a) and the sawtooth voltage u_{saw} (fig. 7.6b) of the saw-toothed wave generator STWG are fed to windings 1 and 2, respectively, of the polarized relay Rel_1. At the times when the signal $u_{rel} = u_{saw} + K_{a1}$ (fig. 7.6c) assumes approximately zero values and the contact Con_1 of the relay Rel_1 is triggered, as a result in the time T_1 a voltage of the frequency $f_{sub\ 1}$ is formed at the output of the summer Σ. If the amplitude and period of the sawtooth are equal to U_m and T, respectively, it is easy to see from figure 7.6c that /296

$$T_1 = \frac{T}{2} + 2\Delta t.$$

Since the triangles ABC and DEC are similar (fig. 7.6c), then

$$\Delta t = \frac{T}{4U_m} K_{a1}.$$

Therefore

$$T_1 = \frac{T}{2}\left(1 + \frac{1}{U_m} K_{a1}\right). \qquad (7.2.5)$$

But since

$$T_2 = T - T_1,$$

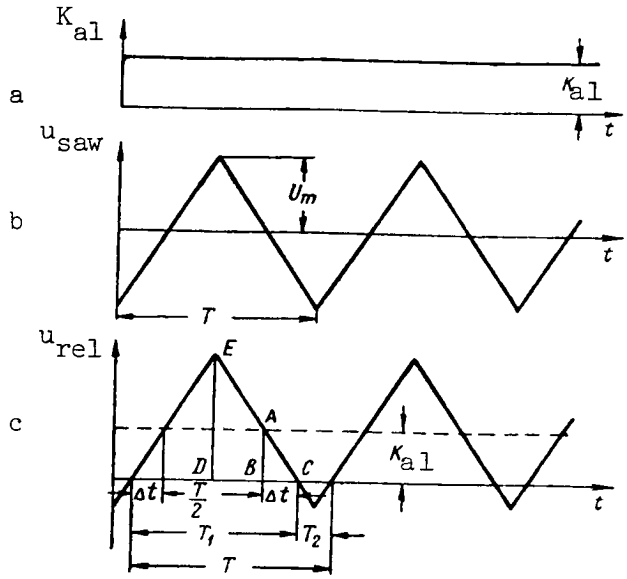

Figure 7.6

then

$$T_2 = \frac{T}{2}\left(1 - \frac{1}{U_m} K_{al}\right). \qquad (7.2.6)$$

On the basis of expressions (7.2.5) and (7.2.6), it can be found that the values of the command K_{Cl} and the command coefficient K_{Ccl} for the first channel at the output of the coder will be determined by formulas (7.2.3) and (7.2.4). This means that despite the difference in different possible circuits, from the point of view of the transfer constants, both considered types of coders are identical. The voltage $u_{\Sigma 2}$, characterizing the command K_{a2}, is formed precisely the same way as the signal $u_{\Sigma 1}$.

In order for the condition $T_1 = T_2 = \frac{T}{2}$ to be satisfied when $K_{al} = 0$, the CCRL coder should be balanced. This means that it is necessary to ensure the selection of a corresponding AD_1 (fig. 7.4a) and also obtain a symmetrical voltage of the "sawtooth" and setting of virtually zero response thresholds of the relays Rel_1 in the coder whose circuit is shown in figure 7.4b. In those cases when the CCRL input signals are the duration of closing or the interval between brief closings of the contacts within the limits of the period T, the functional diagrams of the coders assume the form shown in figure 7.7a, b. /297

In the coder whose functional diagram is shown in figure 7.7a, the input command K_{al} of the first channel constitutes the difference $T_1 - T_2$ of the

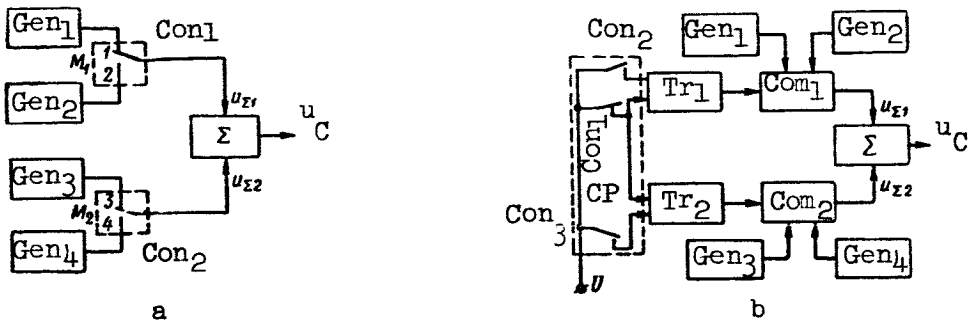

Figure 7.7

durations of closing of the moving contact Con_1 with bars 1 and 2; here $T_1 + T_2 = T$ in the period T of oscillations of contact Con_1, which together with the bars 1 and 2 forms the modulator of the first channel. In the periods T_1 and T_2, subcarrier oscillations from the generators Gen_1 and Gen_2 having the frequencies $f_{sub\ 1}$ and $f_{sub\ 2}$ are fed alternately to the summer Σ. The voltage $u_{\Sigma 1}$ forming at the output of the modulator of the first channel characterizes the output command of the coder K_{C1} for the first channel.

It follows from the principle of operation of the coder that

$$K_{C1} = K_{a1} = T_1 - T_2.$$

This shows that the transfer constant of the coder is equal to unity.

The voltage $u_{\Sigma 2}$, characterizing the command of the second channel, is formed by the modulator M_2 and the generators Gen_3 and Gen_4 which produce sinusoidal subcarrier oscillations with the frequencies $f_{sub\ 3}$ and $f_{sub\ 4}$.

If the output signals of the command pickup CP (fig. 7.7b) for the first channel are periodic closings of the contacts Con_1 and Con_2 at the interval T_1 within the limits of the period T, the trigger Tr_1 and the commutator Com_1 are used for modulation of the Gen_1 and Gen_2 subcarrier oscillations.

The command of the second channel is given by the intervals of time between the times of closing of the contacts Con_1 and Con_3 and its conversion /298

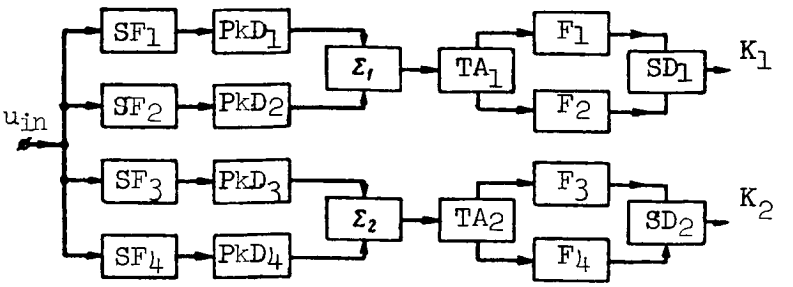

Figure 7.8

to subcarrier oscillations is accomplished by the trigger Tr_2, the commutator Com_2 and the generators Gen_3 and Gen_4.

A coder of the latter type, as well as the coder whose diagram is shown in figure 7.7a, is characterized by transfer constants equal to unity for both channels.

In all four considered types of coders, it is assumed that there are two independent subcarrier generators for each channel. In such a method of design of coders, at the time of switching of frequencies, there is a disruption of the phase continuity of the subcarrier oscillations. This undesirable phenomenon can be eliminated by replacing the two generators with a single generator with commutatable parameters of the oscillatory circuit. In this case, it can be assumed that, in each coder channel, there will be frequency modulation of a sinusoidal voltage by square pulses, which in turn are modulated by the duration of the transmitted command.

It follows from an analysis of the illustrated coder designs that they are virtually inertialess links. A similar conclusion can be drawn with respect to other types of CCRL coders.

When developing models of CCRL decoders with pulse-width modulation of sinusoidal subcarrier oscillations, it is necessary to take into account the problems solved by such apparatus. A possible variant of the functional diagram of the decoder of a two-channel CCRL is shown in figure 7.8.

The voltage u_{in} fed from the CCRL radio receiver, for each moment of time representing the sum of the subcarriers of the first and second channels, is fed to the separation filters SF_1, SF_2, SF_3 and SF_4. These filters transmit subcarriers only with frequencies equal to $f_{sub\ 1}$, $f_{sub\ 2}$, $f_{sub\ 3}$ and $f_{sub\ 4}$, respectively. At the outputs of the separation filters SF_1 and SF_2, groups of sinusoidal oscillations $u'_{sub\ 1}$ and $u'_{sub\ 2}$ are formed (fig. 7.9a, b) with the

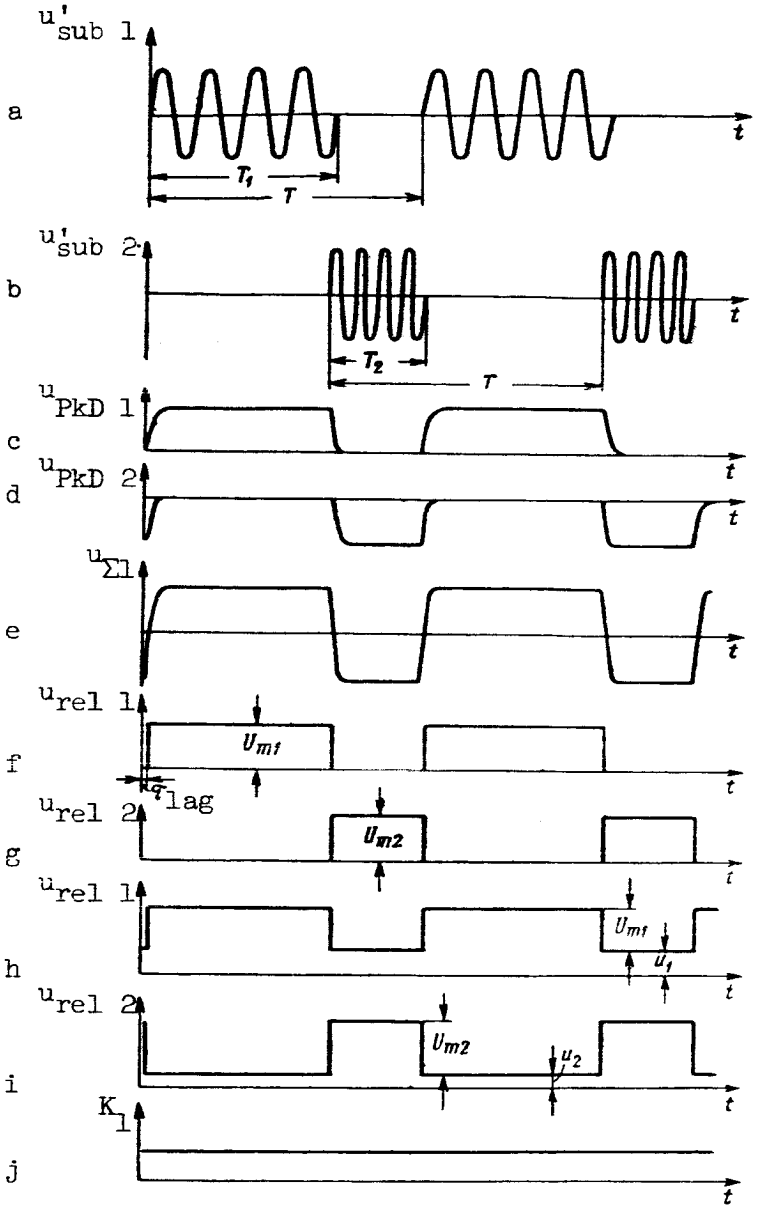

Figure 7.9

durations $T'_{1.1}$ and $T'_{2.1}$, differing from T_1 and T_2 due to transient processes in the CCRL receiver. However, with a sufficiently high degree of accuracy it can be assumed that $T'_{1.1} = T_1$ and $T'_{2.1} = T_2$. /299

By means of the peak detectors PkD_1 and PkD_2, the dc pulses $u_{PkD\ 1}$ and $u_{PkD\ 2}$ (fig. 7.9c, d) are formed from the groups $u'_{sub\ 1}$ and $u'_{sub\ 2}$. The pulses

$u_{PkD\ 1}$ and $u_{PkD\ 2}$ are fed to the summer Σ_1, where the voltage $u_{\Sigma 1}$ is formed (fig. 7.9e).

Under the influence of this voltage, the threshold apparatus TA_1 is "thrown" (see fig. 7.8); a trigger or an electromagnetic relay can serve as the TA.

It is desirable to use a TA because it is necessary to convert the $u_{\Sigma 1}$ into square pulses with a constant amplitude. Since the value of the command is reflected only by the segments T_1 and T_2, the amplitude of the output pulses of the decoder should be constant. However, it can change, for example, due to the effect of noise.

If an electromagnetic relay is used as the TA_1, by means of its moving contact the low-frequency filters F_1 and F_2 are connected to the positive pole of the dc voltage source. This means that F_1 and F_2 are fed the pulses $u_{rel\ 1}$ and $u_{rel\ 2}$, shown in figure 7.9f, g. The times of appearance of these pulses relative to the time of feeding of the signals $u'_{sub\ 1}$ and $u'_{sub\ 2}$ will be shifted by the value τ_{lag}, which indicates that the considered CCRL will transmit commands with a delay. The durations of the pulses $u_{rel\ 1}$ and $u_{rel\ 2}$ are equal to $T_{1.1} \approx T_1$ and $T_{2.1} \approx T_2$, respectively, and their amplitudes are U_{m1} and U_{m2}; in a general case, $U_{m1} \neq U_{m2}$. The same picture is obtained when using a trigger with "grounded" anodes (cathode load).

When a trigger with an anode load is used as the TA, in a general case, the voltages $u_{rel\ 1}$ and $u_{rel\ 2}$, shown in figure 7.9h, i, will be fed from the anodes of its tubes. The beginning of the times of "throwing" of the trigger also is displaced by some value τ_{lag} and the durations of the positive drops are $T_{1.1} \approx T_1$ and $T_{2.1} \approx T_2$.

The minimum and maximum voltages u_1, u_2 and $u_1 + U_{m1}$, $u_2 + U_{m2}$, where U_{m1} and U_{m2} are the amplitudes of the positive voltage drops of the left and right tubes of the trigger, can be different. This depends on whether the

trigger is rigorously symmetrical or not. In addition, the values of these voltages are influenced by the response thresholds of the trigger tubes.

The voltages produced by the trigger act on the filters F_1 and F_2. Since the signals formed by an electromagnetic relay or a trigger with "grounded" anodes are a special case of triggering pulses with an anode load, it will /301 be assumed henceforth that the threshold apparatus TA_1 always produces the voltages $u_{rel\ 1}$ and $u_{rel\ 2}$ shown in figure 7.9h, i.

The low-frequency filters F_1 and F_2 in essence are demodulators of the TA_1 width-modulated video pulses. These devices separate out the mean components u_{F1} and u_{F2} of the voltages $u_{rel\ 1}$ and $u_{rel\ 2}$.

The difference $u_{F1} - u_{F2}$, forming by means of the subtracting device SD_1, whose transfer constant will be assumed equal to 1, constitutes the control command K_1 for the first channel (fig. 7.9j). Thus,

$$K_1 = u_{F1} - u_{F2}.$$

However, in a steady-state regime, during transmission of the command represented by the time segments T_1 and T_2,

$$u_{F1} = k_{F1}u_1 + k_{F1}U_{m1}\frac{T_1}{T} \tag{7.2.7}$$

and

$$u_{F2} = k_{F2}u_2 + k_{F2}U_{m2}\frac{T_2}{T}, \tag{7.2.8}$$

where k_{F1} and k_{F2} are the transfer constants of the filters F_1 and F_2. Then, taking into account expressions (7.2.5), (7.2.6) and (7.2.3), we obtain the following equation for the CCRL decoder of the considered type (for the first channel)

$$\begin{aligned} K_1 = k_{F1}\left(u_1 + \frac{1}{2}U_{m1}\right) - k_{F2}\left(u_2 + \frac{1}{2}U_{m2}\right) \\ + \frac{k_{F1}U_{m1} + k_{F2}U_{m2}}{2}\frac{K_{C1}}{T} = k_{F1}\left(u_1 + \frac{1}{2}U_{m1}\right) - \\ - k_{F2}\left(u_2 + \frac{1}{2}U_{m2}\right) + k_{D1}K_{C1}. \end{aligned} \tag{7.2.9}$$

Here

$$k_{D1} = \frac{k_{F1}U_{m1} + k_{F2}U_{m2}}{2T} \qquad (7.2.10)$$

is the transfer constant of the CCRL decoder for the first channel and $\frac{K_{C1}}{T}$ characterizes the command coefficient at the coder output.

It can be seen from expression (7.2.9) that when $K_{C1} = 0$, the value of the CCRL output signal when $k_{F1}(u_1 + 0.5\ U_{m1}) \neq k_{F2}(u_2 + 0.5\ U_{m2})$ will differ from zero. This means there is a systematic error present. In order to eliminate this error, it is necessary that one of the CCRL output stages has a control device by means of which it is possible to balance the CCRL decoder.

The essence of balancing of the decoder (under the condition that the coder is balanced) is the setting of a zero voltage at the output of the CCRL when transmitting commands $K_{C1} = 0$. /302

If the CCRL is balanced, the following condition is satisfied

$$k_{F2}U_{m2} = 2(k_{F1}u_1 - k_{F2}u_2) + k_{F1}U_{m1}$$

and

$$K_1 = (k_{F1}U_{m1} + k_{F1}u_1 - k_{F2}u_2)\frac{K_{C1}}{T} = k_{D1}K_{C1}, \qquad (7.2.11)$$

where

$$k_{D1} = \frac{1}{T}(k_{F1}U_{m1} + k_{F1}u_1 - k_{F2}u_2). \qquad (7.2.12)$$

Expression (7.2.12) shows that the transfer constant of a balanced decoder is dependent on k_{F1}, k_{F2}, U_{m1}, u_1, u_2 and T. In order for k_{D1} to be maximal, it is necessary to increase the maximum voltage $u_1 + U_{m1}$ fed from the TA and decrease the value u_2.

If the TA is symmetrical, which as will be assumed henceforth corresponds to satisfaction of the condition $u_1 = u_2$ and $U_{m1} = U_{m2} = U_m$, the filters F_1 and F_2 should have identical transfer constants k_{F1} and k_{F2}, equal to k_F. In such CCRL

$$k_{D1} = \frac{1}{T}k_F U_m.$$

The maximum possible value $K_{1\ max}$ of the CCRL output signal will be obtained when $u_{rel\ 1}(t) = u_1 + U_{m1}$ and $u_{rel\ 2}(t) = u_2$; it is

$$K_{1\ max} = k_{F1}U_{m1} + k_{F1}u_1 - k_{F2}u_2.$$

Therefore, on the basis of expression (7.2.11), it can be concluded that the command coefficients K_{c1} and K_{Cc1} at the output of the CCRL coder and decoder are identical and equal to

$$K_{c1} = K_{Cc1} = \frac{T_1 - T_2}{T}.$$

As mentioned, the value K_{Cc1}, and therefore K_{c1}, can vary in the range ±1. However, in actual practice, CCRL are designed in such a way that the values K_{c1} and K_{Cc1} do not exceed ±(0.8-0.9). This can be attributed to the fact that with an increase of K_{c1} there is a decrease of the minimum duration T_{min} of effect of the subcarriers; as a result, there should be an increase of the transmission band of the separation filters and other stages of the CCRL receiver. T_{min} decreases particularly rapidly when $|K_{c1}| > 0.8$. In actuality, when $|K_{c1}| = 0.8$, the value $T_{min} = 0.1\ T$, but when $|K_{c1}| = 0.9$, this value becomes equal to 0.05 T. It follows therefore that with an increase of K_{c1} by only 10 percent, it is necessary to double the width of the passband of a number of decoder stages.

The transfer function of the decoder for the first channel, characterizing the ratio $\frac{K_1(t)}{K_{C1}(t)}$, is determined by the parameters of the filters F_1 /303 and F_2, since all the other decoder stages are virtually inertialess.

Since the radio transmitter and the radio receiver do not change the values of the transmitted command, the transfer constant $k_{CCRL\ 1}$ of the command control radio link for one (the first) channel on the whole is equal to the product of the transfer constants of the coder and decoder, that is

$$k_{CCRL\ 1} = k_{C1}k_{D1}.$$

For example, if the CCRL employs a coder whose functional diagram is shown in figure 7.4a or b, when $k_{F1} = k_{F2}$, $U_{m1} = U_{m2}$ and $u_1 = u_2$

$$k_{CCRL\ 1} = k_{F1}\frac{U_{m1}}{U_m}, \tag{7.2.13}$$

since formula (7.2.3) shows that

$$k_{C1} = \frac{T}{U_m}. \tag{7.2.14}$$

When the CCRL includes a coder constructed as shown in figure 7.7a,

$$k_{CCRL\ 1} = k_{D1}. \tag{7.2.14a}$$

The CCRL transfer function (for the first channel) with identical filters F_1 and F_2 is defined by the following expression

$$L(D) = \frac{K_1(t)}{K_{a1}(t)} = k_{CCRL\ 1}W_{F1}(D), \tag{7.2.15}$$

where $W_{F1}(D)$ is the transfer function of the filter F_1, normalized relative to k_{F1}.

Expression (7.2.15) represents the general form of the CCRL equation.

If the specific form of the equation (7.2.15) is known, it is relatively easy to compute the dynamic and fluctuation errors in transmission of commands for given characteristics of distortions of the input command K_a.

The forming of the command K_2 (fig. 7.8) in the second channel of the decoder is brought about using the separation filters SF_3 and SF_4, peak detectors PkD_3 and PkD_4, summer Σ_2, threshold apparatus TA_2, filters F_3, F_4 and the subtracting device SD_2, exactly as with the signal K_1.

As already mentioned, the CCRL usually is assumed to be an inertialess link, since the delays arising in it are negligibly small.

The output signals of the decoder whose functional diagram is shown in figure 7.8, without any additional conversions, can be used for activating smoothly moving control surfaces.

If CCRL commands are required to activate the spoilers or the oscil- /304
lating control surfaces of the rocket, the low-frequency filters and the subtracting devices are excluded from the decoder, and the value of the command K_1 in the first channel will represent the difference of the time intervals $T_{1.1}$ and $T_{2.1}$ of presence of the TA in different possible states, that is

$$K_1 = T_{1.1} - T_{2.1} \approx T_1 - T_2. \qquad (7.2.16)$$

In this case, the decoder constitutes an inertialess link with the transfer constant $k_{D1} = 1$. The command radio link, producing a command whose value and sign are determined by expression (7.2.16), depending on whether the coder is designed as shown in figure 7.4 or figure 7.7, has a transfer constant for the first channel

$$k_{CCRL\ 1} = k_{C1} = \frac{T}{U_m}$$

or

$$k_{CCRL\ 1} = 1.$$

The transfer function of such a CCRL is equal to $L(D) = k_{CCRL\ 1}$, since its coder and decoder in essence do not contain inertial apparatus.

7.3. CCRL Coders and Decoders with Pulse-Width Modulation of Pulse Subcarrier Oscillations

The intervals T_1 and T_2, discussed in the preceding section, can be reflected not only by sinusoidal oscillations, but as was demonstrated in chapter 5 also using a definite number of periodically repeated video pulses. A CCRL, therefore, can be constructed in such a way that a command of the first channel K_{a1} will be reflected by the signals u_{C1} (groups of pulses) shown in figure 7.10a.

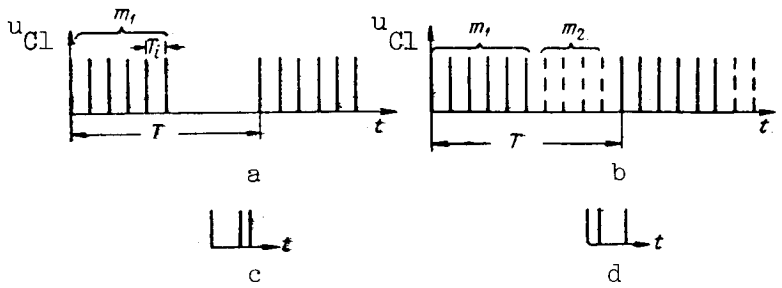

Figure 7.10

With a change of the transmitted command K_{al}, there will be an increase or decrease of the number m_1 of video pulses u_{Cl}, which in essence is equivalent to occurrence of pulse-counting modulation in the CCRL coder. /305

If the video pulses at the coder output reflect only the interval T_1 and the time segment T_2 is determined as the difference $T - T_1$, where T is the command repetition period, a CCRL is obtained with pulse-counting modulation and a passive pause. It also can be assumed that in such a CCRL there will be pulse-width modulation of the pulse subcarrier oscillations.

It is easy to see that the signals shown in figure 7.10a are obtained on the basis of figure 7.3a, if there are video pulses at the point of the zeroes of the sinusoid $u_{sub\ 1}$ with its transition, for example, from negative to positive values.

When the intervals T_1 and T_2 are reflected by video pulses, a CCRL is formed which has pulse-counting modulation and an active pause.

The use of pulse subcarrier oscillations instead of sinusoidal voltages for reflection of the intervals T_1 and T_2, the sum of which is T, in essence leads to conversion of transmitted signals of the analog type (voltage, current, etc.) into a number of pulses, that is, into a digit-pulse code.

In CCRL coders with pulse subcarriers employing the active pause principle, which as in CCRL with sinusoidal subcarriers is the most desirable, the value of the input command K_{al} in the first CCRL channel eventually is converted into the difference of the numbers m_1 and m_2 of the video pulses, separated from one another by the time T_i, and as a sum of the components $m = \frac{T}{T_i}$ of pulses.

It follows from the above that the signal u_{Cl}, characterizing K_{al} at the output of the coder in a CCRL with an active pause should have the form shown in figure 7.10b, and the value of the command K_{Cl} is determined by the following expression

$$K_{Cl} = m_1 - m_2 = k_{Cl}K_{al}. \qquad (7.3.1)$$

Since $K_{Cl\ max} = m$, for the command coefficient at the output of the coder for the first channel, we obtain

$$K_{Ccl} = \frac{m_1 - m_2}{m} = \frac{k_{Cl}}{m} K_{al\ max}K_{icl}, \qquad (7.3.2)$$

where

$$m = m_1 + m_2.$$

In order to be able to determine the numbers m_1 and m_2 at the receiving end, the pulse subcarriers acting on the intervals T_1 and T_2 in some way should differ from one another. In figure 7.10b, this circumstance can be noted from the fact that the signals of the first and second subcarriers are denoted by solid and dashed lines, respectively.

A difference between the two sequences of pulse subcarriers can be en- /306
sured by applying the principles of frequency, time and code selection of signals. Pulse selection on the basis of duration, shape and other criteria also is possible.

The principle of code selection applied to the considered case has as its basis the fact that each subcarrier oscillation represents code groups of pulses with a preset interval between them, rather than individual pulses. Such pulse groups are called timing codes. As an example, figure 7.10c, d shows three-pulse (three-unit) timing codes, also called symbols of the first and second kinds.

When the principle of time selection is applied both subcarrier oscillations represent individual pulses with identical parameters. Special synchronizing signals should be transmitted before each pulse or group of pulses of the subcarriers for separation of such signals. This appreciably complicates the CCRL, especially in the case of a large number of transmitted commands, and therefore the time selection method will not be considered further here.

Frequency selection requires groups of sinusoidal oscillations with different frequencies.

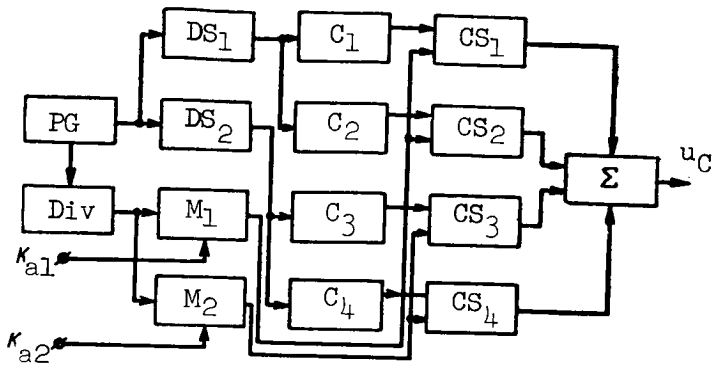

Figure 7.11

If the CCRL must ensure the transmission of N_k commands, it is necessary to have $2N_k$ pulse subcarriers; in this case, each code group of all the channels, when using the principle of code selection, on whose basis all subsequent considerations will be made, must be situated in a definite place within the limits of the interval T_i. Usually, the total number of code groups forming in all channels in the time T must be assumed identical and equal to m.

The functional and block diagrams of a coder can be developed in accordance with the essence of the considered method for transmission of commands. As an example, figure 7.11 shows a diagram of one of the possible variants /307 of a two-channel CCRL with pulse subcarriers which are separated at the receiving end in accordance with the principle of code selection, on the condition that the input commands K_{a1} and K_{a2} are dc voltages.

Synchronization of the operation of all the stages of the coder is accomplished using the pulse generator PG, producing the voltage u_{PG} (fig. 7.12a). This voltage is fed through the delay stages DS_1 and DS_2 to the coders C_1, C_2, C_3 and C_4, whose number is determined by the number of subcarriers, and a pulse frequency divider Div. The divider Div is used to form the pulses u_{div} (fig. 7.12b), the time distance T between which is equal to the repetition rate of the commands. These pulses are triggering pulses for the stages M_1 and M_2, in which there is pulse-width modulation of the video impulses by the commands K_{a1} and K_{a2}. As the modulators M_1 and M_2 which convert voltages into time intervals, it is possible to use the same devices as in a CCRL with sinusoidal subcarriers. The modulator M_1 produces the pulses u_{M1} and u_{M2} (fig. 7.12c, d) with the durations T_1 and T_2 determined by the command K_{a1}, but the duration

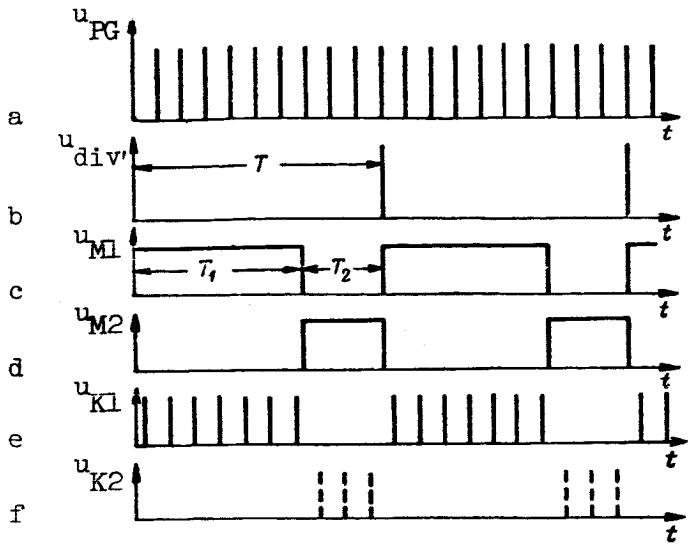

Figure 7.12

of the pulses produced in the modulator M_2 is dependent on the value K_{a2}. The signals u_{M1} and u_{M2} are fed to the coincidence stages CS_1 and CS_2, and the pulses from M_2 are fed to CS_3 and CS_4. In addition, CS_1, CS_2, CS_3 and CS_4 are fed code groups of pulses from the coders C_1, C_2, C_3 and C_4, characterizing the first and second subcarriers of both CCRL channels.

The coincidence stages transmit to the summer Σ the timing codes only /308 during those intervals of time when positive voltages are fed to them from M_1 and M_2.

The output voltage u_C of the coder represents the sum of the signals produced in CS_1, CS_2, CS_3 and CS_4.

CCRL coders with pulse-counting modulation in essence have no inertial elements, and as links of control systems are characterized by transfer constants for the different channels dependent on the form of the transmitted commands.

For example, the transfer constant k_{C1} for the first channel, in a case when the command K_{a1} represents a dc voltage, can be found from expression (7.2.14) when T is replaced by m. Then, when a saw-toothed wave generator and comparison circuits are used as a modulator (fig. 7.4a) we find that

$$K_{Cl} = m_1 - m_2 = \frac{m}{U_{ml}} K_{al}.$$

When K_{al} is given by the difference of the intervals T_1 and T_2, the value $k_{Cl} = \frac{1}{T_i}$, since $m_1 = \frac{T_1}{T_i}$ and $m_2 = \frac{T_2}{T_i}$.

However, it should be noted that all the relations cited in this section for relating the output and input signals in the coder and decoder to one another are correct only for definite discrete values of transmitted commands. This can be attributed to the fact that all possible values of the function $K_a(t)$ cannot be reflected by the finite quantity of numbers formed by the used set of symbols.

On the basis of the above, it can be concluded that the amplitude characteristics of a CCRL with pulse-counting modulation have the form of a stepped curve and that in the transmission process, errors appear which are due to level-quantization of the transmitted commands.

In order to obtain the amplitude characteristic of the first channel of a CCRL corresponding to figure 7.2b, it is necessary that the clipping and the edge of the u_{M1} and u_{M2} pulses (fig. 7.12) develop at the time $\frac{T_i}{2}$ after the last pulse in a symbol of the first kind, under the condition that $m_1 = m_2 = 0.5$ m. Then, taking into account that when $K_{al} = 0$ the intervals T_1 and T_2 are equal, it is required that the CS_1 displace the u_{PG} pulses (fig. 7.12a) by $\tau_{shift} \approx 0.5\, T_i$. As a result, at the outputs of the coincidence stages CS_1 and CS_2, code groups of pulses are formed which have been shown conventionally in figure 7.12e, f.

When $\tau_{shift} = 0.5\, T_i$, the precise proportional dependence between K_{Cl} and K_{al} in expression (7.3.1), and also in the formulas determining the CCRL output signal, will be observed only for $T_1 = m_1 T_i$, although equations (7.3.1) and (7.3.2) remain correct with a change of K_{al} within the limits of the quan- /309 tization interval determined by the interval $T_1 = T_2 = 2T_i$.

In actual practice, the shift τ_{shift} can be selected considerably smaller than $\frac{T_i}{2}$, since the segments between the times of appearance of the edges of the

time-coinciding u_{M1} pulses and the first pulses in the code groups fed from C_1 are not used. However, in the case of transmission of the command K_{a1}, the interval T_2 should be greater than T_1 by a value corresponding to the decrease τ_{shift}. Similar reasoning can be applied also to the second CCRL channel in which the necessary spacing of the timing codes is accomplished using the delay stages DS_2.

Since the amplitude characteristic for any CCRL channel with pulse-counting modulation has a stepped form, when applying the transfer constant of the coder for the considered channel, it is necessary to employ its mean value (section 7.1).

The functional and block diagrams of a CCRL coder with pulse-counting modulation and its principal properties are determined to a considerable degree by the method for analysis of the subcarrier oscillations and the required form of the signals at the CCRL output. Figure 7.13a, b, c, d shows four possible functional diagrams of coders of two-channel CCRL of the considered type.

All these coders are designed for forming commands in the form of dc voltages. However, by removing the filters F_1F_2 and F_3F_4 in the diagrams shown in figure 7.13c and d and by installing a threshold apparatus after SD_1 and SD_2, and also with introduction into the diagrams shown in figure 7.13a and b of apparatus converting the voltages K_1 and K_2 into width-modulated periodic pulses, the considered coders can be used for control of spoilers.

In a coder whose functional diagram is shown in figure 7.13a, the video pulses u_{in} are fed from the output of the radio receiver to decoders which are the coincidence stages CS_1, CS_2, CS_3 and CS_4. These devices, for which a possible layout for one variant for a three-unit timing code is represented in figure 7.14a, are used for separation of the subcarrier oscillations for separate circuits. The coincidence stage contains the tube T of the cathode follower with the delay line DL as a load, the diodes D_1, D_2 and D_3 and the resistances R_1 and R_2. If the three-pulse code of the considered channel is characterized by the intervals Δt_1 and Δt_2 between succeeding pulses (fig. 7.14b), the branches b and c from the DL are situated at such a distance from the point a that, for passage of pulses over the segments ab and ac, a time is required equal to Δt_2 and $\Delta t_1 + \Delta t_2$, respectively. As a result, during the time of existence of the third pulse of the code group (fig. 7.14b) positive

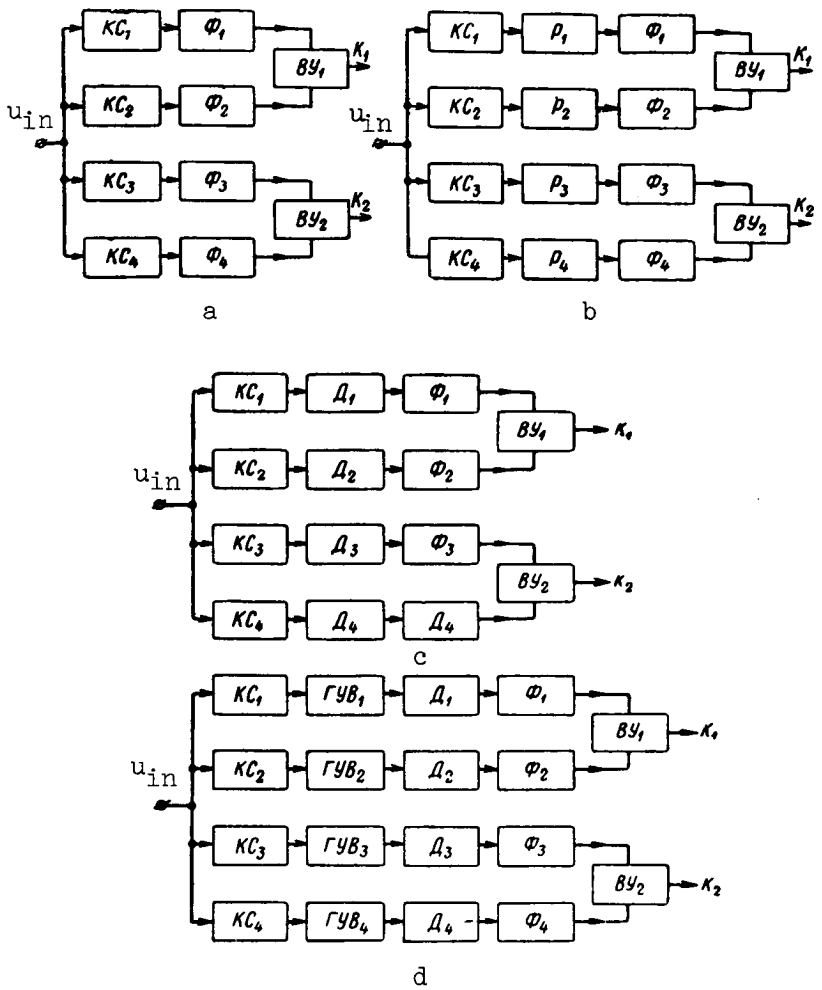

КС = CS
Ф = F
ВУ = SD
Д = PkD
Р = W
ГУВ = RF

Figure 7.13

voltage pulses will be fed to the cathodes of all the diodes D_1, D_2, and /310 D_3. For code groups with intervals not equal to Δt_1 and Δt_2, respectively, the conditions for simultaneous feeding of the signals to the diodes D_1, D_2 and D_3 will not be satisfied.

Usually for high-quality operation of the coincidence stages, it is necessary that $R_1 \gg R_2$. Therefore, the presence of at least one unblocked diode (D_1, D_2 or D_3) maintains the potential of the point A close to zero. If positive pulses of sufficient amplitude are fed simultaneously to D_1, D_2 and D_3 (and this occurs when a code group of the subcarrier oscillation is fed to the

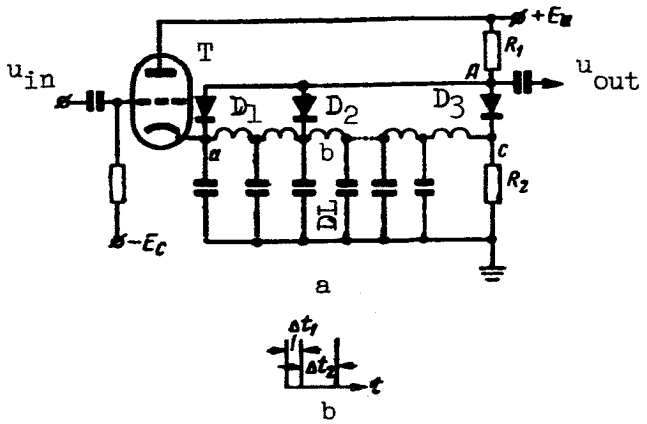

Figure 7.14

input of the tube T, thereby tuning the particular coincidence stage), a positive voltage pulse is formed at the point A. In the case of arrival of a code group with different intervals between pulses, the potential of the point A becomes close to zero, which also occurs in the absence of input signals. /311

Assuming that square pulses with the amplitudes U_{m1} and U_{m2} and the durations τ_{p1} and τ_{p2} are formed at the CS_1 and CS_2 outputs, and that the filters F_1 and F_2 have the transfer constants k_{F1} and k_{F2}, for a stationary regime we find

$$u_{F1} = k_{F1}U_{m1}m_1\frac{\tau_{p1}}{T},$$

$$u_{F2} = k_{F2}U_{m2}m_2\frac{\tau_{p2}}{T}.$$

In these expressions u_{F1} and u_{F2} are dc voltages at the F_1 and F_2 outputs at the time of transmission of a command K_{a1} of constant value. By feeding u_{F1} and u_{F2} to the subtracting device SD_1 with a transfer constant equal to 1, we obtain the voltage K_1, characterizing the output command in the first CCRL channel. The value K_1 is equal to

$$K_1 = k_{F1}U_{m1}m_1\frac{\tau_{p1}}{T} - k_{F2}U_{m2}m_2\frac{\tau_{p2}}{T}. \qquad (7.3.3)$$

This expression shows that in the transmission of a zero command, when $m_1 = m_2$, the value $K_1 \neq 0$, if

$$k_{F1}U_{m1}\frac{\tau_{p1}}{T} \neq k_{F2}U_{m2}\frac{\tau_{p2}}{T}.$$

In order to eliminate the systematic error, it is necessary that the CCRL be balanced. Balancing can be accomplished in the circuits of the subtracting devices. When the CCRL is balanced /312

$$k_{F1}U_{m1}\frac{\tau_{p1}}{T} = k_{F2}U_{m2}\frac{\tau_{p2}}{T}$$

and

$$K_1 = k_{F1}U_{m1}\frac{\tau_{p1}}{T}(m_1 - m_2) = k_{F1}U_{m1}\frac{\tau_{p1}}{T_i}\frac{m_1 - m_2}{m}. \qquad (7.3.4)$$

Expressions (7.3.3) and (7.3.4) represent the equations of a decoder of unbalanced and balanced CCRL.

Taking into account that

$$K_{1\,max} = k_{F1}U_{m1}\frac{\tau_{p1}}{T}m,$$

for the command coefficient at the output of the first channel of the decoder in a balanced CCRL we obtain

$$K_{c1} = \frac{m_1 - m_2}{m} = K_{Cc1} \qquad (7.3.5)$$

By knowing the coder and decoder equations, it is possible to derive the equation for the CCRL as a whole. For example, for CCRL with a coder, whose modulator contains a saw-toothed wave generator and a balanced decoder of the considered type, we will have

$$K_1 = k_{F1}\frac{U_{m1}}{U_m}\frac{\tau_{p1}}{T_i}K_{a1}. \qquad (7.3.6)$$

This expression shows that the CCRL transfer constant for the first channel is equal to

$$k_{CCRL\,1} = k_{F1}\frac{U_{m1}}{U_m}\frac{\tau_{p1}}{T_i}, \qquad (7.3.7)$$

and its frequency characteristic is determined by the type and parameters of the filters of lower frequencies, and also is dependent on a number of CCRL parameters (k_{Fl}, U_{ml}, U_m, τ_{pl} and T_i). The amplitude characteristic of the CCRL has the form shown in figure 7.2b.

The command K_2 of the second channel is formed in a similar way using the coincidence stages CS_3, CS_4, the lower-frequency filters F_3, F_4 and the subtracting device SD_2.

Expression (7.3.7) shows that, for an increase of $k_{CCRL\ 1}$, it is feasible to decrease the "off-duty factor" of the pulses at the CS_1 and CS_2 outputs if this does not worsen the other qualities of the CCRL (such as noise immunity). Decreases of the "off-duty factor" in both CCRL channels can be achieved by the use of the wideners W_1, W_2, W_3 and W_4 (peak detectors with a small time constant, multivibrators, phantastrons, etc.), as shown in the functional diagram of the decoder of the second type (fig. 7.13b). /313

The transfer constant of a CCRL with such a decoder is determined by expression (7.3.7) if τ_{pl} is understood as the duration of the pulse produced by the wideners.

We note that expression (7.3.7) is correct for CCRL with wideners under the assumption that the pulses produced by W_1 and W_2 have identical duration.

A further development of the system shown in figure 7.13b is the system shown in figure 7.13c. Here the functions of wideners are performed by the peak detectors PkD_1, PkD_2, PkD_3 and PkD_4, whose time constants are such that the pulses of the decoders are widened virtually to T_i. This leads to a considerable increase of the CCRL transfer constant.

The method for analyzing subcarriers used in the decoder whose functional diagram is shown in figure 7.13d is somewhat different. In this decoder, the pulses from the decoders are fed to resonance filters RF_1-RF_4, constituting generators with shock excitation. RF_1-RF_4 are used to produce sinusoidal subcarrier oscillations, which continue for a time determined by the lifetime of the corresponding groups of symbols. The resulting sinusoidal subcarrier oscillations are transformed by PkD_1-PkD_4 into square pulses which, after passing through the low-frequency filters F_1, F_2, F_3 and F_4, are fed to the subtracting devices SD_1 and SD_2. The transfer constant of such a decoder can

be determined easily if the parameters of the pulses produced by the peak detectors are known and also the transfer constants of the subtracting devices and of the low-frequency filters.

7.4. CCRL Coders and Decoders with Phase Modulation of the Subcarriers

1. CCRL with Sinusoidal Subcarrier Oscillations

In a CCRL coder with phase modulation of the sinusoidal subcarrier oscillations, the phase difference φ_w and φ_0 of the working and reference sinusoidal voltages changes proportional to the transmitted command: the mean frequencies of both voltages should be identical. Accordingly, the value of the command K_{Cl} and the command coefficient K_{Ccl} at the output of the coder for the first CCRL channel are determined by the following relations

$$K_{Cl} = \varphi_0 - \varphi_w = k_{Cl}K_{al}, \tag{7.4.1}$$

$$K_{Ccl} = \frac{\varphi_0 - \varphi_w}{\Delta\varphi_m} = \frac{k_{Cl}K_{al\ max}}{\Delta\varphi_m} K_{icl} \tag{7.4.2}$$

where k_{Cl} is the transfer constant of the coder for the circuits of the first channel, and $\Delta\varphi_m$ is the maximum value of the phase difference which can occur in the coder.

As in CCRL with pulse-width modulation of sinusoidal subcarriers, the value $\frac{k_{Cl}K_{al\ max}}{\Delta\varphi_m}$ can be less than or equal to 1.

In order to ensure the separation of the signals of the working and reference phases at the receiving end, it is necessary to have two auxiliary subcarrier oscillations with different frequencies. One of these subcarriers is modulated by a voltage with the phase φ_0 and the other with the phase φ_w. In a N_k-channel CCRL, the total number of subcarrier oscillations will be $N_k + 2$, since two subcarrier oscillations common for all channels and one voltage for each channel are used for forming signals with the phases φ_0 and φ_w. /314

One of the possible functional diagrams of a coder of a two-channel CCRL with phase modulation is shown in figure 7.15.

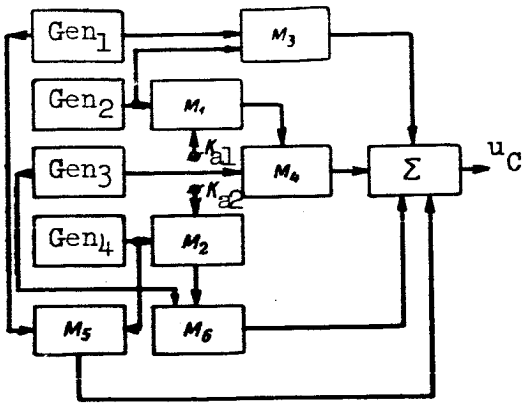

Figure 7.15

A sinusoidal voltage $u_{sub\ 2}$ of the frequency $f_{sub\ 2}$, formed by the generator Gen_2, is fed to the modulator M_1 where there is a change of the phase $u_{sub\ 2}$ under the influence of the command K_{a1} of the first channel. The signal obtained in this way, having the phase φ_w, with modulator M_4 modulates (in phase, frequency or amplitude) the auxiliary subcarrier oscillation $u_{sub\ 3}$, produced by the generator Gen_3. The modulator M_3 performs modulation of another auxiliary subcarrier oscillation $u_{sub\ 1}$, forming at the output of the generator Gen_1, by the voltage $u_{sub\ 2}$. The frequencies of the signals $u_{sub\ 1}$ and $u_{sub\ 3}$ are different and equal to $f_{sub\ 1}$ and $f_{sub\ 3}$, respectively.

In the second channel, voltages of the phases φ_0 and φ_w are formed by the generator Gen_4, tuned to the frequency $f_{sub\ 4} \neq f_{sub\ 2}$, and by the modulators M_2, M_5 and M_6. The summer Σ is used for mixing the oscillations arriving from the modulators M_3, M_4, M_5 and M_6.

Figure 7.15 shows that the value of the transfer constant of the coder for the first and second channels is dependent only on the parameters of the phase modulators M_1 and M_2.

The functional diagram of the coder of a two-channel CCRL with phase modulation has the form shown in figure 7.16. By means of the separation filters SF_1 and SF_2, tuned to the frequencies $f_{sub\ 1}$ and $f_{sub\ 3}$, the modulated auxiliary subcarrier oscillations are separated for individual channels. The

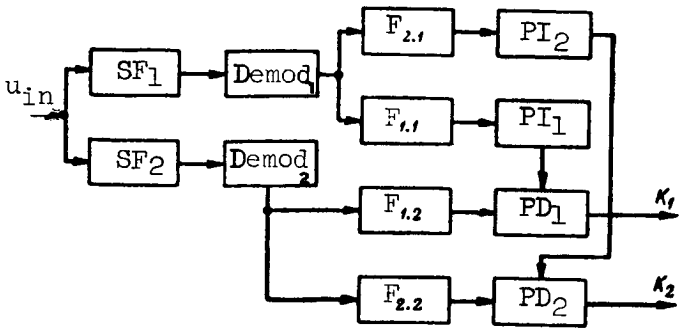

Figure 7.16

demodulators $Demod_1$ and $Demod_2$ produce voltages representing a combination of signals with the phases φ_0 and φ_w for the first and second channels, respectively. The band filters $F_{1.1}$, $F_{2.1}$ and $F_{1.2}$, $F_{2.2}$, tuned to the frequencies $f_{sub\ 2}$ and $f_{sub\ 4}$, separate for the individual circuits voltages with the /315 phases φ_0 and φ_w in the first and second channels. The phase inverters PI_1 and PI_2 change the phases of the reference voltages of each of the channels by $\frac{\pi}{2}$. The latter operation is necessary so that the CCRL signals forming at the outputs of the phase detectors PD_1 and PD_2 will be equal to zero when $K_{a1} = 0$ and $K_{a2} = 0$, that is, when $\varphi_w = \varphi_0$. The output command K_1 (for small values $\varphi_0 - \varphi_w$) constitutes the value

$$K_1(t) = k_{D1} \frac{1}{1 + T_{D1}D} K_{C1}(t),$$

where k_{D1} is the transfer constant of the decoder for the first channel, and T_{D1} is the time constant of the CCRL decoder, determined by the parameters of the PD_1 filter.

But since

$$K_{C1} = k_{C1}K_{a1},$$

we find the following CCRL equation in operator form

$$K_1(t) = \frac{k_{C1}k_{D1}}{1 + T_{D1}D} K_{a1}(t). \qquad (7.4.3)$$

The transfer constants k_{C1} and k_{D1} can be computed if the parameters of all the stages of the coder and decoder are known.

2. CCRL with Pulse Subcarrier Oscillations

The essence of the method for transmission of commands when using phase-modulated pulse subcarriers will be considered using the example of a single-channel CCRL. The command of one channel is transmitted by two periodic pulse sequences--reference (cadence) and working (control) pulses. These pulse sequences differ from one another with respect to timing codes or some other parameters; as a result, they can be separated in separate circuits at the receiving end. In accordance with the value and sign of the transmitted command K_a (the subscript 1 on K_{a1} will be omitted hereafter), there is a change of the intervals T_1 and T_2, in sum forming the repetition interval T of the commands, between the reference and control pulses. Since the most noise-immune CCRL is obtained in a case when the reference and control signals represent timing codes, hereafter we will consider only CCRL with code selection of signals. /316

The mentioned method for transmission of commands is illustrated in figure 7.17, which shows a pulse sequence consisting of three-pulse timing codes. The intervals T_1 and T_2 are changed by movement of the control codes in the limits T. The value of the command K_C at the output of the CCRL is determined by the difference of the intervals T_1 and T_2, that is

$$K_C = T_1 - T_2. \qquad (7.4.4)$$

The identity of the expression for K_C in the CCRL with pulse-phase modulation and pulse-width modulation can be attributed to the fact that CCRL with

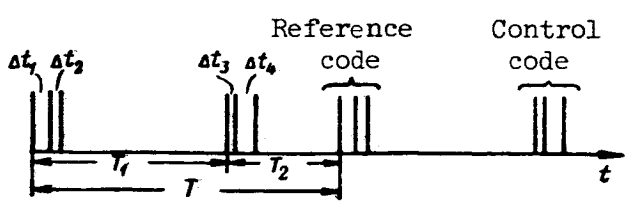

Figure 7.17

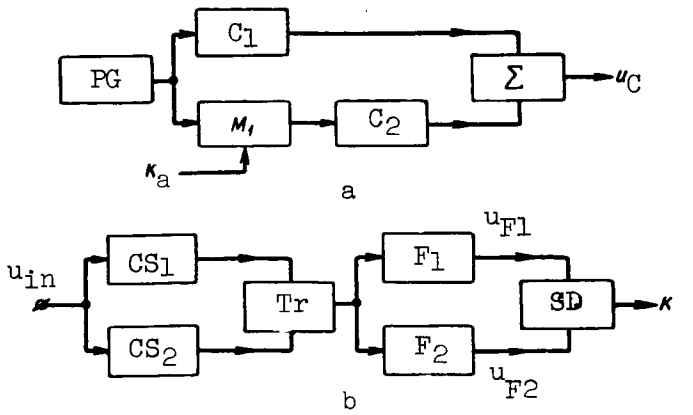

Figure 7.18

pulse-phase modulation with respect to principles of design is a further development of CCRL with pulse-width modulation. In actuality, in a CCRL with pulse-width modulation, the entire length of the intervals T_1 and T_2 is filled by subcarriers, whereas in CCRL with pulse-phase modulation only the limits of these intervals are indicated.

In accordance with the above, the functional diagram of the coder of a single-channel CCRL can be represented as shown in figure 7.18a. The pulse generator PG produces pulses whose repetition interval is T. By means of the coder C_1, the PG pulses are converted into n_0-unit timing codes characterizing the sequence of reference signals.

The modulator M_1 performs pulse-phase modulation of the PG pulses, the transmitted command K_a. The phase-modulated pulses usually are produced by a differentiator and limiter from width-modulated pulses. This means that M_1 includes a video pulse-width modulator, some diagrams of which were considered in section 7.2, a differentiator and limiters. The coder C_2 uses the M_1 pulses to produce n_{con}-unit control codes. The stage Σ is used for summing control /317 and reference codes.

Since the process of differentiation and forming of pulses by limiters introduces virtually no distortions into the intervals T_1 and T_2 obtained in pulse-width modulation, the relationship between the commands K_c and K_a will be determined by the same formulas as for CCRL with pulse-width modulation based on the use of sinusoidal subcarriers.

ОК = reference code
ИК = control code
1, 1st channel
2, 2nd channel
3, i-th channel
4, N_k-th channel

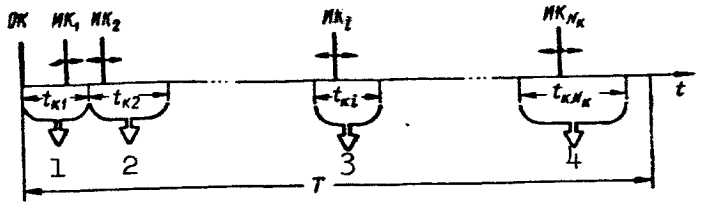

Figure 7.19

The decoder of a single-channel with pulse-phase modulation, whose functional diagram is shown in figure 7.18b, includes the coincidence stages CS_1 and CS_2, the trigger Tr, the low-frequency filters F_1 and F_2 and the subtracting device SD. By means of CS_1 and CS_2, the subcarriers are separated for the individual circuits and the trigger converts pulse-phase modulation into pulse-width modulation. The filters F_1 and F_2 cut into the anode and cathode circuits of the first and second tubes of the trigger Tr are used in detecting the "constants" of the components of the Tr pulses. The subtracting device produces an output command whose stationary value is determined by expression (7.2.9). This can be attributed to the identity of the circuits for analysis of the subcarriers in the CCRL with pulse-phase modulation and in CCRL with pulse-width modulation of sinusoidal subcarriers.

When using a CCRL with pulse-width modulation for transmission of two or of a large number of forms of commands, there can be successive and time-parallel placement of the control code groups (symbols); in this case, in a N_k-channel CCRL there should be at least one reference and N_k control codes. In the successive transmission of N_k commands, their repetition period T is divided by N_k in the general case of unequal intervals (fig. 7.19) called channel intervals.

Within the limits of the interval t_{ki}, assigned for the i-th channel ($i = 1, 2, \ldots, N_k$) within the period T, under the influence of the transmitted command K_{ai}, there is movement of the control pulse of the i-th channel, at the same time that the reference codes (here and in the text which follows assumed to be common for all channels) are formed at the beginning of each cycle of transmission of commands. /318

The coder and decoder of a N_k-channel CCRL with successive placement of channels can be constructed in accordance with the diagrams shown in figure

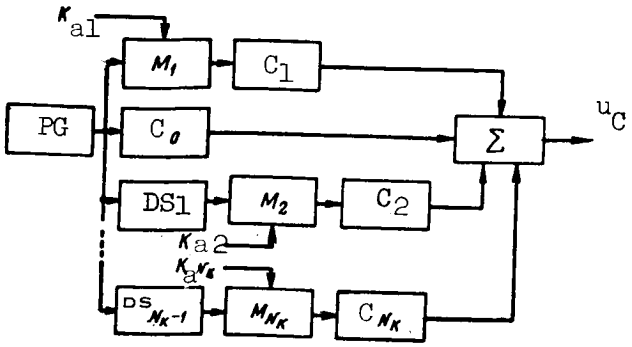

a

KC = CS
Tp = Tr
Φ = F
BУ = SD

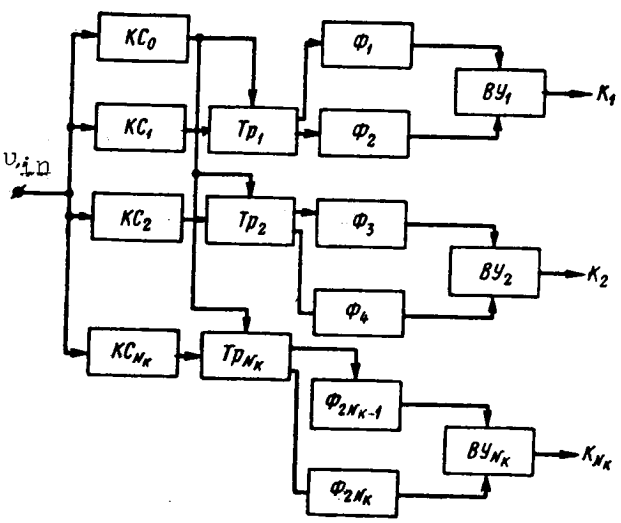

b

Figure 7.20

7.20a, b, provided the commands constitute dc voltages. The pulse generator PG produces pulses u_{PG} (fig. 7.20a) having the repetition period T. These pulses act on the modulator of the first channel M_1, the coder C_0 and the delay stages DS_1 - DS_{N_k-1}. The coder C_0 is used for forming reference codes u_0, shown in figure 7.21b in the form of pairs of pulses with the intervals Δt_0.

The modulator M_1, under the influence of the command K_{a1} and the pulses u_{PG}, performs pulse-phase modulation. As a result, individual pulses are formed at the M_1 output; these pulses are distant from the PG pulses by a time

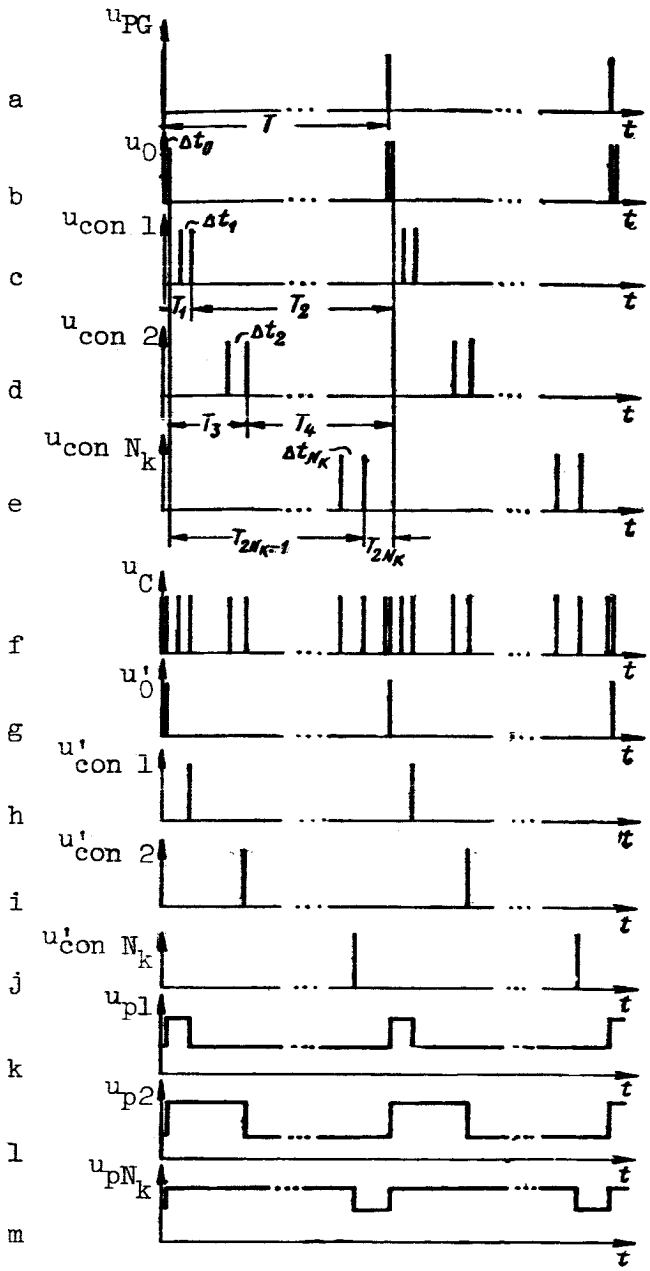

Figure 7.21

determined by the value K_{al}. By means of the coder C_1, these pulses are converted into a timing control code $u_{con\ 1}$, such as a two-pulse code, as shown in figure 7.21c.

The delay stages DS_1 - DS_{N_k-1}, under the influence of the voltage u_{PG}, produce individual pulses which are displaced by corresponding intervals of time

relative to the u_{PG} pulses. The signals produced at the DS_1 output are triggering signals for the second channel modulator M_2, which also is fed the command K_{a2}. The coder C_2 is used to form the control timing codes $u_{con\ 2}$ (fig. 7.21d) for the second channel.

Similar processes occur in all channels. In particular, in the last channel the control codes $u_{con\ N_k}$ are produced by the coder C_{N_k} (fig. 7.21e), to which are fed signals from the modulator M_{N_k}.

The voltages from the C_0, C_1, C_2, ..., C_{N_k-1} outputs are summed by the summer Σ and mixed in a general sequence, and the resulting signals u_C (fig. 7.21f) are fed to the CCRL radio transmitter.

Diagrams of the decoders of a single-channel and each channel of a two-channel CCRL (figs. 7.18 and 7.20b) are identical. In study of figure 7.20b, it is necessary to take into account that the reference pulses discriminated by the coincidence stage CS_0 are used for operation of all the CCRL channels. /321

Time diagrams clarifying the operation of the system shown in figure 7.20b are shown in figure 7.21g-m. It must be remembered that figure 7.21g-j shows the reference and control codes produced by the coincidence stages CS_0-CS_{N_k}, and figure 7.21k-m shows the signals forming at the anode of one of the tubes (such as the left tube) of the triggers Tr_1-Tr_{N_k}.

Distinguishing characteristics of multichannel CCRL with successive placement of channels are a decrease of the transfer constant k_{CCRL} in the i-th channel ($i = 1, 2, \ldots, N_k$) with an increase of N_k and absence of possibilities of "forced" transmission of zero commands in all channels, except in the channel where the zero value of the transmitted command corresponds to the intervals T_1 and T_2, equal to 0.5 T. The latter means that in order to obtain the command $K_i = 0$ at the output of the i-th channel, it is necessary to have a corresponding design of all the converters in the decoder or use of special balancing voltage sources if the equivalent converters have identical parameters.

The characteristics noted here were detected as a result of analysis of the operation of a coder and of a decoder.

By analogy with a single-channel CCRL it can be assumed that the value of the command K_{Ci} for the i-th channel at the ouput of the coder of a

multichannel CCRL with successive placement of channels is determined by the difference of the intervals ΔT_{1i} and ΔT_{2i} forming together the value t_{ki} and read from the time of appearance of the last pulse of the control code of the i-th channel to the beginning and end of the interval t_{ki}, respectively, that is

$$K_{Ci} = \Delta T_{1i} - \Delta T_{2i} = K_{Ci} K_{ai}, \qquad (7.4.5)$$

where k_{Ci} is the transfer constant of the coder for the i-th channel, K_{ai} is the value of the command transmitted in the i-th channel, ΔT_{1i} is the interval between the beginning of the i-th channel interval and the control code of this same i-th channel, and ΔT_{2i} is the interval between the control code and the end of the channel interval of the i-th channel.

By comparing the transfer constants of coders of single-channel and multichannel CCRL with successive arrangement of channels, on the basis of expressions (7.2.1) and (7.4.5), and assuming that $K_{ai} = K_a = K_{al}$, we obtain

$$\frac{k_{Ci}}{k_{Cl}} = \frac{\Delta T_{1i} - \Delta T_{2i}}{T_1 - T_2}.$$

The maximum values ΔT_{1i} and ΔT_{2i} and $T_1 - T_2$ constitute t_{ki} and T, respectively. Therefore

$$k_{Ci} = k_{Cl} \frac{t_{ki}}{T}.$$

It therefore follows that $k_{Ci} < k_{Cl}$.

If the CCRL is designed in such a way that $t_{ki} = \frac{T}{N_k}$, then /322

$$k_{Ci} = \frac{k_{Cl}}{N_k}.$$

This means that the transfer constant of a coder for one of the channels of a multichannel CCRL with identical channel intervals changes inversely proportional to N_k. Since the maximum value $K_{Ci\ max}$ of the command K_{Ci} can be t_{ki}, for the coefficient of the i-th command K_{Cci} we find the following expression

$$K_{Cci} = \frac{\Delta T_i - \Delta T_{2i}}{t_{ki}} = \frac{2\Delta T_{1i}}{t_{ki}} - 1 = \frac{k_{Ci} K_{ai\ max}}{T} K_{ici}. \qquad (7.4.6)$$

Between the times of formation of the last pulses of the reference and control codes of the i-th channel, a time T_{1i} passes which is equal to

$$T_{1i} = \sum_{l=1}^{i-1} t_{kl} + \Delta T_{1i} = \sum_{l=1}^{i-1} t_{kl} + t_{ki} \frac{1 + K_{Cci}}{2}. \qquad (7.4.7)$$

As a result, the trigger Tr_i in the decoder of the i-th channel produces pulse voltages $u_{p1}^{(i)}(t)$ and $u_{p2}^{(i)}(t)$ which are determined as follows

$$\left.\begin{aligned} u_{p1}^{(i)} &= u_1^{(i)} + U_{m1}^{(i)}, \\ u_{p2}^{(i)} &= u_2^{(i)} \end{aligned}\right\} \text{ when } kT \leqslant t < kT + T_{1i} \quad (k = 0, 1, 2, \ldots),$$

$$\left.\begin{aligned} u_{p1}^{(i)} &= u_1^{(i)}, \\ u_{p2}^{(i)} &= u_2^{(i)} + U_{m2}^{(i)} \end{aligned}\right\} \text{ when } kT + T_{1i} \leqslant t < (k+1)T \quad (k = 0, 1, 2, \ldots).$$

In a stationary regime, a command K_i is formed at the output of the i-th channel; this command is in the form of a dc voltage equal to the difference of the constant components of the voltages at the outputs of the low-frequency filters $F_1^{(i)}$ and $F_2^{(i)}$. The filters $F_1^{(i)}$ and $F_2^{(i)}$ are fed the voltages $u_{p1}^{(i)}(t)$ and $u_{p2}^{(i)}(t)$. It then is possible to find that

$$\Phi = F$$

$$K_i = k_{\phi 1}^{(i)} \left[u_1^{(i)} + \frac{U_{m1}^{(i)}}{T} \left(\sum_{l=1}^{i-1} t_{kl} + \frac{t_{ki}}{2} \right) \right] - k_{\phi 2}^{(i)} \left(u_2^{(i)} + U_{m2}^{(i)} \right) - k_{\phi 2}^{(i)} \frac{U_{m2}^{(i)}}{T} \times \left(\sum_{l=1}^{i-1} t_{kl} + \frac{t_{ki}}{2} \right) + \frac{k_{\phi 1}^{(i)} U_{m1}^{(i)} + k_{\phi 2}^{(i)} U_{m2}^{(i)}}{2} \frac{t_{ki}}{T} K_{Cci},$$

where $k_{F1}^{(i)}$ and $k_{F2}^{(i)}$ are the transfer constants of the filters $F_1^{(i)}$ and $F_2^{(i)}$ at the zero frequency.

The derived expression shows that the presence of a symmetrical trigger and of a subtracting device, as well as of identical output filters, in the absence of balancing devices fails to ensure that $K_i = 0$ will be obtained when $K_{Ci} = 0$. This means that with the successive placement of channels there will

be no "forced" transmission of the zero command. By means of selection of the parameters of the trigger, the output filters and the subtracting device /323 can be such that

$$k_{\Phi 1}^{(i)}\left[u_1^{(i)}+\frac{U_{m1}^{(i)}}{T}\left(\sum_{l=1}^{i-1}t_{kl}+\frac{t_{ki}}{2}\right)\right]= k_{\Phi 2}^{(i)}\left[u_2^{(i)}+U_{m2}^{(i)}-\frac{U_{m2}^{(i)}}{T}\left(\sum_{l=1}^{i-1}t_{kl}+\frac{t_{ki}}{2}\right)\right] \tag{7.4.8}$$

and

$$K_i=\frac{k_{\Phi 1}^{(i)}U_{m1}^{(i)}+k_{\Phi 2}^{(i)}U_{m2}^{(i)}}{2}\frac{t_{ki}}{T}K_{Cci}. \tag{7.4.9}$$

But it follows from expression (7.4.8) that

$$k_{\Phi 2}^{(i)}U_{m2}^{(i)}=\frac{T}{T-\left(\sum_{l=1}^{i-1}t_{kl}+0{,}5t_{ki}\right)}\left\{k_{\Phi 1}^{(i)}\left[u_1^{(i)}+\frac{U_{m1}^{(i)}}{T}\left(\sum_{l=1}^{i-1}t_{kl}+0{,}5t_{ki}\right)\right]-k_{\Phi 2}^{(i)}u_2^{(i)}\right\}$$

Therefore

$$K_i = k_D^{(i)}K_{Ci},$$

where $K_{Ci} = K_{Cci}t_{ki}$ determines the value of the command of the i-th channel at the coder output and

$$k_D^{(i)}=\frac{1}{2}\frac{k_{\Phi 1}^{(i)}U_{m1}^{(i)}+k_{\Phi 1}^{(i)}u_1^{(i)}-k_{\Phi 2}^{(i)}u_2^{(i)}}{T-\left(\sum_{l=1}^{i-1}t_{kl}+0{,}5t_{ki}\right)} \tag{7.4.10}$$

characterizes the transfer constant of the decoder of a multichannel CCRL for the i-th channel.

On the basis of expressions (7.2.12) and (7.4.10), it can be found that

$$\frac{k_D^{(i)}}{k_{D1}}=\frac{1}{2}\frac{T}{T-\left(\sum_{l=1}^{i-1}t_{kl}+0{,}5t_{ki}\right)}\frac{k_{\Phi 1}^{(i)}U_{m1}^{(1)}+k_{\Phi 1}^{(i)}u_1^{(i)}-k_{\Phi 2}^{(i)}u_2^{(i)}}{k_{\Phi 1}U_{m1}+k_{\Phi 1}u_1-k_{\Phi 2}u^2} \tag{7.4.11}$$

(Ф = F for all equations on this page)

It follows from an analysis of expression (7.4.11) that if the parameters of the filters and threshold apparatus (triggers) of the decoder in a single-channel CCRL and in the first channel of a multichannel CCRL are identical $k_D^{(i)} < k_{D1}$. This conclusion can be drawn on the basis of the following inequality, which always is satisfied

$$t_{ki} < T.$$

When comparing the transfer constant of the decoder for all other channels with the value k_{D1} in a single-channel radio link, it must be remembered that in a multichannel CCRL the voltages $k_{F1}^{(i)}U_{m1}^{(i)}$ when $i > 1$ should be less than $k_{F1}^{(i)}U_{m}^{(i)}$ when $i = 1$. This can be attributed to the condition that there is balancing of all channels when using threshold apparatus and filters producing signals $k_{F1}^{(i)}U_{m1}^{(i)}$ ($i = 2, 3, \ldots, N_k$) and $k_{F2}^{(i)}U_{m2}^{(i)}$ ($i = 2, 3, \ldots, N_k$) not /324 exceeding $k_{F1}^{(1)}U_{m1}^{(1)}$. In such a method for designing CCRL, the following relationship exists between $k_{F1}^{(i)}U_{m1}^{(i)}$ and $k_{F1}^{(1)}U_{m1}^{(1)}$

$\Phi = F$

$$k_{\phi 1}^{(i)}U_{m1}^{(i)} = \frac{1}{2}k_{\phi 1}^{(1)}U_{m1}^{(1)}\frac{t_{k1}}{\sum_{l=1}^{i-1}t_{kl} + 0{,}5t_{ki}}. \qquad (7.4.12)$$

Expression (7.4.12) was derived on this basis: in the transmission of zero commands through the 1st and i-th chnnels, the constant components $u_{p1}^{(1)}(t)$ and $u_{p1}^{(i)}(t)$ should be equal to one another for identical values $k_{F1}^{(i)}u_1^{(i)}$ and $k_{F2}^{(i)}u_2^{(i)}$, independently of i.

Under the mentioned condition, $k_D^{(i)}$ ($i = 2, 3, \ldots, N_k$) also is less than k_{D1}; with an increase of N_k, the ratio of k_{D1} to $k_D^{(i)}$ increases.

If all the channel intervals in a N_k-channel CCRL are identical and equal to $\frac{T}{N_k}$, then

$\Phi = F$

$$k_D^{(i)} = \frac{N_k\left[k_{\phi 1}^{(i)}U_{m1}^{(i)} + k_{\phi 1}^{(i)}u_1^{(i)} - k_{\phi 2}^{(i)}u_2^{(i)}\right]}{2(N_k - i + 0{,}5)T}$$

and

Φ = F $$\frac{k_D^{(i)}}{k_{D1}} = \frac{N_k}{2(N_k - i + 0{,}5)} \frac{k_{\phi 1}^{(i)} U_{m1}^{(i)} + k_{\phi 1}^{(i)} u_1^{(i)} - k_{\phi 2}^{(i)} u_2^{(i)}}{k_{\phi 1} U_{m1} + k_{\phi 1} u_1 - k_{\phi 2} u_2}.$$

As an illustration we note that when $k_{F1}^{(1)} U_{m1}^{(1)} = k_{F1} U_{m1}$, $k_{F1}^{(1)} u_1^{(1)} = k_{F2}^{(1)} u_2^{(1)}$, $k_{F1} u_1 = k_{F2} u_2$ and $N_k = 2$, the value $k_D^{(1)} = \frac{2}{3} k_{D1}$. The value $k_D^{(2)}$ also is $\frac{2}{3} k_{D1}$, if $k_{F1}^{(2)} u_1^{(2)} = k_{F2}^{(2)} u_2^{(2)}$ and $k_{F1} u_1 = k_{F2} u_2$. In a three-channel CCRL, the values $k_D^{(1)}$, $k_D^{(2)}$ and $k_D^{(3)}$ when $k_{F1}^{(i)} u_1^{(i)} = k_{F2}^{(i)} u_2^{(i)}$ and $k_{F1} u_1 = k_{F2} u_2$, and also with satisfaction of the condition (7.4.12) are equal to $\frac{3}{5} k_{D1}$, $\frac{1}{3} k_{D1}$ and $\frac{3}{5} k_{D1}$, respectively. For a four-channel CCRL, in the same way we obtain $k_D^{(1)} = k_D^{(4)} = \frac{4}{7} k_{D1}$ and $k_D^{(2)} = k_D^{(3)} = \frac{4}{15} k_{D1}$. The cited examples show that in the considered method of design of CCRL, the transfer constants of the decoders for different channels, in a general case, are different and decrease with an increase of N_k. However, by an appropriate selection of t_{ki} and also of the parameters of the threshold apparatus and filters on the basis of expression (7.4.10), it is possible to ensure the identical earlier stipulated values $k_D^{(i)}$, independently of i.

When all the channel intervals should be identical, the voltage $k_{F1}^{(i)} U_{m1}^{(i)} + k_{F1}^{(i)} u_1^{(i)} - k_{F2}^{(i)} u_2^{(i)}$ when $t_{k1} = t_{k2} = \ldots = t_{kN_k} = \frac{T}{N_k}$, as follows from expression (7.4.10), should be computed on the basis of the following condition

Φ = F $$k_{\phi 1}^{(i)} U_{m1}^{(i)} + k_{\phi 1}^{(i)} U_{m1}^{(i)} - k_{\phi 2}^{(i)} u_2^{(i)} = \frac{2(N_k - i + 0{,}5)\, T}{N_k} k_D^{(i)}.$$

In case of a need for creating a decoder for a N_k-channel CCRL in such a way that $k_D^{(i)} = k_{D1}$, independently of i, all the required parameters of the

decoder circuits for any channel can be determined on the basis of expression (7.4.11).

Since for identical channel intervals $k_D^{(i)} < k_{D1}$ and $k_{C1}^{(i)} < k_{C1}$, the /325 transfer constant $k_{CCRL}^{(i)} = k_C^{(i)} k_D^{(i)}$ of a multichannel radio link for the i-th channel will be smaller than $k_{CCRL\ 1} = k_{C1} k_{D1}$ in a single-channel CCRL. Thus, for a two-channel CCRL with identical channel intervals $k_{CCRL}^{(1)} = k_{CCRL}^{(2)} = \frac{1}{3} k_{CCRL\ 1}$. If $N_k = 3$, then $k_{CCRL}^{(1)} = k_{CCRL}^{(3)} = \frac{1}{5} k_{CCRL\ 1}$, and $k_{CCRL}^{(2)} = \frac{1}{9} k_{CCRL\ 1}$. In a four-channel CCRL, $k_{CCRL}^{(1)} = k_{CCRL}^{(4)} = \frac{1}{7} k_{CCRL\ 1}$ and $k_{CCRL}^{(2)} = k_{CCRL}^{(3)} = \frac{1}{15} k_{CCRL\ 1}$.

If in a multichannel CCRL the ratio $\frac{k_D^{(i)}}{k_{D1}}$ should be equal to 1, regardless of i, then $k_{CCRL}^{(i)}$ will be less than $k_{CCRL\ 1}$ by the factor $\frac{T}{t_{ki}}$. When $t_{k1} = t_{k2} = \ldots = t_{kN} = \frac{T}{N_k}$, the ratio $\frac{k_{CCRL}^{(i)}}{k_{CCRL\ 1}} = \frac{1}{N_k}$.

A decrease of $k_{CCRL}^{(i)}$ in comparison with $k_{CCRL\ 1}$ characterizes one of the shortcomings of a CCRL with successive arrangement of channels.

In the case of parallel transmission of commands (parallel placement of channels), the control code of each channel can be moved within the limits of the entire repetition period T of cadence code groups, as a result of which the transfer constant $k_{CCRL}^{(i)}$ remains the same as in a single-channel CCRL. However, for elimination of the possibility of superposing the pulses of the control codes of different channels and the resulting appearance of a reciprocal influence of the channels for the control codes of each channel in the segment T, a number of definite positions are fixed. As an illustration, in figure 7.22, we have shown by the arbitrary points 1, 2 and 3 the possible positions of the

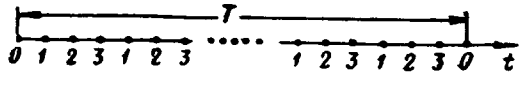

Figure 7.22

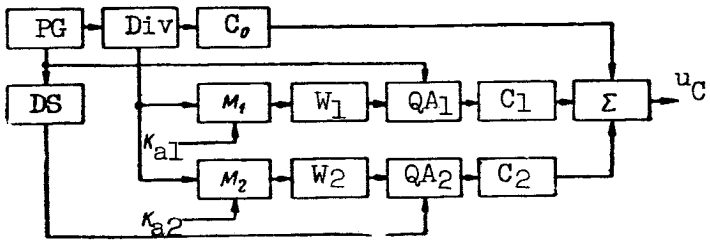

Figure 7.23

control codes of the first, second and third channels in a three-channel CCRL for one period T of transmission of commands. The points 0 in figure 7.22 denote the positions of the reference codes.

Since the control code of each channel cannot occupy any position in the interval T, by use of a CCRL based on the principle of parallel arrangement of subcarriers it is possible to transmit only individual (discrete) values of the commands K_{a1}, K_{a2}, ... This means the presence of errors in the transmission of commands due to level-quantization of the CCRL input signals. The values of the errors caused by quantization of the transmitted commands can be reduced to a necessary minimum if in the development of CCRL the recommendations given in section 7.8 are taken into account.

Another characteristic of a CCRL with parallel placement of subcarrier oscillations is that there can be no precise transmission of the zero values of commands in all channels but one. However, with discrimination for all channels of positions which are situated near the point $\frac{T}{2}$ of the period T, /326 the errors in transmission of a zero command of all the channels will be virtually absent. An additional increase of the accuracy of transmission of zero commands is attained by the use of special correcting voltages at the receiving end.

We will analyze the principles of design of CCRL of the considered type using the example of a two-channel CCRL; the functional diagram of its coder is shown in figure 7.23.

Signals from the pulse generator PG, producing the pulses u_{PG} (fig. 7.24a) with the repetition period T_i, determining the quantization interval, act on the divider Div, quantization apparatus QA_1 and delay stage DS. The pulses u_{div} are fed from the divider (fig. 7.24b); the repetition period of these pulses is T. These pulses act on the coder C_0 of the reference signals. In addition, the signals u_{div} control operation of the modulators M_1 and M_2,

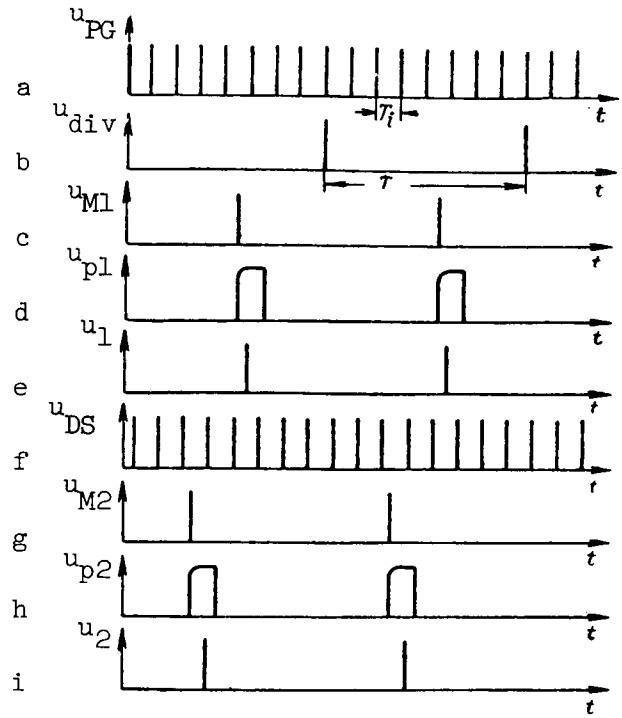

Figure 7.24

where there is pulse-phase modulation by the signals K_{a1} and K_{a2}. The voltages u_{M1} and u_{M2} (fig. 7.24c, g) from the outputs of the modulators M_1 and M_2 are fed to the wideners W_1 and W_2, producing the pulses u_{p1} and u_{p2} (fig. 7.24d, h) with somewhat steepened fronts and durations equal to approximately T_i. The widening of the signals u_{M1} and u_{M2} is necessary to ensure the normal operation of the quantization apparatus QA_1 and QA_2. The QA_1 is fed not only u_{p1}, but also the voltage u_{PG}, and QA_2 is fed not only u_{p2}, but also the pulses u_{DS} (fig. 7.24f) from the delay stage DS, biased by $\frac{T_i}{2}$ relative to the pulses u_{PG}.

Only those PG and DS pulses reach the QA_1 and QA_2 outputs which coincide in time of effect with the signals u_{p1} and u_{p2}. As a result, identical control pulses u_1 and u_2 are formed (fig. 7.24e, i), whose distance from the reference signals u_{div} is determined by the commands K_{a1} and K_{a2} with some error caused by the quantization process. These pulses are converted into timing codes of the coders C_1 and C_2 and are mixed with the C_0 signals in the summer Σ.

In conclusion we point out that the relationship between K_{Cl} and K_{al} /327 for the considered coder is determined by the formula

$$K_{Cl} = m_1 - m_2 = k_{Cl}K_{al},$$

where m_1 and m_2 are the numbers of intervals T_i corresponding to the time segments T_1 and T_2 (fig. 7.17).

We note that in the cited expression, as for CCRL with pulse-counting modulation, the value $m_1 - m_2$ remains constant with a change of K_{al} in limits determined by the quantization interval $2T_i$.

Decoders of multichannel CCRL with parallel placement of channels can be designed using the same models as in cases of successive placement of channels.

The dependence of the output signal K_i for the i-th channel (i = 1, 2, ..., N_k) of a N_k-channel CCRL of the considered type on K_{Ci} in a stationary regime is determined by expression (7.2.9). This can be attributed to the fact that the component elements and processes occurring in any of the channels of the decoder of a CCRL with pulse-phase modulation, in the case of parallel placement of the channels and pulse-width modulation of sinusoidal subcarriers, are identical. However, it must be mentioned that all the mentioned for- /328 mulas will be correct only for individual discrete values of the transmitted commands.

Analysis of a N_k-channel CCRL with pulse-phase modulation when using the principle of parallel placement of channels shows that this CCRL, if the discrete character of transmission of commands is not taken into account, constitutes a set of N_k single-channel CCRL with pulse-phase modulation.

7.5. Principles of Design of CCRL with Pulse-Code Modulation

The values of the transmitted control commands are converted in the CCRL coder into numbers which are reflected by definite combinations of pulses (codes) of subcarrier oscillations. The codes in CCRL with puls -code modulation are designed most frequently on the basis of a binary numbering system. This is due to the relative simplicity of its technical design.

In the process of conversions, the continuous function $K_a(t)$ subject to transmission for a distance first is level-quantized, that is, broken down into a series of intervals.

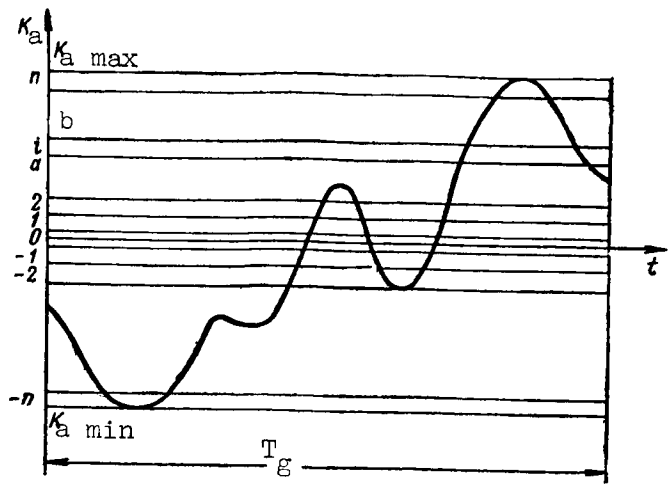

Figure 7.25

Usually the modules of maximum and minimum values $K_a(t)$ are identical, and as a result the number of intervals reflecting positive and negative values $K_a(t)$, which are formed during the time of rocket guidance T_g, will be identical and equal to n (fig. 7.25). In addition, there will be one interval (zero interval) in the neighborhood of the point $K_a = 0$. Thus, the entire range of values K_a is broken down into $2n + 1$ intervals, one of which (the zero interval) is "open," while all the others are "semi-open." We recall that the interval is considered open in a case when its ends are not taken into account.

It should be remembered that the length of the positive (negative) part of the zero interval is half the length of the semi-open interval.

Sequential and parallel binary codes can be used for expression of the numbers. The principal property of codes of the first type is that the pulses determining the individual digits follow one another in time. As is well known, each semi-open interval (a and b in fig. 7.25), satisfying the condition $a \leq K_a < b$, corresponds to one number or set of several numbers expressed by binary codes. The zero open interval also is characterized by a single number or set of several numbers. If a semi-open interval is determined by a single number, for transmission of the entire range of changes K_a, it is necessary to have one numerical sequence which can be sign-variable or constant in sign.

When using several numbers for expressing a single semi-open interval (a, b), the transmission of all values K_a can be accomplished only when there is a corresponding number of numerical sequences and therefore a corresponding

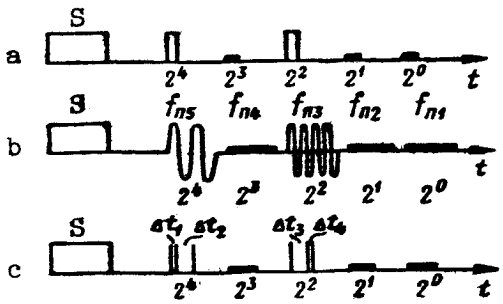

$f_{П} = f_{sub}$

Figure 7.26

number of binary codes. The use of each new sequence of numbers naturally /329 leads to a complication of the CCRL. Therefore, hereafter we will limit ourselves only to a case when the i-th semi-open interval can be expressed by one number or the difference between the numbers $m_{1.i}$ and $m_{2.i}$ of two sequences;

in this case, it is assumed that $m_{1.i} + m_{2.i} = m = \text{const}$. We note that the

latter method of forming commands is similar to the case of pulse-counting modulation. Parallel codes are characterized by the fact that pulses of all digits are transmitted simultaneously.

If the i-th interval (fig. 7.25) is expressed by one number of a sign-variable sequence, in addition to a binary code for each channel in the coder, it is necessary to form a signal characterizing the sign of the transmitted number. This means that commands for one control channel are transmitted by two subcarrier oscillations, one of which is modulated by the signal K_a and

the other is not modulated. The sign signal can constitute a timing code, a pulse differing in width from the pulses of a binary code, etc. For example, if a timing code is used for transmitting the sign, the code parameters change with a transition from transmission of a zero interval to the interval -1. In actual practice, sign signals also can be used for ensuring separation of the pulses of the digits of the binary code at the receiving end by individual circuits, preparation of the CCRL decoder for receiving new values of commands, etc. Very frequently, such signals are called starting (address) pulses or key pulses.

Depending on how the digits of the successive binary codes are ar- /330 ranged, it is possible to distinguish three forms of output signals of a coder during transmission of a command by one sequence of numbers. All these forms, jointly with the starting pulse, are arbitrarily denoted S, shown in figure 7.26 for the example of a five-digit binary code which is used to express the number 20.

Figure 7.26a shows a binary code based on individual video pulses. In this type of code, there is a time separation of digits. The second and third forms of binary codes differ in that the digits are denoted by pulses of sinusoidal oscillations with different frequencies ($f_{sub\ 1}$ - $f_{sub\ 5}$ in fig. 7.26b)

or constitute timing codes (fig. 726c). In such CCRL, the separation of digits for different purposes at the receiving end is based on principles of frequency and code selection of signals. We note that in the second form of coder output signals, the pauses (intervals between digits) may be absent or filled by sinusoidal oscillations of other frequencies.

Parallel binary codes can be formed most easily from pulses of sinusoidal oscillations with different frequencies.

When expressing the i-th interval of the command K_a by one sign-variable sequence of numbers, the zero command is transmitted only by the starting pulse. The value of the output command of the coder K_C when using one sign-variable sequence of numbers can be determined as follows

$$K_C = b\sum_{l=1}^{N} 2^{l-1}\delta_l(i) = k_C K_a, \qquad (7.5.1)$$

where N is the significance of the binary code; b is a coefficient assuming the value +1 or -1 depending on the sign K_a; k_C is the transfer constant of the coder characterizing the number of the single command arriving at the CCRL input; i is a whole number assuming the values -n, -(n - 1), ..., -1, 0, 1, 2, ..., n; $\delta_l(i)$ is a function which for a given value i assumes values 1 or 0 depending on l; and l is the summation index.

For example, if when N = 5 the value i = 13 is transmitted, $\delta_1 = \delta_3$ /331 $= \delta_4 = 1$ and $\delta_2 = \delta_5 = 0$.

As a result of level-quantization of the transmitted commands, the amplitude characteristic of a coder representing the dependence of K_C on K_a, and therefore also the amplitude characteristic of the CCRL as a whole, will have the form of stepped curves. Therefore, by k_C in expression (7.5.1), it is necessary to understand the mean transfer constant of the coder, computed using formula (7.1.1) under the condition that the function $K_C = f(K_a)$ is defined by a curve drawn through the middle of the "steps."

In order to obtain an amplitude characteristic corresponding to figure 7.2b, the precise proportional dependence between K_C and K_a determined by expression (7.5.1) should be observed only for values K_a expressed by 0, 1, 2, ..., n lengths of semi-open intervals. At the same time, conversion from one number to another should be accomplished for K_a determined by the limits

of the semi-open intervals and the value K_C should remain constant when $K_{a(i-1)} \leq K_a < K_{ai}$, where K_{ai} is the value K_a at the limit of the i-th and (i + 1)-th intervals; $K_{a(i-1)}$ is the value K_a at the limit of the (i - 1)-th and i-th intervals. Since the maximum value of the command at the output of the coder is

$$K_{C\ max} = \sum_{l=1}^{N} 2^{l-1} = 2^N - 1,$$

for the command coefficient K_{Cc} at the output of the coder we find

$$K_{Cci} = b \frac{\sum_{l=1}^{N} 2^{l-1} \delta_l(i)}{2^N - 1}. \qquad (7.5.2)$$

It therefore can be seen that k_{Cc} changes discretely in the range ±1.

When expressing the i-th interval of K_a by the difference of two numbers, the need of a sign signal essentially disappears. However, the starting pulses before binary codes usually must be transmitted in this case as well, since they are necessary for ensuring the separation of digits when using the time selection principle or for preparation of the CCRL decoder for reception of the next command. Therefore, in transmission of the command of one channel, at least three types of subcarriers participate: two subcarrier oscillations of binary codes and one subcarrier of the starting pulse. In multichannel CCRL, the same starting pulse can serve several channels. Both subcarrier oscillations of binary codes are modulated by the transmitted command. Modulation is accomplished in such a way that with an increase of the transmitted command, the numbers of one sequence are increased and those of the other sequence are decreased. During the transmission of a zero command, the numbers of both /332 sequences should be identical. In order for the CCRL amplitude characteristic to be symmetrical, the numbers 0 or 2^N - 1 should not be used in both sequences.

As an illustration of the above we will consider the example of conversion of the input command K_a on the assumption that two three-unit binary codes are used, making it possible to obtain two sequences of numbers, 0, 1, 2, 3, 4, 5, 6 and 7. Then, not taking the number 0 into account, we divide the entire range of changes K_a into one open (zero) and 6 semi-open intervals. Each of these intervals is given in accordance with the two numbers given in table 7.1. This same table gives the values of the coder output command.

TABLE 7.1

Number of K_a interval	-3	-2	-1	0	1	2	3
Numbers of first sequence	1	2	3	4	5	6	7
Numbers of second sequence	7	6	5	4	3	2	1
Values of command at coder output	-6	-4	-2	0	2	4	6

In a general case, under the influence of the command characterized by the i-th interval, the numbers $m_{1.i}$ of the first sequence should be formed in conformity to the law

$$m_{1.i} = \sum_{l=1}^{N} 2^{l-1}\delta_l(i).$$

The law of change of the numbers of the second sequence can be found on the basis of the earlier mentioned condition of conservation of the constancy of the sum of the numbers of both sequences. Since a single number of the second sequence is transmitted with the maximum number of the first sequence, the sum of both numbers is 2^N.

Therefore the law of change of the numbers of the second sequence has the form

$$m_{2.i} = 2^N - \sum_{l=1}^{N} 2^{l-1}\delta_l(i).$$

Taking into account the mentioned variants for design of numerical sequences, for a command at the coder output in the case of transmission of the K_a signal expressed by the i-th interval we obtain /333

$$K_C = m_{1.i} - m_{2.i} = 2\sum_{l=1}^{N} 2^{l-1}\delta_l(i) - 2^N = k_C K_a. \qquad (7.5.3)$$

It can be seen from this expression that when transmitting a maximum value K_a, when $\delta_1 = \delta_2 = \ldots = \delta_N = 1$, the sum $\sum_{l=1}^{N} 2^{l-1}\delta_l(i) = 2^N - 1$ and $K_C = K_{C\,max} = 2^N - 2$,

and in the case of transmission of a maximum negative command, when $\delta_1 = \delta_2 = \ldots = \delta_N = 0$, the sum $\sum_{l=1}^{N} 2^{l-1}\delta_l(i) = 1$ and $K_C = K_{C\ min} = -(2^N - 2)$. Therefore, for the command coefficient K_{Cc} we find

$$K_{Cc} = \frac{2\sum_{l=1}^{N} 2^{l-1}\delta_l(i) - 2^N}{2^N - 2} = \frac{2\left[\sum_{l=1}^{N} 2^{l-1}\delta_l(i) - 1\right]}{2^N - 2} - 1. \qquad (7.5.4)$$

We note that formula (7.5.4) in form resembles the expression for the command coefficients in CCRL with pulse-width and pulse-phase modulation, equal to

$$K_{Cc} = \frac{T_1 - T_2}{T} = \frac{2T_1}{T} - 1,$$

if it is recalled that in CCRL with pulse-width and pulse-phase modulation, the value $K_{C\ max} = T$, and in CCRL with pulse-code modulation $K_{C\ max} = 2^N - 2$ and the expression $\sum_{l=1}^{N} 2^{l-1}\delta_l(i) - 1$ is equivalent to T_1.

When a CCRL with pulse-code modulation is based on the use of one sign-constant sequence of numbers, each semi-open and open interval corresponds to one well-defined number.

Since a N-unit binary code ensures that there will be an even number of numbers 2^N, in order for the CCRL amplitude characteristic to be symmetrical relative to the K_a axis, one of the numbers of the sequence should not participate in expression of commands. In theory $K_a = 0$ can be defined by any number, but as will be demonstrated below the simplest coder and decoder are obtained when $K_a = 0$ is expressed by the number 2^{N-1}.

Since at the transmitting end a zero value K_a is fixed by a number not equal to zero, the decoder must have a time-constant voltage equal to the signal produced by the decoder when $K_a = 0$. The presence of this voltage /334 ensures the symmetry of the CCRL amplitude characteristic as a whole. The values of the command and the command coefficient at the coder output when

expressing K_a by a single sequence of numbers of constant sign are determined by the following formulas

$$K_C = \sum_{l=1}^{N} 2^{l-1}\delta_l(i) = k_C K_a + 2^{N-1}, \tag{7.5.5}$$

$$K_{Cc} = \frac{\sum_{l=1}^{N} 2^{l-1}\delta_l(i)}{2^N - 1}. \tag{7.5.6}$$

In such a method for transmission of K_a, the command coefficient K_{Cc} can vary in the range $\frac{1}{2^N - 1}$ to +1 if the number 0 is not used for expressing transmitted commands.

7.6. CCRL Coders and Decoders with Pulse-Code Modulation

Coders with pulse-code modulation usually include elements by means of which pulse-counting or pulse-amplitude modulation is accomplished under the influence of a continuously changing signal, followed by conversion of these forms of modulation into pulse-code modulation. In addition, it is possible to use special electronic or electromechanical devices for converting a continuously changing value into a binary code.

As an illustration of the technical implementation of methods for the conversion of continuous K_a signals into sequences of binary numbers, we will consider possible designs of coders based on primary pulse-counting modulation for a single-channel CCRL with a time method for separation of digits. More detailed information on devices for conversion of continuous signals into binary codes can be found in the book cited as reference 63. The functional diagram of a coder ensuring the production of a starting signal in the form of a timing code and a sequential binary code, formed by individual video pulses, is shown in figure 7.27 for a CCRL with a sign-constant sequence of numbers. /335

The pulse generator PG produces periodic pulses u_{PG} (fig. 7.28a) whose repetition period T_i determines the interval of quantization of the K_a input signals. By means of the frequency divider Div, operating under the influence of the PG, u_{div} pulses are formed (fig. 7.28b) with the repetition period T, characterizing the period (rate) of transmission of commands. These pulses, and also the K_a dc current, are fed to the modulator M, where under the influence of K_a width-modulated video pulses u_M are formed (fig. 7.28c). The

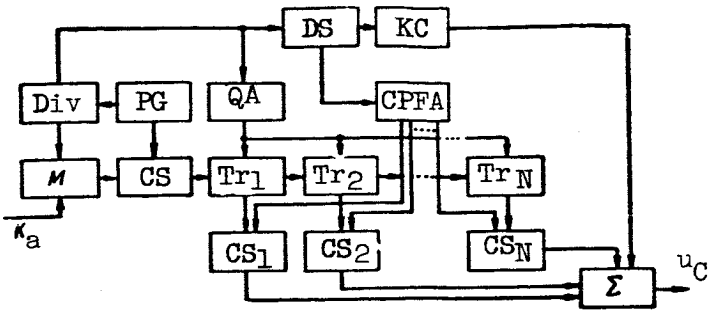

Figure 7.27

modulator M is designed in such a way that with a command corresponding to the lower limit of the n-th interval (fig. 7.25), the duration of the u_M input pulses is n periods of T_i. Pulse-width modulation is converted into pulse-counting modulation in the coincidence stages CS. In order for the amplitude characteristic of the CCRL to be obtained in the form shown in figure 7.2b, the leading edges of the pulses are somewhat steep. It is also possible to use for this purpose the delay stage of u_M signals forming part of the modulator M. /336

As a result of all the mentioned conversions, the number of u_{CS} pulses (fig. 7.28d) produced in the CS during the period T characterizes the value and sign of the transmitted command. The u_{CS} pulses are fed to a binary counter (binary scaler) having the triggers Tr_1, Tr_2, ..., Tr_N (fig. 7.27). The number N of triggers is determined by the type of binary code.

Before beginning formation of the binary code all the right trigger tubes are blocked and the left tubes operate. This is accomplished using a regenerator Reg which produces a pulse acting on the grids of the right tubes.

After the binary counter, whose principle of operation was discussed in chapter 5, is ready for operation, the counting of the number of pulses fed from the CS begins.

The signals from the counter come from the anodes of the left tubes of each trigger, connected to the coincidence stages CS_1, CS_2, ..., CS_N. These stages are fed positive pulses from the apparatus for forming commutating pulses CPFA. The distance between the CPFA pulses should correspond to the intervals between successive pulses denoting the digits of the binary code. The CPFA is controlled by signals produced by the delay stage DS. Under the influence of the voltage u_{div}, the DS is used in forming the pulses u_{DS}

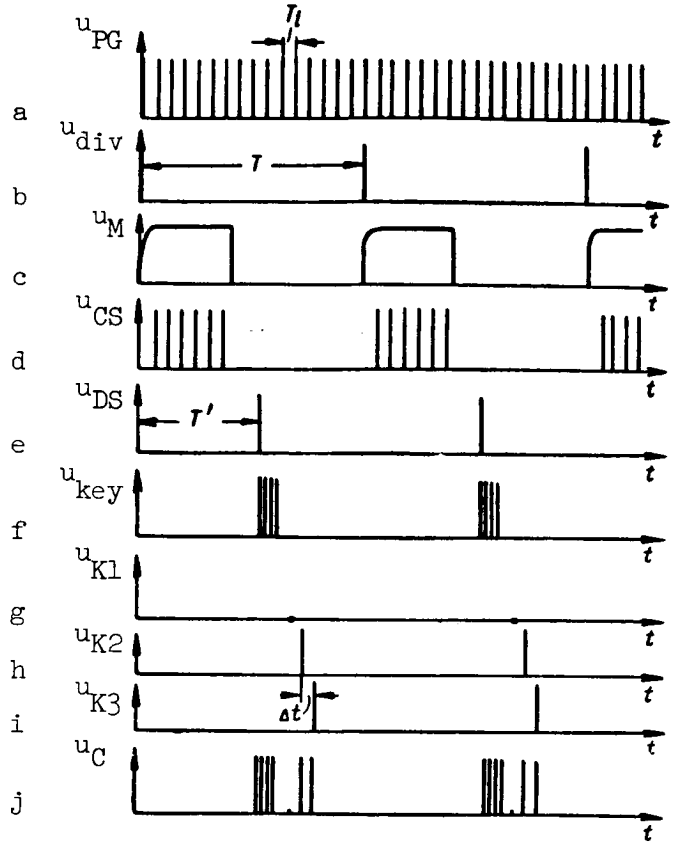

Figure 7.28

(fig. 7.28e) which are separated from the u_{div} signals by the time T', which slightly exceeds the maximum possible duration of the u_M pulses. As a result, the binary code pulses for any K_a are produced after termination of all transient processes in a binary scaler.

In addition to control of the CPFA, the delay stage signals are used for forming the key. This is performed by the key coder KC. Figure 7.28f shows a four-pulse key code. Pulses are fed from the coincidence stages CS_1, CS_2, ..., CS_N to the summer Σ only in those cases when the left tubes of the corresponding triggers are blocked out. For example, if six pulses are formed at the output of the CS stage, there will be no pulses at the CS_1 output (fig. 7.28g), and signals are fed from the CS_2 and CS_3 outputs (fig. 7.28h, i) which characterize digits (twos and fours). The output signal of the coder is u_C pulses produced at the output of the summer (fig. 7.28j).

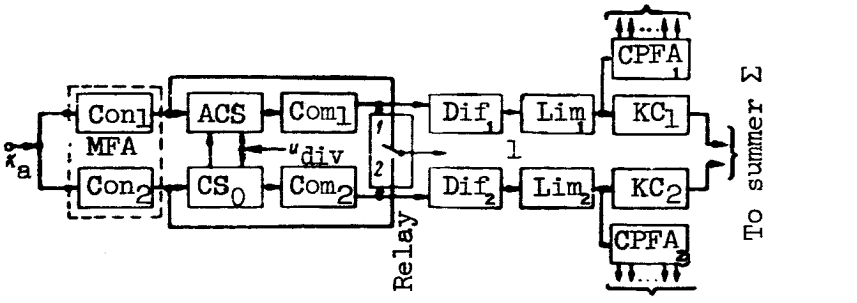

Figure 7.29

If it is necessary to use the principle of code or frequency selection of digits, the pulses produced at the CS_1, CS_2, ..., CS_N outputs should /337

be converted into timing codes or groups of sinusoidal oscillations with different frequencies.

When designing coders for multichannel CCRL, it is necessary to make provision for a corresponding number of binary counters, coincidence stages, key coders, commutators and devices for conversion of K_a into signals modulated in

accordance with the pulse counting modulation law. Here it is necessary to bear in mind that the interval ΔT between the first pulse of the key code in the first channel and the next u_{div} pulse should be such that it can contain

the pulses of all the timing codes of the keys and binary codes if all the primary modulators are triggered simultaneously. In order to ensure the possibility of a uniform distribution of keys and binary codes in the interval T, the apparatus performing pulse-width modulation for the different channels

must be triggered with a time shift of $\frac{T}{N_k}$.

If a sign-variable sequence of numbers is used for transmission of commands, it is essential to convert the odd function $K_a(t)$ into an even function.

In essence this means that the coder must contain devices ensuring determination of the absolute value $|K_a(t)|$. In addition, the coder should form start-

ing pulses with different qualitative criteria during transmission of positive and negative values $K_a(t)$.

For solution of these problems, it is possible to use the apparatus whose functional diagram is shown in figure 7.29.

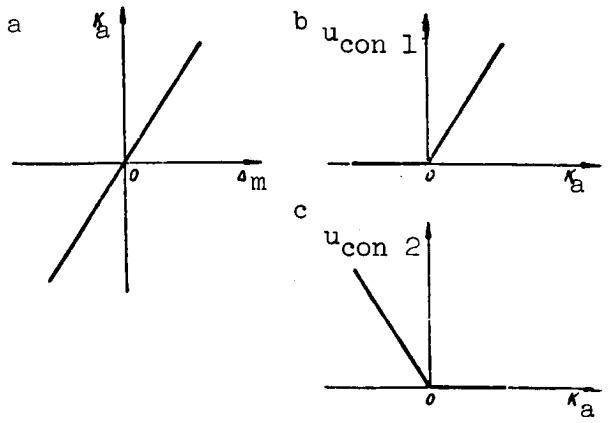

Figure 7.30

By means of the modulus-forming apparatus MFA, containing devices Con_1 and Con_2, the odd function K_a of Δ_m (figure 7.30a) is converted into two voltages. The voltages $u_{con\ 1}$ (fig. 7.30b) is produced by the converter Con_1, trans- /338 mitting to the output only the positive values K_a, and the voltage $u_{con\ 2}$ (fig. 7.30c) is produced as a result of passage of K_a through the converter Con_2, which reacts only to negative values K_a. In Con_2 there is also a change of the polarity K_a. As Con_1 and Con_2 which should have rigorously identical amplitude characteristics, it is possible to use rectifier (diode) instruments with dc amplifiers.

The voltages $u_{con\ 1}$ and $u_{con\ 2}$ can be fed to a circuit for conversion of a dc current to a binary code, one of whose variants is shown in figure 7.27. However, the DS, CPFA and KC should be excluded in this circuit. The voltages $u_{con\ 1}$ and $u_{con\ 2}$ are connected to the modulator M, shown in figure 7.27, by the electromagnetic polarized relay Rel, whose movable contact is closed with the bars 1 and 2 during transmission of positive and negative values K_a.

The position of the movable contact of the relay Rel is controlled by the pulses of the commutators Com_1 and Com_2, to one of which signals are fed from the anticoincidence stage ACS, while signals from the coincidence stage CS_0 are fed to the other.

The coincidence stage CS_0 feeds a brief dc pulse only in those cases when it is fed divider pulses u_{div} (fig. 7.28b), and the value $u_{con\ 2}$ is equal to

or exceeds the voltage u necessary for obtaining one or a large number of pulses at the CS output (fig. 7.27). Pulses are not formed at the CS_0 output if $u_{con\ 2} < u$.

The anticoincidence stage transmits to the output u_{div} pulses in all cases when there are no CS_0 signals. Since the CS_0 forms pulses only during transmission of negative values K_a, the commutator Com_1 will be triggered /339 by the voltage u_{div} during transmission of $K_a \geq 0$.

The commutators Com_1 and Com_2 convert signals fed from CS_0 and ACS into pulses with durations slightly exceeding the width of the signals produced by M (fig. 7.27) when it is fed a maximum command.

The formation of the key codes and the pulses for commutation of the coincidence stages CS_1, CS_2, ..., CS_N (fig. 7.27) is accomplished with the differentiators Dif_1 and Dif_2, the limiters Lim_1 and Lim_2, the key coders KC_1 and KC_2 and also the apparatus for forming commutating pulses $CPFA_1$ and $CPFA_2$ (fig. 7.29). In this case, the position of the first pulses in the key codes corresponds to the times of ending of the feeding of the Com_1 and Com_2 pulses.

The signals forming at the KC_1, KC_2, $CPFA_1$ and $CPFA_2$ outputs (fig. 7.29) should be fed to the summer Σ and the coincidence stages CS_1, CS_2, ..., CS_N, respectively (fig. 7.27).

Figure 7.29 shows that the considered coder will be more complex than a CCRL coder designed for forming commands when using one sign-constant sequence of numbers.

The sign of the command can be expressed not only by key codes, but also by a corresponding spacing of the binary code pulses. For example, it is quite easy to design a coder in which the same key code is formed during the transmission of $K_a \geq 0$ and $K_a < 0$, whereas the binary code pulses when $K_a \geq 0$ and $K_a < 0$ are displaced by equal intervals relative to the key.

Henceforth, depending on the method for setting the sign of the transmitted command, we will distinguish CCRL with one or two key codes.

When transmitting a single command by use of two binary codes, the sum of whose numbers is constant and equal to 2^N for any value K_a, the CCRL coder can be constructed, as follows from equation (7.5.3), in accordance with the

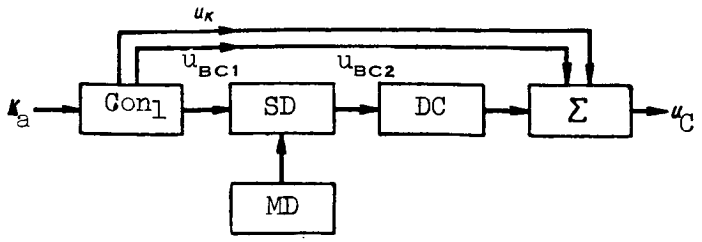

Figure 7.31

diagram shown in figure 7.31. In this figure Con_1 represents the apparatus whose functional diagram is shown in figure 7.27 if the summer Σ is excluded. The voltage $u_{BC\ 1}$, characterizing the first binary code, is fed to /340 the subtracting device SD, which also is fed signals from the memory devices MD. The number 2^N is stored in the MD. At the SD output, the pulses $u_{BC\ 2}$ of the second binary code are formed. After delay of time t_1 by the delay cell DC, these pulses, together with the key pulses u_k and the pulses of the first binary code $u_{BC\ 1}$, are fed to the summer Σ.

We note that in the coder shown in figure 7.31 only one key code is used for both codes and that in the transmission of $K_a = 0$, a code is formed in Con_1 which expresses the number 2^{N-1}.

In the case of use of sinusoidal subcarrier oscillations, the coders can be designed in a similar way.

If it is necessary to transmit several commands for different purposes, coders of the second and third types must include corresponding additional apparatus.

The diagrams of coders are simplified considerably if the command forming apparatus produces signals in the form of numbers in a binary numbering system. In this case, the coder will include only a device for feeding data from the CPFA and stages for forming key codes.

At the output of a CCRL with pulse-code modulation, in most cases, it is necessary to obtain a command K in the form of a voltage or current. This problem can be solved by use of electromechanical, ionic or electronic instruments. In most cases, it is desirable to use electronic apparatus ensuring virtually inertialess operation of the CCRL.

When transmitting K_a commands by a single sequence of numbers of constant sign, the analysis of signals in a single-channel CCRL can be accomplished in

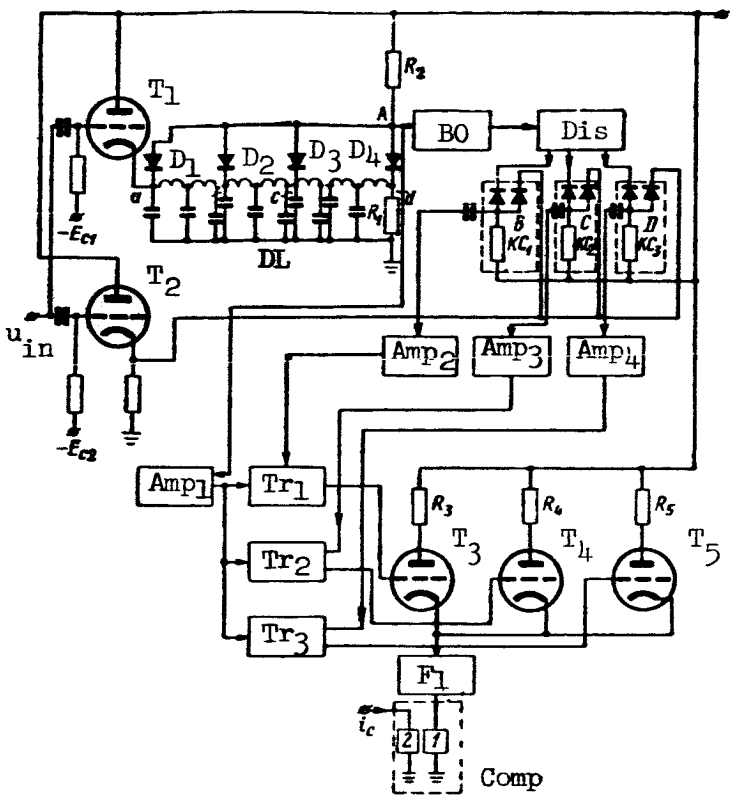

Figure 7.32

the decoder whose diagram, suited for the reception of a three-unit binary code with time separation of digits, is shown in figure 7.32.

The voltage u_{in}, characterizing a four-pulse timing key code, and binary code pulses expressing the number 6 (fig. 7.33a) are fed to the tube T_1 of the coincidence stage and the cathode follower T_2.

In addition to the tube T_1, the coincidence stage contains a delay line DL, diodes D_1-D_4 and resistances R_1 and R_2. The value R_1 is equal to the wave resistance of the DL. The leads from the DL are arranged in such a way that at the point A a pulse u_k is formed (fig. 7.33b) only in a case when the T_1 input is fed a key code. The u_{in} pulse detected in this way from the general sequence of signals, whose position coincides in time with the feeding of the last key code pulse, is used for separation of the binary code digits for different circuits. This problem is solved in the following way. The signals from the point A are fed to the delayed blocking oscillator BO, where square pulses are produced. These pulses are used for control of operation of /341

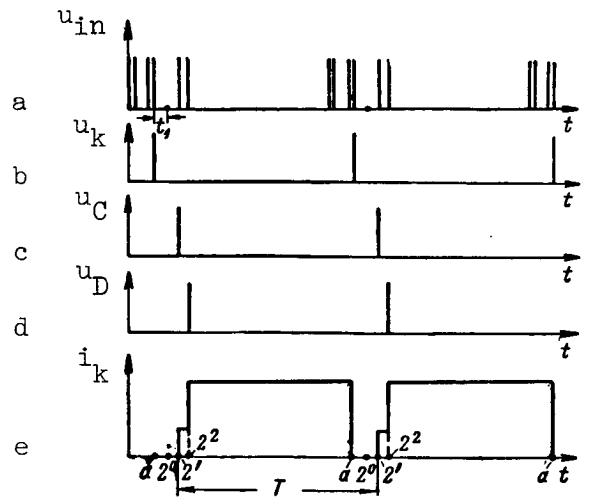

Figure 7.33

the distributor Dis. The latter in the simplest case is a delay line or a tube commutator. The distributor Dis has N outputs (in the considered case, three) at each of which pulses are formed which are separated from the last pulse of the key code by intervals corresponding to the distance of this pulse from the binary code digit pulses.

The signals from Dis and the cathode follower T_2 are fed to the coincidence stages CS_1, CS_2 and CS_3 (fig. 7.32). At the points B, C and D of the circuit, pulses appear which denote the digits of a binary code only under the condition of simultaneous feeding of signals to both diodes in the coincidence stage. For the considered example of CCRL transmission of the number 6, the pulses appear only at the points C and D (fig. 7.33c, d). After amplification of these pulses in Amp_2, Amp_3 and Amp_4, they are fed to the grids of the left tubes of the triggers Tr_1, Tr_2 and Tr_3 forming the decoder. The preliminary preparation of triggers for operation is accomplished by a key pulse amplified in Amp_1, under whose influence the right tubes of all the triggers /342 are blocked out, while the left tubes are triggered. In this case the triodes Tri_3, Tri_4 and Tri_5, which together with the resistances R_3, R_4 and R_5 form the measuring circuit, also are blocked. Under the influence of the signals fed from Amp_2, Amp_3 and Amp_4, the corresponding triggers are operated and the tubes T_3, T_4 and T_5 are unblocked.

In the considered example, in transmission of the number 6, the triodes Tri_4 and Tri_5 are unblocked. The total anode current of the tubes T_3, T_4 and T_5 is fed through the filter F_1 to the winding 1 of an electromagnetic relay

performing the role of a comparison device CD. In order for the value of the output command to correspond to the transmitted communication, the resistances R_3, R_4 and R_5 are selected in accordance with a binary numbering system. The values of the resistances R_3, R_4 and R_5 should be such that the currents i_{a5} and i_{a4} of the tubes T_5 and T_4 are 4 and 2 times greater than the current $i_{a3} = i_{1d}$ of the tube T_3. We note that the current i_{1d} characterizes a single digit of the binary code. The total current i_k in the measuring circuit has a pulse character. As an example, figure 7.33e shows a graph characterizing the dependence of i_k on time t when transmitting the number 6 by a three-digit binary code. In this figure, the points a, 2^0, 2^1 and 2^2 denote the times of appearance of the signals u_k and pulses which determine in a binary code the digits 2^0, 2^1 and 2^2. The amplitude i_{km} of the i_k pulses in figure 7.33e is 6i. In a general case of use of a N-digit binary code, the value i_k is equal to

$$i_{km} = i_{1d} \sum_{l=1}^{N} 2^{l-1} \delta_l(i), \tag{7.6.1}$$

where the function $\delta_l(i)$ assumes the same values as in the expressions determining the coder output command.

It is easy to demonstrate that in order to ensure a proportional dependence between the transmitted number and the mean component i_{mean} of the current $i_k(t)$, it is necessary that the intervals between the binary code pulses be insignificant in comparison with the period T.

Usually, the interval between successive binary code pulses is several units or tens of microseconds, at the same time that the value T exceeds tens and hundreds of thousands of microseconds. In this connection, it can be assumed with a sufficient degree of accuracy that the pulses $i_k(t)$ have a square form and a duration equal to $T - t_1$, where t_1 is the interval between the points a and 2^0 shown in figure 7.33e. Then at the output of the smoothing filter F_1 (fig. 7.32) when K_a = const in a stationary regime we will have

/343

$$i_{mean} = i_{1d} k_{F1} \sum_{l=1}^{N} 2^{l-1} \delta_l(i) \frac{T - t_1}{T}. \tag{7.6.2}$$

where k_{F1} is the transfer constant of the filter F_1 for the constant component of the current.

It is most desirable to construct a CCRL in such a way as to satisfy the condition $t_1 \ll T$. In this case, i_{mean} will virtually coincide with i_{km} and there is no need of a smoothing filter.

Under the influence of the current i_k, fed first to the filter F_1, which sometimes can be absent, ampere turns AT_k are created in the winding 1 of the comparison device CD. We will assume that $t_1 \ll T$. Then

$$AT_k \approx k_{F1} i_{km} W_1 = i_{1d} W_1 \sum_{l=1}^{N} 2^{l-1} \delta_l(i), \qquad (7.6.3)$$

where W_1 is the number of turns in the winding 1 of the comparison device.

In order to obtain an odd CCRL amplitude characteristic, the winding 2 of the comparison device CD is connected to a voltage source ensuring that a comparison current i_c equal to $2^{N-1} i'_{1d}$ will pass through it. Under the influence of this current, comparison ampere turns AT_{mean} are created. Then the CCRL output command, representing the difference of the ampere turns and under whose influence proportional movement of the rocket control surfaces will occur, will be equal to

$$K = AT_k - AT_{mean} = \left[k_{F1} i_{1d} W_1 \sum_{l=1}^{N} 2^{l-1} \delta_l(i) - 2^{N-1} W_2 i'_{1d} \right], \qquad (7.6.4)$$

where W_2 is the number of turns in the winding 2 of the comparison device.

This expression and also all the subsequent formulas used for determination of the value of the command K as well as the coefficient of this command K_c are correct only for segments under the same condition as relation (7.5.1).

Since

$$K_c = \sum_{l=1}^{N} 2^{l-1} \delta_l(i) = k_c K_a + 2^{N-1},$$

then

$$K = K_{F1} W_1 i_{1d} K_c - 2^{N-1} W_2 i'_{1d}$$

or

/344

$$K = k_{Fl} i_{ld} W_l k_C K_a + 2^{N-1}(k_{Fl} i_{ld} W_l - i'_{ld} W_2)$$

$$= k_{Dl} k_C K_a + 2^{N-1}(k_{Dl} - i'_{ld} W_2),$$

where $k_{Dl} = i_{ld} W_l k_{Fl}$ is the transfer constant of the decoder.

It can be seen from the last expression that, in order to obtain K = 0 when $K_a = 0$, it is necessary to ensure the equality $k_{Fl} i_{ld} W_l = i'_{ld} W_2$, which is achieved by balancing the CCRL output stages.

In a balanced CCRL

$$K = i_{ld} W_l k_C K_a, \tag{7.6.5}$$

and the dependence of K on K_C is determined by the following formula

$$K = k_{Fl} i_{ld} W_l (K_C - 2^{N-1}). \tag{7.6.6}$$

We recall that in expression (7.6.5) the value $k_{Fl} i_{ld} W_l k_C$ represents the transfer constant k_{CCRL} of the command control radio link.

Since in accordance with expression (7.6.6)

$$K_{max} = k_{Fl} i_{ld} W_l (2^{N-1} - 1),$$

as the command coefficient K_c at the CCRL output we find

$$K_c = \frac{\sum_{l=1}^{N} 2^{l-1} \vartheta_l(i) - 2^{N-1}}{2^{N-1} - 1} = \frac{\left[\sum_{l=1}^{N} 2^{l-1} \vartheta_l(i) - 1\right]}{2^{N-1} - 1} - 1. \tag{7.6.7}$$

We note that this relation is similar to the expression for K_c in CCRL with pulse-width and pulse-phase modulation.

Taking into account that

$$K_{Cc}=\frac{\sum_{l=1}^{N}2^{l-1}\delta_l(i)}{2^N-1},$$

we also can obtain

$$K_c=\frac{(2^N-1)(K_{Cc}-2^{N-1})}{2^{N-1}-1}. \tag{7.6.8}$$

If the real durations $T_{1.l}$ of pulses forming at the outputs of the decoder triggers when they are fed signals characterizing the digits 2^{l-1} ($l = 1, 2, \ldots, N$) are taken into account, we obtain

$$K=k_{Fl}W_1i_{ld}\sum_{l=1}^{N}2^{l-1}\delta_l(i)\frac{T_{1.l}}{T}-\Delta T_{mean}.$$

If the CCRL is balanced, the following condition should be satisfied /345

$$\Delta T_{mean}=k_{Fl}W_1i_{ld}2^{N-1}\frac{T_{1.N}}{T},$$

where $T_{1.N}$ is the duration of a pulse expressing the digit 2^{N-1}. Then

$$K=k_{Fl}W_1i_{ld}\left[\sum_{l=1}^{N}2^{l-1}\delta_l(i)\frac{T_{1.l}}{T}-2^{N-1}\frac{T_{1.N}}{T}\right].$$

This expression shows that K will not be a linear function of the command $K_C=\sum_{l=1}^{N}2^{l-1}\delta_l(i)$, produced by the coder. However, if the intervals between any successive pulses of a binary code are identical and equal to $\Delta\tau$, the latter expression is reduced to the following form

$$K=k_{Fl}W_1i_{ld}\left[\frac{T_{1.1}}{T}K_C+\frac{\Delta\tau}{T}\sum_{l=1}^{N}2^{l-1}(N-l)\delta_l(i)-2^{N-1}\frac{T_{1.N}}{T}\right]$$

In order to achieve total elimination of the nonlinearity of the CCRL amplitude characteristic, it is necessary that a device be placed between the binary decoding circuit and the filter F_1 for storing the amplitude i_{km} of the

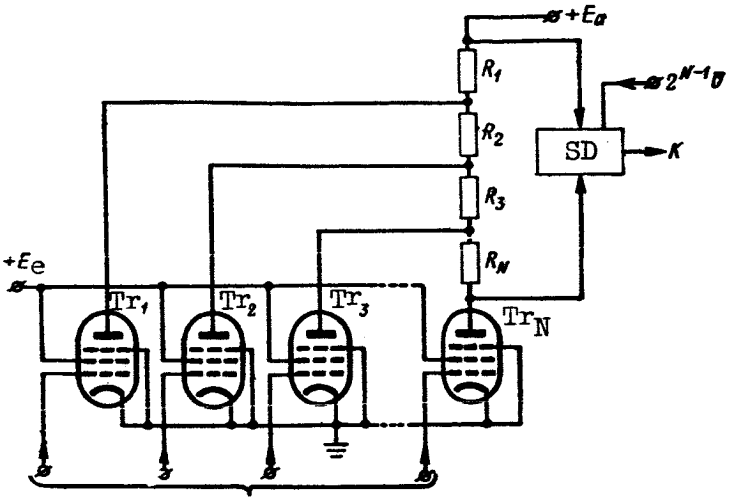

Figure 7.34

current i_k and that the filter F_1 be connected to its output only after termination of transient processes in the decoder.

If it is necessary to obtain a command in the form of a dc voltage at the CCRL output, the measuring apparatus can be designed as shown in figure 7.34. This same figure shows the subtracting device SD to which is fed the comparison voltage $2^{N-1}U$. In this case, the measuring apparatus is an N-stage amplifier, each tube of which is activated by a pulse of a corresponding trigger. The operation of the tubes is selected in such a way that their plate currents will be identical and the voltages created by these currents on the plate resistances will be related as $1:2:4:\ldots:2^{N-1}$. Under these conditions the load resistances $R_1, R_2, R_3, \ldots, R_N$ should be equal to $R_0, R_0, 2R_0, \ldots, 2^{(N-2)}R_0$, where the value R_0 is determined by the characteristics of the tubes and the set range of change of the CCRL output signal. The voltage u_k is fed from the resistances $R_1, R_2, \ldots, R_N$ in the form of dc pulses produced by the measuring apparatus.

If the remarks presented above on the intervals between the binary code pulses and the value t_1 are taken into account, we obtain the following /346

decoder equation for a balanced CCRL

$$K = U\left[\sum_{l=1}^{N} 2^{l-1}\delta_l(i) - 2^{N-1}\right], \qquad (7.6.9)$$

where U is the voltage from the resistance R_1.

As in a decoder with a current measuring circuit, the stability of the output signals K produced by the apparatus whose diagram is shown in figure 7.34 is dependent on fluctuations of the voltages $u_{mean} = 2^{N-1} U$ and u_k, and also on variations of the interval resistances of the tubes T_1, T_2, ..., T_N.

The stability of the CCRL output signals can be increased considerably if the resistances R_1, R_2, ..., R_N (fig. 7.34) are not cut in by the tubes T_1, T_2, ..., T_N, but by means of the contacts of electromagnetic relays. The windings of these relays should be cut into the cathode circuits of the tubes of the cathode followers, which should replace the amplifiers T_1, T_2, ..., T_N shown in figure 7.34.

Some possible variants of diagrams of relay measuring apparatus are shown in figure 7.35a, b, c. The first two variants are based on the principle of use of voltage bridges, and the third uses a current bridge.

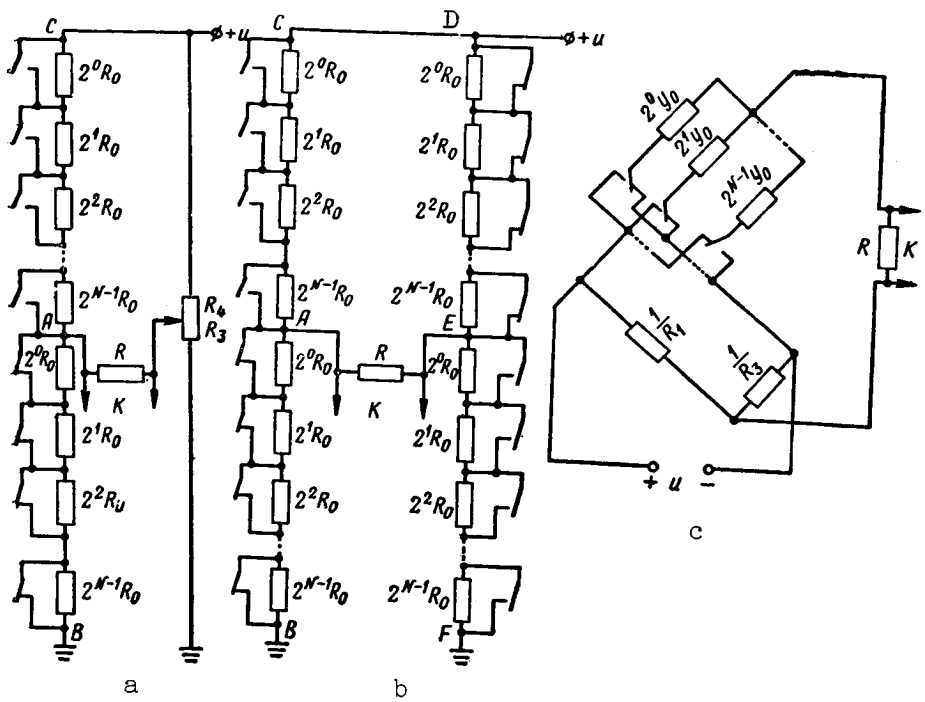

Figure 7.35

In an apparatus of the first type, upon arrival of particular binary code pulses, the corresponding contacts of the relay in the arm AB are opened and those in the arm AC are closed. In the transmission of a zero command, the signal K from the bridge diagonal should be equal to zero. This can be /347

achieved by cutting in the resistance $2^{N-1}R_0$ into the circuit AB and short-circuiting the resistance of this same value in the arm AC, thereby balancing the bridge by a change of R_3 and R_4.

It is known that the output voltage of a bridge (fig. 7.35a) located on the resistance R is equal to

$$K = u\frac{R_1R_4 - R_2R_3}{(R_1+R_2)(R_3+R_4)+\frac{R_1R_2}{R}(R_3+R_4)+\frac{R_3R_4}{R}(R_1+R_2)}. \qquad (7.6.10)$$

During transmission of commands, the resistance R_1 characterizing the arm AB changes in conformity to the law $\sum_{l=1}^{N} 2^{l-1}\delta_l(i)$, and the sum is

$$R_1 + R_2 = (2^N - 1)R_0$$

which remains constant. We note that R_2 corresponds to the resistance in the arm AC (fig. 7.35a).

It is easy to show that in a bridge ensuring K = 0, the following /348

condition should be satisfied when transmitting the number 2^{N-1}

$$\frac{R_3}{R_4} = \frac{R_1}{R_2} = \frac{2^{N-1}}{2^{N-1}-1}.$$

Taking these comments into account, on the basis of expression (7.6.10) we obtain the equation for a decoder using the bridge measuring circuit shown in figure 7.35a

$$K = u\frac{\sum_{l=1}^{N} 2^{l-1}\delta_l(i) - 2^{N-1}}{2^N - 1 + (2^{N-1}-1)\frac{R_3}{R} + \left[2^N - 1 - \sum_{l=1}^{N} 2^{l-1}\delta_l(i)\right] 2^{l-1}\delta_l(i)\frac{R_0}{R}} \qquad (7.6.11)$$

This equation shows that such a decoder has a nonlinear amplitude characteristic drawn through the middle of the steps. However, in selection of the

ratio $\frac{R_0}{R} \ll 1$, the dependence of K on K_C can be made virtually linear for the entire range of changes K_C, that is, we can obtain

$$K \approx u \frac{\sum_{l=1}^{N} 2^{l-1}\delta_l(i) - 2^{N-1}}{2^N - 1 + (2^{N-1}-1)\frac{R_3}{R}} = k_{D1}\left[\sum_{l=1}^{N} 2^{l-1}\delta_l(i) - 2^{N-1}\right], \qquad (7.6.12)$$

where

$$k_{D1} = \frac{u}{2^N - 1 + (2^{N-1}-1)\frac{R_3}{R}}$$

is the decoder transfer constant.

In the measuring circuit shown in figure 7.35b, with the arrival of the pulse of the l-th digit, there will be a switching of the resistances $2^{l-1}R_0$ in all arms of the bridge. As a result, there is approximately a double increase of the decoder transfer constant.

The following expression can be derived for the voltage K from the output of a measuring apparatus based on use of a current bridge (fig. 7.35c)

$$K = u \frac{\sum_{l=1}^{N} 2^{l-1}\delta_l(i) - 2^{N-1}}{2^N - 1 + \frac{R_0}{R} + (2^{N-1}-1)\frac{R_3}{R}}. \qquad (7.6.13)$$

It should be noted that a current bridge, in which there is switching from one arm to another of resistances whose conductivities change in conformity to the binary law, ensures a linear amplitude characteristic of the decoder. The transfer constant of such a decoder, when $\frac{R_0}{R} \ll 1$, is equal /349 to k_{D1} obtained when using a bridge of the first type.

We note in conclusion that the diagrams of bridge measuring apparatus considered here, making it possible to "ground" one pole of the voltage source, do not exhaust all the possible methods for designing CCRL with pulse-code modulation. For example, it is possible to use self-balancing bridges, differential measuring circuits, etc. The problem of what measuring apparatus should actually be used is solved taking into account the specific requirements imposed on the CCRL.

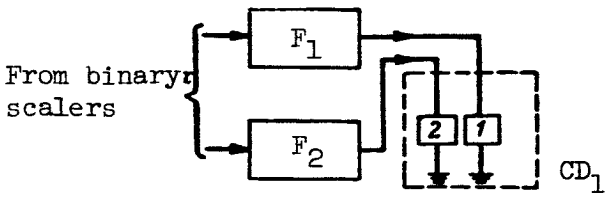

Figure 7.36

CCRL decoders in which the transmission of commands is accomplished using one sign-variable sequence of numbers in essence are a combination of the two apparatuses considered above. If a current measuring circuit is used, the windings 1 and 2 of the comparison device CD_1 (fig. 7.36) are the load for each of these apparatuses.

These windings are fed signals from the low-frequency filters F_1 and F_2, connected to the decoders (binary scalers), one of which operates for positive transmitted commands and the other for negative transmitted commands.

When it is necessary to obtain K in the form of a dc voltage, there must be two corresponding voltage-measuring apparatuses.

The dependence of the CCRL output signal on the value of the command produced by the coder when using measuring circuits shown in figures 7.32 and 7.34, in the case of using one sign-variable sequence of numbers, has the following form

$$K = ak_{F1}AT_1\sum_{l=1}^{N}2^{l-1}\delta_l(i) + (a-1)k_{F2}AT_2\sum_{l=1}^{N}2^{l-1}\delta_l(i) \qquad (7.6.14)$$

and

$$K = aU_1\sum_{l=1}^{N}2^{l-1}\delta_l(i) + (a-1)U_2\sum_{l=1}^{N}2^{l-1}\delta_l(i), \qquad (7.6.15)$$

where AT_1 and AT_2 are the ampere turns produced by the windings 1 and 2 in the comparison device (fig. 7.36), U_1 and U_2 are the voltages formed by the first and second binary circuits during transmission of the minimum values of negative and positive commands, and a is a coefficient equal to +1 when $K_a \geq 0$ and to 0 when $K_a < 0$.

In order to obtain a symmetrical amplitude characteristic, it is necessary to satisfy the condition /350

$$k_{F1}AT_1 = k_{F2}AT_2 = k_FAT \text{ and } U_1 = U_2 = U.$$

When commands are transmitted by the difference of the numbers of two sequences, when using two starting pulses to express the command of one channel, the decoder should be the same as in CCRL with one sign-variable sequence of numbers. If the same starting pulse is used for both binary codes, the decoder should have one rather than two key pulse discriminators and the commutation circuit should be modified accordingly.

The resulting command K at the output of a CCRL based on use of the difference of two sequences of numbers, in the case of use of identical measuring circuits shown in figures 7.32 and 7.34 (if it is assumed that $T_{1.i} \approx T$) is

$$K = k_F i_{1d} W \left[2 \sum_{l=1}^{N} 2^{l-1} \delta_l(i) - 2^N \right] \tag{7.6.16}$$

and

$$K = U \left[2 \sum_{l=1}^{N} 2^{l-1} \delta_l(i) - 2^N \right] \tag{7.6.17}$$

Here i_{1d} and U are the current and voltage produced by the binary decoding circuits during transmission of the number 1, W is the number of turns in windings 1 and 2 (fig. 7.36), and k_F is the transfer constant of the filters F_1 and F_2 (fig. 7.36).

By determining the value K_{max} from expressions (7.6.13), (7.6.14), (7.6.15), (7.6.16) and (7.6.17), is is easy to derive formulas making it possible to determine the command coefficients K_c for different types of CCRL.

Some distinguishing characteristics of CCRL with pulse-code modulation are the possibility of ensuring a high stability of transmission and registry (at the receiving end) of numbers characterizing $K_a = 0$ and the presence of errors in the level-quantized transmitted signals. In addition, it should be noted that it is convenient to couple CCRL to a numerical command forming apparatus, which is not the case for CCRL with pulse-width modulation, pulse-counting modulation and pulse-phase modulation, since their coupling requires devices for conversion of continuous signals into numerical signals. However, whereas the first and third characteristics of a CCRL with pulse-code modulation are advantageous, the second may be regarded as a shortcoming. This can be attributed to the fact that a quantization error leads to the appearance of additional errors of rocket guidance.

We note in conclusion that the considered designs of coders and decoders are based on the use of binary codes which are indicative "incomplete" codes

characterizing a different number of pulses for the expression of different numbers. At the same time, "complete" codes also can be used for command /351 transmission; the characteristic feature of such codes is a constancy of the number of pulses, regardless of the value K_a. For example, an associative code is a "complete" code.

The use of "complete" codes makes it possible to take additional measures for increasing the noise immunity of CCRL. However, it must be remembered that with an identical maximum number of pulses in the code, the number of possible combinations in a "complete" code is considerably less than in an "incomplete" code.

7.7. Command Control Radio Links for Transmission of Single Commands

For transmission of single commands, the CCRL should be designed in such a way that at the receiving end there will be separation of the subcarriers in separate circuits. Single commands usually are irreversible. This means that it is impossible to restore the former state of the actuating apparatus after it has received commands. CCRL designed for transmission of single commands, therefore, should have a high simulation stability. Simulation stability is ensured by the use of such codes as are difficult to reproduce by interference. It should be stated that high simulation stability still does not completely determine the noise immunity of the CCRL because it also is dependent on the characteristics of suppression of the transmitted commands.

Usually single commands in the CCRL coders are reflected by various code groups of pulses. In the simplest case, it is possible to use timing and frequency codes. For example, when a frequency code is used, the single command fed from the command forming apparatus in the form of a dc pulse is converted into pulses of a sinusoidal voltage of a fully determined frequency f_{sub}. Instead of one pulse, there can be several, acting simultaneously or at an interval.

In the case of timing coding, the command is converted into a group of video pulses with intervals between them set in advance.

If frequency codes are used for transmission of commands, the CCRL coders usually contain filters, tuned to the corresponding frequencies, coincidence stages and relays. As an example, figure 7.37 shows the diagram of a decoder for obtaining commands in the form of a dc voltage when a two-pulse frequency code is used in the CCRL coder. It is assumed here that both pulses act simultaneously. Groups of sinusoidal voltages are formed at the output of the filters F_1 and F_2 and these are converted into video pulses by the peak detectors PkD_1 and PkD_2. These video pulses act on the coincidence stage CS, connected to the relay Rel. By use of a contact of the relay Rel, a command /352

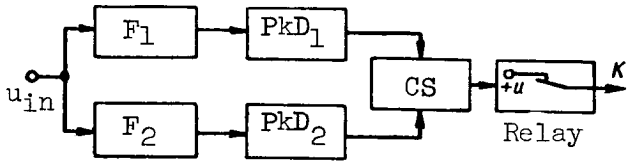

Figure 7.37

K is produced in the form of a dc voltage only under the condition that the input signal is the sum of two sinusoidal oscillations.

In addition to frequency and timing codes, it is possible to employ various kinds of pulse-counting codes. The simplest pulse-counting code is a sequence of a stipulated number of video pulses or pulses of sinusoidal oscillations. In such a method of command transmission, the output stages of the coder should operate on the pulse-counting principle.

In more complex systems, the commands are transmitted by numbers having several digits, each of which expresses a corresponding number of pulses. For example, it is possible to use six-digit numbers expressed by pulses such as in ordinary telephonic apparatus. In such coding the first single command is characterized by a single number (such as 50-37-68), the second by another, etc. If the command expresses the number 50-37-68, the figure 8 is transmitted by eight pulses, the figure 3 by three pulses, etc. Ten pulses are used for zero.

A code of the considered type sometimes is called a six-digit code with a base of 10. It consists of 10 different figures in groups of 6 nonrepeating numbers, entered in different sequence. The apparatus of the CCRL decoder in each channel should operate in such a way that the output command appears only with arrival of signals of a stipulated code.

In addition to frequency, timing and pulse-counting codes, there are other types as well. Selection of a specific type of code is based on the problems to be solved by the CCRL and the conditions under which it operates.

7.8. Selection and Computation of the Principal Parameters of CCRL Numerical Decoders

Certain initial data must be stipulated for developing the CCRL coders and decoders used for transmission of continuous commands. The selection and computation of these data, characterizing the principal parameters of the coders and decoders, should be accomplished taking into account the specific character of the operation of the CCRL as apparatus of the control system of pilotless objects.

The principal parameters of the coders and decoders of a CCRL are: /353

(1) the rate of transmission of commands, determined by the number of commands per unit time;

(2) the transmission bands of the separation filters;

(3) the separation and values of the subcarrier frequencies in the CCRL with frequency separation of signals;

(4) the capacity of the binary codes in a CCRL with pulse-code modulation and the repetition interval T_i in CCRL with pulse-counting modulation and pulse-frequency modulation;

(5) the capacity and structure of the timing codes.

1. Rate of Transmission of Control Commands

In most cases, in all types of CCRL the commands are transmitted discretely in time. This means that the signals K_a are converted into pulses which follow one another at definite intervals of time. These intervals form the command repetition interval T. The value $F = \frac{1}{T}$ is called the rate of command transmission. According to the V. A. Kotel'nikov theorem, for the precise reproduction of a continuously transmitted command $K_a(t)$ with a limited spectrum of frequencies, it is sufficient to transmit only individual values of the function $K_a(t)$ at the time T_{tr} equal to

$$T_{tr} = \frac{1}{2F_h},$$

where F_h is the higher frequency in the signal spectrum $K_a(t)$.

In general the spectrum of the mismatch parameter and, therefore, the spectrum of the transmitted commands can be quite broad. However, the rocket will not react to rapid changes of the command $K_a(t)$. Therefore, the value F_h in the transmitted signal $K_a(t)$ can be limited by the rocket passband ΔF_r. The value ΔF_r can be determined quite easily from equations describing rocket motion (chapter 9).

Since the V. A. Kotel'nikov theorem is based on the condition of use of optimal smoothing devices, which usually is an impossibility under actual conditions, the command transmission rate must be determined from the condition of a decrease of T_{tr} by not less than a factor of 5-10. Therefore

$$F \geq (10\text{-}20)\,\Delta F_r. \qquad (7.8.1)$$

For example, if ΔF_r = (0.5-2) cps, then $F \geq$ (5-40) cps.

2. Transmission Bands of Separation Filters

The separation filters in a CCRL with pulse-width modulation of sinusoidal subcarriers should have a transmission band ΔF_1 which ensures a virtually /354 undistorted transmission of the envelope of pulses having a minimum duration T_{min}. As is well known, it is necessary that

$$\Delta F_1 \geq \frac{2\text{-}3}{T_{min}}.$$

However, since

$$K_c = \frac{2T_1}{T} - 1,$$

taking into account that, when $K_c = K_{c\ min}$, the value $T_1 = T_{min}$, we obtain

$$\frac{T_{min}}{T} = \frac{K_{min} + 1}{2}.$$

Therefore

$$\Delta F_1 \geq \frac{4\text{-}6}{(K_{c\ min} + 1)T}. \qquad (7.8.2)$$

As an illustration, we point out that when $K_{min} = -0.8$ and $T = 0.1$ sec, the band ΔF_1 should be 200-300 cps.

The value ΔF_1 for a CCRL with phase modulation is determined by the spectra of the transmitted signals and the technical possibilities of devising separation filters.

In the final selection of the values ΔF_1 in both CCRL with pulse-width modulation and in CCRL with phase modulation, it is necessary to take into account the instability of the subcarrier frequency.

3. Frequency Separation of Subcarrier Oscillations

In selecting the separation of the subcarrier frequencies in a CCRL with sinusoidal subcarrier oscillations, it is necessary to use as a point of departure the admissible levels of the transient and cross connection distortions. Transient interference arises due to the entry of the components of the spectrum of oscillations of a signal of one subcarrier oscillation into the transmission band of the separation filter of the adjacent subcarrier signal. The level of transient interference is quite low if two adjacent subcarrier frequencies are separated by an interval equal to or exceeding $1.5\ \Delta F_1$.

The cause of cross connection distortions is the nonlinearity of the amplitude characteristics of the command transmission and reception channels. In order for the role of cross connection distortions to be reduced to an admissible minimum, it is necessary to select nonmultiple values of the subcarrier frequencies.

4. Minimum and Maximum Values of the Subcarrier Frequencies in CCRL with Pulse-Width Modulation

The minimum admissible value of the subcarrier frequency is selected on the following basis: in the time of effect of the shortest pulse T_{min} not less than 10-20 periods T_{so} are produced. Otherwise, the edges of the pulses are/355 extremely gently sloping, and as a result there is an increase of the influence of noise on the value of the CCRL output signal. It also should be pointed out that when $T_{so} > 0.1\ T_{min}$, there will be command distortion due to random phase relations of the subcarriers if two independently operating generators are used.

The maximum frequency of the subcarrier oscillation should be as small as possible so that the radio receiver passband will be quite narrow. However, in this case, it is necessary to take into account the admissible levels of transient and cross connection distortions.

5. Capacity of Binary Codes in CCRL with Pulse-Code Modulation and Admissible Repetition Interval of Symbols in CCRL with Pulse-Counting and Pulse-Frequency Modulation

The capacity N of binary codes in CCRL with pulse-code modulation and the period T_i in CCRL with pulse-counting modulation and pulse-frequency modulation are determined in such a way as to ensure that the quantization errors will not exceed admissible values.

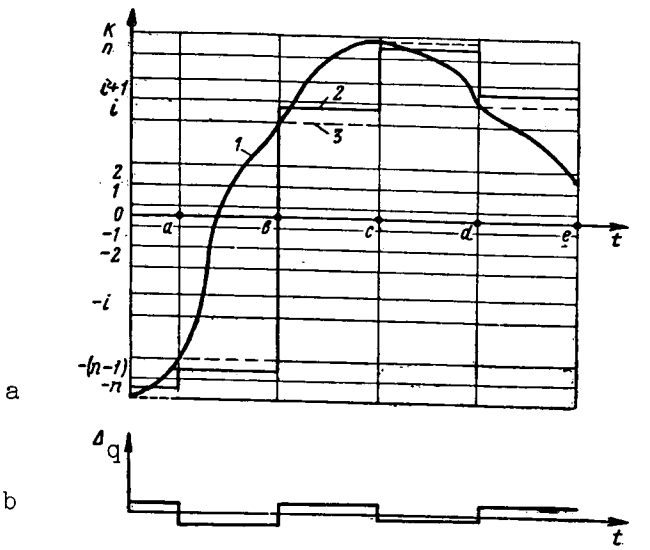

Figure 7.38

In order to determine the statistical characteristics of quantization errors at the output of a CCRL, each channel of which uses only one sequence of numbers, we will consider figure 7.38. If all possible values K_a are transmitted, the signal K, defined by curve 1 (fig. 7.38a) will appear at the CCRL output. Under real conditions, with separation of the entire range of changes of K_a into 2n + 1 intervals, a signal of steplike form, shown by curve 2 in this same figure, will be formed at the CCRL output. Curve 2 was constructed on the condition that the precise values K express the transmitted commands K_a corresponding to the midpoints of the intervals. It should be emphasized that as a result of the short duration of effect of a binary code in comparison with the period of transmission of commands T = ab = bc = cd = de (fig. 7.38a), it can be assumed that in the course of T the height of the step will not change. /356

In essence, this means that the leading edges of the pulses i_k (fig. 7.33e) are vertical and develop at times corresponding to the beginning of the segments T. Comparison of curves 1 and 2 shows that at the time of formation of the leading edges, the true value K at the output of the binary scaler does not coincide with that which can be obtained under real conditions. The difference between the stepped curve 2 and the signal 3, characterizing the precise conversion of the smoothly changing function $K_a(t)$ into a discrete value, is an instantaneous value of the quantization error Δ_q; this can assume either positive or negative values. The dependence of Δ_q on t is shown in figure 7.38b.

It follows from the earlier considered principle of design of a CCRL which uses only one sequence of numbers that the maximum value $\Delta_{q\ max}$ of the error Δ_q is proportional to half the width of one $K_a(t)$ separation interval. Therefore, as a result of level-quantization of $K_a(t)$, the maximum error $\Delta K'_{c\ max}$ of the command coefficient K_c in a CCRL based on the use of numbers of nonvariable sign, in accordance with expression (7.6.7), will be equal to

$$\Delta K'_{c\ max} = \frac{1}{2}\frac{1}{2^{N-1}-1}. \tag{7.8.3}$$

Knowing the value K_{max}, using expression (7.8.3), it is possible to compute quite easily the maximum distortion of the command K caused by level-quantization of the transmitted commands.

For CCRL based on use of two sequences, the maximum distortion of the command coefficient also is determined by formula (7.8.3).

In CCRL with one sign-variable sequence of numbers

$$\Delta K'_{c\ max} = \frac{1}{2}\frac{1}{2^{N}-1}. \tag{7.8.4}$$

In actual practice, it can be assumed that within the limits of a single quantization interval, the value of the command coefficient at the input and therefore at the CCRL output changes in conformity to a uniform law of probability distribution $w(\Delta K'_c) = \frac{1}{2\Delta K'_{c\ max}}$ in the range from $-\Delta K'_{c\ max}$ to $\Delta K'_{c\ max}$. Therefore, the mathematical expectation of the distortions $\Delta\bar{K}'_c$ due to quantization of $K_a(t)$ for CCRL with pulse-code modulation is equal to zero. Under this same condition for the dispersion σ^2_{qK} of distortions of $K_a(t)$ due to quantization of $K_a(t)$, with formulas (7.8.3) and (7.8.4) taken into account, we obtain

$$\sigma^2_{qK} = \int_{-\Delta K'_{c\ max}}^{\Delta K'_{c\ max}} \Delta K'^2_c w(\Delta K'_c)\, d(\Delta K'_c) = \frac{1}{12}\frac{1}{(2^{N-1}-1)^2} \tag{7.8.5}$$

and

$$\sigma^2_{qK} = \frac{1}{12}\frac{1}{(2^N-1)^2}. \qquad (7.8.6)$$

In order to determine the random errors of rocket guidance caused by quantization errors, a knowledge of only the dispersion of command distortion in the interval T is inadequate. This problem cannot be solved without knowing at least the spectral density $G_{\Delta c}(f)$ of the fluctuation component of the signal $\Delta_q(t)$.

We note that $G_{\Delta c}(f)$ determines the continuous part of the spectrum for the signal $\Delta_q(t)$ when $f \geq 0$.

The duration of pulses $\Delta_q(t)$, having a random amplitude, usually does not exceed 0.1-0.2 sec. Therefore, in the passband of the control system as a whole $G_{\Delta c}(f)$ remains virtually constant and is equal to $G_{\Delta c}(0)$. This means that it is not necessary to compute the entire function $G_{\Delta c}(f)$, but only its component when $f = 0$.

The value of $G_{\Delta c}(0)$ for the function $\Delta_q(t)$ can be found as the ratio of the dispersion $\sigma^2_{\Delta c}$ of the signal fluctuations $\Delta_q(t)$, averaged over the time T, to the effective passband ΔF_{ep} which they occupy. Since the function $\Delta_q(t)$ approximately represents square pulses with a random amplitude, constant duration and off-duty factor equal to unity, $\sigma^2_{\Delta c} = \sigma^2_{qK} K^2_{max}$ and $\Delta F_{ep} = \frac{L}{2T}$.

Then

$$G_{\Delta c}(0) = 2\sigma^2_{qK} T K^2_{max}. \qquad (7.8.7)$$

We note that a more detailed derivation of the formula for the spectral density of pulses with a random amplitude is given in reference 33. By dividing expression (7.8.7) by K^2_{max}, it is possible to find the spectral density $G_{qK}(0)$ for the fluctuation component of the command coefficient

$$G_{qK}(0) = 2\sigma^2_{qK} T. \qquad (7.8.8)$$

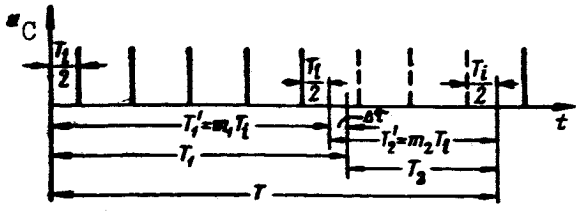

Figure 7.39

By substituting into expression (7.8.7) the values σ^2_{qK} and K^2_{max}, found earlier, it is possible to derive formulas determining $G_{\Delta c}(0)$ for different types of CCRL with pulse-code modulation.

Formulas (7.8.5)-(7.8.8) make it possible to find for different types /358 of CCRL with pulse-code modulation the necessary number of digits N for the binary codes used, if the limiting value $G_{\Delta c}(0)$ is stipulated. The limiting value $G_{\Delta c}(0)$ is determined on the basis of the admissible mean square error of rocket guidance and can be found as a result of analysis of the guidance circuit as a whole.

As an example, we point out that when $G_{\Delta c}(0) = 1 \cdot 10^{-5}$ sec for a CCRL with two sequences of numbers, it is necessary to use a binary code with $N \geq 4$.

As already mentioned, there will be formation of quantization errors in CCRL with pulse-code modulation and pulse-frequency modulation, with parallel arrangement of the subcarriers. At the output of a CCRL coder with pulse-counting modulation, the transmitted value of the command is determined by the intervals $T_1' = m_1 T_i$ and $T_2' = m_2 T_i$ (fig. 7.39). Therefore, in the case of identical parameters of the circuits for analyzing symbols of the first and second kinds in the decoder, the coefficient of the output command in the first channel is determined by expression (7.3.5). At the same time, the actual value of the received signal should be characterized by the command coefficient

$$K_{cf} = \frac{T_1 - T_2}{T}. \tag{7.8.9}$$

However, as can be seen from figure 7.39,

$$T_1 = m_1 T_i + \Delta\tau, \tag{7.8.10}$$

$$T_2 = m_2 T_i - \Delta\tau, \tag{7.8.11}$$

where $\Delta\tau$ can vary in the range $\pm \frac{T_i}{2}$.

On the basis of equations (7.3.5), (7.8.9), (7.8.10) and (7.8.11), taking into account that $T = mT_i$, we derive a formula determining the error for the command coefficient $\Delta K'_c$

$$\Delta K'_c = K_{cl} - K_{cf} = \frac{2\Delta\tau}{T} \text{ when } -0.5\,T_i \leq \Delta\tau \leq 0.5\,T_i. \qquad (7.8.12)$$

With a change of $\Delta\tau$ from $-0.5\,T_i$ to $0.5\,T_i$, the error $\Delta K'_c$ changes linearly and can assume a maximum value

$$\Delta K'_{c\,max} = \frac{T_i}{T}.$$

If it is assumed that the value $\Delta\tau$ changes randomly and within the limits of the interval T_i has a uniform probability distribution $\frac{1}{T_0}$, it is possible to find the following relations determining the mathematical expectation $\overline{\Delta K'_c}$ and the dispersion σ^2_{qK} of the distortion $\Delta K'_c$ /359

$$\overline{\Delta K'_c} = 0. \qquad (7.8.13)$$

$$\sigma^2_{qK} = \frac{1}{3}\frac{T_i^2}{T^2}. \qquad (7.8.14)$$

Formula (7.8.14) makes it possible to compute the necessary repetition interval T_i of code groups, if the admissible values of level-quantization errors of the transmitted signals $K_a(t)$ and the transmission rates of the commands are known.

Since $\Delta K'_c(t)$ represents square pulses with a random amplitude, constant duration and off-duty factor of 1, the spectral densities of the fluctuations of the CCRL output signal and the coefficient of the output command will be determined by formulas (7.8.7) and (7.8.8).

For CCRL with pulse-phase modulation with parallel arrangement of the subcarriers, the relations determining the quantization errors are the same as for a CCRL with pulse-counting modulation.

6. Capacity and Structure of Timing Codes

The selection of the capacity n and structure of timing codes must be accomplished in such a way as to ensure the best operation of the CCRL when it is subjected to radio interference.

Interference can form spurious codes and upon interacting with transmitted signals can cause suppression of one or more useful pulses. The probability p_{nonsup} that a transmitted n-pulse code will not be suppressed is equal to (with an identical probability p_{sup} of any of the pulses)

$$p_{nonsup} = (1 - p_{sup})^n. \qquad (7.8.15)$$

Expression (7.8.15) is correct under the condition that the transmitted code can pass through the coincidence stage only in a case when not one of n pulses is suppressed.

It follows from formula (7.8.15) that, with an increase of n for a particular level of interference, the probability of passage of code groups through the CCRL decoder decreases.

However, with a decrease of n, there is improvement of the conditions for the formation of spurious codes by interference. For example, when the CCRL is affected by pulse interference with random intervals between the pulses, the probability of formation of a spurious code is determined by the following approximate formula (ref. 82)

$$p_k = n(Z\tau_p)^n, \qquad (7.8.16)$$

where Z is the mean number of interference pulses in 1 sec at the coincidence stage input, and τ_p is the pulse duration. /360

We note that formula (7.8.16) determines p_k quite precisely when $Z\tau_p \ll 1$.

It also should be mentioned that in the case of large n, extremely rigorous requirements should be imposed on the stability of the delay lines used in the decoders. Therefore, the values n = 2-5 can be considered most desirable.

In order to decrease the possibility of formation of spurious codes due to the interaction of pulses and interference, for selected n, it is necessary to

select different lengths of the intervals between the successive pulses in the code, usually not multiples (ref. 110). Under this condition, an n-pulse spurious code is formed only with the augmentation of one of the transmitted signals by n - 1 interference pulses. If two or a greater number of intervals in the code are identical, in order to augment the transmitted signals to a code of the specified kind, it is necessary to have a lesser number of interference pulses.

The maximum duration (base) of a timing code is limited by the admissible number of units n_{line} in the delay line used in the coders. It is known that with an increase of n_{line}, the attenuation of the signals occurs approximately in a geometric progression. For practical purposes the timing code bases are not more than several tens of microseconds.

In selecting the structure of the codes, it also is necessary to bear in mind that the minimum intervals Δt_{min} between successive pulses should be not less than 2-3 pulse durations. This is necessary so that the transient processes in different CCRL stages will end in the time $t < \Delta t_{min}$. Naturally, in actual practice, an effort must be made to obtain the minimum code base.

7.9. General Information on the Selection and Computation of the Principal Parameters of CCRL Receiving-Transmitting Apparatus

Radio transmitting and radio receiving apparatus of the CCRL are important components of the control radio link. Despite the fact that the problems solved by the radio transmitter and radio receiver in the CCRL and similar apparatus in radio telephone, radio telegraph, radio telemeter and radio navigation systems have some points in common, there are a number of specific requirements which must be taken into account in the development of the high-frequency channel of the CCRL.

The following factors must be taken into account in the functional and circuit diagrams of the transmitter and receiver of the CCRL, their design and the quality of their operation:

(1) the required directional diagrams of the transmitting and receiving antennas of the CCRL;

(2) the range of wavelengths used;

(3) the necessary strength of radiation; /361

(4) the passband and the general amplification factor of the receiver.

A number of other technical characteristics of the transmitter and receiver can be selected or stipulated on the basis of the general theory of

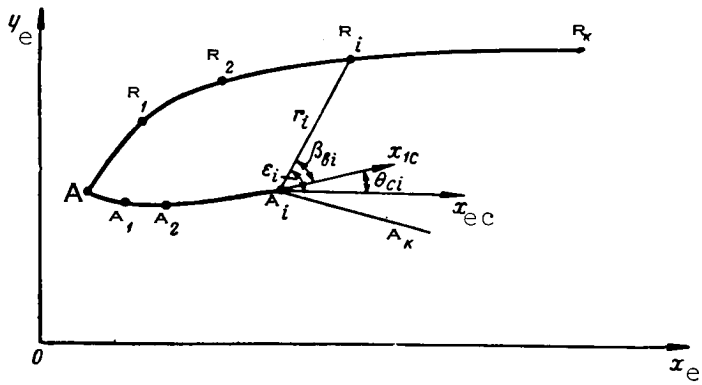

Figure 7.40

characterizing the direction of the radiation maximum relative to the longitudinal axis of the aircraft in the horizontal and vertical planes, and the form of the directional diagram should be selected so as to ensure a stable communication for any possible flight trajectories of an aircraft and rocket, taking into account their oscillations about the centers of mass.

The values θ_{0h}, θ_{0v}, β_h and β_v are determined by constructing the most probable flight trajectories of the rocket carrier and of the rocket, using a ground coordinate system for this purpose. Since the method for computing θ_{0h}, β_h and θ_{0v}, β_v is identical, henceforth we will consider only the vertical plane $oy_e x_e$ (fig. 7.40).

Assume that the aircraft and rocket during the entire time of guidance move along the curves AA_k and AR_k. We will divide the curves AA_k and AR_k into k segments AA_1, A_1A_2, ..., $A_{k-1}A_k$ and AR_1, R_1R_2, ..., $R_{k-1}R_k$, corresponding to constant values of time increment Δt. Obviously, the smaller the value Δt, the more precise will be the results.

By connecting the ends of each segment by a straight line, we obtain the direction of the communication lines for each position of the rocket carrier relative to its longitudinal axis $A_i x_{1c}$. The position of the axis $A_i x_{1c}$ can be determined approximately as the tangent to the direction of motion of the aircraft.

It follows from figure 7.40 that for the moment of time when the aircraft and rocket are situated at the points A_i and R_i, the angle β_{vi} between the communication line $A_i R_i$ and the axis $A_1 x_{1c}$ is equal to

$$\beta_{vi} = \varepsilon_i - \theta_{ci}. \qquad (7.9.1)$$

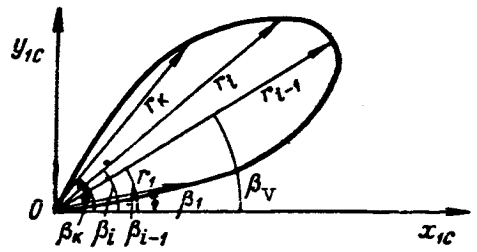

Figure 7.41

Here ϵ_i is the angle of inclination of the communication line relative to /363 the plane tangent to the Earth at point O, and θ_{ci} is the angle between the axes $A_i x_{1c}$ and $A_i x_{ec}$.

Denoting the coordinates of the points R_i and A_i by x_{ri}, y_{ri} and x_{ci}, y_{ci}, we find that

$$\sin \epsilon_i = \frac{y_{ri} - y_{ci}}{r_i},$$

where $r_i = \sqrt{(x_{ri} - x_{ci})^2 + (y_{ri} - y_{ci})^2}$ is the distance from the control point to the rocket.

Since

$$\sin \beta_{vi} = \sin \epsilon_i \cos \theta_{ci} - \cos \epsilon_i \sin \theta_{ci},$$

then

$$\sin \beta_{vi} = \frac{(y_{ri} - y_{ci}) - (x_{ri} - x_{ci}) \operatorname{tg} \theta_{ci}}{r_i} \cos \theta_{ci}. \qquad (7.9.2)$$

If all possible values y_{ri}, y_{ci}, x_{ri}, x_{ci}, θ_{ci} and r_i are determined during the time of rocket guidance T_g, it is possible to find k radii vectors whose lengths are r_i and the angles of inclination to the axis $A_i x_{1c}$ are β_{vi}.

By constructing these radii vectors in a related coordinate system x_{1c}, y_{1c} (fig. 7.41) and connecting their ends with a smooth curve, we obtain the form of the directional diagram on the basis of which it is possible to determine the adjusting angle β_v and the width θ_{0v}.

The diagram obtained in this way should be broadened taking into account the possible oscillations of the rocket and aircraft.

It should be noted that, in some cases, it is possible to obtain forms of diagrams which are infeasible from the technical point of view. In order to overcome this difficulty, it is necessary to increase the width θ_{0v} (or θ_{0h}) so that it is possible to create a quite simple antenna system.

A similar method is used for computing the adjusting angle and the width of the directional diagram carried on the rocket. At the same time, it must be remembered that there are limited possibilities for mounting antennas on small rockets without disrupting their aerodynamic properties. Very frequently, it is necessary to mount the antenna in such a way that it forms one of the elements of the rocket. It therefore follows, in particular, that it is desirable to use small antennas and therefore ultrashort radio waves.

The most important antenna systems for rockets are: /364

(1) a dielectric radiator;
(2) a slotted antenna;
(3) radiators of the "wave channel" type, etc.

2. Wavelengths Used

The following general considerations must be taken into account when selecting the wavelength range for CCRL (ref. 4).

(1) assurance of high stability of the working frequency, which is dictated by the necessity for obtaining a reliable untrimmed communication with a relatively narrow passband of the radio receiver (this is important for increasing the noise immunity of the CCRL);

(2) obtaining the necessary number of fixed waves for interchangeability and creating conditions for easy transfer from one wavelength to another;

(3) assurance of the spatial selection of radio signals when using small antennas;

(4) assurance of a small weight and size of receiving-transmitting apparatus;

(5) the feasibility of the range of working waves from the point of view of the principle of operation of the CCRL.

In addition, the required effective range of the CCRL, the character of the radiated signals (pulse or continuous signals), the screening effect of the gas jet of the jet engine of the rocket causing absorption of energy and distortion of the directional diagram and the characteristics of radio wave propagation exert an appreciable influence on the selection of the range of working waves for the CCRL.

Taking all these factors into account, it can be concluded that when there is geometrical visibility, preference should be given to the region of meter, decimeter and centimeter waves.

Meter and decimeter waves are most suitable for CCRL producing continuous signals or pulses of considerable duration. The merits of these waves are: the possibility of ensuring stable communication with a narrow radio receiver passband by the use of quartz crystals or frequency stabilization; a quite large number of fixed waves is obtained; slight atmospheric attenuation and slight attenuation in the jet of ionized gases of the rocket engine. A shortcoming of meter and decimeter waves is the difficulty of obtaining high-directional radiation and reception.

In actual radio communication with short pulses, only waves in the centimeter wavelength range are used. As is well known, the shorter the wave, the easier it is to form a narrow radiation and reception diagram even with small antennas. At the same time, centimeter waves have shortcomings. The most important of these are:

(1) the low frequency stability of available generators; /365
(2) considerable atmospheric attenuation;
(3) the difficulty in obtaining a considerable number of fixed waves.

Short waves also can be used for communication for considerable distances near the Earth's surface.

3. Necessary Power of the CCRL Radio Transmitter

When computing the necessary power P_σ of radiation of the CCRL radio transmitter, the most important factor is ensuring the required signal strength P_{rec} at the input of the radio receiver during the entire time of rocket guidance. The value P_{rec} is determined in accordance with the required signal-to-noise ratio.

If there is no reflection from the Earth and attenuation in the atmosphere and in the jet of jet engine gases is not taken into account, as is well known, the value P_σ can be computed using the following formula

$$P_\sigma = 16\pi^2 \frac{P_{rec} r_{rr}^2}{G_1 G_2 \lambda^2}, \qquad (7.9.3)$$

where r_{rr} is the distance from the radio transmitter to the radio receiver; G_1 and G_2 are the amplification factors of the transmitting and receiving antennas, respectively, and λ is the wavelength.

If a range of waves is selected whose character of propagation is dependent on the state of the atmosphere and the composition of the jet of gases

from the jet engines, the value P_σ obtained on the basis of the cited expression should be increased by the corresponding number of times.

In control of rockets of the "air-to-ground" class, direct radio waves and radio waves reflected from the Earth reach the input of the CCRL radio receiver. As a result, there is interference of the electromagnetic field along the flight trajectory of the rocket. The maximum and minimum values of the received signals will be formed at the time of arrival of the direct and reflected waves in phase and antiphase, respectively.

Accordingly, computation of the necessary power P_σ of radiation should include allowance for the Earth's influence on the power of the input signals for different possible flight trajectories of the rocket and motion of the point where the radio transmitter is situated.

4. Required Passband and Amplification Factor of Radio Receiver

The minimum necessary passband Δf of the CCRL radio receiver is determined by the spectrum of the radiated oscillations, which is essentially dependent on the type of modulation.

In an N_k-channel CCRL with width-pulse modulation of sinusoidal sub- /366
carrier oscillations, for a case when the principle of an active pause is used, the oscillations produced at the same time by the transmitter generator are modulated in amplitude by N_k "harmonic" signals. For such radio links, the spectrum of the radiated signal, without taking into account the phases of the individual components, when K_a = const in all channels, has the forms shown in figure 7.42, where f_0 is the carrier frequency of the radio transmitter; $f_{sub\ 1}$, ..., $f_{sub\ N_k}$ are the subcarrier frequencies of all the CCRL channels. The upper and lower side components are situated near each subcarrier. The frequency interval between adjacent components of this form is equal to F.

The spectrum shown in figure 7.42 can be found by summation of N_k spectra obtained during modulation of periodic pulses of an identical duration by sinusoidal oscillations with the frequencies $f_{sub\ 1}$, $f_{sub\ 2}$, ..., $f_{sub\ N_k}$. In turn, the radio transmitter is modulated in amplitude by signals having such a total spectrum.

With a change of the transmitted control commands, the amplitudes of all the side components will not remain constant. In addition, the interval

Figure 7.42

between components with the frequency $f_0 + if_{sub\ i}$ $(i = 1, 2, \ldots, N_k)$ and the side component having a zero amplitude will be the greater the lesser the time the considered subcarrier oscillation is effective.

Figure 7.42 shows that the minimum required passband of a CCRL radio receiver with primary pulse-width modulation of sinusoidal subcarriers and secondary amplitude modulation should be equal to

$$\Delta f = 2\left(f_{sub\ N_k} + \frac{1}{2} F_s\right),$$

where F_s is the width of the spectrum of pulses of sinusoidal oscillations with the frequency $f_{sub\ N_k}$.

The value F_s can be determined in the following way

$$F_s = \frac{1 - 2}{T_{N_k min}},$$

where $T_{N_k min}$ is the minimum possible pulse duration in the CCRL channel.

It is also possible to find the value Δf for radio receivers of command control radio links based on the use of phase modulation of sinusoidal subcarrier oscillations. /367

In pulse radio links, the width of the spectrum of radiated oscillations is dependent on pulse duration and the form of pulse modulation. Usually, the transmitted commands are extremely slowly changing functions of time. Therefore, the value Δf can be found, using as a point of departure the stipulated accuracy of reproduction of the envelopes of unmodulated pulses. It is necessary to proceed in the same way in computations of Δf for CCRL with code signal selection. This can be attributed to the fact that the minimum intervals between succeeding pulses in the timing codes always exceed the pulse duration.

In the final selection of the passband of the radio receiver, it is necessary to take into account the frequency instability of the radio transmitter generator and the radio receiver heterodyne.

The general amplification factor of the CCRL receiver is determined so as to ensure the stipulated values of the amplitudes of the subcarrier oscillations at the input of the CCRL decoder.

CHAPTER 8. NOISE IMMUNITY OF COMMAND CONTROL RADIO LINKS

8.1. Mathematical Description of Processes in Command Control Radio Links with Influence of Radio Interference Taken into Account

1. Qualitative Characteristics of Effect of Interference and of a Statistically Equivalent Filter

It follows from the preceding chapter that single-channel command control radio links, depending on the number of subcarrier oscillations used for transmission of $K_a(t)$ commands, can be apparatus of differential or nondifferential type. In CCRL of the nondifferential type only one subcarrier oscillation is modulated by the $K_a(t)$ signal, while in a CCRL of the differential type the command $K_a(t)$ is reflected by two modulated subcarrier oscillations. /368

If as a point of departure we use the properties of conversion of the transmitted signals, in any single-channel CCRL of the nondifferential type with pulse modulation of the subcarrier oscillations, it is possible to distinguish an output filter representing a dynamic link with constant parameters and an inertialess pulse element with parameters changing with time in a jump and connected in series. The pulse element includes a coder, radio transmitter, radio receiver and all the pulse devices of the decoder. In CCRL with continuous forms of modulation, the pulse element, in the coder, is replaced by a system with variable parameters forming, for example, due to the presence in the radio receiver of automatic volume control.

The coder, decoder, radio transmitter and radio receiver of the CCRL usually are such that in the working range of changes of the transmitted command K_a, there is a linear dependence between the output signal K of the CCRL and K_a. Therefore, the CCRL as a whole can be replaced by some linear filter representing the equivalent of the CCRL as one of the links included in the radio control system. /369

The weighting function g(t) of the mentioned filter should be such that the command $K_a(t)$ is amplified by k_{CCRL} times and there is a transient process determined by the inertial properties of the CCRL filter. It can be shown that the same equivalent model is applicable for a CCRL of the differential type, if its output filters have identical characteristics. In actual practice, this condition usually is fully satisfied.

The effect of the instrument noise of the CCRL radio receiver and also external natural and artificial radio interference leads to the partial or complete suppression of the transmitted signals, the formation of spurious signals, exerting an influence on the operating regime of the decoder, and change of the parameters of modulation of the subcarrier oscillations. As a result, depending on the type of CCRL and also on the structure and intensity of the interference, the influence of the latter causes:

(1) formation at the CCRL output of a signal $K_n(t)$ equal to the sum of the command $K(t)$ which would exist in the absence of noise and additive (not dependent on the command K) noise characterizing the distortion of K;

(2) change of the CCRL transfer constant, which can be a random or determined function of time, and the appearance of additive noise at the CCRL output, under the condition that as a dynamic link it remains linear;

(3) the conversion of the CCRL into a nonlinear dynamic link with constant or variable (including random) parameters, at whose output acts a signal which is a function of the transmitted command K_a and additive noise.

When the interference is virtually suppressed, all the transmitted signals overload either one or more stages in the CCRL receiver and a signal is produced at its output which is not dependent on K_a. This means opening of the guidance circuit for the command transmission channel.

It follows from the above that when the CCRL is subjected to interference the weighting function $g(t)$, in a general case, no longer can characterize the conversion properties of the CCRL. At the same time, a knowledge of the CCRL equation determining the relationship between the command $K_n(t)$ (produced by the CCRL with the effect of interference taken into account) and $K_a(t)$ is necessary for determination of the errors of rocket guidance. This can be attributed to the fact, as already noted, that the CCRL is one of the links of a closed control system, and the guidance errors can be determined only by solution of the equations describing the control system as a whole.

Due to the considerable number of nonlinear devices constituting /370
parts of the CCRL and the random change of interference parameters, in actuality, it is difficult to determine the functional dependence between $K_n(t)$ and $K_a(t)$, especially when taking into account the influence of interference of a considerable intensity. In most cases, it is possible to compute analytically or experimentally only the conditional (although sometimes also the unconditional) moments of lower orders for the random signal $K_n(t)$. We recall that the conditional moments for $K_n(t)$ are determined the same as the unconditional

moments, but under the assumption that the values of the input signal $K_a(t)$ are stipulated. The conditional moments are determined more easily than the unconditional moments because when computing the latter, it is necessary to take into account the random character of the change $K_a(t)$, for example, due to fluctuations of the output signal of the coordinator, and to know the law of probability distribution for $K_a(t)$.

In order to overcome the difficulties involved in finding the functional relationship between $K_n(t)$ and $K_a(t)$ as a result of solution of a system of equations describing processes in different stages of the transmitting and receiving apparatus of the CCRL, the latter, taking the influence of radio interference into account, should be replaced by some statistically equivalent converter whose parameters should be determined on the basis of known moments for the command $K_n(t)$. This converter, called a statistically equivalent filter (SEF), when fed the commands $K_a(t)$, should form a signal $K_{ne}(t)$, coinciding with $K_n(t)$ in accordance with the selected criteria for approximation of random functions. The statistically equivalent filter, depending on the type of CCRL and also on the structure and intensity of interference, can be either a linear or nonlinear apparatus with constant or variable (including random) parameters. When the CCRL is replaced by a statistically equivalent filter, it is necessary:

(1) to establish criteria of equivalence of the random functions $K_n(t)$ and $K_{ne}(t)$;

(2) to select an approximating function (type of SEF equation);

(3) to determine the character of change and the necessary characteristics for the parameters of the approximating function.

2. Conditions of Equivalence of CCRL and SEF

For practical purposes, in many cases, a necessary and sufficient condition for equivalence of real CCRL and SEF is an equality of the mathematical expectations and correlation functions (spectral densities) for the commands $K_n(t)$ and $K_{ne}(t)$, respectively.

When an allowance is made for the influence of the instrument noise of the CCRL radio receiver, the $K_n(t)$ output signal usually is a stationary or quasi-stationary (close to stationary) random process. This can be attributed /371 to the fact that the instrument noise of the radio receivers is stationary, whereas the control commands usually are transmitted continuously or periodically. If the CCRL is affected by external radio interference, as a result of the

inconstancy of its parameters and also changes of the coefficients of modulation of interference (especially artificial) and the distance between the interference source and the rocket, the function $K_n(t)$ is nonstationary. However, it must be remembered that the intensity of the external interference arriving at the CCRL input changes considerably more slowly than the random processes that transpire in the elements of the CCRL, which are virtually inertialess links relative to $K_a(t)$. The nonstationary modulating voltages in the interference transmitters should be low frequency so that the interference can pass to the CCRL output. In this connection, it can be assumed that, within the limits of small segments of the rocket flight trajectory, the function $K_n(t)$ also will be quasi-stationary. If the processes transpiring in the CCRL decoder are quasi-stationary and the time constant of the radio control system as a whole, determined by the inertia of the rocket, is considerably greater than the command repetition interval, as the statistical characteristics of the random function $K_n(t)$ it is possible to employ its time-averaged moments without introduction of any significant error.

The use of time-averaged moments for the signal $K_n(t)$ leads to the possibility of obtaining a stationary statistically equivalent filter which can be used in an investigation of the noise immunity of radio control systems, more simply than when the CCRL is replaced by a nonstationary SEF.

Taking the above into account, we will assume that at the CCRL output, when subjected to radio interference, a command $K_n(t)$ is formed which constitutes a stationary or quasi-stationary function of time and that the equivalence of real CCRL and SEF is determined by the following equations

$$\overline{K}_{ne} = \overline{K}_n, \tag{8.1.1}$$

$$R_e(\tau) = R_n(\tau), \tag{8.1.2}$$

where $\overline{K}_{ne}$ and $\overline{K}_n$ are the mathematical expectations or time-averaged mathematical expectations, respectively, for stationary and quasi-stationary signals $K_{ne}(t)$ and $K_n(t)$; $R_e(\tau)$ and $R_n(\tau)$ are the correlation functions or time-averaged correlation functions, respectively, for stationary and quasi-stationary signals $K_{ne}(t)$ and $K_n(t)$; τ is the interval between the moments of time for which is sought a correlation of the functions $K_{ne}(t)$ and $K_n(t)$.

In those cases when the function $K_n(t)$ differs appreciably from a stationary character, even in the case of insignificant movements of the rocket, the equivalence of CCRL and SEF must be established in accordance with the /372 equations of the mathematical expectations and the correlation functions for the signals $K_n(t)$ and $K_{ne}(t)$ without use of time-averaging operations.

Despite the fact that all the subsequent expositions will be presented in accordance with equations (8.1.1) and (8.1.2), the method used in determining the parameters of a stationary SEF is suitable also for a CCRL whose output signal $K_n(t)$ is nonstationary.

3. Linear SEF

If under conditions when radio interference is present a real CCRL remains a linear converter of transmitted commands $K_a(t)$, it can be replaced by a linear SEF in which the output signal is

$$K_{ne}(t) = \xi_0(t) + \xi_1(t)K_a(t), \tag{8.1.3}$$

where $\xi_0(t)$ and $\xi_1(t)$ are coefficients not dependent on $K_a(t)$ and subject to determination in accordance with the stipulated criterion of approximation of the random functions $K_n(t)$ and $K_{ne}(t)$.

It can be assumed that this equation is derived as a result of replacement of $K_n(t)$ by $K_{ne}(t)$ in the expression characterizing the functional relationship between $K_n(t)$ and $K_a(t)$, which would be found from solution of a system of equations reflecting the behavior of a linear CCRL when affected by interference and when the inertia of the CCRL in relation to the transmitted commands is neglected. The necessity for replacement of $K_n(t)$ by $K_{ne}(t)$ can be attributed to the fact that, on the basis of a finite number of known moments for $K_n(t)$, it is impossible to determine fully the random function $K_n(t)$.

We will show that a necessary and sufficient condition for the applicability of equation (8.1.3), for description of processes transpiring in real CCRL subjected to the influence of radio interference, is the satisfaction of the two following relations

$$[\overline{K}_n]_c = b + aK_a(t), \tag{8.1.4}$$

$$[R_n(\tau)]_c = \varphi_0(\tau) + \varphi_1(\tau)K_a(t)K_a(t+\tau) + \varphi_2(\tau)K_a(t) + \varphi_3(\tau)K_a(t+\tau) \tag{8.1.5}$$

Here $[\overline{K_n}]_c$ is the conditional constant component of the output signal $K_n(t)$, representing the conditional mathematical expectation or time-averaged conditional mathematical expectation for stationary and quasi-stationary functions $K_n(t)$, respectively, and computed on the assumption that the value $K_a(t)$ at the time t is given and differs from zero; $[R_n(\tau)]_c$ is the conditional correlation function or the time-averaged conditional correlation function for stationary and quasi-stationary random signals $K_n(t)$, respectively; $[R_n(\tau)]_c$ /373 should be computed for given and nonequivalent and nonzero values $K_n(t)$ and $K_n(t + \tau)$; b and a are constant values not dependent on $K_a(t)$; $\varphi_0(\tau)$, $\varphi_1(\tau)$, $\varphi_2(\tau)$ and $\varphi_3(\tau)$ are functions of the argument τ, not dependent on $K_a(t)$ and $K_a(t + \tau)$.

When there is interference, the conversion properties of the CCRL can be determined or random functions of time. If the conversion properties of real CCRL are not random, then bearing in mind the definition of the conditional correlation function, it can be concluded that $[R_n(\tau)]_c$ will not be dependent on $K_a(t)$ and $K_a(t + \tau)$. However, when the parameters of the CCRL become random under the influence of interference, a relationship between $[R_n(\tau)]_c$ and $K_a(t)$ and $K_a(t + \tau)$ appears. It follows from the above that determination of $[R_n(\tau)]_c$ in the form of formula (8.1.5), in which the third and fourth terms can be absent, indicates the presence of random parameters in a real CCRL when it is subjected to interference.

When expression (8.1.4) does not contain terms dependent on K_a with an exponent greater than unity, the relation (8.1.5) for CCRL with random parameters also determines the necessary and sufficient conditions of linearity of conversion of K_a of a real CCRL subjected to interference. This assertion requires no demonstration because it follows directly from definition of the conditional correlation function.

When the parameters of the CCRL, under the influence of radio interference, do not become random functions of time, on the basis of relation (8.1.5), in which only the first term remains, it is impossible to draw conclusions as to the character of conversion of the signal $K_a(t)$ into the command $K_n(t)$. In this case, the property of linearity of the CCRL relative to K_a can be

determined unambiguously on the basis of expression (8.1.4). In actuality, in accordance with the definition of the conditional mathematical expectation for the function $K_n(t)$, related to $K_a(t)$ and the CCRL parameters, the value $[\bar{K}_n]_c$ for the selected moment of time t will change proportional to the signal $K_a(t)$ only in the case of its linear conversion in the CCRL transmitting and receiving apparatus.

Thus, expression (8.1.5) makes it possible to draw conclusions concerning the parameters of a real CCRL and jointly with formula (8.1.4) makes it possible to judge its linearity relative to K_a.

In the case of a linear CCRL, it is possible to give the following interpretation of the parameters entering into relations (8.1.4) and (8.1.5). The parameter a characterizes the mean value of the CCRL transfer constant. The terms b and $\varphi_0(\tau)$ reflect the mathematical expectation and the correlation function of additive noise forming at the CCRL output. The function $\varphi_1(\tau)$ corresponds to the correlation function for the transfer constant, and $\varphi_2(\tau)$ and $\varphi_3(\tau)$ represent the reciprocal correlation functions of additive noise /374 appearing at the CCRL output due to interference and its random transfer constant.

If the relations (8.1.4) and (8.1.5) are not satisfied, a real CCRL cannot be replaced by a linear statistically equivalent filter.

After it has been established that the considered CCRL is linear, the problem arises of determination of the coefficients $\xi_0(t)$ and $\xi_1(t)$ in equation (8.1.3); for generality, we will assume that $\xi_0(t)$ and $\xi_1(t)$ are random functions of time. Usually, there is a considerable difference between the range of frequencies of effective interference with random parameters and the transmission band of the CCRL output filters. It therefore can be assumed that $\xi_0(t)$ and $\xi_1(t)$ conform to normal laws of probability distribution. Under this assumption, the problem of determination of the coefficients $\xi_0(t)$ and $\xi_1(t)$ is reduced to determining the mathematical expectations and also the correlation and reciprocal correlation functions for $\xi_0(t)$ and $\xi_1(t)$. Then for shortening the writing, the mentioned moments will be called statistical parameters. This term will be used for denoting the mathematical expectations (constant components) and spectral densities (or correlation functions) for all the random functions considered in this chapter.

Since the coefficients $\xi_0(t)$ and $\xi_1(t)$ characterize the internal properties of the CCRL, when determining the statistical parameters for the functions $\xi_0(t)$ and $\xi_1(t)$, it is necessary to proceed in such a way that the corresponding moment of the output signal $K_n(t)$ will be dependent only on the moments and reciprocal moments for $\xi_0(t)$ and $\xi_1(t)$ and are not functions of the moments of the transmitted command. It is easy to see that this requires determination of the conditional moments for $K_n(t)$.

In a case when a real CCRL, acted upon by interference, produces a signal $K_n(t)$ which is linearly dependent on $K_a(t)$, for the conditional mathematical expectation $[\overline{K}_n]_c$, we obtain an expression in the form (8.1.4). At the same time, on the basis of expression (8.1.3), determining the equation of a linear statistically equivalent filter, for the conditional constant component (conditional mathematical expectation or time-averaged conditional mathematical expectation) $[\overline{K}_{ne}]_c$ of the random signal $K_{ne}(t)$, we find

$$[\overline{K}_{ne}]_c = \overline{\xi_0(t)} + \overline{\xi_1(t)}K_a(t), \tag{8.1.6}$$

where $\overline{\xi_0(t)}$ and $\overline{\xi_1(t)}$ are the mathematical expectations (unconditional) for the random functions $\xi_0(t)$ and $\xi_1(t)$.

Comparison of expressions (8.1.4) and (8.1.6) shows that when

$$\overline{\xi_0(t)} = b \tag{8.1.7}$$

and

$$\overline{\xi_1(t)} = a \tag{8.1.8}$$

the satisfaction of condition (8.1.1) is ensured. The conclusion drawn above follows from the fact that when computing $\overline{K}_n$ and $\overline{K}_{ne}$ on the basis of /375 expressions (8.1.4) and (8.1.6), it is necessary to take into account the same function $K_a(t)$.

In determining the correlation and reciprocal correlation functions for $\xi_0(t)$ and $\xi_1(t)$, we also will bear in mind that the equality of the conditional correlation functions (or the time-averaged conditional correlation

functions) $[R_n(\tau)]_c$ and $[R_e(\tau)]_c$ for $K_n(t)$ and $K_{ne}(t)$ ensures the satisfaction of equation (8.1.2). The function $[R_n(\tau)]_c$ for the signal $K_n(t)$, linearly dependent on $K_a(t)$, is determined by formula (8.1.5). For the function $[R_e(\tau)]_c$, under the assumption that $K_a(t)$ and $K_a(t + \tau)$ for the times t and $t + \tau$ are stipulated, from equation (8.1.3) we will have

$$[R_e(\tau)]_c = R_{\xi_1}(\tau) K_a(t) K_a(t+\tau) + R_{\xi_0}(\tau) + R_{0.1}(\tau) K_a(t+\tau) + R_{1.0}(\tau) K_a(t), \tag{8.1.9}$$

where

$$R_{\xi 1}(\tau) = \overline{\xi_1^{\circ}(t)\,\xi_1^{\circ}(t+\tau)}, \quad R_{\xi 0}(\tau) = \overline{\xi_0^{\circ}(t)\,\xi_0^{\circ}(t+\tau)}, \quad R_{0.1}(\tau)$$

$$= \overline{\xi_0^{\circ}(t)\,\xi_1^{\circ}(t+\tau)} \text{ and } R_{1.0}(\tau) = \overline{\xi_1^{\circ}(t)\,\xi_0^{\circ}(t+\tau)}$$

are the correlation and reciprocal correlation functions for $\xi_1(t)$ and $\xi_0(t)$ and

$$\xi_0^{\circ}(t) = \xi_0(t) - \overline{\xi_0(t)}, \qquad \xi_0^{\circ}(t+\tau) = \xi_0(t+\tau) - \overline{\xi_0(t)},$$
$$\xi_1^{\circ}(t) = \xi_1(t) - \overline{\xi_1(t)} \text{ and } \xi_1^{\circ}(t+\tau) = \xi_1(t+\tau) - \overline{\xi_1(t)}$$

Applying the method of equalization of the corresponding coefficients in expressions (8.1.5) and (8.1.9), we find

$$R_{\xi_1}(\tau) = \varphi_1(\tau), \tag{8.1.10}$$
$$R_{\xi_0}(\tau) = \varphi_0(\tau), \tag{8.1.11}$$
$$R_{0.1}(\tau) = \varphi_3(\tau), \tag{8.1.12}$$
$$R_{1.0}(\tau) = \varphi_2(\tau). \tag{8.1.13}$$

It follows from the considered method for determination of the statistical parameters for $\xi_0(t)$ and $\xi_1(t)$ that in an analysis of the problem of the passage of signals and interference through a real CCRL, it is necessary and sufficient to determine $[\overline{K}_n]_c$ and $[R_n(\tau)]_c$, under the condition that the values $K_a(t)$ and $K_a(t + \tau)$ are not equal to zero or to one another. However, in actual practice, the computation of $[R_n(\tau)]_c$ when $K_a(t) \neq K_a(t + \tau)$ in some cases is extremely difficult. The problem therefore arises of determining $R_{\xi_0}(\tau)$, $R_{\xi_1}(\tau)$, $R_{0.1}(\tau)$

and $R_{1.0}(\tau)$ on the basis of a knowledge of the function $[R_n(\tau)]_c$, obtained by computations or experimentation when $K_a(t) = K_a(t + \tau) = K_a = \text{const}$.

If the functions $[\overline{K}_n]_c$ and $[R_n(\tau)]_c$ are determined when $K_a(t) = K_a(t + \tau) = K_a = \text{const}$, it can be concluded that the necessary and adequate conditions for the possibility of replacement of a real single-channel CCRL by a linear statistically equivalent filter involve satisfaction of the following relations /376

$$[\overline{K}_n]_c = b + aK_a, \tag{8.1.14}$$

$$[R_n(\tau)]_c = \varphi_0(\tau) + \varphi_1(\tau) K_a^2 + f(\tau) K_a, \tag{8.1.15}$$

$$\frac{f(\tau)}{\sigma_{\varphi_0}\sigma_{\varphi_1}} \leqslant 2, \tag{8.1.16}$$

where $\sigma^2_{\varphi_0}$ and $\sigma^2_{\varphi_1}$ are the values $\varphi_0(\tau)$ and $\varphi_1(\tau)$ when $\tau = 0$.

In actuality, assuming that the considered CCRL, for which $[\overline{K}_n]_c$ and $[R_n(\tau)]_c$ are determined by expressions (8.1.14) and (8.1.15), can be replaced by a linear statistically equivalent filter, on the basis of equation (8.1.3), when $K_a(t) = K_a(t + \tau) = K_a = \text{const}$, we obtain

$$[\overline{K}_{ne}]_c = \overline{\xi_0(t)} + \overline{\xi_1(t)} K_a, \tag{8.1.17}$$

$$[R_e(\tau)]_c = R_{\xi_0}(\tau) + [R_{0.1}(\tau) + R_{1.0}(\tau)] K_a + R_{\xi_1}(\tau) K_a^2. \tag{8.1.18}$$

However, it is known that

$$R_{\xi_0}(\tau) = \sigma^2_{\xi_0} r_{\xi_0}(\tau), \quad R_{\xi_1}(\tau) = \sigma^2_{\xi_1} r_{\xi_1}(\tau), \quad R_{0.1}(\tau) = \sigma_{\xi_0}\sigma_{\xi_1} r_{0.1}(\tau) \text{ and } R_{1.0}(\tau) = \sigma_{\xi_0}\sigma_{\xi_1} r_{1.0}(\tau),$$

where $r_{\xi_0}(\tau)$ and $r_{\xi_1}(\tau)$ are the correlation functions for the random functions $\xi_0(t)$ and $\xi_1(t)$, but $r_{0.1}(\tau)$ and $r_{1.0}(\tau)$ are the reciprocal correlation coefficients for the random functions $\xi_0(t)$ and $\xi_1(t)$.

Therefore

$$[R_e(\tau)]_c = \sigma^2_{\xi_0} r_{\xi_0}(\tau) + \sigma_{\xi_0}\sigma_{\xi_1} [r_{0.1}(\tau) + r_{1.0}(\tau)] K_a + \sigma^2_{\xi_1} r_{\xi_1}(\tau) K_a^2. \tag{8.1.19}$$

Comparison of the expressions (8.1.14) and (8.1.17) and also the relations (8.1.15) and (8.1.19) shows that the CCRL will be equivalent to a linear statistically equivalent filter in which the processes are described by equation (8.1.3), provided the following conditions are satisfied

$$\overline{\xi_0(t)} = b, \tag{8.1.20}$$

$$\overline{\xi_1(t)} = a, \tag{8.1.21}$$

$$\sigma^2_{\xi_0} r_{\xi_0}(\tau) = \varphi_0(\tau), \tag{8.1.22}$$

$$\sigma^2_{\xi_1} r_{\xi_1}(\tau) = \varphi_1(\tau), \tag{8.1.23}$$

$$\sigma_{\xi_1}\sigma_{\xi_0}[r_{0.1}(\tau) + r_{1.0}(\tau)] = f(\tau), \tag{8.1.24}$$

$$r_{0.1}(\tau) + r_{1.0}(\tau) \leqslant 2. \tag{8.1.25}$$

We note that expression (8.1.25) was written in accordance with the known inequalities $r_{0.1}(\tau) \leq 1$ and $r_{1.0}(\tau) \leq 1$. Since $r_{\xi_0}(\tau)$ and $r_{\xi_1}(\tau)$ when $\tau = 0$ are equal to unity, in accordance with (8.1.22) and (8.1.23) we find that

$$\sigma^2_{\xi_0} = \varphi_0(0),\ \sigma^2_{\xi_1} = \varphi_1(0), \qquad r_{\xi_0}(\tau) = \frac{\varphi_0(\tau)}{\varphi_0(0)} \text{ and } r_{\xi_1}(\tau) = \frac{\varphi_1(\tau)}{\varphi_1(0)}.$$

With the values $\sigma^2_{\xi_0}$ and $\sigma^2_{\xi_1}$ obtained in this way, on the basis of /377 (8.1.24) and (8.1.25), we will have the inequality

$$r_{0.1}(\tau) + r_{1.0}(\tau) = \frac{f(\tau)}{\sqrt{\varphi_0(0)\varphi_1(0)}} \leqslant 2, \tag{8.1.26}$$

coinciding with the condition (8.1.16).

Analysis of (8.1.22)-(8.1.25) shows that when determining $[R_n(\tau)]_c$ for the case when $K_a(t) = K_a(t + \tau) = K_a = \text{const}$, it will be possible to compute unambiguously all the statistical parameters of a linear statistically equivalent filter, with the exception of the reciprocal correlation coefficients $r_{0.1}(\tau)$ and $r_{1.0}(\tau)$. The lack of an additional equation necessary for unambiguous determination of the coefficients $r_{0.1}(\tau)$ and $r_{1.0}(\tau)$ is due to the fact that, in the analysis of the passage of signals and interference through the radio receiver and the CCRL decoder, when $K_a(t) = K_a(t + \tau) = K_a = \text{const}$, there is no dependence detected between $\xi_0(t)$ and $\xi_1(t)$. However, if we proceed on the

basis of condition (8.1.2), assumed previously, we can conclude that it is not mandatory to compute the coefficients $r_{0.1}(\tau)$ and $r_{1.0}(\tau)$ precisely. Therefore, it is admissible to use one of the possible solutions of equation (8.1.24), determining $r_{0.1}(\tau)$ and $r_{1.0}(\tau)$; it also is necessary to have $r_{0.1}(\tau) = r_{1.0}(-\tau)$, $r_{0.1}(\tau) \leq 1$ and $r_{1.0}(\tau) \leq 1$.

Equation (8.1.3) can be used not only with satisfaction of conditions (8.1.4) and (8.1.5) or (8.1.14)-(8.1.16), but also in those cases when the CCRL, under the influence of radio interference, remains quite close to a linear converter of transmitted commands. For clarification of the possibility of replacing a real CCRL with a linear statistically equivalent filter, it is most important to find the conditional constant component and the correlation function of the output signal $K_n(t)$ under the assumption that the input command $K_a(t)$ does not change with time. Then, it is necessary to investigate the influence exerted on $[\bar{K}_n]_c$ and $[R_n(\tau)]_c$ by a CCRL having nonlinearity of the signal $K_a(t) = K_a(t + \tau) = K_a = \text{const}$, first expanding the functions $[\bar{K}_n]_c$ and $[R_n(\tau)]_c$ into a Maclaurin series for the powers of K_a. If it is found that the role of terms proportional to K_a in the second and higher powers in the series for $[\bar{K}_n]_c$ and the terms dependent on K_a in the third and higher powers in the expansion for $[R_n(\tau)]_c$ is insignificant and condition (8.1.16) is satisfied precisely or with a small error, a real CCRL can be considered approximately linear. For such CCRL, the statistical parameters of the coefficients in equation (8.1.3) should be determined the same as for a "purely" linear CCRL.

4. Nonlinear Statistically Equivalent Filter. Principles of Statistical Linearization of CCRL

If a real CCRL subjected to radio interference becomes a nonlinear converter of transmitted commands $K_a(t)$ and the output signal $K_n(t)$ is a continuous function of $K_a(t)$, for description of the processes transpiring in the statistically equivalent filter, it is possible to use a polynomial of the n-th degree. The value n for such a statistically equivalent filter is selected in accordance with the method presented below. Then the relationship between $K_{ne}(t)$ and $K_a(t)$ has the following form /378

$$K_{ne}(t) = \xi_0(t) + \xi_1(t) K_a(t) + \xi_2(t) K_a^2(t) + \ldots + \xi_n(t) K_a^n(t), \qquad (8.1.27)$$

where $\xi_0(t)$, $\xi_1(t)$, ..., $\xi_n(t)$ are coefficients whose character of change and values are to be determined.

We note that expression (8.1.27) can be considered as the aggregate n + 1 of the first terms of a power series used in representing the solution of the equations describing the operation of the CCRL when the latter is acted upon by interference. One of the characteristics of this expression is that $K_{ne}(t)$ is a linear function of the coefficients $\xi_0(t)$, $\xi_1(t)$, ..., $\xi_n(t)$, all or part of which can be random. If the coefficients $\xi_0(t)$, $\xi_1(t)$, ..., $\xi_n(t)$, not dependent on $K_a(t)$, change randomly, as a result of normalization of the process $K_n(t)$ for stipulated values $K_a(t)$, the functions $\xi_0(t)$, $\xi_1(t)$, ..., $\xi_n(t)$ can be considered to have a normal distribution. By a corresponding stipulation of the correlation and reciprocal correlation functions for $\xi_0(t)$, $\xi_1(t)$, ..., $\xi_n(t)$, it is possible to ensure the necessary frequency conversions $K_a(t)$ by a nonlinear statistically equivalent filter. In addition, it should be remembered that equation (8.1.27) is convenient for modeling processes in a real CCRL using electronic computers.

The problem of the character of change of $\xi_1(t)$, $\xi_2(t)$, ..., $\xi_n(t)$ is solved in the same way as for a linear CCRL, on the basis of an analysis of the derived expressions for $[\bar{K}_n]_c$ and $[R_n(\tau)]_c$. In the selection of n and determination of the statistical parameters of the random coefficients entering into equation (8.1.27), the conditional constant component $[\bar{K}_n]_c$ and the conditional correlation function $[R_n(\tau)]_c$, computed for $K_a(t) \neq K_a(t + \tau)$, must be represented in the form of a Maclaurin series for powers of $K_a(t)$ and $K_a(t)$, $K_a(t + \tau)$, respectively. In each of the expansions, it is necessary to discard the terms not exerting a significant influence on $[\bar{K}_n]_c$ and $[R_n(\tau)]_c$. Then it is easy to determine n as the larger of the numbers characterizing the power of the transmitted command $K_a(t)$ in the last remaining terms of the expansions for $[\bar{K}_n]_c$ and $[R_n(\tau)]_c$. If $[R_n(\tau)]_c$ is determined when $K_a(t) = K_a(t + \tau)$ /379 $= K_a = \text{const}$, the exponent n is assumed to be equal to the value of the degree

of the polynomial used to express $[\overline{K}_n]_c$ or to half the exponent of K_a in the last of the remaining terms in the expansion for $[R_n(\tau)]_c$.

The statistical parameters of the random functions $\xi_0(t)$, $\xi_1(t)$, ..., $\xi_n(t)$, entering into equation (8.1.27), can be determined easily if, as a result of analysis of the problem of passage of signals and interference through a real CCRL, when $K_a(t) \neq K_a(t + \tau)$, we compute the functions $[\overline{K}_n]_c$ and $[R_n(\tau)]_c$. This requires use of the method of equalization of the coefficients in the expansions for $[\overline{K}_n]_c$ and $[R_n(\tau)]_c$ and also in the expressions for $[\overline{K}_{ne}]_c$ and $[R_{ne}(\tau)]_c$, obtained on the basis of equation (8.1.27). If $\xi_0(t)$, $\xi_1(t)$, ..., $\xi_n(t)$ are not random, they should be determined by equalization of the corresponding coefficients in the expansion for $[\overline{K}_n]_c$ and in the expression for $[\overline{K}_{ne}]_c$.

As a result of use of the described method, the equation (8.1.27) for a nonlinear statistically equivalent filter will characterize a real CCRL with an accuracy determined by the discarded terms in the corresponding expansions.

If the function $[R_n(\tau)]_c$ is sought for $K_a(t) = K_a(t + \tau) = K_a = \text{const}$, which usually can be done more simply than for $K_a(t) \neq K_a(t + \tau)$, it is easy to show that it is impossible to obtain an unambiguous determination of all the correlation and reciprocal correlation functions for the coefficients entering into equation (8.1.27) for a nonlinear statistically equivalent filter. However, for CCRL in which the correlation time τ_c of the random parameters is such that in the course of τ_c there is virtually no change of the transmitted command, it is possible to ensure conditions (8.1.2) also with an arbitrary stipulation of some of the sought-for correlation and reciprocal correlation functions; however, in this case, it is necessary to take into account the requirement of the necessity for deriving computation formulas convenient for practical use. The problem of determination of the statistical parameters for $\xi_0(t)$, $\xi_1(t)$, ..., $\xi_n(t)$ is simplified appreciably if the polynomial characterizing $[R_n(\tau)]_c$ does not contain terms with the commands $K_a(t)$, having odd exponents. This is because in this case the coefficients $\xi_0(t)$, $\xi_1(t)$, ..., $\xi_n(t)$ can be considered uncorrelated with one another.

If the function $[R_n(\tau)]_c$, determined for $K_a(t) = K_a(t + \tau) = K_a = \text{const}$ and represented in the form of a Maclaurin series for powers of K_a, contains terms with odd exponents on K_a and an arbitrary stipulation of the necessary number of correlation and reciprocal correlation functions for $\xi_0(t)$, $\xi_1(t)$, ..., $\xi_n(t)$ is impossible, the signal $K_{ne}(t)$ can be determined as the sum /380 of the statistically unrelated power and irrational functions of K_a.

In the expansion $[R_n(\tau)]_c$ in order to take into account the terms containing K_a with odd exponents ν, in equation (8.1.27), in addition to the functions $\xi_\nu(t)K_a^\nu(t)$, it is necessary to introduce the terms

$$\zeta_\nu(t)\sqrt{1 \pm K_{ic}^\nu(t)},$$

where ζ_ν is a random function of time with zero mathematical expectation; $K_{ic}(t)$ is the coefficient of the transmitted command.

The sign before $K_{ic}^\nu(t)$ should be the same as in the term containing K_a^ν in the expansion for $[R_n(\tau)]_c$.

If the series of the function $[R_n(\tau)]_c$ includes terms having $-K_a^{2\nu}(t)$ as a cofactor of the function, in equation (8.1.27), in addition to functions of the type $\xi_\nu(t)K_a^{2\nu}(t)$, we should have the functions

$$\zeta_\nu(t)\sqrt{1 - K_a^{2\nu}(t)}.$$

Nonlinear statistically equivalent filters of the considered type also can be used to replace CCRL for which the functions $[\bar{K}_n]_c$ and $[R_n(\tau)]_c$ are reflected by a finite number of terms dependent on K_a under the condition that the functions $[\bar{K}_n]_c$ and $[R_n(\tau)]_c$ contain terms with a fractional exponent on K_a. The same result is obtained in those cases when both functions $[\bar{K}_n]_c$ and

$[R_n(\tau)]_c$ include terms with fractional exponents on K_a or when the functions $[\overline{K_n}]_c$ and $[R_n(\tau)]_c$ are polynomials of K_a.

We will illustrate the above using the example of a CCRL for which

$$[\overline{K_n}]_c = b + aK_a, \tag{8.1.28}$$

$$[R_n(\tau)]_c = \varphi_0(\tau) + \varphi(\tau)K_a. \tag{8.1.29}$$

Then it will be shown that the conditional constant component and the time-averaged conditional correlation function of the output signal of a CCRL with pulse-width modulation, under the influence of high-level interference, are determined by expressions of the form (8.1.28) and (8.1.29) when the former are computed for $K_a(t) = K_a(t + \tau) = K_a = \text{const}$.

Analyzing expressions (8.1.28) and (8.1.29), it can be concluded that the processes transpiring in a statistically equivalent filter replacing the considered CCRL should be described by the following equation

$$K_{ne}(t) = \xi_0(t) + \xi_1(t)K_a + \zeta_1(t)\sqrt{1 + K_{1c}}. \tag{8.1.30}$$

After determining the functions $[\overline{K_{ne}}]_c$ and $[R_e(\tau)]_c$ on the basis of /381 equation (8.1.30), we find that the introduced nonlinear statistically equivalent filter and a real CCRL will be equivalent when

$$\overline{\xi_0(t)} = b; \quad \overline{\xi_1(t)} = a; \quad \overline{\zeta_1(t)} = 0;$$

$$R_{\xi_0}(\tau) = \varphi_0(\tau) - R_{\zeta_1}(\tau); \quad R_{\xi_1}(\tau) = \varphi(\tau)K_{a\max}; \quad R_{\xi_1}(\tau) = 0,$$

where $R_{\xi_0}(\tau)$, $R_{\zeta_1}(\tau)$ and $R_{\xi_1}(\tau)$ are the correlation functions for $\xi_0(t)$, $\zeta_1(t)$ and $\xi_1(t)$.

If the CCRL under the influence of interference is transformed into an essentially nonlinear apparatus, the degree n of the polynomial (8.1.27) becomes very large. Under these conditions, the use of a nonlinear statistically equivalent filter, whose equation is derived taking into account both $[\overline{K_n}]_c$ and $[R_n(\tau)]_c$ is extremely difficult and, therefore, the problem arises of finding such a statistically equivalent converter of the transmitted commands K_a which is feasible (for example, in modeling) by means of quite simple technical solutions.

There are two ways to solve such a problem. The first is based on the fact that there is a considerable deviation of the CCRL from linearity when it is subjected to high-level interference, when the conversion properties of the CCRL and especially the mean value of the transfer constant are distorted appreciably by interference. Under such conditions, the fluctuation components in the output signal $K_n(t)$ exert an insignificant influence on the total error of rocket guidance when the rocket has an extremely small passband. Therefore, a real CCRL can be replaced with a high degree of accuracy by a statistically equivalent converter whose equation has the following form

$$K_{ne}(t) = [\overline{K}_n]_c.$$

In this equation, the command K_a, on which $[\overline{K}_n]_c$ is dependent, should be considered a function of time.

The second way to solve the above-mentioned problem assumes the applicability of the well-known principle of statistical linearization (refs. 84 and 85) to systems with random parameters.

The essence of this principle, developed for nonlinear systems with constant parameters, is the introduction of an inertialess or inertial converter whose parameters are determined in accordance with the selected criterion of approximation of random functions, on the basis of a given law of probability distribution for the input action.

In the statistical linearization of a CCRL, the problem is reduced to finding a linear device which, in contrast to a linear statistically equivalent filter, we will call a statistically equivalent linear converter. Its parameters are determined solely on the basis of the moments (unconditional) /382 for the CCRL input and output signals. When introducing a statistically equivalent linear converter, it is necessary to take into account that as a result of interference a signal is formed at the CCRL output even when $K_a = 0$ and that the CCRL parameters change randomly.

If it is assumed that the conditions of statistical equivalence of a real CCRL and the statistically equivalent linear converter are characterized by the relations (8.1.1) and (8.1.2), as will be seen from the text which follows, the necessary statistical parameters of the statistically equivalent linear converter are determined unambiguously when its equation is written in the following form

$$K_{ne}(t) = c + \xi(t)K_a(t) \qquad (8.1.31)$$

Here c represents the constant value or the determined function of time (in the case of presence of nonstationary interference) and $\xi(t)$ is a random function not dependent on K_a and having a mathematical expectation equal to zero.

In order for the coefficient c not to change randomly in equation (8.1.31) it can be only a function of the statistical parameters for the transmitted command $K_a(t)$. Therefore, bearing in mind that the mathematical expectation for the product $\overline{\xi(t)K_a(t)}$ is equal to zero, in order to ensure satisfaction of equation (8.1.1), it is necessary to apply the concept of mathematical expectation or the time-averaged mathematical expectation (unconditional) $\overline{K}_{ne}$ for the function $K_{ne}(t)$. Then we will have

$$c = \overline{K}_n. \tag{8.1.32}$$

It is easy to see that $\overline{K}_n$ can be computed only when using a known law of probability distribution for $K_a(t)$.

The correlation function or the time-averaged correlation function (unconditional) $R_e(\tau)$ of the random function $K_{ne}(t)$ is

$$R_e(\tau) = R_\xi(\tau)\,\overline{K_a(t)\,K_a(t+\tau)}, \tag{8.1.33}$$

where $R_\xi(\tau)$ characterizes the correlation function of the random coefficient $\xi(t)$, and $\overline{K_a(t)K_a(t+\tau)}$ is the initial or time-averaged initial moment of the second order for the CCRL output signal.

On the basis of expressions (8.1.2) and (8.1.33), we obtain

$$R_\xi(\tau) = \frac{R_n(\tau)}{\overline{K_a(t)\,K_a(t+\tau)}}. \tag{8.1.34}$$

It can be seen from formula (8.1.34) that the function $R_\xi(\tau)$ can be computed if the following are known:

– the correlation function $R_n(\tau)$ of the random signal $K_n(t)$, forming at the output of a real CCRL with allowance for the effect of radio interference and the random character of change of $K_a(t)$;

– the initial or time-averaged initial moment of the second order $\overline{K_a(t)K_a(t+\tau)}$ for the transmitted command $K_a(t)$. /383

The possibility of finding $R_n(\tau)$, dependent on the statistical characteristics not only of radio interference, but also of the transmitted commands, is related to the need for determining in a general case the conditional correlation function $[R_n(\tau)]_c$ with the assumption that the values $K_a(t)$ and $K_a(t + \tau)$ are stipulated, and also the two-dimensional probability density for the random function $K_a(t)$. However, for those values τ for which $R_\xi(\tau)$ differs appreciably from zero, it can be assumed approximately that $K_a(t) \approx K_a(t + \tau)$. In this case, the conditions for finding $R_n(\tau)$ become possible with the stipulation of only the one-dimensional probability density for $K_a(t)$, which also is required for computation of $\overline{K}_n$ for the known function $[\overline{K}_n]_c$. Then expression (8.1.34) assumes the following form

$$R_\xi(\tau) \approx \frac{R_n(\tau)}{\overline{K_a^2(t)}},$$

where $\overline{K_a^2(t)}$ is the second initial moment of the random function $K_a(t)$ (or the time-averaged second initial moment for the quasi-stationary CCRL input signal).

It follows from the above that the replacement of a real essentially nonlinear CCRL by a statistically equivalent linear converter requires more complex operations and a greater quantity of initial data than in the case of use of a statistically equivalent filter based on use of conditional mathematical expectation (constant component) and the conditional correlation function (or the time-averaged conditional correlation function) for the output signal $K_n(t)$.

In addition to a converter which is defined by equation (8.1.31), essentially nonlinear CCRL can be replaced by statistically equivalent linear devices representing inertialess or inertial converters with constant parameters or parameters changing regularly with time.

The parameters of such converters can be determined on the basis of references 84 and 85. It should be mentioned here that when using the mentioned statistically equivalent linear converters for replacement of CCRL, the only values which can be considered stipulated are the moments and the statistical characteristics of the reciprocal relations for the CCRL input and output signals.

It should be noted here that the replacement of a real CCRL by an inertialess statistically equivalent linear converter with constant or variable (but nonrandom) parameters does not make it possible to obtain identical correlation functions for $K_n(t)$ and $K_{ne}(t)$, and the finding of the parameters /384

of an inertial converter with a determined transfer constant in a number of cases, especially under the influence of nonstationary interference, involves considerable technical difficulties (refs. 84 and 85).

In actual practice, the stipulation of the distribution laws of the transmitted commands in a CCRL operating outside a closed circuit usually is not a difficult problem. However, if the CCRL is included as one of the links of an automatic control system, the probability densities of the signals arriving at the CCRL input are unknown in advance. In this case, for determination of the parameters of a statistically equivalent linear converter, it is necessary to use the method of successive approximations in the solution of the equations of the control system as a whole (ref. 84).

The need for solution of the equations of a radio control system for determination of the parameters of a statistically equivalent linear converter is one of the shortcomings of the method of statistical linearization in comparison with the principle of replacement of a real CCRL by a linear or nonlinear statistically equivalent filter. When using a statistically equivalent filter, both the theoretical and experimental investigation of the influence of interference on the CCRL should be conducted without its inclusion in the guidance circuit.

We note, in conclusion, that the methods discussed here for mathematical description of processes in CCRL, with the influence of radio interference taken into account, also can be applied to instruments for measuring the coordinates of targets and rockets and also to data transmission systems.

8.2. Quantitative Characteristics of Noise Immunity of CCRL

As was demonstrated in the preceding section, in order to replace CCRL with a linear or nonlinear statistically equivalent filter, it is necessary to find the functions $[\bar{K}_n]_c$ and $[R_n(\tau)]_c$ for the command $K_n(t)$. If the CCRL under the influence of radio interference is transformed into an essentially nonlinear apparatus, it may be necessary to determine $\bar{K}_n$ and $R_n(\tau)$. The statistical parameters $\bar{K}_n$ and $R_n(\tau)$ can be computed if $[\bar{K}_n]_c$ and $[R_n(\tau)]_c$ are known, as well as the corresponding laws of probability distribution for the signal $K_a(t)$. It therefore follows that a knowledge of the functions $[\bar{K}_n]_c$ and $[R_n(\tau)]_c$ is necessary and adequate or only necessary for evaluation of the influence of interference on the CCRL. Therefore, in an analysis of the effect of interference on the CCRL, it is most important to find the functions $[\bar{K}_n]_c$ and $[R_n(\tau)]_c$. In place of the function $[R_n(\tau)]_c$, in many cases, it is possible to use the more

easily computed spectral density of the random stationary signal $K_n(t)$ or /385 the time-averaged conditional spectral density of this same random signal $K_n(t)$ if it is quasi-stationary. Denoting the mentioned spectral densities when $\omega \geq 0$ by the same symbol $[G(\omega)]_c$, we will have

$$[G(\omega)]_c = 4\int_0^\infty [R_n(\tau)]_c \cos\omega\tau d\tau. \tag{8.2.1}$$

In actuality, the function $[G(\omega)]_c$, which henceforth will be called the conditional spectral density, usually occupies a considerably greater spectrum of frequencies than the effective width of the guidance circuit passband and therefore usually it is sufficient to know the value $[G(0)]_c$. When the spectral density $[G(\omega)]_c$ in an investigation of the control system as a whole can be replaced by $[G(0)]_c$, the function $[R_n(\tau)]_c$ will have the form of a δ-function since

$$[R_n(\tau)]_c = \frac{1}{2\pi}\int_0^\infty [G(\omega)]_c \cos\omega\tau d\tau \approx \frac{1}{2}[G(0)]_c \delta(\tau). \tag{8.2.2}$$

The conditional constant component $[\overline{K}_n]_c$ and the conditional spectral density $[G(0)]_c$ (or the function $R_n(\tau)$), in a general case, are dependent on the properties of the CCRL, the type of interference, the ratio $q_0 = \frac{U_s}{U_n}$ of the effective strengths (mean intensities) of the signal U_s and the interference U_n, the parameters of interference modulation m_n, etc. Therefore, the following relationships can be considered quantitative characteristics of the CCRL noise immunity

$$[\overline{K}_n]_c = F_1(q_0, m_n, \ldots), \tag{8.2.3}$$

$$[G(0)]_c = F_2(q_0, m_n, \ldots). \tag{8.2.4}$$

In addition, in many cases, it is important to know the conditional dispersion, equal to

$$[\sigma^2]_c = \frac{1}{2\pi}\int_0^\infty [G(\omega)]_c d\omega = F_3(q_0, m_n, \ldots). \tag{8.2.5}$$

As already mentioned, the output signal $K_n(t)$ usually consists of two parts, one of which is the additive noise and the other a voltage (current) which is dependent on the transmitted command. As a result, the noise immunity of the CCRL also can be evaluated by the mathematical expectation and correlation function of additive noise $\xi_0(t)$ and the change of the conversion properties of the CCRL, which is characterized by the mean values and the correlation functions of the coefficients $\xi_1(t)$, $\xi_2(t)$, ..., $\xi_n(t)$ in equation (8.1.27) and also the value c and the correlation function of the random parameter $\xi(t)$ in relation (8.1.31). In addition, in some cases as convenient evaluations of the noise immunity of a CCRL, it is possible to use the statistical parameters of distortion of the command /386

$$\Delta K(t) = K_n - K(t). \qquad (8.2.6)$$

These include:

– the conditional mathematical expectation and conditional correlation function (or spectral density) for $\Delta K(t)$ if the process $K_n(t)$ is stationary;

– the conditional time-averaged mathematical expectation (conditional constant component) and correlation function (or spectral density) for $K_n(t)$ if the process is quasi-stationary.

By denoting here and in the text below the conditional mathematical expectation (or conditional constant component) and also the conditional spectral density (or time-averaged conditional spectral density) by the symbols $[\overline{\Delta K}]_c$ and $[G_{\Delta K}(\omega)]_c$, it can be concluded that in the case of presence of wideband interference it is sufficient to determine $[\overline{\Delta K}]_c$ and $[G_{\Delta K}(0)]_c$. Here it should be remembered that $[G_{\Delta K}(\omega)]_c = [G(\omega)]_c$, since each of these functions characterizes the spectral density of fluctuations of the output command $K_n(t)$.

In comparative evaluations of the noise immunity of CCRL of different types and with different kinds of output signals, it is desirable to use the concepts of a command coefficient $K_{cn}(t) = \dfrac{K_n(t)}{K_{max}}$ and distortions of the command coefficient $\Delta K_c(t) = \dfrac{K_n(t) - K(t)}{K_{max}}$.

On the basis of the known conditional and unconditional mathematical expectations (constant component) and the correlation function (or spectral density) or the time-averaged correlation function (time-averaged spectral density)

of the input and output commands, it is possible to determine the corresponding statistical characteristics for $K_{cn}(t)$ and $\Delta K_c(t)$.

If $K_n(t)$ is a nonstationary function of time, it is necessary to use as the quantitative characteristics of the noise immunity of the CCRL the dependence of the conditional mathematical expectation $[\overline{K_n(t)}]_c$ and the so-called instantaneous conditional spectral density $[G(\omega, t)]_c$ or the conditional correlation function $[R_n(t, \tau)]_c$, being functions of t, q_0, m_n, etc. In addition, for CCRL with nonstationary commands $K_n(t)$, it is possible to introduce into consideration the same statistical parameters as for a CCRL in which the signal $K_n(t)$ is a stationary function of time.

It is convenient to solve the problem of evaluation of the noise immunity of a CCRL in several stages. The number of stages usually is equal to the number of nonlinear devices in the radio receiver and CCRL decoder. In actual practice, the analysis of the passage of signals and interference should be accomplished beginning with the CCRL output. /387

The quantitative characteristics of noise immunity of the CCRL introduced above are suitable not only for single-channel but also for multichannel CCRL. The distinguishing characteristic of the statistical parameters of the output signals and their distortions in a multichannel CCRL is a general dependence of these parameters on the transmitted commands for all channels.

The quantitative measure of the noise immunity of CCRL designed for the transmission of single commands is the law of probability distribution of displacement Δt of the CCRL output signals. However, in actual practice, in many cases, it is sufficient to know the mathematical expectation $\overline{\Delta t}$ and the dispersion $\sigma^2_{\Delta t}$ of the random value Δt in dependence on the parameters of the CCRL, signals and interference.

Usually, interference of low and high levels leads to qualitatively different processes transpiring in the CCRL receiver. Therefore, their influence on the output commands of CCRL with different kinds of modulation of subcarrier oscillations, which is the subject of the remaining part of this chapter, will be investigated separately.

8.3. Effect of Low-Level Fluctuation Interference on a CCRL with Pulse-Width Modulation

Now we will consider a CCRL with pulse-width modulation of sinusoidal subcarrier oscillations on the assumption that the decoder is designed as shown

in figure 7.8. Analysis of figure 7.8 makes it possible to draw the conclusion that solution of the problem of the influence of interference on the CCRL should be divided into three stages. In the first stage, we compute the dependence of the statistical characteristics of the output signals of the CCRL on the statistical parameters of the voltages produced by the threshold apparatus TA_1. Then we analyze the relationship between the statistical parameters of the signals forming at the TA_1 output and at the inputs of detectors D_1 and D_2. The problem of the third stage is determination of the moments for the voltages reaching D_1 and D_2 in dependence on the structure and intensity of the signals and interference at the CCRL input.

1. Relationship between the Statistical Characteristics of the CCRL Output Signals and the Threshold Apparatus

In the absence of interference, the threshold apparatus TA_1 is fed bipolar pulses, represented in figure 8.1a (curve 1). At the output of TA_1, having the triggering thresholds $U_{thr\ 1}$ and $U_{thr\ 2}$, the voltages $u_{p1}(t)$ and $u_{p2}(t)$ are formed; these are shown by solid lines in figure 8.1b, c. The voltages $u_{p1}(t)$ and $u_{p2}(t)$ have maximum and minimum values equal to $u_1 + U_{m1}$, $u_2 + U_{m2}$ /388

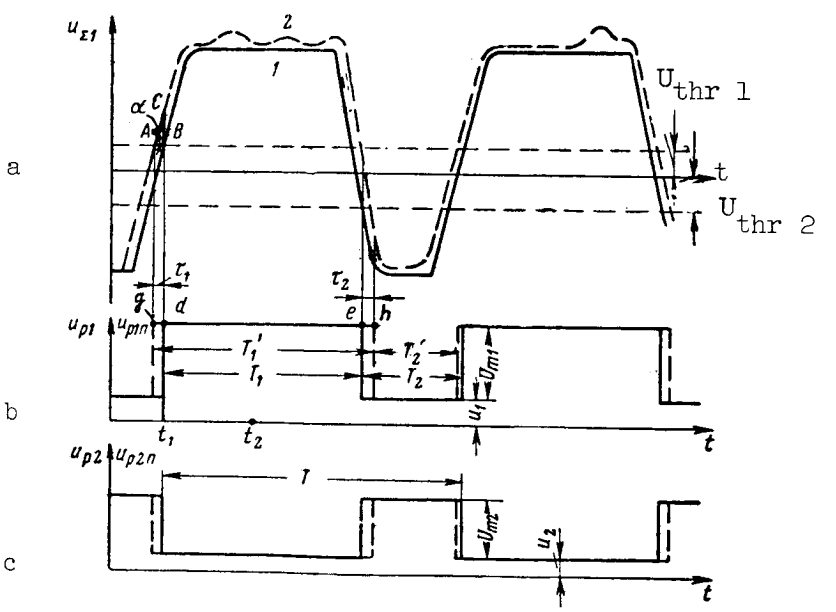

Figure 8.1

and u_1, u_2, respectively. The durations of the positive drops are T_1 and T_2 and the repetition interval is T.

The value of the command K(t), where K(t) here and in the text which follows corresponds to the function $K_1(t)$, mentioned in chapter 7, on the basis of figure 7.8, neglecting the inertial properties of the CCRL, is determined by the following expression

$$K(t) = u_{F1}(t) - u_{F2}(t) = k_{F1}u_{p1} - k_{F2}u_{p2}, \qquad (8.3.1)$$

where $u_{F1}(t)$ and $u_{F2}(t)$ are the output voltages of the filters F_1 and F_2; u_{p1} and u_{p2} are the mean components of the voltages $u_{p1}(t)$ and $u_{p2}(t)$; k_{F1} and k_{F2} are the transfer constants of the filters F_1 and F_2 at the zero frequency.

We note that expression (8.3.1) was written on the assumption that the transfer constant k_{SD} of the subtracting device is included in k_{F1} and k_{F2}.

When there is interference $u_n(t)$, the parameters of the pulses $u_{\Sigma 1}$ are distorted. If the effective value $u_n(t)$ at the output of the detectors D_1 and D_2 is several times less than the amplitude of the useful signals, a voltage u_Σ is created at the Σ_1 output, one of whose possible variants has been shown in figure 8.1a (curve 2). Because of the insignificance of fluctuations in the amplitudes of the pulses $u_{\Sigma 1}(t)$, it is possible, by appropriate selection of the thresholds $U_{thr\ 1}$ and $U_{thr\ 2}$, to restrict interference effects to /389 random oscillations of the moments of formation and durations of the pulses generated by the threshold apparatus. Then the pulses $u_{p1\ n}(t)$ and $u_{p2\ n}(t)$ appear at the TA_1 output; the leading edge and clipping of these pulses are shown by a dashed line in figure 8.1b, c, and their peaks coincide with the plane parts of the signals $u_{p1}(t)$ and $u_{p2}(t)$. For appearance of the voltages shown in figure 8.1b, c, the duration of the positive drops of the pulses $u_{p1\ n}(t)$ and $u_{p2\ n}(t)$ is T_1' and T_2'.

Under the influence of the voltages $u_{p1\ n}(t)$ and $u_{p2\ n}(t)$, the random command $K_n(t)$ is formed at the CCRL output; this command is equal to

$$K_n(t) = u_{1n}(t) - u_{2n}(t) \qquad (8.3.2)$$

Here $u_{1n}(t)$ and $u_{2n}(t)$ are the voltages produced by the filters F_1 and F_2 when there is radio interference.

The expressions (8.3.1) and (8.3.2) make it possible to determine the conditional mathematical expectations $[\overline{K_n(t)}]_c$ and $[\overline{\Delta K(t)}]_c$ for the output signal $K_n(t)$ and the distortion of the command $\Delta K(t)$ if the conditional mathematical expectations $[\overline{u_{1n}(t)}]_c$ and $[\overline{u_{2n}(t)}]_c$ of the voltages $u_{1n}(t)$ and $u_{2n}(t)$ are known.

A knowledge of $[\overline{u_{1n}(t)}]_c$ and $[\overline{u_{2n}(t)}]_c$ also makes it possible to find the conditional mathematical expectations $[\overline{K_{cn}(t)}]_c$ and $[\overline{\Delta K_c(t)}]_c$ for the command coefficient $K_{cn}(t)$ and the distortions of the command coefficient $\Delta K_c(t)$, respectively. For given conditional correlation and reciprocal correlation functions or corresponding spectral and reciprocal spectral densities of the voltages $u_{1n}(t)$ and $u_{2n}(t)$, it is possible to compute the conditional instantaneous spectral densities $[G(t, 0)]_c$ and $[G_c(t, 0)]_c$ at the frequency $\omega = 0$ for the fluctuation components of the output signal $K_n(t)$ and the command coefficient $K_{cn}(t)$.

The voltages $u_{1n}(t)$ and $u_{2n}(t)$ are formed from pulses fed from the threshold apparatus TA_1 and having random durations and times of formation. Such random signals are nonstationary, since their mathematical expectation and correlation function will be dependent on time. This can be seen from the mere fact that for times close to $t = t_1$, the voltage $u_{pl\ n}(t)$ will have an amplitude equal to $u_1 + U_{ml}$, with a lesser probability than at the point t_2 (fig. 8.1b). At the same time, the signal $K_n(t)$ is close to stationary. This can be attributed to the fact that the conditional mathematical expectations and the correlation functions of the voltages $u_{pl\ n}(t)$ and $u_{p2\ n}(t)$, when the CCRL is subjected to stationary or nearly stationary interference, will be periodic functions of time. The repetition interval is T and is an insignificant value /390 in comparison with the time constant of the control system as a whole.

Then the noise immunity of the CCRL can be characterized not by the functions $[\overline{K_n(t)}]_c$, $[\overline{\Delta K(t)}]_c$, $[\overline{K_{cn}(t)}]_c$, $[\overline{\Delta K_c(t)}]_c$, $[G(t, 0)]_c$ and $[G_c(t, 0)]_c$, but by the values, obtained as a result of their time-averaging, $[\overline{K}_n]_c$, $[\overline{\Delta K}]_c$, $[\overline{K}_{cn}]_c$, $[\overline{\Delta K}_c]_c$, $[G(0)]$ and $[G_c(0)]_c$, where $[\overline{K}_{cn}]_c$ and $[\overline{\Delta K}_c]_c$ are the conditional constant components for the coefficient of the output command and its distortion, and $[G_c(0)]_c$ is the conditional spectral density when $\omega = 0$ for the fluctuations $K_{cn}(t)$.

On the basis of expressions (8.3.1) and (8.3.2) we will have

п = n
у = c
ф = F

$$[\overline{K}_n]_y = [\overline{u}_{1n}]_y - [\overline{u}_{2n}]_y, \tag{8.3.3}$$

$$[\overline{\Delta K}]_y = [\overline{u}_{1n}]_y - u_{\phi 1} - \{[\overline{u}_{2n}]_y - u_{\phi 2}\}, \tag{8.3.4}$$

(Note: Key to use for equations (8.3.3) through (8.3.8) only.)

where u_{F1} and u_{F2} characterize the constant components of the signals $u_{F1}(t)$ and $u_{F2}(t)$ in the absence of interference, and $[\overline{u}_{1n}]_c$ and $[\overline{u}_{2n}]_c$ are the conditional constant components of the voltages $u_{1n}(t)$ and $u_{2n}(t)$.

Taking into account the voltages $u_{p1\ n}(t)$, $u_{p2\ n}(t)$, $u_{p1}(t)$ and $u_{p2}(t)$, acting on the F_1 and F_2 inputs in the presence and absence of interference, expressions (8.3.3) and (8.3.4) can be reduced to the following form

$$[\overline{K}_n]_y = k_{\phi 1}[\overline{u}_{p1\,n}]_y - k_{\phi 2}[\overline{u}_{p2\,n}]_y, \tag{8.3.5}$$

$$[\overline{\Delta K}]_y = k_{\phi 1}\{[\overline{u}_{p1\,n}]_y - u_{p1}\} - k_{\phi 2}\{[\overline{u}_{p2\,n}]_y - u_{p2}\}, \tag{8.3.6}$$

where $[\overline{u}_{p1\ n}]_c$ and $[\overline{u}_{p2\ n}]_c$ are the conditional constant components of the voltages $u_{p1\ n}(t)$ and $u_{p2\ n}(t)$, computed on the assumption that the value of the transmitted command $K_a(t)$ does not change.

The maximum value of the command at the CCRL output, in the absence of interference and under the condition that the threshold apparatus TA_1 produces the voltages $u_{p1}(t)$ and $u_{p2}(t)$, is equal to

$$K_{max} = k_{F1}(u_1 + U_{m1}) - k_{F2}u_2.$$

Therefore, the constant components $[\overline{K}_{cn}]_c$ and $[\overline{\Delta K}_c]_c$ for a given value $K_a(t)$ will be

$$[\overline{K}_{cn}]_c = \frac{k_{\phi 1}[\overline{u}_{p1\,n}]_y - k_{\phi 2}[\overline{u}_{p2\,n}]_y}{k_{\phi 1}(u_1 + U_{m1}) - k_{\phi 2}u_2}, \tag{8.3.7}$$

$$[\overline{\Delta K}_c]_c = \frac{k_{\phi 1}\{[\overline{u}_{p1\,n}]_y - u_{p1}\} - k_{\phi 2}\{[\overline{u}_{p2\,n}]_y - u_{p2}\}}{k_{\phi 1}(u_1 + U_{m1}) - k_{\phi 2}u_2}. \tag{8.3.8}$$

It is known that the time-averaged conditional spectral density $[G(\omega)]_c$ which for a CCRL with low-frequency output filters will be denoted by $G_F(\omega)$ and which for brevity will be called simply the conditional spectral density of the random signal $K_n(t)$, determined by the difference between the two voltages $u_{1n}(t)$ and $u_{2n}(t)$, is equal to /391

$$G_f(\omega) = G_1(\omega) + G(\omega) - G_{r1}(\omega) - G_{r2}(\omega),$$

where $G_1(\omega)$, $G_2(\omega)$, $G_{r1}(\omega)$ and $G_{r2}(\omega)$ are the conditional (time-averaged) spectral and reciprocal spectral densities of the voltages $u_{1n}(t)$ and $u_{2n}(t)$ for the frequencies $0 \le \omega < \infty$, determined when $K_a(t) = \text{const}$. But

$$G_1(\omega) = G_{p1}(\omega)\,|Y_1(j\omega)|^2, \tag{8.3.9}$$

$$G_2(\omega) = G_{p2}(\omega)\,|Y_2(j\omega)|^2, \tag{8.3.10}$$

$$G_{r1}(\omega) = G_{1.2}(\omega)\,Y_1^*(j\omega)\,Y_2(j\omega), \tag{8.3.11}$$

$$G_{r2}(\omega) = G_{2.1}(\omega)\,Y_1(j\omega)\,Y_2^*(j\omega). \tag{8.3.12}$$

Here $G_{p1}(\omega)$, $G_{p2}(\omega)$, $G_{1.2}(\omega)$ and $G_{2.1}(\omega)$ are the conditional spectral and reciprocal spectral densities of the voltages $u_{p1\,n}(t)$ and $u_{p2\,n}(t)$, computed when $T_1 = \text{const}$ and $T_2 = \text{const}$; $Y_1(j\omega)$ and $Y_2(j\omega)$ are the frequency characteristics of the filters F_1 and F_2; $Y_1^*(j\omega)$ and $Y_2^*(j\omega)$ are functions conjugate with $Y_1(j\omega)$ and $Y_2(j\omega)$.

Therefore

$$G_f(\omega) = G_{p1}(\omega)\,|\,Y_1(j\omega)\,|^2 + G_{p2}(\omega)\,|\,Y_2(j\omega)\,|^2 -$$
$$- G_{1.2}(\omega)\,Y_1^*(j\omega)\,Y_2(j\omega) - G_{2.1}(\omega)\,Y_1(j\omega)\,Y_2^*(j\omega).$$

If the conditional spectral densities $S_{p1}(\omega)$, $S_{p2}(\omega)$, $S_{1.2}(\omega)$ and $S_{2.1}(\omega)$ of the voltages $u_{p1\ n}(t)$ and $u_{p2\ n}(t)$ are known for the region of frequencies $-\infty \leq \omega \leq \infty$, then

$$G_f(\omega) = 2\,[S_{p1}(\omega)\,|\,Y_1(j\omega)\,|^2 + S_{p2}(\omega)\,|\,Y_2(j\omega)\,|^2 -$$
$$- S_{1.2}(\omega)\,Y_1^*(j\omega)\,Y_2(j\omega) - S_{2.1}(\omega)\,Y_1(j\omega)\,Y_2^*(j\omega)]. \qquad (8.3.13)$$

It therefore follows that the value $G_F(0)$, equal to $G_F(\omega)$ when $\omega = 0$, is

$$G_F(0) = 2[k_{F1}^2 S_{p1}(0) + k_{F2}^2 S_{p2}(0) - 2k_{F1}k_{F2}S_{1.2}(0)]. \qquad (8.3.14)$$

It must be remembered that when writing (8.3.14) we took into account the equality of the real parts of $S_{1.2}(\omega)$ and $S_{2.1}(\omega)$ when $\omega = 0$.

Formula (8.3.14) shows that for given parameters of the filters for determination of $G_F(0)$, it is sufficient to know the spectral and the reciprocal spectral densities of the voltages $u_{p1\ n}(t)$ and $u_{p2\ n}(t)$ acting at the input of the filters F_1 and F_2. /392

If the expressions (8.3.13) and (8.3.14) are divided by

$$K_{max}^2 = [k_{F1}(u_1 + U_{m1}) - k_{F2}U_{m2}]^2,$$

it is possible to derive formulas making it possible to compute the conditional spectral densities $G_{cf}(\omega)$ and $G_{cf}(0)$ of low-frequency fluctuations of the command coefficient at the CCRL output when the CCRL has filters F_1 and F_2 in the decoder.

We will determine the dependence of $[\overline{K_n}]_c$, $[\overline{K_{cn}}]_c$, $[\overline{\Delta K}]_c$, $[\overline{\Delta K_c}]_c$, $G_F(0)$ and $G_{cf}(0)$ on the statistical characteristics of the fluctuations τ_1 and τ_2 of the leading edges of the pulses $u_{p1\ n}(t)$ and $u_{p2\ n}(t)$.

Expression (8.3.1) can be replaced by formula (7.2.9) if it is remembered that

$$\frac{T_1}{T}=\frac{K_C+T}{2T}=\frac{1}{2}\left(1+\frac{k_C K_{a\max}}{T}K_{ic}\right)=$$

$$=\frac{1}{2}(1+k_{tK}K_{ic})=\frac{1}{2}(1+K_{Cc}) \qquad (8.3.15)$$

and

$$\frac{T_2}{T}=\frac{T-K_C}{2T}=\frac{1}{2}(1-k_{tK}K_{ic})=\frac{1}{2}(1-K_{Cc}) \qquad (8.3.16)$$

and the subscript "1" in formula (7.2.9) has been omitted.

Here $k_{tK}=\frac{k_C}{T}K_{a\ max}$ is the transfer constant of the coder for the transmitted command coefficient; in a general case, k_{tK} can be less than 1.

It can be seen from figure 8.1b and c that $u_{pl\ n}(t)$ and $u_{p2\ n}(t)$ can be represented as follows

$$u_{p1\,n}(t)=u_1+u_3(t)+u_4(t), \qquad (8.3.17)$$

$$u_{p2\,n}(t)=u_2+U_{m2}-u_4(t), \qquad (8.3.18)$$

where $u_3(t)$ and $u_4(t)$ are positive voltage pulses having the duration T_1' and amplitudes equal to U_{m1} - U_{m2} and U_{m2}, respectively.

Then for the conditional constant components of the voltages $u_{pl\ n}(t)$ and $u_{p2\ n}(t)$ we find

$$[\bar{u}_{p1\,n}]_c=u_1+(U_{m1}-U_{m2})\frac{[\bar{T}_1']_c}{\bar{T}_p}+U_{m2}\frac{[\bar{T}_1']_c}{\bar{T}_p}=$$

$$=u_1+U_{m1}\frac{[\bar{T}_1']_c}{\bar{T}_p}$$

and

$$[\bar{u}_{p2n}]_c=u_2+U_{m2}-U_{m2}\frac{[\bar{T}_1']_c}{\bar{T}_p}=u_2+U_{m2}\frac{\bar{T}_p-[\bar{T}_1']_c}{\bar{T}_p},$$

where $\bar{T}_p$ is the mean period of repetition (repetition interval) of positive /393 voltage drops of the pulses $u_{pl\ n}(t)$; $[\bar{T}_1']_c$ is the conditional mathematical expectation of the duration of positive drops of the pulses $u_{pl\ n}(t)$, computed on the assumption that $K_a(t)$ = const.

However,

$$T_1'=T_1+\tau_1+\tau_2.$$

Therefore

$\pi = p$
$\Phi = F$

$$[\overline{K}_n]_c = k_{\phi 1}u_1 - k_{\phi 2}u_2 + k_{\phi 1}U_{m1}\frac{T_1 + \overline{\tau}_1 + \overline{\tau}_2}{\overline{T}_n} - \\ - k_{\phi 2}U_{m2}\frac{\overline{T}_n - T_1 - \overline{\tau}_1 - \overline{\tau}_2}{\overline{T}_n} \qquad (8.3.19)$$

and

$$[\overline{K}_{cn}]_c = \frac{k_{\phi 1}u_1 - k_{\phi 2}u_2}{k_{\phi 1}(u_1 + U_{m1}) - k_{\phi 2}u_2} + \\ + \frac{k_{\phi 1}U_{m1}(T_1 + \overline{\tau}_1 + \overline{\tau}_2) - k_{\phi 2}U_{m2}(\overline{T}_n - T_1 - \overline{\tau}_1 - \overline{\tau}_2)}{\overline{T}_n\,|k_{\phi 1}(u_1 + U_{m1}) - k_{\phi 2}u_2|} \qquad (8.3.20)$$

where $\overline{\tau}_1$ and $\overline{\tau}_2$ are the mathematical expectations for τ_1 and τ_2.

The values τ_1 and τ_2 can be either positive or negative. This is dependent on the phase relations of the subcarrier oscillations and the noise voltages. Since in the limits $\pm\pi$ the phase of the noise voltage is characterized by a uniform law of probability distribution, the mathematical expectations $\overline{\tau}_1$ and $\overline{\tau}_2$ are equal to zero. Therefore $[\overline{T}_1]_c = T_1$, $\overline{T}_p = T$, $[\overline{u}_{pl\ n}]_c = u_{pl}$, $[\overline{u}_{p2\ n}]_c = u_{p2}$ and $[\overline{K}_n]_c$ coincides with the value of the command K appearing in the absence of interference. This means that under the influence of fluctuation noise of a low level the mathematical expectation of the error in command transmission is absent.

In determining the conditional spectral density $G_f(0)$, we will bear in mind the absence of a reciprocal statistical relationship between the random shifts τ_1 and τ_2. This can be attributed to the fact that the minimum duration of the pulse of each of the subcarrier oscillations always is greater than the correlation time of the interference, determined by the transmission band of the corresponding separation filter. In the case of the $u_{pl\ n}(t)$ and $u_{p2\ n}(t)$ signals, the continuous part of the energy spectrum is accounted for solely by the pulses

$$x(t) = u_3(t) + u_4(t) \qquad (8.3.21)$$

and

$$y(t) = -u_4(t).$$

Therefore, we need not take into account the voltages u_1 and $u_2 + U_{m2}$ in expressions (8.3.17) and (8.3.18) when determining $S_{pl}(\omega)$ and $S_{p2}(\omega)$.

The voltages x(t) and y(t) are square pulses with the constant amplitudes U_{m1}, U_{m2} and random but equal durations. The mathematical expectation and the dispersion of the duration of these pulses when K_a = const are equal to T_1 and $\sigma_\tau^2 = \overline{\tau}_1^2 + \overline{\tau}_2^2$, respectively, and the mean repetition interval is T. For such random processes, the value of the continuous part of the spectral density at the zero frequency is equal to the ratio of the averaged (for the time T) dispersion of voltage to the effective frequency band occupied by the considered random process. However, the effective frequency band of the mentioned random process in a study of frequencies in the range $-\infty \leq \omega \leq \infty$, as is well known, is equal to $\frac{1}{\sigma_\tau}$, whereas the voltage dispersion averaged for the time T is determined by the product of the square of pulse amplitude and $\frac{\sigma_\tau}{T}$. Therefore, taking into account that the fluctuations of the voltages $u_{p1\,n}(t)$ and $u_{p2\,n}(t)$ are caused by the random signals τ_1 and τ_2, we obtain

$$S_{p1}(0) = U_{m1}^2 \frac{\overline{\tau_1^2} + \overline{\tau_2^2}}{T} \text{ and } S_{p2}(0) = U_{m2}^2 \frac{\overline{\tau_1^2} + \overline{\tau_2^2}}{T}.$$

We note that a detailed analysis of the spectral density of pulses with random durations is given in reference 33. The reciprocal conditional spectral densities $S_{1.2}(0)$ and $S_{2.1}(0)$ can be determined as the Fourier transform of the corresponding time-averaged reciprocal conditional correlation functions $R_{p1.2}(\tau)$ and $R_{p2.1}(\tau)$ for the voltages $u_{p1\,n}(t)$ and $u_{p2\,n}(t)$. Denoting the time-averaging operation by a wavy line over the averaged function, we will have

$\Pi = n$
$y = c$

$$R_{p1.2}(\tau) = \widetilde{\left[\overline{u^0_{p1\,n}(t)\, u^0_{p2\,n}(t+\tau)}\right]_y},$$

$$R_{p2.1}(\tau) = \widetilde{\left[\overline{u^0_{p2\,n}(t)\, u^0_{p2\,n}(t+\tau)}\right]_y},$$

where

$$u^0_{p1\,n}(t) = u_{p1\,n}(t) - \left[\overline{u_{p1\,n}(t)}\right]_y$$

and

$$u^0_{p2\,n}(t) = u_{p2\,n}(t) - \left[\overline{u_{p2\,n}(t)}\right]_y.$$

Substituting the values $u_{p1\,n}(t)$ and $u_{p2\,n}(t)$ from formulas (8.3.17) and (8.3.18) into the expressions for $R_{p1.2}(\tau)$ and $R_{p2.1}(\tau)$ and making the appropriate transformations, we find

$$R_{p1.2}(\tau)=R_{p2.1}(\tau)=-\left[\overline{u_3^0(t)\,u_4^0(t+\tau)}\right]_c-\left[\overline{u_4^0(t)\,u_4^0(t+\tau)}\right]_c,$$

where

$$u_3^0(t)=u_3(t)-\left[\overline{u_3(t)}\right]_c \text{ and } u_4^0(t)=u_4(t)-\left[\overline{u_4(t)}\right]_c$$

are the centered random functions $u_3(t)$ and $u_4(t)$ when K_a = const.

In order to obtain a more graphic means for computation of $S_{1.2}(0)$ /395 and $S_{2.1}(0)$, the voltages $u_3(t)$ and $u_4(t)$ are represented in the following form

$$u_3(t)=(U_{m1}-U_{m2})f_1(t),$$
$$u_4(t)=U_{m1}f_2(t),$$

where $f_1(t)$ and $f_2(t)$ are functions describing the pulses $u_3(t)$ and $u_4(t)$ with different amplitude. Obviously, $f_1(t) = f_2(t) = f(t)$, since the pulses $u_3(t)$ and $u_4(t)$ differ only in amplitude. Then

$$R_{p1.2}(\tau)=R_{p2.1}(\tau)=-U_{m1}U_{m2}\left[\overline{f(t)\,f(t+\tau)}\right]_c. \qquad (8.3.22)$$

However $\left[\overline{f(t)f(t+\tau)}\right]_c$ characterizes the correlation function of square pulses with a unique amplitude and random durations whose mathematical expectation is T_1, with a dispersion $\sigma_\tau^2 = \overline{\tau}_1^2 + \overline{\tau}_2^2$ and a constant mean repetition interval T. Therefore

$$S_{1.2}(0)=S_{2.1}(0)=-U_{m1}U_{m2}\frac{\overline{\tau_1^2}+\overline{\tau_2^2}}{T}.$$

Substituting the determined values $S_{p1}(0)$, $S_{p2}(0)$, $S_{1.2}(0)$ and $S_{2.1}(0)$ into expression (8.3.14), we obtain

$$G_f(0)=2\frac{\overline{\tau_1^2}+\overline{\tau_2^2}}{T}(k_{F1}U_{m1}+k_{F2}U_{m2})^2. \qquad (8.3.23)$$

It can be seen from this expression that for given values T, k_{F1}, k_{F2}, U_{m1} and U_{m2} the value $G_f(0)$ can be determined if $\overline{\tau_1^2}$ and $\overline{\tau_2^2}$ are known.

Since the maximum positive command is $K_{max} = k_{F1}(u_1 + U_{m1}) - k_{F2}u_2$, the conditional spectral density $G_{cf}(0)$ at the zero frequency for distortion of the command coefficient is

$\Phi = F$

$$G_{cf}(0) = 2\frac{\overline{\tau_1^2} + \overline{\tau_2^2}}{T}\frac{(k_{\Phi 1}U_{m1} + k_{\Phi 2}U_{m2})^2}{[k_{\Phi 1}(u_1 + U_{m1}) - k_{\Phi 2}u_2]^2}. \quad (8.3.24)$$

It was demonstrated earlier that the CCRL should be designed in such a way that the conditions $k_{F1}U_{m1} = k_{F2}U_{m2} = k_F U_m$ and $k_{F1}u_1 = k_{F2}u_2$ are satisfied. In this case

$$G_f(0) = 8k_F^2 U_m^2 \frac{\overline{\tau_1^2}\,\overline{\tau_2^2}}{T} \quad (8.3.25)$$

and

$$G_{cf}(0) = 8\frac{\overline{\tau_1^2} + \overline{\tau_2^2}}{T}. \quad (8.3.26)$$

This completes the first stage of investigation of the noise immunity of a CCRL of the considered type and we can proceed to the second stage in which $\overline{\tau_1^2}$ and $\overline{\tau_2^2}$ are determined as a function of the parameters of the signals /396 and interference acting at the inputs of D_1 and D_2 (fig. 7.8).

2. Dependence of $G_f(0)$ and $G_{cf}(0)$ on the Signal-to-Noise Ratio at the Input of the CCRL Decoder and Radio Receiver

First, it is necessary to determine the dependence between the shifts τ_1 and τ_2 and the intensity of the interference reaching the input of the threshold apparatus TA_1 and their dependence on the parameters of the pulses produced by the summer Σ_1 in the absence of interference. In order to obtain more graphic and simpler results, we will assume that the separation filters SF_1 and SF_2 and the detectors D_1 and D_2 are identical. The value τ_1 can be found with a sufficient degree of accuracy using figure 8.2, where curves 1 and 2 characterize the leading edges of the pulses $u_{\Sigma 1}(t)$ near the triggering threshold

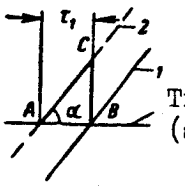

Triggering threshold TA_1 (at $U_{thr\ 1}$ level)

Figure 8.2

$U_{thr\ 1}$ without and with the presence of interference, respectively. The displacement of the curve 2 by the segment τ_1 is caused by the noise voltage u_{n1} = BC which remains virtually constant within a short interval of time. If the effective value of the voltage u_{n1} is many times less than the maximum value of the pulse $u_{\Sigma 1}(t)$ in the absence of interference, the triangle ABC can be considered linear and therefore

$$\tau_1 = \frac{u_{n1}}{|S_1|}, \tag{8.3.27}$$

where S_1 is the steepness of the leading edge of the pulse $u_{\Sigma 1}$ obtained in the absence of interference at the level $U_{thr\ 1}$.

Similarly we find that

$$\tau_2 = \frac{u_{n2}}{|S_2|}, \tag{8.3.28}$$

where S_2 is the steepness of the clipping of the pulse $u_{\Sigma 1}$, obtained in the absence of interference at the level $U_{thr\ 2}$.

On the basis of expressions (8.3.27) and (8.3.28), taking into account $\bar{u}_{n1} = \bar{u}_{n2} = 0$, we obtain

$\Pi = n$

$$\overline{\tau_1^2} = \frac{\overline{u_{n1}^2}}{S_1^2}, \tag{8.3.29}$$

$$\overline{\tau_2^2} = \frac{\overline{u_{n2}^2}}{S_2^2}. \tag{8.3.30}$$

The signals u_{n1} and u_{n2} represent the sum of the noise voltages u_{D1} /397
and u_{D2} from the detectors D_1 and D_2. In the case of a considerable separation of the subcarrier frequencies, the signals u_{D1} and u_{D2} can be considered uncorrelated and therefore

$$\overline{u_{n1}^2} = \overline{u_{n2}^2} = \overline{u_{D1}^2} + \overline{u_{D2}^2}.$$

The detectors D_1 and D_2 usually are fed voltages with quite large amplitudes. The stages D_1 and D_2 therefore can be considered "linear."

If we consider the problem of the joint passage of sinusoidal signals and low-level noise through linear detectors with identical parameters, it is possible to obtain the following expressions for $\overline{u_{D1}^2}$ and $\overline{u_{D2}^2}$ (ref. 34)

$$\overline{u_{D1}^2} = \overline{u_{D2}^2} = 2\frac{k^2 k_D^2 \sigma_n^2}{\pi^2}\frac{\Delta F_D}{\Delta F_1},$$

where k_D is the transfer constant of the detectors D_1 and D_2, characterizing the value of the current at the D_1 and D_2 outputs when they are fed voltages with the amplitude 1 v; σ_n^2 is the dispersion of noise voltages at the D_1 and D_2 inputs; k is a proportionality factor taking into account the value of the voltage at the Σ_1 output for a unit current of the detector; ΔF_1 is the effective transmission bands of the separation filters SF_1 and SF_2; ΔF_D is the effective passbands of the detectors D_1 and D_2.

Since

$$\Delta F_D \approx \frac{\Delta F_1}{2},$$

then

$$\overline{u_{D1}^2} = \overline{u_{D2}^2} = \frac{k^2 k_D^2 \sigma_{D1}^2}{\pi^2}. \qquad (8.3.31)$$

In computation of S_1 and S_2, it can be assumed that the principal change of the slope of the leading edges of the pulses occurs as a result of the

passage of sinusoidal subcarriers through the separation filters. Therefore, when the separation filters used are individual resonance circuits, which are the simplest and at the same time perform their functions quite well, for the envelopes $u_{1.1}$ and $u_{1.2}$ of the front and clipping of the pulses at the SF_1 output we obtain:

Ф = F

$$u_{1.1} = U_{mp}(1 - e^{-\alpha_\Phi t}), \tag{8.3.32}$$

$$u_{1.2} = U_{mp}e^{-\alpha_\Phi t}, \tag{8.3.33}$$

where U_{mp} is the pulse amplitude at the SF_1 output in a steady-state regime; $\alpha_F = 2\Delta F_1 = \pi f_{nl} d$, and d is the circuit attenuation. /398

Similar formulas are derived for the envelopes $u_{2.1}$ and $u_{2.2}$ of the leading edge and clipping of the pulse forming at the SF_2 output, that is

Ф = F

$$u_{2.1} = U_{mp}(1 - e^{-\alpha_\Phi t}), \tag{8.3.34}$$

$$u_{2.2} = U_{mp}e^{-\alpha_\Phi t}. \tag{8.3.35}$$

We note that in expressions (8.3.32)-(8.3.35) the time should be read from the times of formation and ending of the pulses appearing at the SF_1 and SF_2 outputs.

In the resulting pulse $u_{\Sigma 1}$, the leading edge and the clipping $u_1(t)$ and $u_2(t)$ will change in conformity to the following laws

Д = D
Ф = F

$$u_1(t) = \frac{kk_д}{\pi}(u_{1.1} - u_{2.2}) = \frac{kk_д}{\pi}U_{mp}(1 - 2e^{-\alpha_\Phi t})$$

and

$$u_2(t) = \frac{kk_д}{\pi}(u_{2.1} - u_{1.2}) = \frac{kk_д}{\pi}U_{mp}(1 - 2e^{-\alpha_\Phi t}).$$

If the thresholds $U_{thr\ 1}$ and $U_{thr\ 2}$ are close to one another in absolute value, assuming that $|U_{thr\ 1}| \approx |U_{thr\ 2}| = U_{thr}$, and using the notation $k_{TA} = \frac{\pi U_{thr}}{kk_D U_{mp}}$, on the basis of the last two expressions, it is possible to obtain the following formula determining the time t_1 necessary for attaining the voltages $u_1(t)$ and $u_2(t)$ of the threshold U_{thr}

$$t_1 = \frac{1}{2\Delta F_1} \ln \frac{1}{1 - k_{TA}}.$$

Here t_1 characterizes the time reckoned from the times of beginning of the leading edge and the clipping of the pulses produced by the filter SF_1. In this case, it is found that

$$|S_1| = |S_2| = \frac{du_1(t)}{dt}\Big|_{t=t_1} = \frac{du_2(t)}{dt}\Big|_{t=t_1} = \frac{2}{\pi} k k_D U_{mp} \Delta F_1 (1 - k_{TA}).$$

Substituting the determined values $\overline{u_{n1}^2}$, $\overline{u_{n2}^2}$, S_1 and S_2 into expressions (8.3.29) and (8.3.30), we obtain formulas determining $\overline{\tau_1^2}$ and $\overline{\tau_2^2}$. Then, in accordance with expression (8.3.23) we will have

Φ = F

$$G_f(0) = \frac{(k_{\Phi 1} U_{m1} + k_{\Phi 2} U_{m2})^2}{T \Delta F_1^2 q_1^2 (1 - k_{TA})^2}. \qquad (8.3.36)$$

Similarly, we find

/399

$$G_{cf}(0) = \frac{(k_{\Phi 1} U_{m1} + k_{\Phi 2} U_{m2})^2}{|k_{\Phi 1}(u_1 + U_{m1}) - k_{\Phi 2} u_2|^2} \frac{1}{T \Delta F_1^2 q_1^2 (1 - k_{TA})^2}. \qquad (8.3.37)$$

In the last two relations, the value q_1^2, equal to

$$q_1^2 = \frac{U_{mp}^2}{2\sigma_n^2},$$

characterizes the ratio of the effective signal and noise at the D_1 and D_2 inputs. These inputs in essence also constitute the noise input for the CCRL decoder.

Analysis of formulas (8.3.36) and (8.3.37) shows that the proper selection of k_{TA} and q_1, with stipulation of the other parameters, can ensure admissible values $G_f(0)$ and $G_{cf}(0)$. The minimum values $G_f(0)$ and $G_{cf}(0)$ are obtained when $k_{TA} = 0$. This can be attributed to the fact that when $k_{TA} = 0$, the leading edges and clipping of the $u_{\Sigma 1}$ pulses have maximum steepness. A decrease of

$G_f(0)$ and $G_{cf}(0)$ with an increase of ΔF_1 can be attributed to the fact that the steepness of the leading edge of the pulse changes inversely proportional to ΔF_1, whereas the noise intensity at the SF_1 and SF_2 output increases in conformity to the law $\sqrt{\Delta F_1}$.

If it is necessary to know the dispersions σ_f^2 and σ_{cf}^2 of distortion of the command and the command coefficient, it is necessary to integrate expression (8.3.13) for all frequencies. In a case when both filters F_1 and F_2 have identical effective transmission bands equal to ΔF, on the basis of formulas (8.3.36) and (8.3.37), we obtain

Ф = F
Ш = TA

$$\sigma_f^2 = \frac{(k_{\phi 1}U_{m1} + k_{\phi 2}U_{m2})^2}{T\Delta F_1^2 q_1^2 (1 - k_{\text{ш}})^2}\Delta F \qquad (8.3.38)$$

and

$$\sigma_{cf}^2 = \frac{(k_{\phi 1}U_{m1} + k_{\phi 2}U_{m2})^2 \Delta F}{[k_{\phi 1}(u_1 + U_{m1}) - k_{\phi 2}u_2]^2\, T\Delta F_1^2 q_1^2 (1 - k_{\text{ш}})^2}. \qquad (8.3.39)$$

Computation of the dependence q_1 on the ratio q_0 of the effective signal and noise voltages at the radio receiver input characterizes the last stage of solution of the considered problem. The relationship between q_1 and q_0, in a general case, is determined to a considerable degree by the type of detector used in the radio receiver. It can be shown that for the considered single-channel CCRL, using a linear detector in the radio receiver and $q > 2$, we obtain with an adequate degree of accuracy the following approximate relation

$$q_1 \approx m q_0 \sqrt{\frac{\Delta f_e}{2\Delta F_1}}, \qquad (8.3.40)$$

where m is the coefficient of modulation of the carrier caused by the effect of one subcarrier oscillation, and Δf_e is the effective passband of the intermediate frequency amplifier.

If the CCRL output signal is a current rather than a voltage, it can /400 be found that the conditional constant component of command distortion will be equal to zero and the conditional spectral density at the zero frequency is determined by the earlier derived formulas if the voltages in them are replaced by the corresponding currents.

Under the influence of fluctuation low-level noise in the CCRL, the signals of which are intended for moving the spoilers, the duration of effect of the subcarrier oscillation changes randomly. As a result (fig. 8.1)

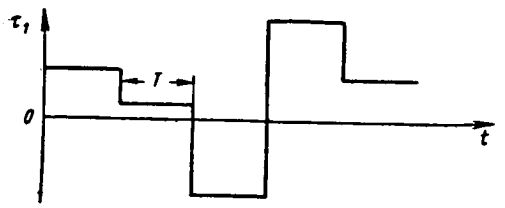

Figure 8.3

$$K_n(t) = T_1 - T_2 + 2(\tau_1 + \tau_2). \tag{8.3.41}$$

Since $\bar{\tau}_1 = \bar{\tau}_2 = 0$, the conditional mathematical expectation of the output command when radio interference is present will coincide with the value $K = K_C$ and $[\Delta\bar{K}]_c = 0$.

Taking into account that τ_1 and τ_2 are uncorrelated and have zero mathematical expectations, for the conditional spectral densities $[G(0)]_c$ and $[G_c(0)]_c$ of the output command $K_n(t)$ and the command coefficient $K_{cn}(t)$ we obtain

$$[G(0)]_c = 4[G_{\tau 1}(0) + G_{\tau 2}(0)] \quad \text{when} \quad 0 \leqslant \omega \leqslant \infty$$

and

$$[G_c(0)]_c = \frac{4}{T^2}[G_{\tau 1}(0) + G_{\tau 2}(0)] \quad \text{when} \quad 0 \leqslant \omega \leqslant \infty,$$

where $G_{\tau 1}$ and $G_{\tau 2}$ are the spectral densities at the zero frequency for the random functions $\tau_1(t)$ and $\tau_2(t)$.

The random functions $\tau_1(t)$ and $\tau_2(t)$ are square pulses having the fluctuating amplitudes τ_1 and τ_2, the constant durations T and a repetition interval T. As an illustration, figure 8.3 shows one of the possibilities of dependence of τ_1 on t. Therefore,

$$G_{\tau 1}(0) = 2\bar{\tau}_1^2 T$$

and

$$G_{\tau 2}(0) = 2\bar{\tau}_2^2 T.$$

Then

$$[G(0)]_c = 8T(\bar{\tau}_1^2 + \bar{\tau}_2^2) \tag{8.3.42}$$

and

$$[G_c(0)]_c = 8\frac{\bar{\tau}_1^2 + \bar{\tau}_2^2}{T}. \tag{8.3.43}$$

Taking into account the earlier determined values $\overline{\tau_1^2}$ and $\overline{\tau_2^2}$ under the condition that the decoder of the considered CCRL is designed as shown in figure 7.8, with the low-frequency filters and subtracting devices eliminated from it, we obtain

П = ТА

$$[G(0)]_c = \frac{4T}{\Delta F_1^2 q_1^2 (1 - k_n)^2} \tag{8.3.44}$$

and

/401

$$[G_c(0)]_c = \frac{4}{T\Delta F_1^2 q_1^2 (1 - k_n)^2} \tag{8.3.45}$$

On the basis of these formulas, we find that the conditional dispersions σ^2 and σ_c^2 of distortion of the command and the command coefficient are

П = ТА

$$\sigma^2 = [G(0)]_c \Delta F_{1.1} = \frac{2}{\Delta F_1^2 q_1^2 (1 - k_n)^2} \tag{8.3.46}$$

and

$$\sigma_c^2 = [G_c(0)]_c \Delta F_{1.1} = \frac{2}{T^2 \Delta F_1^2 q_1^2 (1 - k_n)^2}, \tag{8.3.47}$$

where $\Delta F_{1.1}$ is the effective band of the spectrum of fluctuations $K_n(t)$ in the case of its propagation at the frequency $0 \leq \omega \leq \infty$. Obviously, $\Delta F_{1.1} = \frac{1}{2T}$. In the expressions (8.3.44)-(8.3.47), the dependence of q_1 on q_0 is determined by the relation (8.3.40).

Comparison of formulas (8.3.47) and (8.3.39) under the condition of the equality $k_{F1}U_{m1} = k_{F2}U_{m2} = k_F U_m$ shows that

$$\sigma_{cf}^2 = 2\Delta F T \sigma_c^2.$$

Since good quality of detection of the mean component from the pulses $u_{p1}(t)$ and $u_{p2}(t)$ requires satisfaction of the condition $\Delta FT < 0.5$, then $\sigma_{cf}^2 < \sigma_c^2$. This means that a CCRL with filters at the output are more noise immune than CCRL without filters.

At the same time, the spectral densities $G_{cf}(0)$ and $[G_c(0)]_c$ determined by relations (8.3.26) and (8.3.43) for CCRL with and without filters are identical (which is physically obvious).

In conclusion of consideration of the problem of the influence of low-level interference on CCRL with pulse-width modulation of sinusoidal

subcarriers it should be noted that all the conclusions drawn apply to a case when there is identity of the characteristics of the separation filters SF_1 and SF_2 and the detectors D_1 and D_2. If these devices have different parameters, there will be a change of the quantitative values only of the spectral densities and dispersions of command distortions. The method for computing the fluctuation errors remains as before.

It also should be pointed out that the effect of low-level interference does not change the CCRL transfer function and the only result is that a fluctuation component of the command is added to the output signal formed in the absence of radio interference. Therefore, the equation describing processes in CCRL with and without filters SF_1 and SF_2 (fig. 7.8) will have the form

$$K_n(t) = k_{CCRL}K(t) + \Delta K(t). \qquad (8.3.48)$$

In this equation, the random function $\Delta K(t)$ has a zero mathematical expectation and a spectral density determined by formula (8.3.36) or (8.3.44) in dependence on the decoder design.

8.4. Effect of High-Level Interference on a CCRL with Pulse-Width Modulation

If the effective strength of interference at the output of the separa- /402
tion filters SF_1 and SF_2 is commensurable with or exceeds the amplitudes of the useful signals at the input of the detectors D_1 and D_2 (fig. 7.8), the oscillations of amplitudes of the pulses $u_{\Sigma 1}$ will be considerable and the instantaneous values of the voltage $u_{\Sigma 1}$ within the intervals T_1 and T_2 can by several times exceed the lower and upper triggering thresholds of the threshold apparatus TA_1 (fig. 7.8). The parasitic perturbations responsible for the described effect will be called high-level interference.

As an illustration, figure 8.4a (curve 2) shows one of the possible variants of the voltage $u_{\Sigma 1}(t)$ in the case of a high level of fluctuation interference; the same figure (curve 1) shows the voltage $u_{\Sigma 1}(t)$ in the absence of interference. As a result of considerable changes of the amplitudes of $u_{\Sigma 1}(t)$ at the TA_1 output, the signals $u_{p1\,n}(t)$ and $u_{p2\,n}(t)$ appear, the possible form

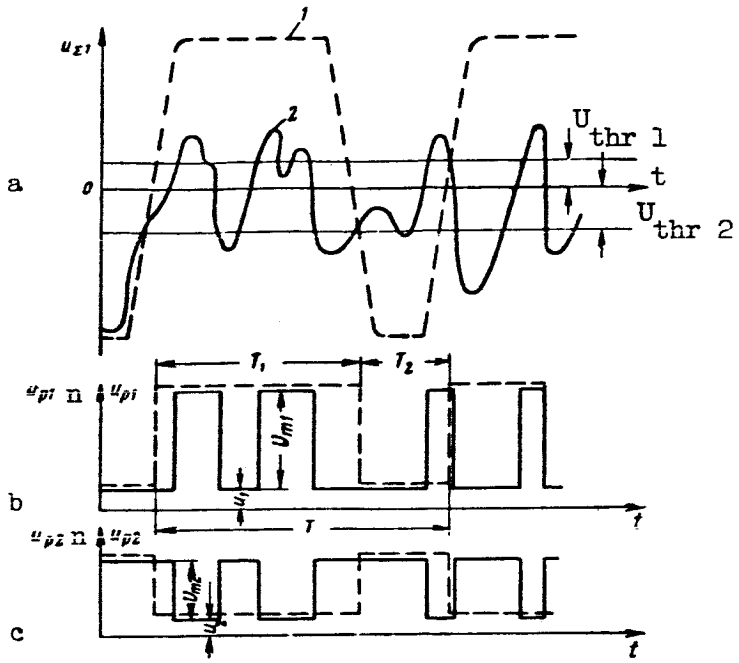

Figure 8.4

of which can be seen in figure 8.4b and c (solid lines). This same figure shows (by dashed lines) the voltages $u_{p1}(t)$ and $u_{p2}(t)$ forming at the TA_1 output in the absence of interference. We note that the difference in the values of the signals $u_{p1}(t)$, $u_{p2}(t)$, $u_{p1\ n}(t)$ and $u_{p2\ n}(t)$ is introduced only for greater clarity.

Figure 8.4b and c shows that in the case of strong interference, the /403 voltages $u_{p1\ n}(t)$ and $u_{p2\ n}(t)$ are square pulses with constant maximum and minimum amplitudes, but with random durations and repetition interval.

Essentially, the effect of strong interference leads to a breakdown of the transmitted pulses of the subcarrier oscillations, which causes distortions of the CCRL output signals. In the case of a breakdown with small fluctuations, the leading edges of the $u_{\Sigma 1}$ pulses (fig. 8.1a) need not be taken into account.

The effect of spurious "tripping" of TA_1 (breakdown of pulses) can be attributed to the fact that at certain times in the interval T the sum of the positive and negative voltages forming at the D_1 and D_2 output in absolute value attains values exceeding $U_{thr\ 1}$ or $U_{thr\ 2}$ (fig. 8.4a).

Thus, in the segment T_1 the formation of a positive voltage jump $u_{p2\,n}(t)$ is possible in those cases when the sum of voltages of different polarity, fed from the detectors D_1 and D_2 and passing through the summer Σ_1, becomes less than $U_{thr\,2}$. The appearance of positive voltage surges $u_{p1\,n}(t)$ in the interval T_2 is possible only when the threshold $U_{thr\,1}$ is exceeded by the voltage $u_{\Sigma 1}$.

The value of an output command of a CCRL with filters when affected by high-level interference is determined, as in the case of low-intensity interference, by equation (8.3.2). If there is no interference, the signal produced by the CCRL can be found using (8.3.1).

In accordance with relations (8.3.1) and (8.3.2) in the preceding section, we obtained formulas (8.3.5) and (8.3.6) by means of which we computed the values $[\bar{K}_n]_c$ and $[\overline{\Delta K}]_c$. These formulas also remain correct for a CCRL under the influence of high-level noise.

It can be seen from expressions (8.3.5) and (8.3.6) that, in order to find $[\bar{K}_n]_c$ and $[\overline{\Delta K}]_c$, it is necessary to compute the constant components u_{p1}, u_{p2}, $[\bar{u}_{p1\,n}]_c$ and $[\bar{u}_{p2\,n}]_c$ of the voltages $u_{p1}(t)$, $u_{p2}(t)$, $u_{p1\,n}(t)$ and $u_{p2\,n}(t)$ under the condition that the value $K_a(t)$ is known. First, we will find $[\bar{u}_{p1\,n}]_c$, assuming that the threshold apparatus used in the CCRL is inertialess.

Since

$$u_{p1\,n}(t) = u_1 + u_3(t) + u_4(t) \tag{8.3.17}$$

or

$$u_{p1\,n}(t) = u_1 + x(t),$$

where

$$x(t) = u_3(t) + u_4(t),$$

then

$$[\bar{u}_{p1n}]_c = u_1 + [\bar{x}]_c. \tag{8.4.1}$$

We note that the voltage $x(t)$ can assume the value U_{m1} if $u_{\Sigma 1}(t)$ ex- /404 ceeds the threshold $U_{thr\,1}$, or 0 if $u_{\Sigma 1}(t)$ is less than $U_{thr\,2}$. For determination of $[\bar{x}]_c$ we divide the intervals T_1 and T_2 into Q_1 and Q_2 equal parts with

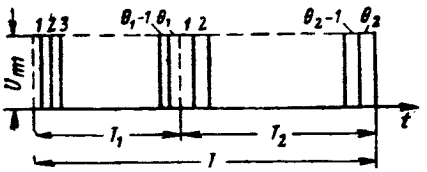

Figure 8.5

the durations Δt_1 and Δt_2 and the heights U_{m1} (fig. 8.5). Here the values Δt_1 and Δt_2 are selected on the basis of the following conditions

$$\Delta t_1 \approx \tau_{c1} \approx \frac{1}{\Delta F_1},$$

$$\Delta t_2 \approx \tau_{c2} \approx \frac{1}{\Delta F_2},$$

where τ_{c1} and τ_{c2} are the noise correlation times at the outputs of the separation filters SF_1 and SF_2 with effective transmission bands ΔF_1 and ΔF_2.

Pulses with the durations Δt_1 and Δt_2 and the amplitudes U_{m1}, in contrast to the command pulses, will be called elementary pulses.

In addition to the elementary pulses, a dashed line in figure 8.5 has been used to denote pulses with the durations T_1 and T_2, determined by the value of the transmitted command.

The entire period T (fig. 8.5) consists of $Q = Q_1 + Q_2$ uncorrelated square elementary pulses. When there is no interference, the amplitudes of the elementary pulses acting in the time T_2 with a probability of 1 are equal to zero and those pulses which fall in the interval T_1 with the same probability have the amplitude U_{m1}.

When there is interference, the elementary pulses with the amplitude U_{m1} can appear at any time. Obviously, an elementary pulse is formed in a case when the voltage $u_{\Sigma 1}$ exceeds the threshold $U_{thr\ 1}$. This can be attributed to the fact that in this case there is a "tripping" of the threshold apparatus TA_1 or it will remain in its former state if TA_1 produces a voltage U_{m1}. When $u_{\Sigma 1}$ is less than $U_{thr\ 2}$, the amplitude of an elementary pulse x(t) becomes

equal to zero. Under these conditions, the constant component $[\bar{x}]_c$ of the voltage x(t) can be determined in the following way

$$[\bar{x}]_c = U_{m1} \frac{[\bar{T}_{dur}]_c}{T},$$

where $[\bar{T}_{dur}]_c$ is the total conditional mathematical expectation of the durations of the elementary pulses having the amplitude U_{m1}.

Denoting by $\overline{\Delta t}_1$ and $\overline{\Delta t}_2$ the mean durations of the elementary pulses /405 with the amplitudes U_{m1} acting during the inervals T_1 and T_2, we obtain

$$[\bar{T}_{dur}]_c = [\bar{T}_{dur\ 1}]_c + [\bar{T}_{dur\ 2}]_c = Q_1\overline{\Delta t}_1 + Q_2\overline{\Delta t}_2,$$

where $[\bar{T}_{dur\ 1}]_c$ and $[\bar{T}_{dur\ 2}]_c$ are the total conditional mathematical expectations of the durations of the pulses produced in TA_1 in the intervals T_1 and T_2.

Since in the interval T_1 the value Δt_1 of the i-th pulse (i = 1, 2, ..., Q_1) is part of T_{dur} only under the condition that the i-th elementary pulse is positive, then

$$\overline{\Delta t_1} = \Delta t_1 (1 - p_1),$$

where p_1 is the probability that in the interval T_1, in the limits Δt_1, the condition $u_{\Sigma 1} < U_{thr\ 2}$ is satisfied.

Similarly, we find that

$$\overline{\Delta t_2} = \Delta t_2 p_2,$$

where p_2 is the probability that in the interval T_2 the signal $u_{\Sigma 1}$, in the limits Δt_2, is greater than $U_{thr\ 1}$.

Then

$$[\bar{T}_{dur}]_c = Q_1\Delta t_1 (1 - p_1) + Q_2\Delta t_2 p_2$$

and therefore

$$[\bar{x}]_c = \frac{U_{m1}}{T} [T_1 (1 - p_1) + T_2 p_2].$$

Substituting the determined value $[\bar{x}]_c$ into expression (8.4.1), we obtain

$$[\bar{u}_{p1n}]_c = u_1 + \frac{U_{m1}}{T}[T_1(1-p_1) + T_2 p_2].$$

Similarly, we find that

$$[\bar{u}_{p2n}]_c = u_2 + \frac{U_{m2}}{T}[T_1 p_1 + T_2(1-p_2)].$$

Therefore

Ф = F

$$[\bar{K}_n]_c = k_{\phi 1}u_1 - k_{\phi 2}u_2 + k_{\phi 1}\frac{u_{m1}}{T}[T_1(1-p_1) + T_2 p_2] - k_{\phi 2}\frac{U_{m2}}{T}[T_1 p_1 + T_2(1-p_2)]. \quad (8.4.2)$$

Taking into account formulas (8.3.15) and (8.3.16), and also that /406
$K_C = TK_{Cc} = k_C K_a$, on the basis of expression (8.4.2) we obtain

$$[\bar{K}_n]_c = K_{1.1} + K_{1.2}, \quad (8.4.3)$$

where

$$K_{1.1} = \frac{k_{\phi 1}U_{m1} + k_{\phi 2}U_{m2}}{2T}(1 - p_1 - p_2)\, k_C K_a =$$

Ф = F

$$= \frac{k_{\phi}U_{m1} + k_{\phi 2}U_{m2}}{2}(1 - p_1 - p_2)\, K_{ic}; \quad (8.4.4)$$

$$K_{1.2} = k_{\phi 1}u_1 - k_{\phi 2}u_2 + \frac{k_{\phi 1}U_{m1}}{2}(1 - p_1 + p_2) - \frac{k_{\phi 2}U_{m2}}{2}(1 + p_1 - p_2); \quad (8.4.5)$$

$K_{Cc} = K_{ic} = \frac{k_C K_a}{T}$ is the command coefficient of the coder if it is assumed that $T = k_C K_{a\,max}$.

An analysis of the derived expression shows that the conditional constant component of the CCRL output signal consists of two parts, one of which ($K_{1.1}$) is dependent on the value of the transmitted command K_a and the other ($K_{1.2}$) is not so dependent. We now will consider expression (8.4.5) in greater detail. It can be seen from this expression that the component A of the signal $K_{1.2}$ is

$$A = k_{F1}u_1 - k_{F2}u_2 + \frac{k_{F1}U_{m1} - k_{F2}U_{m2}}{2},$$

and is caused only by the nonidentity of the coefficients k_{F1} and k_{F2} and also the asymmetry of the threshold apparatus TA_1, which is related to the appearance of different values u_1, u_2, U_{m1} and U_{m2}.

As already mentioned in the preceding chapter, the influence of a signal causing an error of constant value, in the absence of interference, can be compensated by corresponding adjustments (balancing) in the output stages of the CCRL or by selection of identical values k_{F1} and k_{F2} and use of a rigorously symmetrical threshold apparatus.

The voltage

$$u = \frac{k_{F1}U_{m1} + k_{F2}U_{m2}}{2}(p_2 - p_1),$$

being the second part of the component $K_{1.2}$, characterizes the mathematical expectation of the error in transmission of commands, dependent on the probabilities p_1 and p_2, the voltages U_{m1} and U_{m2} and the coefficients k_{F1} and k_{F2}.

This error cannot be eliminated by balancing the CCRL or by selection /407 of identical filters F_1 and F_2 and a symmetrical threshold apparatus. Its compensation requires such a CCRL decoder design so as to satisfy the equality $p_1 = p_2 = p_0$. A CCRL for which $p_1 = p_2 = p_0$ henceforth will be said to be symmetrical relative to interference.

The value $K_{1.1}$ changes proportional to the value of the transmitted command. However, if the CCRL transfer constant in the absence of interference is equal to

$$k_{CCRL} = \frac{k_{F1}U_{m1} + k_{F2}U_{m2}}{2T}k_C,$$

then when interference is present the mean value of this coefficient decreases by the value

$$\frac{k_{F1}U_{m1} + k_{F2}U_{m2}}{2T}(p_1 + p_2)k_C$$

and becomes equal to

$$(k_{CCRL})_n = k_{CCRL}(1 - p_1 - p_2). \qquad (8.4.6)$$

In the case of a CCRL for which $k_{F1}u_1 = k_{F2}u_2$, $k_{F1}U_{m1} = k_{F2}U_{m2}$ and $p_1 = p_2 = p_0$

$$[\bar{K}_n]_c = k_{F1}U_{m1}(1 - 2p_0)K_{Cc} = (k_{CCRL})_n K_a, \tag{8.4.7}$$

where

$$(k_{CCRL})_n = k_{CCRL}(1 - 2p_0). \tag{8.4.7a}$$

Since the maximum value of the command in such CCRL is $K_{max} = k_{F1}U_{m1}$ and $K_c = K_{Cc}$, for the conditional constant component of the command coefficient at the CCRL output we find

$$[\bar{K}_{cn}]_c = (1 - 2p_0)K_{Cc} = (1 - 2p_0)K_{ic}. \tag{8.4.8}$$

The conditional constant components of distortions of the command and of the command coefficient for a CCRL symmetrical when interference is present, as follows from formulas (8.4.7) and (8.4.8), are equal respectively to

$$[\overline{\Delta K}]_c = [\bar{K}_n]_c - K = -2k_{F1}U_{m1}p_0 \frac{k_C}{T} K_a \tag{8.4.9}$$

$$[\overline{\Delta K_c}]_c = [\bar{K}_{cn}]_c - K_c = -2p_0 K_{ic} \tag{8.4.10}$$

where

$$K = k_{F1}U_{m1}\frac{k_C}{T}K_a = k_{F1}U_{m1}K_{ic}.$$

The minus sign in expressions (8.4.9) and (8.4.10) means that the interference in a CCRL of such a type always leads to a decrease of the modulus of the signal which will be fed to the control components.

The formulas determining $[\bar{K}_{cn}]_c$, $[\overline{\Delta K}]_c$ and $[\overline{\Delta K_c}]_c$ for a general case /408 of design of a CCRL can be obtained on the basis of expression (8.4.3) if it is remembered that

$$K_{max} = k_{\Phi 1}(u_1 + U_{m1}) - k_2 u_2,$$

and

$$K = k_{\Phi 1}\left(u_1 + \frac{U_{m1}}{2}\right) - k_{\Phi 2}\left(u_2 + \frac{U_{m2}}{2}\right)$$

Φ = F

$$+ \frac{k_{\Phi 1}U_{m1} + k_{\Phi 2}U_{m2}}{2} K_{ic}$$

In determining the spectral density $G_f(0)$ for the fluctuation components of the CCRL output signal, we will use as a point of departure expression (8.3.14), suitable for any level of interference.

First we will find the value $S_{pl}(0)$, characterizing the time-averaged conditional spectral density of the fluctuation components of the voltage $u_{pl\,n}(t)$. As already noted, in computing $S_{pl}(0)$ it is sufficient to consider only the voltage determined by formula (8.3.21). As in the determination of $[\bar{x}]_c$, we will separate out in the intervals T_1 and T_2, respectively, Q_1 and Q_2 uncorrelated elementary pulses with random amplitudes and constant durations Δt_1 and Δt_2. The repetition interval of each of the elementary pulses is T and their amplitude can assume the value 0 or U_{ml}.

Since the elementary pulses are mutually uncorrelated, the conditional spectral density $S_{pl}(0)$ is

$$S_{p1}(0) = Q_1 S_{e1}(0) + Q_2 S_{e2}(0),$$

where $S_{e1}(0)$ and $S_{e2}(0)$ are the conditional spectral densities at the zero frequency for elementary pulses acting in the intervals T_1 and T_2.

However, for pulses with a random amplitude and a constant duration and repetition interval, the spectral density at the zero frequency is equal to the ratio of the dispersion of the voltage, averaged over the period T, to the effective frequency band occupied by the elementary pulse. Therefore

$$S_{e1}(0) = \frac{\sigma_1^2}{\Delta f_1} \tag{8.4.11}$$

and

$$S_{e2}(0) = \frac{\sigma_2^2}{\Delta f_2}, \tag{8.4.12}$$

where σ_1^2 and σ_2^2 are the dispersions of the elementary pulses forming in the intervals T_1 and T_2, averaged for the period T; $\Delta f_1 = \frac{1}{\Delta t_1}$ and $\Delta f_2 = \frac{1}{\Delta t_2}$ /409

are the effective frequency bands of the spectra of the square elementary pulses with the durations Δt_1 and Δt_2.

The elementary pulses forming in the time T_1 can have the amplitude 0 or U_{m1} with probabilities equal to p_1 and $(1 - p_1)$, respectively. Therefore

$$\sigma_1^2 = U_{m1}^2 \frac{\Delta t_1}{T} p_1 (1 - p_1).$$

The probability of appearance of a pulse with the amplitude U_{m1} in the interval T_2 is p_2, and the probability of the absence of this signal in this same interval is $1 - p_2$; as a result

$$\sigma_2^2 = U_{m1}^2 \frac{\Delta t_2}{T} p_2 (1 - p_2).$$

Substituting the determined values σ_1^2 and σ_2^2 into expressions (8.4.11) and (8.4.12) we obtain

$$S_{e1}(0) = U_{m1}^2 \frac{\Delta t_1^2}{T} p_1 (1 - p_1),$$

$$S_{e2}(0) = U_{m1}^2 \frac{\Delta t_2^2}{T} p_2 (1 - p_2).$$

Then

$$S_{p1}(0) = U_{m1}^2 \frac{1}{T} \left[T_1 \frac{1}{\Delta F_1} p_1 (1 - p_1) + T_2 \frac{1}{\Delta F_2} p_2 (1 - p_2) \right].$$

In a similar way we find that

$$S_{p2}(0) = U_{m2}^2 \frac{1}{T} \left[\frac{T_1}{\Delta F_1} p_1 (1 - p_1) + \frac{T_2}{\Delta F_2} p_2 (1 - p_2) \right].$$

Then we determine the reciprocal conditional spectral densities $S_{1.2}(0)$ and $S_{2.1}(0)$ at the zero frequency for the voltages $u_{p1\,n}(t)$ and $u_{p2\,n}(t)$. Using the principle of separation of the period T into Q parts and bearing in mind expression (8.3.22) for the reciprocal correlation functions $R_{p\,1.2}(\tau)$ and $R_{p\,2.1}(\tau)$, we obtain

$$S_{1.2}(0) = S_{2.1}(0) = -U_{m1} U_{m2} \frac{1}{T} \left[\frac{T_1}{\Delta F_1} p_1 (1 - p_1) + \frac{T_2}{\Delta F_2} p_2 (1 - p_2) \right].$$

Substituting the values $S_{p1}(0)$, $S_{p2}(0)$ and $S_{1.2}(0)$ into expression (8.3.14) we find /410

$$G_f(0) = \frac{2}{T}(k_{F1}U_{m1} + k_{F2}U_{m2})^2\left[\frac{T_1}{\Delta F_1}p_1(1-p_1) + \frac{T_2}{\Delta F_2}p_2(1-p_2)\right]. \quad (8.4.13)$$

If the values T_1 and T_2 are replaced, using for this purpose expressions (8.3.15) and (8.3.16) and also the relation $K_C = k_C K_a$, we obtain

$$G_f(0) = (k_{F1}U_{m1} + k_{F2}U_{m2})^2\left\{\frac{p_1(1-p_1)}{\Delta F_1} + \frac{p_2(1-p_2)}{\Delta F_2} + \frac{1}{T}\left[\frac{p_1(1-p_1)}{\Delta F_1} - \frac{p_2(1-p_2)}{\Delta F_2}\right]k_C K_a\right\}. \quad (8.4.14)$$

It can be seen from expression (8.4.14) that the conditional spectral density $G_f(0)$ when $\omega = 0$ consists of two parts, one of which is dependent only on interference and on the CCRL parameters, and the other, in addition, is a function of the transmitted command.

If the CCRL is symmetrical relative to interference, which also occurs when $\Delta F_1 = \Delta F_2$ and $p_1 = p_2 = p_0$, the second component $G_f(0)$ becomes equal to zero, the fluctuations of the CCRL output signal are not dependent on the value of the transmitted command and

$$G_f(0) = 2(k_{F1}U_{m1} + k_{F2}U_{m2})^2\frac{p_0(1-p_0)}{\Delta F_1}. \quad (8.4.15)$$

We note that the condition $p_1 = p_2$ denotes equiprobability of spurious tripping of TA_1 in the intervals T_1 and T_2.

It can be seen from (8.4.15) that with an increase of the intensity of interference, when $p_0 \to 0.5$, the value $G_f(0)$ increases monotonically, attaining a maximum equal to

$$G_{f\,max}(0) = \frac{(k_{F1}U_{m1} + k_{F2}U_{m2})^2}{2\Delta F_1}.$$

If a CCRL, symmetrical relative to interference, contains a symmetrical threshold apparatus ($u_1 = u_2$ and $U_{m1} = U_{m2} = U_m$) and filters F_1 and F_2 with identical coefficients $k_{F1} = k_{F2} = k_F$, then

$$G_f(0) = \frac{8p_0(1-p_0)}{\Delta F_1} k_F^2 U_m^2. \qquad (8.4.16)$$

Hence, for the spectral density of distortion of the command coefficient we obtain

$$G_{cf}(0) = \frac{8p_0(1-p_0)}{\Delta F_1}. \qquad (8.4.17)$$

Determination of the dispersions σ_f^2 and σ_{cf}^2 for a completely symmetrical CCRL can be accomplished by multiplying $G_f(0)$ and $G_{cf}(0)$ by ΔF. Then /411

$$\sigma_f^2 = \frac{8k_F^2 U_m^2 p_0(1-p_0)\Delta F}{\Delta F_1}, \qquad (8.4.18)$$

$$\sigma_{cf}^2 = \frac{8p_0(1-p_0)\Delta F}{\Delta F_1}. \qquad (8.4.19)$$

In a general case, the value $G_{cf}(0)$ can be found by dividing the function $G_f(0)$ by the square of the maximum value of the command, and the dispersion of the output command is computed by integration of expression (8.3.13).

The curves shown in figure 8.6 serve as an illustration of the functions $\frac{[\overline{K}_{cn}]_c}{K_{ic}} = f_1(p_0)$ and $\frac{G_{cf}(0)\Delta F_1}{8} = f_2(p_0)$, determined by formulas (8.4.8) and (8.4.17), for a symmetrical CCRL.

Determination of the dependence of the conditional constant components and spectral densities of the CCRL output signal and command coefficient, and also of the conditional constant components and spectral densities for distortion of commands and command coefficient, on the ratios $q_{1.1}$ and $q_{1.2}$ of the effective strengths of signal and interference at the output of the separation filters SF_1 and SF_2 requires determination of the relationship between p_1 and $q_{1.1}$ and p_2 and $q_{1.2}$. For this reason, we will establish under what conditions and /412 in what way tripping of the threshold apparatus occurs under the influence of the voltage $u_{\Sigma 1}(t)$.

During the time T_1, the summer Σ_1 is fed a voltage u_1 from the detector D_1; this voltage is a mixture of signal and noise. Only noise u_2 is fed from

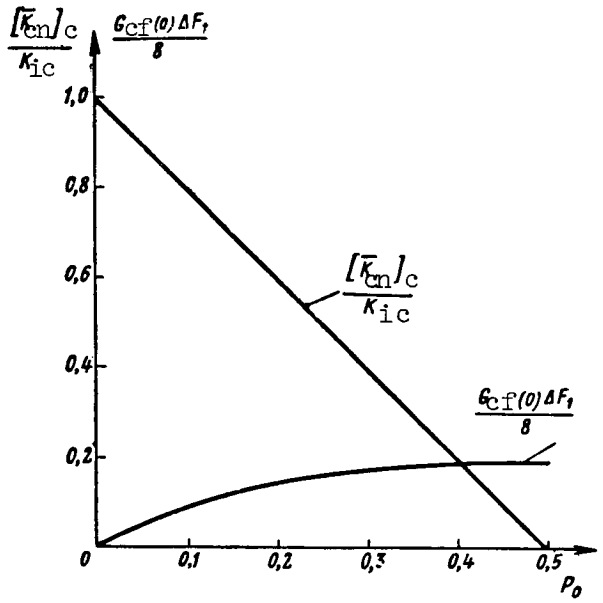

Figure 8.6

the detector D_2. The following condition must be satisfied for the threshold apparatus TA_1 to be tripped at some point t_1 of the interval T_1

$$u_2 \geq \left|U_{thr\ 2}\right| + u_1. \tag{8.4.20}$$

On this basis, it can be asserted that the value p_1 characterizes the probability of satisfaction of the inequality (8.4.20), that is

$$p_1 = p(u_2 \geq \left|U_{thr\ 2}\right| + u_1).$$

Here $p_1(u_2 \geq \left|U_{thr\ 2}\right| + u_1)$ is the probability that $u_2 \geq \left|U_{thr\ 2}\right| + u_1$.

Since the transmission bands of the filters SF_1 and SF_2 to all intents and purposes do not overlap, the voltages u_1 and u_2 can be considered uncorrelated and therefore

$\Pi = thr$
$$p_1 = \int_0^\infty W_1(u_1)\,du_1 \int_{|U_{n2}|+u_1}^\infty W_2(u_2)\,d\,u_2\,, \tag{8.4.21}$$

where $W(u_1)$ and $W(u_2)$ are the probability densities for the random signals u_1 and u_2.

If linear detectors with transfer constants for the envelope which are identical and equal to unity are used in the CCRL decoder, it is well known (ref. 34) that

$$W_1(u_1) = \frac{u_1}{\sigma^2_{n1}} \exp\left[\frac{-u_1^2 + E^2_{c1}}{2\sigma^2_{n1}}\right] I_0\left(\frac{u_1 E_{c1}}{\sigma^2_{n1}}\right)$$

and

$$W_2(u_2) = \frac{u_2}{\sigma^2_{n2}} \exp\left[-\frac{u_2^2}{2\sigma^2_{n2}}\right],$$

c = s
п = n

where E_{s1} is the amplitude of signal strength acting on the D_1 input; σ^2_{n1} is the interference dispersion at the D_1 input; $I_0\left(\frac{u_1 E_{s1}}{\sigma^2_{n1}}\right)$ is the Bessel function of the zero order of the fictitious argument; σ^2_{n2} is the interference dispersion at the D_2 input.

Substituting the values $W_1(u_1)$ and $W_2(u_2)$ into expression (8.4.21) and assuming that the thresholds $U_{thr\ 1} = U_{thr\ 2} \approx 0$, we obtain

$$p_1 = \frac{1}{2a^2} \exp\left[-q^2_{1.1}\left(1 - \frac{1}{2a^2}\right)\right], \qquad (8.4.22)$$

п = n

where $a^2 = \frac{1}{2}\left(1 + \frac{\sigma^2_{n1}}{\sigma^2_{n2}}\right)$ is a coefficient dependent on the effective transmission bands ΔF_1 and ΔF_2 of the filters SF_1 and SF_2, since when there is an /413 equality of the transfer constants of SF_1 and SF_2 at the resonance frequency the condition $\frac{\sigma^2_{n1}}{\sigma^2_{n2}} = \frac{\Delta F_1}{\Delta F_2}$ is satisfied. Similarly we find

where

$$p_2 = \frac{1}{2b^2} \exp\left[-q^2_{1.2}\left(1 - \frac{1}{2b^2}\right)\right],$$

п = n

$$b^2 = \frac{1}{2}\left(1 + \frac{\sigma^2_{n2}}{\sigma^2_{n1}}\right) = a^2 - \frac{1}{2}\left(\frac{\sigma^2_{n1}}{\sigma^2_{n2}} + \frac{\sigma^2_{n2}}{\sigma^2_{n1}}\right). \qquad (8.4.23)$$

When $\sigma^2_{n1} = \sigma^2_{n2}$, which corresponds to the case of a CCRL symmetrical relative to interference,

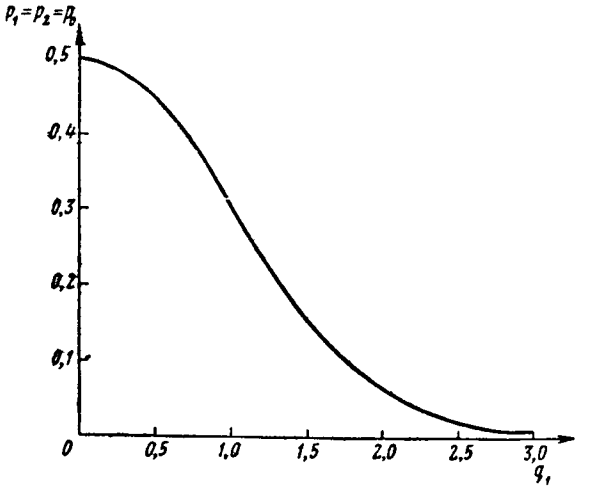

Figure 8.7

$$p_1=p_2=\frac{1}{2}\exp\left(-\frac{q_1^2}{2}\right), \tag{8.4.24}$$

where

$$q_1^2=q_{1.1}^2=q_{1.2}^2.$$

Figure 8.7 shows a curve of the function $p_0 = p_1 = p_2 = F(q_1)$, constructed on the basis of formula (8.4.24). This curve shows that when the effective interference exceeds the signal by a factor of 2 we have $p_1 = p_2 \approx 0.45$.

The dependence of $q_{1.1}$ and $q_{1.2}$ on q_0, in the case of a high level of interference, for the case of identical filters F_1 and F_2 is determined approximately using the following formula (ref. 34)

$$q_{1.1}^2=q_{1.2}^2=\frac{2q_0^4m^2}{2(2+m^2)q_0^2+\sqrt{2}}\cdot\frac{\Delta f_e}{\Delta F_1}. \tag{8.4.25}$$

On the basis of the derived formulas, it is possible to find the relationship of $[\overline{K}_n]_c$, $[\overline{\Delta K}]_c$, $[\overline{K}_{cn}]_c$, $[\overline{\Delta K}_c]_c$, $G_f(0)$, $G_{cf}(0)$, σ_f^2 and σ_{cf}^2 and the value q_0. Figure 8.8 is a pair of curves illustrating the influence of q_0 on $G_{cf}(0)$ and $[\overline{K}_{cn}]_c$ for a symmetrical CCRL. In this figure, the dashed straight line represents the value of the command coefficient K_c which would characterize the CCRL output signal in the absence of interference. The approach of the /414

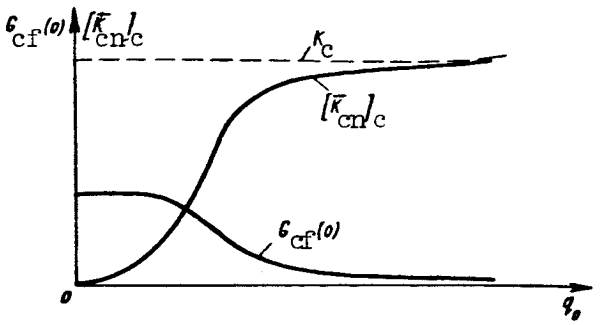

Figure 8.8

value $[\bar{K}_{cn}]_c$ to zero with a decrease of q_0 means the appearance of the effect of opening of the control system (guidance circuit) for the regular component of the received commands; in this case, the opening occurs in such a way that the control surfaces of the rocket, for a given form of guidance, on the average will be in a neutral position. Figure 8.6 shows that virtually complete opening sets in when $p_0 \geq 0.4\text{-}0.45$, which corresponds to $q_1 \leq 0.5\text{-}0.6$ (fig. 8.7). At the same time, with a decrease of q_0 the spectral density attains a maximum value, increasing monotonically from zero when interference is absent (fig. 8.8).

If the CCRL is asymmetrical relative to interference, which corresponds to the condition $p_1 \neq p_2$, with an increase of intensity (strength) of fluctuations, one of the probabilities (p_1 or p_2) approaches 1 and the other approaches 0. In such CCRL, in the case of a very high level of interference, the value $[\bar{K}_n]_c$ does not become equal to zero. Thus, when $p_1 = 1$ and $p_2 = 0$, on the basis of expression (8.4.3) we obtain

$$[\bar{K}_n]_c = k_{F1}u_1 - k_{F2}u_2 - k_{F2}U_{m2}. \qquad (8.4.26)$$

When $p_2 = 1$ and $p_1 = 0$, we will have

$$[\bar{K}_n]_c = k_{F1}u_1 - k_{F2}u_2 + k_{F1}U_{m1}. \qquad (8.4.27)$$

Formulas (8.4.26) and (8.4.27) show that in the case of a very high level of interference at the output of an asymmetrical CCRL, in most cases, a minimum

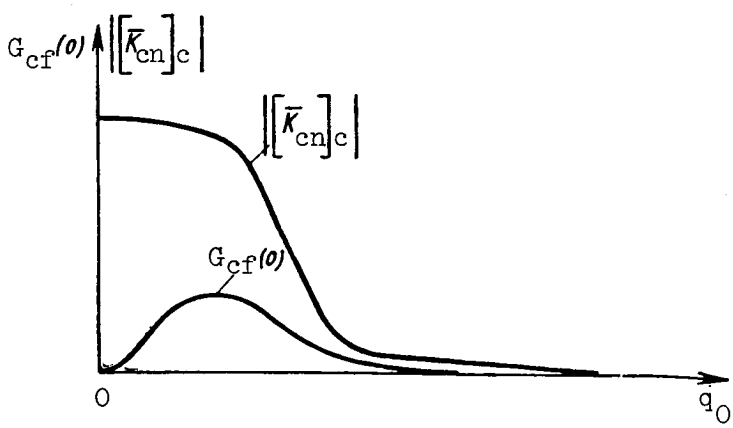

Figure 8.9

or maximum output signal is formed which within limits is not dependent on the transmitted command. This means that the guidance circuit will be opened for the "constant" component of the received commands, but in such a way that, in the majority of cases, the control surfaces of the rocket will be in one of the extreme positions. /415

The spectral density of the CCRL output signals when $p_1 = 1$ and $p_2 = 0$ or when $p_1 = 0$ and $p_2 = 1$ also becomes equal to 0, which is equivalent to opening of the guidance circuit for the fluctuation components of the CCRL output signal.

Figure 8.9 shows the typical appearance of the dependence $\left|\left[\bar{K}_{cn}\right]_c\right|$ and $G_{cf}(0)$ when $K_a = 0$ on q_0 for an asymmetrical CCRL.

On the basis of the considerations presented above, it can be concluded that when designing a CCRL it is necessary to ensure that it is symmetrical relative to interference. Then, it is important to emphasize the desirability of using a symmetrical threshold apparatus and identical output filters. This can be attributed, in particular, to the fact that under the mentioned conditions the maximum of the transfer constant of the CCRL is ensured.

We note, in conclusion, that the derived expressions for $\left[\bar{K}_n\right]_c$ and $G_f(0)$ make it possible to find the equation of a mathematical model of a CCRL of the considered type. For example, for a symmetrical CCRL we will have

$$K_{ne}(t) = (k_{CCRL})_n K_a(t) + \Delta K(t). \qquad (8.4.28)$$

In this equation $(k_{CCRL})_n$ is determined using formula (8.4.7a) and the random function $\Delta K(t)$, which can be considered white noise, has a zero mathematical expectation and spectral density $G_f(0)$, computed using formula (8.4.15).

If the CCRL is not symmetrical relative to interference, the processes transpiring in the statistically equivalent filter should be described by equation (8.1.30). In this equation, the mathematical expectations $\overline{\xi_0(t)}$, $\overline{\xi_1(t)}$, $\overline{\zeta_1(t)}$ and the spectral densities (at the frequency $\omega = 0$) $G_{\xi 0}(0)$, $G_{\xi 1}(0)$ and $G_{\xi 1}$, determined from expressions (8.4.3), (8.4.4), (8.4.5) and (8.4.14), /416 should be equal to

$$\overline{\xi_0(t)} = K_{1.2}, \quad \overline{\zeta_1(t)} = 0, \quad \overline{\xi_1(t)} = \frac{K_{1.1}}{K_a}.$$

$$G_{\xi 0}(0) = (k_{F1}U_{m1} + k_{F2}U_{m2})^2 \left[\frac{p_1(1-p_1)}{\Delta F_1} + \frac{p_2(1-p_2)}{\Delta F_2}\right] - G_{\xi 1}(0),$$

$$G_{\xi 1}(0) = (k_{F1}U_{m1} + k_{F2}U_{m2})^2 k_{tK}\left[\frac{p_1(1-p_1)}{\Delta F_1} - \frac{p_2(1-p_2)}{\Delta F_2}\right]$$

$$G_{\xi 1}(0) = 0.$$

The CCRL output signal, used for moving the spoilers, is equivalent to the voltage difference between $u_{p1}(t)$ and $u_{p2}(t)$ in a CCRL containing the output filters F_1 and F_2, if it is assumed that $u_{p1}(t)$ and $u_{p2}(t)$ have different amplitudes and $u_1 = u_2 = 0$. Therefore, the conditional mathematical expectations and spectral densities of the command coefficients in both types of CCRL should be identical.

Then, on the basis of expressions (8.4.3) and (8.4.14) when $k_{F1} = k_{F2}$, for CCRL without filters we obtain

$$[\bar{K}_{cn}]_c = p_2 - p_1 + K_{Cc}(1 - p_1 - p_2), \tag{8.4.29}$$

$$[G_c(0)]_c = 4\left\{\frac{p_1(1-p_1)}{\Delta F_1} + \frac{p_2(1-p_2)}{\Delta F_2} + K_{Cc}\left[\frac{p_1(1-p_1)}{\Delta F_1} - \frac{p_2(1-p_2)}{\Delta F_2}\right]\right\}. \tag{8.4.30}$$

In order to find $[\bar{K}_n]_c$ and $[G(0)]_c$, it is sufficient to multiply expressions (8.4.29) and (8.4.30) by T and T^2, respectively; $[\Delta\bar{K}_c]_c$ and $[\Delta\bar{K}]_c$ can be computed from the known formulas for $[\bar{K}_{cn}]_c$ and $[\bar{K}_n]_c$ after subtracting $K_c = K_{Cc}$ from them and also $K = K_C = T_1 - T_2 = k_C K_a$.

The value

$$[\bar{K}_n]_c = T(p_2 - p_1) + k_C K_a(1 - p_1 - p_2) \qquad (8.4.31)$$

consists of two parts. The first part, equal to $T(p_2 - p_1)$, characterizes the mathematical expectation of error in transmission of command and can be made equal to zero if the CCRL is designed in such a way that the equality $p_1 = p_2 = p_0$ is satisfied.

The term $k_C K_a(1 - p_1 - p_2)$ changes proportional to the transmitted command K_a and is dependent on the noise intensity.

The mean CCRL transfer constant decreases due to interference by the value $p_1 + p_2$ and becomes equal to

$$(k_{CCRL})_n = k_C(1 - p_1 - p_2). \qquad (8.4.32)$$

If the CCRL is symmetrical relative to interference, in the case of very strong interference $[\bar{K}_n]_c$ approaches zero and the guidance circuit is opened so that the control surfaces of the rocket, under the influence of radio interference, in most cases occupy a neutral position. The mean (statistical) transfer constant of such a CCRL is

$$(k_{CCRL})_n = k_{OC}(1 - 2p_0). \qquad (8.4.33)$$

In an asymmetrical CCRL, when $p_1 = 1$ and $p_2 = 0$ or $p_1 = 0$ and $p_2 = 1$, /417 the value $[\bar{K}_n]_c$ is equal to -T and T, respectively. This means that the opening of the circuit, for the most part, occurs when there is a maximum deflection of the spoiler in one direction or the other.

It follows from the above that it is desirable to design a CCRL in such a way that it is symmetrical relative to interference. This requires a rigorous identity of the like stages for handling the subcarrier oscillations of the considered channel in the decoder.

The dependence of $[\bar{K}_n]_c$, $[\bar{K}_{cn}]_c$, $[\overline{\Delta K}]_c$ and $[\overline{\Delta K_c}]_c$ on $q_{1.1}$ and $q_{1.2}$, and also on q_0 can be determined quite easily by using formulas (8.4.22), (8.4.23) and (8.4.25).

It was noted earlier that it is desirable to design a CCRL which is symmetrical relative to interference when $p_1 = p_2 = p_0$ and $\Delta F_1 = \Delta F_2 = \Delta F_{eff}$. As can be seen from expression (8.4.30), for such CCRL $[G(0)]_c$ ceases to be dependent on K_a and accordingly is equal to

$$[G(0)]_c = \frac{8T^2}{\Delta F_1} p_0(1-p_0). \tag{8.4.34}$$

At the same time

$$[G_c(0)]_c = \frac{8}{\Delta F_1} p_0(1-p_0). \tag{8.4.35}$$

The relationship between $[G(0)]_c$ and $[G_c(0)]_c$ and between $q_{1.1}$, $q_{1.2}$ and q_0 can be obtained on the basis of expressions (8.4.22), (8.4.23) and (8.4.25). Analysis of formula (8.4.30) reveals that $[G_c(0)]_c$ in a CCRL without filters changes qualitatively with an increase of the interference level as it does in a CCRL with low-frequency output filters.

If it is necessary to know the dispersion of fluctuations of the CCRL output signal, for a symmetrical CCRL, the functions $[G(0)]_c$ and $[G_c(0)]_c$ must be multiplied by the effective band of fluctuations when $0 \leq \omega \leq \infty$ is equal to $\frac{1}{2T}$.

Then we obtain

$$\sigma^2 = 4\frac{T}{\Delta F_1} p_0(1-p_0) \tag{8.4.36}$$

and

$$\sigma_c^2 = \frac{4}{\Delta F_1 T} p_0(1-p_0). \tag{8.4.37}$$

Comparison of the dispersions σ_{cf}^2 and σ_c^2 reveals that

$$\sigma_{cf}^2 = 2\Delta F T \sigma_c^2.$$

We recall that this same expression was obtained for CCRL with low-frequency output filters.

8.5. Effect of Low-Level Fluctuation Interference on a CCRL with Pulse-Counting Modulation

The output signals in a CCRL with pulse-counting modulation are determined quite simply by using the decoder whose functional diagram is shown in figure

7.13b. The distinguishing characteristic of this apparatus is that it contains wideners for the pulses fed from the coincidence stages CS_1 and CS_2. /418

When a CCRL with wideners in the decoder is subjected to fluctuations interference whose level is low in comparison with the amplitude of the working signals, the conditional constant component of distortion of the received commands is equal to zero. This is because for the stipulated value of the transmitted command, when interference is present or absent, during the time T the wideners form the same number of pulses with constant amplitudes and durations.

At the same time, groups of pulses $u_{p1\ n}(t)$ and $u_{p2\ n}(t)$ will act at the W_1 and W_2 outputs (fig. 7.13b) when interference is present; the times of formation of these groups change randomly.

Since in the case of pulses which are position modulated randomly the value of the spectral density at the zero frequency is equal to zero (ref. 33), in a study of the problem of the noise immunity of CCRL with wideners in the decoder it is necessary to know $G_f(\omega)$, rather than $G_f(0)$, where $G_f(\omega)$, as before, is the conditional spectral density of the signal $K_n(t)$ in a CCRL with output filters.

Determination of $G_f(\omega)$ requires a knowledge of the functions $G_1(\omega)$ and $G_2(\omega)$, characterizing the spectral densities of the voltages $u_{p1\ n}(t)$ and $u_{p2\ n}(t)$ for all frequencies ω. For a given value of the transmitted command, reflected using m_1 and m_2 symbols of the first and second kind, the voltage $u_{p1\ n}(t)$ can be considered as consisting of m_1 pulse sequences, in each of which there is phase (position) fluctuation of the pulses; the mean pulse repetition interval is constant and equal to T. In addition, the amplitudes and durations of the pulses in all sequences are identical and equal to U_{m1} and τ_{p1}, respectively.

Taking into account that, in any sequence, the pulses are formed independently of one another and that all sequences are uncorrelated with one another, we can write

$$G_1(\omega) = m_1 G_{1i}(\omega), \tag{8.5.1}$$

where $G_{1i}(\omega)$ is the continuous part of the spectral density of the i-th of m_1 pulse sequences with random phase modulation.

It is known (ref. 33) that for square pulses forming at random times

$$G_{1l}(\omega)=\frac{8}{T\omega^2}U_{m1}^2\sin^2\frac{\omega\tau_{p1}}{2}[1-|\theta_1(\omega)|^2], \qquad (8.5.2)$$

where $\theta_1(\omega)$ is the characteristic function of deviation of the time of appearance of the pulses $u_{pl\ n}(t)$ from the mean value.

If the probability density of deviation $\xi_{\tau 1}$ of the time of formation /419 of a pulse relative to its mean value is denoted $W(\xi_{\tau 1})$, then

$$\theta_1(\omega)=\int_{-\infty}^{\infty}W_1(\xi_{\tau 1})e^{j\omega\xi_{\tau 1}}d\xi_{\tau 1}.$$

However

$$\xi_{\tau 1}=\tau_1-\overline{\tau}_1,$$

where τ_1 and $\overline{\tau}_1$ are the instantaneous and mean values of displacement by interference of the leading edges of the $u_{pl\ n}(t)$ pulses.

It follows therefore that the possibility of computing $W_1(\xi_{\tau 1})$ involves the necessity for determining the distribution density of the probabilities $W(\tau_1)$ for τ_1. The latter can be determined by an analysis of the fluctuations of the times of appearance of the pulses $u_{CS\ 1}$, produced by the coincidence stage CS_1.

The process of formation of these fluctuations for the case when CS_1 produces a signal when under the influence of a two-pulse timing code is illustrated in figure 8.10. The solid and dashed lines in figure 8.10a and b show the position of the leading edges and the clipping of the first and second code pulses in the absence and in the presence of interference, respectively, before and after passing through the delay line in the coincidence stage; figure 8.10c shows the output signal.

The square pulses at the CS_1 input can be obtained using a so-called normalizer, which consists of a bilateral limiter, delay multivibrator, blocking oscillator, etc. Figure 8.10 shows the pulses for a case when the role of a normalizer is performed by a bilateral limiter. If a delay multivibrator or a blocking oscillator is used, the signals shown in figure 8.10a and b will be position modulated on the time axis, rather than being width modulated.

The operation of the decoder deteriorates appreciably when there is no normalizer in the CCRL radio receiver. This is because video pulses are formed

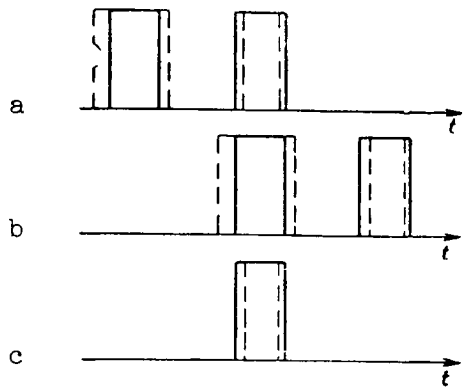

Figure 8.10

at the radio receiver output which in shape are close to triangular. If there are fluctuations of their leading edges, there will be appreciable oscillations of the amplitudes of the $u_{CS\ 1}$ output pulses of the coincidence stage CS_1, resulting in unfavorable conditions for passage of the signals through the subsequent circuits of the decoder. Therefore, henceforth we will assume that the input pulses of the coincidence stage are normalized in shape and are square. Under this condition it can be found (ref. 105) that /420

$$W(\tau_1) = n_1 W_0(\tau_1) \left[\int_0^{\tau_1} W_0(\Delta t)\, d(\Delta t) \right]^{n-1} \qquad (8.5.3)$$

where $W_0(\Delta t)$ is the probability density for fluctuations of the leading edge of a single pulse at the CS_1 input, and n_1 is the capacity of the timing code to which the coincidence stage CS_1 is tuned.

It can be shown that the fluctuations Δt in the case of a low noise level have a zero mathematical expectation and with an adequate degree of accuracy have a normal probability distribution, that is

$$W_0(\Delta t) = \frac{1}{\sqrt{2\pi}\sigma_\tau} \exp\left(-\frac{\Delta t^2}{2\sigma_\tau^2}\right),$$

where σ_τ^2 is the dispersion of fluctuations of the leading edge for any of the normalizer output pulses.

Substituting the cited value $W_0(\Delta t)$ into the expression for $W(\tau_1)$ and integrating, we obtain

$$W(\tau_1)=\frac{n_1}{2^{n_1-1}\sigma_\tau\sqrt{2\pi}}\left[1+\Phi\left(\frac{\tau_1}{\sqrt{2}\sigma_\tau}\right)\right]^{n_1-1}\exp\left(-\frac{\tau_1^2}{2\sigma_\tau^2}\right) \tag{8.5.4}$$

Here $\Phi\left(\frac{\tau_1}{\sqrt{2}\sigma_\tau}\right)=\frac{2}{\pi}\int_0^x e^{-t}dt$ is the probability integral representing the tabulated function.

By knowing $W(\tau_1)$, in accordance with the rules of transformation of the probability distribution laws for functions of the random values, we obtain

$$W(\xi_{\tau 1})=\frac{n_1}{2^{n_1-1}\sqrt{2\pi}\sigma_{\tau 1}}\left[1+\Phi\left(\frac{\bar{\tau}_1+\xi_{\tau 1}}{\sqrt{2}\sigma_{\tau 1}}\right)\right]^{n_1-1}\times\exp\left[-\frac{(\bar{\tau}_1+\xi_{\tau 1})^2}{2\sigma_{\tau 1}^2}\right], \tag{8.5.5}$$

where

$$\bar{\tau}_1=\int_{-\infty}^{\infty}\tau_1 W(\tau_1)\,d\tau_1; \tag{8.5.6}$$

$$\sigma_{\tau 1}^2=\int_{-\infty}^{\infty}(\tau_1-\bar{\tau}_1)^2 W(\tau_1)\,d\tau_1. \tag{8.5.7}$$

We note that in a general case the integrals (8.5.6) and (8.5.7) are not expressed through elementary functions and the values $\bar{\tau}_1$ and $\sigma^2_{\tau 1}$ must be computed using the methods of numerical integration. /421

After $W(\xi_{\tau 1})$ is known, it is possible to determine the characteristic function $\theta_1(\omega)$, and then, using formulas (8.5.1) and (8.5.2), also find the values $G_1(\omega)$.

Considering in this way the processes transpiring at the output of the coincidence stage CS_2 and the widener W_2, we obtain

$$G_2(\omega)=m_2 G_{2i}(\omega), \tag{8.5.8}$$

where $G_{2i}(\omega)$ is the continuous part of the spectral density of the i-th sequence (of the total number m_2) of pulses forming at the W_2 output.

Since at the CS_2 output each sequence represents square pulses with random phase modulation, then

p = w

$$G_{2i}(\omega) = \frac{8}{T\omega^2} U_{m2}^2 \sin^2 \frac{\omega\tau_{p2}}{8} [1 - |\theta_2(\omega)|^2]. \qquad (8.5.9)$$

Here

$$\theta_2(\omega) = \int_{-\infty}^{\infty} W_2(\xi_{\tau 2}) e^{j\omega\xi_{\tau 2}} d\xi_{\tau 2}$$

is the characteristic function for the deviation $\xi_{\tau 2}$ of the time of appearance of the pulses of the widener W_2 on the mean value;

$$W_2(\xi_{\tau 2}) = \frac{n_2}{2^{n_2-1}\sqrt{2\pi}\sigma_{\tau 2}} \left[1 + \Phi\left(\frac{\bar{\tau}_2 + \xi_{\tau 2}}{\sqrt{2}\sigma_{\tau 2}}\right)\right]^{n_2-1} \exp\left[-\frac{(\bar{\tau}_2 + \xi_{\tau 2})^2}{2\sigma_{\tau 2}^2}\right]$$

is the probability density for $\xi_{\tau 2}$;

$$\bar{\tau}_2 = \int_{-\infty}^{\infty} \tau_2 W(\tau_2)\, d\tau_2$$

is the mean displacement by interference of the leading edge of the pulse $u_{CS\ 2}$, forming at the CS_2 output;

$$\sigma_{\tau 2}^2 = \int_{-\infty}^{\infty} (\tau_2 - \bar{\tau}_2)^2 W(\tau_2)\, d\tau_2$$

is the dispersion of displacement by interference of the leading edge of the pulse $u_{CS\ 2}$; τ_{w2} is the duration of the pulses produced by the widener W_2; U_{m2} is the amplitude of pulses produced by the widener W_2.

Then after determining $G_1(\omega)$ and $G_2(\omega)$ we find that

$$G_f(\omega) = \frac{m}{2} [(1 + K_{Cc}) G_{1i}(\omega) |Y_1(j\omega)|^2 + (1 - K_{Cc}) G_{2i}(\omega) |Y_2(j\omega)|^2]. \qquad (8.5.10)$$

It can be seen from expression (8.5.10) that for different parameters of pulses produced in the CS_1 and CS_2 and for different characteristics /422

of the CCRL output filters, the conditional spectral density of distortion of the command is dependent not only on the intensity of the interference, but also on the value of the transmitted command K_a.

In order to exclude the influence of K_a on $G_f(\omega)$ it is necessary to satisfy the following conditions: $G_{1i}(\omega) = G_{2i}(\omega)$ and $Y_1(j\omega) = Y_2(j\omega)$. These

conditions mean that $G_f(\omega)$ will be constant for a given level of interference and frequency ω for any K_a if CS_1, CS_2, W_1 and W_2 have identical corresponding characteristics and the capacity of the codes of the first and second kinds are equal to one another.

If the CCRL decoder is designed as shown in figure 7.13a, for the conditional constant component of the CCRL output signal we obtain

Ф = F
П = n

$$[\overline{K_n}]_c = \frac{m}{2T}[k_{\phi 1}U_{m1}\bar{\tau}_{n1} - k_{\phi 2}U_{m2}\bar{\tau}_{n2} + K_{Cc}(k_{\phi 1}U_{m1}\bar{\tau}_{n1} + k_{\phi 2}U_{m2}\bar{\tau}_{n2})], \quad (8.5.11)$$

where $\bar{\tau}_{n1}$ and $\bar{\tau}_{n2}$ are the mathematical expectations of the durations of the pulses formed by the coincidence stages CS_1 and CS_2 when interference is present.

It can be seen from expression (8.5.11) that when interference is present the CCRL output signal consists of two parts, one of which is characterized by the parameters of the filters F_1 and F_2, the amplitudes of the pulses U_{m1} and U_{m2} and the pulse durations τ_{n1} and τ_{n2}, while the other, in addition, is dependent on the transmitted command coefficient $K_{ic} = K_{Cc}$.

The mean transfer constant of the CCRL, equal to

$$(k_{CCRL})_n = \frac{k_C}{2T}(k_{F1}U_{m1}\bar{\tau}_{n1} + k_{F2}U_{m2}\bar{\tau}_{n2}),$$

is dependent on the values $\bar{\tau}_{n1}$ and $\bar{\tau}_{n2}$, which are functions of the intensity of interference and the structure of the timing codes. We note that the expression for $(k_{CCRL})_n$ was written taking into account the equality $K_{Cc} = \frac{k_C}{m}K_a$.

In accordance with formula (8.5.11) and the expression determining the output command K in the absence of interference, for the conditional constant component of command distortion we obtain

И = p
П = n
Ф = F

$$[\overline{\Delta K}]_c = \frac{m}{2T}[k_{\phi 1}U_{m1}(\bar{\tau}_{n1} - \tau_{и1}) - k_{\phi 2}U_{m2}(\bar{\tau}_{n2} - \tau_{и2}) + K_{Cc}[k_{\phi 1}U_{m1}(\bar{\tau}_{n1} - \tau_{и1}) + k_{\phi 2}U_{m2}(\bar{\tau}_{n2} - \tau_{и2})]. \quad (8.5.12)$$

If both circuits handling the subcarrier oscillations have identical characteristics, when $k_{F1}U_{m1} = k_{F2}U_{m2} = k_F U_m$ and $\tau_{p1} = \tau_{p2} = \tau_p$, and the /423

capacities of the timing codes of the considered channel are n, then

п = n
и = p
ф = F

$$\bar{\tau}_{n1} = \bar{\tau}_{n2} = \bar{\tau}_n,$$

$$K = \frac{k_\phi U_m k_C \tau_и}{T} K_a, \tag{8.5.13}$$

$$[\overline{K}_n]_c = \frac{k_\phi U_m k_C \bar{\tau}_n}{T} K_a \tag{8.5.14}$$

and

$$[\overline{\Delta K}]_c = [\overline{K}_n]_c - K = \frac{k_\phi U_m k_C}{T} (\bar{\tau}_n - \tau_и) K_a.$$

Under these conditions

$$K_{max} = \frac{m}{T} k_\phi U_m \tau_и,$$

$$K_c = K_{Cc} = \frac{k_C}{m} K_a, \tag{8.5.15}$$

$$[\overline{\Delta K}_c]_c = \frac{\bar{\tau}_n - \tau_и}{\tau_и} K_{Cc}$$

and

$$[\overline{K}_{cn}]_c = \frac{\bar{\tau}_n}{\tau_и} K_c = \frac{\bar{\tau}_n}{\tau_и} K_{Cc}. \tag{8.5.16}$$

If follows from expressions (8.5.13) and (8.5.14) that when there is interference present, the mean transfer constant of a CCRL with a symmetrical decoder, that is, an apparatus having identical circuits for handling the subcarrier oscillations, changes by $\frac{\bar{\tau}_n}{\tau_p}$ times, where $\frac{\bar{\tau}_n}{\tau_p} < 1$.

The conditional spectral density $G_f(0)$ of the fluctuations of the CCRL output command at the zero frequency can be determined as the sum of the spectral densities $G_{f1}(0)$ and $G_{f2}(0)$ of the voltages $u_{F1}(t)$ and $u_{F2}(t)$, produced by the filters F_1 and F_2. This is because the signals $u_{F1}(t)$ and $u_{F2}(t)$ are uncorrelated due to the absence of a statistical relationship between the pulses $u_{CS\,1}(t)$ and $u_{CS\,2}(t)$, forming at the outputs of the coincidence stages CS_1 and CS_2. However, $G_{f1}(0)$ is equal to the product of the square of the transfer constant k_{F1}^2 of the filter F_1 and the value of the conditional spectral density $G_1(0)$ at the zero frequency for the voltage $u_{CS\,1}(t)$, that is,

$$G_{f1}(0) = k_{F1}^2 G_1(0).$$

Similarly

$$G_{f2}(0) = k_{F2}^2 G_2(0),$$

where $G_2(0)$ is the spectral density at the zero frequency for the voltage $u_{CS\ 2}$.

The spectral density $G_1(0)$ can be found as the sum of the spectral densities $G_{1i}(0)$ $(i = 1, 2, \ldots, m_1)$ at the zero frequency for m_1 pulse sequences of the coincidence stage CS_1, in each of which the pulses have a constant amplitude, a constant mean repetition interval T and a random duration. In a general case, the times of formation of both the leading edge and the clipping of the pulse change randomly. /424

In actual practice, the product of pulse duration in the radio receiver passband is selected in such a way that the fluctuations of the leading edge and the clipping of each pulse can be considered independent. The successive pulses in any of m_1 sequences are uncorrelated.

Therefore, $G_{1i}(0)$ can be represented as the sum $G_{i\ ed}(0) + G_{i\ cl}(0)$, where $G_{i\ ed}(0)$ and $G_{i\ cl}(0)$ are the spectral densities at the zero frequency, forming due to fluctuations of the leading edge and clipping of the pulse of the i-th sequence of m_1 considered pulses. However, much as was done before, we find

$$G_{i\ ed}(0) = 2U_{m1}^2 \frac{\sigma_{\tau 1}^2}{T},$$

$$G_{i\ cl}(0) = 2U_{m1}^2 \frac{(\sigma'_{\tau 1})^2}{T},$$

where $(\sigma'_{\tau 1})^2$ is the dispersion of the fluctuations of the clipping of the pulse produced by the coincidence stage CS_1. Therefore

$\Phi = F$

$$G_1(0) = 2k_{\Phi 1}^2 U_{m1}^2 m_1 \frac{\sigma_{\tau 1}^2 + (\sigma'_{\tau 1})^2}{T}.$$

Similarly, we obtain

$$G_2(0) = 2k_{\Phi 2}^2 U_{m2}^2 m_2 \frac{\sigma_{\tau 2}^2 + (\sigma'_{\tau 2})^2}{T},$$

where $\sigma_{\tau 2}^2$, $(\sigma'_{\tau 2})^2$ are the dispersions of the fluctuations of the leading edge and clipping of the pulse, produced by the coincidence stage CS_2.

In actual practice, the pulses forming at the radio receiver output can be considered symmetrical. Then

$$\sigma_{\tau 1} = \sigma'_{\tau 1},\ \sigma_{\tau 2} = \sigma'_{\tau 2},$$

Φ = F

$$G_1(0) = 4k_{\phi 1}^2 U_{m1}^2 m_1 \frac{\sigma_{\tau 1}^2}{T},$$

$$G_2(0) = 4k_{\phi 2}^2 U_{m2}^2 m_2 \frac{\sigma_{\tau 2}^2}{T}$$

and

$$G_f(0) = 4k_{\phi 1}^2 m_1 U_{m1}^2 \frac{\sigma_{\tau 1}^2}{T} + 4k_{\phi 2}^2 m_2 U_{m2}^2 \frac{\sigma_{\tau 2}^2}{T}. \qquad (8.5.17)$$

Since

/425

$$m_1 = \frac{m}{2}(1 + K_{Cc}) \text{ and } m_2 = \frac{m}{2}(1 - K_{Cc}),$$

then

$$G_f(0) = 4k_{\phi 1}^2 (1 + K_{Cc}) \frac{m}{2} U_{m1}^2 \frac{\sigma_{\tau 1}^2}{T} + 4k_{\phi 2}^2 \frac{m}{2}(1 - K_{Cc}) U_{m2}^2 \frac{\sigma_{\tau 2}^2}{T}. \qquad (8.5.18)$$

It can be seen therefore that $G_f(0)$ is a function not only of the intensity of interference, but also of the value of the transmitted command, on which K_{Cc} is dependent. In order to exclude the dependence of $G_f(0)$ on K_{Cc}, it is necessary that the following conditions be observed

$$k_{F1}U_{m1} = k_{F2}U_{m2} = k_F U_m \text{ and } \sigma_{\tau 1}^2 = \sigma_{\tau 2}^2 = \sigma_{\tau c}^2.$$

These conditions will be satisfied if identical filters F_1 and F_2 are used, the coincidence stages CS_1 and CS_2 are identical and also if codes of identical capacity are selected. Then

$$G_f(0) = 4k_F^2 m U_m^2 \frac{\sigma_{\tau c}^2}{T}. \qquad (8.5.19)$$

Bearing in mind that when $k_{F1}U_{m1} = k_{F2}U_{m2} = k_F U_m$ the square of the maximum command will be equal to

$$k_{max}^2 = k_F^2 m^2 U_m^2 \frac{\tau_p^2}{T^2},$$

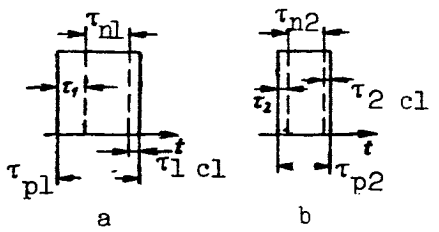

Figure 8.11

on the basis of expression (8.5.19) we obtain

И = p
К = c

$$G_{cf}(0)=\frac{4\sigma_{\tau K}^2 T}{m\tau_{и}^2}=4T_i\frac{\sigma_{\tau K}^2}{\tau_{и}^2}. \qquad (8.5.20)$$

It follows from expression (8.5.20) that the conditional spectral density $G_{cf}(0)$ of fluctuations of the command coefficient at the zero frequency can be computed if the interval T_i, pulse duration τ_p and dispersion $\sigma_{\tau c}^2$ are known.

The dispersion of the command distortion σ_f^2 and the command coefficient σ_{cf}^2 can be computed by multiplying expressions (8.5.19) and (8.5.20) by the effective transmission band of the CCRL output filter. If the output filters have different effective transmission bands ΔF_{e1} and ΔF_{e2}, the value σ_f^2 can be determined using expression (8.5.17) if its first and second terms on the right-hand side are multiplied by ΔF_{e1} and ΔF_{e2}, respectively.

For determination of the values $\bar{\tau}_{n1}$ and $\bar{\tau}_{n2}$, we will consider figure 8.11. The solid lines in figure 8.11a and b denote the pulses forming at the CS_1 and CS_2 outputs in the absence of interference, and the dashed line denotes one of the possible variants of these pulses when there is interference.

Since the instantaneous value of the duration τ_{n1} of a pulse produced /426 in CS_1 is

$$\tau_{n1} = \tau_{p1} - \tau_1 - \tau_{1\,cl},$$

then

$$\bar{\tau}_{n1} = \bar{\tau}_{p1} - \bar{\tau}_1 - \bar{\tau}_{1\,cl}.$$

Similarly, we obtain (fig. 8.11b)

$$\bar{\tau}_{n2} = \bar{\tau}_{p2} - \bar{\tau}_2 - \bar{\tau}_{2\ cl}.$$

It can be seen from the last two expressions that $\bar{\tau}_{n1}$ and $\bar{\tau}_{n2}$ can be determined easily if the probability densities $W(\tau_1)$, $W(\tau_2)$, $W(\tau_{1\ cl})$ and $W(\tau_{2\ cl})$ of the random values τ_1, τ_2, $\tau_{1\ cl}$, and $\tau_{2\ cl}$ are known. A knowledge of these functions also is completely adequate for computation of $\sigma_{\tau 1}$, $\sigma_{\tau 2}$, $\sigma'_{\tau 1}$ and $\sigma'_{\tau 2}$.

The probability density of the random value τ_1 is determined by formula (8.5.4). This same formula also can be used for computation of the probability densities $W(\tau_2)$, $W(\tau_{1\ cl})$ and $W(\tau_{2\ cl})$. When determining $W(\tau_{1\ cl})$ in formula (8.5.4) it is necessary to replace τ_1 by $\tau_{1\ cl}$ and σ^2_τ by $\sigma^2_{\tau\ cl}$, where $\sigma^2_{\tau\ cl}$ is the dispersion of the fluctuations of clipping of the pulses of the normalizer placed before the coincidence stages. When $W(\tau_2)$ is determined, it is necessary to replace τ_1 and n_1 in expression (8.5.4) by τ_2 and n_2, and when computing $W(\tau_{2\ cl})$ it is necessary to replace the parameters τ_1, n_1 and σ_τ by $\tau_{2\ cl}$, n_2 and $\sigma_{\tau\ cl}$.

After determining $\sigma_{\tau 1}$, $\sigma'_{\tau 1}$, $\sigma_{\tau 2}$ and $\sigma'_{\tau 2}$ as functions of σ_τ, $\sigma_{\tau\ cl}$, n_1 and n_2, they can be determined as a function of q_0 and the CCRL parameters in accordance with the method considered below.

If the pulses of the coincidence stages are widened in the CCRL to the value T_i, the values $[\bar{K}_n]_c$, $[\bar{K}_{cn}]_c$, $G_f(0)$ and $G_{cf}(0)$ can be computed using formulas (8.3.19), (8.3.20), (8.3.23) and (8.3.24), provided $\bar{\tau}_1$, $\bar{\tau}_2$, $\bar{\tau}^2_1$ and $\bar{\tau}^2_2$ in them are replaced by the mathematical expectations and dispersions $\bar{\tau}_1$, $\bar{\tau}_2$, $\sigma^2_{\tau 1}$ and $\sigma^2_{\tau 2}$ of the fluctuations of the leading edges and clippings of the pulses $u_{p1\ n}(t)$ and $u_{p2\ n}(t)$. Here it must be remembered that the "tripping" of the threshold apparatus in the CCRL, when it is subjected to low-level interference, is accomplished by the first of the arriving pulses which are produced by the coincidence stages CS_1 and CS_2 (fig. 7.13c).

It follows from an analysis of the expressions which determine $W(\tau_1)$ and $W(\tau_2)$ that when $n_1 \neq n_2$ the conditional constant component $[\overline{\Delta K}]_c$ of distortion

of the command at the CCRL output is not equal to zero. If it is not compensated by special apparatus in the control system, this will lead to the /427 appearance of a mathematical expectation of the error of rocket guidance.

In order to exclude the undesirable phenomenon caused by the error $[\Delta\bar{K}]_c$, the CCRL must be designed in such a way that $n_1 = n_2 = n$. In such a method of command transmission, only random guidance errors will appear which are dependent on $\sigma^2_{\tau 1}$ and $\sigma^2_{\tau 2}$.

If $n_1 = n_2 = n$, the dispersions $\sigma^2_{\tau 1}$ and $\sigma^2_{\tau 2}$ are equal to one another and are determined unambiguously through σ^2_τ. The computations made for n = 1, 2, 3 show that $\sigma^2_{\tau 1} - \sigma^2_{\tau 2}$ when n = 1, 2, 3 are equal to σ^2_τ, 0.64 σ^2_τ and 0.55 σ^2_τ, at the same time that for these same values n the values $\bar{\tau}_1 = \bar{\tau}_2$ are 0, 0.6 σ_τ and 0.71 σ_τ. It follows therefore that with an increase of n, the rocket guidance errors caused by the effect of low-level interference decrease. With the selection of an appropriate number n, it becomes possible to compute the necessary excess of signal over noise, proceeding on the basis of the admissible values of the conditional dispersions and spectral density for distortion of the CCRL output command when $\omega = 0$. This requires only a knowledge of the dependence of σ^2_τ on the ratio q^2_0 of the effective intensities of signal and noise at the CCRL receiver input.

If the normalizer has one triggering threshold $U_{thr\ n}$, which is the case when using a delay multivibrator and a blocking oscillator, or two slightly separated triggering thresholds, which is typical of a bilateral limiter, then

$$\sigma^2_\tau = \frac{\sigma^2_1}{S^2},$$

where σ^2_1 is the noise dispersion at the normalizer input; S is the steepness of the leading edge of the pulse at the normalizer input at a point corresponding to the triggering threshold or the midpoint between the two triggering thresholds.

Approximately

$$S \approx \frac{U_n}{\tau_{ed}},$$

where U_n is the pulse amplitude at the normalizer input, and τ_{ed} is the duration of the leading edge of the pulse.

However,

$$\tau_{ed} \approx \frac{1}{2F_{va}},$$

where F_{va} is the equivalent width of the passband of the receiver video amplifier.

Therefore,

$$\sigma_\tau^2 = \frac{\sigma_1^2}{4U_n^2 F_{va}^2}.$$

We note that F_{va} usually is half the passband of the dc amplifier.

In the case of a low level of interference, the ratio of the intensity of noise entering the dc amplifier passband to the pulse power of the signal P_s at the radio receiver input remains the same as for the output of the video amplifier. This means that /428

$$\sigma_\tau^2 = \frac{1}{4q_p^2 F_{va}^2},$$

where q_p^2 is the ratio of the pulse power of the signal P_s to the effective intensity of the noise P_n at the radio receiver input; in such cases, P_n is proportional to σ_1^2.

In addition to the ratio q_p^2, it is possible to use the ratio q_0^2 of the mean power of the signal $\bar{P}_s$ to the effective intensity of noise P_n. It is known that, when using square pulses, the pulse power of the signal is

$$P_s = \frac{\bar{P}_s T}{\tau_{dur} n_{tc}}.$$

Here τ_{dur} is the pulse duration at the input of the CCRL receiver, and n_{tc} is the total number of pulses fed to the input of the CCRL during the period T of command transmission.

Then

$$q_0^2 = \frac{U_s^2}{U_{thr}^2} = \frac{\bar{P}_s}{P_n} = q_p^2 \frac{\tau_{dur} n_{tc}}{T} \qquad (8.5.21)$$

and

$$\sigma_\tau^2 = \frac{\tau_{dur}^3 n_{tc}}{q_0^2 T},$$

since $\tau_{ed} \approx \tau_{dur}$.

In the case of CCRL without output filters, the values $[\bar{K}_n]_c$ and $[G(0)]_c$ can be determined by multiplying by T and T^2 the values $[\bar{K}_{cn}]_c$ and $G_{cf}(0)$ of corresponding CCRL with filters. This is because the mathematical expectations and spectral densities for the command coefficients in both types of CCRL are identical if $k_{F1}U_{m1} = k_{F2}U_{m2}$.

It follows from an analysis of the results presented in this section that CCRL with pulse-counting modulation have a higher noise immunity than CCRL with pulse-width modulation of sinusoidal subcarrier oscillations, if identical output apparatus is used.

We note, in conclusion, that the equations of statistically equivalent filters for CCRL with pulse-counting modulation, depending on the circuitry of the decoders, are the same in form as for CCRL with pulse-width modulation of sinusoidal subcarrier oscillations with a low or high interference level.

8.6. Effect of High-Level Interference on a CCRL with Pulse-Counting Modulation

Under the influence of interference of considerable intensity on a /429
single-channel CCRL with pulse-counting modulation, the transmitted commands are distorted as a result of the suppression of the transmitted signals and the formation of spurious timing codes (symbols) during the interaction of interference with the received pulses and also due to the effect of interference alone. In addition, it must be remembered that the parameters of each of the pulses produced by the coincidence stages will change randomly.

If the CCRL is multichannel, additional command distortions appear which arise due to the formation of spurious commands for the considered channel, caused by the interaction of interference with the received pulses of the other channels.

In considering the influence of high-level interference on a single-channel CCRL with wideners W_1 and W_2 in the decoders (fig. 7.13b), we will

assume that W_1 and W_2 produce pulses with identical durations τ_w and amplitudes U_m. We will also assume identity of the transfer constants k_{F1} and k_{F2} of the filters F_1 and F_2, which leads to satisfaction of the condition $k_{F1} = k_{F2} = k_F$, and also inclusion of the amplification factor of the subtracting device in k_{F1} and k_{F2}.

Then in the absence of interference, the value of the command K at the CCRL output for a steady-state regime is equal to

p = w
Φ = F

$$K = k_\Phi U_m \frac{\tau_p}{T_i} \frac{m_1 - m_2}{m}. \tag{8.6.1}$$

Under these assumptions, the conditional constant component $[\bar{K}_n]_c$ when interference is present obviously will be

$$[\bar{K}_n]_c = k_\Phi U_m \frac{\tau_p}{T_i} \frac{[\bar{M}_1]_c - [\bar{M}_2]_c}{m}, \tag{8.6.2}$$

where $[\bar{M}_1]_c$ and $[\bar{M}_2]_c$ are the mean number of pulses appearing at the W_1 and W_2 outputs during the time T under the condition that the value of the transmitted command remains constant.

On the basis of expressions (8.6.1) and (8.6.2), taking into account that the maximum value of the command appearing at the CCRL output in the absence of interference is $\frac{k_F U_m \tau_w}{T}$, we find

y = c

$$[\overline{\Delta K}]_c = k_\Phi U_m \frac{\tau_p}{T_i} \left(\frac{[\bar{M}_1]_y - [\bar{M}_2]_y}{m} - K_{Cc} \right), \tag{8.6.3}$$

$$[\bar{K}_{cn}]_c = \frac{[\bar{M}_1]_y - [\bar{M}_2]_y}{m}, \tag{8.6.4}$$

$$[\overline{\Delta K}_c]_c = \frac{[\bar{M}_1]_y - [\bar{M}_2]_y}{m} - K_{Cc}, \tag{8.6.5}$$

/430

where

$$K_{Cc} = \frac{m_1 - m_2}{m}.$$

It follows from expressions (8.6.2)-(8.6.5) that $[\bar{K}_n]_c$, $[\overline{\Delta K}]_c$, $[\bar{K}_{cn}]_c$ and $[\overline{\Delta K}_c]_c$ can be computed if the values $[\bar{M}_1]_c$ and $[\bar{M}_2]_c$ are known.

When determining $[\bar{M}_1]_c$ it is necessary to take into account that in the time T_1 the coincidence stage CS_1 is fed pulses of timing codes to which CS_1 is "tuned" and interference; in the interval T_2, in addition to interference, it is fed pulses of timing codes of the second kind. Therefore, it is feasible to assume that

$$[\bar{M}_1]_c = \bar{M}_{1.1} + \bar{M}_{1.2},$$

where $\bar{M}_{1.1}$ and $\bar{M}_{1.2}$ are the mean numbers of pulses produced by the coincidence stages CS_1 in the times T_1 and T_2, respectively.

If a pulse normalizer is placed in front of CS_1, it can be assumed that the following conditions are satisfied:

(1) square pulse signals and interference with constant amplitudes appear at the input of the coincidence stage CS_1;

(2) the probability density $W(x_1)$ for intervals x_1 between any successive interference pulses at the CS_1 output is $W(x_1) = \lambda_1 e^{-\lambda_1 x_1}$, where λ_1 is the mathematical expectation of the number of interference pulses produced by the CS_1 coincidence stage;

(3) the probabilistic characteristics of different interference pulses at the W_1 input are mutually independent;

(4) each pulse forming at the CS_1 output is capable of "tripping" the widener W_1;

(5) transmitted codes of the first kind to which the CS_1 is "tuned" are not suppressed by interference.

Then, in the time T_1, pulses with a probability of 1 will be fed to the widener W_1 at regular intervals T_i. In addition, there will be random pulses formed whose mean number in the time T_1 will be $\lambda_1 T_1$. The mean number of pulses $\bar{M}_{1.1}$ forming in this case at the W_1 output can be determined as indicated in reference 101.

In the interval T_2, the widener W_1 is fed pulses which appear at the CS_1 output, as a result of addition of interference to the transmitted pulses forming timing codes (symbols) of the second kind to a code group of the first

kind and also due to the formation of symbols of the first kind by interference only. Due to the assumption of an exponential probability distribution of the intervals between successive spurious pulses at the CS_1 output, the value $\bar{M}_{1.2}$ can be found on the basis of an analysis of the effect of randomly following pulses on the widener W_1. $[\bar{M}_2]_c$ is determined in a similar way if it is remembered that, in the time T_1, the coincidence stage CS_2 is fed symbols of the first kind as well as interference and, in the interval T_2, timing codes of the second kind. /431

If timing codes with an identical number n of pulses are used in a single-channel CCRL with pulse-counting modulation, when its decoder is subjected to the influence of pulse interference of the Poisson type (probability density for the intervals is exponential), and under the condition that the constant components of the voltages at the F_1 and F_2 outputs are proportional to $[\bar{M}_1]_c$ and $[\bar{M}_2]_c$, independently of the values $[\bar{M}_1]_c$ and $[\bar{M}_2]_c$, it can be found that

$p_к = p_{code}$, $\tau_p = \tau_w$

$$[\bar{K}_{cn}]_c = K_c p_к \frac{n^2 - n + ZT_l - \alpha n}{\alpha + \tau_p F_l p_к [(n^2 - n + ZT_l)(1 + 2\alpha + \alpha n)] + \rightarrow}, \quad (8.6.6)$$
$$\rightarrow + \tau_p^2 F_l^2 p_к^2 (1 + \alpha)(n^2 - n + ZT_l)(n^2 + ZT_l)$$

$$[\overline{\Delta K}_c]_c = K_{cc} \left\{ p_к \frac{n^2 - n + ZT_l - \alpha n}{\alpha + \tau_p F_l p_к [(n^2 - n + ZT_l)(1 + 2\alpha + \alpha n)] + \rightarrow} - 1 \right\}. \quad (8.6.7)$$
$$\rightarrow + \tau_p^2 F_l^2 p_к^2 (1 + \alpha)(n^2 - n + ZT_l)(n^2 + ZT_l)$$

In these expressions, Z is the mean number of interference pulses acting at the inputs of the coincidence stages CS_1 and CS_2 in 1 sec; $F_i = 1/T_i$ is the repetition interval of the symbols; p_{code} is the probability of formation of an n-unit timing code due to addition of interference to the transmitted pulse: α is a function dependent on the ratios $\frac{\tau_w}{T_i}$ and $\mu = \frac{2Z_{nl}}{m(1 + K_{ic})}$; Z_{nl} and $0.5\, m(1 + K_{ic})$ are the mean numbers of interference pulses and regular pulses fed to the widener W_1 in the interval T_1.

The value α can be computed using the formulas given in reference 101.

In deriving formulas (8.6.6) and (8.6.7), it was assumed that interference could be added to a timing code of a particular type of not only one but any of the transmitted pulses. In this case, for the selected value n, we obtain

the minimum number of spurious codes appearing as a result of interaction with the transmitted pulses and the CCRL has the greatest noise immunity.

It can be seen from expressions (8.6.6) and (8.6.7) that $[\bar{K}_{cn}]_c$ and /432 $[\Delta K_c]_c$ change directly proportional to the transmitted command since $K_{ic} = K_{Cc} = K_c = \frac{k_{CCRL}K_a}{K_{max}}$. This characteristic is a property of only CCRL with equistable codes. It is assumed that two timing codes are equistable if an identical number of spurious codes of a specified kind are formed in 1 sec during the interaction of interference with each of the codes. In the case of "purely" Poisson interference, codes with an identical capacity n are equistable.

Analysis of expression (8.6.6) shows that in the absence of interference, when $Z = 0$, $p_{code} = 0$ and $\alpha = 0$, the equality $[\bar{K}_{cn}]_c = K_{ic}$ is satisfied. When $Z \to \infty$, the rocket guidance circuit for the constant component of received commands is opened in such a way that the rocket control surfaces usually are in a neutral position. For all practical purposes, the opening of the circuit occurs when there is a finite value Z.

If output apparatus is used in a CCRL which does not ensure proportional communication of the constant components of the output voltages with $[\bar{M}_1]_c$ and $[\bar{M}_2]_c$ for any values $[\bar{M}_1]_c$ and $[\bar{M}_2]_c$, the breaking of the guidance circuit occurs at a lesser value Z than in the case of an "absolutely" linear CCRL.

If

$$K_{Cc} = K_{ic} = K_c = \frac{k_{CCRL}K_a}{K_{max}} \text{ and } [\bar{K}_n]_c = [\bar{K}_{cn}]_c K_{max},$$

the transfer constant $(k_{CCRL})_n = \frac{[\bar{K}_n]_c}{K_a}$ for CCRL when subjected to interference is

$p_K = p_{code}$, $\tau_p = \tau_w$

$$(k_{CCRL})_n = k_{CCRL}\, p_K \frac{n^2 - n + ZT_i - \alpha n}{\alpha + \tau_p F_i p_K [(n^2 - n + ZT_i)(1 + 2\alpha + \alpha n)] + \ldots + \tau_p^2 F_i^2 p_K^2 (1 + \alpha)(n^2 - n + ZT_i)(n^2 + ZT_i)} \quad (8.6.8)$$

If the CCRL is N_k-channel, the factor N_k appears before n^2 in expressions (8.6.6)-(8.6.8). The degree of the relationship between $(k_{CCRL})_n$ and N_k is essentially dependent on pulse duration τ_w of the pulses produced by the wideners W_1 and W_2.

With exclusion of W_1 and W_2 from the decoder circuit, when $\tau_w = 0$ and $\alpha = p_{code}(N_k n^2 - n + ZT_i)$, the values $[\overline{K}_{cn}]_c$ and $[\overline{\Delta K}_c]_c$ cease to be functions of N_k and become equal to

$$[\overline{K}_{cn}]_c = K_{ic}(1 - np_{code}) \tag{8.6.9}$$

and

$$[\overline{\Delta K}_c]_c = -np_{code}K_{ic} \tag{8.6.10}$$

We recall that expressions (8.6.9) and (8.6.10) are correct under the condition of absence of suppression of the transmitted pulses by interference, that is, when $np_{code} < 1$. If $\tau_w \neq 0$, it is impossible to avoid an influ- /433
ence of N_k on $[\overline{K}_{cn}]_c$.

Formulas (8.6.9) and (8.6.10) can be derived not only on the basis of expressions (8.6.6) and (8.6.7) with the substitution in them of

$$\alpha = p_{code}(N_k n^2 - n + ZT_i) \text{ and } \tau_w = 0,$$

but also as a result of direct analysis of the processes transpiring in the decoder.

With the interaction of interference with each of the pulses entering into a symbol of the first kind, a maximum of (n - 1) spurious timing codes can be formed, to which the coincidence stage CS_1 will react. This is because such a pulse in the spurious code can be at any place except that which it occupies in the transmitted code. If the probability of addition of this pulse by interference to the corresponding code is denoted p_{code}, the mean number of spurious codes of the considered type will be $p_{code}(n - 1)$. As a result, during the time T_1, an average of $\overline{M}_{1.1} = p_{code}m_1 n(n - 1) + Z_1 + m_1$ pulses is formed at the CS_1 output, where Z_1 is the mean number of symbols of the first kind appearing during the time T_1 under the influence of interference, and m_1 is the number of symbols of the first kind fed to the input of the CCRL radio receiver during this same time T_1.

Interference, interacting with any of the pulses forming a timing code to which the coincidence stage CS_1 is not "tuned," can create n^2 spurious symbols of the first kind. Then, bearing in mind that m_2 symbols of the second kind

are transmitted in the interval T_2, we find that $\bar{M}_{1.2} = p_{code} m_2 n^2 + Z_2$, where Z_2 is the mean number of symbols of the first kind appearing in the time T_2 due to interference only.

By knowing $\bar{M}_{1.1}$ and $\bar{M}_{1.2}$, we obtain

$p_K = p_{code}$

$$[\bar{M}_1]_c = p_K m n^2 + m_1 (1 - p_K n) + Z_1 + Z_2. \tag{8.6.11}$$

Similarly, it can be found that

$$[\bar{M}_2]_c = p_K m n^2 + m_2 (1 - p_K n) + Z_1 + Z_2. \tag{8.6.12}$$

We note that in expression (8.6.12) the sum $Z_1 + Z_2$ was written on the assumption of equistability of the timing codes used in the analyzed CCRL. Substituting the values $[\bar{M}_1]_c$ and $[\bar{M}_2]_c$, determined by expressions (8.6.11) and (8.6.12), into relations (8.6.4) and (8.6.5), we obtain formulas (8.6.9) and (8.6.10).

In order to obtain the necessary quantitative evaluations $[\bar{K}_n]_c$, $[\bar{K}_{cn}]_c$, $[\overline{\Delta K}]_c$ and $[\overline{\Delta K_c}]_c$ as a function of the ratio of the mean intensities of the received signals and interference at the CCRL radio receiver input, it is necessary to know the formulas determining Z and p_{code} as a function of q_0. This problem can be solved under the condition that the statistical parameters of the effective interference are given.

For example, when the CCRL is subjected to interference in the form of randomly following pulses with the duration τ_p, the value Z corresponds to the mean number of these pulses appearing in 1 sec, and p_{code} is equal to approximately (ref. 82)

$$p_{code} \approx n(Z\tau_p)^{n-1}. \tag{8.6.13}$$

If it is assumed that the input of the radio receiver of a single-channel CCRL is fed square pulses of signals and interference with identical durations and amplitudes, then

$$q_0^2 = \frac{nmF}{Z}. \tag{8.6.14}$$

Expressions (8.6.6), (8.6.7), (8.6.13) and (8.6.14) and the formula /434 determining the function α (ref. 101) make it possible to compute $[\overline{K}_{cn}]_c$ and $[\overline{\Delta K}_c]_c$ for different parameters of the command signals, CCRL decoder and values Z of random pulse interference.

As an illustration, figures 8.12 and 8.13 show the dependence of $-\frac{[\overline{\Delta K}_c]_c}{K_{ic}}$ and $-[\overline{\Delta K}_c]_c$ on $\frac{1}{q_0^2}$ for CCRL in which the constant components of the voltages of the output filters F_1 and F_2 change directly proportional to $[\overline{M}_1]_c$ and $[\overline{M}_2]_c$, and for CCRL in which the constant component of the voltage forming at the F_1 output remains a constant value when $[\overline{M}_1]_c \geq m$.

The curves in figure 8.12 show that the minimum command distortions are obtained in CCRL without wideners (curve 1). It can be shown that with an increase of $\frac{\tau_w}{T_i}$ from 0 to 0.5-0.6, the values $[\overline{\Delta K}_c]_c$ increase sharply. A further increase of the ratio $\frac{\tau_w}{T_i}$ slows down the rate of increase of the errors $[\overline{\Delta K}_c]_c$ and when $\frac{\tau_w}{T_i} = 1$ (curve 2) the distortions $\overline{\Delta K}_c$ for the same ratio $\frac{1}{q_0^2}$ become

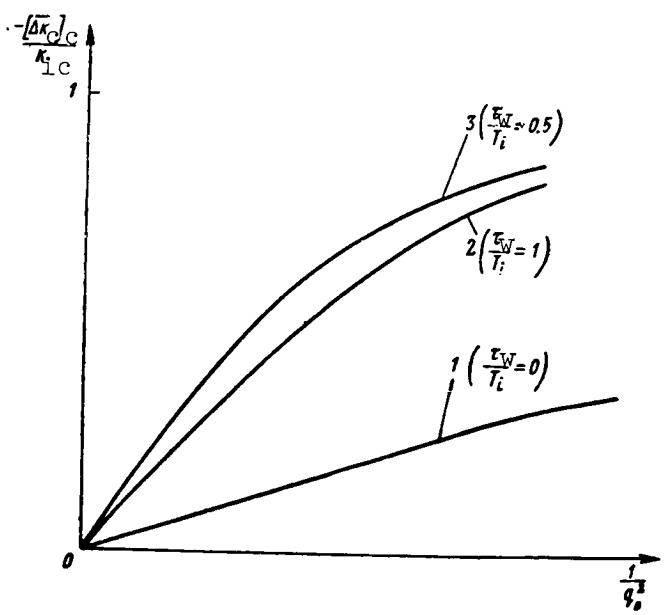

Figure 8.12

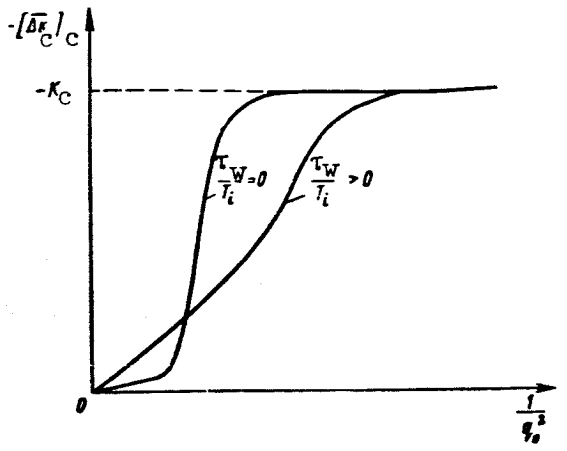

Figure 8.13

smaller than when $\frac{\tau_w}{T_i} = 0.5\text{-}0.6$. However, they considerably exceed $[\overline{\Delta K_c}]_c$ /435 when $\tau_w = 0$. With an increase of N_k, the distortions $[\overline{\Delta K_c}]_c$ increase for all $\tau_w \neq 0$.

It follows from figure 8.13, where the dashed line denotes the value of the command coefficient K_c which we would have if there was no interference, that for a single-channel CCRL with a linearly limited amplitude characteristic of the filter F_1, the changes of $[\overline{\Delta K_c}]_c$ with $\frac{1}{q_0^2}$ have a threshold character. This means that beginning with some value $\frac{1}{q_0^2}$, the value $[\overline{\Delta K_c}]_c$ increases greatly and then becomes equal to $-K_c$. The threshold phenomenon is manifested most sharply for small K_c. When $\frac{\tau_w}{T_i} > 0$, the change of $\left|[\overline{\Delta K_c}]_c\right|$ occurs more smoothly.

If $\frac{\tau_w}{T_i} = 1$, CCRL with linear and linear-limited amplitude characteristics become identical. An increase of N_k (all other conditions being equal) leads to a decrease of the ratio $\frac{1}{q_0^2}$ at which the guidance circuit for the mean component of received commands opens. In a general case, the appearance of nonlinearity in the amplitude characteristic leads to a decrease of CCRL noise immunity.

If the effect of suppression of transmitted signals is taken into account, it can be concluded that the mathematical expectation of the distortions

$[\overline{\Delta K_c}]_c$ increases. With an increase of $\frac{1}{q_0^2}$ and K_{ic}, the difference $[\Delta K_c]_c$ when $p_{sup} = 0$ and $p_{sup} \neq 0$, where p_{sup} is the probability of suppression of the /436 transmitted pulse by interference, increases. In a CCRL with a linearly-limited amplitude characteristic, the presence of the suppression effect leads to a decrease of the values Z at which the threshold effect sets in.

These conclusions apply to a CCRL based on use of equistable timing codes. If the codes are not equistable, it is necessary to add to the right-hand side of expression (8.6.6) a term which is a function of Z and which is not dependent on the transmitted command K_a. However, such a CCRL, in contrast to the earlier considered asymmetrical CCRL with pulse-width modulation, opens the guidance circuit so that the control surfaces of the rocket usually are in a neutral position.

The conditional spectral density $G_f(\omega)$ and $G_f(0)$ for any intensity of interference is determined most easily for a CCRL without wideners. If wideners W_1 and W_2 are part of the CCRL decoder, the theoretical solution of the problem of computation of $G_f(\omega)$, in a general case, involves considerable mathematical difficulties. However, in approximate evaluations of the fluctuating components present in the output signal $K_n(t)$, for cases when the value $\frac{\tau_w}{T_i}$ is several tens of percent, it can be taken into account that W_1 and W_2 produce signals which are randomly following pulses. With such a formulation of the problem, we will obtain somewhat exaggerated values $G_f(\omega)$ for relatively small values of the ratio $\frac{1}{q_0^2}$ at which the value $[\overline{\Delta K_c}]_c$ differs insignificantly from zero and extremely precise results for the values $\frac{1}{q_0^2}$ at which $(k_{CCRL})_n$ becomes close to zero.

Since there is virtually no reciprocal correlation between the random signals produced by the coincidence stages CS_1 and CS_2, in accordance with expression (8.3.2) we will have

$$G_f(\omega) = G_1(\omega)\,|\,Y_1(j\omega)\,|^2 + G_2(\omega)\,|\,Y_2(j\omega)\,|^2, \qquad (8.6.15)$$

where $G_1(\omega)$ and $G_2(\omega)$ are the spectral densities of the fluctuating components of the voltages produced by the corresponding coincidence stages for CCRL without wideners and by the stages W_1 and W_2 for CCRL with wideners.

By dividing $G_f(\omega)$ by $K^2_{max} = k^2_{Fl} U^2_{ml} \frac{\tau^2_w}{T^2_i}$, we obtain the following formula determining the spectral density $G_{cf}(\omega)$

$\Phi = F$
$p = w$

$$G_{cf}(\omega) = \frac{T_i^2}{k^2_{\phi 1} U^2_{m_1} \tau^2_p} [G_1(\omega) | Y_1(j\omega)|^2 + G_2(\omega) | Y_2(j\omega)|^2].$$

We note that here τ_w is the duration of pulses fed to the filters F_1 and F_2. /437

Since τ_w usually is much less than the time constant of each of the filters F_1 and F_2, then

$$G_{cf}(\omega) \approx \frac{T_i^2}{k^2_{\phi 1} U^2_{m_1} \tau^2_p} [G_1(0) | Y_1(j\omega)|^2 + G_2(0) | Y_2(j\omega)|^2],$$

and in the case of identical frequency characteristics of the filters, that is, when

$$Y_1(j\omega) = Y_2(j\omega) = Y(j\omega) \text{ and } k_{\phi 1} = k_{\phi 2} = k_\phi,$$

we will have

$$G_{cf}(\omega) \approx \frac{T_i^2}{k^2_\phi U^2_m \tau^2_p} [G_1(0) + G_2(0)] | Y(j\omega)|^2. \qquad (8.6.16)$$

For CCRL with wideners in the decoder, the approximate computation of $G_{cf}(0)$ when $\omega = 0$ can be found using the following formula which follows from expression (8.6.16)

$$G_{cf}(\omega) \approx \frac{\sigma_1^2 + \sigma_2^2}{U^2_m F_i^2 \tau^2_p k^2_\phi \Delta F_{ebw}} | Y(j\omega)|^2, \qquad (8.6.17)$$

where

$$G_1(0) \approx \frac{\sigma_1^2}{\Delta F_{ebw}}; \qquad G_2(0) \approx \frac{\sigma_2^2}{\Delta F_{ebw}};$$

$\Delta F_{ebw} = \frac{1}{2\tau_w}$ is the effective band of fluctuations forming at the W_1 and W_2 output for frequencies $\omega \geq 0$, and σ_1^2 and σ_2^2 are the dispersions of the voltages produced by the wideners W_1 and W_2.

It follows from expression (8.6.17) that it is necessary to find σ_1^2 and σ_2^2. Since it is assumed that the W_1 output signals are "purely" random, the

probability p_{pl} of the widener W_1 forming a pulse with the amplitude U_m will be $p_{pl} = [\bar{M}_1]_c \tau_w$, where $[\bar{M}_1]_c$ is the mean number of pulses appearing at the W_1 output in 1 sec. Then for any fixed time

(see key below) $$\sigma_1^2 = \bar{u}_{p1}^2 - \bar{u}_{p1}^2 = U_m^2 \tau_p [\bar{M}_1]_y (1 - \tau_p [\bar{M}_1]_y).$$

Similarly, we obtain

$$\sigma_2^2 = U_m^2 \tau_p [\bar{M}_2]_y (1 - \tau_p [\bar{M}_2]_y).$$

By substituting the values σ_1^2 and σ_2^2 into expression (8.6.17) we obtain

y = c
$\tau_p = \tau_w$

$$G_{cf}(\omega) = 2|Y(j\omega)|^2 \frac{[\bar{M}_1]_y (1 - [\bar{M}_1]_y \tau_p) + [\bar{M}_2]_y (1 - [\bar{M}_2]_y \tau_p)}{F_i^2 k_F^2}. \quad (8.6.18)$$

If it is sufficient to know $G_{cf}(\omega)$ when $\omega = 0$ (in this case, $Y(j\omega) = k_F$), we will have /438

$$G_{cf}(0) = 2 \frac{[\bar{M}_1]_y (1 - [\bar{M}_1]_y \tau_p) + [\bar{M}_2]_y (1 - [\bar{M}_2]_y \tau_p)}{F_i^2}. \quad (8.6.19)$$

It can be seen from expressions (8.6.18) and (8.6.19) that as a result of computation of $[\bar{M}_1]_c$ and $[\bar{M}_2]_c$ it becomes possible to compute $G_{cf}(\omega)$. Since $[\bar{M}_1]_c$ and $[\bar{M}_2]_c$ increase with an increase of Z, the dependence $G_{cf}(0)$ on $\frac{1}{q_0^2}$ will have the form shown in figure 8.14 (curve 1). However, for a given value ω, the value $G_{cf}(\omega)$ will be the smaller the larger is τ_w.

At the same time, it should be noted that $G_{cf}(\omega)$ in the case of a high level of interference has virtually no dependence on K_a and becomes close to zero for the value $\frac{1}{q_0^2}$ corresponding to the conditions of opening of the CCRL for the mean component of the received commands.

For CCRL without wideners in the decoder, the functions $G_1(\omega)$ and $G_2(\omega)$ can be found in accordance with the method described in reference 81. In this case, each of the voltages formed by the coincidence stages CS_1 and CS_2 must be considered as consisting of two parts. One part of the signal at the output, such as of the coincidence stage CS_1, consists of pulses $u_1(t)$, forming

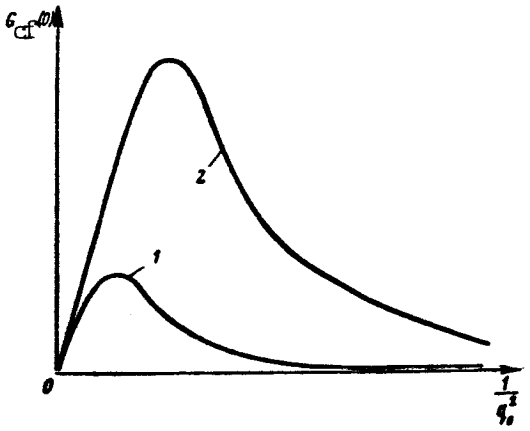

Figure 8.14

as a result of the interaction of interference and the transmitted signals, and the other consists of the signals $u_n(t)$ forming due to the effect of interference alone. The voltage $u_1(t)$ in turn is divided into Q pulse sequences, in each of which the signals have a random amplitude and duration and which on the average appear at the interval T.

It can be shown that in a N_k-channel CCRL without wideners, with n-unit symbols of the first and second kinds, the conditional spectral density $G_{cf}(\omega)$ is

$$G_{cf}(\omega) = 2(1-p_п)^n \left\{ \frac{4}{\tau_и^2 \omega^2 F m} \int_0^{\tau_и} \sin^2 \frac{\omega x}{2} W_{1\tau}(x)\, dx \right.$$

$$\left. - \frac{(1-p_п)^n}{\tau_и^2 \omega^2 F m} |\theta_{1\tau}(\omega)|^2 \left| \int_0^{\tau_и} (1 - e^{-j\omega x}) W_{1\tau}(x)\, dx \right|^2 \right\}$$

$p_П = p_{sup}$

$\tau_И = \tau_p$

$p_К = p_{code}$

/439

$$+ 2n(2N_К n - 1) p_К (1-p_п) \left\{ \frac{4}{F m \tau_и^2 \omega^2} \int_0^{\tau_и} \sin^2 \frac{\omega x}{2} W_\tau(x)\, dx \right.$$

$$\left. - \frac{p_К (1-p_п)^n}{m F \tau_и^2 \omega^2} |\theta_\tau(\omega)|^2 \left| \int_0^{\tau_и} (1 - e^{-j\omega x}) W_\tau(x)\, dx \right|^2 \right\}$$

$$+ 16 Z p_К \frac{1}{m^2 F^2 \tau_и^2 \omega^2} \int_0^{\tau_и} \sin^2 \frac{\omega x}{2} W_\tau(x)\, dx - 8 Z p_К^2 \frac{1}{m^2 F^2 \tau_и^2 \omega^2}$$

$$\times \operatorname{Re} \left\{ \frac{\theta_{\tau*}(\omega)[1 - \theta_\tau(\omega)]^2}{1 - \theta_\mu(\omega)} \right\} \qquad (8.6.20)$$

when $0 \leqslant \omega \leqslant 2\pi\Delta F$.

Here

$W_{1\tau}(x)$ is the probability density for durations of pulses forming at the CS_1 and CS_2 outputs as a result of nonsuppression of the timing codes;

$W_{\tau}(x)$ is the probability density for duration of pulses forming at the CS_1 and CS_2 outputs as a result of interaction of interference and the transmitted signals;

$\theta_{1\nu}(\omega)$ and $\theta_{\nu}(\omega)$ are the characteristic functions for the moments of displacement of the pulses appearing at the CS_1 and CS_2 outputs as a result of nonsuppression of the transmitted codes and due to the interaction of interference with the transmitted signals, relative to their mathematical expectations;

$\theta_{\tau*}(\omega)$, $\theta_{\tau}(\omega)$ and $\theta_{\mu}(\omega)$ are the characteristic functions for the intervals between two successive pulses and also the durations and times of formation of pulses produced at the CS_1 and CS_2 outputs solely due to the effect of interference;

$\Delta F_1 = \Delta F_2 = \Delta F$ are the effective transmission bands of the filters F_1 and F_2.

It follows from expression (8.6.20) that for a fixed frequency ω, the function $G_{cf}(\omega)$, with an increase of Z (when the probabilities p_{code} and p_{sup} begin to increase), increases monotonically beginning from zero, attains a maximum, then decreases and when $Z \to \infty$ tends to zero. This means that, as a result of the effect of high-level interference on the CCRL, the rocket guidance circuit can be opened not only with respect to the mathematical expectation of the received commands $K_n(t)$, but also with respect to the fluctuating components of the signal $K_n(t)$.

It should be noted further that with an increase of N_k, the value $G_{cf}(\omega)$ for the fixed frequency ω increases, whereas the probability p_{sup} for a number n of several units exerts virtually no influence on the value $G_{cf}(\omega)$. Since τ_p usually does not exceed several microseconds, for practical values ΔF it is sufficient to take into account only the frequency $\omega = 0$.

If formula (8.6.20), where the relationship of p_{sup}, p_{code} and Z to q_0^2 is determined for a particular structure of CCRL interference and signals, is used for computing the dependence of $G_{cf}(0)$ on $\frac{1}{q_0^2}$, it is possible to obtain the curve 2 shown in figure 8.14. It can be seen from expression (8.6.20) that, in a CCRL without wideners in the decoder, the spectral density $G_{cf}(0)$ is not dependent on the values of the transmitted commands.

We note, in conclusion, that a single-channel CCRL with pulse-counting modulation, subjected to high-level interference, can be replaced by a /440 statistically equivalent filter with the equation (8.4.28), if identical circuits are used for handling both subcarrier oscillations. This assertion is supported by the fact that $[\bar{K}_n]_c$ changes proportional to K_a, but $G_{cf}(\omega)$ is not dependent or is virtually nondependent on K_a.

8.7. Effect of Low-Level Fluctuating Interference on a CCRL with Pulse-Phase Modulation

The decoder of a CCRL with pulse-phase modulation of pulse subcarriers, constituting timing codes, contains not only coincidence stages, but also usually a threshold apparatus TA. It usually is based on an electronic relay with two stable states of equilibrium (trigger).

If the CCRL is designed for driving spoilers, the windings of an electromagnetic relay are cut into the plate circuits of the trigger tubes or the amplifier connected to it. When the CCRL output signal should be a dc voltage, low-frequency filters are cut into the trigger; the signals from these filters are fed to a subtracting device.

It follows from the above that the output stages and the threshold apparatus in a decoder with pulse-phase modulation is designed much as in CCRL with pulse-width modulation of sinusoidal subcarrier oscillations. Therefore, computation of the conditional constant components and spectral densities for the output command and its coefficient in a CCRL with or without the output filters F_1 and F_2 is possible using formulas (8.3.19), (8.3.20), (8.3.23), (8.3.24), (8.3.42) and (8.3.43). However, in this case, the values $\bar{\tau}_1^2$ and $\bar{\tau}_2^2$ in expressions (8.3.23), (8.3.24), (8.3.42) and (8.3.43) must be replaced by the dispersions $\sigma_{\tau 1}^2$ and $\sigma_{\tau 2}^2$, respectively. The dependence of $\sigma_{\tau 1}^2$, $\sigma_{\tau 2}^2$, $\bar{\tau}_1$ and $\bar{\tau}_2$ on σ_τ can be computed using the formulas cited in section 8.5 and the relationship of σ_τ^2 and q_0^2 is determined by the relation (8.5.21) if n_{tc} in it

is replaced by n_{tp}, where n_{tp} is the total number of pulses fed to the input of a CCRL radio receiver with pulse-phase modulation during the period T of command transmission.

Obviously, as in a CCRL with pulse-width modulation of pulse subcarrier oscillations, in order to eliminate the mathematical expectation of distortion of commands in a CCRL with pulse-phase modulation, it is necessary to have identity of the characteristics of CS_1 and CS_2, F_1 and F_2, and also the parameters of both "arms" of the threshold apparatus. In this case, the conditions are

$$[\Delta \overline{K}_c]_c = 0, \tag{8.7.1}$$

$$[G_{cf}(0)]_c = [G_c(0)]_c = 16 a_1 \frac{\tau_0^3 n_{tp}}{q_0^2 T^2}, \tag{8.7.2}$$

where

$$a_1 = \frac{1}{\sigma_\tau^2} \int_{-\infty}^{\infty} (\tau_1 - \bar{\tau}_1)^2 W(\tau_1)\, d\tau_1.$$

Formula (8.7.2) makes it possible to compute the necessary value q_0, using the admissible value $G_{cf}(0)$ as a point of departure. /441

If the conditional spectral densities at a zero frequency are compared for a CCRL with pulse-phase modulation and a CCRL with pulse-counting modulation during expansion of pulses produced in CS_1 and CS_2 in the decoder of the latter to T_i, for identical values q_0 it is possible to find that

$$\frac{[G_{cf}(0)]_{PPM}}{[G_{cf}(0)]_{PCM}} = \frac{n_{tp}}{n_{tc}}.$$

Here, the subscripts "PPM" and "PCM" apply to the conditional spectral densities of the fluctuations of the command coefficients in single-channel CCRL with pulse-phase and pulse-counting modulation, respectively. It follows from the cited expression that CCRL with pulse-phase modulation are more noise immune than CCRL with pulse-counting modulation.

In actuality, if all the timing codes in single-channel CCRL with pulse-phase and pulse-counting modulation have identical capacities n, then $n_{tp} = 2n$ and $n_{tc} = \frac{T}{T_i} n$. Therefore, taking into account admissible quantization errors, we will have

$$\frac{[G_c(0)]_{PPM}}{[G_c(0)]_{PCM}} = \frac{2T_i}{T} \ll 1.$$

Similar computations can be made when comparing CCRL with pulse-phase and pulse-counting modulation without expanders in the decoder, since formulas (8.7.2) and (8.5.20) show that

$$\frac{[G_{cf}(0)]_{PPM}}{[G_{cf}(0)]_{PCM}} = \frac{4\tau_p^2(\sigma_{\tau c}^2)_{PPM}}{TT_i(\sigma_{\tau c}^2)_{PCM}} = \frac{4\tau_p^2 n_{tp}}{TT_i n_{tc}},$$

where $(\sigma_{\tau c}^2)_{PPM} = (a_1\sigma_\tau^2)_{PPM}$ and $(\sigma_{\tau c}^2)_{PCM}$ are the dispersions of the displacements of the leading edges of the pulses forming at the CS_1 and CS_2 outputs in CCRL with PPM and PCM.

The equation of a statistically equivalent filter for a single-channel CCRL with pulse-phase modulation, when under the influence of low-level interference, will have a form determined by expression (8.3.48).

8.8. Effect of High-Level Interference on CCRL with Pulse-Phase Modulation

The following are possible under the influence of high-level interference in a CCRL designed as shown in figure 7.18:

(1) nonpassage of part or all of the reference and control codes through the coincidence stages CS_1 and CS_2 as a result of suppression of one or a large number of pulses in each of the transmitted codes;

(2) formation of spurious reference and control codes, which we will call "quasi-regular," due to the addition of interference to the transmitted /442 pulses to a code of the corresponding structure;

(3) formation of spurious reference and control codes by interference pulses only.

If the CCRL is multichannel, as a result of the interaction of interference and the signals of other channels, there will also be formation of additional spurious reference and control codes.

The appearance of spurious codes and the suppression of transmitted codes leads to disruption of the rhythm of operation of the trigger Tr and, as a result, during the times T_1 and T_2 there can be a considerable number of "trippings" of the trigger. This means that here high-level interference, as in CCRL with pulse-width modulation, leads to the breakup of pulse signals produced by the trigger Tr in the absence of interference.

Spurious "trippings" of Tr during the formation of codes only by interference can occur at any time, whereas the triggering of Tr by signals forming during the interaction of interference and transmitted pulses occurs near the reference and control codes.

A precise theoretical analysis of the influence of all possible signals produced by the coincidence stages CS_1 nd CS_2 when the CCRL is subjected to interference leads to extraordinarily unwieldy computation formulas. However, an allowance for the specific characteristics of the structure of the codes makes it possible to find relatively simple ways to investigate the noise immunity of CCRL, and the computation relations obtained in this process have sufficient accuracy and can be used without recourse to special computing apparatus.

A distinguishing characteristic of a CCRL of the considered type is that the intervals between successive pulses in timing codes usually do not exceed several microseconds, whereas the minimum duration of a pulse formed by the trigger in the absence of interference is not less than $T_{min} = (0.05\text{-}0.1)T$. As a result of the extremely small timing code base in comparison with T_{min}, the spurious pulses forming during the interaction of interference with transmitted pulses lead only to insignificant fluctuations of the times of "tripping" of Tr. These times can be not more than one code base to the right or left of the last pulse in the code. Then, without introducing a large error, for the single-channel CCRL which will be considered in detail below, it will be assumed that the "tripping" of Tr by quasi-regular signals occurs only at points t_0 and t_{con}, characterizing the times of formation of the last pulses in the reference and control codes. However, in order to take into account the influence of all possible quasi-regular spurious codes, it must be assumed that at points t_0 and t_{con} the "tripping" signals appear with the probabilities $p_{1.1}$ and $p_{2.2}$ of formation of at least one pulse at the CS_1 and CS_2 outputs when subjected to reference and control codes and interference.

It can be shown that, in the case of timing code capacities $n \leq 3\text{-}4$, /443 the values $p_{1.1}$ and $p_{2.2}$ are extremely close to 1, regardless of the interference level. In particular, this can be attributed to the fact that, with an increase of the intensity of interference, there is an increase of both the probability of suppression of a code and the probability of augmentation by interference of each of the transmitted pulses to the corresponding timing code.

The two assumptions introduced here mean that, at points $t_0 = kT$ and $t_{con} = T_1 + kT$, where $k = 0, 1, 2, \ldots$, there will always be tripping of Tr by

the reference and control pulses, respectively, but in the intervals T_1 and T_2, making up the period T, there can be a random effect of the signals on Tr.

Assuming further that the trigger Tr (fig. 7.18) and the threshold apparatus TA_1 (fig. 7.8) produce signals with identical parameters, we conclude that the conditional constant components $[\overline{K}_n]_c$ and $[\overline{\Delta K}]_c$, $[\overline{K}_{cn}]_c$ and $[\overline{\Delta K_c}]_c$, and also the conditional spectral densities $G_f(\omega)$ and $G_f(0)$ of the fluctuations of the output signal $K_n(t)$ in a CCRL with pulse-phase modulation will be determined by formulas (8.3.5)-(8.3.8), (8.3.13) and (8.3.14). Division of $G_f(\omega)$ and $G_f(0)$ by the square of the maximum value of the output command K^2_{max}, obtained in the absence of interference, makes it possible to compute the conditional spectral densities $G_{cf}(\omega)$ and $G_{cf}(0)$ of fluctuations of the command coefficient. If there are no output filters in a CCRL with pulse-phase modulation, which should be the case when it is necessary to connect it to spoilers, the values $[\overline{K}_{cn}]_c$ and $[\overline{\Delta K_c}]_c$ can be computed using formulas (8.3.7) and (8.3.8), and for finding the functions $[G_c(\omega)]_c$ and $[G_c(0)]_c$, it is necessary to use expressions (8.3.13) and (8.3.14), divided by $K^2_{max} = T^2$.

In this case, it must be assumed that the pulses $u_{p1\,n}(t)$ and $u_{p2\,n}(t)$ have a single amplitude, $k_{F1} = k_{F2} = 1$ and $u_1 = u_2 = 0$.

Using the notations $p_1(t)$ and $p_2(t)$ for the probabilities that the trigger Tr, in the intervals T_1 and T_2, produces a voltage equal to $u_1 + U_{m1}$, for the conditional constant components $[\overline{K}_{cn}]_c$ and $[\overline{\Delta K_c}]_c$ in CCRL with the filters F_1 and F_2 we find

$\Phi = F$

$$[\overline{K}_{cn}]_c = \frac{1}{k_{\phi 1}(u_1 + U_{m1}) - k_{\phi 2}u_2}\left\{k_{\phi 1}u_1 - k_{\phi 2}(u_2 + U_{m2}) + \frac{k_{\phi 1}U_{m1} + k_{\phi 2}U_{m2}}{T}\left[\int_0^{T_1} p_1(t)\,dt + \int_{T_1}^{T} p_2(t)\,dt\right]\right\}, \tag{8.8.1}$$

$$[\Delta\overline{K}_c]_c = \frac{1}{k_{\phi 1}(v_1 + U_{m1}) - k_{\phi 2}v_2}\left\{k_{\phi 1}u_1 - k_{\phi 2}(u_2 + U_{m2}) - (k_{\phi 1}u_{p1} - k_{\phi 2}u_{p2}) + \frac{k_{\phi 1}U_{m1} + k_{\phi 2}U_{m2}}{T}\left[\int_0^{T_1} p_1(t)\,dt + \int_{T_1}^{T} p_2(t)\,dt\right]\right\}. \tag{8.8.2}$$

The dependence of the probabilities $p_1(t)$ and $p_2(t)$ on time can be /444 attributed to the fact that the possibility of "tripping" of Tr is determined by its state in the preceding time interval. However, with the assumptions made here the values $p_1(t)$ and $p_2(t)$ are repeated at the interval T. As a result, in the case of a constant or slowly changing intensity of interference, the signal $K_{cn}(t)$ will be almost stationary.

As a result of the periodic character of change of the function $p_1(t)$, during its determination it is sufficient to consider the time interval T_1 only within the limits of the single period T, the beginning of which corresponds to the time t = 0. Then, when $0 \leq t < T_1$, the trigger, constituting an essentially inertialess device, will produce a voltage $u_1 + U_{m1}$, provided that in some time interval t_i-$t_i + dt_i$, where $0 \leq t_i < t$, the trigger is tripped for the last time by a reference pulse, and that in the interval t_i-t not a single control code is formed at the Tr input. Since t_i can fall at any point of the interval 0-t, we obtain a number of mutually exclusive events favoring the formation of the voltage $u_1 + U_{m1}$ by the trigger at the time t. Therefore

$$p_1(t) = \int_0^t p_c(t_i, t)\, W_{ref}(t_i)\, dt_i + p_c(0, t) \qquad \text{when} \qquad 0 \leqslant t < T_1, \tag{3.8.3}$$

where $p_c(t_i, t)$ is the probability that not one control pulse will appear at the CS_2 output in the time t_i-t; $p_c(0, t)$ is the probability of the absence of control pulses at the CS_2 output in the time interval from 0 to t; $W_{ref}(t_i)dt_i$ is the probability that at least one reference pulse appears at the CS_1 output in the time interval t_i-$t_i + dt_i$, "tripping" the trigger.

It is easy to see that

$$W_{ref}(t_i)\, dt_i = [1 - p_1(t_i)]\, W_1(t_i)\, dt_i,$$

where $1 - p_1(t_i)$ is the probability that by the time t_i the trigger is in a position determined by the control pulse; $W_1(t_i)dt_i$ is the conditional probability of appearance of at least one reference pulse in the interval dt_i.

Then

$$p_1(t) = \int_0^t p_c(t_i,\ t)\,[1 - p_1(t_i)]\,W_1(t_i)\,dt_i + p_c(0,\ t)$$

$$\text{when } 0 \leq t < T_1. \tag{8.8.4}$$

Similarly, we obtain the following integral equation for $p_2(t)$ /445

$$p_2(t) = 1 - \left[\int_{T_1}^t p_0(t_i,\ t)\,p_2(t_i)\,W_2(t_i)\,dt_i + p_0(T_1,\ t)\right]$$

$$\text{when } T_1 \leq t < T. \tag{8.8.5}$$

Here

$p_0(t_i, t)$ and $p_0(T_i, t)$ are the probabilities of nonappearance of even one reference pulse in the intervals t_i-t and T_1-t, where $T_i \leq t < T$;

$W_2(t_i)dt_i$ is the conditional probability of the appearance of at least one control pulse in the interval dt_i;

$p_2(t_i)$ is the probability that by the time t_i ($T_1 \leq t_i < T$) the trigger is in a position determined by the control pulse.

The functions $W_1(t_i)$, $W_2(t_i)$, $p_0(T_1, t)$, $p_c(t_i, t)$, $p_0(t_i, t)$ and $p_c(0, t)$ are dependent on the type of effective interference and the structure of the timing codes used.

For example, if the times of appearance of interference pulses at the output of the coincidence stages conform to a Poisson distribution, which in actual practice often can be assumed, then

$$p_c(0,\ t) = e^{-\lambda_2 t},\ p_0(T_1,\ t) = e^{-\lambda_1 (t - T_1)},\ p_c(t_i,\ t) = e^{-\lambda_2 (t - t_i)},$$

$$p_0(t_i,\ t) = e^{-\lambda_1 (t - t_i)},\ W_1(t_i)dt_i = \lambda_1 dt_i,$$

$$W_2(t_i)\,dt_i = \lambda_2 dt_i,$$

where λ_1 and λ_2 are the mean numbers of interference pulses forming at the CS_1 and CS_2 outputs, respectively, in 1 sec.

Under these conditions it can be found that

$$p_1(t) = \frac{\lambda_1}{\lambda_1 + \lambda_2} + \frac{\lambda_2}{\lambda_1 + \lambda_2}\left[e^{-(\lambda_1 + \lambda_2)t}\right] \text{ when } 0 \leqslant t < T_1, \tag{8.8.6}$$

$$p_2(t) = \frac{\lambda_1}{\lambda_1 + \lambda_2}\left[1 - e^{-(\lambda_1 + \lambda_2)(t - T_1)}\right] \text{ when } T_1 \leqslant t < T. \tag{8.8.7}$$

Substituting the determined values $p_1(t)$ and $p_2(t)$ into expression (8.8.1) and multiplying the result by $K_{max} = k_{F1}(u_1 + U_{m1}) - k_{F2}u_2$, for the conditional constant component $[\bar{K}_n]_c$ of the output command $K_n(t)$ we will have

$$[\bar{K}_n]_c = K_{n1} + K_{n2}, \tag{8.8.8}$$

where

Φ = F
Π = n

/446

$$K_{n1} = (k_{\phi 1}U_{m1} + k_{\phi 2}U_{m2})\left(\frac{\lambda_1}{\lambda_1 + \lambda_2} + \frac{\lambda_2 - \lambda_1}{(\lambda_1 + \lambda_2)^2 T}\right) + k_{\phi}u_1 - k_{\phi 2}(u_2 + U_{m2}) \tag{8.8.9}$$

$$K_{n2} = \frac{k_{\phi 1}U_{m1} + k_{\phi 2}U_{m2}}{T}\left\{\frac{\lambda_1}{(\lambda_1 + \lambda_2)^2}\exp\left[-\frac{\lambda_1 + \lambda_2}{2}T \times (1 - K_{Cc})\right] - \frac{\lambda_2}{(\lambda_1 + \lambda_2)^2}\exp\left[-(\lambda_1 + \lambda_2)T\frac{1 + K_{Cc}}{2}\right]\right\} \tag{8.8.10}$$

It can be seen from expression (8.8.9) that K_{n1} is not dependent on the values of the transmitted commands $K_a = \frac{K_C}{k_C} = T\frac{K_{Cc}}{k_C}$ and is a function only of the intensity of interference and the parameters of the transmitted codes and the decoder. However, if the CCRL is balanced, which corresponds to satisfaction of equality $k_{F1}(u_1 + 0.5\,U_{m1}) = k_{F2}(u_2 + 0.5\,U_{m2})$, with use of equistable reference and control codes $\lambda_1 = \lambda_2 = \lambda$, and the constant component K_{n1} becomes equal to zero. When $\lambda_1 \ll \lambda_2$, which determines a case when the reference code is considerably more noise immune than the control code,

$$K_{n1} \approx \frac{k_{\phi 1}U_{m1} + k_{\phi 2}U_{m2}}{\lambda_2 T} + k_{\phi 1}u_1 - k_{\phi 2}(u_2 + U_{m2}). \tag{8.8.11}$$

It therefore follows that with an increase of λ_2, the value K_{n1} will approach the minimum possible value of the voltage $k_{F1}u_1 - k_{F2}(u_2 + U_{m2})$, whereas

$K_{n2} \to 0$. This makes it possible to conclude that it is infeasible to have autonomous synchronization of a CCRL without taking any other measures since, when strong interference is present, the rocket for the most part begins to move along a curve close to a circle, regardless of K_a. If the control code ($\lambda_2 \gg \lambda_1$) is more noise immune, then

$$\begin{matrix}\Phi = F \\ \Pi = n\end{matrix} \qquad K_{n1} \approx (k_{\phi 1} U_{m1} + k_{\phi 2} U_{m2})\left(1 - \frac{1}{\lambda_1 T}\right) + k_{\phi 1} u_1 - k_{\phi 2}(u_2 + U_{m2})$$

and when $\lambda_1 \to \infty$, in most cases, the maximum possible signal, equal to $k_{F1}(u_1 + U_{m1}) - k_{F2} u_2$, will appear at the CCRL output.

Analysis of expression (8.8.10) leads to the following conclusions:

(1) in a general case, the value K_{n2} is not a linear function of the transmitted commands;

(2) when equistable codes ($\lambda_1 = \lambda_2 = \lambda$) are used, the dependence of K_{n2} on $K_a(t)$ will be symmetrical relative to the y-axis;

(3) when $\lambda_2 \to \infty$ and $\lambda_1 \to \infty$, the value K_{n2} tends to zero.

It can be seen from the above that it is desirable to design CCRL with equistable reference and control codes. In such CCRL, when $k_{F1} u_1 = k_{F2} u_2$ and $k_{F1} U_{m1} = k_{F2} U_{m2} = k_F U_m$, /447

$$[\overline{K}_c]_c = K_{n2} = \frac{k_\phi U_m}{2\lambda T}\{\exp[-\lambda T(1 - K_{Cc})] - \exp[-\lambda T(1 + K_{Cc})]\}. \qquad (8.8.12)$$

Expression (8.8.12) shows that CCRL with pulse-phase modulation, when acted upon by high-level interference, are transformed into a nonlinear link whose amplification properties decrease with an increase of λ. At the limit, $[\overline{K}_n]_c$ becomes equal to zero, which is equivalent to the effect of opening the rocket guidance circuit. Under conditions when $\lambda_1 = \lambda_2 = \lambda$, the control surfaces of the rocket in most cases are set in a neutral position. If $\lambda_1 \neq \lambda_2$, the opening of the guidance circuit occurs in such a way that the control surfaces of the rocket, in most cases, will be in one of the extreme positions. If the transfer constant for a CCRL under the influence of interference is determined by the value of the derivative $\frac{dK_{nc}}{dK_a}$ when $K_a = 0$, on the basis of

expression (8.8.12), after replacement of K_{Cc} by $\frac{k_C K_a}{T}$, for the mathematical expectation $(k_{CCRL})_n$ of this coefficient we obtain

$$(k_{CCRL})_n = k_{CCRL} e^{-\lambda T}, \tag{8.8.12a}$$

where

$$k_{CCRL} = \frac{k_F U_m k_C}{T}.$$

In those cases when $\lambda T(1 + |K_{Cc}|) \leq 0.1\text{-}0.2$, expression (8.8.12) can be reduced to the following form

$$[\bar{K}_n]_c = k_F U_m (1 - \lambda T) K_{Cc}. \tag{8.8.13}$$

On the basis of relations (8.8.12) and (8.8.13), it is possible to derive the following formulas which make it possible to compute $[\bar{K}_{cn}]_c$ and $[\overline{\Delta K_c}]_c$

кп = cn
y = c
к = c
кш = Cc

$$[\bar{K}_{кп}]_y = \frac{1}{2\lambda T}\{\exp[-\lambda T(1 - K_{кш})] - \exp[-\lambda T(1 + K_{кш})]\}, \tag{8.8.14}$$

$$[\Delta\bar{K}_к]_y = \frac{1}{2\lambda T}\{\exp[-\lambda T(1 - K_{кш})] - \exp[-\lambda T(1 + K_{кш})]\} - K_{кш} \tag{8.8.15}$$

for any value λ (if $\lambda_1 = \lambda_2 = \lambda$).

When $\lambda T(1 + |K_{Cc}|) \leq 0.1\text{-}0.2$,

$$[\bar{K}_{кп}]_y = (1 - \lambda T) K_{кш}, \tag{8.8.16}$$

$$[\Delta\bar{K}_к]_y = -\lambda T K_{кш}. \tag{8.8.17}$$

Figure 8.15 shows the dependence of $[\bar{K}_{cn}]_c$ on λT and K_{Cc} when /448 $K_{Cc} = 0.2$, 0.5 and 0.8. The values λT as functions of q_0^2 can be determined if the statistical characteristics of the effective interference and structure of the reference and control codes are known. However, in all cases, λT increases with an increase of the intensity of interference.

The functional relationship between $[\bar{K}_{cn}]_c$ and K_{Cc} for different values λT is shown in figure 8.16 and the function $\frac{(k_{CCRL})_n}{k_{CCRL}} = f(\lambda T)$ for CCRL in which

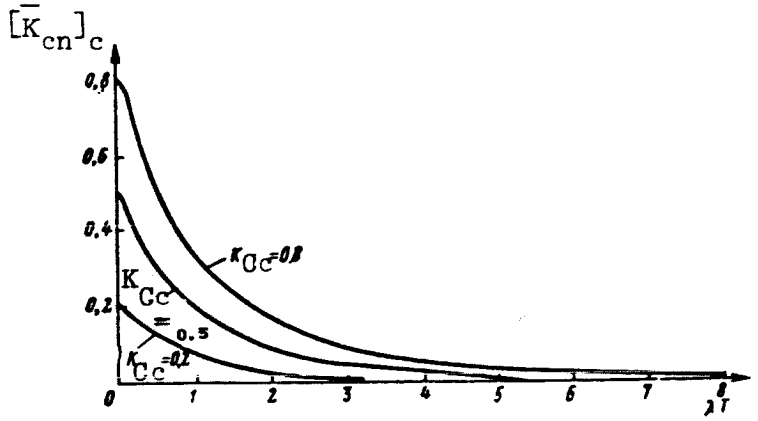

Figure 8.15

$\lambda_1 = \lambda_2 = \lambda$, in figure 8.17 (curve 1). The curves in figure 8.18 illustrate the change of $[\bar{K}_{cn}]_c$ for CCRL with autonomous synchronization when $\lambda_1 = 0$. These curves were constructed on the basis of expression (8.8.8) under the condition that $k_{F1}u_1 = k_{F2}u_2$ and $k_{F1}U_{m1} = k_{F2}U_{m2} = k_F U_m$. The ratio $\frac{(k_{CCRL})_n}{k_{CCRL}}$ in such a radio link changes as shown in figure 8.17 (curve 2).

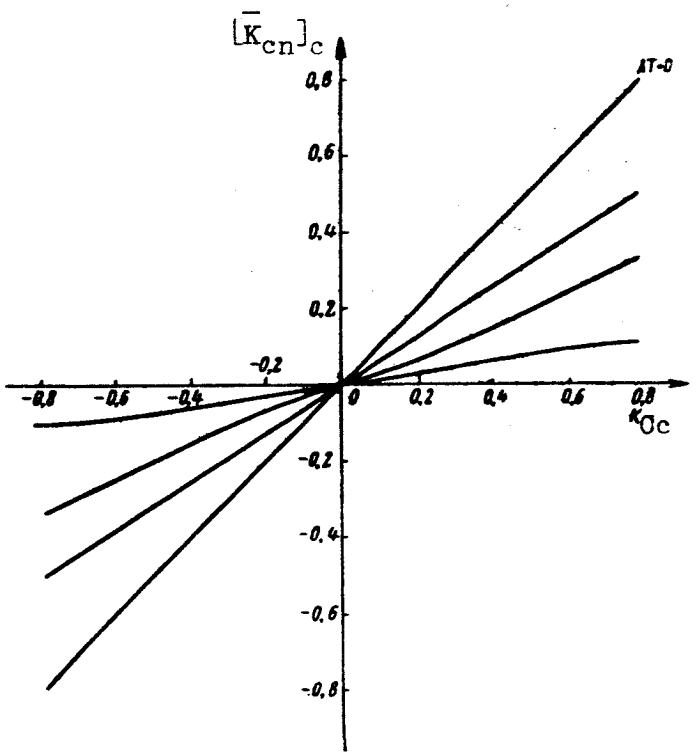

Figure 8.16

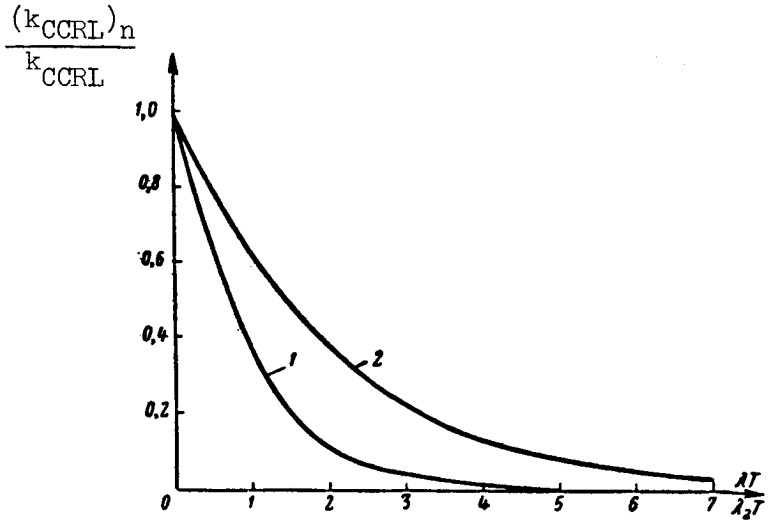

Figure 8.17

Consideration of the problem of the influence of high-level interference on multichannel CCRL with arrangement of channels in series leads to the conclusion that such CCRL, even when equistable reference and control codes are used, at the limit result in the opening of the guidance circuit in such a way that the control surfaces of the rocket will not be in a neutral position. The worst conditions for operation will be in those channels whose control codes move in small intervals at the beginning and end of the period T of transmission of commands. This can be attributed to the fact that the conditional constant component $[\overline{K}_{nj}]_c$ of the output command $K_{nj}(t)$ in the j-th channel differs from zero due to the dc voltage source, ensuring balancing of the j-th channel in the absence of interference.

In a multichannel CCRL with arrangement of channels in parallel, the /450 change of the conditional constant component of the output signal in the j-th channel ($j = 1, 2, \ldots, N_k$) on $\frac{1}{q_0^2}$ occurs qualitatively in the same way as in a single-channel CCRL. However, with an increase of N_k the opening of the guidance circuit sets in with decreasing values $\frac{1}{q_0^2}$.

In order to determine the conditional spectral density $G_f(\omega)$ or $G_f(0)$, it is first desirable to find the functions $R_{p1}(\tau)$, $R_{p2}(\tau)$, $R_{p1.2}(\tau)$ and $R_{p2.1}(\tau)$, being the result of time-averaging of the conditional correlation and reciprocal correlation functions for the voltages $u_{p1\ n}(t)$ and $u_{p2\ n}(t)$.

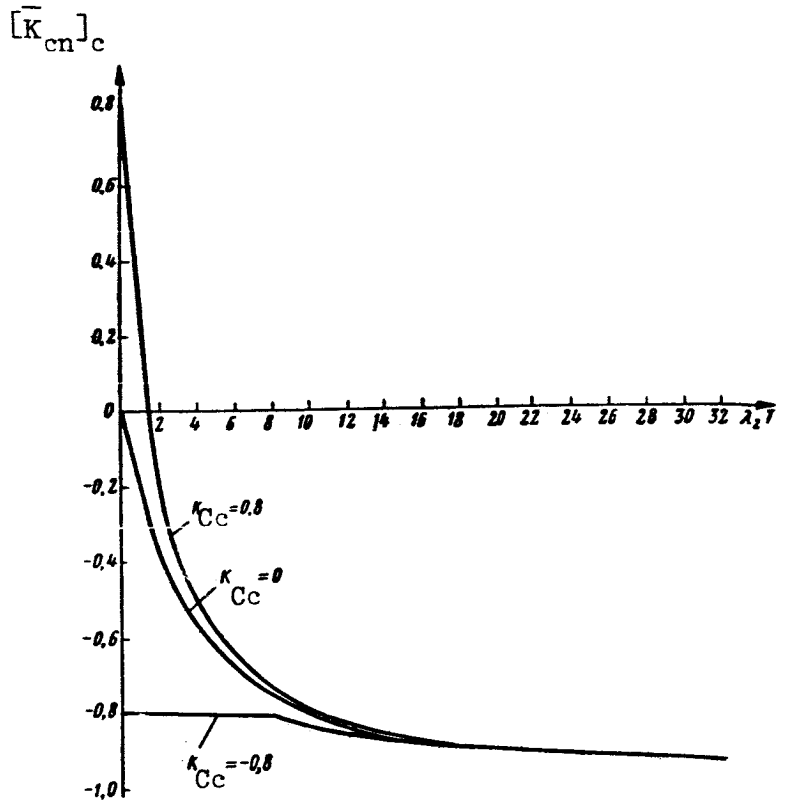

Figure 8.18

When determining $R_{p1}(\tau)$, $R_{p2}(\tau)$, $R_{p1.2}(\tau)$ and $R_{p2.1}(\tau)$, we will assume that the CCRL is single-channel.

In accordance to the definition we have

$$\begin{matrix} \text{п} = \text{n} \\ \text{y} = \text{c} \end{matrix} \qquad R_{p1}(\tau) = \left[\overbrace{\{u_{p1n}(t) - [\overline{u_{p1n}(t)}]_y\}\{u_{p1n}(t+\tau) - [\overline{u_{p1n}(t+\tau)}]_y\}}\right]_y.$$

Here the wavy line denotes time-averaging. /451

With the earlier made assumptions on the probabilities p_1 and p_2, the voltages $u_{pl\ n}(t)$ and $u_{p2\ n}(t)$ will be correlated only in the limits of one period T, whose components are $o \leq t < T_1$ and $T_1 \leq t < T$ should be considered separately.

In the time intervals $0 \leq t < T_1$, the function $u_{pl\ n}(t)$ assumes values $u_1 + U_{ml}$ or u_1 with the probabilities $p_1(t)$ and $1 - p_1(t)$.

Therefore the difference $u_{pl\ n}(t) - \overline{[u_{pl\ n}(t)]}_c$ can be $U_{ml}[1 - p_1(t)]$ or $-U_{ml}p_1(t)$, and the value $u_{pl\ n}(t + \tau) - [u_{pl\ n}(t + \tau)]_c$ can be equal to $U_{ml}[1 - p_1(t + \tau)]$ or $-U_{ml}p_1(t + \tau)$. Then for the product $x = [\{u_{pl\ n}(t) - \overline{[u_{pl\ n}(t)]}_c\}\{u_{pl\ n}(t + \tau) - \overline{[u_{pl\ n}(t + \tau)]}_c\}]_c$, we obtain the following complete set of possible values x_1, x_2, x_3 and x_4

$$x_1 = U_{ml}^2[1 - p_1(t)][1 - p_1(t + \tau)], \quad x_2 = -U_{ml}^2[1 - p_1(t)]p_1(t + \tau),$$
$$x_3 = -U_{ml}^2 p_1(t)[1 - p_1(t + \tau)], \quad x_4 = U_{ml}^2 p_1(t)p_1(t + \tau).$$

Denoting the probabilities of formation of these values through p_{x1}, p_{x2}, p_{x3} and p_{x4}, we obtain

$$R_1(t, \tau) = x_1 p_{x1} + x_2 p_{x2} + x_3 p_{x3} + x_4 p_{x4} \text{ when } 0 \leqslant t < T_1 - \tau, \quad 0 \leqslant \tau < T_1,$$

where $R_1(t, \tau)$ is the nontime-averaged conditional correlation function of the voltage $u_{pl\ n}(t)$ when $0 \leq t < T_1$.

However,

$$p_{x1} = p_1(t)p_{1y}(t + \tau), \quad p_{x2} = p_1(t)[1 - p_{1y}(t + \tau)],$$
$$p_{x3} = [1 - p_1(t)]p_{2y}(t + \tau)$$

and

$$p_{x4} = [1 - p_1(t)][1 - p_{2y}(t + \tau)],$$

where $p_{1y}(t + \tau)$ is the probability that at the time $t + \tau$ the voltage $u_{pl\ n}(t + \tau) = u_1 + U_{ml}$, if at the point t it is equal to this same value; $p_{2y}(t + \tau)$ is the probability of satisfaction of the equality $u_{pl\ n}(t + \tau) = u_1 + U_{ml}$ under the condition that $u_{pl\ n}(t) = u_1$.

In turn, $p_{1y}(t + \tau)$ and $p_{2y}(t + \tau)$ are equal to the values $p_1(t)$ and $p_2(t)$ when $t = \tau$. Therefore

$$R_1(t, \tau) = U_{ml}^2 p_1(t)[1 - p_1(t)][p_1(\tau) - p_2(\tau)]$$

$$\text{when } 0 \leq t < T_1 - \tau \text{ and } 0 \leq \tau < T_1. \tag{8.8.18}$$

Similarly, for the second part of the period we obtain

$$R_2(t, \tau) = U_{m1}^2 p_2(t)[1 - p_2(t)][p_1(\tau) - p_2(\tau)]$$

when $T_1 \leq t < T - \tau$, $0 \leq \tau < T_2$.

Then, taking into account that the function $R_{p1}(\tau)$ is even for a case when $T_1 > T_2$, we obtain

$$R_{p1}(\tau) = \frac{1}{T} U_{m1}^2 [p_1(\tau) - p_2(\tau)] \left\{ \int_0^{T_1 - |\tau|} p_1(t)[1 - p_1(t)]\, dt + \int_{T_1}^{T - |\tau|} p_2(t)[1 - p_2(t)]\, dt \right\}$$

when $0 \leq \tau < T_1$ and $T_1 < \tau \leq 0$:

$$R_{p1}(\tau) = \frac{1}{T} U_{m1}^2 [p_1(\tau) - p_2(\tau)] \int_{T_1}^{T - |\tau|} p_2(t)[1 - p_2(t)]\, dt$$

when $T_1 \leq \tau < T_2$ and $-T_2 < \tau \leq T_1$;

$$R_{p1}(\tau) = 0$$ /452

when $\tau > T_2$ and $\tau < -T_2$.

When $T_1 < T_2$,

$$R_{p1}(\tau) = \frac{1}{T} U_{m1}^2 [p_1(\tau) - p_2(\tau)] \left\{ \int_0^{T - |\tau|} p_1(t)[1 - p_1(t)]\, dt + \int_{T_1}^{T - |\tau|} p_2(t)[1 - p_2(t)]\, dt \right\}$$

when $0 \leq \tau < T_2$ and $-T_2 < \tau \leq 0$:

$$R_{p1}(\tau) = \frac{1}{T} U_{m1}^2 [p_1(\tau) - p_2(\tau)] \int_0^{T_1 - |\tau|} p_1(t)[1 - p_1(t)]\, dt$$

when $T_2 \leq \tau < T_1$ and $-T_1 < \tau \leq -T_2$;

$$R_{p1}(\tau) = 0$$

when $\tau > T_1$ and $\tau < -T_1$.

Thus, in the same way we find that

$$R_{p2}(\tau) = \frac{U_{m2}^2}{U_{m1}^2} R_{p1}(\tau), \quad R_{p1.2}(\tau) = R_{p2.1}(\tau) = -\frac{U_{m2}}{U_{m1}} R_{p1}(\tau).$$

Applying the Fourier transform to the functions $R_{p1}(\tau)$, $R_{p2}(\tau)$, $R_{p1.2}(\tau)$ and $R_{p2.1}(\tau)$, we find $S_{p1}(\omega)$, $S_{p2}(\omega)$, $S_{p1.2}(\omega)$ and $S_{p2.1}(\omega)$. Then, on the basis of expression (8.3.13) we obtain

$$G_f(\omega) = \frac{4}{T}\{U_{m1}^2 |Y_1(j\omega)|^2 + U_{m2}^2 |Y_2(j\omega)|^2 + U_{m1}U_{m2}[Y_1^*(j\omega)Y_2(j\omega) + Y_2^*(j\omega)Y_1(j\omega)]\} \times \left\{\int_0^{T_1}[p_1(\tau) - p_2(\tau)]\cos\omega\tau d\tau \int_0^{T_1-\tau} p_1(t)[1-p_1(t)]\,dt + \int_0^{T_2}[p_1(\tau) - p_2(\tau)\,d\tau\cos\omega\tau d\tau \int_{T_1}^{T-\tau} p_2(t) \times [1-p_2(t)]\,dt\right\} \text{ when } 0 \le \omega \le \infty. \quad (8.8.19)$$

If $p_1(t)$ and $p_2(t)$ are determined by formulas (8.8.6) and (8.8.7), then

$$G_f(0) = G_{f1}(0) + G_{f2}(0). \quad (8.8.20)$$

where

$$G_{f1}(0) = \frac{2(k_{\phi1}U_{m1} + k_{\phi2}U_{m2})^2}{T(\lambda_1+\lambda_2)^3}\left(2\lambda_1\lambda_2 T + \frac{\lambda_1^2 + \lambda_2^2 - 8\lambda_1\lambda_2}{\lambda_1+\lambda_2}\right); \quad (8.8.21)$$

Ф = F
КШ = Cc

$$G_{f2}(0) = \frac{2(k_{\phi1}U_{m1} + k_{\phi2}U_{m2})^2}{T(\lambda_1+\lambda_2)^3} \times \left\{\frac{\lambda_1^2\left[1 - e^{-(\lambda_1+\lambda_2)T(1-K_{кш})}\right] + \lambda_2^2\left[1 - e^{-(\lambda_1+\lambda_2)T(1+K_{кш})}\right]}{\lambda_1+\lambda_2}\right. \quad /453$$

$$+ \frac{4\lambda_1\lambda_2\left[e^{-\frac{\lambda_1+\lambda_2}{2}T(1+K_{кш})} + e^{-\frac{\lambda_1+\lambda_2}{2}T(1-K_{кш})} - 2\right]}{\lambda_1+\lambda_2}$$

$$\left. - \lambda_2(\lambda_2-\lambda_1)T(1+K_{кш})e^{-\frac{\lambda_1+\lambda_2}{2}T(1+K_{кш})} - \right.$$

$$\left. - \lambda_1(\lambda_1-\lambda_2)(1-K_{кш})e^{-\frac{\lambda_1+\lambda_2}{2}T(1-K_{кш})}\right\}. \quad (8.8.22)$$

(Note: This key applies also to the following equations in this section.)

The component $G_{f1}(0)$ is not dependent on the transmitted command and is only a function of λ_1, λ_2, T, k_{F1}, k_{F2}, U_{m1} and U_{m2}. The function $G_{f1}(0)$ first increases with an increase of λ_1 and λ_2, attains a maximum and then begins to decrease, and at the limit when $\lambda_1 \to \infty$ and $\lambda_2 \to \infty$ it becomes equal to zero.

The component $G_{f2}(0)$ is dependent not only on the intensity of interference, but also on the values of the transmitted command. The character of its change with an increase of λ_1 and λ_2 is qualitatively the same as for $G_{f1}(0)$.

If the CCRL uses equistable codes and $k_{F1}U_{m1} = k_{F2}U_{m2} = k_F U_m$, then

$$G_f(0) = \frac{U_m^2 k_\phi^2}{2T\lambda^2}\left[4\lambda T - 6 - e^{-2\lambda T(1+K_{km})} - e^{-2\lambda T(1-K_{km})} + 4e^{-\lambda T(1+K_{km})} + 4e^{-\lambda T(1-K_{km})}\right]. \quad (8.8.23)$$

When $2\lambda T(1 + |K_{Cc}|) \leq 0.1\text{-}0.2$, this expression is reduced approximately to the following form

$$G_f(0) = \frac{2}{3} U_m^2 k_\phi^2 \lambda T^2 (1 + 3K_{km}^2). \quad (8.8.24)$$

The presence of the term $2U_m^2 k_F^2 \lambda T^2 K_{Cc}^2$ in (8.8.24) indicates that a linearized and balanced CCRL with pulse-phase modulation, based on the use of equistable codes, can be replaced by a statistically equivalent filter with the equation

$$K_{ne}(t) = \xi_1(t) K_a(t) + \Delta K(t),$$

where $\xi_1(t)$ and $\Delta K(t)$ are random functions of time, not related to one another.

The mathematical expectation $\overline{\Delta K}(t)$ of the function $\Delta K(t)$ is zero, but $\overline{\xi_1(t)} = (k_{CCRL})_n = (1 - \lambda T)k_{CCRL}$. The spectral densities of the random functions $\Delta K(t)$ and $\xi_1(t)$ at the frequency $\omega = 0$ are $\frac{2}{3}\lambda T^2 k_F^2 U_m^2$ and $2k_{CCRL}^2 \lambda T^2$, respectively.

Since when $k_{F1}U_{m1} = k_{F2}U_{m2} = k_F U_m$ the maximum command is $K_{max} = k_F U_m$, then

$$G_{cf}(0) = \frac{1}{2T\lambda^2}\left[4\lambda T - 6 - e^{-2\lambda T(1+K_{km})} - e^{-2\lambda T(1-K_{km})} + 4e^{-\lambda T(1+K_{km})} + 4e^{-\lambda T(1-K_{km})}\right]. \quad (8.8.25)$$

We recall that this expression is correct for CCRL, regardless of whether they have output filters. /454

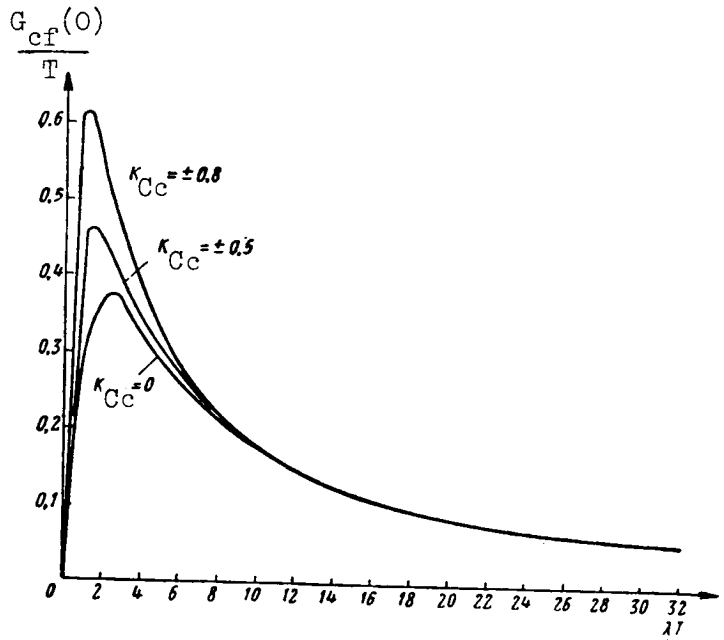

Figure 8.19

Figures 8.19 and 8.20 show curves characterizing the dependence of $\frac{G_{cf}(0)}{T}$ on λT and K_{Cc} for cases when random pulse interference is fed to the input of a decoder of a single-channel CCRL and $\lambda_1 = \lambda_2 = \lambda$.

Here it should be noted that, all other conditions being equal, the opening of the rocket guidance channel for the fluctuating component of the received command sets in at larger values $\frac{1}{q_0^2}$ than for the mathematical expectation of the received commands.

If the CCRL has autonomous synchronization, with the opening of the circuit for the mathematical expectation of the received commands, the random components of the CCRL output signals also become virtually equal to zero.

In a multichannel CCRL with successive (in series) arrangement of channels, in the case of identical intensity of interference, the fluctuations of the output signals are greater than in a single-channel CCRL if, in both types of CCRL, the transfer constants are identical. However, the breaking of the guidance circuit for the fluctuating component sets in at a lesser value $\frac{1}{q_0^2}$ in a multichannel CCRL. The influence of any of the adjacent channels increases with an increase of the interval between the control codes. /455

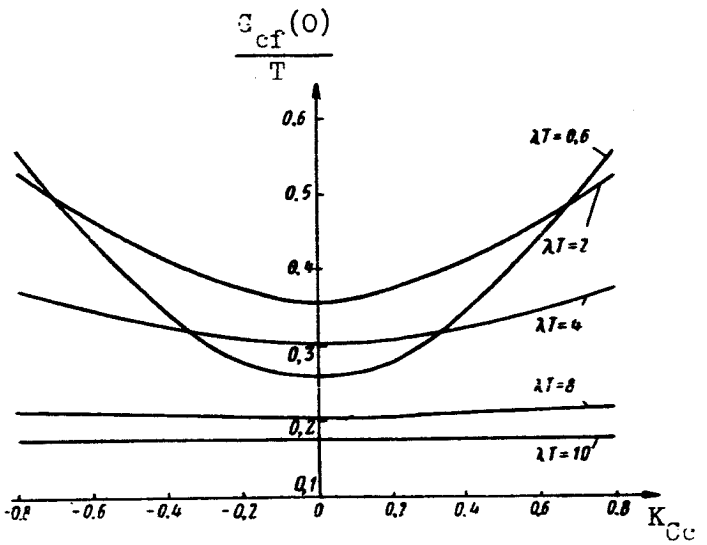

Figure 8.20

In a multichannel CCRL with parallel (in-parallel) arrangement of channels, the value $G_f(0)$ for the j-th channel, all other conditions being equal, also is determined by the separation of the control codes of all the other channels. However, as a result of the possibility of fitting the control code of the j-th channel into specified intervals of time within the entire period T, the fluctuations in a CCRL of the latter type can be more intense. At the same time, in the case of identical values of the commands transmitted in all channels, CCRL with parallel arrangement of channels are less "noisy." This is due to the relative closeness of arrangement of all the control codes under the mentioned condition.

We note, in conclusion, that when multichannel CCRL with either in-series or in-parallel arrangement of channels are subjected to interference, they are transformed from linear into nonlinear converters with random parameters.

8.9. Influence of Fluctuating Low-Level Interference on CCRL with Pulse-Code Modulation

1. Qualitative Characteristics of Effect of Interference

The output signal of the summer of a binary scaler is current pulses $i_{sc}(t)$ or voltage $u_{sc}(t)$. Assuming, as before, that the CCRL output command is a voltage, the pulses $u_{sc}(t)$ for a CCRL based on the use of one sign-constant or sign-variable sequence of numbers can be represented as shown in figure 8.21.

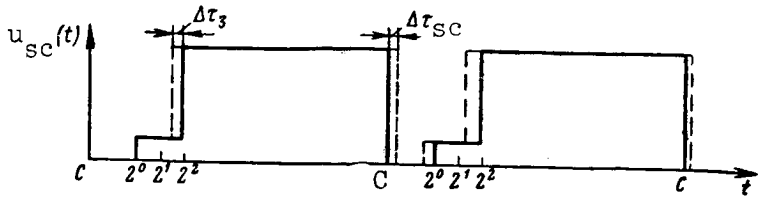

Figure 8.21

The voltage $u_{sc}(t)$ shown in figure 8.21 by solid lines is obtained /456 under the condition that the transmitted command is converted in the coder into number 5 and the binary code is three-unit. The points C, 2^0, 2^1 and 2^2 in figure 8.21 correspond to the times of appearance of synchronizing pulses and pulses of the binary code expressing the digits 2^0, 2^1 and 2^2.

When there is low-level interference, there is a fluctuation of the times of formation of the binary code pulses and the synchronizing pulses produced by the coincidence stage. As a result, the triggers in the binary scalers will be tripped irregularly, thereby causing random changes of the durations of the $u_{sc}(t)$ pulses.

The dashed lines in figure 8.21 denote the possible deviations $\Delta\tau_1 = 0$ and $\Delta\tau_3 \neq 0$ of the leading edges of the pulses from the points 2^0 and 2^2. In addition, figure 8.21 shows the displacement $\Delta\tau_{sc}$ of the time of the ending of the pulse $u_{sc}(t)$ due to fluctuations of the position of the leading edge of the synchronizing pulse.

Despite the small values of the fluctuations of the leading edges of the $u_{sc}(t)$ pulses, an evaluation of the distortions of the received commands when there is weak interference is necessary to confirm that, in the absence of suppression of transmitted pulses and the formation of spurious signals by interference, the distortions of the received commands will not exceed the admissible values and, in case of necessity, to determine more precisely the required strength of the radio transmitter and the sensitivity of the CCRL radio receiver.

As a result of change of the parameters of the voltage $u_{sc}(t)$ by interference, the output commands $K_n(t)$ for a CCRL with one sign-constant, one sign-variable and two sequences of numbers will be equal to

$$K_{\text{п}}(t) = u_{\text{п1}}(t) - u_{\text{mean}}, \tag{8.9.1}$$

п = n

$$K_{\text{п}}(t) = a u_{\text{п1}}(t) + (a-1)\, u_{\text{п2}}(t), \tag{8.9.2}$$

$$K_{\text{п}}(t) = u_{\text{п1}}(t) - u_{\text{п2}}(t), \tag{8.9.3}$$

where $u_{n1}(t)$ and $u_{n2}(t)$ are the voltages produced by the CCRL output filters, with the influence of interference taken into account.

Expressions (8.9.1)-(8.9.3) make it possible to find the output signals for different kinds of single-channel CCRL with pulse-code modulation under the condition that they are designed for connection to continuous-action control surface apparatus. In those cases when spoilers must be operated, there must be apparatus for conversion of voltages into pulses with constant amplitude and repetition interval T. The duration of these pulses should change proportional to the converted voltage. /457

If the CCRL is multichannel, in the case when there is low-level interference, there are no additional distortions of the received signals in the considered channel.

2. Conditional Constant Components of Output Signals and Their Distortions

First, we will consider a CCRL with one sign-constant sequence of numbers. In accordance with expression (8.9.1) and taking into account that the summer of the binary scaler produces the voltage $u_{sc}(t)$ shown in figure 8.21, we will have

$$[\overline{K}_{\text{п}}]_{\text{у}} = k_{\phi 1} U_1 \sum_{l=1}^{N} 2^{l-1} \delta_l(i) \frac{[\overline{\tau}_{1.l}]_{\text{у}}}{T} - u_{\text{ср}}, \tag{8.9.4}$$

п = n
ср = mean
у = c
ф = F
кп = cn
к = c
кру = CCRL
с = sc
ку = ic
(subscripts)

$$[\Delta\overline{K}]_{\text{у}} = [\overline{K}_{\text{п}}]_{\text{у}} - K = k_{\phi 1} U_1 \left[\sum_{l=1}^{N} 2^{l-1} \delta_l(i) \frac{[\overline{\tau}_{1.l}]_{\text{у}}}{T} - \sum_{l=1}^{N} 2^{l-1} \delta_l(i) \frac{T_{1.l}}{T} \right], \tag{8.9.5}$$

$$[\overline{K}_{\text{кп}}]_{\text{у}} = \frac{k_{\phi 1} U_1 \sum_{l=1}^{N} 2^{l-1} \delta_l(i) \frac{[\overline{\tau}_{1.l}]_{\text{у}}}{T} - u_{\text{ср}}}{k_{\phi 1} U_1 \sum_{l=1}^{N} 2^{l-1} \frac{T_{1.l}}{T} - u_{\text{ср}}}, \tag{8.9.6}$$

$$[\Delta\overline{K}_{\text{к}}]_{\text{у}} = \frac{k_{\phi 1} U_1 \left[\sum_{l=1}^{N} 2^{l-1} \delta_l(i) \frac{[\overline{\tau}_{1.l}]_{\text{у}}}{T} - \sum_{l=1}^{N} 2^{l-1} \delta_l(i) \frac{T_{1.l}}{T} \right]}{k_{\phi 1} U_1 \sum_{l=1}^{N} 2^{l-1} \frac{T_{1.l}}{T} - u_{\text{ср}}} \tag{8.9.7}$$

In these expressions, $T_{1.i}$ and $\tau_{1.i}$ ($i = 1, 2, \ldots, N$) are the durations of the pulses produced by the i-th unit of the binary scaler under the influence of pulses of a binary code characterizing the digit 2^{i-1} in the absence and in the presence of interference, respectively; U_1 is the amplitude of the voltage pulse forming at the output of the summer of a binary scaler when signals /458 expressing the number 1 are fed to the decoder.

Since

$$\tau_{1.i} = T_{1.i} + \Delta\tau_i + \Delta\tau_c,$$

where $\Delta\tau_i$ ($i = 1, 2, \ldots, N$) is the displacement of the leading edge of the pulse $u_{sc}(t)$ due to fluctuations of the leading edge of a pulse expressing the digit 2^{i-1} in a binary code; then

$$[\bar{\tau}_{1.i}]_y = T_{1.i} + \Delta\bar{\tau}_i + \Delta\bar{\tau}_c.$$

(Note: See key accompanying equations (8.9.4)-(8.9.7) which also applies to following equations through (8.9.14).)

In the preceding chapter, we noted that it is necessary to select small intervals between successive pulses in a binary code so that the amplitude characteristic of the CCRL will be linear. If this requirement is satisfied, it can be assumed that with a sufficiently high degree of accuracy $T_{1.i} \approx T$. In addition, in a balanced CCRL, the voltage $u_{mean} = k_{Fl} U_1 2^{N-1} \frac{T_{1.N}}{N}$, and with the use in the binary code of pulses with the identical parameters $\Delta\bar{\tau}_1 = \Delta\bar{\tau}_2 = \ldots = \Delta\bar{\tau}_N$. Then for $[\bar{K}_n]_c$ and $[\bar{K}_{cn}]_c$ we will have

$$[\bar{K}_n]_y = k_{кру}\left(1 + \frac{\Delta\bar{\tau}_1 + \Delta\bar{\tau}_c}{T}\right) K_a + 2^{N-1} k_{\phi 1} U_1 \frac{\Delta\bar{\tau}_1 + \Delta\bar{\tau}_c}{T}, \tag{8.9.8}$$

$$[\bar{K}_{кп}]_y = K_{ку}\left(1 + \frac{\Delta\bar{\tau}_1 + \Delta\bar{\tau}_c}{T}\right) + \frac{2^{N-1}}{2^{N-1} - 1} \frac{\Delta\bar{\tau}_1 + \Delta\bar{\tau}_c}{T}. \tag{8.9.9}$$

In expression (8.9.8)

$$(k_{кру})_п = k_{кру}\left(1 + \frac{\Delta\bar{\tau}_1 + \Delta\tau_c}{T}\right) \tag{8.9.10}$$

characterizes the mean transfer constant for the CCRL when it is subjected to interference and $2^{N-1} k_{Fl} U_1 \frac{\Delta\bar{\tau}_1 + \Delta\bar{\tau}_{sc}}{T}$ is the constant component of some additive noise leading to displacement of the zero of the CCRL amplitude characteristic.

The results show that in a general case, under the influence of low-level interference, there will be a change of the transfer constant and a constant component of error will appear. In order to eliminate the mentioned phenomena, it is necessary to ensure satisfaction of the equality $\Delta\bar{\tau}_1 = -\Delta\bar{\tau}_{sc}$. These same results will be obtained when $\Delta\bar{\tau}_1 = \Delta\bar{\tau}_{sc} = 0$. In order for $\Delta\bar{\tau}_1 = -\Delta\bar{\tau}_{sc}$, it is necessary to select identical parameters of the key code and the binary code signals, and as a result the triggering and completion of the operation of any i-th unit of the binary scaler, in most cases, will occur with an identical lag or lead relative to the times of its triggering in the absence of interference. For example, for this purpose it is possible to use equi-/459 stable timing codes for formation of the key and the digits of the binary code or memory devices can be used in the decoder, cut into the output stages of the CCRL after transient processes are ended during the reception of the binary code.

If the CCRL is designed as shown in figure 7.32, in formulas (8.9.9) and (8.9.10), the displacement is $\Delta\bar{\tau}_1 = 0$ and $\Delta\bar{\tau}_{sc} \neq 0$. As a result, in a CCRL of such a type in all cases $[\bar{K}_n]_c \neq K$. It should be remembered that the maximum distortions will occur when transmitting the maximum command.

The values $\Delta\bar{\tau}_1$ and $\Delta\bar{\tau}_{sc}$, in the case when they are not equal to zero, can be computed as a function of q_0 in accordance with the method described in section 8.5.

If a balanced CCRL with a single sign-variable sequence of numbers is considered in the same way, in the case of identical binary circuits we obtain the following formulas determining $[\bar{K}_n]_c$ and $[\bar{K}_{cn}]_c$

$$[\bar{K}_n]_y = ak_{xpy}\left(1+\frac{\Delta\bar{\tau}_1+\Delta\bar{\tau}_c}{T}\right)K_a + \\ +(a-1)\left(1+\frac{\Delta\bar{\tau}_1+\Delta\bar{\tau}_{c1}}{T}\right)k_{xpy}K_a. \qquad (8.9.11)$$

$$[\bar{K}_{xn}]_y = a\left(1+\frac{\Delta\bar{\tau}_1+\Delta\bar{\tau}_c}{T}\right)K_{xy} + \\ +(a-1)\left(1+\frac{\Delta\bar{\tau}_1+\Delta\bar{\tau}_{c1}}{T}\right)K_{xy}, \qquad (8.9.12)$$

(key p. 515)

where $\Delta\bar{\tau}_{sc\,1}$ is the mathematical expectation for displacement of the leading edge of the synchronizing pulse characterizing negative commands.

It can be seen from expressions (8.9.11) and (8.9.12) that, in the considered CCRL, low-level interference leads only to a change of the mean value of the transfer constant. However, with the formation of pulses of different duration by the i-th units of both binary scalers, there will be an asymmetry of the CCRL amplitude characteristic during the transmission of positive and negative commands. If we compare CCRL based on one sign-constant and one sign-variable sequence of numbers, it can be concluded that the use of a sign-variable sequence of numbers is more desirable if $\Delta\bar{\tau}_1 \neq 0$ and $\Delta\bar{\tau}_{sc} \neq 0$.

In CCRL with two sequences of numbers, under the condition that the durations of the pulses produced by the i-th units of both binary circuits virtually coincide with the command repetition interval, the values $[K_n]_c$ /460 and $[\bar{K}_{cn}]_c$ are equal to

$$[\bar{K}_n]_y = k_{кру}K_a + k_{\phi 1}U_1 \sum_{i=1}^{N} 2^{i-1}\frac{(\Delta\bar{\tau}_{i1} + \Delta\bar{\tau}_{c1})\,\delta_i(i)}{T} - k_{\phi 2}U_2 \sum_{j=1}^{N} 2^{j-1}\frac{\Delta\bar{\tau}_{j2} + \Delta\bar{\tau}_{c2}}{T}\delta_j(i), \tag{8.9.13}$$

$$[\bar{K}_{кп}]_y = K_{ку} + \frac{1}{T}\times$$

(key p. 515)

$$\frac{k_{\phi 1}U_1 \sum_{i=1}^{N} 2^{i-1}(\Delta\bar{\tau}_{i1} + \Delta\bar{\tau}_{c1})\,\delta_i(i) - k_{\phi 2}U_2 \sum_{j=1}^{N} 2^{j-1}(\Delta\bar{\tau}_{j2} + \Delta\bar{\tau}_{c2})\,\delta_j(i)}{k_{\phi 1}U_1\left(2^N - 1 - \frac{k_{\phi 1}U_1}{k_{\phi\phi 2}U_2}\right)}, \tag{8.9.14}$$

where $\Delta\bar{\tau}_{i1}$ and $\Delta\bar{\tau}_{j2}$ are the mathematical expectations of the changes of the durations of the pulses produced by the i-th and j-th units of the first and second binary scalers and caused by the fluctuations of the leading edges of the binary code pulses;

$\Delta\bar{\tau}_{sc\ 1}$ and $\Delta\bar{\tau}_{sc\ 2}$ are the mathematical expectations of the fluctuations of the leading edges of the synchronizing pulses used for control of the operation of the first and second binary scalers;

U_2 is the amplitude of the voltage pulse forming at the output of the summer of the second binary scaler when fed signals expressing the number 1.

In order to eliminate changes of the transfer constant in CCRL of the last two types by interference, the same measures are suitable as in CCRL based on one sign-constant sequence of numbers.

3. Conditional Spectral Densities of Fluctuations of Output Signals

Under the influence of low-level interference, the signals forming at the summer output (the cathode circuit of amplifiers Amp_3, Amp_4 and Amp_5 in figure 7.32) of a CCRL with one sign-constant sequence of numbers are pulses whose leading edges and clippings fluctuate independently of one another. For such signals in the transmission of the i-th command, the spectral density $G_{fi}(0)$ of the random components, as is well known, can be represented by the sum of the two terms: $G_{f1}(\omega)$ and $G_{f2}(\omega)$.

These terms characterize the spectral densities caused by the fluctuations of the leading edges and clippings of the $u_{sc}(t)$ pulses, respectively. However, the leading edge of the voltage $u_{sc}(t)$ is formed by the addition of pulses characterizing those digits which form part of the binary code when transmitting the command expressed by the number i. The times of formation of pulses of the latter type are unrelated since the minimum interval between successive pulses in a binary code always is greater than the interference correlation time. Therefore /461

$$G_{f_1}(\omega)=\sum_{l=1}^{N} G_l(\omega)\delta_l(i), \tag{8.9.15}$$

where $G_l(\omega)$ is the spectral density of the voltage fluctuations $u_{sc}(t)$ caused by random changes of the position of the leading edge of the pulse formed by the l-th unit of the binary scaler.

Then

$$G_{fi}(\omega)=\sum_{l=1}^{N} G_l(\omega)\delta_l(i)+G_{f2}(\omega).$$

For practical purposes, it is sufficient to know $G_f(\omega)$ when $\omega = 0$. Therefore we will have

$$G_{fi}(0)=\sum_{l=1}^{N} G_l(0)\delta_l(i)+G_{f2}(0). \tag{8.9.16}$$

However, $G_l(0)$ is equal to the ratio of the dispersion of a voltage pulse with the amplitude $2^{l-1}U_1$ and the mean square duration $\sigma_{\tau l}$, averaged for the period T, to the effective frequency band occupied by the fluctuations and being $\frac{1}{2\sigma_{\tau l}}$ for the region of frequencies $0 \leq \omega \leq \infty$. At the same time, the

value $G_{f2}(0)$ is determined by the ratio of the dispersion of the pulse $u_{sc}(t)$, caused by fluctuations of its clipping, averaged for the time T, to the effective frequency band of these fluctuations. Therefore

$$G_{fi}(0) = U_1^2\left\{\sum_{l=1}^{N} 2^{(2l-1)}\frac{\sigma_{\tau l}^2}{T}\delta_l(i) + 2\frac{\sigma_{\tau 3}^2}{T}\left[\sum_{l=1}^{N} 2^{l-1}\delta_l(i)\right]^2\right\}, \qquad (8.9.17)$$

where $\sigma_{\tau 3}^2$ is the dispersion of displacement of the clipping of the pulse $u_{sc}(t)$.

By multiplying $G_{fi}(0)$ by the square of the transfer constant k_{F1}^2 of the filter F_1 (fig. 7.32), we obtain the following expression for the conditional spectral density $G_f(0)$ of the fluctuating components of the output signal $K_n(t)$

$$G_f(0) = k_{F1}^2 U_1^2\left\{\sum_{l=1}^{N} 2^{(2l-1)}\frac{\sigma_{\tau l}^2}{T}\delta_l(i) + 2\frac{\sigma_{\tau 3}^2}{T}\left[\sum_{l=1}^{N} 2^{l-1}\delta_l(i)\right]^2\right\}. \qquad (8.9.18)$$

Analysis of formula (8.9.18) shows that $G_f(0)$ is dependent not only /462 on the level of interference, but also on the value of the transmitted command: the larger the value K_a, the greater is the value $G_f(0)$.

The relationship between $G_f(0)$ and the intensity of interference at the CCRL radio receiver input is established by determination of $\sigma_{\tau l}^2$ and $\sigma_{\tau 3}^2$, which can be done in accordance with the method considered in section 8.5.

The spectral density of the command coefficient $G_{cf}(0)$ obviously will be equal to

$$G_{cf}(0) = \frac{1}{(2^{N-1}-1)^2}\left\{\sum_{l=1}^{N} 2^{(2l-1)}\frac{\sigma_{\tau l}^2}{T}\delta_l(i) + \frac{2\sigma_{\tau 3}^2}{T}\left[\sum_{l=1}^{N} 2^{(l-1)}\delta_l(i)\right]^2\right\} \qquad (8.9.19)$$

since

$$K_{max}^2 \approx k_{F1}^2 U_1^2 (2^{N-1}-1)^2. \qquad (8.9.20)$$

If we compare the spectral densities when $\omega = 0$ for the considered CCRL with pulse-code modulation and pulse-phase modulation, when there is an equality of the maximum possible amplitude of the $u_{sc}(t)$ pulses and the height of the $u_{pl\ n}(t)$ pulses, constant values $\sigma_{\tau l}^2$, regardless of l, and when there are

identical values of the dispersions of fluctuations of the leading edges of the $u_{pl\ n}(t)$ pulses in CCRL with pulse-phase modulation, it can be concluded that CCRL with pulse-code modulation have greater noise immunity. This is due to the absence of correlation of the fluctuations of the leading edges of the pulses produced by the i-th units of the binary scaler. At the same time, it should be emphasized that there is one specific difference between CCRL with pulse-code modulation and earlier considered types of CCRL with pulse-width modulation and pulse-phase modulation. This difference is that CCRL with pulse-code modulation, when subjected to low-level interference, are transformed into nonlinear apparatus with random conversion properties.

In those cases when it is necessary to know $G_f(\omega)$ for any values of the frequency ω, the functions $G_i(\omega)$ and $G_{i2}(\omega)$ can be found using the formulas given in reference 33.

Considering CCRL with one sign-variable sequence using different codes characterizing positive and negative commands, in the same way we obtain

$$G_f(0)=a^2k_{F1}^2U_1^2\left\{\sum_{i=1}^{N}2^{(2i-1)}\frac{\sigma_{\tau i}^2}{T}\delta_i(i)+2\frac{\sigma_{\tau 3}^2}{T}\left[\sum_{i=1}^{N}2^{i-1}\delta_i(i)\right]^2\right\}+(a-1)^2k_{F2}^2U_2^2\times\left\{\sum_{i=1}^{N}2^{(2i-1)}\frac{\sigma_{\tau i}^2}{T}\delta_i(i)+2\frac{\sigma_{\tau 31}^2}{T}\left[\sum_{i=1}^{N}2^{i-1}\delta_i(i)\right]^2\right\}, \quad (8.9.21)$$

where $\sigma_{\tau 3\ 1}^2$ is the dispersion of the variations of the time of formation /463 of the leading edge of the synchronizing pulse denoting negative commands.

Dividing the expression (8.9.21) by $k_{Fl}^2U_1^2(2^N-1)^2$, we find the formula for $G_{cf}(0)$.

In those cases when positive and negative commands are denoted by the same or two different but equistable timing codes, the dependence of $G_f(0)$ on K_a will be symmetrical relative to the y-axis.

Comparison of CCRL with one sign-constant and one sign-variable sequence of numbers, in the case of the same capacity of the binary codes, reveals:

(1) in a CCRL with a sign-variable sequence of numbers, in the transmission of the command $K_a = 0$, there are no fluctuations of the output signal, whereas in CCRL with a sign-constant sequence of numbers they differ from zero;

(2) in the transmission of maximum positive commands, the spectral density of the output signal for both types of CCRL is the same, but in the case of transmission of maximum negative commands a CCRL of the first type has the greater noise immunity.

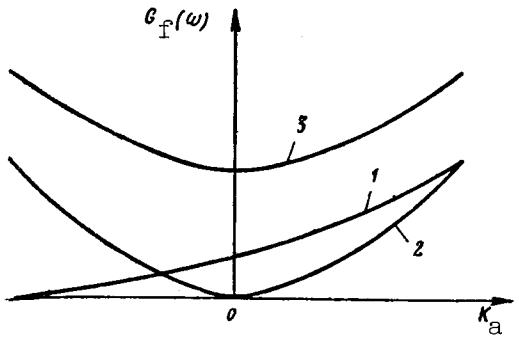

Figure 8.22

The qualitative dependence of $G_f(0)$ on K_a for the same level of interference and identical parameters of the analytical circuits, for CCRL with one sign-constant and one sign-variable sequence of numbers, has been shown in figure 8.22 by curves 1 and 2, respectively.

In the case of CCRL with two sequences of numbers, on the assumption that different key codes are used for each of the binary codes, we will have

$$G_f(0) = 2k_{F1}^2 U_1^2 \left\{ \sum_{l=1}^{N} 2^{2(l-1)} \frac{\sigma_{\tau l}^2}{T} \delta_l(i) + \frac{\sigma_{\tau 3}^2}{T} \left[\sum_{l=1}^{N} 2^{(l-1)} \delta_l(i) \right]^2 \right\}$$
$$+ 2k_{F2}^2 U_2^2 \left\{ \sum_{j=1}^{N} 2^{2(j-1)} \frac{\sigma_{\tau j}^2}{T} \delta_j(i) + \frac{\sigma_{\tau 3 l}^2}{T} \left[\sum_{j=1}^{N} 2^{(j-1)} \delta_j(i) \right]^2 \right\}. \qquad (8.9.22)$$

We note that expression (8.9.22) was derived under the condition that there is no reciprocal correlation of the processes transpiring in the first and second binary scalers.

In the considered CCRL, the intensity of the fluctuations (fig. 8.22, curve 3) is greater than in CCRL of the two preceding types. A common characteristic of all three types of CCRL with pulse-code modulation is nonlinearity and the random character of conversion of the input signals when there is low-level interference. /464

8.10. Effect of High-Level Interference on a CCRL with Pulse-Code Modulation

1. Qualitative Characteristics of Influence of Interference

First, we will consider a single-channel CCRL with one sign-variable sequence of numbers, assuming that such a CCRL is designed as shown in figure 7.32, and that the structure of the command signal has the form shown in figure

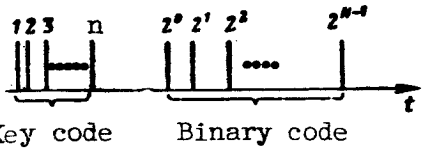

Figure 8.23

8.23. Figure 8.23 shows that the transmitted command is sent using an n-unit timing key code and an N-unit binary code.

When such a CCRL is subjected to high-level interference, there can be:

– suppression of the key code, resulting in the pulses of the binary code being unable to exert an effect on the binary scaler, and at the CCRL output the value of the signal transmitted in the preceding cycle will remain as before;

– suppression of one or a large number of transmitted binary code pulses and the formation of spurious pulses in the free positions of a binary code under the condition that the key code is not suppressed;

– formation of a spurious command signal by the transmitted pulses due to the addition of interference and the appearance of spurious binary code pulses;

– formation of spurious keys and binary codes only due to effective interference;

– formation of such spurious keys only by the effect of interference, which ensures the passage of one or a large number of transmitted pulses (it is unimportant which) to the input of the i-th unit of a binary scaler.

In addition, in a multichannel CCRL spurious keys can be formed during the interaction of interference with the transmitted signals of all the channels, and any of the pulses of all channels except the considered channel can play the role of binary code signals for the particular channel.

In the CCRL whose diagram is shown in figure 7.32, each successive key, however soon it forms after the preceding one, does not terminate the effect of the latter with respect to the formation of the gating pulses, which are intended for the separation of the binary code pulses expressing the different digits in separate circuits. Such a CCRL is characterized by the fact that at any time the voltage $u_i(t)$ can be formed at the output of the i-th unit of the binary scaler. Therefore, the output voltage $u_{sc}(t)$ of the summer will be equal to

/465

$$u_{sc}(t)=\sum_{i=1}^{N} u_i(t). \qquad (8.10.1)$$

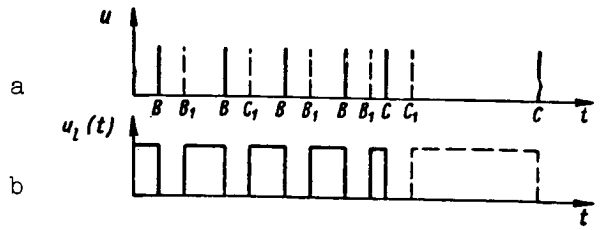

Figure 8.24

The voltage $u_l(t)$ constitutes square pulses. These pulses form after the appearance of the synchronizing pulses, after a time characterizing the interval between the pulse of the digit 2^{l-1} in the binary code and the signal C, and end at the time of arrival of the pulses C (fig. 8.21). The amplitude of the $u_l(t)$ pulses can be zero or $2^{l-1}U_1$. One of the possible variants of the function $u_l(t)$ is shown in figure 8.24b; figure 8.24a shows the synchronizing pulses (solid lines) and the pulses occupying the place of the l-th digit in a binary code. The points B denote the times of formation of the synchronizing pulses forming as a result of the interaction of interference with one of the transmitted signals and the points C--as a result of the effect of interference only. At the times corresponding to the points B_1 and C_1, binary code pulses appear associated with the transmitted signals. It should be noted here that under the influence of interference the transmitted signal can simultaneously perform the functions of pulses of all the digits of a binary code, provided that synchronizing pulses are fed in the corresponding intervals.

As an illustration of the above, figure 8.25 shows the synchronizing pulses C_1, C_2, ..., C_N, formed by interference, and the transmitted pulse TP. The intervals between the pulses TP and the C_1, C_2, ..., C_N pulses correspond to the intervals between the transmitted synchronizing pulses and the binary code pulses expressing the digits 2^0, 2^1 and 2^{N-1} in the considered CCRL.

All the $u_l(t)$ pulses forming in the time T can be divided into the following three groups, differing in their statistical properties and forming as a

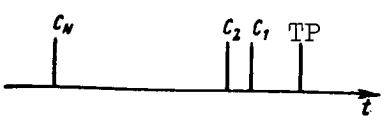

Figure 8.25

whole k + 1 pulse sequences (series), where k is the total number of synchronizing pulses which can be formed in the period T during the interaction of interference with transmitted signals as a result of nonsuppression of the key code: /466

(1) the pulses forming with nonsuppression of the key code (one sequence);

(2) the pulses appearing as a result of the addition by interference to a spurious key code of each of the transmitted signals (k - 1 sequences);

(3) the pulses appearing as a result of the formation of spurious keys by interference alone (one sequence).

During the time T in each of the groups there is a random number of $u_t(t)$ pulses. However, the first group and any of the sequences of the second group cannot include more than one pulse.

If only one transmitted pulse can be added simultaneously to the key code by interference, for a single-channel CCRL

$$k-1=n(n-1)+nN_{ri},$$

where n is the capacity of the key code, and N_{ri} is the number of pulses present in the binary code in transmission of the i-th command.

Considering the processes of formation of the voltage $u_t(t)$ in this way it can be assumed that $u_t(t)$ consists of one "purely" random sequence of pulses and "regular" sequences of pulses forming at the points of formation of the "regular" gating pulses which are the result of nonsuppression of the transmitted key code and the interaction of interference with the transmitted command.

Then expression (8.10.1) assumes the following form

$$u_{sc}(t)=\sum_{t=1}^{N}\sum_{s=1}^{k+1}u_{t.s}(t), \qquad (8.10.2)$$

where $u_{t.s}(t)$ is the voltage of the s-th sequence of pulses expressing the t-th digit in the binary code.

Accordingly, for the output signal $K_n(t)$ we obtain

$$K_n(t)=\sum_{t=1}^{N}\sum_{s=1}^{k+1}\int_0^t u_{t.s}(t)\,h_1(t-\tau)\,d\tau-u_{mean}, \qquad (8.10.3)$$

where $h_1(t)$ is the weighting function of the filter F_1.

In a case when a CCRL with one sign-variable sequence of numbers is subjected to interference, it is necessary to take into account the processes transpiring in the first and second binary scalers. If positive commands are transmitted, the same signal will be formed in the first binary scaler as in a CCRL with one sign-constant sequence of numbers. At the same time, the second binary scaler will produce signals due to:

-formation of a spurious synchronizing pulse in the place of the effect of the last pulse in the key code expressing a positive command, resulting in formation of gating pulses ensuring passage of signals of the binary code if the sign of the command is given by different key codes; /467

-the appearance of spurious synchronizing pulses during the interaction of interference with each of the transmitted signals, as a result of which the interference and some of the transmitted pulses can play the role of binary code symbols;

-formation of synchronizing pulses only under the influence of interference, so that each of the transmitted pulses begins to perform the functions of a signal of the i-th ($i = 1, 2, \ldots, N$) digit in the binary code;

-the creation of spurious synchronizing pulses and binary code pulses only under the influence of interference.

Then the output signal $K_n(t)$ of a CCRL with a sign-variable sequence of numbers can be represented in the following way

$$K_n(t) = \sum_{i=1}^{N} \sum_{s=1}^{k_1+1} \int_0^t u_{i.s}(t)\, h_1(t-\tau)\, d\tau - \sum_{i=1}^{N} \sum_{s=1}^{k_2+1} \int_0^t u'_{i.s}(t) h_2(t-\tau)\, d\tau, \qquad (8.10.4)$$

where k_1 and k_2 are the maximum values of the numbers of the "regular" synchronizing pulses acting on the first and second binary scalers in the time T; $u_{i.s}(t)$ and $u'_{i.s}(t)$ are the voltages of the s-th sequence of pulses expressing the i-th digit in the binary code and acting at the outputs of the summers of the first and second binary scalers; $h_2(t)$ is the weighting function of the filter F_2 (fig. 7.36).

When transmitting negative commands, the functions of the first and second binary scalers are changed to opposite signs in comparison with the case $K_a > 0$. However, the command $K_n(t)$ will be determined by the same expression (8.10.4) under the condition of corresponding computation of the values k_1 and k_2.

If in a CCRL with a sign-variable sequence of numbers the sign of the transmitted command is determined by the displacement of the binary code pulses, in contrast to the preceding CCRL, the formation of a spurious synchronizing pulse as a result of nonsuppression of the transmitted key does not lead to a possibility of passage of the binary code pulses to the second binary scaler.

In determining the output signal $K_n(t)$ in a CCRL with two sequences of numbers, it is also possible to use expression (8.10.4) if it is taken into account that k_1 and k_2 should be computed with allowance for the specific /468 characteristics of operation of the first and second binary scalers. The fact is that both the first and second binary scalers will be affected by interference and the transmitted signals characterizing the first and second sequences of numbers.

2. Conditional Constant Components of Output Commands and Their Distortions

First, we will consider a single-channel CCRL with one sign-variable sequence of numbers. On the basis of expression (8.10.3), for a steady-state regime we find

$$[\overline{K_n}]_c = k_{F1} \sum_{l=1}^{N} \sum_{s=1}^{k+1} [\overline{u}_{l.s}]_c - u_{mean}, \qquad (8.10.5)$$

where $[\overline{u}_{l.s}]_c$ is the time-averaged conditional mathematical expectation of the voltage $u_{l.s}(t)$, computed on the assumption that the value of the transmitted command is specified.

Since in the absence of interference the duration of the pulse produced by the l-th unit of the binary scaler is virtually equal to T, then

$$K = k_{F1} U_1 \sum_{l=1}^{N} 2^{l-1} \delta_l(i) - u_{mean}$$

and for the conditional constant component $[\overline{\Delta K}]_c$ of the distortion of the output command we will have

$$[\Delta \overline{K}]_c = k_{F1} \sum_{l=1}^{N} \sum_{s=1}^{k+1} [\overline{u}_{l.s}]_c - k_{F1} U_1 \sum_{l=1}^{N} 2^{l-1} \delta_l(i). \qquad (8.10.6)$$

Dividing expressions (8.10.5) and (8.10.6) by the maximum value of the command

$$K_{max} \approx k_{F1} U_1 (2^N - 1) - u_{mean},$$

it is possible to find formulas determining $[\overline{K}_{cn}]_c$ and $[\overline{\Delta K}_c]_c$.

As already mentioned, pulses of the s-th sequence have random amplitude $a_{l.s}$, duration $\tau_{l.s}$ and time of formation $t_{l.s}$. Therefore

$$[\overline{u}_{l.s}]_c = \overline{a}_{l.s}\overline{\tau}_{l.s}Z_{l.s},$$

where $\overline{a}_{l.s}$ and $\overline{\tau}_{l.s}$ are the conditional mean amplitude and duration of the $u_{l.s}(t)$ pulses, and $Z_{l.s}$ is the mean number of $u_{l.s}(t)$ pulses forming in 1 sec.

The product $\overline{\tau}_{l.s}Z_{l.s}$ is the probability of an event in which, with the shifting of a point to the sequence of segments formed by the bases of the pulses of the s-th sequence and the intervals between them, this point falls on the base of one of the pulses. /469

Taking into account the specific character of the statistical properties of different sequences, it is desirable to determine the value

$$[\overline{u}_l]_c = \sum_{s=1}^{k+1} [\overline{u}_{l.s}]_c$$

in the following way

$$[\overline{u}_l]_c = \overline{a}_{l.1}\overline{\tau}_{l.1}Z_{l.1} + \sum_{s_1} \overline{a}_{l.s_1}\overline{\tau}_{l.s_1}Z_{l.s_1} + \sum_{\mu} \overline{a}_{l.\mu}\overline{\tau}_{l.\mu}Z_{l.\mu} + \sum_{s_2} \overline{a}_{l.s_2}\overline{\tau}_{l.s_2}Z_{l.s_2} + \overline{a}_{l.\nu}\overline{\tau}_{l.\nu}Z_{l.\nu}, \quad (8.10.7)$$

where $\overline{a}_{l.1}\overline{\tau}_{l.1}Z_{l.1}$ is the conditional constant component of the voltage produced by the l-th unit of the binary scaler under the influence of the transmitted keys and a pulse of the l-th digit in the binary code;

s_1 is the summation index, applied to the spurious "regular" synchronizing pulses, under whose influence are created gating pulses which coincide with the transmitted pulses;

s_2 is the summation index, applied to those spurious "regular" synchronizing pulses responsible for appearance of gating pulses not coinciding with the transmitted pulses;

μ is the summation index, applied to the synchronizing pulses forming due to interference only and which then cause formation of gating pulses coinciding with the transmitted pulses;

$\bar{a}_{l.s_1}$, $\bar{\tau}_{l.s_1}$, $Z_{l.s_1}$, $\bar{a}_{l.\mu}$, $\bar{\tau}_{l.\mu}$, $Z_{l.\mu}$, $\bar{a}_{l.s_2}$, $\bar{\tau}_{l.s_2}$ and $Z_{l.s_2}$ are the conditional mean values of the amplitudes, durations and number of pulses in 1 sec in the s_1-th, μ-th and s_2-th sequences;

$\bar{a}_{l.\nu}$, $\bar{\tau}_{l.\nu}$ and $Z_{l.\nu}$ are the conditional mean values of the amplitude, duration and number of pulses per 1 sec in a sequence caused by the influence of interference only.

Since a periodic transmission of commands is assumed, then

$$\Pi = \sup \quad Z_{l.1} = p_1 F = (1 - p_n)^n F;\ Z_{l.s_1} = Z_{l.s_2} = p_k F \quad \text{and} \quad Z_{l.\mu} = p_{kn} F,$$

where $p_1 = (1 - p_{sup})^n$ is the probability of nonsuppression of a transmitted key code; p_k is the probability of augmentation of a transmitted pulse to a key code by interference; p_{kn} is the probability of formation of a spurious key code by interference only; $F = \frac{1}{T}$.

However, /479

$$\bar{\tau}_{l.\nu} Z_{l.\nu} = 1 - p_{la},$$

where p_{la} is the probability of an event in which, with the shifting of a point to the sequences of segments formed by the bases of the $u_l(t)$ pulses and the intervals between them, this point falls on the base of one of the pulses.

It can be found that

$$\bar{\tau}_{l.\nu} Z_{l.\nu} = 1 - F\left[\bar{\tau}_{l.1}(1 - p_n)^n + p_k\left(\sum_{s_1} \bar{\tau}_{l.s_1} + \sum_{s_2} \bar{\tau}_{l.s_2}\right) + p_{kn} \sum_{\mu} \bar{\tau}_{l.\mu}\right].$$

Next we determine $\bar{a}_{l.1}$, $\bar{a}_{l.s_1}$, $\bar{a}_{l.s_2}$ and $\bar{a}_{l.\mu}$. In the case of transmission of a pulse characterizing the l-th digit in a binary code, it can be suppressed with the probability p_{sup}, but in the absence of this pulse a spurious signal can be formed by interference with the probability p_{spur}. The amplitude of the pulse produced by the l-th unit of the binary scaler is $U_1 2^{l-1}$. Therefore,

П = sup
Л = spur

$$\bar{a}_{l.1} = U_1 2^{l-1}\{(1-p_п)\delta_l(i) + p_л[1-\delta_l(i)]\}.$$

(Note: This key applies to the present and following equations.)

Similarly, we obtain

$$\bar{a}_{l.s_1} = U_1 2^{l-1}\{(1-p_п)\delta_{l.s_1}(i) + p_л[1-\delta_{l.s_1}(i)]\},$$

$$\bar{a}_{l.s_2} = \bar{a}_{l.\nu} = 2^{l-1}U_1 p_л$$

and

$$\bar{a}_{l.\mu} = 2^{l-1}U_1(1-p_п)\delta_{l.\mu}(i),$$

where $\delta_{l.s_1}(i)$ and $\delta_{l.\mu}(i)$ are functions equal to 1 or 0, depending on whether or not the s_1-th and μ-th pulses are transmitted when the CCRL coder is subjected to the influence of the i-th command.

After substituting the values $[\bar{u}_l]_c$, $Z_{l.1}$, $Z_{l.s_1}$, $Z_{l.s_2}$, $\bar{a}_{l.1}$, $\bar{a}_{l.s_1}$, $\bar{a}_{l.s_2}$, $\bar{a}_{l.\mu}$, $\bar{a}_{l.\nu}$ and $\bar{\tau}_{l.\nu}Z_{l.\nu}$ into expression (8.10.5) we find that

$$[\bar{K}_п]_c = K_1 + K_2, \tag{8.10.8}$$

where

$$K_1 = k_{F1}U_1 p_л(2^N - 1) - u_{mean}; \tag{8.10.9}$$

$$K_2 = k_{F1}U_1(1-p_п-p_л)\sum_{l=1}^{N}2^{l-1}\Big((1-p_п)^n\bar{\tau}_{l.1}\delta_l(i) + \sum_{s_1}p_к^{\bar{\tau}_{l.s_1}}\delta_{l.s_1}(i) + p_{кп}\sum_{\mu}\bar{\tau}_{l.\mu}\delta_{l.\mu}(i)\Big). \tag{8.10.10}$$

The value K_1 is dependent only on k_{F1}, U_1, p_{spur}, N and u_{eff} and is not a function of the transmitted commands. Therefore, it cannot be considered a constant component of the signal produced by some noise source. With an increase of interference, $p_{spur} \to 1$ and K_1 assumes a value equal to the /471 maximum command forming at the CCRL output.

The component K_2 is a function of interference, the structure of the CCRL and the transmitted command. As follows from expression (8.10.10), in the presence of interference, the CCRL decoder is transformed into a nonlinear apparatus. However, if the decoder is divided into N units, the signals from whose outputs are fed to a summer, it is possible to detect N links which are linear relative to the transmitted symbols 2^0, 2^1, ..., 2^N. At the output of

the l-th link we will have the constant component $2^{l-1}k_{Fl}U_1p_{spur}$, regardless of whether or not the digit 2^{l-1} is transmitted, and the signal

$$K_2^{(l)} = k_{F_1}U_1(1-p_n-p_{sp})\left[(1-p_n)^n\bar{\tau}_{l.1} + \sum_{s_1} p_k^{\bar{\tau}_{l.s_1}}\frac{\delta_{l.s_1}(i)}{\delta_l(i)} + p_{kn}\sum_{\mu}\bar{\tau}_{l.\mu}\frac{\delta_{l.\mu}(i)}{\delta_l(i)}\right]2^{l-1}\delta_l(i).$$

In this expression the factor standing before $2^{l-1}\delta_l(i)$ characterizes the mean value of the transfer constant of the l-th link.

It then follows from expression (8.10.10) that with increase of the intensity of interference, the value $(1 - p_{sup} - p_{spur})$ decreases and at the limit tends to -1. At the same time, with an increase of the interference level, $\bar{\tau}_{l.1}$, $\bar{\tau}_{l.\mu}$ and $\bar{\tau}_{l.s_1}$ continuously decrease approaching zero. This means that the effect of interference leads to a decrease of the amplification properties of the CCRL.

In order to decrease the influence of all the transmitted pulses except the pulse characterizing the digit 2^{l-1} in the binary code, it is necessary to satisfy the equation $\delta_{l.s_1}(i) = 0$. Therefore, in developing a CCRL it is necessary to have such a separation of signals in which gating pulses coinciding with the transmitted pulses are not formed under the influence of spurious "regular" synchronizing pulses.

The dependence of $[\bar{K}_n]_c$ on the ratio $\frac{1}{q_0^2}$ has the form shown in figure 8.26.

With sufficiently small values of the ratio $\frac{1}{q_0^2}$, as the ratio increases, the principal role is played by the formation of spurious pulses at the CCRL radio receiver output and spurious regular synchronizing pulses. Therefore, the component K_2 decreases rather rapidly, primarily due to $\bar{\tau}_{l.1}$, $\bar{\tau}_{l.s_1}$ and $\bar{\tau}_{l.\mu}$. At the same time, the increase of the signal K_1 occurs relatively slowly. As a result, and also due to the presence of the voltage u_{mean} at some point a, the command $[\bar{K}_n]_c$ becomes equal to zero and then assumes negative values.

When p_{spur} is 10-20 percent, the number of spurious synchronizing /472 pulses becomes so great that $\bar{\tau}_{l.1}$, $\bar{\tau}_{l.s_1}$ and $\bar{\tau}_{l.\mu}$ are equal to zero and the

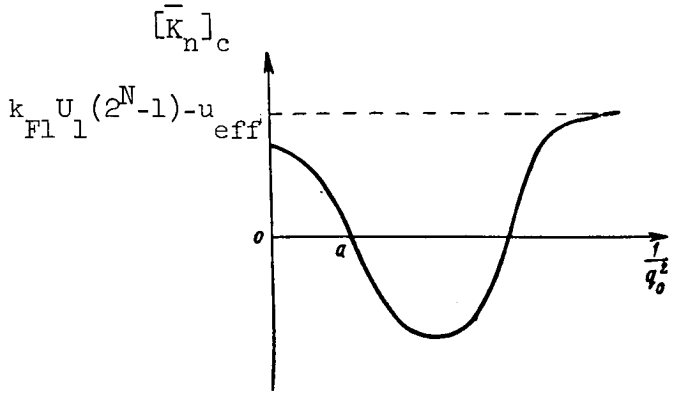

Figure 8.26

influence of the transmitted commands on the CCRL output signal comes to an end. In essence, this means an opening of the rocket guidance circuit. However, since p_{spur} still is not very large, the guidance circuit for all practical purposes opens when there is a maximum negative voltage at the CCRL output. The latter assertion is based on the fact that when $K_2 \approx 0$ a set of spurious commands resulting from the influence of interference only occurs relatively rarely in comparison with the formation of spurious regular synchronizing pulses. This can be attributed to the fact that the formation by interference of a spurious key and at least one pulse corresponding to a binary code signal is equivalent to the creation by interference of a spurious timing code of a greater capacity than the key code used.

A further increase of $\frac{1}{q_0^2}$ causes an increasingly strong appearance of commands corresponding to increasing values i due to the effect of interference only and the suppression of the transmitted pulses. As a result, the number of units of a binary scaler which at each time is in a working state increases and $[\bar{K}_n]_c$ approaches to

$$k_{Fl}U_1(2^N - 1). - u_{mean} = K_{max}.$$

If the CCRL is multichannel, the guidance circuit is opened at a lesser interference level.

A study of a CCRL with one sign-variable sequence of numbers in the same way makes it possible to draw the following conclusions:

(1) When there are identical circuits for analysis of the signals used in transmission of positive and negative commands, the output signal $[\bar{K}_n]_c$ does not contain a component not dependent on K_a.

(2) In order to decrease the influence of all the transmitted pulses /473 on the value $[\bar{K}_n]_c$, it is necessary to select the structure of the command signals in such a way that the spurious "regular" synchronizing pulses which appear do not create gating pulses which coincide in time of effect with the transmitted pulses.

(3) With an increase of the intensity of the interference, the amplification properties of the CCRL, which becomes a nonlinear link, deteriorate and at the limit the value $[\bar{K}_n]_c$ becomes equal to zero, which leads to opening of the guidance circuit when (on the average) the control surfaces of the rocket are in a neutral position.

(4) In order to obtain a symmetrical mean amplitude characteristic representing the dependence of $[\bar{K}_n]_c$ on K_a, when interference is present, it is necessary to use equistable key codes. In a CCRL with one common key in the transmission of positive and negative commands, the value $[\bar{K}_n]_c = 0$ when $K_a = 0$, and in a CCRL with different keys this condition is satisfied approximately.

(5) The absolute value $[\bar{K}_n]_c$ is larger in a CCRL with one common code; however, in order for the mean amplitude characteristic of such a CCRL to be close to symmetrical, the displacement of the binary code pulses must not be for any considerable interval of time in the transmission of negative commands.

The curve characterizing the dependence $[\bar{K}_{cn}]_c = f(q_0^2)$ for one value K_a is shown in figure 8.27 (curve 1).

The effect of high-level interference on CCRL with two sequences of /474 numbers causes qualitatively the same processes as in a CCRL with one sign-variable sequence of numbers. However, in order to obtain the mean amplitude characteristic undisplaced relative to zero, in addition to satisfying the requirement that the key codes are equistable, it is necessary to ensure a corresponding displacement of the binary code pulses in the limits of the period T. At the same time, it should be noted that, for the same value $\frac{1}{q_0^2}$, the value $[\bar{K}_{cn}]_c$ is smaller than in a CCRL with one sign-variable sequence of numbers (fig. 8.27, curve 2). This is because virtually identical values $[\bar{K}_n]_c$ will be observed in both types of compared CCRL for the same mean number of pulses of effective interference. At the same time, when using two sequences of pulses

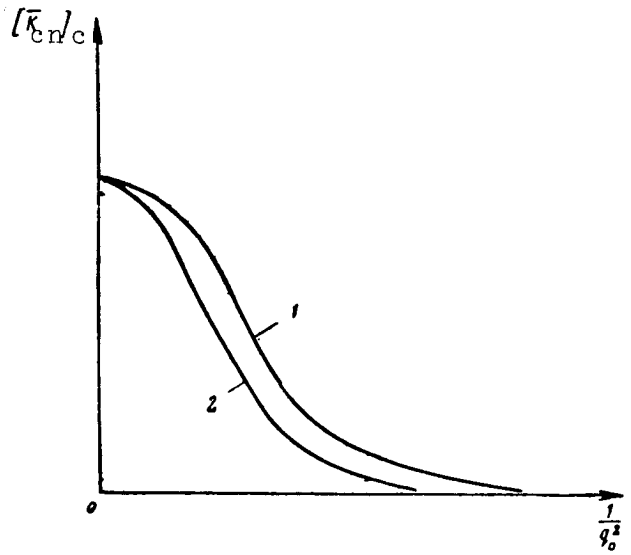

Figure 8.27

for transmission of a particular command, a greater power is expended than in CCRL with one sign-variable sequence of numbers.

3. Conditional Spectral Densities of Fluctuations of Output Signals

In the case of a CCRL with pulse-code modulation, subjected to high-level interference, it is simplest to compute the conditional correlation function. Obviously, it first is necessary to find the conditional correlation function $R_{sc}(t, t + \tau)$ of the signal $u_{sc}(t)$ formed by the summer of the binary scaler.

We will consider a single-channel CCRL with one sign-constant sequence of numbers.

Taking into account $u_{sc}(t) = \sum_{l=1}^{N} \sum_{s=1}^{k+1} u_{l.s}(t)$, on the basis of expression (8.10.2), we find

$$R_{sc}(t,\ t+\tau) = \sum_{l=1}^{N} R_l(t,\ t+\tau) + \sum_{\substack{l=1 \\ l \neq \rho}}^{N} \sum_{\rho=1}^{N} R_{l.\rho}(t,\ t+\tau), \qquad (8.10.11)$$

where

$$R_l(t,\ t+\tau) = \overline{u_l^0(t)\, u_l^0(t+\tau)}$$

is the conditional autocorrelation function of the voltage produced by the l-th unit of the binary scaler;

$$R_{l.\rho}(t,\ t+\tau) = \overline{u_l^0(t)\, u_\rho^0(t+\tau)}$$

is the conditional reciprocal correlation function of the voltages produced by the i-th and ρ-th units of the binary scaler;

$$u_i^0(t) = u_i(t) - [\overline{u_i(t)}]_c$$

is the centered function $u_i(t)$ for a given value of the input command.

The second term in expression (8.10.11) is negligibly small. This is due to the extremely low probability that both the i-th and ρ-th units will be activated by the same pulse forming at the output of the CCRL radio receiver output (since only under this condition will the voltages $u_i(t)$ and $u_\rho(t)$ be correlated). /475

Then

$$R_{sc}(t,\ t+\tau) = \sum_{i=1}^{N} R_i(t,\ t+\tau) = \sum_{i=1}^{N} \overline{u_i^0(t)\, u_i^0(t+\tau)}.$$

The product $u_i^0(t)u_i^0(t+\tau)$ can be equal to one of the following values:

– the square of the amplitude $b_{i.s}^2$ $(s = 1, 2, \ldots, k+1)$ of the centered signal $u_{i.s}(t)$, if the times t and $t+\tau$, corresponding to the beginning and end of the segment with the length τ, lie on the base of the same pulse of the s-th sequence;

– the product $b_{i.s}b'_{i.s}$, where $b'_{i.s}$ is the amplitude of the centered signal $u_{i.s}(t)$ at the time $t+\tau$, under the condition that the times t and $t+\tau$ coincide with the bases of two different pulses of the same s-th sequence;

– the product $b_{i.s}b_{i.\varkappa}$ $(s = 1, 2, \ldots, k+1;\ \varkappa = 1, 2, k+1;\ s \neq \varkappa)$, where $b_{i.\varkappa}$ is the amplitude of a signal of the $\varkappa$-th sequence, under the condition that the times t and $t+\tau$ are situated at the bases of the pulses of the s-th and $\varkappa$-th sequences, respectively.

Therefore

$$R_i(t,\ t+\tau) = \sum_{s=1}^{k+1} p_{1.s}\overline{b}_{i.s}^2 + \sum_{s=1}^{k+1} p_{2.s}\overline{b}_{i.s}\overline{b}'_{i.s} + \sum_{s=1}^{k+1}\sum_{\varkappa=1}^{k+1} p_{s.\varkappa}\overline{b}_{i.\varkappa}\overline{b}_{i.s}, \qquad (8.10.12)$$

where $p_{1.s}$, $p_{2.s}$ and $p_{s.\varkappa}$ are the probabilities that both ends of the segment of the length τ will be situated on the base of the same pulse of the s-th

sequence, two different pulses of the s-th sequence and two pulses of the s-th and $\varkappa$-th sequences, respectively.

In writing expression (8.10.12), an allowance was made for the nondependence of the change of the amplitudes of the pulses of the s-th and $\varkappa$-th sequences and also of the same s-th sequence.

Since $\overline{b}_{i.s} = 0$ and $\overline{b}_{i.\nu} = 0$, as a result of the fact that $u_i^0(t)$ is the centered function of the voltage $u_i(t)$, then

$$R_{sc}(t, t+\tau) = \sum_{i=1}^{N} \sum_{s=1}^{k+1} p_{1.s} \overline{b}_{i.s}^2 = p_{1.1} \overline{b}_{i.1}^2 + \sum_{\mu} p_{1.\mu} \overline{b}_{i.\mu}^2 + p_{1.\nu} \overline{b}_{i.\nu}^2 + \sum_{s_1} p_{1.s_1} \overline{b}_{i.s_1}^2 + \sum_{s_2} p_{1.s_2} \overline{b}_{i.s_2}^2. \quad (8.10.13)$$

Here s_1, s_2 and μ are the indices of summation, having the same sense as /476 in expression (8.10.7);

$\overline{b}_{i.\mu}^2$ and $\overline{b}_{i.\nu}^2$ are the dispersions of the amplitudes of the voltage produced by the i-th unit of the binary scaler under the influence of the μ-th transmitted pulse and the interference pulse, respectively, forming at the output of the CCRL radio receiver;

$\overline{b}_{i.1}^2$, $\overline{b}_{i.s_1}^2$ and $\overline{b}_{i.s_2}^2$ are the dispersions of the amplitudes of the voltage produced by the i-th unit of the binary scaler under the influence of a pulse characterizing the digit 2^{i-1} in a binary code, the transmitted pulse and the s_1-th "regular" spurious synchronizing pulse and also an interference pulse and the s_2-th "regular" spurious synchronizing pulse, respectively.

In transmission of a pulse characterizing the digit 2^{i-1} in a binary code, the voltage at the output of the i-th unit, under the condition that it is "tripped" by this pulse, can be $2^{i-1}U_1$, or 0 with probabilities of $1 - p_{sup}$ and p_{sup}, respectively. If the pulse determining the digit 2^{i-1} is not transmitted in a binary code, the formation of the output signal of the i-th unit with the amplitudes $2^{i-1}U_1$ and 0 will occur with the probabilities p_{spur} and $(1 - p_{spur})$. On this basis we obtain

П = sup
Л = spur

$$\overline{b}_{i.1}^2 = 2^{2(i-1)} U_1^2 \{(1-p_{\text{п}}) p_{\text{п}} \delta_i(i) + p_{\text{л}}(1-p_{\text{л}})[1-\delta_i(i)]\}.$$

Similarly, we find

$$\bar{b}^2_{l.\,s_1}=2^{2(l-1)}U_1^2\{(1-p_{\text{п}})p_{\text{п}}\delta_{l.\,s_1}(i)+p_{\text{л}}(1-p_{\text{л}})[1-\delta_{l.\,s_1}(i)]\},$$

$$\bar{b}^2_{l.\,s_2}=\bar{b}^2_{l.\,\nu}=2^{2(l-1)}U_1^2p_{\text{л}}(1-p_{\text{л}});$$

$$\bar{b}^2_{l.\,\mu}=2^{2(l-1)}U^2p_{\text{п}}(1-p_{\text{п}})\delta_{l.\,\mu}(i).$$

The probability $p_{1.s}$ is

$$p_{1.\,s}=p_sp(0,\ t,\ t+\tau),$$

where p_s ($s = 1, 2, \ldots, k+1$) is the probability of an event in which, with the shifting of a point to the sequence of segments formed by the bases of the pulses of the s-th sequence and the intervals between them, this point falls on the base of one of the pulses;

$p(0, t, t+\tau)$ is the probability that in the interval of time t-$t+\tau$ not a single synchronizing pulse is formed under whose influence, as already mentioned, the next "tripping" of the l-th unit of the binary scaler occurs.

The value p_s is determined by the ratio of the mean duration of pulses of the s-th sequence to their mean repetition interval. Therefore /477

П = sup
К = k
КП = kn
Л = spur
В = inter

$$p_{1.\,1}=\bar{\tau}_{l.\,1}(1-p_{\text{п}})^nFp(0,\ t,\ t+\tau),$$

$$p_{1.\,s_1}=\bar{\tau}_{l.\,s_1}p_{\text{к}}Fp(0,\ t,\ t+\tau),$$

$$p_{1.\,s_2}=\bar{\tau}_{l.\,s_2}p_{\text{к}}Fp(0,\ t,\ t+\tau),$$

$$p_{1.\,\mu}=\bar{\tau}_{l.\,\mu}p_{\text{кп}}Fp(0,\ t,\ t+\tau).$$

(Note: This key may be used also for equations through (8.10.15).)

Similarly, we find that

$$p_{1.\,\nu}=p_\nu p(0,\ t,\ t+\tau),$$

where $p_{1.\nu}$ is the probability of the left end of the segment of the length τ falling on the base of a pulse of the ν-th sequence. However,

$$p_{1.\,\nu}+\tau_{l.\,1}(1-p_{\text{п}})^nF+\sum_{s_1}\bar{\tau}_{l.\,s_1}p_{\text{к}}F+\sum_{s_2}\bar{\tau}_{l.\,s_2}pF+\sum_{\mu}\bar{\tau}_{l.\,\mu}Fp_{\text{кп}}=1.$$

Therefore

$$p_{1.\,\nu}=1-F\left[\bar{\tau}_{l.\,1}(1-p_{\text{п}})^n+\sum_{s_1}\bar{\tau}_{l.\,s_1}p_{\text{к}}+\sum_{s_2}\bar{\tau}_{l.\,s_2}p_{\text{к}}+\sum_{\mu}\bar{\tau}_{l.\,\mu}p_{\text{кп}}\right].$$

By substituting the determined values $p_{1.1}$, $p_{1.\mu}$, $p_{1.\nu}$, $p_{1.s_1}$, $p_{1.s_2}$, $\bar{b}^2_{1.1}$, $\bar{b}^2_{1.\mu}$, $\bar{b}^2_{1.\nu}$, $\bar{b}^2_{1.s_1}$ and $\bar{b}^2_{1.s_2}$ into expression (8.10.13), we obtain

$$R_{sc}(t,\ t+\tau)\approx p(0,\ t,\ t+\tau)\,U_1^2\sum_{l=1}^{N}2^{2(l-1)}\Big\{p_л(1-p_л)+F\left[p_п(1-p_п)-p_л(1-p_л)\right]\Big[(1-p_п)^n\bar{\tau}_{l.1}\delta_l(i)+p_к\sum_{s_1}\bar{\tau}_{l.s_1}\delta_{l.s_1}(i)+p_{кп}\sum_{\mu}\bar{\tau}_{l.\mu}\delta_{l.\mu}(i)\Big]\Big\}. \qquad (8.10.14)$$

In the case of a constant intensity of interference, $R_{sc}(t,\ t+\tau)$ is a periodic function of time t. Its period is T. Since the value T is considerably less than the time constant of the CCRL output stages, it is possible to use the time-averaged correlation function $R_{sc\ 1}(\tau) = \overline{R_{sc}(t,\ t+\tau)}$. This same function is suitable for investigation of control systems in the case of a slow change of the intensity of interference for individual parts of the trajectory of motion of the rocket, when the pertinent slowly changing coefficients can be "frozen."

Then, taking into account the condition $\overline{p(0,\ t,\ t+\tau)} = p_{sup}(\tau)p_{inter}(\tau)$, where $p_{sup}(\tau)$ is the probability that in the interval τ interference does not create a single synchronizing pulse, and $p_{inter}(\tau)$ is the time-averaged probability that in the interval τ not a single synchronizing pulse is formed during the interaction of interference and the transmitted signals, we obtain /478

$$R_{sc}(\tau)=p_п(\tau)\,p_в(\tau)\,U^2\sum_{l=1}^{N}2^{2(l-1)}\Big\{p_л(1-p_л)+F\left[p_п(1-p_п)-p_л(1-p_л)\right]\Big[(1-p_п)^n\bar{\tau}_{l.1}\delta_l(i)+p_к\sum_{s_1}\bar{\tau}_{l.s_1}\delta_{l.s_1}(i)+p_{кп}\sum_{\mu}\bar{\tau}_{l.\mu}\delta_{l.\mu}(i)\Big]\Big\}. \qquad (8.10.15)$$

By knowing the correlation function and the frequency characteristic $Y_1(j\omega)$ of the filter F_1, we obtain the following expression for the conditional spectral density $G_f(\omega)$ of fluctuations of the output signal $K_n(t)$

$$G_f(\omega)=4\,|Y_1(j\omega)|^2\int_0^{\infty}R_{sc}(\tau)\cos\omega\tau\,d\tau, \qquad (8.10.16)$$

where $R_{sc}(\tau)$ is determined by formula (8.10.15).

Dividing both sides of formula (8.10.16) by the square of the maximum value of the output command in the absence of interference, we obtain the conditional spectral density $G_{cf}(0)$ for the fluctuating components of the command coefficient.

The probabilities $p_{sup}(\tau)$, $p_{inter}(\tau)$, p_{spur} and p_{sup} and also the values $\overline{\tau}_{1.1}$, $\overline{\tau}_{1.s_1}$ and $\overline{\tau}_{1.\mu}$ can be computed if the parameters of the signals and the statistical characteristics of interference are known.

It follows from an analysis of expressions (8.10.15) and (8.10.16) that:

(1) the conditional correlation function $R_{sc}(\tau)$ and the spectral density $G_f(\omega)$ consist of two parts, one of which is not dependent on the transmitted commands, whereas the other is a function of the transmitted commands;

(2) the conversion properties of the CCRL are random, as indicated by the presence of the functions $\delta_1(i)$, $\delta_{1.s_1}(i)$ and $\delta_{1.\mu}(i)$ in expression (8.10.15), dependent in turn on K_a;

(3) for virtually complete elimination of the influence of transmitted commands on $R_{sc}(\tau)$ and $G_f(0)$, it is necessary to create a CCRL in which $p_{sup} = p_{spur}$; under this condition, the random character of the conversion properties of the CCRL can be neglected;

(4) with an increase of the intensity of interference, the values $R_{sc}(\tau)$ and $G_f(\omega)$ for fixed values τ and ω first increase monotonically, then attain a maximum and then begin to decrease, at the limit approaching zero. For all practical purposes, the breaking of the guidance circuit for the fluctuating components of the signal sets in at a larger ratio $\frac{1}{q_0^2}$ than for the constant component;

(5) for a decrease of the influence of the individual transmitted pulses on $R_{sc}(\tau)$ and $G_f(\omega)$, the CCRL must be designed in such a way that the condition $\delta_{1.s_1}(i) = 0$ is satisfied;

(6) the influence of the term proportional to p_{kn}, in the case of a small number of transmitted pulses, is negligibly small because /479

$$p_{kn} \ll p_k \text{ and } p_{kn} \ll (1 - p_{sup})^n.$$

If a CCRL with a sign-constant sequence of numbers is a multichannel apparatus, then $R_{sc}(\tau)$ and $G_f(\omega)$ decrease with an increase of N_k as a result of the decrease of the values $p_{inter}(\tau)$, $\overline{\tau}_{i.1}$, $\overline{\tau}_{i.s_1}$ and $\overline{\tau}_{i.\mu}$.

The conditional spectral density of fluctuations of the output signal in a CCRL with one sign-variable sequence of numbers can be found if the conditional spectral and reciprocal spectral densities or the conditional correlation and reciprocal correlation functions of the voltages $u_{sc\ 1}(t)$ and $u_{sc\ 2}(t)$ produced by the first and second scalers are known. However, without making significant errors, it is possible to neglect the mutual relationship between the voltages $u_{sc\ 1}(t)$ and $u_{sc\ 2}(t)$ and also between the voltages formed by the i-th and ρ-th units in both the first and second binary scalers.

Under these conditions,

$$G_f(\omega) = G_{F_1}(\omega)\,|\,Y_1(j\omega)\,|^2 + G_{F_2}(\omega)\,|\,Y_2(j\omega)\,|^2,$$

where $G_{f1}(\omega)$ and $G_{f2}(\omega)$ are the spectral densities of the voltages $u_{sc\ 1}(t)$ and $u_{sc\ 2}(t)$ without taking into account the reciprocal correlation between the signals produced by the i-th and ρ-th units in both the first and second scalers.

The functions $G_{f1}(\omega)$ and $G_{f2}(\omega)$ are determined most easily as the Fourier transform of the time-averaged conditional correlation functions for the voltages $u_{sc\ 1}(t)$ and $u_{sc\ 2}(t)$. The latter, however, can be computed as was done in an investigation of a CCRL with one sign-constant sequence of numbers.

As a result of an analysis of the expression determining $G_f(\omega)$ it can be concluded:

(1) $G_f(\omega) = f(q_0^2)$ changes the same as in a CCRL with one sign-constant sequence of numbers.

(2) The value $G_f(\omega)$ in a CCRL with a sign-variable sequence of numbers, when $\frac{1}{q_0^2} > \left(\frac{1}{q_0^2}\right)_{max}$, where $\left(\frac{1}{q_0^2}\right)_{max}$ is the ratio corresponding to the $G_f(\omega)$ maximum, is approximately twice as great as in a CCRL with a sign-constant sequence of numbers; however, this does not mean that, in all cases, the

dispersion of the rocket also will be greater since the transfer of the sign of the command is equivalent to an increase by a unit of the capacity of the code in a CCRL with a sign-constant sequence of numbers.

(3) When $\frac{1}{q_0^2} < \left(\frac{1}{q_0^2}\right)_{max}$ the fluctuations in a CCRL with a sign-variable sequence of numbers are considerably greater than in a CCRL with one sign-constant sequence of numbers.

(4) Opening of the rocket guidance circuit for the fluctuating components of the signal occurs at virtually the same values $\frac{1}{q_0^2}$ as for the constant component of the received commands. /480

(5) In order to decrease the influence of individual transmitted pulses and elimination of the random properties of conversion, it is necessary to take into account the recommendations given for a CCRL with a sign-constant sequence of numbers.

(6) With an increase of the number of channels N_k, the value $G_f(\omega)$ at the fixed frequency ω decreases.

When determining the spectral density $G_f(\omega)$ for a CCRL with two sequences of numbers, it is necessary to proceed as in study of a CCRL with one sign-variable sequence of numbers.

As a result of investigation of the derived computation formulas, it can be confirmed that the fluctuations in CCRL of the last two types, for the same interference level, are approximately identical for ratios $\frac{1}{q_0^2} > \left(\frac{1}{q_0^2}\right)_{max}$

However, in CCRL with two sequences of numbers, the maximum value $G_f(\omega)$ is somewhat smaller; this can be attributed to the transmission of a large number of pulses in the period T.

The qualitative character of the dependence of $G_f(0)$ on $\frac{1}{q_0^2}$ for all types of CCRL with pulse-code modulation, for a given value K_a, is the same as for CCRL with pulse-counting and pulse-phase modulation.

We note, in conclusion, that as a result of the usually insignificant discreteness of the dependence of $[\bar{K}_n]_c$ and $G_f(\omega)$ on K_a, when determining the

statistically equivalent filters for CCRL with pulse-code modulation, the step functions $[\bar{K}_n]_c = f_1(K_a)$ and $G_f(\omega) = f_2(K_a)$ should be replaced by continuous functions of the argument K_a, using well-known interpolation methods for this purpose.

CHAPTER 9. THE ROCKET AS AN OBJECT OF AUTOMATIC CONTROL. ROCKET AUTOMATIC PILOTS

9.1. Rocket Equations of Motion

The behavior of a rocket as an object of automatic control is characterized by a quite complex system of differential equations relating the change of the position of the control components to the parameters of rocket motion (angles of attack, pitching and banking, the value and direction of the velocity vector, etc.). /481

The complexity of the mathematical description of the spatial motion of the rocket and also the fact that, in many cases, the rocket is stabilized for banking and the control signals are transmitted through two independent channels make it desirable to divide spatial movement into two plane movements: longitudinal and lateral. Such a separation makes it possible to make a detailed analysis of control systems. In the final elaboration of a control system, it is necessary to analyze the spatial movement of the rocket, especially for the solution of problems involved in rocket stability and evaluation of the effect of radio interference. This can be attributed to the fact that with separation of general motion into two plane motions, it is possible to neglect cross connections between the course, pitching and banking channels which in actuality exist and sometimes exert an important influence on the character of motion of the rocket. We note that in the spatial motion of a rocket as an object of control, the rocket constitutes an apparatus with several inputs and outputs. The rocket inputs are the changes of position of its control components and the outputs are the parameters characterizing its motion.

The equations of longitudinal motion of a rocket can be obtained by assuming that its motion occurs in a vertical plane, that is, that the plane of symmetry of the rocket ox_1y_1 is vertical and its velocity vector v at all times remains in this vertical plane.

Figure 9.1 shows the position of the rocket in the vertical plane. /482 The figure also shows the forces acting on it in flight and the parameters characterizing its longitudinal motion.

The following notations are used in the figure: ox_1y_1 is the related coordinate system, oxy is the flow coordinate system, T_r is the thrust of the engine whose direction is assumed to coincide with the longitudinal axis of the rocket, Y is the lift, X is the force of head resistance, $G = mg$ is gravity, α is the angle of attack, ϑ is the pitching angle, and θ is the angle of inclination of the velocity vector.

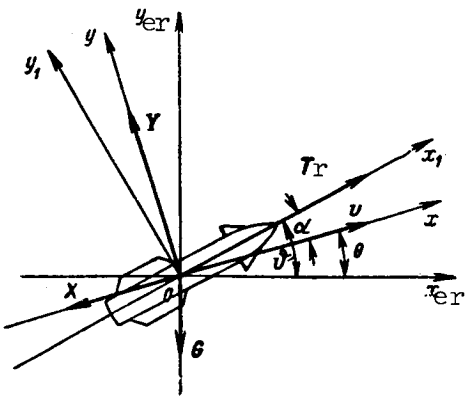

Figure 9.1

The angles ϑ and θ are read relative to the nonrotating coordinate system $ox_{er}y_{er}$, whose origin o is situated at the center of mass of the rocket; the axes are parallel to the corresponding axes of the ground coordinate system.

By projecting the forces G, X, Y and T_r onto the ox and oy axes of the flow coordinate system, we obtain the equation of longitudinal forces

$$m\dot{v} = T_r \cos \alpha - G \sin \theta - X \tag{9.1.1}$$

and the equation of normal forces

$$mv\dot{\theta} = T_r \sin \alpha - G \cos \theta + Y. \tag{9.1.2}$$

The equation of momenta relative to the lateral axis oz_1 has the form

$$J_{z1}\ddot{\vartheta} = M_{z1}. \tag{9.1.3}$$

Here J_{z1} is the moment of inertia of the rocket relative to the oz_1 axis, and M_{z1} is the sum of the momenta acting on the rocket.

In the three above equations, the unknowns are v, α, θ and ϑ. As the still lacking fourth equation we use an equation for the relationship between the angles

$$\vartheta = \theta + \alpha. \tag{9.1.4}$$

All the forces and momenta entering into equations (9.1.1), (9.1.2) and (9.1.3) can be expressed through the design elements of the rocket and the parameters of its flight regime.

The thrust T_r created by the jet engine of the rocket, in a general /483 case, represents a function of three arguments

$$T_r = T_r(v, p_0, t^\circ),$$

where p_0 is the atmospheric pressure, and t° is the temperature of the surrounding medium.

If the rocket has a jet engine, then, as is well known (ref. 13),

$$T_r = \frac{G_s}{g} w_a + F_a (p_a - p_0).$$

Here G_s is the fuel consumption per second, w_a is the escape velocity of the combustion products, F_a is the area of the exit section, and p_a - p_0 is the pressure difference in the exit section of the nozzle and in the atmosphere.

The lift Y and the head resistance X are determined by the formulas

$$Y = c_y \frac{\rho v^2}{2} S, \tag{9.1.5}$$

$$X = c_x \frac{\rho v^2}{2} S, \tag{9.1.6}$$

where $\frac{\rho v^2}{2}$ is the velocity head, S is the characteristic area (the area of the wing for rockets with plane symmetry and the midsection for axially symmetrical rockets), and c_y and c_x are the lift and head resistance coefficients, respectively.

For angles of attack α not exceeding 10-15°,

$$\left.\begin{aligned} c_y &\approx c_y^\alpha \alpha, \\ c_x &= \text{const}, \end{aligned}\right\} \tag{9.1.7}$$

where c_y^α is the derivative of the lift coefficient for an angle of attack not dependent on α.

Then

$$Y = c_y^{\alpha} \frac{\rho v^2}{2} S\alpha. \tag{9.1.8}$$

The total aerodynamic moment M_{z1} consists of the static, damping and active torques.

The static torque M_{α} is created by the lift effect. This torque characterizes the stability of the rocket relative to the angle of attack α. If the lift is applied behind the center of mass of the rocket, then $M_{\alpha} < 0$ and the rocket is stable. In actuality, with an increase of α, Y increases and as a result the rocket tends to turn in the direction of a decrease of the angle of attack. If $M_{\alpha} > 0$, which occurs in a case when Y is applied in front of the center of mass, the rocket is unstable. Rockets for which $M_{\alpha} = 0$ are called statically neutral. /484

The value of the static torque is determined by the formula

$$M_{\alpha} = -m_{\alpha} \frac{\rho v^2}{2} Sl, \tag{9.1.9}$$

where $m_{\alpha} = m_z^{\alpha}\alpha$ is the dimensionless coefficient of static longitudinal moment, and l is the characteristic dimension of the rocket (the mean aerodynamic chord of the wing for rockets with plane symmetry or the length of the fuselage for axially symmetrical rockets).

When the rocket rotates relative to the oz_1 axis, there will be a damping moment

$$M_{\dot{\vartheta}} = -m_{\dot{\vartheta}} \frac{\rho v^2}{2} Sl. \tag{9.1.10}$$

Here $m_{\dot{\vartheta}} = m_z^{\bar{\omega}_z} \frac{l}{v} \dot{\vartheta}$ is the dimensionless coefficient of the longitudinal damping moment.

This moment is primarily the result of a change of the angle of attack of the horizontal fins during the rotation of the rocket relative to the center of mass. Since the air medium hinders the rotation of the rocket, the damping moment is directed in the direction opposite the rotation.

The active torque created by turning of the control surfaces is

$$M_{\delta} = m_{\delta} \frac{\rho v^2}{2} Sl. \tag{9.1.11}$$

In this expression $m_\delta = m_z^\delta \delta_r$ is the dimensionless coefficient of the active torque and δ_r is the value of deflection of the control surface from a neutral position.

By substituting M_α, M_ϑ and M_δ into the right-hand side of equation (9.1.3), we obtain

$$J_{z1}\ddot{\vartheta} = -m_z^\alpha \frac{\rho v^2}{2} Sl\alpha - m_z^{\bar{\omega}_z} \frac{\rho v}{2} Sl^2 \dot{\vartheta} + m_z^\delta \frac{\rho v^2}{2} Sl\delta_r. \qquad (9.1.12)$$

Hence we obtain

$$\ddot{\vartheta} + a_\vartheta \dot{\vartheta} + a_\alpha \alpha = a_\delta \delta_r, \qquad (9.1.13)$$

where $a_\vartheta = \frac{m_z^{\bar{\omega}_z}}{J_{z1}} \frac{\rho v S l^2}{2}$ is the relative coefficient of aerodynamic damping,

$a_\alpha = \frac{m_z^\alpha}{J_{z1}} \frac{\rho v^2}{2} Sl$ is the relative coefficient of static stability, and /485

$a_\delta = \frac{m_z^\delta}{J_{z1}} \frac{\rho v^2}{2} Sl$ is the relative coefficient of efficiency of the control surface.

By substituting the values Y and X from expressions (9.1.8) and (9.1.6) into equations (9.1.1) and (9.1.2) and taking into account that the angle of attack does not exceed 10-15°, when $\sin\alpha \approx \alpha$ and $\cos\alpha \approx 1$, we rewrite the equations of longitudinal motion of the rocket

$$\left.\begin{aligned} m\dot{v} &= T_r - c_x \frac{\rho v^2}{2} S - G\sin\theta, \\ mv\dot{\theta} &= T_r \alpha + c_y^\alpha \frac{\rho v^2}{2} S\alpha - G\cos\theta, \\ \ddot{\vartheta} + a_\vartheta \dot{\vartheta} + a_\alpha \alpha &= a_\delta \delta_r, \\ \vartheta &= \theta + \alpha. \end{aligned}\right\} \qquad (9.1.14)$$

In equations (9.1.14) the values m, T_r, G, c_x, ρ, S, c_y^α, a_ϑ, a_α and a_δ, in a general case dependent on time, are considered known in the solution of the problem of rocket motion.

In these equations, the unknown variables are v, θ, ϑ and α. The angle of deflection of the control surface δ_r in the analysis of the dynamic properties of the rocket, as a link in the automatic control system, is given as an input action. In an investigation of the entire control circuit, δ_r also will

be an unknown value, determined by the parameters of the circuit and the conditions under which the rocket is used.

The first and second equations of system (9.1.14) describe the motion of the center of mass of the rocket and determine, respectively, the relationship between rocket velocity v and thrust T_r (velocity channel of the rocket) and the angle of inclination of the trajectory θ and the angle of attack α (inclination of the rocket velocity vector channel). The third equation of system (9.1.14) characterizes the angular motion of the rocket about its center of mass.

Motions of the rocket along the normal to the trajectory and its angular motions about its center of mass are of the greatest interest for an analysis of the control circuit because the control system regulates these specific parameters. For this reason, the first equation of system (9.1.14) will not be considered hereafter.

Introducing into the second equation of system (9.1.14) the notation

$$T_v = \frac{mv}{T_r + c_y^\alpha \frac{\rho v^2}{2} S}, \tag{9.1.15}$$

we obtain

$$T_v \dot{\theta} = \alpha - T_v \frac{g}{v} \cos\theta. \tag{9.1.16}$$

The second term on the right-hand side of equation (9.1.16) is for the gravitational effect. In the case of high flight velocities, the value of this term is small but it changes with a change of the angle θ. Since changes of $T_V \frac{g}{v} \cos\theta$ exert an insignificant influence on the character of the guidance process, hereafter we will assume this term to be constant and equal to its maximum value $A_0 = T_V \frac{g}{v}$. /486

The value T_V determines the rate of turning of the rocket for a particular angle of attack, thereby characterizing the maneuvering properties of the rocket. Because of this, T_V sometimes is called the aerodynamic time constant of the rocket.

In general, the value T_V is a function of time and the flight regimes of the rocket. However, changes of T_V in the course of guidance will be quite slow in comparison with the changes of the angles ϑ and α. Therefore, in many cases in the investigation of rocket motion the value T_V is "frozen," being considered constant for a particular flight regime.

Now we will transform the equation of moments (the third equation of the system (9.1.14), excluding the pitching angle $\vartheta = \theta + \alpha$ from it. Then

$$\ddot{\alpha} + \left(\frac{1}{T_v} + a_{\dot{\vartheta}}\right)\dot{\alpha} + \left(\frac{a_{\dot{\vartheta}}}{T_v} + a_\alpha - \frac{\dot{T}_v}{T_v^2}\right)\alpha = a_\delta(\delta_r + \delta_0). \tag{9.1.17}$$

Here $\delta_0 = \frac{a_{\dot{\vartheta}} g}{a_\delta v}\cos\theta + \frac{1}{a_\delta}\frac{d}{dt}\left(\frac{g}{v}\cos\theta\right)$ is the adjusting angle of the control surface, caused by the necessity for compensating gravity.

We introduce the notations

$$\omega_0^2 = \frac{a_{\dot{\vartheta}}}{T_v} + a_\alpha - \frac{\dot{T}_v}{T_v^2}, \tag{9.1.18}$$

$$2d\omega_0 = \frac{1}{T_v} + a_{\dot{\vartheta}}, \tag{9.1.19}$$

where ω_0 is the natural frequency of oscillations of the angle of attack, and d is the coefficient of attenuation of these oscillations.

In final form, equations (9.1.16) and (9.1.17) are written in the form

$$T_v\dot{\theta} = \alpha - A_0, \tag{9.1.20}$$

$$\ddot{\alpha} + 2d\omega_0\dot{\alpha} + \omega_0^2\alpha = a_\delta(\delta_r + \delta_0). \tag{9.1.21}$$

The derived equations can be used for constructing the block diagram of the rocket for its longitudinal motion.

In order to derive the transfer functions characterizing the lateral motion of the rocket, it is necessary to derive equations in the first approximation describing the motion of the rocket in a horizontal plane similar to what was done for longitudinal motion. The process of writing lateral motion equations has been described in detail in reference 7. For this reason, we will discuss only certain peculiarities of lateral motion of a rocket. These peculiarities arise because the process of control of lateral motion will not be identical for rockets with different aerodynamic properties. For example, in the case of rockets with axial aerodynamic symmetry, a change of flight direction is accomplished by deflection of the rudder δ_{rud} and the resulting formation of the angle of slip α_s. The appearance of the angle α_s leads to the creation of a lateral force which turns the velocity vector. In most cases, banking in such rockets is held close to zero ($\gamma_b = 0$) by ailerons. Under

/487

these conditions, it can be assumed that the lateral motion of the rocket consists of two independent motions: course motion and banking motion.

Course control of a rocket having plane aerodynamic symmetry by use of the rudder when $\gamma_b = 0$ is quite ineffective because the lateral force is created in this case only by the surfaces of the fuselage and the vertical fins so that its value will be extremely small in comparison with the lift.

Therefore, course control of a plane-symmetrical rocket is accomplished by changes of the banking angle, and the rudder is used for maintaining the angle of slip arising during rocket banking to a zero value (coordinated turning). Thus, in rockets with plane symmetry, the lateral force changing the flight direction is created by the horizontal component of lift appearing during banking of the rocket.

9.2. Rocket Block Diagrams

It was mentioned before that the coefficients entering into equations (9.1.20) and (9.1.21) are dependent on time and on the flight regime of the rocket. In constructing a block diagram, it is customary to apply to it the principle of "freezing" of the coefficients. This simplifies the problem of investigation of the system of equations. Such an investigation naturally can give only an approximate idea of the behavior of a rocket during its guidance to a target.

Writing equations (9.1.20) and (9.1.21) in symbolic form, we obtain

$$T_v D\theta = \alpha - A_0, \tag{9.2.1}$$

$$(D^2 + 2d\omega_0 D + \omega_0^2)\alpha = a_\delta(\delta_r + \delta_0). \tag{9.2.2}$$

Figure 9.2 shows a block diagram constructed on the basis of equations (9.2.1) and (9.2.2). Figure 9.2 shows that the block diagram of a rocket moving in a vertical plane consists of oscillatory and integrating links. The oscillatory link with the transfer function /488

$$W_{\frac{\alpha}{\delta_r}}(D) = \frac{\alpha(t)}{\delta_r(t)} = \frac{a_\delta}{D^2 + 2d\omega_0 D + \omega_0^2} \tag{9.2.3}$$

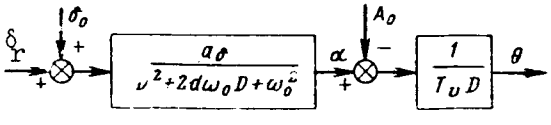

Figure 9.2

establishes the relationship between the angle of attack α and the deflection of the elevator δ_r, and the integrating link having the transfer function

$$W_{\frac{\theta}{\alpha}}(D)=\frac{\theta(t)}{\alpha(t)}=\frac{1}{T_v D}, \tag{9.2.4}$$

relates the change of the angle of inclination of the trajectory θ to the deflection of the angle of attack α.

Using equations (9.2.3) and (9.2.4) and taking into account the relationship between the angles $\vartheta = \theta + \alpha$, it is easy to obtain the transfer functions of the rocket $W_{\frac{\theta}{\delta_r}}(D)$ and $W_{\frac{\vartheta}{\delta_r}}(D)$ relating the angle of deflection of the control surface to the angle of inclination of the trajectory θ and the pitching angle ϑ

$$W_{\frac{\theta}{\delta_r}}(D)=\frac{\theta(t)}{\delta_r(t)}=\frac{k_{V_r}\omega_0^2}{D\left(D^2+2d\omega_0 D+\omega_0^2\right)}, \tag{9.2.5}$$

$$W_{\frac{\vartheta}{\delta_r}}(D)=\frac{\vartheta(t)}{\delta_r(t)}=\frac{(T_v D+1)\,k_{V_r}\omega_0^2}{D\left(D^2+2d\omega_0 D+\omega_0^2\right)}. \tag{9.2.6}$$

where $k_{V_r}=\frac{a_\delta}{T_v\omega_0^2}$ is the "gain coefficient" of the rocket for the pitching channel and has the dimensionality 1/sec.

The presence of the factor D in the denominator of the transfer functions (9.2.5) and (9.2.6) indicates the integrating properties of the rocket as an object of control in relation to flight direction, characterized by the angle θ and the position of its longitudinal axis ϑ. In particular, this means that with deflection of the control surface by a constant angle, the direction of flight will change continuously. In a steady-state regime, that is, after attenuation of transient processes caused by the factor enclosed in parentheses, the value θ will change proportional to the time elapsing from the time of deflection of the control surface. If the control surface now is returned to its initial (zero) position, the new steady-state value θ will differ from its initial value.

It sometimes is desirable to have the available normal accelerations $j_n = v\dot{\theta}$ as an output parameter. The transfer function $W_{\frac{j_n}{\delta_r}}(D)$, relating j_n to deflections of the control surface, has the form /489

$$W_{\frac{j_n}{\delta_r}}(D)=\frac{v k_{V_r}\omega_0^2}{D^2+2d\omega_0 D+\omega_0^2}. \tag{9.2.7}$$

The value vk_{V_r} is called the controllability of the rocket. It shows by how many times normal acceleration changes with deflection of the control surface by one radian. It should be noted that the controllability of the rocket is dependent on its velocity.

The transfer functions of an axially symmetrical rocket, characterizing the changes of its course during lateral motion, will be similar in form to the transfer functions for longitudinal motion.

For example, the transfer function $W_{\frac{\psi}{\delta_{rh}}}(D)$, relating the angle of yawing (course) of the rocket ψ to the deflection of the rudder δ_{rh} has the form

$$W_{\frac{\psi}{\delta_{rh}}}(D) = \frac{(T_{vh}D + 1)\, kV_{rh}\, \omega_{0h}^2}{D\left(D^2 + 2d_h\omega_{0h}D + \omega_{0h}^2\right)}, \tag{9.2.8}$$

and the transfer function $W_{\frac{\alpha_s}{\delta_{rh}}}(D)$, establishing the relationship between the angle of slip α_s and the change of the angle δ_{rh}, is expressed by the formula

$$W_{\frac{\alpha_s}{\delta_{rh}}}(D) = \frac{a_{\delta h}}{D^2 + 2d_h\omega_{0h}D + \omega_{0h}^2}. \tag{9.2.9}$$

The subscript "h" on the coefficients of the transfer functions (9.2.8) and (9.2.9) indicates that these coefficients were computed for the motion of the rocket in a horizontal plane. For rockets with cruciform wings, they do not differ, for all intents and purposes, from the coefficients of the transfer functions for longitudinal motion. Comparing formulas (9.2.3), (9.2.9) and (9.2.7), (9.2.8), it is easy to note that the angle ψ of lateral motion corresponds to the pitching angle ϑ in longitudinal motion and the angle α_s to the angle α. Therefore, the angle of inclination of the trajectory $\theta = \vartheta - \alpha$ will correspond to the angle $\theta_h = \psi - \alpha_s$, characterizing the direction of flight in a horizontal plane. The transfer function of a rocket with the output coordinate θ_h is similar to expression (9.2.5). The same can be said with respect to the transfer function for normal acceleration.

We note that, whereas the factor D in the denominator of (9.2.6) is obtained on the assumption of a constancy of rocket flight velocity, the similar factor in (9.2.8) is caused by the property of neutrality of the rocket /490

in relation to the angle ψ. In particular, this means that if the rocket is deflected from its initial course under the influence of external perturbations, after the cessation of their effect the initial course is not restored.

The banking channel for the considered type of rocket is autonomous in relation to the principal control channels. The transfer function establishing the dependence of the banking angle γ_b on the angle of deflection of the ailerons δ_a has the form

$$W_{\frac{\gamma}{\delta_a}}(D)=\frac{\gamma_b(t)}{\delta_a(t)}=\frac{k_\gamma}{D(T_\gamma D+1)}, \qquad (9.2.10)$$

where k_γ is the "gain coefficient" of the rocket for the banking channel, and T_γ is the time constant of the rocket for the banking channel.

The values k_γ and T_γ are expressed through the aerodynamic moments and the moment of inertia of the rocket relative to the ox_1 axis in the following way

$$k_\gamma=\frac{M_x^{\delta_a}}{M_x^{\omega_x}}, \quad T_\gamma=\frac{J_{x1}}{M_x^{\omega_x}},$$

where $M_x^{\omega_x}$ is the derivative of the damping moment for the angular velocity of banking, $M_x^{\delta_a}$ is the derivative of the torque created by the ailerons, and J_{x1} is the moment of inertia of the rocket relative to the ox_1 axis.

On the basis of expressions (9.2.8), (9.2.9) and (9.2.10), it is easy to construct block diagrams reflecting the process of lateral motion of an axially symmetrical rocket.

The lateral motion of a rocket with plane aerodynamic symmetry is described by two transfer functions. One of them $W_{\frac{\gamma}{\delta_a}}(D)$ relates the angle of deflection of the ailerons δ_a to the banking of the rocket γ_b, the other $W_{\frac{\psi}{\gamma}}(D)$ relates the angle γ_b to the yawing angle ψ. The expression for the first transfer function was obtained earlier (9.2.10).

The second transfer function is equal to (ref. 7)

$$W_{\frac{\psi}{\gamma}}(D)=-\frac{\psi(t)}{\gamma_b(t)}=\frac{g}{v_h D}. \qquad (9.2.11)$$

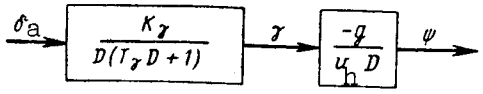

Figure 9.3

We note that the minus sign in formula (9.2.11) is caused by the rule of taking into account the signs of the angles. The angle ψ is considered positive when the turning of the axis of the rocket is to the left and the angle of banking γ_b is to the right.

The block diagram of the lateral motion control channel for a rocket with plane aerodynamic symmetry is shown in figure 9.3. The transfer function for lateral motion of the rocket $W_{\frac{\psi}{\delta_a}}(D)$ is equal to /491

$$W_{\frac{\psi}{\delta_a}}(D) = \frac{\psi(t)}{\delta_a(t)} = \frac{-k_\gamma \frac{g}{v_h}}{D^2(T_\gamma D + 1)}. \qquad (9.2.12)$$

We note in conclusion that the angle ψ in formulas (9.2.11) and (9.2.12) indicates both the direction of the longitudinal axis of the rocket and the direction of its flight in a horizontal plane, since it was assumed that $\alpha_s = 0$.

9.3. Functional Diagram of the Automatic Pilot

The automatic pilot is part of a control system whose elements are related directly to the control components of the rocket. It is designed for stabilization of the angular motions of the rocket relative to the center of mass and the control of the motion of the center of mass itself in accordance with the commands arriving from the radio apparatus aboard the rocket.

The rocket is a relatively complex object of automatic control. Effective control in a dynamic system such as a rocket is possible only when there is a high perfection of the controller, whose role is performed by the automatic pilot and electronic apparatus.

The most important characteristics of a rocket as an object of control are stability, characterized by its capability of returning to the initial flight regime after termination of a perturbation, and controllability, determined by the reaction of the rocket to the controlling signal. In a certain sense the requirements on the stability and controllability of a rocket are contradictory. For example, an attempt to increase the reserve of stability of the rocket due to a change of its aerodynamic characteristics frequently is reflected unfavorably in controllability and vice versa. Therefore, an increase of rocket stability with respect to certain parameters and the introduction of the necessary damping (when the damping of the rocket is small)

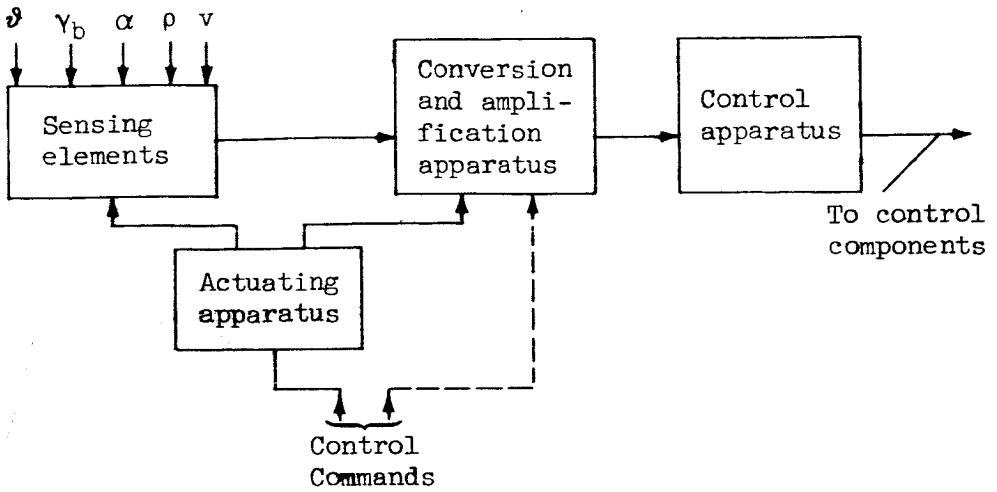

Figure 9.4

can be brought about artificially--by introducing additional signals into the control command. These signals are proportional to those parameters of motion of the rocket which exert an influence on rocket stability and ensure the attenuation of transient processes. These additional signals are formed /492 by the set of measuring instruments included in the automatic pilot.

In addition, the automatic pilot includes measuring instruments producing signals used for stabilization of the rocket in its angular motions if such stabilization is necessary. Thus, for example, in the case of guidance of an axially symmetrical rocket from a control point, it should be stabilized for banking because its rotation around its longitudinal axis will lead to disruption of matching of the axes of the command and control coordinate systems, which in turn causes a disruption of the guidance process.

The automatic pilot of a rocket, whose functional diagram is shown in figure 9.4, includes sensing elements, conversion-amplification apparatus, control apparatus (control surface mechanisms) and master controls. The sensing elements of the automatic pilot are used in measuring the necessary parameters of motion of the rocket and forming additional control signals. The conversion-amplification apparatus converts the measured values, sums them and amplifies them, thereby forming controlling signals which are fed to the control apparatus. The control apparatus acts on the control surfaces of the rocket.

Command signals from the output of the radio apparatus aboard the rocket are fed either to the actuating mechanisms, which under their influence change the tuning of the measuring system of the sensing elements, or are fed directly to the conversion-amplification apparatus. In addition, the actuating mechanisms are used for introducing programmed signals and commands. Each automatic pilot usually has three control channels: pitching, course and banking.

A special requirement imposed on the automatic pilot, related to its use in an object of one-time operation, is a requirement on the reliability and simplicity of its operation. The number and character of the group of sensing elements, being the most complex and precise part of the automatic pilot, are determined by the types of problems to be solved and should facilitate the attainment of the stipulated quality of control of the rocket-automatic pilot system. /493

9.4. Sensing Elements of the Automatic Pilot

Position and velocity gyroscopes, linear acceleration sensors (accelerometers) and instruments for measuring velocity head are used as the sensing elements of automatic pilots in most cases.

A position (three-power) gyroscope is used for measurement of the angular deflections of a rocket relative to some fixed frame of reference (fig. 9.5). The gyroscope rotor 1 is attached in two frames 2 and 3 of a gimbal suspension having free rotation relative to the axes $o_m x_m$ and $o_m z_m$. The rotor rotates with the angular velocity Ω_h relative to the $o_m y_m$ axis, called the main axis of the gyroscope.

The use of a position gyroscope as a measuring instrument is based on the property of stability of its main axis in the absence of external moments so that the position of the main axis can be used as the origin of some coordinate system.

If such a gyroscope is installed on a rocket, its turning in space leads to a turning of the main axis of the gyroscope relative to the body of the rocket. Depending on the position of the gyroscope axes relative to the axes of the related coordinate system, a position gyroscope can be used for measurement of the course, pitching or banking angles. Accordingly, such gyroscopes are called course, pitching or banking gyroscopes.

In order to obtain an instrument analog of the measured angle, the gyroscope is connected to some kind of pickup. These can be of various types (potentiometric, capacitive, inductive, etc.). Figure 9.5 shows a banking gyroscope with a potentiometric pickup. The body 4 of the potentiometric pickup is connected to the body of the rocket and the slide 5 is connected to the $o_m x_m$ axis of the outer frame of the gyroscope. Prior to launching of the rocket, the gyroscope is locked in such a position that the directions of its axes coincide with the directions of the axes of the related coordinate system; the $o_m x_m$ axis is directed along the longitudinal axis of the rocket. In this case, a zero voltage is fed from the potentiometric pickup. At the time of rocket launching, the gyroscope is unlocked. If the rocket assumes some banking angle γ_b relative to its position corresponding to the time of the launching, the potentiometer slide is moved relative to its body. The voltage /494

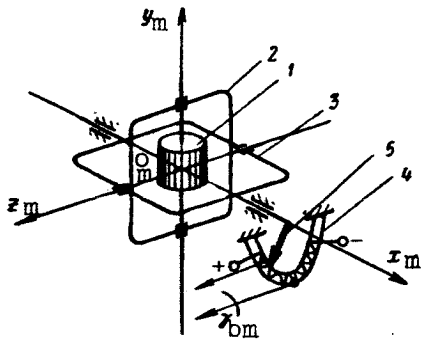

Figure 9.5

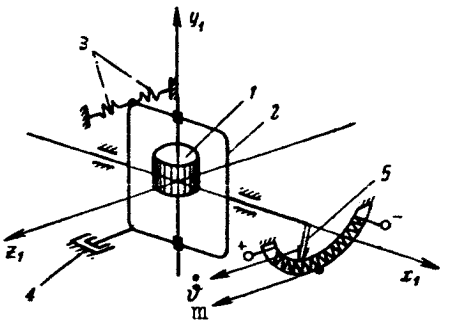

Figure 9.6

from the potentiometer in a steady-state regime will be proportional to the angle γ_b. Banking and yawing gyroscopes are designed in a similar way.

If the rocket flight continues for a considerable time, there will be appreciable departures of the main axis of the gyroscope caused by various perturbing moments. In order to decrease these departures, the position gyroscope is supplied with a correction system which returns the main axis to the required position.

Henceforth the position gyroscope, as an angle-measuring instrument, will be characterized by the transfer coefficient k with a subscript for the angle which it measures.

A velocity (two-power) gyroscope is designed for measurement of the angular velocities of the rocket relative to the related axes ox_1, oy_1, oz_1.

Figure 9.6 is a diagram of a velocity gyroscope. The rotor 1 of the gyroscope rotates around the axis oy_1, attached to the frame 2. The axes of rotation

of the rotor and frame of the gyroscope are perpendicular to that axis of the rocket relative to which its angular velocity is measured. The gyroscope shown in figure 9.6 is designed for measurement of the angular velocity of pitching of the rocket. With the turning of the rocket about the axis oz_1

with an angular velocity $\dot{\vartheta}$ a gyroscopic moment develops which tends to turn the frame and the rotor relative to the ox_1 axis. The value of this moment is

proportional to the angular velocity $\dot{\vartheta}$ and the sign is dependent on the direction of rotation.

The gyroscope frame begins to experience precession under the influence of the applied moment. The spring 3 counteracts the precession of the gyroscope. With the deformation of the spring, a counteracting moment develops which is proportional to the angle of deflection of the frame, which equalizes the gyroscopic moment. When these moments are equalized, there will be no further motion of the frame. Therefore, the angle by which the gyroscope

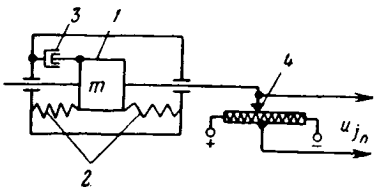

Figure 9.7

frame is deflected will be proportional to the angular velocity of rotation of the rocket. The damper 4 is used for damping the possible oscillations of the system. A voltage proportional to the angular velocity of the rocket is fed from the pickup 5.

The linear accelerations or overloads acting on the rocket are measured by linear acceleration pickups--accelerometers. The design and circuitry of /495 accelerometers can be quite different. Figure 9.7 is an example of a linear acceleration pickup whose principle of operation is based on the change of the position of a weight, balanced by a spring, under the influence of the external medium. The weight 1 of the mass m is balanced by the spring 2. The weight is moved under the influence of the applied weight. The movement of the weight counteracts the spring and it is stopped when the force of the counteraction of the spring becomes equal to the external force. Thus, for a given mass of the weight m its deflection from a mean position will be proportional to the effective force and therefore to the acceleration developed by the rocket in the direction of movement of the weight. The mentioned displacement is measured by the pickup 4. The damper 3 is used for eliminating oscillation of the weight. The accelerometer is placed on the rocket in such a way that the direction of movement of the weight coincides with that axis of the rocket along which acceleration is measured.

The voltage measured by the pickup in a steady state will be

$$u_{jn} = k_a j_n$$

where $k_a = \frac{k_{tr} c}{m}$ is the transfer constant of the accelerometer, k_{tr} is the transfer ratio of the pickup, c is the stiffness of the spring, and m is the mass of the weight.

Since normal acceleration j_n is related to the overload n by the following dependence $n = \frac{j_n}{g}$, it can be said that the accelerometer measures the overloads acting on the rocket. If the measurement axis of the accelerometer lies in the plane of operation of an aerodynamic force, such as lift, it is easy to

show that in the case of small angles of attack and a constant rocket velocity the accelerometer readings will be proportional to these angles of attack.

9.5. Automatic Pilot Control Apparatus

In the classification of control apparatus, it is customary to take into account the form of energy which is used for movement of the control components. On the basis of this criterion, it is possible to distinguish the following types of control apparatus:

(1) pneumatic;
(2) hydraulic;
(3) electrical, divided in turn into electric motor and electromagnetic.

The selection of the type of control apparatus is determined by the /496
required power of the control components, the admissible values of signal delay in the control surfaces channel, the type of current available aboard the rocket, the flight duration of the rocket, etc.

A pneumatic control apparatus is of relatively small size and weight but its use involves expenditure of a large quantity of compressed gas. Such a drive, therefore, can be used in rockets of a relatively short effective range. The compressed gas is fed either from cylinders carried aboard the rocket or it can be obtained from a separate, slowly burning cordite charge which is ignited at the time of rocket launching.

A hydraulic control apparatus has a shorter lag in producing a controlling signal and is capable of overcoming great loads. However, the weight of a hydraulic system exceeds the weight of a pneumatic system.

Electrical control apparatus is quite general-purpose in use and is characterized by simplicity of the channelization of the energy fed to it. At the same time, its use on a rocket requires the presence there of a quite powerful current source.

A hydraulic control apparatus, shown diagrammatically in figure 9.8, combines a hydraulic amplifier and an actuating element (servomotor). The working fluid is fed under pressure into channel 1. If the position of the valve 2 is such that both entrances of the channel 3 of the working cylinder are shut off, the piston 4 and the output rod will be fixed in position. With displacement of the valve to the left of its initial position, the working fluid will be fed under pressure into the channel 5 and then into the left cavity of the working cylinder. The right cavity of the working cylinder in this case will communicate with the drain channel 6. Due to the pressure difference, the working cylinder together with the output rod will be moved to the right. If the valve is displaced to the right of its initial position, the working fluid will be fed under pressure through the channel 7 into the right cavity of the working cylinder. The piston together with the rod will move to the left. The /497
rod control of the valve mechanism is accomplished by use of an electromagnet

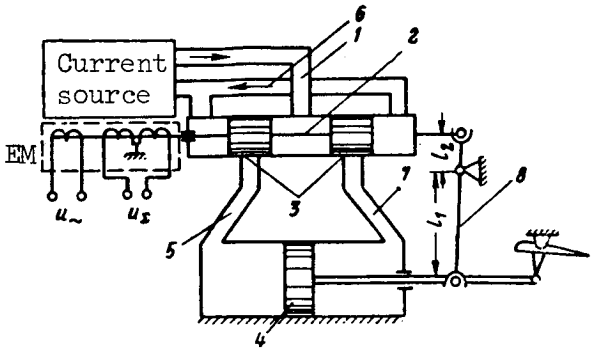

Figure 9.8

EM which has two windings. A controlling voltage u_Σ is fed to one of the windings. The second winding is used for decreasing the zone of stagnation of the drive characteristic. This winding is fed an alternating voltage of small amplitude. Under the influence of this voltage, the valve undergoes small oscillations. Such an apparatus improves the linearity of the drive.

In order for the deflection of the rod of the working piston to be proportional to the controlling voltage, a rigid feedback is introduced into the apparatus. Such a feedback can be designed, in particular, in the form of a lever transmission 8, connecting the output rod to the body of the valve mechanism. With displacement of the valve to the right, the piston begins to move to the left. Movement of the piston and rod by the lever causes movement of the body of the valve to the left. This movement will continue until the entrances are again covered. Movement in the system ceases.

If the feedback is eliminated, with certain simplifying assumptions, the considered servodrive is equivalent in its dynamic properties to an integrating link (ref. 30). This means that the rate of movement of the working rod $\dot{x}_{rod}$ will be proportional to the linear displacement of the valve x_{val}, that is

$$\dot{x}_{rod} = k_{hy} x_{val}, \tag{9.5.1}$$

where k_{hy} is the proportionality factor determined for the most part by the design of the hydraulic amplifier.

The transfer function $W_{hy}(D)$ of the servodrive without a feedback will be equal to

$$W_{hy}(D) = \frac{x_{rod}}{x_{val}} = \frac{k_{hy}}{D}. \tag{9.5.2}$$

When a rigid negative feedback with the transmission ratio $i = \frac{l_1}{l_2}$ is used with the mentioned link, it is transformed into an inertial link with the transfer function

$$F_1(D) = \frac{W_{hy}(D)}{1 + W_{hy}(D)} = \frac{k_1}{T_{dr}D + 1}, \qquad (9.5.3)$$

where

$$k_1 = \frac{1}{i}; \quad T_{dr} = \frac{1}{k_{hy}i}.$$

We will assume that the movement of the valve x_{val} is related linearly to the controlling voltage u_Σ, that is, $x_{val} = k_{val}u_\Sigma$, and the angle of deflection of the control surface δ_r is proportional to the movement of the working rod, that is, $\delta_r = k_{rod}x_{rod}$. Then the transfer function of the control sur- /498 face drive with a control surface apparatus of the hydraulic type can be written as

$$F(D) = \frac{\delta_r}{u_\Sigma} = \frac{k_{dr}}{T_{dr}D + 1}, \qquad (9.5.4)$$

where $k_{dr} = k_1k_{val}k_{rod}$ is the transfer constant of the drive.

The apparatus for pneumatic drive of the control components of the rocket in many respects resembles the hydraulic servomotor considered above. As the amplifiers in this case, choke-coupled and jet amplifiers are used. Since the diagram of a pneumatic servomotor with a choke-coupled amplifier is virtually the same as the diagram for the earlier discussed hydraulic servomotor (fig. 9.8), as an example, we will consider a servodrive with a jet amplifier. Such amplifiers are used in systems operating at relatively low pressure.

Figure 9.9 is a diagram of this drive. The jet tube 1 is rotated about the axis o by the electromagnet EM to which is fed a controlling signal u_Σ and a feedback signal. In the absence of the mentioned signals, the jet tube is set precisely at the midpoint between the inlets of the receiving channels 2 and 3 by means of the springs S_1 and S_2. In this case, the pressure in the right and left cavities of the pressure cylinder will be identical and the piston 4 will remain fixed.

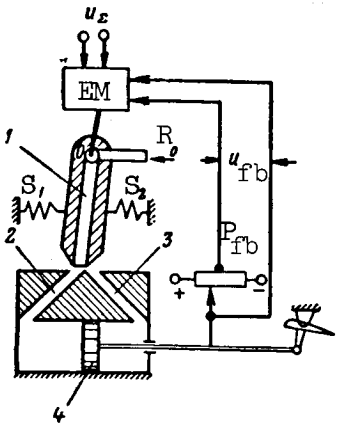

Figure 9.9

With the turning of the jet tube under the influence of a controlling cylinder, more compressed gas will be fed into one cavity of the pressure cylinder from the nozzle of the jet tube than into the other. The developing pressure drop causes movement of the piston and of the working rod. The rod is connected to the control surface and to the slide of the feedback potentiometer P_{fb}. The feedback voltage u_{fb} is fed to the winding of the feedback of the electromagnet EM, wound opposite to the turns of the controlling signal winding. When the total ampere turns become equal to zero, the jet tube is set in the initial position and the piston no longer moves.

It can be shown that the dynamic properties of the considered drive also are described by the transfer function of an inertial link similar to (9.5.4). The transfer constant of the drive k_{dr} and its time constant T_{dr} are determined by the particular design of the pneumatic engine. /499

The actuating mechanism of the electric motor drive is a dc or ac motor. As a power amplifier the dc motor uses electrical and relay amplifiers. For amplification of the power in an ac drive, it is more convenient to use magnetic amplifiers.

The functional diagram of a dc electric motor drive is shown in figure 9.10. The controlling voltage u_Σ is fed to the power amplifier PA and then to the armature of the motor M which is connected through the reducer Red to a control surface and the feedback potentiometer P_{fb}. The feedback voltage u_{fb} is subtracted from the controlling voltage and therefore, in a stationary regime, the angle of deflection of the control surface will be proportional to the controlling signal u_Σ. If it is assumed that the transfer function of the motor is expressed by the formula

$$W_M(D) = \frac{k_M}{D(TD+1)}. \qquad (9.5.5)$$

where k_M is the transfer constant of the motor, T is the time constant of the motor, and the remaining elements of the drive are inertialess, the transfer function of the drive is written as

$$F(D) = \frac{\delta_r}{u_\Sigma} = \frac{k_1}{TD^2 + D + k_2} \qquad (9.5.6)$$

Here $k_1 = k_{PA}k_M k_{Red}$ is the amplification factor of the open drive system, k_{PA} is the transfer constant of the power amplifier, k_{Red} is the transfer constant of the reducer, $k_2 = k_1 k_{fb}$ is the feedback amplification factor, and k_{fb} is the transfer constant of the feedback potentiometer.

In the case of a small time constant T of the motor, when the condition $Tk_2 \ll 1$ is satisfied, the electric motor drive in its dynamic properties is equivalent to an inertial link with the transfer function /500

$$F(D) = \frac{\delta_r}{u_\Sigma} = \frac{k_{dr}}{T_{dr}D + 1}, \qquad (9.5.7)$$

where $k_{dr} = \frac{k_1}{k_2}$ is the transfer constant of the control surface channel, and $T_{dr} = \frac{1}{k_2}$ is the time constant.

An electromagnetic drive is used on rockets where the control components are spoilers. Figure 9.11a shows the diagram of an electromagnetic actuating apparatus. The spoilers Sp_1 and Sp_2 are rigidly connected to the armature Arm of the electromagnets EM_1 and EM_2. If the drive circuit is de-energized, the armature is held in a neutral position by springs. Bipolar voltage pulses u_p

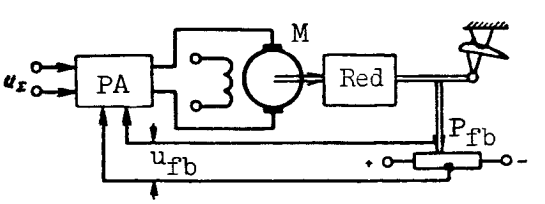

Figure 9.10

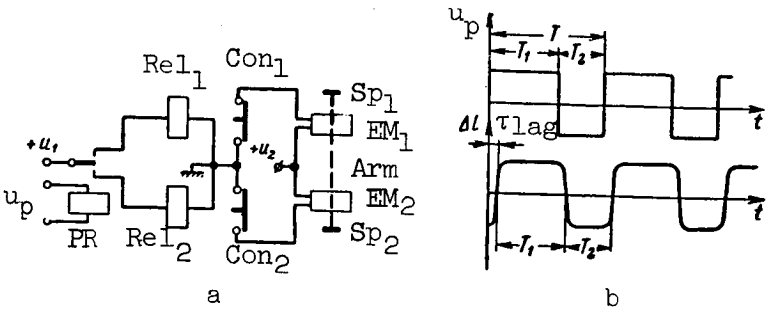

Figure 9.11

(fig. 9.11b) are fed to the winding of the polarized relay PR. These pulses control the position of the polarized relay armature. In the case of a positive voltage wave the armature of the PR relay is thrown upward and the contacts Con_1 of the power relay Rel_1 are triggered. As a result, a current is fed to the winding of the electromagnet EM_1 and the spoiler plate is moved upward. In the case of a negative wave of controlling voltage, the armature of the relay PR moves onto the lower contact, triggers the power relay Rel_2 and through its contacts Con_2 the winding of the electromagnet EM_2 is cut in. The spoiler plate moves into the lower position.

The law of movement $\Delta l = \Delta l(t)$ of the spoilers is illustrated in figure 9.11b. It can be seen from the time diagram that the pulses $\Delta l(t)$ differ from square pulses. This can be attributed to the influence of considerable inductance of the windings of the electromagnets. However, if the duration of the shortest pulse at the input of the polarized relay exceeds the triggering time of the electromagnet, the resulting durations of positive and negative pulses $T_{1\sim}$ and $T_{2\sim}$ (fig. 9.11b) are approximately equal to T_1 and T_2, respectively. Since the polarized relay, power relays and electromagnets are not triggered instantaneously, there is a lag τ_{lag} between the controlling voltage fed to the drive and the deflections of the spoiler. /501

Applied to the considered type of control components, we introduce the concept of mean deflection of the spoilers, expressed by the formula

$$\delta_{mean} = \delta_m \frac{T_{1\sim} - T_{2\sim}}{T}, \qquad (9.5.8)$$

where δ_m is the maximum deflection of the spoiler plate.

If it is assumed that the input of the drive apparatus is fed the command $K(t) = T_1 - T_2$, taking into account the lag of operation of the control components of the rocket in comparison with the output signals, we obtain

$$\delta_{mean} = \frac{\delta_m}{T} K(t - \tau_{lag}). \tag{9.5.9}$$

The value of the lag τ_{lag} is determined by the type and design of the relays and electromagnets used. In many cases, in an approximate analysis, the lag τ_{lag} is not taken into account. Then the actuating apparatus will be characterized by the transfer constant

$$k_{dr} = \frac{\delta_m}{T}. \tag{9.5.10}$$

In a case when spoilers are used the controlling voltage is applied in the form of a slowly changing function of time; it must be converted into bipolar pulses of the duration T_1 and T_2.

9.6. Actuating Apparatus of the Automatic Pilot

In most cases, the actuating apparatus in the automatic pilot of an aircraft plays an auxiliary role. In the automatic pilots of rockets, it is of extremely great importance due to the complete automation of flight control. The actuating apparatus is designed for change of the flight regime in accordance with a prestipulated program or in conformity to controlling signals fed from the output of the electronic apparatus carried aboard the rocket.

The simplest programming apparatus cuts in and cuts out the individual components of the apparatus aboard the rocket upon completion of a definite, preset time. It consists of a timing mechanism and cam gears with contact groups. The timing mechanism usually used is an electric motor with a stabilized rate of rotation.

A more complex actuating apparatus performs reorganization of the automatic pilot for the purpose of changing the flight regime of the rocket. As /502 an example, we will consider the programming apparatus for changing the angle of pitching of a ballistic rocket (ref. 4). The slide of the potentiometer of the base mechanism 2 (fig. 9.12) is attached to the gyroscope 1. In the initial position (in the case of vertical launching) the slide is situated opposite the midpoint of the potentiometer and the voltage fed from it is equal to zero.

The position gyroscope is oriented in such a way that its measurement axis coincides with the longitudinal axis of the rocket. If for any reason the

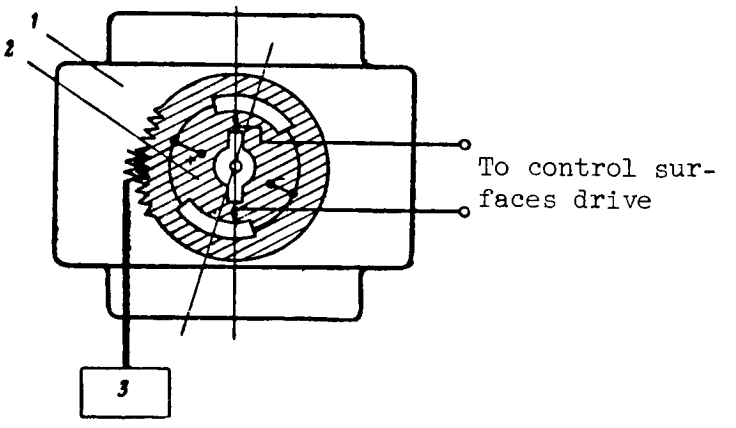

Figure 9.12

longitudinal axis of the rocket is deflected from its initial (vertical) position, a mismatch voltage is formed between the houding of the potentiometer (related to the position of the longitudinal axis of the rocket) and its slide. After amplification, this voltage is fed to the control surfaces drive. The control surfaces are deflected in such a way that the longitudinal axis of the rocket returns to its initial position.

After some time, the motor of the programming apparatus 3 begins to turn the base which supports the potentiometer housing at a fixed velocity relative to the body of the rocket. This causes formation of a mismatch signal which, when fed to the control surfaces, causes the longitudinal axis of the rocket to begin to turn relative to the initial position at approximately the same velocity.

If the angular position of the rocket relative to some fixed direction should be changed not in conformity to a program, but in accordance with commands formed by the control system, a similar base mechanism can be used for returning the measuring system of the sensing element. However, in this case, the turning of the base should be accomplished by a motor which is controlled by the formed commands, rather than by a timing mechanism.

9.7. Rocket Banking Control Channel

In the guidance process, as a result of the effect of different random perturbations, there can be changes of the angular position of the rocket relative to its center of mass. It is quite probable that there will be rotation of the rocket about its longitudinal axis because the moment of inertia relative to this axis is relatively small. /503

In the case of the rotation of an axially symmetrical rocket about its longitudinal axis in some control systems, such as beam-riding guidance or a command control system, there will be a change in the operation of the control

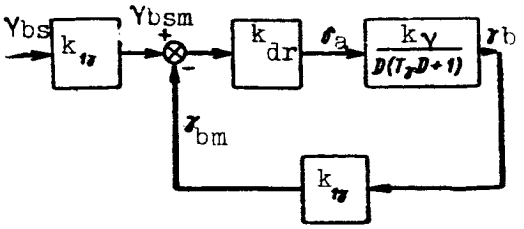

Figure 9.13

surfaces: the rudder begins to perform the function of the elevator and vice versa. Therefore, steps must be taken to ensure the normal controllability of the rocket during the entire time of its flight. Stabilization apparatus preventing the rotation of the rocket about its longitudinal and lateral axes and apparatus ensuring the introduction of corrective signals to the control surfaces with a change in the direction of their control planes are used for this purpose.

Next, for the sake of brevity, we will refer to the first group of apparatus as apparatus for stabilization of the axes of a rocket in space, and the second group will be referred to as apparatus with automatic change of operation of the control surfaces. In axially symmetrical rockets, the lateral stabilization systems usually are autonomous in relation to systems for control of the position of the center of mass of the rocket.

With respect to rockets with plane aerodynamic symmetry, when the control of the lateral motion of the center of mass of the rocket is accomplished by banking, the lateral stabilization is necessary so that the banking angle will change in conformity to a law determined only by the controlling signals.

Figure 9.13 is the block diagram of a system for control of banking. The deviation of the banking angle from the stipulated value γ_{bs} is fixed by a sensing element; a banking position gyroscope (gyro-vertical) is used for this purpose. The transfer constant of the measuring instrument, relating the actual value of the banking angle γ_b to its measured value γ_{bm}, will be denoted k_{1_γ}. In addition, we will assume that the inertia of the drive of the ailerons can be neglected in comparison with the inertia of determination of the banking angle of the rocket itself, that is, in the earlier derived formulas for the transfer functions of actuating apparatus of different types, we assume $T_{dr} = 0$, and the conversion properties of the drive will be characterized by the transfer coefficient k_{dr}.

In the regime of control of banking, the stipulated value γ_{bsm}, rep- /504 presented in the form of a voltage or the angle of rotation of the base of the actuating apparatus, is changed in conformity to the change of the control

commands. In the regime of stabilization of banking, this value remains constant and is proportional to the value of the angle of banking γ_{bs} which the rocket had at the time of unlocking of the position gyroscope if the latter does not have correction of the vertical. When there is such a correction γ_{bs} will be equal to zero.

The transfer function of the channel for control of banking $W_{\frac{\gamma_b}{\gamma_{bs}}}(D)$, relating the stipulated value of the angle of banking to its true value, will be equal to

$$W_{\frac{\gamma_b}{\gamma_{bs}}}(D) = \frac{k_{dr} k_\gamma k_{1\gamma}}{T_\gamma D^2 + D + k_{dr} k_\gamma k_{1\gamma}}. \qquad (9.7.1)$$

It follows from formula (9.7.1) that the system for stabilization of banking, together with the rocket, forms an oscillatory link. The process of setting the banking angle of the rocket occurs in the following way. With deflection of the banking angle γ_b from the stipulated value, a difference signal $\gamma_{bsm} - \gamma_{bm}$ appears at the summer output; after amplification, this difference signal is fed to the control surfaces mechanism. The control surfaces mechanism deflects the ailerons until the feedback signal of the control surfaces channel becomes equal to the mismatch signal γ_{bsm}. In the case of small angles of banking, the angle of deflection of the ailerons will be proportional to the mismatch $\gamma_{bsm} - \gamma_{bm}$.

Deflection of the ailerons leads to a banking moment which will return the rocket to the initial position. As the banking angle is restored to the stipulated value, the angle δ_a will tend to 0. All the time that the ailerons are deflected in one direction, the rocket will be acted upon by a moment of a single sign, also causing acceleration of the same sign. Therefore, the angular velocity of the rocket about its longitudinal axis increases, which leads to an increase of the moment of the natural damping of the rocket, whose sign is opposite the sign of the acting moment.

Usually the natural damping of rockets is small and the total moment does not change its sign. Therefore, with return of the rocket to the initial position, the angular velocity of its rotation relative to the longitudinal axis will differ from zero. As a result, the angle of banking passes through the stipulated value and changes its sign. Thus, the process of setting the banking angle will have an oscillatory-attenuating character. It is easy to find the parameters determining this process. We reduce expression (9.7.1) to the form

$$W_{\frac{\gamma_b}{\gamma_{bs}}}(D) = \frac{\omega_{0b}^2}{D^2 + 2d\omega_{0b}D + \omega_{0b}^2}, \qquad (9.7.2)$$

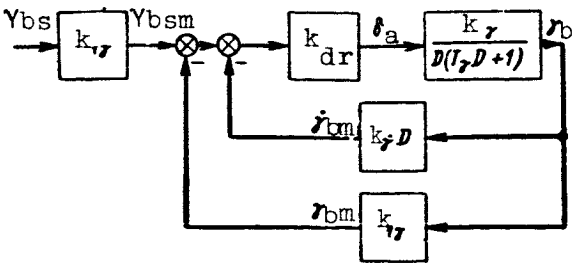

Figure 9.14

where $\omega_{0b}=\sqrt{\frac{k_{dr}k_{1\gamma}k_\gamma}{T_\gamma}}$ is the natural frequency of rocket banking oscillations.

and $d=\frac{1}{2\sqrt{k_{dr}k_\gamma k_{1\gamma}T_\gamma}}$ is the attenuation factor. /505

The adjustable parameter in a banking control system usually is the transfer constant $k_{1\gamma}$ of the sensing element. It follows from (9.7.2) that, for an increase of attenuation of the transient process, this coefficient must be decreased. However, it can be shown that, with a decrease of $k_{1\gamma}$, there is an increase of the error which sets in under the influence of the constant perturbing moment. It therefore is unfeasible to use this approach for obtaining the desired characteristics of the banking control system.

The best results are obtained using the signal of the derivative of the banking angle in the feedback circuit. Such a signal is formed by a velocity gyroscope. The block diagram of a banking control channel with introduction of a banking signal and its derivative is shown in figure 9.14. Here the conversion properties of the velocity gyroscope are characterized by the transfer function $W_{\dot{\gamma}}(D) = k_{\dot{\gamma}}D$.

It is easy to show that in this case the structure of the transfer function of the banking control channel is maintained, but there is a change of the value of the attenuation factor. It will be equal to

$$d=\frac{1+k_{dr}k_\gamma k_{\dot{\gamma}}}{2\sqrt{k_{dr}k_{1\gamma}k_\gamma T_\gamma}}. \qquad (9.7.3)$$

By changing the value $k_{\dot{\gamma}}$ within quite broad limits, it is possible to change the character of setting of the banking angle. The cited example shows that by use of an additional signal, formed in the automatic pilot, it is possible to change the dynamic characteristics of the rocket-automatic pilot system without changing the aerodynamic configuration of the rocket.

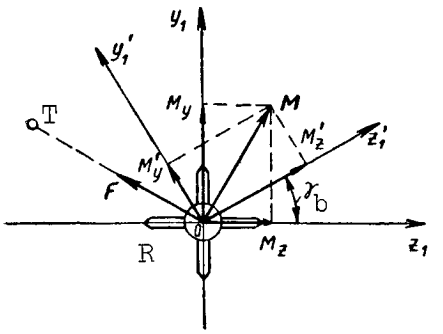

Figure 9.15

The important factor in operation of apparatus with automatic change of operation of the control surfaces is that, by their use, it is possible to ensure conversion of the control commands fed to the control surfaces of the /506 course and pitching channels, in accordance with the value of the banking angle of the rocket. This conversion is accomplished in such a way that the vectors of the aerodynamic forces and moments acting on the rocket, due to deflection of the control surfaces, do not change during the rotation of the rocket about its longitudinal axis. If at any time the rocket R occupies the position in space shown in figure 9.15, the projections of the effective moment M onto the axes oy_1 and oz_1 of the related coordinate system will be equal to M_y and M_z, respectively. The values of the moments M_y and M_z are dependent on the deflections of the course and pitching control surfaces which are determined by the course and pitching control commands K_z and K_y. The total moment causes an angular velocity of the rocket ω_r about the center of mass and the appearance of a controlling force F in the plane in which it is necessary to change the rocket trajectory. This plane passes through the rocket velocity vector and the target point T.

With the rotation of the rocket about the longitudinal axis by the angle γ_b, the vectors M and F should remain unchanged in space if the target remains in its former position. Turning of the rocket is accompanied by turning of the related coordinate system: the lateral axis occupies the direction oz_1' and the vertical axis the direction oy_1'. Figure 9.15 shows that the vector of the moment M, in this case, remains unchanged if the moments created by the control surfaces of the pitching and course channels of the rocket are equal to M_z' and M_y'.

The values M_y' and M_z' are determined by the equations

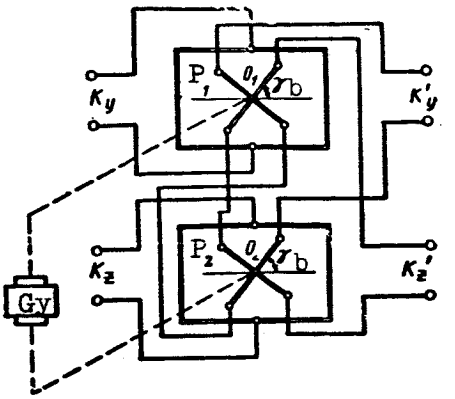

Figure 9.16

$$\left.\begin{aligned} M'_y &= M_y \cos\gamma_b - M_z \sin\gamma_b, \\ M'_z &= M_z \cos\gamma_b + M_y \sin\gamma_b. \end{aligned}\right\} \qquad (9.7.4)$$

If the pitching and course control surfaces are deflected by the angles at which the required values M'_y and M'_z are created, the rocket will continue to move in the necessary direction to the target.

It follows from expressions (9.7.4) that determination of the necessary values M'_y and M'_z will be ensured if the control commands K_y and K_z, under whose influence the moments are produced, are converted in accordance with turning of the oy_1 and ox_1 axes of the rocket. Therefore, the following control commands are fed to the apparatus for driving the course and pitching control surfaces

$$\left.\begin{aligned} K'_y &= K_y \cos\gamma_b - K_z \sin\gamma_b, \\ K'_z &= K_z \cos\gamma_b + K_y \sin\gamma_b. \end{aligned}\right\} \qquad (9.7.5)$$

With such a conversion of the control commands K_y and K_z on the rocket, /507 its rotation about the longitudinal axis does not disrupt the control process.

The considered problem of conversion of control commands can be solved using an apparatus consisting of a position gyroscope Gy which measures the angle of banking γ_b and the sine-cosine potentiometers P_1 and P_2 (fig. 9.16).

The bodies of these potentiometers are attached rigidly to the body of the rocket, and their brushes are attached to the outer frame of the gyroscope Gy. The design of such potentiometers has been described in section 4.10. If the

voltages of the commands K_y and K_z are applied to the input plates of the potentiometers, the voltages K'_y and K'_z are formed at their output; these are determined by formulas (9.7.5).

Apparatus for automatic changing of the operation of the control surfaces is installed on axially symmetrical rockets, the position of whose longitudinal axis is difficult to stabilize by quite simple technical solutions.

9.8. Channels for Control of the Longitudinal and Lateral Motions of a Rocket

The process of automatic control of the angle of pitching in the stabilization regime is somewhat more complex than the process of stabilization of the angle of banking. Whereas the latter is related only to the rotation of the rocket relative to its longitudinal axis and is described only by the lateral momenta equation, in the control of the pitching angle it is necessary to take into account both the rotation of the rocket relative to its lateral axis and the turning of the velocity vector. Therefore, in an analysis of the longitudinal motion, the longitudinal momenta and normal forces equations must be considered.

Figure 9.17 shows the block diagram of the longitudinal motion control channel. Here, in addition to the pitching angle feedback signal formed by the position gyroscope, there are two additional control signals. One of them, measured by the velocity gyroscope, is proportional to the angular velocity of rotation of the longitudinal axis of the rocket $\dot{\vartheta}$ and the second, formed by the linear acceleration sensor, is proportional to the angle of attack α.

The voltage u_Σ, fed to the control surfaces channel, is the sum of /508 the mentioned signals, that is

$$u_\Sigma = k_\vartheta(\vartheta_{st} - \vartheta) - k_{\dot\vartheta}\dot\vartheta - k_\alpha\alpha. \tag{9.8.1}$$

By using expression (9.8.1), as well as the longitudinal motion equations (9.1.20) and (9.1.21), it is easy to obtain an equation relating the mismatch signal $k_\vartheta(\vartheta_{st} - \vartheta)$ to the angle of attack α of the rocket

$$\ddot\alpha + (2d\omega_0 + a_3 k_{dr} k_{\dot\vartheta})\dot\alpha + \left(\omega_0^2 + a_3 k_{dr} k_\alpha + \frac{1}{T_v} a_3 k_{dr} k_\vartheta\right)\alpha = \\ = a_3 k_{dr} k_\vartheta (\vartheta_{st} - \vartheta). \tag{9.8.2}$$

After analyzing expression (9.8.2), it is possible to draw the following conclusions. The signal of the velocity gyroscope artificially changes the

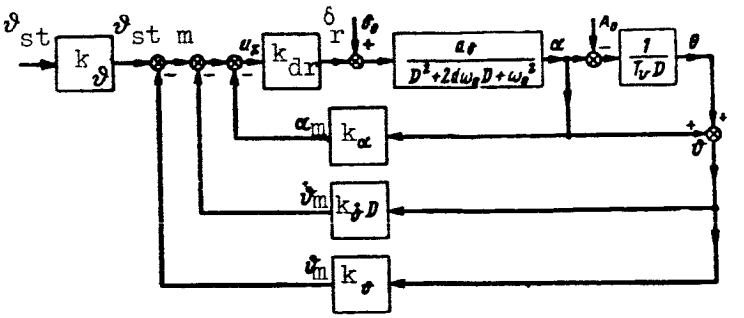

Figure 9.17

damping coefficient of the rocket and the natural frequency of its oscillations. Its introduction into the controlling voltage is desirable when the natural damping of the rocket is inadequate. The signal formed by the accelerometer increases the natural frequency of oscillations of the rocket, thereby improving its controllability considerably. By varying the coefficients k_ϑ and k_α, it is possible to change the dynamic properties of the rocket in broad limits, achieving the desired quality of the control process.

We now will discuss briefly the regime of rocket flight altitudinal stabilization. Figure 9.18 is a simplified block diagram of control of flight altitude. It is assumed here that the angle of attack is established instantaneously with deflection of the control surfaces. In addition, the gravitational components of the rocket are taken into account. The link with the /509 transfer constant k_H characterizes an apparatus which measures the current flight altitude and compares it with the stipulated value. The relationship between the angle of inclination of the trajectory θ and altitude H is established by a kinematic link with the transfer function $W_{\frac{H}{\theta}}(D) = \frac{V}{D}$.

The control circuit contains two integrating links and therefore it will be unstable. The equation relating the actual value of flight altitude to the stipulated value has the form

$$\frac{T_v\omega_0^2}{k_H k_{dr} a_\delta v}\frac{d^2H}{dt^2}+H=H_{st}. \qquad (9.8.3)$$

The process of change of H, described by equation (9.8.3), is a nonattenuating sinusoidal oscillation. Therefore, the structure of the circuit should be modified. This change is achieved in two ways. The first way is to introduce a differentiating link into the channel for measuring the mismatch signal H_{st} - H. Then the transfer function of the k_H measuring instrument can be

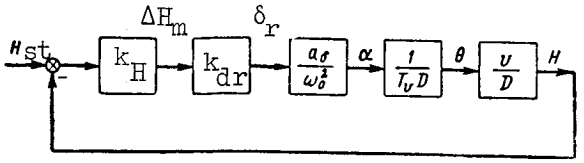

Figure 9.18

represented in the form $k_H = k_{H1} + k_H^{\cdot} D$ and the equation of motion is written as

$$\frac{T_v \omega_0^2}{k_{dr} k_{H1} a_\delta v} \frac{d^2H}{dt^2} + \frac{k_{\dot{H}}}{k_{H1}} \frac{dH}{dt} + H = H_{st} + \frac{k_{\dot{H}}}{k_{H1}} \frac{dH_{st}}{dt}. \quad (9.8.4)$$

When H_{st} = const, the last term on the right-hand side of equation (9.8.4) will be equal to zero. As follows from (9.8.4), by change of the coefficients k_{H1} and $k_H^{\cdot}$, it is possible to achieve the desired transient process of establishing the flight altitude of the rocket.

It should be noted that the determination of the derivative of the controlling signal frequently involves considerable technical difficulties. In addition, when measuring flight altitude by electronic methods, the differentiation of the controlling signal leads to amplification of the high-frequency fluctuation components.

For this reason, in some cases, it is preferable to use a second method for damping oscillations during flight altitude control. In this method, a voltage is introduced into the control signal which is proportional to the pitching angle, measured by the position gyroscope. Figure 9.19 is a simplified block diagram of the flight altitude control channel. The equation for attaining the stipulated altitude has the form

$$\frac{T_v \omega_0^2 + a_\delta k_{dr} k_\theta T_v}{k_{dr} k_H a_\delta v} \frac{d^2H}{dt^2} + \frac{k_\theta}{k_H v} \frac{dH}{dt} + H = H_{st}. \quad (9.8.5)$$

It follows from the cited equation that a signal proportional to the pitching angle performs the function of a damping signal during flight altitude stabilization. At the same time, equation (9.8.5) shows that the introduction of a pitching signal increases the inertia of the altitude determination system and therefore worsens the controllability of the rocket. /510

Signals of the velocity gyroscope and accelerometer can be used as additional signals in control of the flight altitude of a rocket, much as in the earlier considered example of control of the pitching angle. On the basis of the considered examples, it is possible to write a general automatic pilot equation which will reflect the relationship between the deflection of the

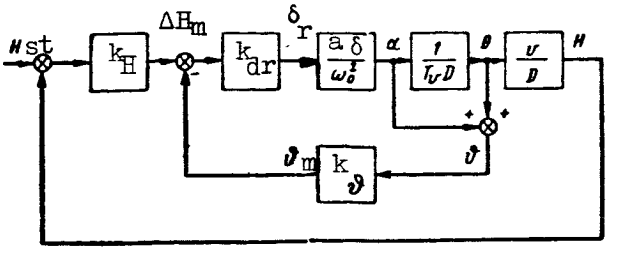

Figure 9.19

rocket control surfaces δ_r and the control command K and the additional signals for the vertical plane. This equation has the form

$$\delta_r = F(D)\left[K + \sum_{i=1}^{n_\vartheta} W_{\vartheta i}(D)\, Q_i\right] \qquad (9.8.6)$$

Here F(D) is the transfer function for the drive of the control surfaces, Q_i is the i-th additional control signal, and $W_{\vartheta i}(D)$ is the transfer function of the i-th instrument for measuring the additional signal.

Henceforth, in most cases, we will use one of the special forms of equation (9.8.6) when position and velocity gyroscopes or accelerometers are used as instruments for measuring the additional signals. Then the automatic pilot equation is written as

$$\delta_r = F(D)\,[K + W_\vartheta(D)\,\vartheta + W_\alpha(D)\,\alpha]. \qquad (9.8.7)$$

If the inertia of the measuring elements and control apparatus is neglected, that is, if a steady-state regime is considered, equations (9.8.6) and (9.8.7) express the control law. The principal component of the control law is the command K, which, being related functionally to the mismatch parameter, determines to a considerable degree the requirements imposed on the radio apparatus for transmission of commands and on the coordinators.

The control of lateral motion of the rocket has much in common with the control of its longitudinal motion. This similarity is manifested most /511
clearly in rockets with axial aerodynamic symmetry, with banking stabilization. The turning of the velocity vector and therefore the change of the flight trajectory of the rocket are the result, in this case, of a lateral force arising due to the angle of slip, caused by deflection of the rudder.

The ailerons are the principal organs of control of the lateral motion of a rocket with plane aerodynamic symmetry. The rudder is used for elimination

of the angle of slip, appearing during the banking of the rocket, and which is necessary for coordinated turning. The automatic pilot of such a rocket contains interconnected banking and yawing (or course) channels.

Additional control signals are used for change of the dynamic properties of the rocket-automatic pilot system in both mentioned types of rockets. These signals are formed by pickups similar to the pickups of the longitudinal motion control channel. It is most common to use velocity gyroscopes for increasing the damping coefficient of the rocket and accelerometers for increasing vane stability.

In order to stabilize the center of mass of the rocket in the stipulated trajectory, it is necessary to introduce into the controlling signal not only a voltage proportional to the lateral deflection of the rocket from the stipulated trajectory, but also either the derivative of this deflection or the aywing angle signal; the yawing is measured by a yawing position gyroscope. If this is not done, the control process will be unstable. Here we have a full analogy with the stabilization of rocket flight altitude in longitudinal motion.

9.9. Self-Tuning of the Rocket Control System

It has been emphasized repeatedly above that a rocket constitutes a relatively complex object of automatic control whose parameters change in quite broad limits during the change of the flight regime.

The control process is influenced considerably by changes of flight altitude and therefore by atmospheric density, flight velocity and the weight of the rocket.

For this reason, the selection of the transfer constants for the radio apparatus on the rocket and the automatic pilot which ensure an acceptable quality of the transient process for certain flight conditions is unsatisfactory when there is a change of these conditions. It follows therefore that the control apparatus should change its parameters, and in some cases its structure, in accordance with changes of environmental conditions, that is, possess the property of self-tuning. In a self-tuning rocket control system, the functions of a self-tuning correcting apparatus are imposed on the apparatus carried aboard the rocket.

There are three principal types of systems with self-tuning correcting apparatus: systems with open circuits for tuning of the correcting apparatus, systems with closed circuits for self-tuning and control of the characteristics, and systems with extremal tuning of the correcting apparatus. /512

In a system of the first type, the parameters of the correction circuit are changed by signals from sensors which measure the change of environmental conditions. The simplest example of such a system is a control system in which the amplification of the controlling signal changes in a jump when the rocket passes through a stipulated altitude. In actuality, with an increase of

altitude (with flight velocity held constant) the efficiency of the control and aerodynamic surfaces of the rocket decreases. Hence, the same mismatch and therefore the same control command, at a greater altitude, should correspond to a greater angle of deflection of the control surfaces. In a similar way, it is also possible to take flight velocity into account.

Instruments of different types for measurement of velocity head can be used as the sensor for combined measurement of the change of atmospheric density and of the air velocity of the rocket.

A shortcoming of this system is the complexity of measuring all the acting perturbations; hence, its low accuracy.

In systems of the second type, the change of the parameters of the correcting apparatus is accomplished by a comparison of the actual characteristics of the closed control system with standard parameters (characteristics) determined in advance. In such a system, it is possible to take into account a great number of prestabilizing factors, some of which are not subject to direct measurement. Under certain conditions of rocket use, however, the standard characteristics used in the tuning of the guidance circuit can be less than optimal.

Systems of the third type do not have this shortcoming. In these, there is a control of the parameters of the correcting apparatus in which the parameters assume values corresponding to the extremum of the used evaluation of the quality of the control process. The actual design of such systems naturally involves considerable technical difficulties.

CHAPTER 10. FUNCTIONAL AND BLOCK DIAGRAMS OF RADIO CONTROL SYSTEMS

10.1. Functional Diagrams of Radio Control Systems

1. Functional Diagrams of Homing Systems

The functional diagram of a homing system is determined primarily by /513
the type of coordinator. If only the means ensuring a change of rocket trajectory are taken into account, for cases when fixed and moving coordinators are used, we obtain the functional diagrams shown in figure 10.1a and b.

The input action for the coordinator is the angular position of the rocket-target line, forming at the output of the kinematic link, which is used to characterize the relative motion of the centers of mass of the rocket and target.

The angular position of the rocket-target line in a fixed coordinator is compared with the angular position of the longitudinal axis of the rocket $o_r x_1$, and in a moving coordinator, with the equisignal direction. The output signals of fixed and moving coordinators are voltages (currents) characterizing the deflections of the axis $o_r x_1$ from the direction to the target and the angular velocity of the rocket-target line, respectively.

The control commands in homing systems usually are formed in the automatic pilot. The additional control signals necessary for stabilization of the rocket and improvement of the dynamic properties of the guidance circuit also are measured and appropriately converted in the automatic pilot.

Under the influence of a control signal produced by the automatic pilot, the control surfaces of the rocket are moved in such a way as to eliminate the appearing disruption of coherence which is imposed on the rocket motion.

Figure 10.1 shows that a homing system contains not only a guidance /515
circuit in which the feedback is closed through a kinematic link, but also a number of internal circuits for automatic control.

An electronic homing system contains one, two or three open links which can be subject to the effect of artificial interference. The most vulnerable are the rocket nosecone radio receiver and the radar set for scanning of the target. It is considerably more difficult to create interference at the input of "tail-end" radio receivers used in semiactive homing systems. This can be attributed to the fact that the antenna of the "tail-end" receiver can be used

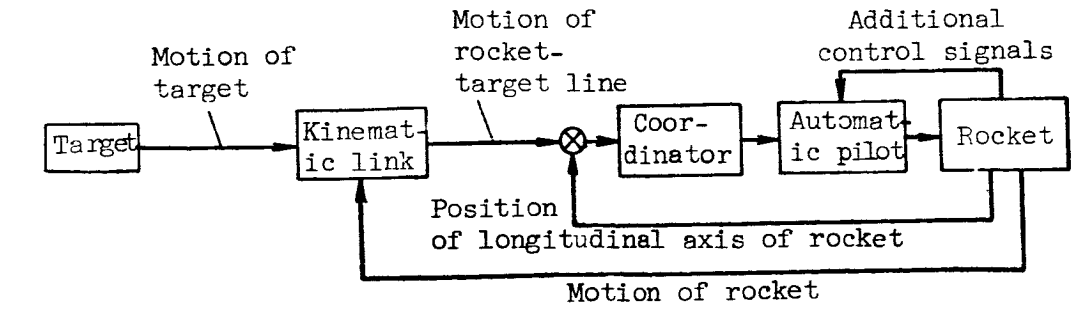

a

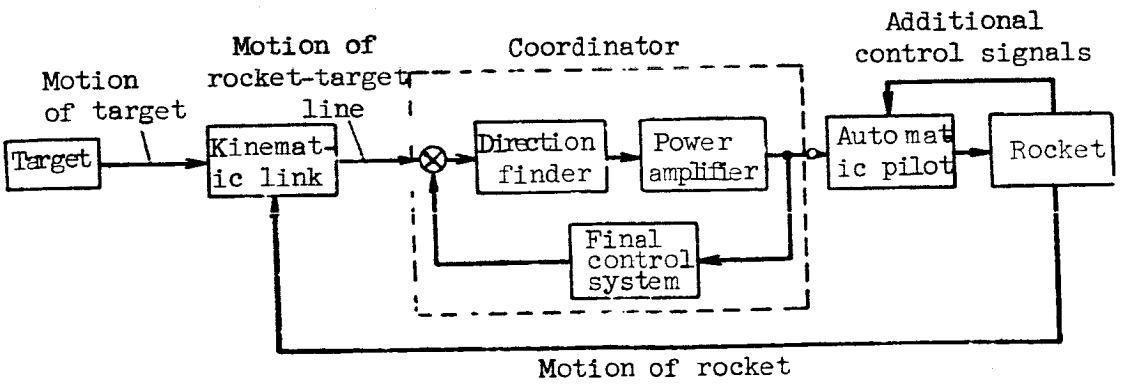

b

Figure 10.1

in most cases only within the limits of a quite small solid angle with directions opposite those in which the rocket is moving.

The presence of open links through which the external guidance circuit is closed is one of the important shortcomings of electronic homing systems. At the same time, because of these links, a homing rocket seemingly is guided by the target to be damaged itself, which makes possible extremely precise guidance of the rocket to rapidly moving and maneuvering targets.

2. Functional Diagrams of Radio Zone (Beam-Riding) Control Systems

In a beam-riding control system, whose standard functional diagram for the case of rocket guidance by the coincidence method is shown in figure 10.2, the coordinator consists of a radar set RS, located at the control point, and the radio apparatus carried aboard the rocket, constituting a direction finder. The relative motion of the target and control point, reflected by the kinematic link I, leads to a change of the position of the control point-target line. The movement of this line is detected by the radar set RS and is converted into the movement of the radio beam (equisignal direction). The angle between the equisignal direction and the control point-rocket line, whose position is determined by the kinematic link II characterizing the relative motion of the control point and the rocket, is the input action for the direction finder. This apparatus produces voltages (currents) which are related functionally to the

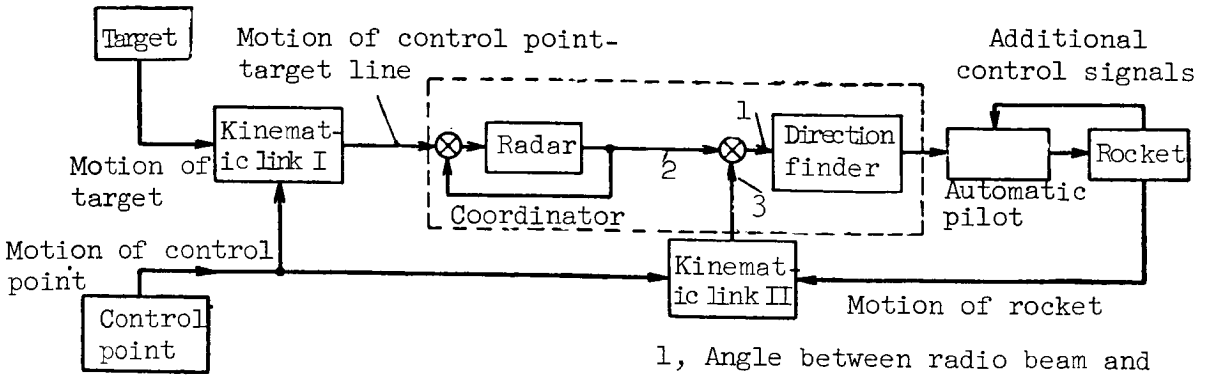

1, Angle between radio beam and rocket-control point line
2, Motion of controlling beam
3, Motion of control-point rocket line

Figure 10.2

linear deflections of the center of mass of the rocket from an equisignal direction in the planes of its longitudinal and lateral motions.

The voltages (currents) received from the direction finder are used in the automatic pilot for forming control commands and controlling signals which cause deflection of the control surfaces of the rocket in such a way that the latter is held on the equisignal direction.

The instruments carried on the rocket and ensuring its flight in the radio beam form an independent tracking system which in essence compares the motion of the target and rocket.

This system contains two open links caused by the presence of radio receivers both in the radar set and aboard the rocket. /517

If the beam-riding control system is used for guiding the rocket to a forward point, the radar set for tracking the target must be supplemented by a radar control station. Its antenna system should form an equisignal line in the direction of the forward point. This problem can be solved by use of a computer Com in which signals characterizing the coordinates of the target are received at the input. The Com output signals are used for turning the axis of the antenna of the radar control station in vertical and horizontal planes. It is easy to see that more unwieldy apparatus is required for guiding a rocket to a forward point, although this apparatus of course is away from the rocket.

The rocket radio apparatus of beam-riding control systems is quite simple because it includes only a direction finder. However, when guiding a rocket from an aircraft to an air target, when for all practical purposes there can be control by the coincidence method, there are limitations on the maneuvering of the carrier. This restricts the region of applicability of beam-riding control systems.

If the rocket is intended for damaging fixed targets, it is possible to use radio navigation equipment ensuring the creation of a radio zone of some

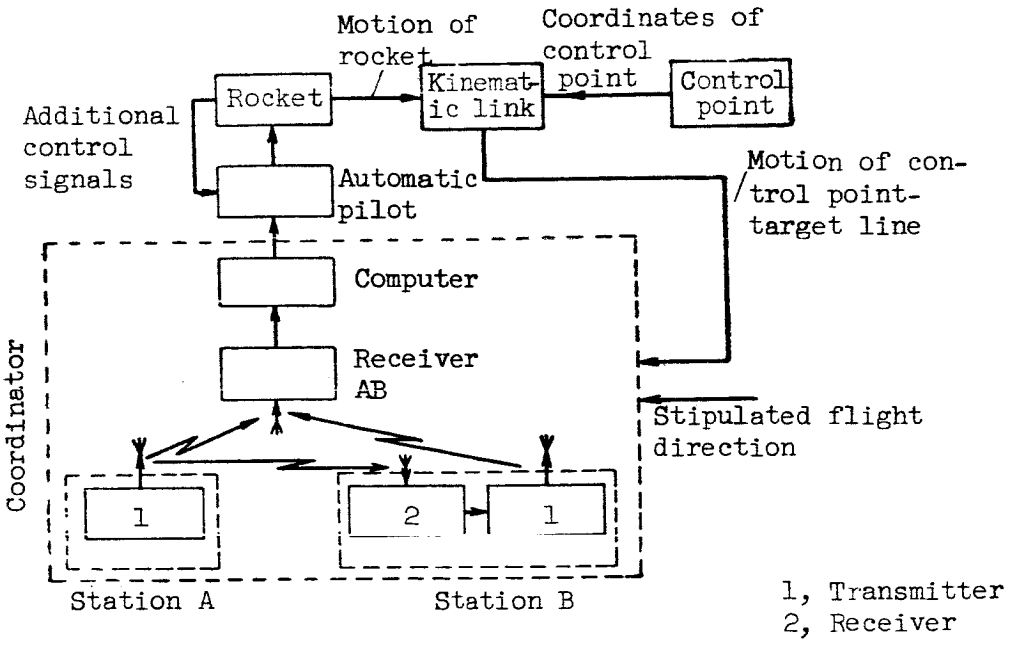

Figure 10.3

type. The number of functional diagrams of control systems based on radio navigation zones can be very great. However, their difference from the diagrams of beam-riding control systems will be primarily in the structure and the functions performed by individual components of the coordinator. For example, when using an add-subtract– range-finding navigation system, a rocket guidance system can be created whose functional diagram is shown in figure 10.3. By use of such a system, it is possible to control the rocket in its course. In this case, the projection of the radio zone onto the ground, in a general case, is represented by a hyperbola which is characterized by a fully determined difference of the distances to the master and controlled stations A and B.

The signals of the transmitters of stations A and B are fed to the receiver AB, situated aboard the rocket, and then to the computer Com. The computer measures the difference of the distances R_A and R_B from the rocket to the stations A and B, and this determines the deflection of the center of mass of the rocket from the stipulated hyperbola. The resulting mismatch signal acts on the automatic pilot, thereby eliminating the appearing disruption of coherence which is imposed on the rocket motion.

The determination of the guidance process also is accomplished using the Com, which produces the necessary voltage (current) under the influence of the signals of another pair of ground stations.

One of the merits of a radio zone control system, based on use of an /518 add-subtract– range-finding radio navigation system, is its great transmitting

capacity. This means that the same ground stations can service a considerable number of launching sites simultaneously. Such a property is inherent in a number of other types of radio zone control systems.

3. Functional Diagrams of Command Control Systems

Two forms of command control systems can be distinguished. A characteristic feature of systems of the second kind is determination of the coordinates of the target using apparatus carried aboard the rocket. In all other methods for measurement of the parameters of motion of the target a command control system of the first type is used.

The functional diagram of a command control system of the first kind can be represented as shown in figure 10.4a. It follows from figure 10.4a that the coordinates of the target relative to the control point, fixed by the kinematic link I, are determined by the target coordinates measuring instrument TCI. The relative coordinates of the rocket and control point, whose relative motion is reflected by the kinematic link II, are determined by the rocket coordinates measuring instrument RCI. The output signals of the TCI and RCI are fed to the computer Com.

In the case when the TCI and RCI are situated at control points, they are connected to the computer without using any special apparatus. If these /520 measuring instruments are situated away from the control point, wire or electronic data transmission systems DTS I and DTS II are used; these are shown in figure 10.4a by a dashed line. In actual practice, TCI and RCI can be two different apparatuses or a single radar station, for example, with linear scanning of the antenna system beam, and the coordinates of the target and rocket need not be measured only relative to the control point.

A signal in the form of a voltage (current) or special codes is created at the output of the computer of the automatic control system. This signal is a measure of the disruption of the coherence imposed on the motion of the rocket by the used guidance method. Under the influence of the mismatch signal, the apparatus for forming commands CF produces a command which is transmitted to the rocket by the command control radio link CCRL. If the system is non-automatic, the mismatch parameter is determined using an optical sighting apparatus or from the images on the screen of the cathode-ray tube, and the computer is replaced by an operator and a command pickup. In those cases when the target is fixed, the instrument for measuring its coordinates is dispensed with and replaced by an apparatus fixing the program of motion of the rocket.

The functional diagram of a command control system of the second kind is shown in figure 10.4b. The TRCI apparatus measures the coordinates of the target relative to the rocket. The relative motion of the target and rocket is reflected by the kinematic link. The output signals of the TRCI, by means of a data transmission system DTS, which is an essential element of this control system, are relayed to the indicator (the screen of a television receiver, radar station, etc.) where target and rocket pips are formed. The operator O, by use of the command unit CU, controlling the operation of the command control radio link CCRL, should produce commands in such a way as to ensure coincidence of these pips.

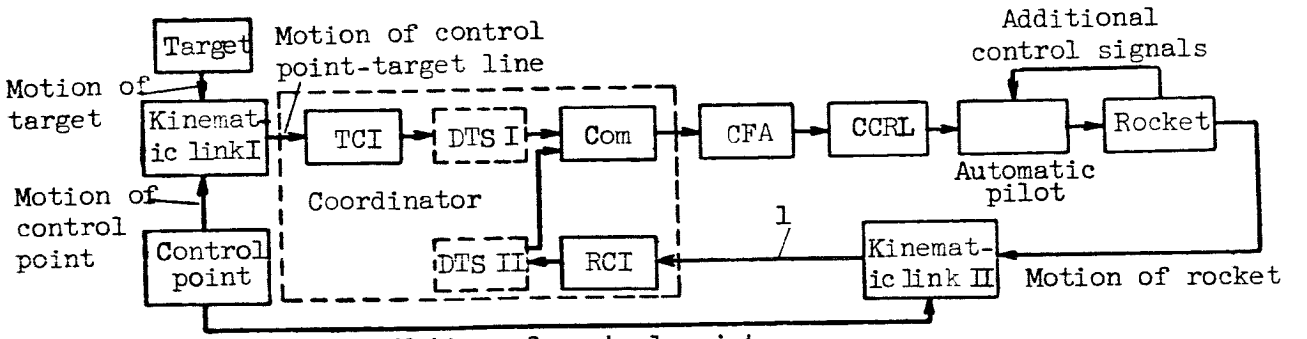

a

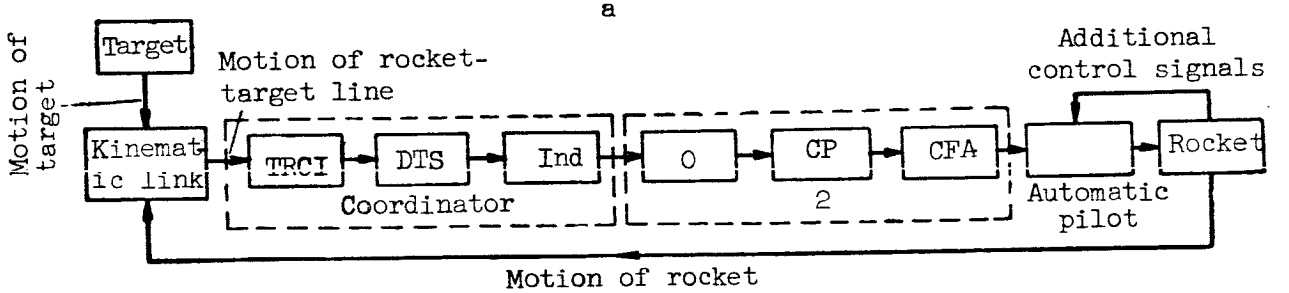

b

1, Motion of control point-rocket line
2, Apparatus for forming and transmitting commands

Figure 10.4

Comparison of figures 10.1 and 10.4b shows some common features of command control systems of the second type and of homing systems: the coordinator measuring instruments are carried on the rocket. The basic difference between command control systems of the second kind and homing systems is that the measurement results are converted into command signals not on the rocket itself but at the control point CP. The need for relaying of data from the rocket to the CP considerably complicates the control apparatus as a whole and especially the equipment carried on the rocket. Nevertheless, the use of control systems of the second kind can be desirable, since when there is an operator it ensures better target resolution, a great flexibility of the guidance process and a decrease of the effect of interference. At the same time, the limitations of such systems must not be forgotten; these limitations are caused by the /521 subjective nature of the operator and also by the great complexity and cost of their manufacture.

The controlling signal acting on the control surfaces of the rocket in both forms of command control systems is formed by the automatic pilot on the basis of the received command and additional signals measured by autonomous transducers.

A command control system contains a considerable number of open links. For example, when individual radar stations are used for determination of the

coordinates of the rocket and target, the system will include at least three of four radio receivers, two of which will be on the rocket and one or two at the control point or near it. When there are two receivers aboard the rocket, one of them is used in receiving control commands and the other is for ensuring the operation of the radar responder, which usually is necessary due to the extremely small reflectivity of the rocket surface.

A number of advantages (simplicity of rocket equipment, large effective range, etc.), characteristic of command control systems, have led to their extensive use for guidance of rockets of different types.

At the same time, it should be noted that, with respect to accuracy of operation, command control systems of the first kind are less accurate than homing systems.

4. Functional Diagram of an Autonomous Control System

The standard functional diagram of an autonomous control system, which can be used for guidance of rockets to fixed targets or targets whose parameters of motion are known, is shown in figure 10.5. Data on the coordinates of the target and the launching point, determining the stipulated trajectory of motion of the rocket, are introduced into the computer Com. The current position of the center of mass of the rocket is determined by an autonomous coordinate-measuring instrument RCI and the command and controlling signals are formed in the automatic pilot. The kinematic link relates the angular motions of the rocket to the motion of its center of mass.

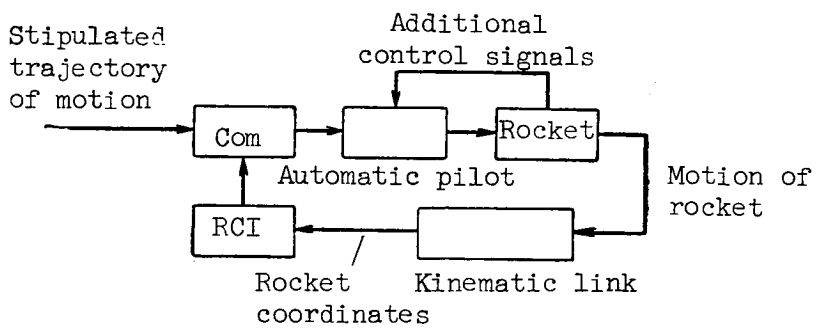

Figure 10.5

10.2. General Description of the Equations and the Principal Problems in Investigation of Radio Control Systems

/522

In accordance with the general functional diagram shown in figure 1.3, we can name the following groups of equations describing the operation of the control system:

– rocket equations, characterizing the relationships between the output parameters of the rocket, representing the angles of inclination of the velocity

vector v or the components of the normal acceleration vector j_n and the movements of the control surfaces of the rocket;

– automatic pilot equations, defining the deflections of the control surfaces of the rocket as a function of the course and pitching controlling signals;

– equations of the apparatus for forming and transmission of the control commands, establishing the dependence between the control commands and the measured values of the components of the mismatch parameter for the corresponding control planes of the rocket;

– coordinator equations, relating the components of the vector Δ_m to the parameters of motion of the rocket and target, defining the coherence which is imposed on motion of the rocket.

In addition, the general system of equations includes kinematic equations. In the case of homing and command control systems of the second kind, these equations are used to characterize the relative velocity of movement of the centers of mass of the rocket and target along the vector r and along the normal to it. In the case of radio zone control systems and command control systems of the first kind, the kinematic equations establish the relationship between the relative velocities of approach of the rocket and target and also the target and control point to the parameters of motion of these objects, considered as geometrical points. Kinematic equations reflecting the dependence of the change of the coordinates of the center of mass of a rocket on its angular movements are used for description of autonomous control systems.

As already mentioned, in analytical investigations of the spatial motion of a rocket, in many cases, it is desirable to separate the longitudinal and lateral motions which are considered independent of one another. However, it must be remembered that the results obtained in a separate analysis of the longitudinal and lateral movements of the rocket can be considered only preliminary. In the final development of a control system, it usually is necessary to consider the spatial motion of the rocket. In particular, this can be attributed to the fact that, in the case of different characteristics of longitudinal and lateral motions, such as in a four-winged rocket, even when there is stability of the course and pitching channels separately, the rocket as a whole can be unstable. An important characteristic of the equations /523 describing the motion of the rocket is a temporal change of the coefficients which they contain.

The processes transpiring in the automatic pilot and characterizing the laws of control of a rocket in course and pitching are described by two equations which are dependent on one another. In most cases, in the working range they are linear differential equations with constant coefficients. These same properties are characteristic of the equations for the apparatus for forming commands and also for the command control radio link and the coordinator when there is no radio interference. The guidance method, the type of command control radio link, the type of apparatus for forming the commands and the types of measuring instruments and computers used exert an appreciable influence

on the specific forms of the equations for these types of apparatus. The number and type of kinematic equations for each of the control planes are dependent on the type of control system. In a general case, these equations are nonlinear differential equations with variable coefficients.

It follows from the above that the control system as a whole is characterized by a system of nonlinear differential equations of a relatively high degree. In the selected guidance method, determined to a considerable degree by the purpose of the rocket, the analysis of the control system essentially involves primarily an investigation of its stability. As a result of such an investigation, it is possible to establish the control law and the principal parameters of all the apparatus forming the control system. Later it is possible to determine the errors of rocket guidance caused by the dynamic properties of the guidance circuit and the different perturbations acting in the guidance process. The impeding perturbations include atmospheric turbulence, the instrument noise of the radio receivers, fluctuations of the signals received from the targets at the input of the radar receivers, change of radio wave propagation conditions, etc.

Since the motion of a controlled rocket is described by a complex system of nonlinear differential equations, solutions of problems involved in investigation of the guidance circuit can be obtained only by use of electronic computers. However, determination of the exhaustive characteristics of a control system by the use of computers requires the expenditure of a great amount of time and work. In addition, prior to carrying out modeling, it usually is necessary to represent the expected results at least in approximate form.

In this connection, the problem arises of an approximate theoretical analysis of the properties of the projected control system. Methods for investigation of linear systems of automatic control with constant parameters presently are the best developed.

The presence of variable coefficients in a number of equations describing the rocket guidance process does not make possible direct use of the concept of transfer functions which is employed widely in the theory of stationary linear automatic control systems. /524 However, by using the methods of linearization of nonlinear functions and the "freezing" principle for slowly changing coefficients, it is possible in the case of individual segments of trajectories to analyze radio control systems by the well-known methods of the theory of linear stationary dynamic systems.

In those cases when the principle of "freezing" of the coefficients is not applicable, on the basis of the linearized equations it is possible to find the transfer functions of radio control systems which are dependent on time.

10.3. Block Diagrams of Electronic Homing Systems

If a rocket is intended for damage of fixed or nearly stationary targets, it is customary to use the direct guidance method (approximate guidance along a pursuit curve). In those cases when the target to be attacked is moving

rapidly, the most suitable method is parallel approach or the proportional navigation method.

The general system of equations describing the homing process for an axially symmetrical rocket guided by the direct method in a vertical plane is derived using expressions (9.1.14), (9.1.20), (9.1.21), (2.7.1), (9.8.7), (3.8.2) and (5.8.1). In this case, it must be assumed that $S_{com} = 0$ and K_a, Δ_m and $L_1(D)$ should be replaced by K, Δ_m and L(D). The system of equations derived in this way has the form

$$\left.\begin{aligned}
m\dot{v} &= T_r - C_x \frac{\rho v^2}{2} S - G\sin\theta,\\
T_y\dot{\theta} &= \alpha - A_0,\\
\ddot{\alpha} + 2d\omega_0\dot{\alpha} + \omega_0^2\alpha &= a_s(\delta_r + \delta_0),\\
\vartheta &= \theta + \alpha,\\
\dot{r} &= v_t\cos q_t - v\cos q,\\
r\dot{\varepsilon} &= -v_t\sin q_t + v\sin q,\\
q &= \varepsilon - \theta,\\
q_t &= \varepsilon - \theta_t,\\
\delta_r &= F(D)\,[K + W_\alpha(D)\,\alpha + W_\vartheta(D)\,\vartheta],\\
K &= L(D)\,\Delta_m,\\
\Delta_m &= u_{DF} = k_{DF}\gamma,\\
\gamma &= \varepsilon - \vartheta.
\end{aligned}\right\} \qquad (10.3.1)$$

The represented equation contains 12 equations with 12 unknowns: v, θ, /525 α, ϑ, δ_r, q, ε, K, Δ_m, r, q_t and γ. The value v_t and inclination θ_t of the velocity vector v_t for the motion of the rocket in a vertical plane or the projection of this rocket in the case of spatial motion of the rocket are stipulated functions of time, determining the input action in the homing system. The parameters A_0 and δ_0 are known.

In most cases of the practical use of a rocket guided by the direct method, the angles q_t and q_r will be small, and therefore it can be assumed without great error that $\cos q_t \approx 1$, $\cos q \approx 1$, $\sin q_t \approx q_t$ and $\sin q \approx q$. Under such a condition, the kinematic equations become linear.

The first equation of system (10.3.1) characterizes the change of velocity v and for the reasons pointed out in chapter 9 need not be considered in an analysis of control systems.

Then, taking into account that the value A_0 in the second equation can be considered constant, we will have the following linearized equations for the considered homing system

$$\left.\begin{aligned} T_v\dot{\theta} &= \alpha - A_0, \\ \ddot{\alpha} + 2d\omega_0\dot{\alpha} + \omega_0^2\alpha &= a_\delta(\delta_r + \delta_0), \\ \delta_r &= F(D)\,[K + W_\alpha(D)\,\alpha + W_\vartheta(D)\,\vartheta], \\ K &= L(D)\,\Delta_m, \\ \Delta_m &= u_{DF} = k_{DF}\gamma, \\ \gamma &= \varepsilon - \vartheta, \\ \vartheta &= \theta + \alpha, \\ r\dot{\varepsilon} &= -v_t(\varepsilon - \theta_t) + v(\varepsilon - \theta). \end{aligned}\right\} \qquad (10.3.2)$$

In the derived system of linear differential equations, the unknowns are θ, α, δ_r, K, Δ_m, γ, ε and ϑ.

If the conditions that q_t and q be small are not satisfied, in order to be able to construct the block diagram, it is necessary to linearize the kinematic equations relative to those values q_t and q which would be obtained in the case of rocket guidance along a reference trajectory. In this case, as already noted, the mismatch parameter Δ_m is assumed equal to zero.

Without discussing at length the linearization of system (10.3.1) for arbitrary angles q_t and q, we will continue our consideration of equations (10.3.2). It was demonstrated in chapter 2 that the last equation in system (10.3.2), with the equation $\dot{r} \approx v_t - v$ taken into account, can lead to the following form

$$\frac{d(r\varepsilon)}{dt} = v_t\theta_t - v\theta. \qquad (10.3.3)$$

Then we will have

/526

$$\left.\begin{aligned} \dot{\theta} &= \frac{1}{T_v}(\alpha - A_0), \\ \ddot{\alpha} + 2d\omega_0\dot{\alpha} + \omega_0^2\alpha &= a_\delta(\delta_r + \delta_0), \\ \delta_r &= F(D)\,[K + W_\alpha(D)\,\alpha + W_\vartheta(D)\,\vartheta], \\ K &= L(D)\,\Delta_m, \\ \Delta_m &= u_{DF} = k_{DF}\gamma, \\ \gamma &= \varepsilon - \vartheta, \\ \vartheta &= \theta + \alpha, \\ \frac{d(r\varepsilon)}{dt} &= v_t\theta_t - v\theta. \end{aligned}\right\} \qquad (10.3.4)$$

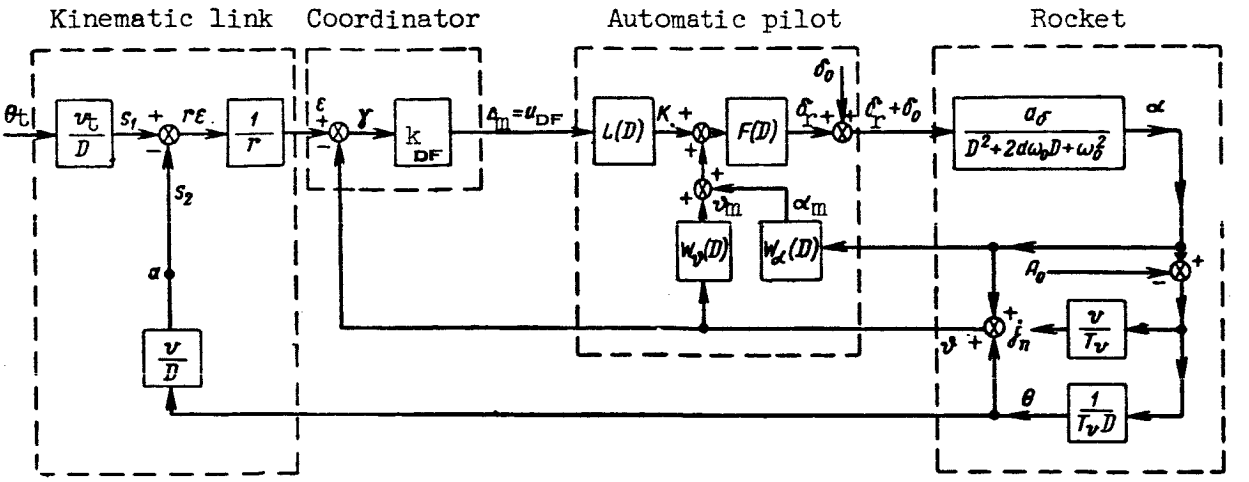

Figure 10.6.

A number of variable coefficients are present in the derived equations. The most rapidly varying of these is the value r, which tends to zero with approach of the rocket to the target. Because of this, the application of the principle of "freezing" of the coefficients for such systems, in some cases, is possible only when making very approximate estimates.

The block diagram corresponding to equations (10.3.4) is shown in figure 10.6. This figure also shows a link with the transfer function $\frac{v}{T_v}$, whose output is normal acceleration j_n. We recall that by knowing j_n, it is easy to find the normal overloads experienced by the rocket in the course of its guidance.

It can be seen from figure 10.6, where all components of the homing system have been denoted in accordance with the functional diagram shown in figure 10.1a, that the kinematic link in turn is divided into three links. The links with the transfer functions $\frac{v_t}{D}$ and $\frac{v}{D}$ are the converters of the angles θ_t and θ, while the link having the variable transfer coefficient 1/r is used for forming the angle ε, which represents the input action for the coordinator.

The block diagram of the system for guidance of a rocket with axial aerodynamic symmetry for lateral motion also can be obtained in the form shown in figure 10.6 if the angles θ_t, ε, α, etc., are replaced by the parameters of motion and transfer functions characterizing rocket flight in a horizontal plane.

Figure 10.6 also applies as the block diagram of the control system for longitudinal motion for rockets with plane aerodynamic symmetry. The block diagram of a homing system for lateral motion of such a rocket can be obtained from figure 10.6 if the transfer functions in it

$$W_{\frac{\alpha}{\delta_r}}(D)=\frac{a_\delta}{D^2+2d\omega_0 D+\omega_0^2} \text{ and } W_{\frac{\theta}{\alpha}}(D)=\frac{1}{T_v D}$$

are replaced by the functions

/528

$$W_{\frac{\gamma}{\delta_a}}(D)=\frac{\gamma_b(t)}{\delta_a(t)}=\frac{k_\gamma}{D(T_\gamma D+1)} \text{ and } W_{\frac{\psi}{\gamma}}(D)=-\frac{\psi(t)}{\gamma_b(t)}=\frac{g}{v_H D}.$$

In addition, all other signals and functions indicated in figure 10.6 should be replaced by the corresponding parameters and transfer functions for the horizontal control plane.

It follows from figure 10.6 that with approach of the rocket to the target, the transfer coefficient k_r of an open system increases continuously with a break in the circuit at the point a. As a result, at some value $r = r_{min}$, the homing system becomes unstable and the guidance process is disrupted. In order to ensure a stable rocket flight in a given range of change of distance r, there must be a corresponding selection of the transfer coefficient k_r of the open guidance circuit. The control law also exerts a great influence on the stability of the homing process.

In those cases when it is desirable to have a closing of the block diagram for the acceleration circuit j_n, it is necessary to modify the first and last equations in system (10.3.4). Taking into account that $j_n = v\dot{\theta}$, the equation $\dot{\theta} = \frac{1}{T_v}(\alpha - A_0)$ can be replaced by

$$j_n=\frac{v}{T_v}(\alpha-A_0). \tag{10.3.5}$$

In order for system (10.3.4) to remain closed with the replacement of $\dot{\theta}$ by j_n, it is necessary to differentiate the last equation of the system. We will have

$$\frac{d^2(r\varepsilon)}{dt^2}=v_t\dot{\theta}_t+\dot{v}_t\theta_t-j_n-\dot{v}\theta.$$

If v_t and v are virtually not dependent on time, then

$$\frac{d^2(r\varepsilon)}{dt^2} \approx v_t \dot{\theta}_t - j_n.$$

Since the closing of the guidance circuit through acceleration j_n for all types of control systems is accomplished as a result of the mentioned transformation of the equation $\dot{\theta} = \frac{1}{T_v}(\alpha - A_0)$ and the differentiation of the kinematic equations, this problem will not be considered hereafter, and will be represented in the block diagrams only by a link with the transfer function $\frac{v}{T_v}$.

The diagram in figure 10.6 and therefore the system of equations (10.3.4) represent one of the forms of the block diagrams and equations of homing systems for the direct guidance method. A characteristic of this form of guidance is absence of a signal characterizing the rocket miss, knowledge of /529 which, as already pointed out, is of very great importance in an investigation of the influence of various parasitic perturbations on the rocket, electronic apparatus, etc.

We recall that by rocket "miss" is understood the distance in the reference plane by which the rocket passes by the target. In determining the miss of a homing missile, it is necessary to take into account that in the course of several tenths of a second of flight, when the distance between the rocket and the target becomes equal to r_K, the rocket in actuality ceases to be controlled (for example, due to the dead zone of the radar coordinate-measuring apparatus, rocket inertia, etc.), its velocity remains unmodified and the target can complete no maneuvering. As will be demonstrated below, in investigations of control systems, it is also desirable to employ the concept of "current" miss, characterizing the value of deflection of the rocket from the target in the reference plane on the assumption that beginning with a particular time t the guiding process ceases and the rocket and target velocity vectors remain unmodified.

Hereafter, for simplicity in exposition, the miss and its current value will be defined only for the longitudinal motion of the rocket and will be denoted by the symbols h and h_t.

In order to have the value $h_t = 0$, it is necessary and sufficient to ensure the coincidence of the relative velocity vector v_0 of approach of the rocket to the target and the vector r. If there is some angle ν between these vectors (figure 10.7), assuming that h_t is read from the target T along the normal to the vector v_0, we obtain

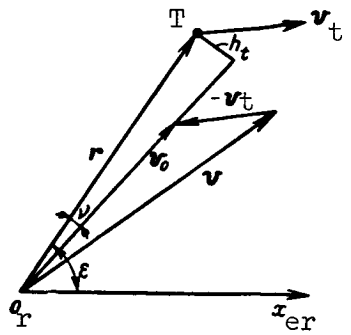

Figure 10.7

$$h_t = r \sin \nu.$$

Bearing in mind that

$$\dot{\varepsilon} = \frac{v \sin(\varepsilon - \theta) - v_t \sin(\varepsilon - \theta_t)}{r} = \frac{v_0 \sin \nu}{r}, \tag{10.3.6}$$

we find

$$h_t = \frac{\dot{r}^2 \varepsilon}{v_0}. \tag{10.3.7}$$

We note that h_t is considered positive if the rocket flies ahead of the target. Using (10.3.7) it is possible to find h, provided that the value r in expression (10.3.7) is replaced by r_K.

The "current" miss h_t is introduced into the block diagram by differentiating the last equation in system (10.3.4) for t and multiplying the result by r. Then we obtain

$$r^2\ddot{\varepsilon} + 2\dot{r}r\dot{\varepsilon} + r\ddot{r}\varepsilon = rv_t\dot{\theta}_t + r\dot{v}_t\theta_t - rv\dot{\theta} - r\dot{v}\theta.$$

But

/530

$$r^2\ddot{\varepsilon} + 2r\dot{r}\dot{\varepsilon} = \frac{d}{dt}(r^2\dot{\varepsilon}) = \frac{d(v_0 h_t)}{dt}.$$

If the values $\ddot{r}$, $\dot{v}_t$ and $\dot{v}$ can be neglected, we find

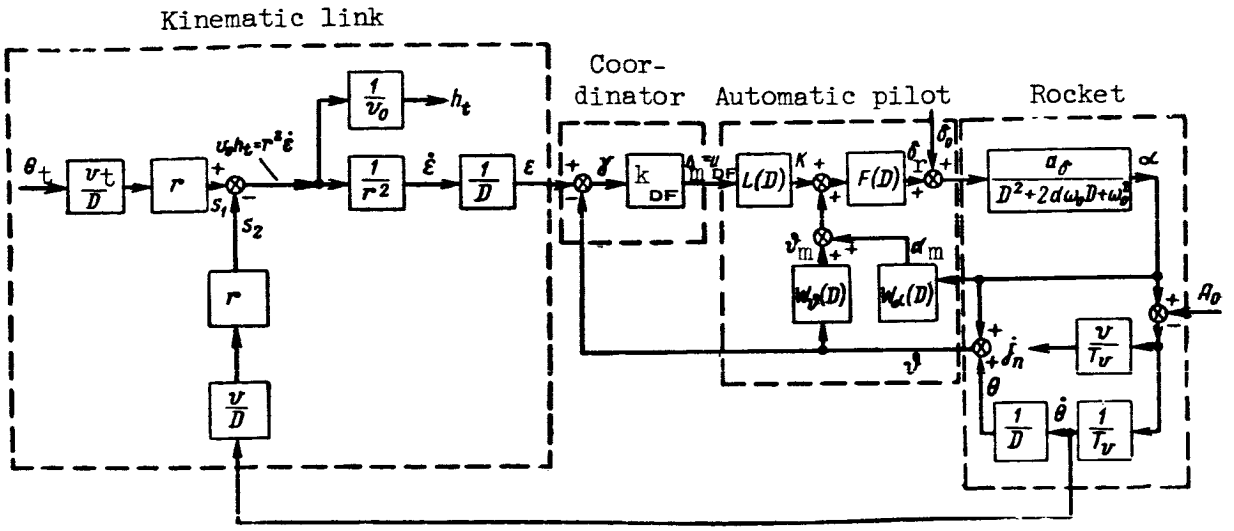

Figure 10.8.

$$\frac{d(v_0 h_t)}{dt} = r\left(v_t \dot{\theta}_t - v\dot{\theta}\right). \qquad (10.3.8)$$

Taking equations 1-6 in system (10.3.4) into account and also the relations (10.3.7) and (10.3.8), we obtain the block diagram shown in figure 10.8. Figures 10.8 and 10.6 show that only the kinematic links differ in form in these diagrams. In actual practice the second form of block diagram frequently is more desirable, especially when modeling homing processes.

In accordance with the considered method, there is no difficulty in constructing a second form of block diagram also for the horizontal control plane of a rocket for the cases of both plane and axial aerodynamic symmetry.

In the case of rocket guidance by the parallel approach method, the block diagram of a homing system can be constructed using the system of equations (10.3.4) if the coordinator equation in it is modified. It was demonstrated in chapter 3 (3.9.9) that at the output of the coordinator power amplifier, used in forming the mismatch parameter in the parallel approach method for a rocket in a vertical plane, a voltage $\Delta_m = u_c$ is formed, which is equal to

$$\Delta_m = u_c = \frac{k_{DF} k_a}{T_a D^2 + D + k_V} \dot{\varepsilon}.$$

Then for the first and second forms of writing of the kinematic equations, we obtain block diagrams shown in figures 10.9 and 10.10. These figures show

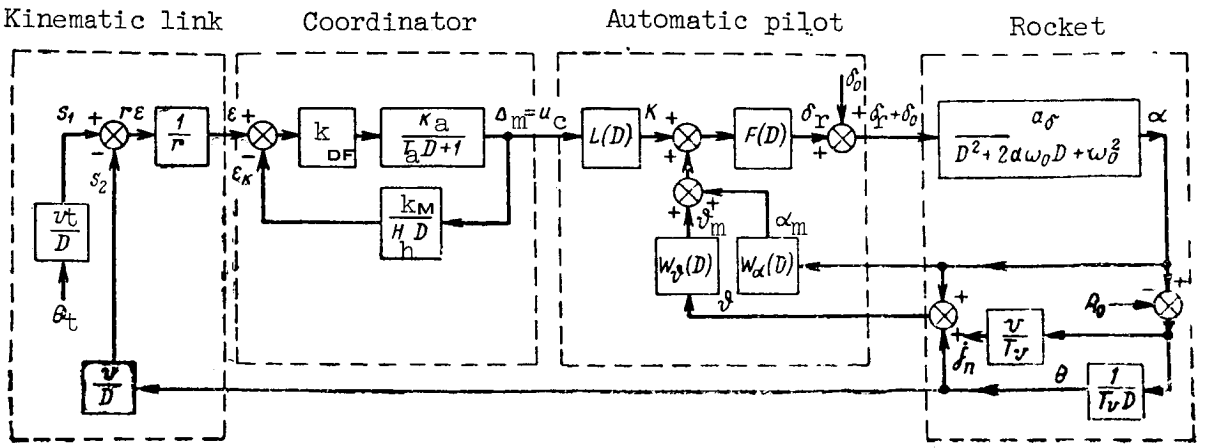

Figure 10.9

that the transfer coefficient of the guidance circuit changes inversely proportional to distance r and is dependent on the transfer properties of the coordinator. In the case of a horizontal control plane, the block diagrams can be obtained using figures 10.9 and 10.10 after a corresponding replacement of the transfer functions and all actuating signals.

If the rocket is guided by proportional guidance, the first and second forms of the block diagrams of homing systems for a vertical plane can be obtained also from figures 10.9 and 10.10. However, in this case it is necessary to take into account that the measured value of the mismatch parameter Δ_m, in accordance with formula (2.6.16), is determined by the following expression

$$\Delta_m = u_{cl} = \frac{ak_{DF}k_a}{T_a D^2 + D + k_V}\dot{\varepsilon} - k_\theta^{\cdot}\dot{\theta},$$

where $k_\theta^{\cdot}$ is the transfer coefficient of the θ measuring instrument.

On the basis of the block diagrams for given transfer functions L(D), F(D), $W_\vartheta(D)$ and $W_\alpha(D)$, it is possible to find the characteristic equation of a closed guidance circuit and determine the necessary conditions of stability of the homing system. With a change of the control law, the structure of the homing system and therefore its characteristic equation will change. /532

For example, if $\delta_r = k_{pr}[K + W_\alpha(D)\alpha]$, in the case $W_\alpha(D) = k_\alpha$ (where k_α is the transfer coefficient for the angle of attack measuring instrument) and in the case of an inertialess apparatus for forming commands K, the homing system in the case of parallel approach and proportional guidance will be

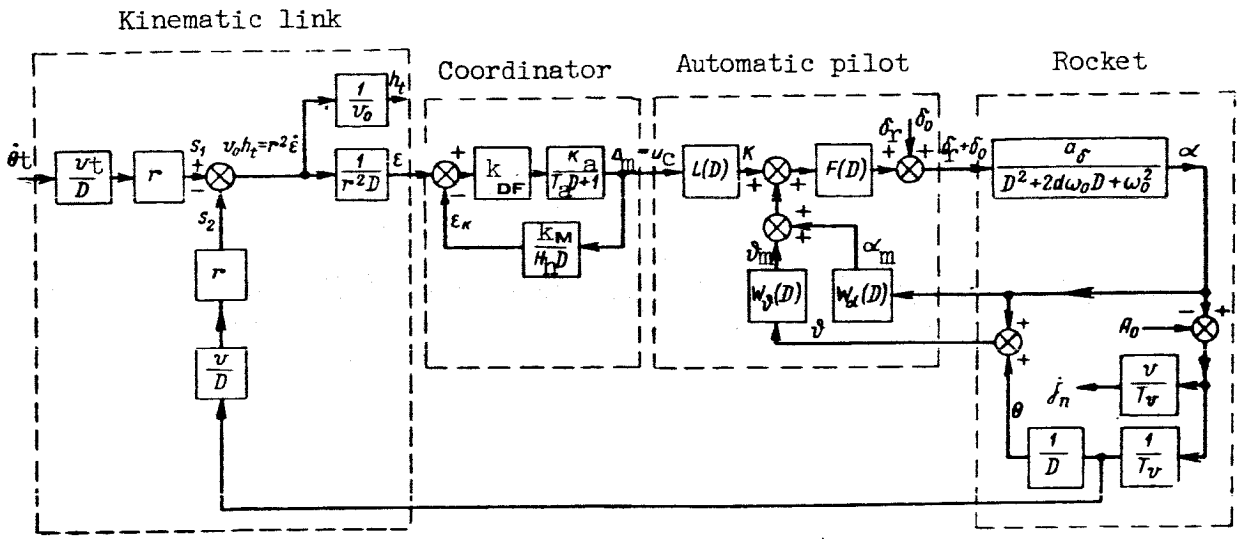

Figure 10.10

structurally unstable. This can be attributed to the fact that, in addition to inertialess amplifiers, the circuit will include two links with the transfer functions $\frac{1}{T_V D}$ and $\frac{v}{D}$, not included in the feedback, and one oscillatory link. The oscillatory link is obtained as a result of conversion of the links with the transfer functions $F(D) = k_{pr}$, $W_\alpha D = k_\alpha$ and $\frac{a_\delta}{D^2 + 2d\omega_0 D + \omega_0^2}$. It must be remembered at the same time that the mentioned oscillatory link will possess high natural frequency and damping in comparison with the link having the transfer function $\frac{a_\delta}{D^2 + 2d\omega_0 D + \omega_0^2}$. As a result, the introduction of a link with the transfer function $W_\alpha(D) = k_\alpha$ leads to a decrease of the duration of transient processes.

In order for the system to be stable when $\delta_r = k_{pr}[K + W_\alpha(D)\,\alpha]$, where $W_\alpha(D) = k_\alpha$, it is necessary to differentiate the mismatch parameter. However, the presence of noise in the coordinator radio receiver and the fluctuations of the signals arriving from the target leads, as is well known, to an appreciable distortion of the differentiated signal.

In the selection of a control law of the form $\delta_r = k_{pr}[K + W_\vartheta(D)\,\vartheta]$ one of the integrating links will be included in the feedback and the guidance circuit

will be stable even with performance of integration functions by the link L(D). At the same time, the time constant of the system increases and as a result, there is an increase of the time of the transient processes.

A compromise solution of the problem of ensuring structural stability of the homing system and the admissible time of transient processes is the use of a control law in which the movement of the control surface is dependent not only only on ϑ, but also on α. If the duration of transient processes does not play a special role, it is not necessary to introduce the signal α into the control law.

10.4. Block Diagrams of Radio Zone (Beam-Riding) Control Systems

First, we will construct the block diagram for a beam-riding control system, assuming for generality that the control point at which the radar station is situated and which forms the radar beam is moving. Then, we will consider the control process in a vertical plane, assuming that the rocket is guided by the coincidence method. /534

The general system of equations, derived on the basis of expressions (9.1.20), (9.1.21), (2.9.1), (2.9.2), (9.8.7), (4.5.5), (4.5.1), (4.5.2) and (5.8.1) when $K_a = K_a$, $\Delta_m = \Delta_m$, $S_{com} = 0$, and under the condition that the subscripts "v" in formulas (4.5.1), (4.5.2) and (4.5.5) are omitted has the following form

$$\left.\begin{aligned}
T_v\dot{\vartheta} &= \alpha - A_0,\\
\ddot{\alpha} + 2d\omega_0\dot{\alpha} + \omega_0^2\alpha &= a_\delta(\delta_r + \delta_0),\\
\vartheta &= \theta + \alpha,\\
\dot{r}_t &= v_t\cos q_t - v_c\cos q_c,\\
r_t\dot{\varepsilon}_t &= -v_t\sin q_t + v_c\sin q_c,\\
\dot{r}_r &= v\cos q_r - v_c\cos q_{1c},\\
r_r\dot{\varepsilon}_r &= -v\sin q_r + v_c\sin q_{1c},\\
q_r &= \varepsilon_r - \theta,\\
q_t &= \varepsilon_t - \theta_t,\\
q_c &= \varepsilon_t - \theta_c,\\
q_{1c} &= \varepsilon_r - \theta_c,\\
\delta_r &= F(D)\,[K + W_\alpha(D)\,\alpha + W_\vartheta(D)\,\vartheta],\\
K &= L(D)\,\Delta_m,\\
\Delta_m &= u_a = k_{DF}\varepsilon_{1R},\\
\varepsilon_{1R} &= \varepsilon_R - \varepsilon_r,\\
\varepsilon_R &= W_R(D)\,\varepsilon_t.
\end{aligned}\right\} \qquad (10.4.1)$$

The system (10.4.1) contains 16 equations with 16 unknowns: θ, α, ϑ, δ_r, r_t, q_t, q_c, ε_t, r_r, q_r, q_{1c}, ε_r, K, Δ_m, ε_R and ε_{1R}, where ε_R is the angle of inclination of the equisignal direction produced by the radar set whose tracking system has the transfer function $W_R(D)$.

The values v_t, v_c, θ_c and θ_t, in a general case representing the projections of the vectors $\mathbf{v}_t$ and $\mathbf{v}_c$ onto the vertical plane $o_c x_{ce} y_{ce}$, are given. The parameters A_0 and δ_0 also are considered known.

In order that there be no inadmissibly great overloads, in the course of rocket guidance by the coincidence method, the rocket should fly in the direction of motion of the target. The control point should adhere to this same path so that its radar set will ensure stable automatic tracking of the target. Under these conditions, the angles q_t, q_c, q_{1c} and q_r are small and the kinematic equations assume the following form

/535

$$\begin{aligned}
\dot{r}_t &= v_t - v_c,\\
\dot{r}_r &= v - v_c,\\
r_r\dot{\varepsilon}_r &= v_c(\varepsilon_r - \theta_c) - v(\varepsilon_r - \theta),\\
r_t\dot{\varepsilon}_t &= v_c(\varepsilon_t - \theta_c) - v_t(\varepsilon_t - \theta_t).
\end{aligned}$$

After transformation of these equations, we obtain

$$\frac{d(r_r\varepsilon_r)}{dt} = v\theta - v_c\theta_c, \tag{10.4.2}$$

$$\frac{d(r_t\varepsilon_t)}{dt} = v_t\theta_t - v_c\theta_c. \tag{10.4.3}$$

Then we will have the following linearized equations for a beam-riding control system

$$\left.\begin{aligned}
\dot{\theta} &= \frac{1}{T_v}(\alpha - A_0),\\
\ddot{\alpha} + 2d\omega_0\dot{\alpha} + \omega_0^2\alpha &= a_\vartheta(\delta_r + \delta_0),\\
\dot{\delta}_r &= F(D)[K + W_\vartheta(D)\vartheta + W_\alpha(D)\alpha],\\
K &= L(D)\Delta_m,\\
\Delta_m &= u_a = k_{DF}\varepsilon_{1R},\\
\varepsilon_{1R} &= \varepsilon_R - \varepsilon_r,\\
\varepsilon_R &= W_R(D)\varepsilon_t,\\
\frac{d(r_r\varepsilon_r)}{dt} &= v\theta - v_c\theta_c,\\
\frac{d(r_t\varepsilon_t)}{dt} &= v_t\theta_t - v_c\theta_c.
\end{aligned}\right\} \tag{10.4.4}$$

We recall that according to formula (4.5.3) k_{DF} changes proportionally to the distance between the control point and the rocket.

A block diagram corresponding to the system of equations (10.4.4) is shown in figure 10.11. We note that figure 10.11 also shows circuits characterizing the "current" miss of the rocket h_t, read along the perpendicular to the vector r_t and the normal acceleration j_n. In this case, h_t obviously represents the value of the mismatch parameter, expressed in linear units under the condition that the rocket is situated at the distance r_r from the control point. In accordance with this definition, we have /536

$$h_t = r_r(\varepsilon_t - \varepsilon_r). \tag{10.4.5}$$

When $r_r = r_t$, formula (10.4.5) determines the guidance error (miss of the rocket. As before, we will assume that the lag of the center of mass of the rocket from the vector r_t causes a negative miss.

Figure 10.11 shows that the transfer coefficient k_r of an open system with the breaking of the circuit at the point a is virtually not dependent on the distance r_r, which is caused by the presence of a range potentiometer in the coordinator. This is one of the important differences between homing and beam-riding control systems.

The same conclusions can be drawn with respect to the influence of the form of the control law on the dynamic properties of the guidance circuit as were drawn for homing systems.

The system of equations (10.4.4) and the diagram in figure 10.11 reflect the first form of the equations and the block diagrams for beam-riding control systems.

If the kinematic relationship of the rocket, target and control point is established on the basis of the velocity of deflection of the center of mass of the rocket along the normal to the vector r_t, it is possible to obtain a second form of block diagram. In accordance with figure 2.15, under the condition that the current miss h_t is considered positive, if the rocket outstrips the target, we have

$$\dot{h}_t = v \sin(\varepsilon_t - \theta) - v_c \sin(\varepsilon_t - \theta_c) + r_r\dot{\varepsilon}_t.$$

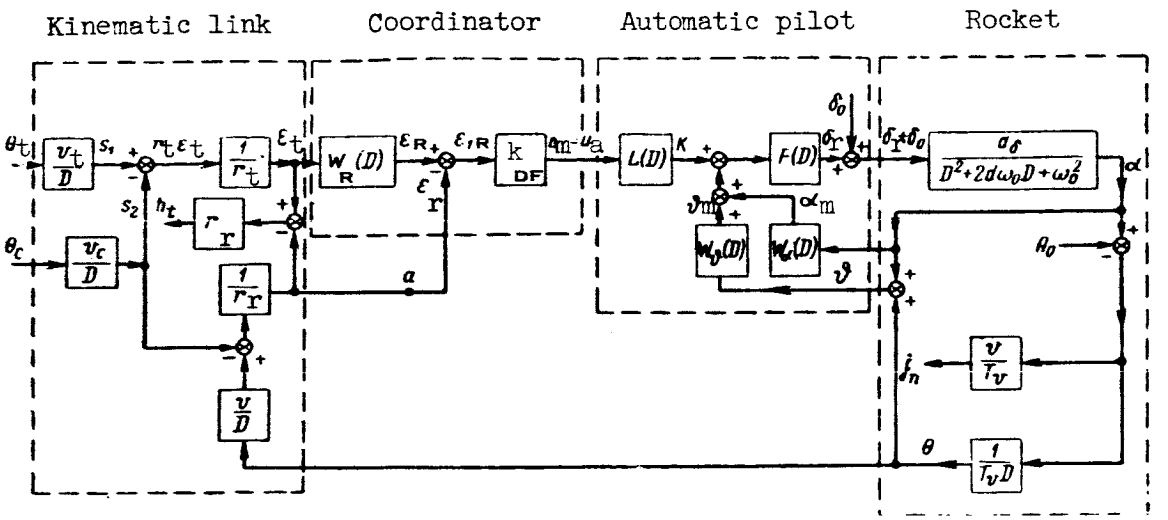

Figure 10.11

We note that such an equation is obtained on the basis of the kinematics of plane-parallel motion of bodies.

As already noted, in some cases, it can be assumed in the coincidence method that $\sin(\varepsilon_t - \theta) \approx \varepsilon_t - \theta$ and $\sin(\varepsilon_t - \theta_c) \approx \varepsilon_t - \theta_c$, but $r \approx r_t - r_r$. Therefore

$$\dot{h}_t = \frac{d}{dt}(r_r \varepsilon_t) - v\theta + v_c\theta_c. \tag{10.4.6}$$

It must be remembered that in writing expression (10.4.6), the approximate equality $\dot{r}_r \approx v - v_c$ was taken into account; this was obtained for $\cos(\varepsilon_r - \theta) \approx 1$ and $\cos(\varepsilon_r - \theta_c)$. But

$$\text{Ц} = \text{t} \qquad \dot{\varepsilon}_{\text{ц}} = \frac{v_c \sin(\varepsilon_{\text{ц}} - \theta_c) - v_{\text{ц}} \sin(\varepsilon_{\text{ц}} - \theta_{\text{ц}})}{r_{\text{ц}}} \approx \frac{v_c(\varepsilon_{\text{ц}} - \theta_c) - v_{\text{ц}}(\varepsilon_{\text{ц}} - \theta_{\text{ц}})}{r_{\text{ц}}}.$$

From the latter expression, taking into account that the condition $v_t - v_c \approx \dot{r}_t$ is satisfied for small angles q_t and q_c, we obtain

$$\frac{d(\varepsilon_t r_t)}{dt} = v_t\theta_t - v_c\theta_c. \tag{10.4.7}$$

The expression (10.4.7) determines the relationship beteen ε_t and the given functions v_t, θ_t, v_c and θ_c. /538

For the closure of the control system, which is obtained from (10.4.1), with the introduction of the kinematic equation (10.4.7), it is necessary to have an expression relating the angle ε_r with the miss h_t. This relation which follows from formula (10.4.5) has the following form

$$\varepsilon_r = \varepsilon_t - \frac{h_t}{r_r}. \tag{10.4.8}$$

Taking expressions (10.4.1), (10.4.6), (10.4.7) and (10.4.8) into account, we find the second form of linearized equations describing the rocket guidance process in the vertical plane by means of a beam-riding control system

$$\left.\begin{aligned}
\dot{\theta} &= \frac{1}{T_v}(\alpha - A_0),\\
\ddot{\alpha} + 2d\omega_0\alpha + \omega_0^2\alpha &= a_\delta(\delta_r + \delta_0),\\
\delta_r &= F(D)\,[K + W_\alpha(D)\,\alpha + W_\vartheta(D)\,\vartheta],\\
K &= L(D)\,\Delta_m,\\
\Delta_m &= u_a = k_{DF}\varepsilon_{1R},\\
\varepsilon_{1R} &= \varepsilon_R - \varepsilon_r,\\
\varepsilon_r &= \varepsilon_t - \frac{h_t}{r_r},\\
\varepsilon_R &= W_R(D)\,\varepsilon_t,\\
\dot{h}_t &= \frac{d}{dt}(r_r\varepsilon_t) - v\theta + v_c\theta_c,\\
\frac{d}{dt}(\varepsilon_t r_t) &= v_t\theta_t - v_c\theta_c.
\end{aligned}\right\} \tag{10.4.9}$$

The block diagram corresponding to the system of equations (10.4.9) is shown in figure 10.12. This diagram differs from figure 10.11 only in the structure of the kinematic link.

In those cases when a beam-riding control system is used for rocket guidance toward a fixed target from a fixed control point, the block diagrams are simplified considerably.

As an illustration, we will consider a system of lateral guidance of a rocket with plane aerodynamic symmetry. The equations describing the guidance process under the mentioned conditions, under the assumption that the angle of slip $\alpha_s = 0$, will have the following form /549

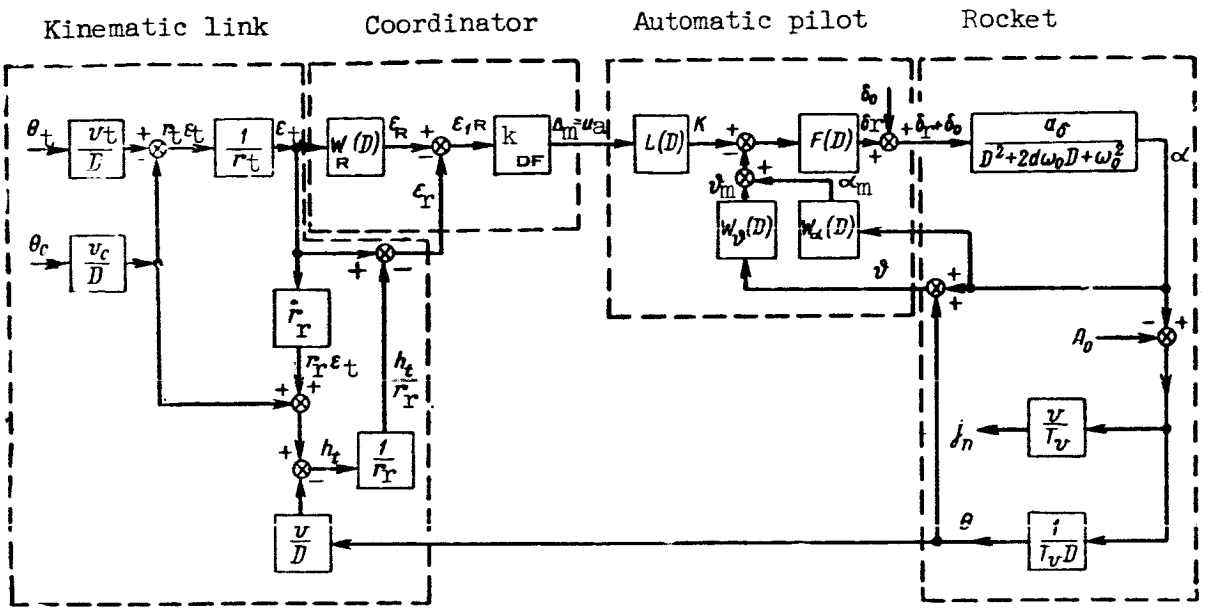

Figure 10.12

$$
\left.
\begin{aligned}
\gamma_b &= \frac{k_\gamma}{D(T_\gamma D+1)}\delta_a,\\
\psi &= -\frac{g}{v_h D}\gamma_b,\\
\delta_a &= F_h(D)\,[K_h + W_\gamma(D)\gamma_b],\\
K_h &= L_h(D)\,\Delta_{mh},\\
\Delta_{mh} &= u_z = k_{DF}\varepsilon_{1Rh},\\
\varepsilon_{1Rh} &= \varepsilon_{Rh} - \varepsilon_{rh},\\
\varepsilon_{Rh} &= \varepsilon_{th} + \Delta\varepsilon_{th},\\
\frac{d}{dt}(r_{rh}\varepsilon_{rh}) &= v_h\psi,
\end{aligned}
\right\} \qquad (10.4.10)
$$

where the first two equations were written on the basis of relations (9.2.10) and (9.2.11).

The subscripts "h" in all the equations (10.4.10) indicate that the signals K_h, Δ_{mh}, ε_{1Rh}, ε_{rh}, ε_{th} and r_{rh} define, respectively, the values of the commands, the measured value of the mismatch parameter, the angle between the equisignal line and the direction to the rocket, the azimuth of the rocket and of the target, and the range to the rocket in the horizontal plane. These same subscripts "h" characterize the transfer functions $F_h(D)$ and $L_h(D)$ for apparatus ensuring deflection of the ailerons under the influence of commands

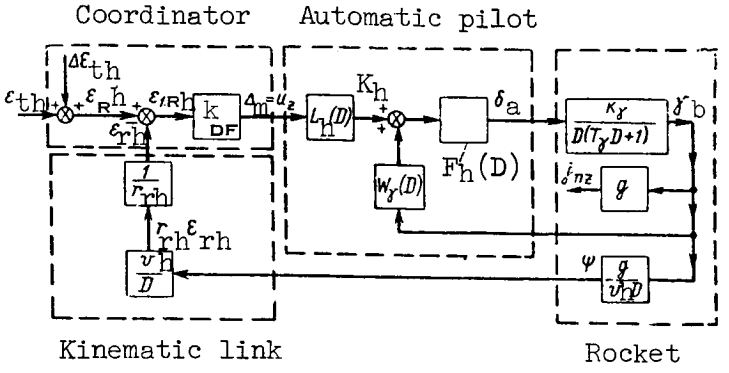

Figure 10.13

K_h and additional control signals and also for apparatus forming the commands K_h in a horizontal plane.

In the derived system of eight equations (10.4.10), the unknowns are ψ, γ_b, δ_a, K_h, Δ_{mh}, ϵ_{1Rh} and ϵ_{rh}, and $\Delta\epsilon_{th}$ characterizes the setting of the angle ϵ_{th}.

The block diagram corresponding to equations (10.4.10) is shown in figure 10.13. This figure also shows the link determining the relationship of γ_b to the signal j_{nz} characterizing the normal acceleration of the rocket in the /541 horizontal plane. If one of the axes of the rectangular coordinate system whose origin is situated at the control point is superposed with the direction to the target, the angle $\epsilon_t = 0$ and the arc - $r_{rh}\epsilon_{rh}$ in equations (10.4.10) for small deflections of the rocket from the straight line connecting the target to the control point will approximately characterize the linear error of rocket guidance h_{zt} for a given value r_{rh}. When $r_{rh} = r_t$ the value h_{zt} will represent the miss of the rocket.

In addition, in the sixth equation of system (10.4.10), the angle ϵ_{rh} must be considered equal to

$$\epsilon_{rh} = \epsilon_{th} - \frac{h_{zt}}{r_{rh}}.$$

Under these conditions, the block diagram shown in figure 10.14 is obtained.

If the radio zone control system uses radio navigation measurement instruments for determination of rocket coordinates, depending on their type, it is

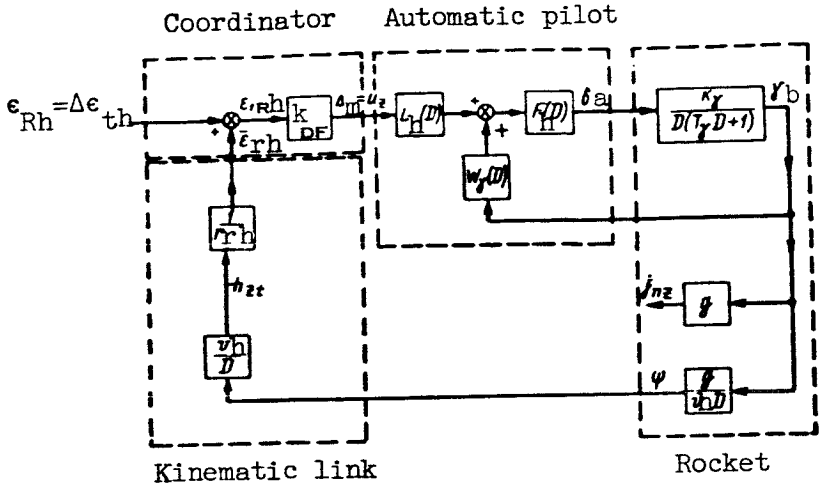

Figure 10.14

possible to obtain a considerable number of equations and block diagrams characterizing the guidance process. Since the method for solution of the problem of the block diagram of a particular control system is common for all, we will consider only one form of the radio zone control system. We will assume that the coordinator is based on an add-subtract- range-finding system and that the guided rocket has plane aerodynamic symmetry only in the horizontal plane. In addition, we will assume that the trace of the reference trajectory coincides with the perpendicular to the base, passing through its middle.

In accordance with expression (4.12.18), the coordinator of the considered type is described by the following equation /542

$$u_z = k_z \Delta_z,$$

where

$$\Delta_z \approx r_r \epsilon_{1R} = r_r(\epsilon_{th} - \epsilon_{rh}).$$

If the value of the angle $\Delta\epsilon_{th}$ is assumed to equal zero, and the link with the transfer coefficient $k_{DF\ h}$ is replaced by two links connected in series having the transfer coefficients k_z and r_r, we obtain the block diagram shown in figure 10.13.

We note in conclusion that in comparing the block diagrams shown in figures 10.11 to 10.14, it was assumed that the instruments for conversion of mismatch signals into commands are situated in the automatic pilot unit. Under real

conditions, the apparatus having the transfer functions L(D) and $L_h(D)$ can be fully incorporated into the coordinator or form an independent unit.

10.5. Block Diagrams of Command Control Systems

If we wished to consider all possible methods for design of coordinators and command control radio links, it would be possible to present a very great number of types of systems of command radio control for the same rocket guidance method.

We will consider first the problem of the block diagram of a command radio control system of the first kind for a case when the rocket is guided by the coincidence method. In order for the block diagram to be most general, we will assume that the coordinates of rocket and target are determined by different measuring instruments RCI and TCI and the target and control point are moving. At the same time, we will assume that the RCI and TCI are situated quite close to one another so that the system includes no computer for producing signals for compensation of parallax errors.

As already mentioned repeatedly, in most cases, it is possible to consider separately the processes of guidance in vertical and horizontal (or oblique) control planes. Hereafter, we will investigate control only in a vertical plane. All the conclusions which will be drawn can be applied also to the lateral motion of the rocket, taking into account its equations and the transfer functions of all the control apparatus.

The general system of equations obtained on the basis of expressions (9.1.20), (9.1.21), (2.9.1), (2.9.2), (9.8.7), (7.1.2) and (5.8.1) when $K_a = K_a$, $\Delta_m = \Delta_m$ and $S_{com} = 0$, has the following form /543

$$
\left.
\begin{gathered}
T_v\dot{\theta} = \alpha - A_0, \\
\ddot{\alpha} + 2d\omega_0\dot{\alpha} + \omega_0^2\alpha = a_\delta(\delta_r + \delta_0), \\
\vartheta = \theta + \alpha, \\
\dot{r}_t = v_t\cos q_t - v_c\cos q_c, \\
r_t\dot{\varepsilon}_t = -v_t\sin q_t + v_c\sin q_c, \\
\dot{r}_r = v\cos q_r - v_c\cos q_{1c}, \\
r_r\dot{\varepsilon}_r = -v\sin q_r + v_c\sin q_{1c}, \\
q_r = \varepsilon_r - \theta, \\
q_t = \varepsilon_t - \theta_t, \\
q_c = \varepsilon_t - \theta_c, \\
q_{1c} = \varepsilon_r - \theta_c, \\
\dot{\delta}_r = F(D)\,[K + W_\alpha(D)\,\alpha + W_\vartheta(D)\,\vartheta], \\
K = L(D)\,K_a, \\
K_a = L_1(D)\,\Delta_m, \\
\Delta_m = u_h = k_{pot}\delta_{pr}^r\,[W_t(D)\,\varepsilon_t - W_r(D)\,\varepsilon_r].
\end{gathered}
\right\} \qquad (10.5.1)
$$

In the derived system (10.5.1) there are 15 equations; the unknown functions are θ, α, δ_r, ϑ, r_t, q_t, q_c, ε_t, q_r, ε_{lc}, ε_r, r_r, K, u_h and K_a. Among these equations, the first three characterize the motion of the rocket, equations 4-11 define the kinematic relations and the other four equations describe the processes transpiring in the automatic pilot, the command control radio link, the apparatus for forming the commands and the coordinator.

It follows from system (10.5.1), representing one of the forms of the equations defining the guidance process in the coincidence method, that the current miss of the rocket h_t, that is, the deflection of its center of mass along the normal to the control point-target line for the current time, is not included in explicit form in the guidance circuit. However, this parameter, equal to

$$h_t = r_r(\varepsilon_t - \varepsilon_r), \tag{10.5.2}$$

can be determined from the given values r_r and ε_t and also on the basis of the computed value of the angle ε_r.

If all the considerations expressed during the discussion of beam-riding control systems are taken into account, system (10.5.1) can be reduced to the following form /544

$$\left.\begin{aligned}
\dot{\theta} &= \frac{1}{T_v}(\alpha - A_0),\\
\ddot{\alpha} + 2d\omega_0\dot{\alpha} + \omega_0^2\alpha &= a_\delta(\delta_r + \delta_0),\\
\delta_r &= F(D)\,[K + W_\alpha(D)\,\alpha + W_\vartheta(D)\,\vartheta],\\
K &= L(D)\,K_a,\\
K_a &= L_1(D)\,\Delta_m,\\
\Delta_m = u_h &= k_{pot}\partial r_{pr}\,[W_t(D)\,\varepsilon_t - W_r(D)\,\varepsilon_r],\\
\frac{d(r_r\dot{r}_r)}{dt} &= v\theta - v_c\theta_c,\\
\frac{d(r_t\dot{r}_t)}{dt} &= v_t\theta_t - v_c\theta_c.
\end{aligned}\right\} \tag{10.5.3}$$

The block diagram corresponding to equations (10.5.3), with expression (10.5.2) taken into account, is shown in figure 10.15. A comparison of this diagram with figure 10.11 reveals that the command radio control system differs from a beam-riding control system (in both cases during rocket guidance by the coincidence method) with respect to the structure of the coordinator, automatic pilot and an additional link characterizing the apparatus for forming commands. A common feature of both is the presence of two integrating links $\frac{1}{T_v D}$ and $\frac{v}{D}$, connected in series.

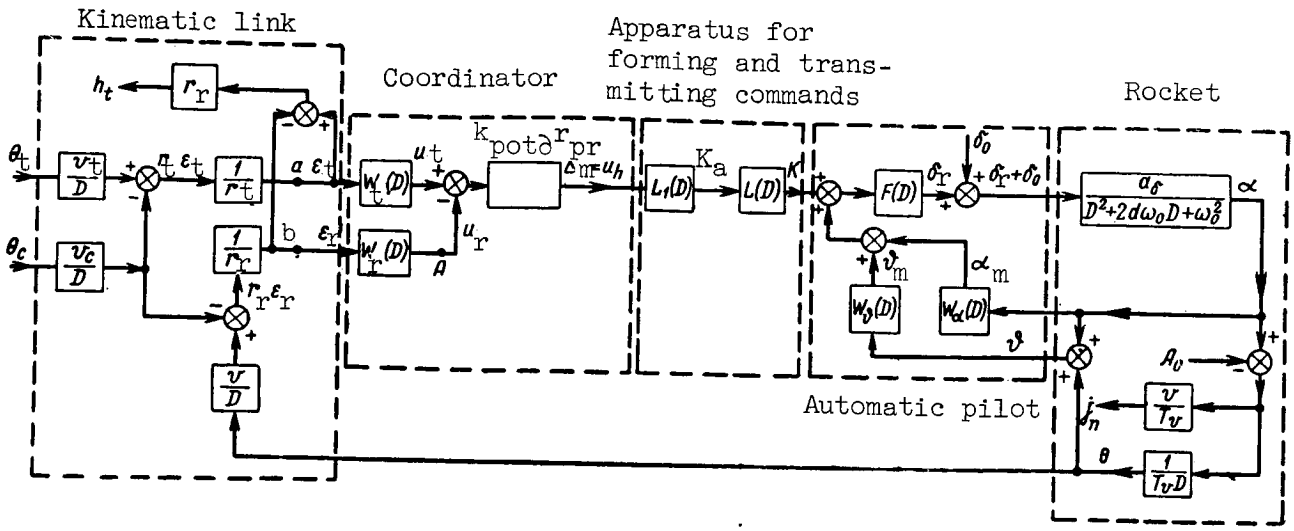

Figure 10.15

If the control system contains only one radar set, operating, for example, by the group method and ensuring the measurement of the difference in angular coordinates $\varepsilon_t - \varepsilon_r$, the coordinator equation is modified. In this case, the block diagram of the control system can be obtained on the basis of the diagram in figure 10.15 by connecting the apparatus shown in figure 10.6 to the points a and b and by eliminating the links $W_t(D)$, $W_r(D)$ and $k_{pot}\partial^r_{pr}$.

We note that in figure 10.16 the radar set is represented by a link with the transfer function $W_R(D)$, whose output signal is the voltage $u_{\varepsilon 1}$, characterizing the angle ε_1.

In a case when the control system is nonautomatic, the apparatus for forming the commands is characterized by the following equations (section 5.9)

$$K_a = k_{\partial c}\Delta_{lev} \quad \text{and} \quad \Delta_{lev} = k_o(1 + T_o D)\,\Delta_m\,(t - \tau_{lag}).$$

Then when an inertialess instrument is used for measuring the difference between the angles ε_t and ε_r, and under the condition that the rocket is stabilized for banking, and only control commands K are fed to the control surface apparatus, we obtain the block diagram shown in figure 10.17.

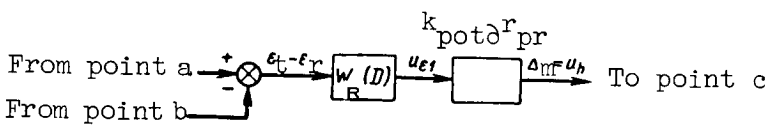

Figure 10.16

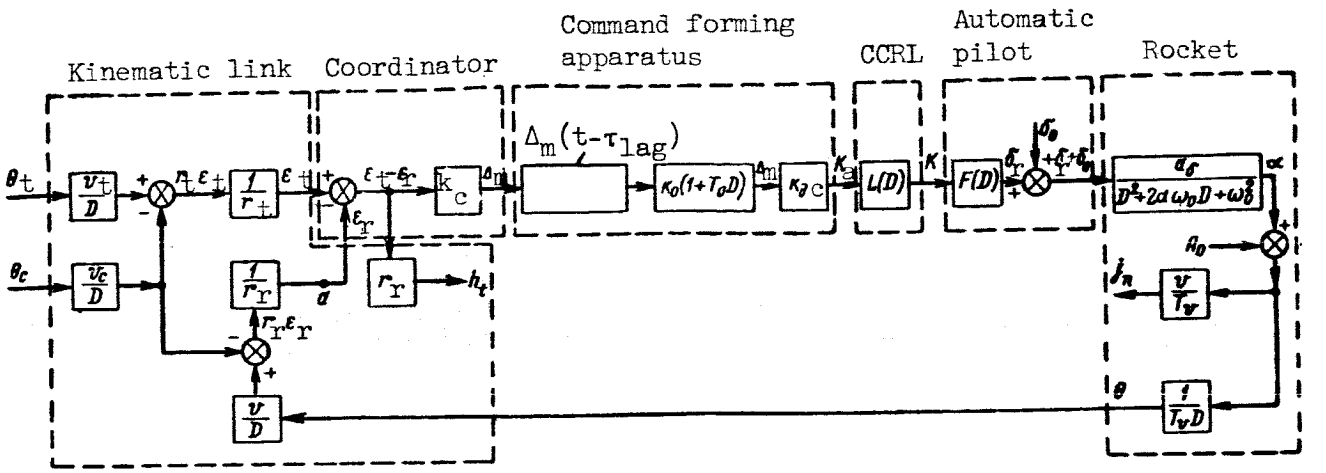

Figure 10.17

In this case /546

$$\Delta_m = k_c(\varepsilon_t - \varepsilon_r),$$

where k_c is the transfer coefficient of the coordinator (such as an optical coordinator).

Since the signal K_a is a fluctuating signal, it is infeasible to develop a command control radio link and a control surface control apparatus in such a way that they will perform amplification operations and differentiation functions. These apparatuses are essentially inertialess. Under such conditions, for the guidance circuit to be stable it is necessary to impose extremely rigorous requirements on the actions performed by the operator. This can be attributed to the fact that the portion of the effect for the derivative of Δ_m, that is, the coefficient characterizing the value δ_r for an individual rate of change of Δ_m should be quite large and at the same time limited both at the top and at the bottom. The need for thorough training of the operator disappears when using more rational control laws. In automatic control systems with fixed rocket parameters, this can be achieved by the selection of a control law and a transfer coefficient k_r open at the point A (fig. 10.15) of the guidance circuit.

In command control systems, it is easier to ensure the necessary value k_r by the use of adjustable components in the circuits of the measuring instruments, computer and command control radio link.

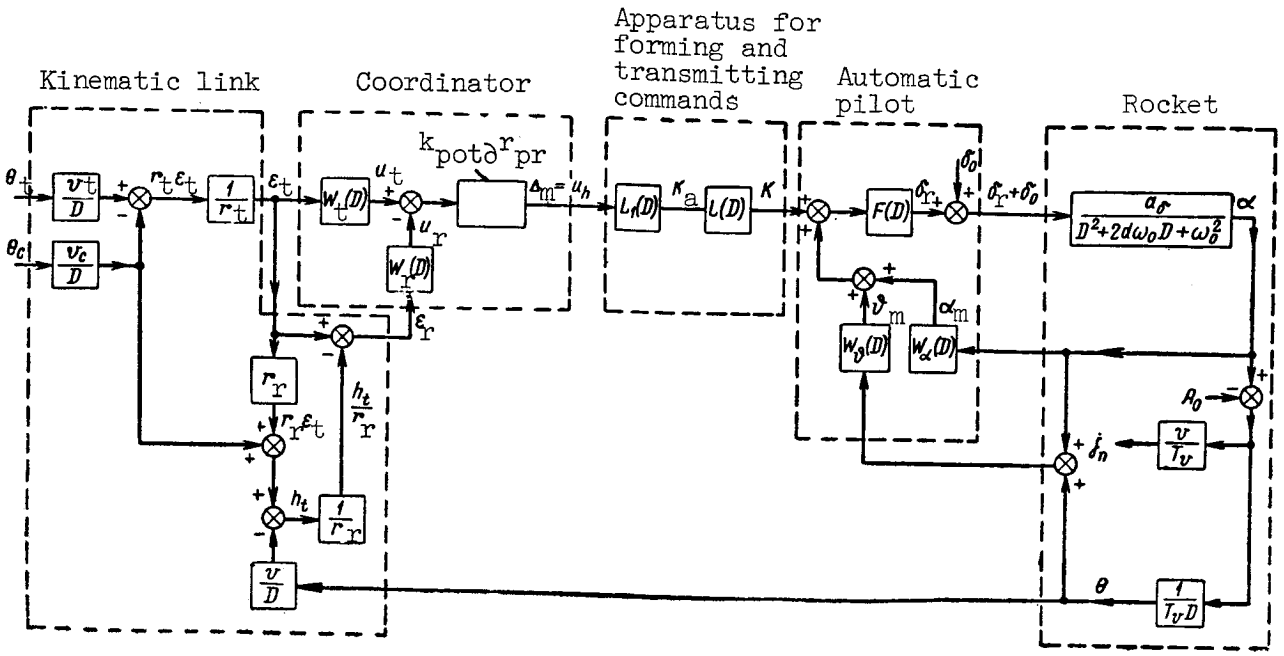

Figure 10.18

Figure 10.15 shows that with the use of the value and sign of the linear deflection of the center of mass of the rocket along the normal to the vector $\mathbf{r}_t$ as the mismatch parameter, the transfer coefficient k_r of the open guidance circuit is not dependent on r_r if $r_{pr} = r_r$. At the same time, when the mismatch parameter is the value and sign of the angle formed by the vectors $\mathbf{r}_r$ and $\mathbf{r}_t$, the value k_r decreases with an increase of r_r (fig. 10.17).

If the first kinematic equation in system (10.5.3) is replaced by relation (10.4.6), a second form of block diagram of a command radio control system is obtained (fig. 10.18). The principal characteristic of this diagram is that the signal h_t enters directly into the guidance circuit. The diagram shown in figure 10.17 also can be transformed in a similar way.

The problem of the stability of the circuit for different control laws and the selection of the necessary transfer coefficient k_r should be solved on /548 the basis of known methods of the theory of automatic control systems.

The processes transpiring in command radio control systems during the guidance of a rocket by the approximate parallel approach method are described by the system of equations (10.5.3) if the coordinator equation in it is replaced by the relation

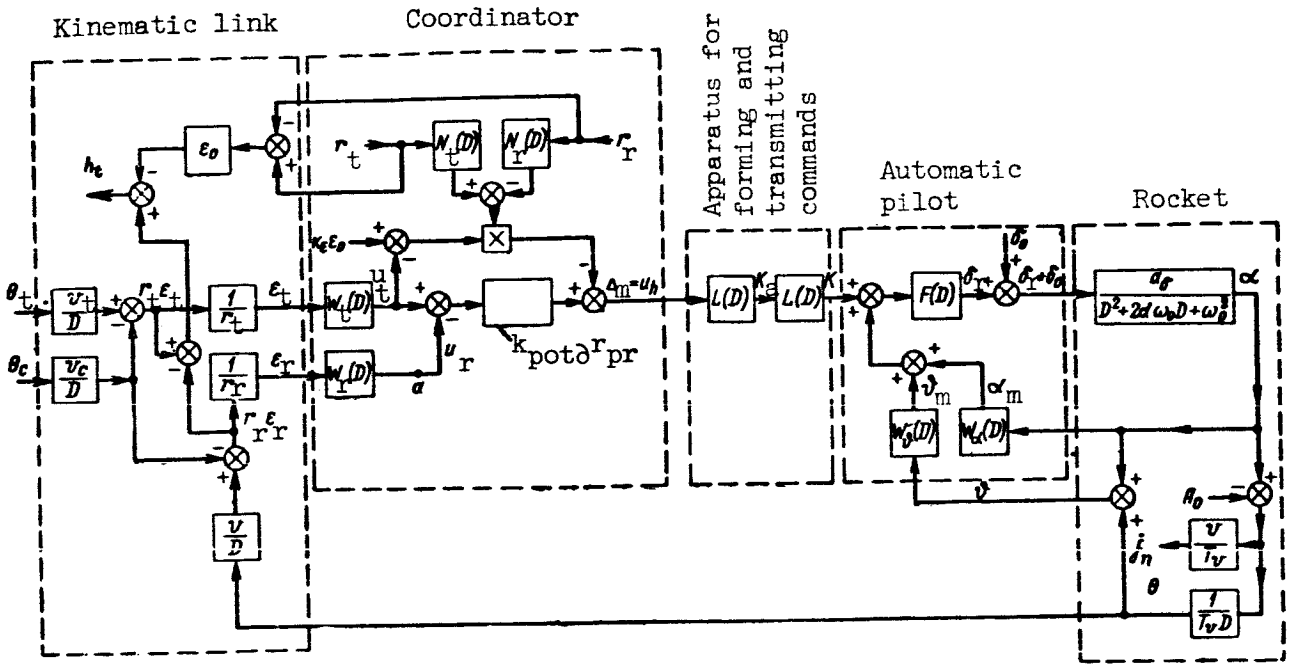

Figure 10.19

$$\Delta_m = u_h = k_{pot}\partial^{r}_{pr}\left\{W_t(D)\epsilon_t - W_r(D)\epsilon_r - \right.$$

$$\left. - \frac{N_t(D)r_t - N_r(D)r_r}{k_{pot}\partial^{r}_{pr}}\left[k_\epsilon\epsilon_0 - W_t(D)\epsilon_t\right]\right\}. \qquad (10.5.4)$$

In this expression, which is derived on the basis of equation (5.5.6), r_t, r_r, ϵ_0 and $r_{pr} = r_r$ are considered given functions of time and $k_\epsilon\epsilon_0$ characterizes the voltage $u_\epsilon(t)$ in (5.5.6).

Then it is possible to obtain the first form of the block diagram shown in figure 10.19.

The value of the guidance error h_t, noted in figure 10.19, is

$$h_t = r_r(\epsilon_K - \epsilon_r),$$

where ϵ_K is the angle between the axis $o_c x_{ec}$ and the straight line on which the center of mass of the rocket should be situated during its motion along the reference (kinematic) trajectory.

For the approximate method of parallel approach

$$\epsilon_K = \epsilon_t - \frac{r_t - r_r}{r_{pr}} (\epsilon_0 - \epsilon_t). \tag{2.8.7}$$

Therefore, assuming that $r_{pr} = r_r$, we will have

$$h_t = r_t\epsilon_t - (r_t - r_r)\epsilon_0 - r_r\epsilon_r. \tag{10.5.5}$$

It therefore can be seen that for the end of the guidance process, when $r_t = r_r$,

$$h_t = r_t(\epsilon_t - \epsilon_r). \tag{10.5.6}$$

It should be noted that equation (10.5.4) is nonlinear. Therefore, the resulting diagram (fig. 10.19) can be considered a block diagram only conditionally. When the principle of "freezing" of ranges r_t and $r_r \approx r_{pr}$ is applied, equation (10.5.4) is transformed into a linear equation, and it is then possible to construct easily a block diagram of a fully linearized control system.

For finding the second form of the block diagram of a command radio control system for the approximate method of parallel approach of the rocket to the target, it is also possible to use system (10.5.3) if the coordinator equation in it is replaced by relation (10.5.4) and the first kinematic equation is written in the following form

$$\dot{h}_t = v \sin(\varepsilon_K - \theta) + r_r \dot{\varepsilon}_K - v_c \sin(\varepsilon_K - \theta_c). \tag{10.5.7}$$

When the guidance process is such that /551

$$\sin(\varepsilon_K - \theta) \approx \varepsilon_K - \theta$$

and

$$\sin(\varepsilon_K - \theta_c) \approx \varepsilon_K - \theta_c,$$

we obtain

$$\dot{h}_t = \frac{d}{dt}(r_t\varepsilon_t - r\varepsilon_0) - v\theta + v_c\theta_c. \tag{10.5.8}$$

We note that in deriving the equation (10.5.8), the expression for ϵ_K and the formula $\dot{r}_r \approx v - v_c$ were taken into account.

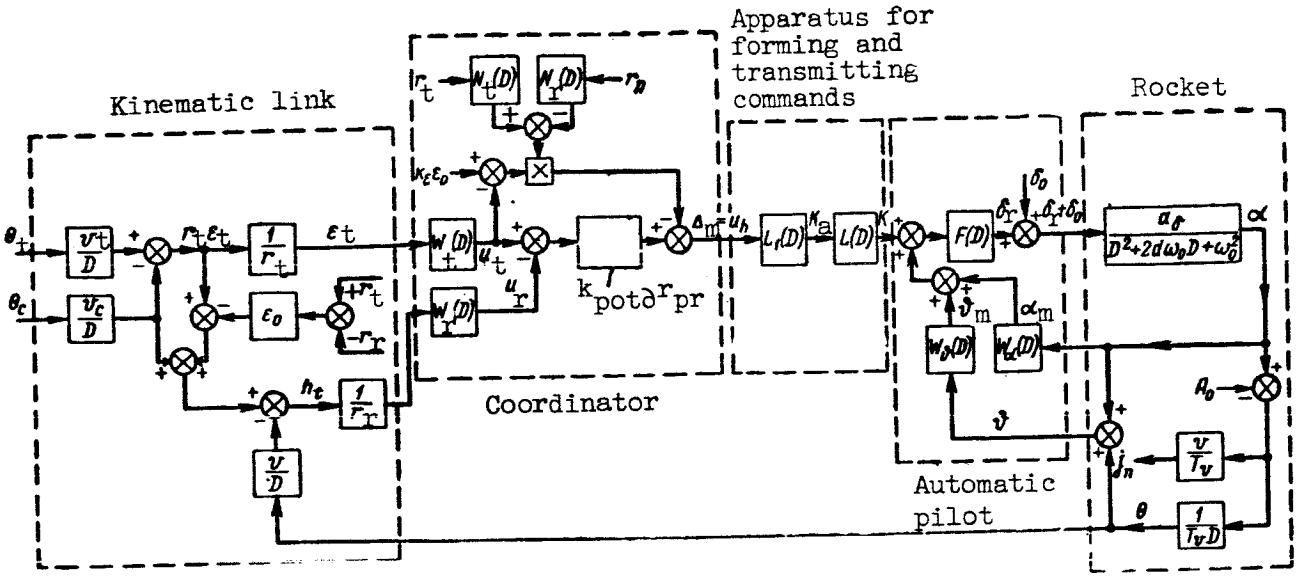

Figure 10.20

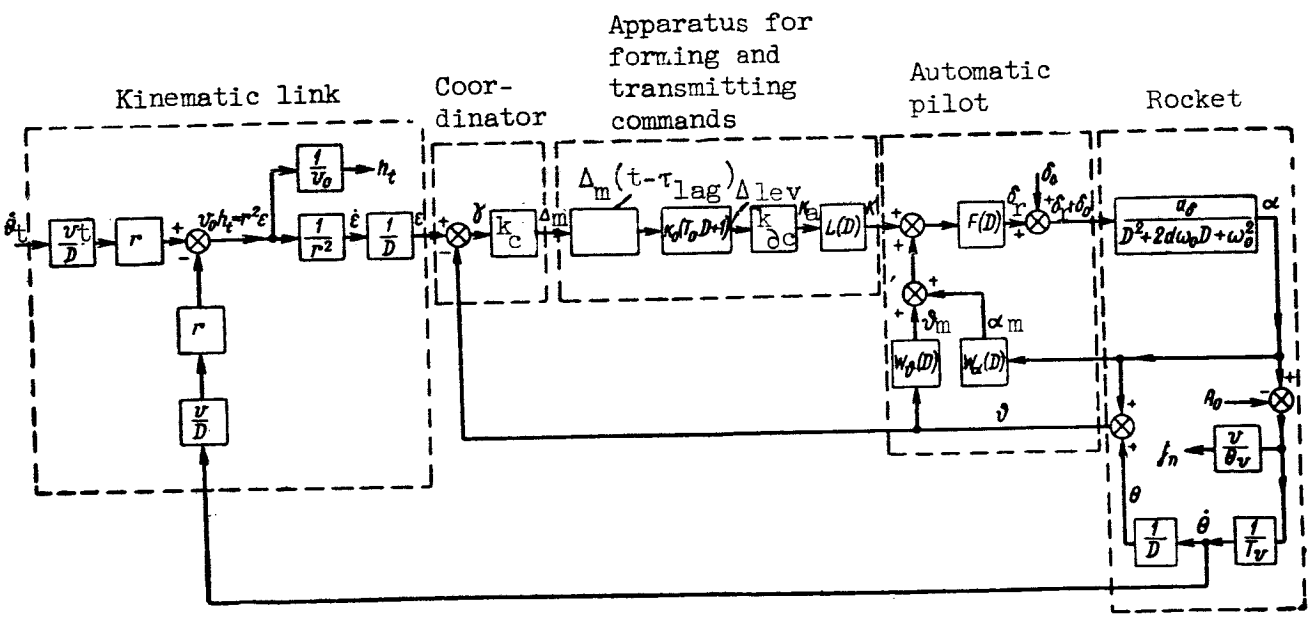

Figure 10.21

Then, after replacement of the coordinator equation and the first kinematic equation in (10.5.3) by the relations (10.5.4) and (10.5.8) and taking expression (10.5.5) into account, it is possible to construct the block diagram shown in figure 10.20. With the "freezing" of the distances r_r and r_t, we obtain a block diagram in which the coordinator will be represented by a linearized equation.

The block diagrams of command radio control systems of the second kind can be obtained from the corresponding diagrams of homing systems if they include equations characterizing the data transmission system, the action of the operator, an apparatus for forming commands and a command radio link.

As an example, figure 10.21 shows the block diagram of a command radio control system by means of which the rocket is guided by the direct method.

Linearized equations for such a system in a case when the miss of the rocket is one of the signals acting within the guidance circuit has the following form

$$\left.\begin{gathered}
\dot{\theta}=\frac{1}{T_v}(\alpha-A_0),\\
\ddot{\alpha}+2d\omega_0\dot{\alpha}+\omega_0^2\alpha=a_\delta(\delta_r+\delta_0),\\
\delta_r=F(D)\,[K+W_\vartheta(D)\,\vartheta+W_\alpha(D)\,\alpha],\\
K=L(D)\,K_a,\\
K_a=k_{\partial c}\Delta_{lev},\\
\Delta_{lev}=k_0(1+T_cD)\,\Delta_m(t-\tau_{lag}),\\
\Delta_m=u_{DF}=k_c\gamma,\\
\gamma=\varepsilon-\vartheta,\\
\vartheta=\theta+\alpha,\\
\frac{d(v_0h_t)}{dt}=r\left(v_t\dot{\theta}_t-\frac{v}{T_v}\dot{\theta}\right),\\
h_t=\frac{r^2\dot{\varepsilon}}{v_0}.
\end{gathered}\right\} \qquad (10.5.9)$$

We note that in this system of equations k_c is the transfer coefficient of the coordinator, including an instrument for measuring the angle γ, which is carried on the rocket, a system for transmission of data from aboard the rocket to the control point and an indicator set up at the control point. /553

10.6. Block Diagrams of Autonomous Control Systems

In autonomous control systems, the mismatch parameter characterizes the linear deflection of the center of mass of the rocket from a fixed trajectory in a horizontal (or oblique) and a vertical plane.

If the process of rocket guidance in a vertical plane is considered, we obtain the following linearized equations describing the operation of an autonomous control system

$$\left.\begin{aligned}
\dot{\theta} &= \frac{1}{T_v}(\alpha - A_0),\\
\ddot{\alpha} + 2d\omega_0\dot{\alpha} + \omega_0^2 &= a_\delta(\delta_r + \delta_0),\\
\delta_r &= F(D)\,[K + W_\vartheta(D)\,\vartheta + W_\alpha(D)\,\alpha],\\
K &= L(D)\,\Delta_m,\\
\Delta_m &= u_a = u_{st} - u_h,\\
u_h &= W_h(D)\,H,\\
\dot{H} &= v\theta.
\end{aligned}\right\} \qquad (10.6.1)$$

Here $W_h(D)$ is the transfer function of the instrument for measuring the flight altitude of the rocket, u_h is the voltage (current) produced by the instrument for measuring altitude H, u_{st} is the voltage (current) characterizing the stipulated flight altitude of the rocket.

The kinematic equation

$$\dot{H} = v\theta \qquad (2.4.2)$$

is written on the assumption that $\theta = \theta_v$.

System (10.6.1) corresponds to the block diagram shown in figure 10.22. It is a characteristic of this block diagram that part of the apparatus of the coordinator (instrument for measuring altitude H) is placed in the feedback circuit of the external guidance circuit. The apparatus forming the command K can be included within the automatic pilot unit or outside it.

The behavior of the autonomous control system in the horizontal plane is determined by equations similar to those which enter into system (10.6.1). For example, if the rocket has plane aerodynamic symmetry and $\alpha_s = 0$, we obtain the following system of equations /554

$$\left.\begin{aligned}
\gamma_b &= \frac{k_\gamma}{D\,(T_\gamma D + 1)}\,\delta_a,\\
\psi &= -\frac{g}{v_h D}\,\gamma_b,\\
\delta_a &= F_h(D)\,[K_h + W_\gamma(D)\,\gamma_b],\\
K_h &= L_h(D)\,\Delta_{mh},\\
\Delta_{mh} &= -u_z,\\
u_z &= W_z(D)\,z,\\
z &= v_h\psi,
\end{aligned}\right\} \qquad (10.6.2)$$

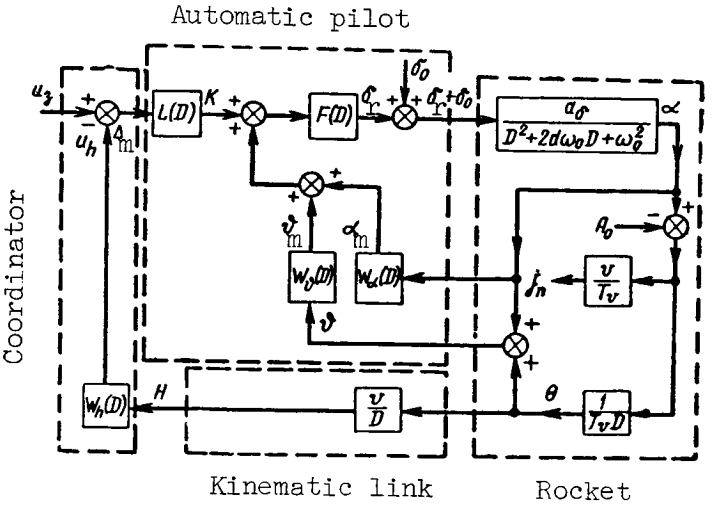

Figure 10.22

where u_z is the voltage produced by the instrument measuring the linear deflection of the center of mass of the rocket from a fixed trajectory in the horizontal plane, and $W_z(D)$ is the transfer function of the instrument for measurement of the linear deflection of the center of mass of the rocket from a fixed trajectory in the horizontal plane.

On the basis of equations (10.6.2) it is quite easy to obtain a block diagram which, in form, will correspond to a considerable degree to figure 10.22. There will be a still greater correspondence between the block diagrams of the systems for control in the vertical and horizontal guidance planes when the rocket has axial aerodynamic symmetry.

CHAPTER 11. ACCURACY OF ROCKET GUIDANCE AND NOISE IMMUNITY OF RADIO CONTROL SYSTEMS

11.1. Principal Sources of Errors in Rocket Guidance

As already mentioned, it is desirable to characterize the quality of /555
the control system by the guidance error (miss) of the rocket. The value of the miss is determined by dynamic, instrument and fluctuation errors.

The dynamic errors are caused by the fact that the rocket itself and the regulating apparatus of the control system have inertia, and as a result the input actions occur with a lag. Depending on the structure of the control system, the value of the dynamic error $h_д$ is dependent on the form of the controlling action, which in turn is determined by the trajectories of motion of the target and of the control point.

The character of motion of the target and of the control point influences the kinematic (reference) trajectory along which the rocket should move. With an increase of the curvature of the kinematic trajectory, the error $h_д$ increases. If the controlling action is a random function of time, at each moment of time the value $h_д$ can assume some value with a particular probability. In the case of random initial conditions of the launching of rockets, $h_д$ will be random even for an identical character of motion of the target. In actual practice, the computation of the dynamic error in many cases is accomplished conveniently by working on the basis of a specific hypothesis on the motion of the target and of the control point, and also on the assumption that the parameters of the control system are known. It then can be assumed that, for a specific moment of time, $h_д$ is a determined value.

The instrument guidance errors h_{in} include the errors of the instruments for measuring the coordinates of the target and rocket, computer, apparatus for forming commands, command control radio link, automatic pilot and the de- /556
sign tolerances in manufacture of the rocket. The reasons for these errors can be shortcomings in the design and circuitry of this apparatus, presence of free play in moving parts of individual instruments, inaccuracy of calibration, etc. So-called systematic errors frequently are included in this same group, that is, errors caused by imperfections of the methods used for measurement of the coordinates of the target and rocket, and also the errors arising due to skewing of coordinate systems.

We note that the concept of skewing of coordinate systems refers to the lack of parallelism between the final control and all other coordinate systems used in the control system.

The instrument errors h_{in} of each of the apparatuses in the control system has regular and random components. As a result, it is possible to determine the mathematical expectation and correlation function (or dispersion) of the error h_{in}. Usually the regulating apparatus of the control system is constructed in such a way that the value h_{in} is negligibly small.

The fluctuation errors of guidance are caused by perturbations acting on the control system. The principal sources of this group of errors are:

(1) fluctuations of amplitude and the effective center of reflection of radio signals arriving from the target to radar coordinate measuring instruments;

(2) fluctuations of signal parameters caused by instability of the conditions for propagation of radio waves, especially in the jet of gases of the jet engine of the rocket;

(3) instrument noise of the radio receivers included in radio control systems;

(4) fluctuations of the velocity vector of the wind, caused by atmospheric turbulence;

(5) active and passive interference organized by the enemy;

(6) fluctuations arising during the quantization of transmitted signals, with respect to both level and time.

The analysis of the accuracy of guidance of controlled rockets is an important part of the theory of radio control systems. As already mentioned in the preceding chapter, the direct method of analysis of guidance errors involves the solution of differential equations describing the processes of rocket control. Since a large percentage of these equations are nonlinear, it is not possible to make a separate determination of the dynamic, instrument and fluctuation guidance errors. As a rule, the total error can be determined only by modeling the guidance process using electronic computers. In theoretical investigations, it is possible to compute only the approximate value of the miss. The miss is computed most easily by solution of the linearized equations of the radio control system with application of the principle of "freezing" of slowly varying coefficients. Under these conditions, the accuracy of /557
rocket guidance can be determined in accordance with the methods of analysis of stationary linear automatic control systems. We note that the possibility of applying the principle of "freezing" of the variable coefficients should be considered separately for each investigated control system. Further simplification of the problem of determining rocket guidance errors is based on the

assumption that it is possible to neglect the small inertia of such apparatus as the command control radio link, automatic pilot, computers and instruments for measuring the coordinates of the rocket and target. It follows that such an assumption is legitimate from the fact that all the mentioned links have broader passbands than the rocket and that the input actions themselves represent slowly and smoothly changing functions of time in which the higher derivatives are insignificant.

However, it must be remembered that the application of the theory of linear systems of automatic control, and the principle of "freezing" of coefficients is possible only in those cases when the parasitic perturbations acting on the radio control system do not lead to a random or a determined law of change of its parameters. In this connection, it is most important to establish what processes will occur in the elements of the radio control system when it is acted upon by different kinds of perturbations.

The objective of the discussion which follows is examination of the problems involved in the method for determination of the dynamic and fluctuation errors of rocket guidance for linearized homing systems, radio zone control systems, command control systems and autonomous control systems. In order to shorten the length of the book, we will assume that all the sources of fluctuation errors in guidance (except atmospheric turbulence) form interference which act upon the electronic apparatus of the radio control system and that they have specific statistical characteristics.

No special consideration will be given to the influence of instrument errors and atmospheric turbulence in this chapter, although their influence can be taken into account in conjunction with the method discussed here.

11.2. Dynamic Errors in Rocket Guidance

In an investigation of the spatial motion of a rocket, the dynamic error can be represented in the form of the vector h_∂ in the reference plane $oy_r z_r$. If the components of this vector along the axes oy_r and oz_r are denoted $h_{\partial y}$ and $h_{\partial z}$, the value of the dynamic error h_∂ will be equal to

$$h_\partial = \sqrt{h_{\partial y}^2 + h_{\partial z}^2},$$

and the inclination of the vector h_∂ in relation to the oz_r axis forms the angle /558

$$\beta_\partial = \arctan \frac{h_{\partial y}}{h_{\partial z}}.$$

Since the same method is used for determination of $h_{\partial y}$ and $h_{\partial z}$, it is sufficient to consider the errors for only one guidance plane. In this section, it will be assumed that the motion of the rocket occurs in the vertical plane. Then $h_{\partial} = h_{\partial y}$.

In homing systems, the input action is the value v_t and the direction θ_t of the velocity vector v_t of the target. When a rocket is guided by a beam-riding control system and a command control system from a moving control point, the input signal is determined by the angles θ_t and θ_c, and also the values v_t and v_c of the vectors v_t and v_c. If the linearized equations of the control system are considered, in accordance with the superposition principle, the value h_{∂}, with θ_t, θ_c, v_t and v_c taken into account, will be equal to

$$h_{\partial} = h_1 + h_2,$$

where h_1 and h_2 are the dynamic guidance errors caused by the motion of the target and control point, respectively.

The error h_1 should be computed on the assumption that there is a fixed control point and h_2 on the assumption that $v_t = 0$.

It is known that for the dynamic error y_{∂} of a linear stationary automatic control system, in which the transfer function of the open circuit is $W(D)$ and the input and output signals represent the functions $x_{in}(t)$ and $x_{out}(t)$, for a steady-state regime, we have the following formula

$$y_{\partial}(t) = c_0 x_{\text{вх}}(t) + c_1 \frac{dx_{\text{вх}}(t)}{dt} + \frac{1}{2}\frac{d^2x_{\text{вх}}(t)}{dt^2} + \ldots + \frac{1}{k!} c_k \frac{d^k x_{\text{вх}}(t)}{dt^k} + \ldots, \qquad (11.2.1)$$

вх = in

where $c_k = \left.\frac{d^k [W_o(D)]}{dD^k}\right|_{D=0}$ is the error coefficient of the (k + 1)-th term, and $W_o(D)$ is the transfer function of the error.

Radio control systems are nonstationary. However, command control systems and radio zone control systems, especially in the case of rocket guidance by the coincidence method, are close to stationary. This can be attributed to the fact that with a sufficiently precise formulation of the law for $r_{pr}(t)$, the

parameters of the guidance circuit in the case of using the coincidence method vary with time only due to a change of the coefficients a_δ, d, ω_0 and T_v, characterizing the rocket as an object of control.

In systems of command radio control ensuring guidance by the parallel approach method, the guidance circuit parameters are influenced not only by a_δ, d, ω_0 and T_v, but by distance r_t as well. However, the change of a_δ, d, ω_0, T_v and r_t with time occurs relatively slowly. Therefore, when determining /559 the dynamic errors of beam-riding control systems and command control systems for a specific segment of the rocket trajectory, when a small interval of time is considered, all the coefficients in the equations of these systems can be considered constant and equal to their values at the time of flight by the rocket through the middle of the investigated segment of the trajectory. Then, when finding the dynamic error of rocket guidance, it is possible to use formula (11.2.1).

Computation of the value h_∂ using this same formula for homing systems, whose transfer constant is dependent not only on the properties of the rocket, but also on the distance r, involves great errors and can be accomplished only if the principle of "freezing" of variable coefficients is applicable.

The purpose of this section is a discussion of the problem of use of the formula (11.2.1) for different types of linearized systems of radio control and different methods of rocket guidance.

It follows from expression (11.2.1) that for determination of the dynamic error h_∂ of a radio control system, it is most important to find the transfer function $W_0(D)$ which gives the relationship between the current miss h_t and the input actions. It is easy to see that $W_0(D)$ will be dependent not only on the type of system but also on the guidance method.

If rocket guidance is accomplished by the coincidence method, using a command control system, in accordance with the block diagrams shown in figures 10.15 and 10.17 and expression (11.2.1) for the dependence of the current miss h_t on ε_t and $x_c = \int_0^t v_c \theta_c dt$, we obtain

$$h_t = \left[1 - \frac{W_c(D)}{1 + W_c(D)} \frac{W_t(D)}{W_r(D)}\right] \varepsilon_t r_r + \frac{1}{1 + W_c(D)} x_c. \qquad (11.2.2)$$

Here $W_c(D) = \frac{u_r(t)}{u_t(t)}$ is the transfer function of the external guidance circuit open at point a, with the signals $u_t(t)$ and $u_r(t)$ or $\varepsilon_t(t)$ and $\varepsilon_r(t)$ at the input and output (figs. 10.15 and 10.17).

The value ε_t entering into expression (11.2.2) is equal to (fig. 10.15)

$$\varepsilon_t = \varepsilon_{t1} - \varepsilon_{t2}, \tag{11.2.3}$$

where

$$\varepsilon_{t1} = \frac{1}{r_t}\int_0^t v_t \theta_t dt, \tag{11.2.4}$$

$$\varepsilon_{t2} = \frac{x_c}{r_t} = \frac{1}{r_t}\int_0^t v_c \theta_c dt. \tag{11.2.4a}$$

Therefore it is possible to write /560

$$h_t = h_{1t} + h_{2t},$$

where

$$h_{1t} = \left[1 - \frac{W_c(D)}{1 + W_c(D)} \frac{W_t(D)}{W_r(D)}\right] \varepsilon_{t1} r_r$$

is the component of the current miss, caused by the motion of the target and dependent on the distance r_r and the transfer functions $W_c(D)$, $W_t(D)$ and $W_r(D)$:

$$h_{2t} = \left\{\frac{r_t}{1 + W_c(D)} - \left[1 - \frac{W_c(D)}{1 + W_c(D)} \frac{W_t(D)}{W_r(D)}\right] r_r\right\} \varepsilon_{t2}$$

is a component of the current miss caused by the motion of the control point and dependent on the distances r_r and r_t, and also on the transfer functions $W_c(D)$, $W_t(D)$ and $W_r(D)$.

The value of the dynamic error of rocket guidance h_∂ in the region where it encounters the target will be equal to the value h_t when $r_r = r_t$, that is

$$h_{\partial} = h_t\Big|_{r_r=r_t} = h_{1t}\Big|_{r_r=r_t} + h_{2t}\Big|_{r_r=r_t}. \qquad (11.2.5)$$

In accordance with formula (11.2.1), for the stipulated distance r_r for the component h_{1t} we will have

$$\text{ц} = \text{t} \qquad h_{1t} = c'_0\varepsilon_{t1}r_r + c'_1 r_r \frac{d\varepsilon_{t1}}{dt} + \frac{1}{2}c'_2 r_r \frac{d^2\varepsilon_{t1}}{dt^2} + \ldots + \frac{1}{k!}c'_k r_r \frac{d^k\varepsilon_{t1}}{dt^k} + \ldots \qquad (11.2.6)$$

Here

$$c'_k = \frac{d^k W_{01}(D)}{dD^k}\Big|_{D=0};$$

$$W_{01} = 1 - \frac{\overline{W}_c(D)}{1+\overline{W}_c(D)}\frac{\overline{W}_t(D)}{\overline{W}_r(D)}.$$

If the functions $W_c(D)$, $W_t(D)$ and $W_r(D)$, and also the laws of change of v_t, θ_t and r_r with time are known, it is possible to compute the coefficients c'_k (k = 0, 1, 2, ...) and the derivatives $\frac{d^k\varepsilon_{t1}}{dt^k}$, after which all the terms in expression (11.2.6) are determined. Usually, since the function $\varepsilon_{t1}(t)$ changes slowly with time, it is necessary to take into account no more than 3-5 terms of series (11.2.6) and sometimes only the first non-zero term.

It is simplest to compute h_{1t} when the transfer functions $W_t(D)$ and $W_r(D)$ are identical, when

$$W_{01} = \frac{1}{1+\overline{W}_c(D)}$$

The form of the function $W_c(D)$ is dependent on the control law and the /561 structure of the automatic pilot, and also on the structure of the apparatus for forming and transmitting commands. However, in a general case, it is possible to write

$$W_c(D) = \frac{1}{D^{\nu}}\frac{Q(D)}{A(D)},$$

where ν is a whole number characterizing the degree of astaticism of the system, and Q(D) and A(D) are polynomials also containing free (not dependent on D) terms.

Usually, it is very difficult to design a stable system whose degree of astaticism is greater than 2. Therefore, in most cases, it is necessary to deal with transfer functions $W_c(D)$ for which ν is equal to 1 or 2.

If $\nu = 1$, when $W_t(D) = W_r(D)$

$$W_{o1}(D) = \frac{1}{1 + \frac{1}{D}\frac{Q(D)}{A(D)}} = \frac{Q_1(D)}{A_1(D)} = \frac{b_n D^n + b_{n-1}D^{n-1} + \ldots + b_1 D}{a_n D^n + a_{n-1}D^{n-1} + \ldots + a_1 D + a_0}$$

and the values of the first four error coefficients are equal to

$$c_0' = 0,\ c_1' = \frac{1}{k_v},\ c_2' = \frac{1}{k_v}\left(b_2 - \frac{a_1}{k_v}\right),\ c_3' = \frac{1}{k_v}\left[b_3 - \frac{a_2}{k_v} - \frac{a_1}{k_v}\left(b_2 - \frac{a_1}{k_v}\right)\right],$$

where $k_v = DW_c(D)\Big|_{D=0}$ is the transfer coefficient of the open external velocity guidance circuit.

For second-degree astatic systems

$$W_{o1} = \frac{1}{1 + \frac{1}{D^2}\frac{Q(D)}{A(D)}} = \frac{Q_2(D)}{A_2(D)} = \frac{b_n D^n + b_{n-1}D^{n-1} + \ldots + b_2 D^2}{a_n D^n + a_{n-1}D^{n-1} + \ldots + a_1 D + a_0},$$

where $Q_2(D) = D^2A(D)$ and $A_2(D) = D^2A(D) + Q(D)$, it can be found that

$$c_0' = 0,\ c_1' = 0,\ c_2' = \frac{1}{k_{1r}},\ c_3' = \frac{1}{k_{1r}}\left(b_3 - \frac{a_1}{k_{1r}}\right)$$

We note that in the expressions determining c_2' and c_3', the value $k_{1r} = D^2W_c(D)\Big|_{D=0}$ characterizes the transfer coefficient of the input signal of the acceleration radio control system.

Now for the component $h_1 = h_{1t}\Big|_{r_r=r_t}$ of the dynamic error h_∂ in first- and second-degree astatic systems, we obtain, respectively /562

$$h_1 = \frac{1}{k_v} r_{\text{ц}} \frac{d\varepsilon_{\text{ц}1}}{dt} + \frac{1}{2k_v}\left(b_2 - \frac{a_1}{k_v}\right) r_{\text{ц}} \frac{d^2\varepsilon_{\text{ц}1}}{dt^2} +$$

$$+ \frac{1}{6k_v}\left[b_3 - \frac{a_2}{k_v} - \frac{a_1}{k_v}\left(b_2 - \frac{a_1}{k_v}\right)\right] r_{\text{ц}} \frac{d^3\varepsilon_{\text{ц}1}}{dt^3} + \ldots, \qquad (11.2.7)$$

ц = t
р = r

$$h_1 = \frac{1}{2k_{1\text{р}}} r_{\text{ц}} \frac{d^2\varepsilon_{\text{ц}1}}{dt^2} + \frac{1}{6k_{1\text{р}}}\left(b_3 - \frac{a_1}{k_{1\text{р}}}\right) r_{\text{ц}} \frac{d^3\varepsilon_{\text{ц}1}}{dt^2} + \ldots \qquad (11.2.8)$$

It can be seen from expressions (11.2.7) and (11.2.8) that in systems with first-degree astaticism, the error h_1 is not dependent on the value ϵ_{t1}, and in systems with second-degree astaticism, the value h_1 also is not influenced by the rate $\dot{\epsilon}_{t1}$ of change of ϵ_{t1}. It then should be noted that, whereas in the case of rocket guidance from a moving control point h_1 characterizes one of two components of the dynamic error of guidance h_∂, in the case of a fixed control point h_1 represents the total dynamic error h_∂.

In order to decrease h_1 for a specific function $\epsilon_{t1}(t)$, it is necessary to increase the coefficients k_v and k_{1r} which, as already noted, are dependent on the transfer properties of all the elements forming the guidance circuit. However, the maximum values k_v and k_{1r} are limited by the requirement of ensuring stability of the process of guidance and the technical possibilities of the automatic pilot, etc.

For the component $h_{2t}\big|_{r_r=r_t}$, which can be found the same as $h_{1t}\big|_{r_r=r_t}$, we obtain

$$h_{2t}|_{r_r=r_t} = h_2 = h_1' - h_{1t}'|_{r_r=r_t}, \qquad (11.2.9)$$

where the value h_1' for first- and second-degree astatic systems is determined by formulas (11.2.7) and (11.2.8) with the replacement of ϵ_{t1} in them by ϵ_{t2}, and the error $h_{1t}'\big|_{r_r=r_t}$ should be computed using formula (11.2.6) with the replacement of the function $\epsilon_{t1}(t)$ in it by $\epsilon_{t2}(t)$ and r_r by r_t. If $W_t(D) = W_r(D)$, then $h_2 = 0$.

As an illustration of the results, we will consider the example of determination of the dynamic errors $h_\partial = h_{\partial I}$ and $h_{\partial II}$ in first- and second-degree

astatic systems when $W_t(D) = W_r(D)$ for a case when the control point is fixed and the target moves uniformly and linearly with the velocity v_t at the angle θ_t to the horizontal plane. In this case, it will be assumed that the values $h_{\partial I}$ and $h_{\partial II}$ are characterized with a high degree of accuracy only by the first terms in the series (11.2.7) and (11.2.8). Then on the basis of expression (11.2.7) we find

$$h_{\partial I} = \frac{1}{k_v} r_t \dot{\varepsilon}_t. \qquad (11.2.10)$$

But in accordance with the kinematic equation /563

Ц = t $$r_{ц}\varepsilon_{ц} = \int_0^t v_{ц}\theta_{ц}dt = v_{ц}\theta_{ц}t + r_{ц0}\varepsilon_{ц0}, \qquad (11.2.11)$$

where ε_{t0} and r_{t0} are the angle of inclination ε_t of the vector r_t relative to the horizontal plane and to the distance between the control point and the target, respectively, at the time t = 0.

We therefore find that

Ц = t $$\dot{\varepsilon}_{ц} = \frac{v_{ц}r_{ц0}(\theta_{ц} - \varepsilon_{ц0})}{r_{ц}^2}$$

We note that in obtaining the latter expression, the approximate equation $r_t = r_{t0} + v_t t$ was taken into account.

Substituting the determined value $\dot{\varepsilon}_t$ into formula (11.2.10) and assuming that in the expression derived in this way r_t characterizes the distance between the rocket and the control point at the termination of the guidance process, we will have

Ц = t $$h_{\partial I} = \frac{v_{ц}r_{ц0}(\theta_{ц} - \varepsilon_{ц0})}{k_v r_{ц}} \qquad (11.2.12)$$

Formula (11.2.12), where, as it is easy to find

Ц = t $$r_{ц} = \frac{v}{v - v_{ц}} r_{ц0},$$

shows that the increase of $\theta_t - \varepsilon_{t0}$ from 0 to 90°, with constant values r_{t0}, r_t, v_t and k_v, leads to an increase of the error $h_{\partial I}$.

If in a similar way for $v_c = 0$ we consider a radio control system with second-degree astaticism, we obtain

Ц = t

$$h_{\partial II} = \frac{v_{ц}^2 r_{ц0}(\varepsilon_{ц0} - \theta_{ц})}{k_{1p} r_{ц}^2} \qquad (11.2.13)$$

The method for determination of dynamic errors considered here also is applicable for analysis of other types of radio control systems for different guidance methods. Therefore, we will limit ourselves hereafter to the derivation of formulas characterizing the current miss of the rocket h_t for beam-riding control systems when guiding rockets by the coincidence method, command control systems for the method of parallel approach and homing systems ensuring a direct guidance method and the parallel approach method. In addition, we note the principal characteristics inherent in the analyzed systems.

For beam-riding control systems, by means of which a rocket is guided by the coincidence method, in accordance with figure 10.11 or 10.12, it can be found that

$$h_t = \left[1 - \frac{W_c(D)}{1 + W_c(D)} W_R(D)\right] \varepsilon_t r_r + \frac{1}{1 + W_c(D)} x_c. \qquad (11.2.14)$$

Here $W_c(D)$ is the transfer function of a system open at point a, with the signals ε_R and ε_r at the input and output (fig. 10.11).

A similar expression also is obtained from formula (11.2.2) if it is assumed in it that $W_r(D) = 1$ and $W_t(D)$ is replaced by $W_R(D)$. At the same time, it must be remembered that in a general case the transfer functions $W_c(D)$ for command control systems and beam-riding control systems do not coincide with one another. /564

The value of the current miss for a command control system for rocket guidance by the parallel approach method can be found using figures 10.19 and 10.20.

For the "frozen" values r_t and r_r, we obtain

Ц = t
р = r
к = c
пд = potd

$$h_t = \left[1 - \frac{W_к(D)}{1 + W_к(D)} \frac{W_ц(D)}{W_р(D)}\right] \varepsilon_ц r_р - \frac{1}{k_{пд}} \left[\frac{r_ц}{r_р} N_ц(D) - N_р(D)\right] \left[\frac{W_к(D)}{1 + W_к(D)} \frac{k_в}{W_р(D)} \varepsilon_0 r_р - \frac{W_к(D)}{1 + W_к(D)} \frac{W_ц(D)}{W_р(D)} \varepsilon_ц r_р\right] + \frac{x_c}{1 + W_к(D)}, \quad (11.2.15)$$

where $W_c(D)$ is the transfer function of a system open at point a, with the signals u_t and u_r at the input and output (fig. 10.19). If r_r is replaced by r_t, formula (11.2.15) makes it possible to compute the dynamic error $h_д = h_t\big|_{r_r=r_t}$ Expression (11.2.15), when $r_r = r_t$, becomes the same as for command control systems ensuring the guidance of a rocket by the coincidence method, if $N_t(D) = N_r(D)$.

In the direct method of guidance of a homing rocket the value h_t, as follows from figure 10.6 or 10.8, for a case when v_t = const and v = const and the coefficient r is "frozen," is equal to

$$h_t = r \frac{v_t}{v_0} \frac{1}{1 + W_c(D)} \theta_t, \quad (11.2.16)$$

where $W_c(D)$ is the transfer function of a system open at point a, with the signals S_1 and S_2 at the input and output (fig. 10.6).

A formula of similar external appearance, making it possible to compute h_t, is also obtained for homing systems ensuring the guidance of rockets by the parallel approach and proportional guidance methods.

11.3. Quantitative Characteristics of Noise Immunity of a Radio Control System and Their Relationship to Fluctuation Errors of Rocket Guidance

Each of the radio receivers included in the control system reacts not only to the controlling signals, but also to the parasitic random perturbations which in a general case are formed by the fluctuations of reflected signals, instrument noise and artificially created interference. The controlling /565 signals themselves usually are of a random character.

In the preceding chapters, it was demonstrated that the effect of different kinds of radio interference leads to a change of the conversion (dynamic) properties of the radio links of the control system and to the appearance of errors in the transmission of commands and determination of the coordinates of the target and rocket. In the long run, all this leads to the appearance of additional errors of rocket guidance.

The rocket miss caused by interference is dependent both on the structure and intensity (power) of the interfering signals and on the properties of the radio apparatus used. Different complexes of apparatus used in rocket guidance will react differently to fluctuations of instrument noise and to radio interference created especially for disruption of the guidance process.

The capability of a radio control system to withstand reconnaissance of the radio signal parameters in the electronic apparatus used and to ensure rocket guidance when there is radio interference present is called noise immunity. Quantitative noise immunity is evaluated by the probability p_{ni} that, under the influence of radio interference, the center of mass of the rocket will be deflected along the oy_r and oz_r axes in the dispersal plane $oy_r z_r$ at the distance h_{my} and h_{mz}, not exceeding some values h_{myl} and h_{mzl}. Knowledge of p_{ni} representing the distribution function (integral law of distribution of probabilities) of rocket guidance errors makes it possible to determine the probability of a rocket striking in the specified region in the reference plane and also the two-dimensional differential rocket dispersion law, and as a result it becomes possible to determine the conditional probability $p_{st\,c}$ of striking the target necessary for computation of the unconditional probability p_{st} of striking the target.

If the radio control system includes n radio receivers and the probability that interference will be created at the input of the i-th radio receiver ($i = 1, 2, \ldots, n$) is p_{0i}, the value p_{ni} can be found in the following way. With interference at the input of only the i-th radio receiver, with some conditional probability p_{ci}, characterizing the conditional distribution function, the rocket will be deflected from the target along the oy_r and oz_r axes by the distance $h_{my} \leq h_{myl}$ and $h_{mz} \leq h_{mzl}$.

In a general case, interference appears at the inputs of several radio receivers simultaneously. Then, as a result of the nonlinearity of conversions of the transmitted communications (control command and measured coordinates) by the electronic apparatus when interference is present, the probability that $h_{my} \leq h_{myl}$ and $h_{mz} \leq h_{mzl}$, with the influence of interference on the i-th radio receiver taken into account, will be dependent on the probabilities of the

deflections $h_{my} \leq h_{myl}$ and $h_{mz} \leq h_{mzl}$ caused by interference which is present at the inputs of radio receivers with numbers less than i. Therefore, the value p_{ci} should be computed under the condition that radio interference is received by the receivers with the designation 1, 2, ..., i - 1, together with signals. /566

In order to take into account the mentioned circumstance we introduce the notation $p\left(\frac{A_i}{A_1, A_2, \ldots, A_{i-1}}\right)$ defining the probability of appearance of the deflections $h_{my} \leq h_{myl}$ and $h_{mz} \leq h_{mzl}$ arising due to the effect of interference on the i-th radio receiver, under the condition that all the receivers from the first to the (i - 1)-th were also subjected to the effect of radio interference. Then, taking into account the formula for the total probability and the introduced notations, we find that

$$p_{ni} = \prod_{i=1}^{n}(1-p_{oi}) + \sum_{i=1}^{n} p_{oi}p_{ci}\prod_{\substack{j=1\\ j\neq i}}^{n}(1-p_{oj}) +$$

$$+\sum_{\substack{i=1\\ j=2\,(j>i)}}^{n} p_{oi}p_{oj}p_{ci}p\left(\frac{A_j}{A_i}\right)\prod_{\substack{k=1\\ k\neq i,\,j}}^{n}(1-p_{ok}) + \sum_{\substack{i=1,\,j=2\\ l=3\,(l>j>i)}}^{n} p_{oi}p_{oj}p_{ol}p_{ci}p\left(\frac{A_j}{A_i}\right)\times$$

$$\times p\left(\frac{A_l}{A_i, A_j}\right)\prod_{\substack{r=1\\ r\neq i,\,j;\,l}}^{n}(1-p_{or}) + \ldots + p_{c1}\,p\left(\frac{A_2}{A_1}\right)p\left(\frac{A_3}{A_1, A_2}\right)\ldots\times$$

$$\times p\left(\frac{A_n}{A_1, A_2, \ldots, A_{n-1}}\right)\prod_{i=1}^{n} p_{oi}. \qquad (11.3.1)$$

Expression (11.3.1) makes it possible to compute p_{ni} when there is both natural and artificial interference. In addition, it is possible to compute p_{ni} by taking into account the joint effect of these kinds of interference. In the latter case, "n" should be understood as double the number of actually used radio receivers, and when determining p_{ni} by means of formula (11.3.1) it is necessary to find $\frac{n}{2}$ the values p_{0i} on the assumption that there is noise of natural origin.

The value n can vary in rather considerable limits, depending on the type of radio control system. For example, there is one radio receiver in active

and passive homing systems; beam-riding control systems, ensuring rocket guidance by the coincidence method have two: and command radio control systems and semi-active homing systems usually contain not less than three or four radio receivers.

If one radio receiver is used, with both artificial interference and instrument noise taken into account /567

$$p_{ni} = (1 - p_{o1}) p_{c2} + p_{o1} p_{c1} p\left(\frac{A_2}{A_1}\right). \qquad (11.3.2)$$

When the system contains two radio receivers,

$$p_{ni} = (1 - p_{o1})(1 - p_{o3}) p_{c2} p\left(\frac{A_4}{A_2}\right) + p_{o1}(1 - p_{o3}) p_{c1} p\left(\frac{A_2}{A_4}\right) \times$$
$$\times p\ \frac{A_4}{A_1, A_2} + p_{o3}(1 - p_{o1}) p_{c2} p\left(\frac{A_3}{A_2}\right)\left(\frac{A_4}{A_2, A_3}\right) +$$
$$+ p_{o1} p_{o3} p_{c1} p\left(\frac{A_2}{A_1}\right) p\left(\frac{A_3}{A_1, A_2}\right) p\left(\frac{A_4}{A_1, A_2, A_3}\right). \qquad (11.3.3)$$

In writing expressions (11.3.2) and (11.3.3), the sources of artificial interference and instrument noise were assigned odd and even numbers, respectively.

It follows from expression (11.3.2) that in the absence of artificial interference, when $p_{01} = 0$, the value p_{ni} is determined only by the influence of instrument noise. When $p_{01} = 1$, the rocket miss is dependent both on instrument noise and on artificial interference. If the artificial interference is insufficiently effective, $p_{c1} \approx 1$ and $p_{ni} \approx p\left(\frac{A_2}{A_1}\right)$. When $p_{01} = 1$ and the value $p_{c1} \approx 0$, the control system does not ensure the necessary quality of rocket guidance.

In a control system with two radio receivers, the absence of artificial interference causes a miss resulting solely from instrument noise. The fact that p_{01} or p_{03} is not equal to zero, and also that p_{01} and p_{03} are not equal to zero, exerts an appreciable influence on the value p_{ni}.

In a general case, the p_{ni} distribution function is dependent very complexly on the probabilities p_{0i} (i = 1, 2, ..., n) and a considerable number of conditional distribution functions. At the same time, it should be noted that

in all cases when interference exerts no influence on the conversion properties of the radio links and the radio control system remains virtually linear, all the conditional distribution functions $p\left(\frac{A_j}{A_i}\right)$, $p\left(\frac{A_l}{A_iA_j}\right)$, etc., become independent of whether or not interference affects the preceding radio receivers. This can be attributed to the nondependence of the sources of instrument noise and to the different range of operation of each of the radio receivers.

The probabilities p_{0i}, entering into expression (11.3.1), characterize the secretiveness of operation of the radio control system in the i-th receiving channel, that is, the property of making difficult the detection of radio radiations, reconnaissance of the parameters of the radiated signals and creation of radio interference. It is possible to distinguish secretiveness of the radio control system for the CCRL channels, the coordinate measuring instruments RCI and TCI, the data transmission system and the total secretiveness of the /568 radio control system. The latter can be determined by the probability that interference will not be created at the inputs of any of n radio receivers.

The conditional distribution functions entering into expression (11.3.1) characterize the noise immunity of the radio control system, that is, its capacity to withstand natural and artificial interference when their effect on the radio signal receiving channels 1, 2, ..., n is taken into account. It therefore follows that in determining noise immunity, it is necessary to assume the presence of interference at the inputs of the corresponding number of radio receivers.

The noise immunity of a radio control system for the i-th channel (i = 1, 2, ..., n) alone for radio signal reception is characterized by the value $p_{nc}^{(i)} = p_{ci}$. Taking into account the effect of interference in the i-th and j-th channels (i = 1, 2, ..., n; j = 2, 3, ..., n; j > i), it is feasible to speak of noise immunity for two reception channels with stipulated numbers. The conditional distribution function $p_{nc}^{(i,j)}$ determining the noise immunity of the radio control system for two reception channels is determined, as can be seen from expression (11.3.1), by the following formula

$$p_{nc}^{(i,\,j)} = p_{ci}\,p\left(\frac{A_j}{A_i}\right).$$

Similarly, it is possible to find the quantitative characteristics of noise immunity of a radio control system taking into account the effect of interference on three, four, or more channels. If it is assumed that there is interference acting on all n radio receivers, the conditional distribution function

$$p_{nc}=p_{nc}^{(1,2,\ldots,n)}=p_{c1}p\left(\frac{A_2}{A_1}\right)p\left(\frac{A_3}{A_1,A_2}\right)\cdots$$
$$\times p\left(\frac{A_n}{A_1,A_2,\ldots,A_{n-1}}\right),$$

determined on the basis of expression (11.3.1), represents a quantitative measure of the total noise immunity of the radio control system, frequently simply called the noise immunity of the radio control system.

It follows from the above that, in a general case, the quantitative measure of the noise immunity of a radio control system for s signal reception channels (s = 1, 2, ..., n) should be the two-dimensional conditional integral law of probability distribution for deflections of the center of mass of the rocket along the axes oy_r and oz_r of the coordinate system oy_rz_r in the dispersal plane. In some special cases, the measure of noise immunity of the radio control system for the corresponding number of signal reception channels can be the probability of striking of the rocket in the stipulated region and in this same dispersal plane.

The conditional distribution functions entering into expression (11.3.1) are dependent on the structure and intensity of the effective signals and interference. Therefore, the noise immunity of the radio control system should be characterized by the dependence of p_{nc} on the ratio $\frac{U_{ni}}{U_{si}}$ (i = 1, 2, ..., n) of the effective values of the strength of the interference and signals, and also on the modulation parameters M_{ni} (i = 1, 2, ..., n) of interference at the input of the i-th radio receiver. Therefore, we find that in an evaluation of the total noise immunity of a radio control system, it is necessary to determine the relationships

/569

$$\begin{matrix}\text{п} = \text{n}\\ \text{с} = \text{s}\end{matrix} \qquad p_{nc}=f\left(\frac{U_{n1}}{U_{c1}},\ \frac{U_{n2}}{U_{c2}},\ \ldots,\ \frac{U_{nn}}{U_{cn}},\ M_{n1},\ M_{n2},\ \ldots,\ M_{nn}\right) \qquad (11.3.4)$$

for different classes of interference.

It should be noted here that in addition to the parameters mentioned in expression (11.3.4), in the case of some types of interference, the values p_{nc} are determined more conveniently as a function of the number of pulses in the timing code, the mean number of interference pulses reaching the input of the corresponding radio receiver in 1 sec, etc.

However, similar functions also can be used for evaluation of the influence of interference for s (s = 1, 2, ..., n) signal reception channels.

It can be seen from expression (11.3.1) that for computation of $p_{nc}^{(i)}$, $p_{nc}^{(i,j)}$, ..., p_{nc}, it is necessary to know

$$p_{ci},\quad p\left(\frac{A_j}{A_i}\right),\ p\left(\frac{A_l}{A_i,A_j}\right),\ \ldots,\ p\left(\frac{A_n}{A_1, A_2, \ldots, A_{n-1}}\right).$$

There are considerable difficulties involved in separate determination of the mentioned probabilities.

The values $p_{nc}^{(i)}$, $p_{nc}^{(i,j)}$, ..., p_{nc} can be computed more easily by first determining the fluctuation errors of rocket guidance, taking into account the effect of interference on the corresponding radio signal reception channels. This can be attributed to the fact that the effective natural or artificial radio interference with one or a large number of randomly changing parameters usually are wide-band for the guidance circuit. Under this condition, the fluctuation errors of rocket guidance h_{my} and h_{mz}, in the dispersion plane, with a high degree of accuracy can be considered to have a normal distribution law. Then, as is known, the functions $p_{nc}^{(i)}$, $p_{nc}^{(i,j)}$, ..., p_{nc} can be computed relatively easily if the following have been determined:

(1) the mathematical expectations $\overline{h}_{my}$ and $\overline{h}_{mz}$ of the random deflections h_{my} and h_{mz}, characterizing the coordinates of the mean point at which the center of mass of the rocket will strike;

(2) the correlation coefficient r_{yz} and the dispersions σ_{my}^2 and σ_{mz}^2 of the random values h_{my} and h_{mz}.

In order to know the dependence of $p_{nc}^{(i)}$, $p_{nc}^{(i,j)}$, ..., p_{nc} on the structure and intensity of the effective signals and interference, it is obviously necessary, in an investigation of the noise immunity of a radio control system, to determine the following functions /570

$h_{\Pi} = h_m$
$\sigma_{\Pi} = \sigma_m$
$U_{\Pi} = U_n$
$U_C = U_s$
$M_{\Pi} = M_n$

$$\overline{h}_{ny} = f_1\left(\frac{U_{n1}}{U_{c1}}, \frac{U_{n2}}{U_{c2}}, \ldots, \frac{U_{nn}}{U_{cn}}, M_{n1}, M_{n2}, \ldots, M_{nn}\right),$$
$$\overline{h}_{nz} = f_2\left(\frac{U_{n1}}{U_{c1}}, \frac{U_{n2}}{U_{c2}}, \ldots, \frac{U_{nn}}{U_{cn}}, M_{n1}, M_{n2}, \ldots, M_{nn}\right),$$
$$\sigma_{ny}^2 = f_3\left(\frac{U_{n1}}{U_{c1}}, \frac{U_{n2}}{U_{c2}}, \ldots, \frac{U_{nn}}{U_{cn}}, M_{n1}, M_{n2}, \ldots, M_{nn}\right),$$
$$\sigma_{nz}^2 = f_4\left(\frac{U_{n1}}{U_{c1}}, \frac{U_{n2}}{U_{c2}}, \ldots, \frac{U_{nn}}{U_{cn}}, M_{n1}, M_{n2}, \ldots, M_{nn}\right),$$
$$r_{yz} = f_5\left(\frac{U_{n1}}{U_{c1}}, \frac{U_{n2}}{U_{c2}}, \ldots, \frac{U_{nn}}{U_{cn}}, M_{n1}, M_{n2}, \ldots, M_{nn}\right).$$

The statistical characteristics of the rocket miss under which we henceforth will understand the combination of values $\bar{h}_{my}$, $\bar{h}_{mz}$, σ^2_{my}, σ^2_{mz} and r_{yz} can be determined experimentally or theoretically. The experimental investigation of the noise immunity of the radio control system should be made using all apparatus and real sources of radio interference. Such an investigation can be made only after the radio control system has been created. Theoretical analysis of noise immunity is based on an analytical or computer solution of the equations describing the radio control system with the effect of radio interference taken into account. Since the parameters of electronic apparatus in a general case change under the influence of interference, in the theoretical solution of the problem of the noise immunity of a radio control system, it is most important to find equations which describe the processes transpiring in the mentioned apparatus. Then, it is necessary to determine the most desirable method for solution of the derived system of equations and compute the mathematical expectations, dispersions and correlation coefficient of the fluctuation errors of rocket guidance.

We note in conclusion that investigation of the noise immunity of radio control systems is of great importance, if for no other reason than that a knowledge of the formulas determining $\bar{h}_{my}$, $\bar{h}_{mz}$, σ^2_{my}, σ^2_{mz} and r_{yz} makes it possible to compute the necessary strengths of the radio transmitters used and to select the structure of the methods for analyzing the received oscillations in such a way that the noise immunity of the radio control system satisfies the stipulated requirement.

In an analysis of artificial interference, the instrument noise of radio receivers and fluctuations of the input signals usually can be neglected because, in an intelligently planned system, their role will be extremely small. For this reason, it is desirable to consider separately the method for determination of fluctuation errors of guidance for low and high levels of interference as was done in the preceding chapters.

11.4. Fluctuation Errors of Rocket Guidance in Command Control

In systems of command radio control, the fluctuation errors of rocket guidance are caused by the instrument noise of the radio receivers included in the CCRL, data transmission systems and instruments for determination of target and rocket coordinates and also fluctuations of the parameters of the received radio signals. In addition, artificial radio interference can exert a considerable influence. /571

In most cases, it can be assumed with a high degree of accuracy that the effect of the instrument noise of the radio receivers and fluctuations of the received signals leads only to the appearance of errors in measurement of coordinates and transmission of commands and does not change the conversion

properties of the measuring instruments, data transmission systems and CCRL. In this connection, in application to the vertical control plane, for example, the fluctuation rocket guidance errors will be caused by random distortions u_{nc} of the voltage characterizing the output signal of the coordinator and by the distortions $\Delta K(t)$ of the received control commands.

The voltage u_{nc}, related to the function $h_{mn}(t)$, whose method of determination was considered in chapter 5, is formed due to errors of the data transmission systems and of the target and rocket coordinate measuring instruments. In an intelligently designed system, the effective values $u_{nc}(t)$ and $\Delta K(t)$ are small, and therefore analysis of the fluctuation errors of rocket guidance can be made on the basis of linearized equations describing the operation of the control system. For example, when taking into account the influence of the instrument noise of the radio receivers and the random changes of the parameters of the received signals for a radio control system of the first kind ensuring rocket guidance by the coincidence method in a vertical plane, we obtain the following system of equations

$$\left.\begin{aligned}
\dot{\theta} &= \frac{1}{T_v}(\alpha - A_0),\\
\ddot{\alpha} + 2d\omega_0\dot{\alpha} + \omega_0^2\alpha &= a_\delta(\delta_r + \delta_0),\\
\delta_r &= F(D)\,[K + \Delta K + W_\vartheta(D)\,\vartheta + W_\alpha(D)\,\alpha],\\
K &= L(D)\,K_a,\\
K_a &= L_1(D)\,(u_h + u_{nc}),\\
u_h = \Delta_m &= [W_t(D)\,\varepsilon_t - W_r(D)\,\varepsilon_r]\,k_{pot}\,\partial_{pr},\\
\varepsilon_r &= \varepsilon_t - \frac{h_t}{r_r},\\
\dot{h}_t &= \frac{d(r_r\varepsilon_t)}{dt} - v\theta + v_c\theta_c,\\
\frac{d(r_t\varepsilon_t)}{dt} &= v_t\vartheta_t - v_c\theta_c.
\end{aligned}\right\} \qquad (11.4.1)$$

We note that equations (11.4.1) were written on the basis of equations (10.5.3) and differ from them in the sixth equation, for which (10.4.6) was used, and the presence of the additional perturbations $u_{nc}(t)$ and $\Delta K(t)$. In a case when a command control system of the first kind is used for rocket guidance by the parallel approach method, allowance for the effect of the distortions $u_{nc}(t)$ and $\Delta K(t)$ makes it necessary that in system (11.4.1) the equations determining h_t, ε_r and u_h be replaced by the expressions (10.5.8), (10.5.5) and (10.5.4). /572

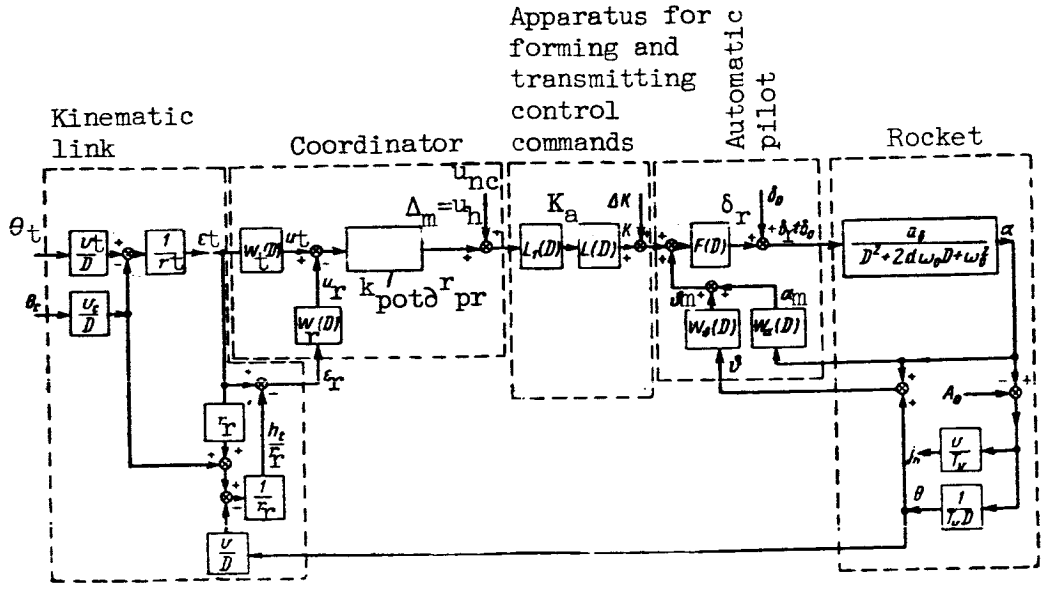

a

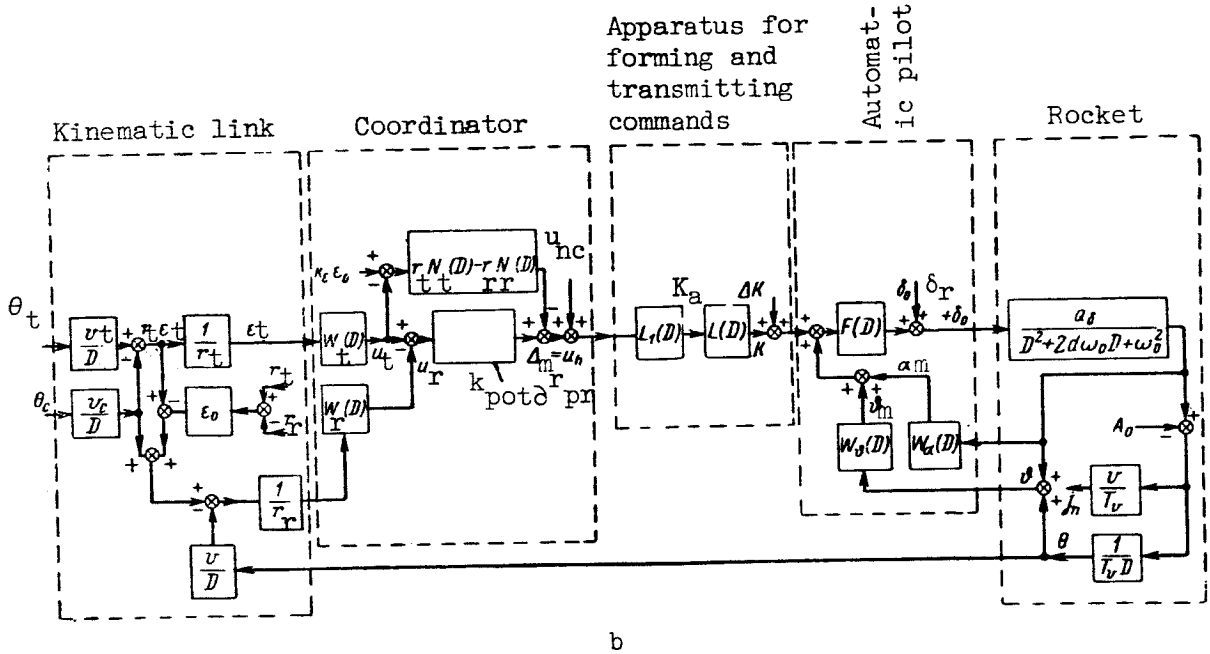

b

Figure 11.1

The systems of equations which are characterizing the processes of rocket guidance in a vertical plane either by the coincidence method or by the parallel approach method, when there are distortions $u_{nc}(t)$ and $\Delta K(t)$, correspond to the block diagrams shown in figure 11.1a, b. Figure 11.1a, b shows that

allowance for the random perturbations $u_{nc}(t)$ and $\Delta K(t)$ means that the signals $u_h + u_{nc}$ and $K + \Delta K$ will act on the output of the coordinator and CCRL instead of the mismatch parameter $\Delta_m = u_h$ and the command K, respectively.

The equations and block diagrams for command control systems of the second kind, with u_{nc} and ΔK taken into account, are derived as for systems of the first kind, and therefore here and in the text which follows they are not considered.

As already mentioned, command control systems are nonstationary. However, as a result of the quite slow change of the coefficients, it is possible to use the method of "freezing" of coefficients. Then, on the assumption of a stationary or almost stationary character of the change of $u_{nc}(t)$ and $\Delta K(t)$, which in some cases actually occurs, for an approximate determination of the probabilistic characteristics of the parameters α, δ_r, h_t, etc., we can use the methods employed in an analysis of the problems of passage of stationary random signals through linear dynamic systems with constant coefficients. In this case, of course, the control system equations should be solved for small parts of the rocket trajectory. The interval of time when $r_r \approx r_t$ is of the greatest importance for determination of the fluctuation errors of rocket guidance.

When there is interference $u_{nc}(t)$ and $\Delta K(t)$, the error in rocket guidance in the vertical plane for the time of the end of the guidance process, when $r_t = r_r$, can be represented in the form of a sum

$$h = h_t\Big|_{r_r=r_t} = h_{\partial in} + h_{my}, \qquad (11.4.2)$$

where $h_{\partial in}$ is the component of the miss associated with dynamic and instrument errors, h_{my} is the component of the miss associated with the effect of radio interference causing the distortions $u_{nc}(t)$ and $\Delta K(t)$.

It should be noted here that the separation of h into $h_{\partial in}$ ahd h_{my} is admissible only for a case when the radio control system is linear. In addition, it must be remembered that expression (11.4.2) is suitable for any guidance method.

Analyzing the system of equations (11.4.1), it can be concluded that /575 h_{my} is the current miss h_t for $r_t = r_r$ and under the condition that the

input actions θ_t, θ_c, A_0, δ_0 and the signals reflecting the instrument errors of the individual links are equal to zero and $u_{nc}(t) \neq 0$ and $\Delta K(t) \neq 0$. It therefore follows that the mathematical expectation $\bar{h}_{my}$ and the dispersion σ^2_{my} of the random function h_{my} in rocket guidance by the coincidence method are determined by solution of the system of equations (11.4.1) relative to h_t when $r_{pr} = r_r = r_t$, $\theta_c = \theta_t = \delta_0 = A_0 = 0$, $u_{nc}(t) \neq 0$ and $\Delta K(t) \neq 0$.

If the rocket is guided by the parallel approach method, the error h_{my} will be equal to the current miss h_t, computed in solution of the equations corresponding to the block diagram shown in figure 11.1b and relative to the same values r_{pr}, r_r, θ_c, θ_t, δ_0, A_0, $u_{nc}(t)$ and $\Delta K(t)$ as in the preceding case.

Since the interference acting on the coordinate measuring instruments, CCRL and data transmission systems is created by different sources, the random functions $u_{nc}(t)$ and $\Delta K(t)$ are independent. This makes it possible to determine separately the influence of $u_{nc}(t)$ and $\Delta K(t)$ on the value of the fluctuaerror. Then the values $\bar{h}_{my}$ and σ^2_{my} can be found using the following formulas

$$\bar{h}_{my} = \bar{h}_{m1} + \bar{h}_{m2}, \tag{11.4.3}$$

$$\sigma^2_{my} = \sigma^2_{m1} + \sigma^2_{m2}, \tag{11.4.4}$$

where $\bar{h}_{m1}$ and σ^2_{m1} are the mathematical expectation and dispersion of the random function $h_m(t)$, appearing due to the effect of interference on the coordinator, which leads to distortion of $u_{nc}(t)$ under the condition that $\Delta K(t) = 0$; $\bar{h}_{m2}$ and σ^2_{m2} are the mathematical expectation and dispersion of the random function $h_m(t)$, arising due to the effect of interference on the CCRL or on the assumption that $u_{nc}(t) = 0$.

First, we will determine the values $\bar{h}_{m1}$, σ^2_{m1}, $\bar{h}_{m2}$ and σ^2_{m2} for a system ensuring rocket guidance by the coincidence method. Figure 11.1a shows that when $\delta_0 = \theta_c = \theta_t = A_0 = 0$ and $r_{pr} = r_r = r_t$

$$h_{m1}(t) = \frac{W_1(D)}{1 + W_c(D)}\, u_{nc}(t), \qquad (11.4.5)$$

$$h_{m2}(t) = \frac{W_2(D)}{1 + W_c(D)}\, \Delta K(t). \qquad (11.4.6)$$

Here $W_1(D)$ is the transfer function of the direct circuit of a control system in which the signals $u_{nc}(t)$ and $h_t(t)\big|_{r_r=r_t}$ act at the input and output when $r_r = r_t$, $A_0 = \delta_0 = \theta_c = \theta_t = 0$ and $\Delta K(t) = 0$; $W_2(D)$ is the transfer function of the direct circuit of a control system in which the input and output signals are $\Delta K(t)$ and $h_t(t)\big|_{r_r=r_t}$ when $r_r = r_t$, $A_0 = \delta_0 = \theta_t = \theta_c = 0$ and $u_{nc}(t) = 0$. /576

The transfer functions $W_1(D)$, $W_2(D)$ and $W_c(D)$ can be determined quite easily using the block diagram of the considered control system (fig. 11.1a). On the basis of expressions (11.4.5) and (11.4.6) we will have

$$\bar{h}_{m1} = \frac{W_1(D)}{1 + W_c(D)}\, \bar{u}_{nc} = F_1(D)\bar{u}_{nc}, \qquad (11.4.7)$$

$$\bar{h}_{m2} = \frac{W_2(D)}{1 + W_c(D)}\, \Delta\bar{K} = F_3(D)\Delta\bar{K}, \qquad (11.4.8)$$

where $F_1(D) = \dfrac{h_t\big|_{r_r=r_t}}{u_{nc}}$ is the transfer function of a closed control system at whose input and output act the signals $u_{nc}(t)$ and $h_t(t)\big|_{r_r=r_t}$ when $r_{pr} = r_r = r_t$, $A_0 = \delta_0 = \theta_t = \theta_c = 0$ and $\Delta K(t) = 0$; and $F_2(D) = \dfrac{h_t\big|_{r_r=r_t}}{\Delta K}$ is the transfer function of a closed control system whose input is $\Delta K(t)$ and whose output is $h_t(t)\big|_{r_r=r_t}$ when $r_{pr} = r_r = r_t$, $A_0 = \delta_0 = \theta_c = \theta_t = 0$ and $u_{nc}(t) = 0$.

Hence, for a steady-state regime we find

$$\overline{h}_{m1} = F_1(0)\overline{u}_{nc}, \tag{11.4.9}$$

$$\overline{h}_{m2} = F_2(0)\Delta\overline{K}. \tag{11.4.10}$$

Depending on the form of the transfer functions of the links forming the control system, the latter with respect to the constant component of the signals $u_{nc}(t)$ and $\Delta K(t)$ can be either static or astatic.

For example, if it is required that the mathematical expectation of the miss $\overline{h}_{my} = 0$ when $\Delta\overline{K} \neq 0$, it is necessary to have at least one integrating link between the points of arrival of the signals h_t and ΔK in figure 11.1a.

In order to find the dispersions σ^2_{m1} and σ^2_{m2}, it is necessary to know the spectral densities $G_{nc}(\omega)$ and $G_{\Delta K}(\omega)$ of the random signals $u_{nc}(t)$ and $\Delta K(t)$, and also the frequency characteristics $F_1(j\omega)$ and $F_2(j\omega)$ obtained by the replacement of D by $j\omega$ in the functions $F_1(D)$ and $F_2(D)$.

If $G_{nc}(\omega)$, $G_{\Delta K}(\omega)$, $F_1(j\omega)$ and $F_2(j\omega)$ are given, it is known that /577

$$\sigma^2_{m1} = \frac{1}{2\pi}\int_0^\infty G_{nc}(\omega)\,|F_1(j\omega)|^2\,d\omega. \tag{11.4.11}$$

$$\sigma^2_{m2} = \frac{1}{2\pi}\int_0^\infty G_{\Delta K}(\omega)\,|F_2(j\omega)|^2\,d\omega. \tag{11.4.12}$$

Usually, the output elements of the coordinator and CCRL are such that within the limits of the passband of the guidance circuit $G_{nc}(\omega)$ and $G_{\Delta K}(\omega)$ are approximately equal to the values of these functions when $\omega = 0$. Under these conditions

$$\sigma^2_{m1} \approx \frac{1}{2\pi}G_{nc}(0)\int_0^\infty |F_1(j\omega)|^2\,d\omega = k_1^2 G_{nc}(0)\,\Delta F_{ep1}, \tag{11.4.13}$$

$$\sigma^2_{m2} \approx \frac{1}{2\pi}G_{\Delta K}(0)\int_0^\infty |F_2(j\omega)|^2\,d\omega = k_2^2 G_{\Delta K}(0)\,\Delta F_{ep2}, \tag{11.4.14}$$

where $\Delta F_{ep1} = \frac{1}{2\pi}\frac{1}{k_1^2}\int_0^\infty |F_1(j\omega)|^2 d\omega$ and $\Delta F_{ep2} = \frac{1}{2\pi}\frac{1}{k_2^2}\int_0^\infty |F_2(j\omega)|^2 d\omega$ are the effective

passbands of systems with the frequency characteristics $F_1(j\omega)$ and $F_2(j\omega)$; $k_1 = F_1(0)$ and $k_2 = F_2(0)$ are the transfer constants of systems with the frequency characteristics $F_1(j\omega)$ and $F_2(j\omega)$ at the frequency $\omega = 0$.

For those cases when the control system is astatic relative to the signals $u_{nc}(t)$ and $\Delta K(t)$, k_1 and k_2 in expressions (11.4.13) and (11.4.14) denote the transfer constants when $\omega = \omega_1$ and $\omega = \omega_2$, where ω_1 and ω_2 are the frequencies at which the functions $F_1(j\omega)$ and $F_2(j\omega)$ attain maximum value. At the same time, it should be noted that frequently it is more convenient to omit computation of ΔF_{epl} and ΔF_{ep2} and instead compute directly the integrals entering into relations (11.4.13) and (11.4.14).

If more precise computations of the dispersion σ^2_{ml} are required, formula (11.4.13) will be inapplicable. This is because the coordinator includes a device which multiplies the input signals by $k_{pot}\partial^{r}_{pr} = k_{pot}\partial^{r}_{r}$, and therefore the function $u_{nc}(t)$ is not stationary. However, it can be represented in the following form

$$u_{nc}(t) = x_{ran}(t) \cdot r_r(t),$$

where $x_{ran}(t)$ is a stationary random function of time.

Then, as can be demonstrated (ref. 32), when representing $r_r(t)$ as the sum of exponential functions $\sum_{i=1}^{n} a_i e^{\mu_i t}$, the dispersion σ^2_{ml} will be equal to /578

$$\sigma^2_{ml} = \frac{1}{2\pi}\int_0^{\infty} G_x(\omega)\left|\sum_{i=1}^{h} a_i F_1(j\omega + \mu_i)\, e^{\mu_i t}\right|^2 d\omega, \qquad (11.4.15)$$

where $G_x(\omega)$ is the spectral density of the random function $x_{ran}(t)$. Here, as might be expected, the dispersion σ^2_{ml} is dependent on time. Expression (11.4.15) is extremely unwieldy and inconvenient for practical computations. At the same time, formula (11.4.13) does not lead to significant errors, especially in an investigation of small segments of the rocket trajectory, and makes it

possible to determine σ_{m1}^2 with a lesser expenditure of time in computation work.

The components $\bar{h}_{m1}$, $\bar{h}_{m2}$, σ_{m1}^2 and σ_{m2}^2 of the miss h_{my} in rocket guidance by the parallel approach method are determined on the basis of the block diagram shown in figure 10.1b in exactly the same way as for the system by which a rocket is guided by the coincidence method. All the formulas derived above are also correct in this case if the transfer functions $W_1(D)$ and $W_2(D)$ entering into them are appropriately determined.

After $\bar{h}_{m1}$, $\bar{h}_{m2}$, σ_{m1}^2 and σ_{m2}^2 are determined, it is possible to find $\bar{h}_m$ and σ_m^2 as a function of $\bar{u}_{nc}$, $\Delta\bar{K}$, $G_{nc}(\omega)$ and $G_{\Delta K}(\omega)$. If as a result of investigation of the problem of the influence of interference on the coordinator and the CCRL we find the dependence of $\bar{u}_{nc}$, $\Delta\bar{K}$, $G_{nc}(\omega)$ and $G_{\Delta K}(\omega)$ on the parameters of the electronic apparatus, received signals and effective interference, there is no difficulty in obtaining expressions for $\bar{h}_m$ and σ_m^2, in the long run determining the quantitative measure of noise immunity of the radio control system. In addition, on the basis of the stipulated values $\bar{h}_{my}$ and σ_{my}^2, it is possible to formulate requirements on the parameters of the electronic apparatus for ensuring $\bar{u}_{nc}$, $\Delta\bar{K}$, $G_{nc}(\omega)$ and $G_{\Delta K}(\omega)$ not exceeding admissible values.

As an illustration of the use of the described method for computation of the fluctuation error of rocket guidance in the vertical plane, we will analyze a radio control system which includes a nonelectronic (such as optical) coordinator and a CCRL. The block diagram of such a system is shown in figure 11.2, and its equations have the following form /579

$$\left.\begin{aligned}
\dot{\theta} &= \frac{1}{T_\sigma}(\alpha - A_0),\\
\ddot{\alpha} + 2d\omega_0\dot{\alpha} + \omega_0^2\alpha &= a_\delta(\delta_p + \delta_0),\\
\delta_p &= k_\delta(K + \Delta K),\\
K &= k_{кру}K_y,\\
K_y &= k_{уф}(1 + T_{уф}D)\,\Delta_и,\\
\Delta_и &= k_{кр}\frac{h_t}{r_p},\\
\dot{h}_t &= \frac{d(r_p\varepsilon_и)}{dt} - v\theta,\\
\frac{d(r_и\varepsilon_и)}{dt} &= v_и\theta_и.
\end{aligned}\right| \qquad (11.4.16)$$

р	= r
кру	= CCRL
у	= a
уф	= CFA
и	= m
кр	= c
ц	= t
пу	= my
эр	= ep
к	= c
макс	= max
(subscripts)	

(Note: This key may be used for this equation and some of the following equations in section 11.4.)

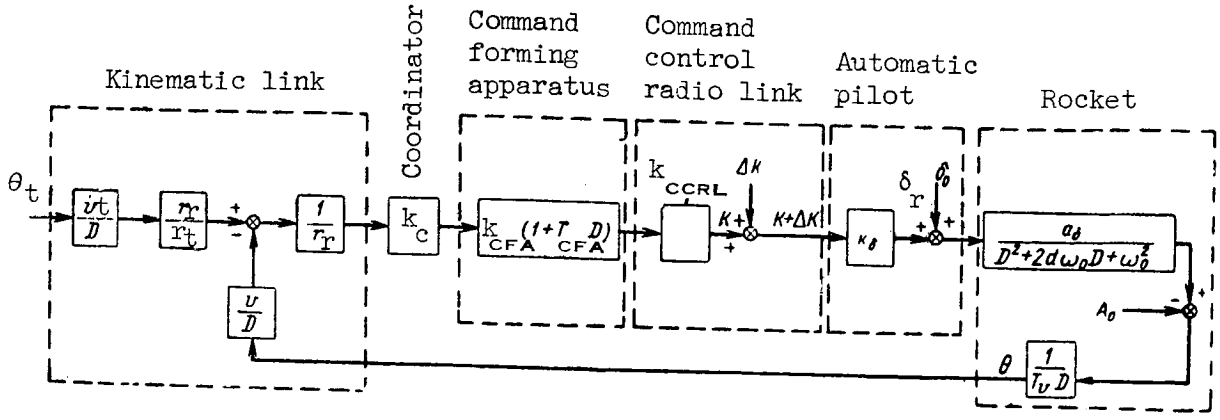

Figure 11.2

As follows from figure 11.2 and equations (11.4.16), which are derived on the basis of (11.4.1), in the considered example the command radio link, automatic pilot and coordinator are considered inertialess links with the transfer constants k_{CCRL}, k_δ and k_c and the apparatus for forming the commands is a differentiating link with the transfer constant k_{CFA} and the time constant T_{CFA}. Then, it is assumed that rocket guidance is accomplished from a fixed control point and that the coordinator produces a signal Δ_m, proportional to the angle $\epsilon_t - \epsilon_r = \frac{h_t}{r_r}$. Since only the signal $\Delta K(t)$ changes randomly, then

$$\overline{h}_{my} = \overline{h}_{m2}, \tag{11.4.17}$$

$$\sigma^2_{my} = \sigma^2_{m2}. \tag{11.4.18}$$

Solving the system of equations (11.4.16) when $r_r = r_t$, we find that when $A_0 = \delta_0 = \theta_t = 0$

$$F_2(D) = \frac{h_{ny}(t)}{\Delta K(t)} = \frac{h_t|_{r_p=r_n}}{\Delta K(t)} = \frac{r_n k_\delta a_\delta v}{r_n T_v D^2\left(D^2+2d\omega_0 D+\omega_0^2\right)+\rightarrow} \cdot$$
$$\rightarrow + k_{kp}k_\delta v a_\delta k_{y\phi}k_{kpy}(1+T_{y\phi}D)$$

It therefore can be seen that the considered system is static relative to $\Delta K(t)$ and the coefficient k_2 is equal to

$$k_2 = \frac{r_t}{k_c k_{CFA} k_{CCRL}}. \qquad (11.4.19)$$

In accordance with the above-cited formula for ΔF_{ep2}, the effective passband of the system is equal to

$$\Delta F_{ep2} = \frac{1}{2\pi} \frac{k_\Delta^2}{r_n^2} \int_0^\infty |F_2(j\omega)|^2 d\omega,$$

where $F_2(j\omega)$ is derived from the expression $F_2(D)$ after replacement of D by $j\omega$ and $k_\Delta = k_c k_{CFA} k_{CCRL}$.

Using formulas (11.4.10) and (11.4.17), we arrive at the following expression for the mathematical expectation of the miss $\bar{h}_{my}$ in a steady-state regime /581

$$\bar{h}_{my} = r_t \frac{\Delta\bar{K}}{k_c k_{CFA} k_{CCRL}}. \qquad (11.4.20)$$

Analysis of the derived expression shows that for a decrease of $\bar{h}_{my}$, it is necessary to increase the transfer constants k_c, k_{CFA} and k_{CCRL} and design a CCRL in such a way that interference causes the smallest possible values $\Delta\bar{K}$. In addition, it is desirable to eliminate the dependence of k_2 on r_t.

Then on the basis of expressions (11.4.14) and (11.4.18) we find

$$\sigma_{my}^2 = \frac{1}{k_\Delta^2} K_{max}^2 r_t^2 G_c(0) \Delta F_{ep2}, \qquad (11.4.21)$$

where $G_c(0)$ is the spectral density of the fluctuations of the command coefficient at the frequency $\omega = 0$.

It can be seen from expression (11.4.21) that for finding σ_{my}^2 for stipulated values k_Δ, K_{max} and $G_c(0)$, it is sufficient to compute ΔF_{ep2}.

We have

$$\Delta F_{эр2} = \frac{1}{2\pi}\int_0^{\infty} \frac{v^2 a_\delta^2 k_\delta^2 k_\Delta^2 d\omega}{\left| r_ц T_v (j\omega)^2 \left[(j\omega)^2 + 2jd\omega_0\omega + \omega_0^2\right] + \right.} \quad (11.4.22)$$
$$\left. + jk_{кр}k_\delta v a_\delta k_{уф} k_{кру} T_{уф}\omega + k_{кр}k_\delta v a_\delta k_{уф} k_{кру}^2 \right|$$

It is known that values of integrals of the type

$$I = \frac{1}{2\pi j}\int_{-\infty}^{\infty} \frac{G_n(\omega)}{H_n(\omega) H_n(-\omega)}\, d\omega, \quad (11.4.23)$$

where
$$H_n^{(\omega)} = a_0\omega^n + a_1\omega^{n-1} + \ldots + a_n,$$
$$G_n(\omega) = b_0\omega^{2n-2} + b_1\omega^{2n-4} + \ldots + b_{n-1},$$

under the condition that all the roots of the polynomial $H_n(\omega)$ are in the upper half-plane, are cited in a number of textbooks in tabular form. For example, such tables can be found in reference 31.

In expression (11.4.22), determining ΔF_{ep2}, the numerator and denominator of the integrand are represented easily in the form of polynomials $G_n(\omega)$ and $H_n(\omega)$. In this case, it can be shown that if the control system is stable, the roots of the polynomial $H_n(\omega)$ lie in the upper half-plane. Then it is necessary to note that in expression (11.4.23) the degree of the polynomial is smaller than the degree of the polynomial of the denominator, and that all the terms of the function $G_n(\omega)$ contain frequencies ω only in an even degree. If under real conditions the latter property of the polynomial in the numerator is not satisfied, it is necessary to discard all the terms with odd degrees ω because they will give a zero value of the integral as a result of the evenness of the function $\left|H_n(\omega)\right|^2$ and the selected integration limits.

Taking all the above considerations into account, we reduce relation (11.4.22) to the following form

$$\Delta F_{эр2} = \frac{1}{2\cdot 2\pi j}\int_{-\infty}^{\infty} \frac{jv^2 a_\delta^2 k_\delta^2 k_\Delta^2 d\omega}{\left| r_ц T_v \left(\omega^4 - j2d\omega_0\omega^3 - \omega_0^2\omega^2\right) + \right.} \quad (11.4.24)$$
$$\left. + jk_{кр}k_\delta v a_\delta k_{уф} k_{кру} T_{уф}\omega + k_{кр}k_\delta v a_\delta k_{уф} k_{кру}^2 \right|$$

It therefore follows that the polynomial $H_n(\omega)$ has the degree n = 4. /582

When n = 4, the value of the integral I is (ref. 31)

$$I = \frac{b_0(-a_1a_4 + a_2a_3) - a_0a_3b_1 + a_0a_1b_2 + \frac{a_0b_3}{a_4}(a_0a_3 - a_1a_2)}{2a_0\left(a_0a_3^2 + a_1^2a_4 - a_1a_2a_3\right)}. \qquad (11.4.25)$$

Comparison of expressions (11.4.23) and (11.4.24) shows that for the considered example $a_0 = r_t T_v$, $a_1 = -j2d\omega_0 T_v r_t$, $a_2 = -r_t T_v \omega_0^2$, $a_3 = jk_c k_\delta v a_\delta k_{CFA} k_{CCRL} T_{CFA}$, $a_4 = k_c k_\delta v a_\delta k_{CFA} k_{CCRL}$, $b_0 = 0$, $b_1 = 0$, $b_2 = 0$, $b_3 = jv^2 a_\delta^2 k_\delta^2 k_\Delta^2$.

Substituting the values of the coefficients a_0, a_1, a_2, a_3, a_4, b_0, b_1, b_2 and b_3 into expression (11.4.25) and taking into account that $\Delta F_{ep2} = \frac{1}{2} I$, we obtain

$$\Delta F_{ep2} = \frac{2r_\Pi T_v d\omega_0^3 - a_\delta v k_\delta k_\Delta T_{y\phi}}{4\left(2r_\Pi T_v d\omega_0^3 T_{y\phi} - a_\delta v k_\delta k_\Delta T_{y\phi}^2 - 4r_\Pi T_v d^2\omega_0^2\right)}.$$

We finally obtain

$$\sigma_{ny}^2 = \frac{r_\Pi^2 K_{макс}^2 G_K(0)}{4k_{kp}^2 k_{y\phi}^2 k_{kpy}^2} \cdot \frac{2r_\Pi T_v d\omega_0^3 - a_\delta v k_\delta k_\Delta T_{y\phi}}{2r_\Pi T_v d\omega_0^3 T_{y\phi} - a_\delta v k_\delta k_\Delta T_{y\phi}^2 - 4r_\Pi T_v d^2\omega_0^2}. \qquad (11.4.26)$$

It can be seen from the derived expression, which makes it possible to compute the dispersion of the rocket miss for stipulated values of the parameters of a radio control system and the spectral density for fluctuations of the control command, that the value σ_{my}^2, like $\bar{h}_{my}$, is essentially dependent on distance r_t. In order to exclude such a dependence, it is necessary to introduce into the control circuit a link with a variable transfer constant r_r which at the end of the guidance process becomes equal to r_t. It can be shown that in such a method for construction of the control system when $r_r = r_t$

$$\bar{h}_{my} = \frac{\Delta\bar{K}}{k_c k_{CFA} k_{CCRL}}$$

and

$$\sigma_{\text{пу}}^2 = \frac{K_{\text{макс}}^2 G_{\text{к}}(0)}{4k_{\text{кр}}^2 k_{\text{уф}}^2 k_{\text{кру}}^2} \frac{2T_{\text{в}} d\omega_0^3 - a_{\delta} v k_{\delta} k_{\text{кр}} k_{\text{уф}} k_{\text{кру}} T_{\text{уф}}}{2T_{\text{в}} d\omega_0^3 T_{\text{уф}} - a_{\delta} v k_{\delta} k_{\text{кр}} k_{\text{уф}} k_{\text{кру}} T_{\text{уф}}^2 - 4T_{\text{в}} d^2 \omega_0^2}.$$

In this case $\bar{h}_{my}$ and σ_{my}^2 are not functions of r_t but are determined only by the fluctuations $\Delta K(t)$ and the parameters of the control system; here in the last expression the coefficient k_{Δ} has a different dimensionality than it had in expression (11.4.26).

If the rocket is guided on the basis of the angular deflection of the center of mass of the rocket from the vector $\mathbf{r}_t$, when $k_{\Delta} = k_c k_{CFA} k_{CCRL} = 100$ v/rad, $K_{max} = 30$ v, $r_t = 10$ km, $T_v = 3$ sec, $2d\omega_0 = 0.7$ 1/sec, $a_{\delta} = 50$ 1/sec^2, $v = 200$ m/sec, $T_{CFA} = 0.4$ sec, $\omega_0^2 = 50$ 1/sec^2, $\Delta\bar{K}_{cm} = 0.01$, $G_c(0) = 9 \cdot 10^{-5}$ sec and $k_{\delta} = 0.5$ rad/v, in accordance with formulas (11.4.20) and (11.4.26) we find that $\bar{h}_{my} \approx 30$ m and the mean square value of the miss is $r_{ms} = \sqrt{\sigma_{my}^2} \approx 25$ m.

The cited example shows that under certain conditions of guidance and certain values of the parameters of the control system, even extremely insignificant distortions of the command coefficient ΔK_c can cause quite large fluctuation errors of guidance. /583

The method considered here and the formulas cited for computation of fluctuation errors of guidance usually are suitable only when taking into account the effect of weak interference (for example, instrument noise) and fluctuations of the parameters of the received signals.

Artificial interference can be created for all electronic channels of a command radio control system. However, it is simplest to ensure the effect of such interference on the apparatus for measurement of target coordinates. The most complex problem is the creation of artificial interference for the radio receiving apparatus whose antennas are placed in the rear part of the rocket. Nevertheless, it is possible to create radio interference for the channels of this apparatus as well, because in the case of rocket guidance for a great distance, it will be over enemy territory for a considerable time. In such cases, noise transmitters can be set up near defended objects and such apparatus can be effective in disrupting operation of the radio receiving apparatus carried on the rocket.

The conclusion therefore can be drawn that it is necessary to develop radio control systems which will ensure a quite high quality of rocket guidance, even when there are extremely effective radio countermeasures for all the electronic channels present in the system.

Determination of guidance errors caused by artificial interference also involves solution of radio control system equations. However, such

interference leads not only to the appearance of distortions u_{nc} and ΔK, representing additive noise, but also to a change of the conversion properties of the coordinate measuring instruments, CCRL and data transmission systems, and also to a breakoff of automatic tracking. As already mentioned, in a general case under the influence of strong interference, the coordinate measuring instruments and the CCRL become nonlinear dynamic links with random parameters. This makes it necessary to use electronic computers for solution of the equations of the radio control system for determination of the rocket miss. Since highly effective interference leads to a considerable increase of h_{my}, in the processes of modeling the guidance circuit it is possible to neglect the instrument noise of the radio receivers and the fluctuations of the received signals. In addition, the inertias of the coordinate measuring instruments, data transmission systems and CCRL can be neglected. Then, when using the equations of electronic apparatus, it becomes possible to apply mathematical modeling of the rocket guidance process by relatively simple methods.

However, it must be remembered that, in mathematical modeling, the /384 use of the radio apparatus equations found in the preceding chapters makes it possible to obtain only approximate estimates of the rocket miss. However, even an approximate knowledge of the miss h_m makes it possible to find means increasing the noise immunity of the radio control system. More precise results are obtained in the case of physical modeling when real radio equipment and interference sources are used.

In some cases, additional requirements which the electronic apparatus must satisfy are noted in the process of taking into account the effect of strong interference on them, and the guidance errors can be computed analytically. Under this condition, the modeling should be done only for refinement of the selected and computed parameters of the radio control system.

It is simplest to establish the limiting possibilities of radio countermeasures, which usually essentially involve a cutoff of the processes of determination of the target and rocket coordinates and also a breaking of the guidance circuit, as was mentioned in the preceding chapters.

11.5. Fluctuation Errors of Rocket Guidance in Radio Zone (Beam-Riding) Control

In beam-riding control systems interference can act on two radio receivers: the receiver of the radar set used for automatic tracking of the target and the receiver carried aboard the rocket. If the effect of artificial interference is not taken into account, the parameters of the signals produced by the radar will change under the influence of the instrument noise of the radio receiver and the fluctuations of the oscillations arriving from the target. The noise and fluctuations cause random oscillations of the radio beam relative

to the line of sight, coinciding with the vector r_t and change the transfer constant of the radar tracking system. As a result, the center of mass of the rocket is deflected from the necessary flight direction. The linear error of rocket guidance increases with an increase of r_r despite the same angular error in the position of the radar beam. Therefore, the effect of interference is the more dangerous the closer the rocket is to the target.

Distortions of the mismatch parameter and change of the conversion properties of the coordinator also are caused by the effect of the instrument noise of the rocket radio receiver and fluctuations of signals received by it. The latter occur as a result of passage of the radio waves through the jet of the rocket engine. In actuality, the role of the instrument noise of the rocket radio receiver is negligibly small due to the considerable strength of the received signals.

It also should be noted that the random oscillations of the transfer constants of the radar tracking system and the radio equipment aboard the rocket under the influence of instrument noise and natural fluctuations are insignificant, as was demonstrated in chapters 3 and 4. Therefore, without introducing any significant errors, it can be assumed that the conversion properties of the guidance circuit do not change because of this interference. /586
Then the fluctuation errors of guidance of rockets which are controlled by the coincidence method can be computed on the basis of the block diagram shown in figure 11.3. This block diagram is shown in accordance with the diagram in figure 10.12 and differs from it only in that, at the output of the coordinator, in addition to the mismatch parameter $\Delta_m = u_a$, there will be the error u_{nc} caused by the influence of all kinds of fluctuations of received signals and instrument noise of the radio receivers.

Strictly speaking, a beam-riding control system is nonstationary because of the variability of the coefficients in the equations describing the motion of the rocket and the error u_{nc} is dependent on the distance r_r. However, when computing the miss when $r_r = r_t$, it is sufficient to limit ourselves to an analysis of rocket motion for a short interval of time when the circuit parameters should be considered constant and the value r_r entering into the formula can be "frozen."

Then the mathematical expectation $\bar{h}_{my}$ and the dispersion σ^2_{my} of the miss h_{my} of a rocket guided in a single (vertical) plane will be determined by expressions (11.4.3) and (11.4.4) when $\bar{h}_{m2} = 0$ and $\sigma^2_{m2} = 0$. For computation of $\bar{h}_{m1}$ and σ^2_{m1}, it is possible to use relations (11.4.9) and (11.4.13), in which $F_1(j\omega)$ is understood as the frequency characteristic of a closed control system

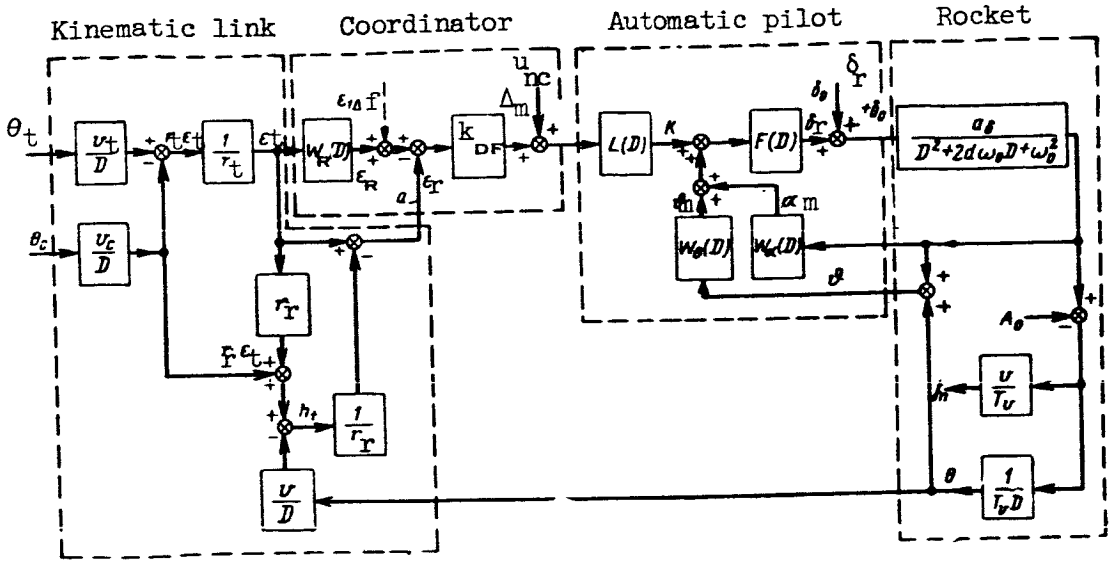

Figure 11.3

with the input action $u_{nc}(t)$ and the output signal $h_t(t)\Big|_{r_r = r_t}$ when

$\theta_t = \theta_c = \delta_0 = A_0 = 0$ (fig. 11.3).

Since in a number of cases the errors caused by the radio equipment of the rocket are negligibly small, there is no special need for converting the random oscillations of the radio beam to the coordinator ouput. Under this condition, instead of the random perturbation u_{nc}, it is necessary to take into account the random effect $\epsilon_{1\Delta f}$ (fig. 11.3) characterizing the angular error in tracking of the target by the radar set associated with fluctuations of the received signals and radio interference. Then the mathematical expectation $\bar{h}_{my}$ and the dispersion σ^2_{my} of the miss in a steady-state regime will be equal to

$$\bar{h}_{my} = F(0)\bar{\epsilon}_{1\Delta f}, \tag{11.5.1}$$

$$\sigma^2_{my} \approx k_1^2 G_\Delta(0)\Delta F_{ep}, \tag{11.5.2}$$

where $G_\Delta(0)$ is the spectral density of the random function $\epsilon_{1\Delta f}(t)$ when /587

$\omega = 0$; $\Delta F_{ep} = \frac{1}{2\pi k_1^2}\int_0^\infty |F(j\omega)^2 d\omega|$ is the effective passband of a closed control

system in which the input and output signals are $\epsilon_{1\Delta f}(t)$ and $h_t\big|_{r_r = r_t}$ when $\theta_t = \theta_c = \delta_0 = A_0 = 0$, respectively; k_1 and $F(j\omega)$ are the transfer constant and the frequency characteristic of the mentioned system, respectively.

It should be noted here that the considered system is static relative to the parasitic perturbation $\overline{\epsilon_{1\Delta f}(t)}$.

It can be seen from formulas (11.5.1) and (11.5.2) that the fluctuation errors of guidance are dependent on the transfer function of the guidance circuit and on the radar set error, which is related to the parameters of its tracking system and effective interference.

As an illustration of the method for computing $\overline{h}_{my}$ and σ^2_{my} we will use formulas (11.5.1) and (11.5.2) to consider a system of beam-riding control taking into account only the amplitude fluctuations of the signals arriving from the target. We note here as a rule the mentioned source of errors is most important because the radar set ensures stable tracking of the target only when there is a considerable value of the signal-to-noise ratio, and the process of rocket guidance is ended at a rather great distance between the control point and the target. When computing $\overline{h}_{my}$ and σ^2_{my}, we will use as a point of departure the structural diagram shown in figure 11.3, under the condition that $\theta_t = \theta_c = \delta_0 = A_0 = 0$, $W_\vartheta(D) = 0$ and $W_\alpha(D) = 0$. In addition, we will assume that $L(D)F(D) = k_a(T_\partial D + 1)$.

Since the deflection of the radio beam under the influence of the interfering effect is equiprobable in either direction, $\overline{\epsilon}_{1\Delta f} = 0$ and therefore

$$\overline{h}_{my} = 0.$$

According to the diagram in figure 11.3, when $\theta_t = \theta_c = \delta_0 = A_0 = 0$, $W_\vartheta(D) = W_\alpha(D) = 0$, the function $F(D)$ when $r_r = r_t$ is equal to

р = r
ц = t
ф = f
эр = ep
ну = my

$$F(D) = \frac{h_t(t)\big|_{r_p = r_u}}{\epsilon_{1\Delta\phi}(t)} = \frac{r_u k_p (T_\partial D + 1)}{T_p^2 D^4 + 2dT_p D^3 + D^2 + k_p T_\partial D + k_p}, \qquad (11.5.3)$$

(Note: This key may be used for this and following equations in this section.)

where $k_r = \frac{k_{DF}k_a a_\delta v}{T_v r_t \omega_0^2}$ is the transfer constant of an open acceleration system (when the guidance circuit is broken at the point a), and $T_r = \frac{1}{\omega_0}$.

It follows from expression (11.5.3) that

$$k_1^2 = r_t$$

and therefore

$$\Delta F_{ep} = \frac{1}{2\pi}\int_0^\infty \left| \frac{k_p (jT_\partial \omega + 1)}{T_p^2 (j\omega)^4 + 2dT_p (j\omega)^3 + (j\omega)^2 + k_p T_\partial j\omega + k_p} \right|^2 d\omega.$$

Computing the derived integral in the same way as was done in the preceding section, we obtain /588

$$\Delta F_{ep} = \frac{2dT_\partial^2 k_p - T_p T_\partial k_p + 2d}{4\left(2T_\partial d - T_p T_\partial^2 k_p - 4d^2 T_p\right)}. \qquad (11.5.4)$$

Substituting the values k_1^2 and ΔF_{ep} into expression (11.5.2) and taking into account that

$$G_\Delta(0) = \frac{2G_m(\Omega)}{k_m^2},$$

we find

$$\sigma_{my}^2 = \frac{r_u^2 G_m(\Omega)}{2k_m^2} \frac{2dT_\partial k_p - T_p T_\partial k_p + 2d}{2T_\partial d - T_p T_\partial^2 k_p - 4d^2 T_p}. \qquad (11.5.5)$$

The derived formula characterizes the dispersion of the miss as a function of the distance r_t, the parameters of the guidance circuit, the steepness of the directional diagram of the radar set antenna and the spectral density of the fluctuations of the modulation coefficient m of the signal received by the radar at the scanning frequency Ω.

For example, if $k_r = 0.8$ 1/sec^2, $T_\partial = 0.4$ sec, $T_r = 0.14$ sec, $d = 0.05$, $G_m(\Omega) = 3.6 \cdot 10^{-4}$ sec and $k_m = 30$ %/degree, the value σ_{my} is 17 m.

Decreases of the value σ_{my}^2 can be achieved by an appropriate selection of Ω, k_m, T_∂, k_r, T_r and d. Formula (11.5.5) also makes it possible to formulate

requirements on the admissible value $\frac{G_m(\Omega)}{k_m^2}$ for stipulated values σ_{my}^2, r_t and the parameters of the guidance circuit.

The mathematical expectation and the dispersion of the rocket miss can be computed on the basis of expressions (11.5.1) and (11.5.2) also when taking into account the effect of artificial interference on the radar set, if the interference does not change the conversion properties of the set. When artificial interference causes the radar set to be converted from a regime of automatic tracking of the target on the basis of angular coordinates to a search regime, the rocket guidance process virtually ceases and it will fly as an uncontrolled object in accordance with the last value of the received command.

The effect of artificial interference on the radio receiver of the rocket causes distortion of the reference signals and the envelope of the received pulses. If this interference is sufficiently effective, the guidance circuit is opened, and depending on the particular circuitry the control surfaces of the rocket in general are set in a neutral position or in one of the extreme positions.

The fluctuation errors of a beam-riding control system ensuring rocket guidance with a forward point can be computed as in the coincidence method. However, in this case it is necessary to take into account the change of structure of the guidance circuit associated with the kinematic equations and the mismatch equation.

It is necessary to proceed in this way when computing the fluctuation errors of guidance of rockets which are controlled by nonautonomous systems based on use of radio navigation apparatus. However, it should be remembered that in a general case, in radio zone control systems based on radio navigation, coordinate measuring instruments interference can exert an influence on all the radio receivers used, although the rocket radio equipment, when directional antennas are used, will have greater noise immunity than ground radio apparatus. /589

11.6. Fluctuation Errors of Rocket Guidance during Homing

First we will consider the fluctuation errors in the absence of artificial interference. For active and passive homing systems, the random errors of rocket guidance are caused by fluctuations of signals received from the target and the instrument noise of the radio receiver. As the rocket approaches the target, the role of instrument noise decreases and exerts virtually no influence on the rocket miss.

As already mentioned, in semi-active homing systems there are usually three radio receivers: the receiver of the radar set scanning the target and

also the "tail" and "nose" radio receivers of the rocket. In a general case, fluctuating signals to which instrument noise is added reaches the input of each of these radio receivers. However, the "tail" receiver of the rocket, designed for synchronization of the system, does not cause the appearance of errors of the mismatch parameter when there is low-level interference. The same can be said of the radar set if the stability of tracking of the target is not disrupted. At the same time, the random oscillations of the radar antenna system should be taken into account when computing the effective range of the homing system.

Thus, in the absence of artificial interference the sources of random errors of guidance of a rocket controlled by a semi-active homing system are the instrument noise of the "nose" radio receiver of the rocket and fluctuations of the signals reflected by the target. In the case of a small distance r between the rocket and the target, the principal role is played by angular fluctuations. Amplitude fluctuations are of lesser importance and the instrument noise of the radio receiver exerts virtually no influence.

It was demonstrated in chapter 3 that radio interference of the type of fluctuations of received signals does not lead to an appreciable change of the conversion properties of the direction finder of the rocket and of the coordinator as a whole. Therefore, if there are sufficiently small values $q = \varepsilon - \theta$ and $q_t = \varepsilon_t - \theta_t$, homing systems can be considered linear. Then the influence of interference is reduced to the appearance of additive noise at the output of the coordinator, and the block diagrams of homing systems for rocket guidance by the direct method and the parallel approach method will have the form represented in figure 11.4a, b. /590

We note that figure 11.4a, b was obtained on the basis of figures 10.8 and 10.10 with the replacement of Δ_m in the latter by $\Delta_m + u_{nc}$, where u_{nc} is the noise signal at the coordinator output.

The approximate value of errors of rocket guidance by such systems can be found in accordance with the method described in section 11.4 if we apply the principle of "freezing" of the variable coefficients, including distance r. However, it must be remembered that the application of the principle of "freezing" of the coefficients with respect to homing systems, in some cases, can lead to a relatively low accuracy of computation of $\bar{h}_{my}$ and σ^2_{my}. At the same time, considerable difficulties often will arise when determining $\bar{h}_{my}$ and σ^2_{my}, as a result of solution of the systems of homing equations when taking into account the change of the coefficients in these equations.

If it is assumed that the homing system is linearized and that the principle of "freezing" of variable coefficients is applicable, in accordance with the block diagrams shown in figure 11.4, we obtain

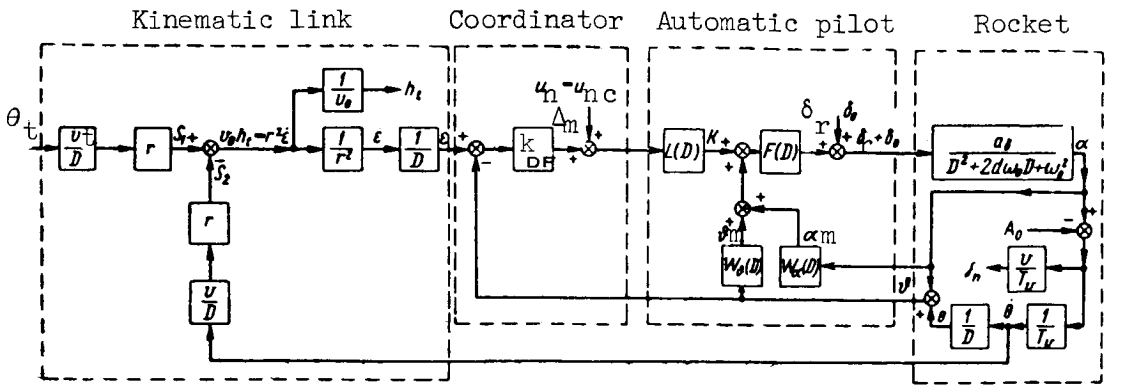

a

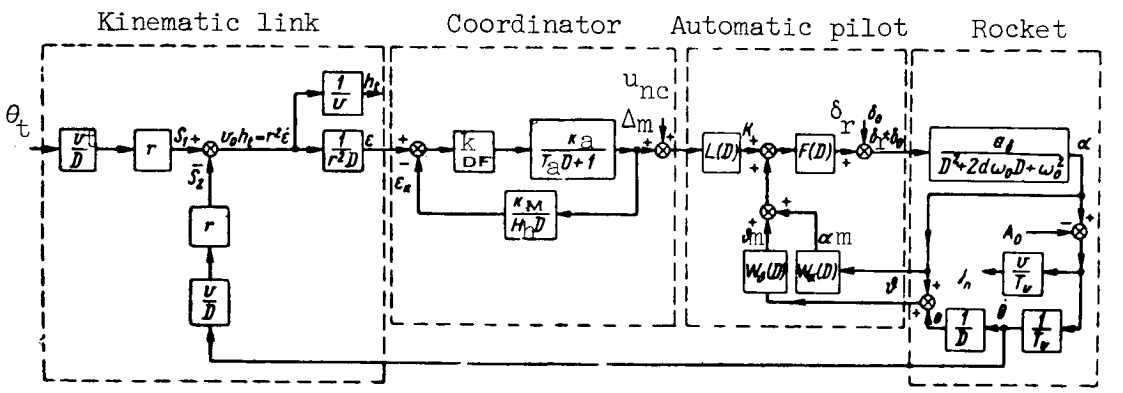

b

Figure 11.4

$$h_{my} = h_t(t)\Big|_{r=r_K}, \qquad (11.6.1)$$

where $h_t(t)_{r=r_K}$ is the rocket miss, determined by formula (10.3.7) when $r = r_K$ and $\theta_t = \delta_0 = A_0 = 0$; r_K is the distance between the rocket and the target at the time when the control command ceases.

On the basis of expression (11.6.1) we obtain

$$\overline{h}_{my} = \overline{h_t(t)}\Big|_{r=r_K}$$

and

$$\sigma_{my}^2 = \sigma_h^2,$$

where σ_h^2 is the dispersion of the random function $h_t(t)\Big|_{r=r_K}$ when $\theta_t = \delta_0 = A_0 = 0$ and $u_{nc} \neq 0$.

However, as follows from the block diagrams shown in figure 11.4

$$h_t(t)\Big|_{r=r_K} = F_c(D)u_{nc}(t),$$

where $F_c(D) = \dfrac{h_t(t)\Big|_{r=r_K}}{u_{nc}(t)}$ is the transfer function of the closed control system in which the signals $u_{nc}(t)$ and $h_t(t)$ act at the input and output, respectively, when $r = r_K$ and $\theta_t = \delta_0 = A_0 = 0$.

Then for a steady-state regime, we obtain /592

$$\bar{h}_{my} = F_c(0)\bar{u}_{nc}, \tag{11.6.2}$$

$$\sigma_{my}^2 = \frac{1}{2\pi}\int_0^\infty |F_c(j\omega)|^2 G_{nc}(\omega)\, d\omega, \tag{11.6.3}$$

where $G_{nc}(\omega)$ is the spectral density of signal fluctuations $u_{nc}(t)$.

If within the limits of the passband of the guidance circuit, the spectral density $G_{nc}(\omega)$ remains virtually constant and remains equal to the value of this function when $\omega = 0$, expression (11.6.3) is simplified and assumes the following form

$$\sigma_{my}^2 \approx \frac{1}{2\pi} G_{nc}(0)\int_0^\infty |F_c(j\omega)|^2 d\omega. \tag{11.6.3a}$$

Under real conditions, the function $F_c(j\omega)$ can characterize either an astatic or a static system. For example, it can be seen from figure 11.4a that a homing system ensuring the direct method of rocket guidance is astatic relative to the signal $\bar{u}_{nc}(t)$ and the miss h_t. This means that the mathematical expectation of the rocket miss will be equal to zero even when $\bar{u}_{nc} \neq 0$. At

the same time, the system whose block diagram is shown in figure 11.4b is static relative to the signal $\overline{u}_n$, provided the output is the miss h_t. It therefore follows that, in contrast to the preceding case, the integrator does not contain a feedback since the coordinator ensures a differentiation of the input signal.

The fluctuation signal u_{nc} appears as a result of conversion of the noise voltage u_n produced by the direction finding component of the coordinator. It is easy to see that the relatively constant component of the voltage u_n of the homing system in the parallel approach method is astatic.

Thus, in parallel approach of a rocket to the target, the mathematical expectation (systematic component) of the guidance error due to the effect of interference can appear only when there are errors in measurement of the angular velocity of the "rocket-target" line, provided the transfer function $F_c(D)$ characterizes a static system.

By introducing additional integrating links into the circuit between the points of cutting in of the signals h_t and u_{nc}, it is possible to achieve an absence of the mathematical expectation of rocket guidance error even in the presence of u_{nc}, $\left(\frac{\overline{du}_{nc}}{dt}\right)$, etc.

In those cases when $F_c(j\omega) \neq 0$ when $\omega = 0$, expression (11.6.3a) should be written in the following form

$$\sigma_{my}^2 = k_{dc\ c}^2 {}_cG_{nc}(0)\Delta F_{ep\ c}, \qquad (11.6.4)$$

where $k_{dc\ c}$ and $\Delta F_{ep\ c}$ are the transfer constant for direct current and the effective passband of a system with the frequency characteristic $F_c(j\omega)$. /593

If $F_c(j\omega)$ characterizes an astatic system, the dispersion of the miss must be computed on the basis of expression (11.6.3a) or (11.6.3).

As an illustration of the method of determination of fluctuation errors in systems of homing by the direct method and the parallel approach method, we find computed relations making it possible to compute $\overline{h}_{my}$ and σ_{my}^2 for the homing systems whose block diagrams are shown in figure 11.4a, b. Here it will be assumed that $W_\alpha(D) = 0$ and $W_\vartheta(D) = k_\vartheta(T_\vartheta D + 1)$, where k_ϑ and T_ϑ are the

transfer constant and the time constant of the apparatus measuring the angle ϑ, respectively.

On the basis of figure 11.4a, when $\theta_t = \delta_0 = A_0 = 0$ and $r = r_K$, we obtain

$$h_f(t)|_{r=r_K} = \frac{1}{v_0} \frac{r_K^2 D W_4(D) W_5(D)}{r_K^2 D + k_{DF} r_K^2 D W_2(D) W_5(D) - k_{DF} W_4(D) W_5(D)} u_{nc}(t),$$

where

$$W_4(D) = \frac{v}{T_v D} r_K; \quad W_2(D) = 1 + \frac{1}{T_\vartheta D}, \quad W_5(D) = L(D) F_1(D);$$

$$F_1(D) = \frac{W_1(D)}{1 + W_1(D) W_2(D) W_3(D)}; \quad W_1(D) = \frac{a_\delta F(D)}{D^2 + 2d\omega_0 D + \omega_0^2}.$$

After replacement of $W_4(D)$, $W_5(D)$ and $W_2(D)$ by their values, we find

$$h_f(t)|_{r=r_K} = \frac{1}{v_0} \frac{r_K^2 v L(D) F(D) a_\delta D}{Q_1(D)} u_{nc}(t). \tag{11.6.5}$$

Here

$$Q_1(D) = r_K D \left[T_v D \left(D^2 + 2d\omega_0 D + \omega_0^2\right) + a_\delta k_\vartheta F(D) (T_v D + 1) (T_\vartheta D + 1)\right] + k_{DF} r_K D (T_v D + 1) a_\delta L(D) F(D) - k_{DF} v a_\delta L(D) F(D).$$

From expression (11.6.5), we obtain the earlier expressed assertion that a homing system based on the direct method is astatic. It also is found that the form of the transfer functions F(D) and L(D) cannot decrease the degree of astaticism.

Assuming that within the limits of the passband of the guidance circuit the spectral density $G_{nc}(\omega) \approx G_{nc}(0)$, in accordance with formulas (11.6.2) and (11.6.3) we will have

$$\overline{h}_{my} = 0,$$

$$\sigma_{my}^2 = \frac{1}{v_0^2} G_{nc}(0) \frac{1}{2\pi} \int_0^\infty \left| \frac{j r_K^2 v L(j\omega) F(j\omega) a_\delta \omega}{Q_1(j\omega)} \right|^2 d\omega. \tag{11.6.6}$$

For example, if L(D) = k_1 and F(D) = k_2, we find that

$$F_c(D) = \frac{1}{v_0} \frac{r_K^2 v k_1 k_2 a_\delta D}{D r_K \left[T_v D \left(D^2 + 2d\omega_0 D + \omega_0^2\right) + a_\delta k_\vartheta k_2 (T_v D + 1) (T_\vartheta D + 1)\right] + \rightarrow + k_{DF} r_K D k_1 k_2 a_\delta (T_v D + 1) - k_{DF} v a_\delta k_1 k_2}$$

Using the method for computing the integral entering into expression (11.6.3a) considered in section 11.4, we find /594

$$\sigma^2_{my} = \frac{1}{v_0^2} G_{nc}(0) \frac{r_K^3 v^2 a_\delta k_1 k_2 (2d\omega_0 T_v + a_\delta k_\vartheta k_2 T_v T_\vartheta)}{4(a-b-c)}, \tag{11.6.7}$$

where

$$a = r_K k_{DF} k_2 a_\delta (2d\omega_0 T_v + a_\delta k_\vartheta k_2 T_\vartheta T_v)(k_\vartheta T_v + k_\vartheta T_\vartheta + k_{DF} k_1 T_v);$$
$$b = k_{DF} v (2d\omega_0 T_v + a_\delta k_\vartheta k_2 T_\vartheta T_v)^2;$$
$$c = T_v r_K k_{DF}^2 k_1 k_2 a_\delta.$$

The derived expression (11.6.7) makes it possible to compute σ^2_{my} if the parameters of the homing system and the spectral density $G_{nc}(0)$ of the signal fluctuations $u_{nc}(t)$ are known. Naturally, $G_{nc}(0)$ is essentially dependent on the structure of the received interference. Thus, when taking into account the influence of the amplitude fluctuations of the signals received from the target, in accordance with formula (3.9.24) we find that

$$G_{nc}(0) = \frac{2G_m(\Omega)}{k_m^2} k_{DF}^2.$$

For a system in which r_K = 500 m, v = 100 m/sec, a_δ = 50 1/sec^2, k_1 = 4, k_{DF} = 50 v/rad, k_2 = 0.01 rad/v, $2d\omega_0$ = 0.7, T_v = 3 sec, k_ϑ = 50 v/rad, T_ϑ = 0.5 sec, v_0 = 300 m/sec and $G_{nc}(0)$ = 0.2 v^2·sec, the mean square value of the miss is approximately 8 m.

It follows from the block diagram shown in figure 11.4b that when $\theta_t = \delta_0 = A_0 = 0$

$$F_c(D) = \frac{1}{v_0} \frac{L(D) W_3(D) v r_K^2 D}{T_v r_K D^2 + L(D) W_3(D) v W_c(D)},$$

where

$$W_3(D) = \frac{W_1(D)}{1 + W_1(D) W_2(D)}; \quad W_1(D) = \frac{F(D) a_\delta}{D^2 + 2d\omega_0 D + \omega_0^2};$$
$$W_2(D) = k_\vartheta (T_\vartheta D + 1)\left(1 + \frac{1}{T_v D}\right);$$
$$W_c(D) = \frac{k_{DF} k_a H_n D}{H_n D (T_a D + 1) + k_{DF} k_a k_\vartheta}.$$

After transformation of this expression, taking into account that the voltage

$$u_{n\,c}(t)=\frac{k_a D}{D(T_a D+1)+k_V}u_n(t),$$

where $k_V=\frac{k_{DF}k_a k_\partial}{H_\partial}$ is the amplification factor of the velocity coordinator, and $u_n(t)$ is the fluctuation voltage acting at the output of the link with the transfer constant k_{DF}, we obtain

$$F_c(D)=\frac{h_t(t)|_{r=r_к}}{u_n(t)}=\frac{1}{v_0}\frac{L(D)\,vr_к^2 a_\delta k_\vartheta F(D)\,D}{r_к\left[T_v D\left(D^2+2d\omega_0 D+\omega_0^2\right)+F(D)\times\right.\rightarrow}\cdot \qquad (11.6.8)$$
$$\rightarrow\times a_\delta k_\vartheta(T_v D+1)]\,[D(T_a D+1)+k_V]+\rightarrow$$
$$\rightarrow+va_\delta k_{DF}k_a L(D)F(D)$$

Formula (11.6.8) makes it possible to compute σ^2_{my} for stipulated parameters of the homing system and the spectral density $G_n(0)$ at the zero frequency for the voltage $u_n(0)$. In addition, this formula makes it possible to select the circuit coefficients in such a way that for a given value $G_n(0)$ the dispersion of the miss does not exceed the admissible value. /595

Now, on the basis of expression (11.6.3) when $L(D)=k_1$, $F(D)=k_2$ and $T_a=0$, we will have

$$\sigma^2_{my}=\frac{1}{v_0^2}G_n(0)\frac{v^2r_к^2k_1^2k_2^2a_\delta^2k_a^2(T_v k_v+2d\omega_0T_v+k_2a_\delta k_\vartheta T_v T_\vartheta)}{4(a_1-b_1-c_1)}, \qquad (11.6.9)$$

where

$$a_1=(T_v k_v+2d\omega_0T_v+k_2a_\delta k_\vartheta T_v T_\vartheta)\left(2d\omega_0T_v k_V+T_v\omega_0^2+k_2a_\delta k_\vartheta T_v T_\vartheta k_V\right.$$
$$\left.+k_2a_\delta k_\vartheta T_v+k_2a_\delta k_\vartheta T_\vartheta\right)\left(T_v\omega_0^2k_V+k_2a_\delta k_\vartheta T_v k_v+k_2a_\delta k_\vartheta T_\vartheta k_V+k_2a_\delta k_\vartheta\right);$$
$$b_1=T_v\left(T_v\omega_0^2k_V+k_2a_\delta k_v T_v k_V+k_2a_\delta k_\vartheta\right)^2;$$
$$c_1=(T_v k_V+2d\omega_0T_v+k_2a_\delta k_\vartheta T_v T_\vartheta)^2\left(k_2a_\delta k_\vartheta k_V+\frac{vk_1k_2a_\delta k_{DF}k_a}{r_к}\right).$$

With the same parameters as in the preceding case and also with $k_a=1$ and $k_V=5$ 1/sec, we find that the mean square miss of a rocket guided by the parallel approach method for $G_n(0)=0.2$ $v^2\cdot$sec is approximately 1.7 m.

We note that the cited examples have a purely illustrative character and cannot serve as a basis for the conclusion that the mean square value of miss of a rocket guided by the parallel approach method in all cases will be less than in the direct guidance method.

In homing systems, artificial interference can exert an influence on the radar stations used in scanning the target (in the case of semi-active homing) and radio receivers carried on the rocket. If the interference acting on the "nosecone" receiver of the rocket does not change the conversion properties of the coordinator, the rocket miss can be computed on the basis of the earlier cited formulas. Otherwise, it is most important to determine the coordinator equation taking into account the influence of interference on it and then solve the derived system of equations. The effect of artificial interference on a radar set for scanning the target can cause a cutoff of the regime of automatic tracking, resulting in a disruption of the homing process. The same result can be caused by the effect of interference in the channel of the instrument used for measuring angular coordinates and the range and velocity target selection apparatus.

11.7. Skewing of Coordinate Systems and Its Influence on the Quality of Rocket Guidance

In a general case, the formation of the mismatch parameter, the output of control commands and the creation of the acceleration vector j_n of a rocket is accomplished in different coordinate systems frequently called measurement, command and control coordinate systems. The different character of motion /596 of these coordinate systems leads to their skewing, which, as already mentioned, is expressed in absence of parallelism between the axes of the control and all other coordinate systems used in the control system.

Skewing can be represented most simply by using the example of a command radio control system of the second kind for a case when a rocket is guided by the vane method.

We will assume that the corresponding axes $o_r x_K$, $o_r x_m$, $o_r y_K$, $o_r y_m$, $o_r z_K$ and $o_r z_m$ of the command and measurement coordinate systems $o_r x_K y_K z_K$ and $o_r x_m y_m z_m$ coincide in direction. In addition, we will assume that the coordinate systems $o_r x_K y_K z_K$ and $o_r x_m y_m z_m$ cannot rotate about the axes $o_r x_K$ and $o_r x_m$, which coincide with the air velocity vector **v** of the rocket. Then, taking into account that in winged rockets the control (related) and flow coordinate systems $o_r x_1 y_1 z_1$ and $o_r xyz$ coincide with one another with a sufficient degree of accuracy, it is easy to confirm the absence of angles between the axes $o_r x$,

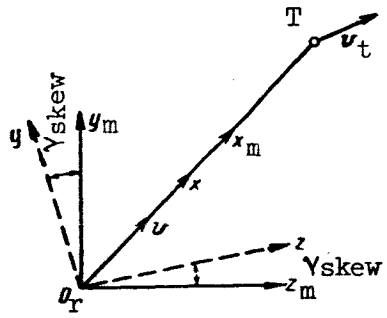

Figure 11.5

$o_r x_m$, $o_r y$ and $o_r y_m$ and $o_r z$, $o_r z_m$, if they are oriented correctly initially and if the rocket is stabilized for banking. However, if the rocket is not stabilized for banking, there can be a turning of the system $o_r xyz$ around the axis $o_r x_m$, which leads to the appearance of angles γ_{skew} between the axes $o_r z$, $o_r z_m$ and $o_r y$, $o_r y_m$ (fig. 11.5).

We note that in constructing the diagram shown in figure 11.5, we took into account the presence of a common origin of the systems $o_r xyz$ and $o_r x_m y_m z_m$ at the point o_r, corresponding to the center of mass of the rocket.

We arrive at the same results under the condition that the rocket is stabilized for banking but the vane base can turn about the axis $o_r x_m$. The value γ_{skew} will be characterized by the total effect of rotation of both coordinate systems $o_r x_m y_m z_m$ and $o_r xyz$ if they are not stabilized.

The skewing resulting from the relative rotation of the considered coordinate systems about the coinciding axes $o_r x$ and $o_r x_m$ usually is called plane skewing. Plane skewing can be illustrated sufficiently clearly using the example of a beam-riding control system ensuring rocket guidance by the coincidence method.

We will assume that the control point o_R, where a radar station is situated (fig. 11.6) is fixed and the axis $o_r x$ of the flow coordinate system coincides precisely with the longitudinal axis of the rocket and the equisignal direction. We will assume further that the rocket is stabilized for banking and that the direction of the radio beam is changed by the turning of the antenna system of the radar station about the axes $o_R z_v$ and $o_R y_v$; the presence of the angular velocity y_v causes turning of the axis $o_R z_v$. /597

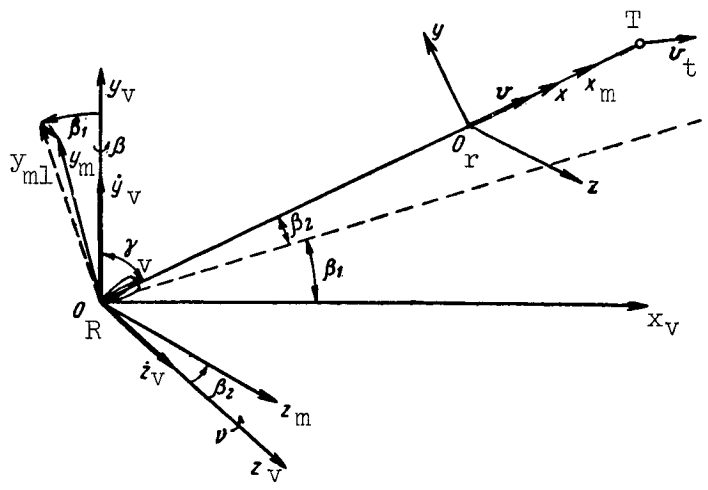

Figure 11.6

Figure 11.6 shows that the coincidence of the beam $o_R x_m$ with the direction to the target T is achieved by turning the antenna in the plane $o_R x_v y_v$ by the angle $\beta = \beta_1$ and about the axis $o_R y_v$ by the angle $\nu = \beta_2$. The axes $o_R y_m$ and $o_R z_m$ of the measurement coordinate system $o_R x_m y_m z_m$ of the radar station formed thereby characterize the coordinate grid transmitted to the rocket by a reference voltage. As a result of the different character of the movement of the axes $o_R y_m$, $o_R z_m$ and $o_r y$, $o_r z$, the grid is turned by some angle γ_{skew} relative to the coordinate system $o_r xz$ in which the reference signal was formed at the beginning of the guidance process. The value γ_{skew} is determined by the following expression

$$\gamma_{skew} = \int_0^t \dot{\gamma}_{skew}(t)dt,$$

where $\dot{\gamma}_{skew}(t)$ is the angular velocity of the turning of the coordinate system $o_R x_m y_m z_m$ about the axis $o_R x_m$.

However, since the system $o_R x_m y_m z_m$ changes its position due to the angular velocities $\dot{y}_v$ and $\dot{z}_v$, then

$$\dot{\gamma}_{skew}(t) = \dot{y}_{vl} + \dot{z}_{vl},$$

where $\dot{y}_{v1}$ and $\dot{z}_{v1}$ are the projections of the angular velocities $\dot{y}_v$ and $\dot{z}_v$ onto the axis $o_R x_m$.

In accordance with the selected method of change of direction of the equisignal line, the horizontal axis of rotation is always normal to the straight line $o_R T$, and as a result $\dot{z}_v = 0$. Then, under the condition that at the /598 time of rocket launching the angle $\beta_2 = 0$, we will have

$$\gamma_{skew} = \int_0^t \frac{d\beta}{dt} \cos \gamma_R dt = \int_0^{\beta_2} \cos \gamma_R d\beta.$$

Here β_2 is the azimuth of the axis of the beam at the current moment of time of rocket flight.

If at the beginning of the guidance process the azimuth of the rocket is not equal to zero, but forms the angle β_0, then

$$\gamma_{skew} = \int_{\beta_0}^{\beta_2} \cos \gamma_R d\beta. \qquad (11.7.1)$$

It follows from expression (11.7.1) that with an increase of the position angle of the target, equal to $90^\circ - \gamma_R$, the angle of skew γ_{skew}, all other conditions being equal, increases and when $\gamma_R < 30^\circ$ the following approximate equation is correct

$$\gamma_{skew} \approx \beta_2 - \beta_0.$$

In actual practice, the values γ_{skew} can attain 180° or more. For example, in the case of linear flight of a target along the horizontal straight line $T_0 T_k$ (fig. 11.7), where the points T_0 and T_k correspond to the times of the beginning and end of the guidance process, the beam of the radar station RS moves in the limits of the angle $T_0 R S T_k$. In this case, if the projection of the point characterizing the position of RS on a horizontal plane passing through the straight line $T_0 T_k$ corresponds to the point 0, in the case of a sufficiently great position angle of the target, the value γ_{skew} will be equal to

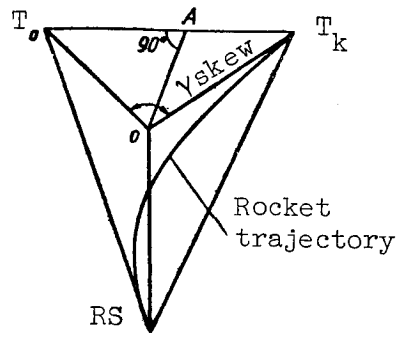

Figure 11.7

the angle T_0OT_k. Figure 11.7 shows that the shorter the length of the perpendicular OA, called the target parameter, the greater is γ_{skew}, and in the case of a very short length of the segment OA the angle γ_{skew} is extremely close to 180°.

When the target moves curvilinearly, it is easy to demonstrate that the skewing can attain 360° or more if, during the time of rocket guidance, the target can fly more than one circle.

The use of the parallel approach method in beam-riding control systems leads to $\gamma_{skew} = 0$, if the target moves uniformly and linearly. This can be attributed to the fact that the direction of the equisignal line, which coincides with the set forward point, remains constant during the entire time of rocket flight. However, in those cases when the target maneuvers, the values γ_{skew} in the case of parallel approach of the rocket to the target can be 180° or more. /599

In command control systems of the first kind, characterizing the spatial separation and different laws of motion of the measurement and control coordinate systems, plane skewing can be found approximately the same as in beam-riding control systems. Depending on the type of measuring instruments included in the coordinator, the character of motion of the target and the rocket guidance method, the range of change of γ_{skew} is rather great: from zero to several hundred degrees.

Plane skewing in homing systems is caused by the possibility of relative turning of the measurement and control coordinate systems, and when stabilization apparatus is used does not exceed several degrees.

In most cases, under real conditions, there is spatial rather than plane skewing of the measurement and control coordinate systems. This can be attributed to the fact that the axis o_rx is displaced (is set forward) relative to

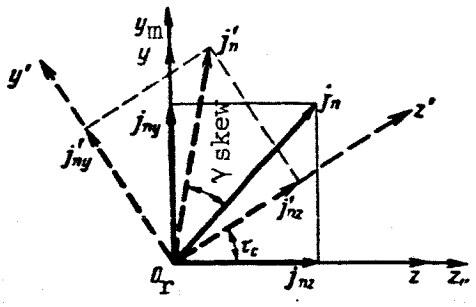

Figure 11.8

the axis $o_r x_m$, usually coinciding with the straight line between the rocket and the target or the control point and the target.

An exception is the pursuit method in homing, when the velocity vector v is directed to the point where the target is situated. The maximum angle of deflection is required in parallel approach methods. However, in accordance with the information in chapter 2, it can be established that when $v_t/v < 0.5$, the mismatch of the axes $o_r x$ and $o_r x_m$, sometimes called "deflection," does not exceed 30-40° (ref. 1). Such deflection values lead to changes γ_{skew} which in the worse case are 20-30°, but most frequently only several degrees. Therefore, in the first approximation the value γ_{skew} can be computed only on the basis of an analysis of plane skewing.

After it has been established that the angles γ_{skew} can vary in the range from several to several hundreds of degrees, the problem arises of the influence of the phenomenon of skewing of coordinate systems on the quality of rocket guidance.

It is found that small angles γ_{skew} lead to lengthening of transient processes in the control system and greater angles to a total loss of stability of the guidance circuit.

For confirmation of this conclusion and determination of the admissible values γ_{skew} we will analyze the influence of plane skewing arising due to spatial turning only of the control coordinate system relative to the coinciding measurement and command coordinate systems. In this process, we will assume first that a Cartesian control of the rocket is used. We will assume that at some time t the axes $o_r z_m$, $o_r z$, $o_r y_m$ and $o_r y$ are oriented as shown in figure 11.8 by solid lines, and we will assume that lateral acceleration /600 was formed under the influence of the coordinator signals

$$j_n = j_{nz} + j_{ny},$$

where j_{nz} and j_{ny} are accelerations arising with the deflection of the rudder and elevators, respectively.

If in the course of further guidance of the rocket, the axes $o_r z$ and $o_r y$ are turned by the angle γ_{skew} and occupy the position $o_r y'$ and $o_r z'$, with the formation of this same mismatch signal at the coordinator as at the time t, the elevators and rudder are deflected to their former angles. As a result, accelerations appear whose vectors j'_{nz} and j'_{ny} will coincide with the axes $o_r z'$ and $o_r y'$. The moduli $|j'_{nz}|$ and $|j'_{ny}|$ will be equal to $|j_{nz}|$ and $|j_{ny}|$, respectively. Summation of j'_{nz} and j'_{ny} gives the acceleration vector j'_n, turned by the angle γ_{skew} relative to the vector j_n. At the same time, $|j'_n| = |j_n|$. It is easy to see that the same results can be obtained in a case when the turning of the axes $o_r y$ and $o_r z$ is absent but the axes $o_r y_m$ and $o_r z_m$ rotate.

It follows from the above that in the case of Cartesian rocket control, the skewing of the coordinate systems $o_r y_m z_m$ and $o_r yz$ by the angle γ_{skew} leads to the turning of the acceleration vector j'_n created by the control surfaces by the same angle γ_{skew} relative to the direction of the vector j_n which would be obtained in the absence of the skewing phenomenon.

Similar conclusions also are drawn for the case of rocket control in polar coordinates. However, if the content of the preceding chapters is recalled, it can be concluded that the skewing phenomenon leads to the same influence on the quality of the rocket guidance process as the dephasing of the rocket-borne radio apparatus included in the coordinators of homing systems and beam-riding guidance systems.

It therefore can be assumed that the limiting value of the skewing angle γ_{skew} is determined primarily by the inertial properties of the radio control system. However, angles γ_{skew} exceeding 45° are inadmissible, because additional factors causing deflections of the vector j'_n (errors in measurement of the mismatch parameter, dephasing, etc.) usually result in loss of stability of

the control system (ref. 1). A further decrease of the angle γ_{skew} is /601

dependent on the reserve of stability of the system: the greater the inertia of the control system and the lesser its reserve of stability, the smaller are the admissible values γ_{skew}. In rough estimates, it is assumed that the angle γ_{skew} should not exceed 10° (ref. 1).

More precise values γ_{skew}, for which there is an insignificant worsening of the quality of the rocket guidance process, can be found by modeling of the guidance process using electronic computers.

Thus, on the one hand, if special measures are not taken, it is possible to obtain very large angles γ_{skew}, and on the other hand values $\gamma_{skew} \leq 10^{\circ}$ are admissible. Therefore, in developing radio control systems, it is necessary to use methods decreasing the influence of skewing of coordinate systems. One of these methods involves elimination of the factors responsible for the relative rotation of coordinate systems. Skewing can be virtually completely eliminated most easily in homing systems and command control systems of the second kind, based on the use of direct and vane guidance methods.

In all cases of rocket homing with deflection and also rocket guidance using beam-riding and command control systems, the elimination of the skewing phenomenon is essentially impossible. This can be attributed to deflection of the axes. However, since the deflection usually exerts a small influence on γ_{skew}, by an appropriate innovation of a radio control system it is possible to achieve an appreciable decrease of the angle γ_{skew}. Thus, a radical measure decreasing γ_{skew} for the above-mentioned beam-riding control system (fig. 11.6) is the stabilization of the measurement coordinate system in such a way that there is no rotation of the system about the x-axis. If for some reason this method for displacement of the beam is inapplicable, it is possible to change the direction of the axes of rotation of the antenna system of the radar station. By an appropriate selection of these axes, it is possible that the skewing will be insignificant in the case of large position angles $90^{\circ} - \gamma_R$, rather than for small angles.

The second method for decreasing the influence of the skewing effect involves measurement of the angle γ_{skew} and the introduction of corresponding corrections into the controlling signals fed to the control surface apparatus. In homing, autonomous control and command control systems of the second kind, when the measurement, command and control coordinate systems are placed on the rocket, determination of the angle γ_{skew} and its introduction into the controlling signal usually involves no significant difficulties. Such a problem can

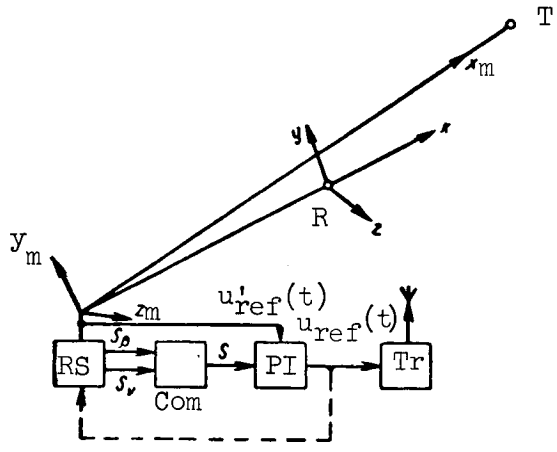

Figure 11.9

be solved, for example, as was described in section 9.7 in discussion of the problem of automatic change of operation of the rocket control surfaces.

In beam-riding control systems, whose basic idea is illustrated in figure 11.6, the value of the angle γ_{skew} is determined approximately by /602

expression (11.7.1) and the signal obtained in this way can be used for shifting the phase of the reference voltage at the control point, in order to change the angular position of the axes of the coordinate grid transmitted by the radar station to the rocket.

One of the possible variants for realization of this idea is shown in figure 11.9. The signals S_β and S_ν, characterizing the position angles and the azimuth of the target β and ν, which are measured by the radar set RS, are fed to the computer Com. This instrument is used to produce a voltage (current) S, reflecting the angle γ_{skew}. Under the influence of the signal S, the phase inverter PI changes the phase of the reference voltage $u_{ref}(t)$ formed by the generator, which is connected rigidly to the motor for rotation of the directional diagram. The voltage $u'_{ref}(t)$ at the PI output is a corrected reference signal which can be transmitted to the rocket by a special radio transmitter or by modulation of the radar station pulses.

11.8. Concise Information on Determination of Rocket Guidance Errors by the Modeling Method

As already mentioned, analytical methods for solution of the equations describing the processes of rocket guidance make it possible to obtain only

extremely approximate results. At the same time, in the creation of the individual units of a control system, an insistent need arises for refining their parameters so that the finally created complex of apparatus will ensure performance of the tasks imposed upon it. In addition to obtaining more precise data on the dynamic properties of the control system, it is extremely important to determine the effectiveness of the influence of different types of fluctuations and, in some cases, artificial radio interference as well. In other words, a sufficiently precise allowance for all the factors characterizing the error in rocket guidance is an extremely important problem /603 at all stages in planning a radio control system.

The solution of this problem is facilitated to a considerable degree by methods of modeling guidance processes, although final conclusions on the quality of the control system can be drawn only on the basis of data from polygon (testing grounds) and other forms of rocket tests.

As is well known, by modeling is meant the simulation of the processes transpiring in a real control system, using other apparatus which usually can be constructed more simply and whose characteristics can be varied quite easily. In actual practice analog and digital computers are used as such apparatus.

Mathematical and mixed modeling of a radio control system can be distinguished in accordance with the methods of use of the modeling apparatus. In mathematical modeling, the operation of all the elements of the investigated system is represented in mathematical form and the equations obtained in this way are solved by computers. In mixed modeling, one part of the guidance circuit is formed by real apparatus and the other is formed by equations.

Mathematical modeling makes it possible to obtain less exact results than mixed modeling. This can be attributed to the fact that in derivation of the equations replacing the real links, it is necessary to make a number of simplifying assumptions, especially in the analysis of radio apparatus under the influence of a high level of interference, including artificial interference. This circumstance is a shortcoming of mathematical modeling. However, the use of mathematical models exclusively makes it possible to investigate rocket guidance processes not only at the true time scale, but also with a lag or acceleration. The latter is very important because, in a relatively short time, it is possible to obtain a great quantity of varied information. Hence it follows that the solution of the problem of finding equations which with a high degree of accuracy reflect processes in each of the links of a radio control system for different methods and environmental conditions of its use is timely.

For mixed modeling, in many cases, it is necessary to create an extremely unwieldy and expensive apparatus. In addition, it must be remembered that mixed modeling can be accomplished only at the true time scale.

When carrying out mixed modeling it is most feasible to use analog computers. This is due to the simplicity of coupling the units of the model to real apparatus. At the same time, it must be remembered that digital computers ensure a considerably higher accuracy of solution of equations although

the preparation of a program for their operation in some cases involves extremely time-consuming processes.

The principles of operation and the design of digital and analog electronic computers and also their use for modeling various physical processes now are described quite fully in the literature (refs. 64 and 65). Therefore, in this section we will consider briefly only the principles of mathematical and mixed modeling using analog computers from the point of view of determining the output parameters of the system analyzed under the influence of parasitic random or nonrandom perturbations. /604

As pointed out, mathematcial modeling is the machine solution of a system of differential equations describing processes which transpire in a real radio control system. As a result of appropriate transformations, the system of equations can be reduced to a single equation. After the equation which is to be investigated has been derived, it should be appropriately prepared. The preparation involves replacement of the modeled functions by electrical signals and the selection of a time scale M_t. Determination of a suitable value M_t is of great importance because when an excessively long time is required for solution of the equation on the electronic computer, there will be considerable errors due to the instability of the current sources and the zero "drift" of the voltages produced by the computer. At the same time, a short integration time distorts the solution as a result of the influence of transient processes in the computer.

It has been established by experience that the time scale should be selected in such a way that all the coefficients in the equation prepared for machine solution differ insignificantly from unity, and naturally it is also necessary to take into account the total time τ_o which is required for obtaining a solution. If τ_o is too long or too short, it is necessary to modify the value M_t.

In order to obtain a more graphic idea concerning the operations of preparing and compiling an electronic model, we will consider a control system described by a fourth-degree linear differential equation with the constant coefficients

$$\Pi = m \qquad b_4 \frac{d^4 h_\Pi}{dt^4} + b_3 \frac{d^3 h_\Pi}{dt^3} + b_2 \frac{d^2 h_\Pi}{dt^2} + b_1 \frac{dh_\Pi}{dt} + b_0 h_\Pi = u_1(t), \qquad (11.8.1)$$

where $h_m(t)$ is the output signal of the investigated system, and $u_1(t)$ is a function characterizing the input action.

For clarity in exposition, we will assume that the above equation, which can be derived on the basis of the block diagrams of command radio control

systems and beam-riding control systems, neglecting all derivatives of functions whose power is greater than four, characterizes the rocket miss $h_t(t)$ under the influence of noise acting at the coordinator output or CCRL output when $\theta_t = \theta_c = \delta_0 = A_0 = 0$ and $r_r = r_t$.

The coefficients b_4, b_3, b_2, b_1 and b_0 can be found in accordance /605 with the block diagrams shown in figures 11.1 and 11.3.

After converting the modeled value h_m into a voltage and replacing the mathematical time t by the computer time τ (using the scale factors M_h and M_t having the dimensionality $\left[\frac{v}{m}\right]$, ref. 1), we will have

$$\left.\begin{aligned} h_m &= \frac{1}{M_h} u, \\ t &= \frac{\tau}{M_t} \end{aligned}\right\} \tag{11.8.2}$$

and

$$b_4 \frac{1}{M_h} M_t^4 \frac{d^4u}{d\tau^4} + b_3 \frac{1}{M_h} M_t^3 \frac{d^3u}{d\tau^3} + b_2 \frac{1}{M_h} M_t^2 \frac{d^2u}{d\tau^2} + b_1 \frac{1}{M_h} M_t \frac{du}{d\tau} + b_0 \frac{1}{M_h} u = u_1(\tau), \tag{11.8.3}$$

where $u_1(\tau)$ is the voltage $u_1(t)$ obtained with the replacement of t by τ.

Under real conditions in most cases $b_4 < b_3 < b_2 < b_1 < b_0$. Therefore, by an appropriate selection of the value $M_t > 1$, after dividing the left and right-hand sides of equation (11.8.3) by $b_4 \frac{1}{M_h} M_t^4$, we find that the coefficients standing before the function u(t) and its derivatives differ little from 1. As a result of division by $b_4 \frac{1}{M_h} M_t^4$, we obtain the following computer equation (electronic model equation) for the investigated control system

$$\frac{d^4u}{d\tau^4} + a_3 \frac{d^3u}{d\tau^3} + a_2 \frac{d^2u}{d\tau^2} + a_1 \frac{du}{d\tau} + a_0 u = b u_1(\tau). \tag{11.8.4}$$

Here

$$a_3 = \frac{b_3}{M_t b_4}; \quad a_2 = \frac{b_2}{M_t^2 b_4}; \quad a_1 = \frac{b_1}{M_t^3 b_4}; \quad a_0 = \frac{b_0}{M_t^4 b_4}; \quad b_0 = \frac{M_h}{b_4 M_t^4}.$$

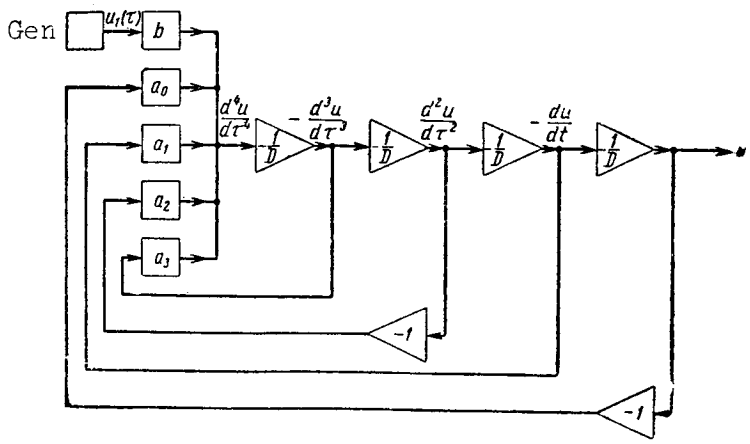

Figure 11.10

Since the analog computer does not contain differentiators, the equation (11.8.4) should be solved relative to the higher derivative, whose integration, with the initial conditions taken into account, makes it possible to find all the lower-order derivatives. Using such an approach, we obtain the diagram of the program shown in figure 11.10, with the assumption that the initial conditions are zero conditions. In this diagram, the elements with the coefficients b, a_0, a_1, a_2 and a_3 reflect amplifiers with transfer constants equal to b, a_0, a_1, a_2 and a_3, respectively. It is assumed that the sign of the input signals is not changed by such amplifiers. The symbols $-\frac{1}{D}$ and -1 in figure 11.10 denote the integrators and amplifiers performing the corresponding conversions of the output voltages with change of their sign (polarity). /606

The random voltage $u_1(\tau)$, reflecting the input action, is produced by the generator Gen. The latter should be designed in such a way that the two-dimensional distribution laws, or at least the mathematical expectations and the correlation functions of the signal forming at the output of the generator Gen and the voltage $u_1(\tau)$ will be identical.

If it is necessary to investigate the dynamic errors of rocket guidance, the method described above must be applied to the equation relating the miss $h_t(t)$ to the motion of the target and control point.

When modeling a nonlinear radio control system, the superposition principle is inapplicable, and therefore the values of the output parameter must be determined under the condition of taking into account all possible external effects simultaneously.

We will consider the principle of mixed modeling using the example of a beam-riding control system, on the assumption that the control point and the

target are fixed and the radio equipment of the rocket is used as the real apparatus. In addition, we will assume that a rocket stabilized for banking, an automatic pilot and a kinematic link for the vertical guidance plane are described by linear differential equations, on the basis of which we have shown the corresponding links of the block diagram in figure 10.12. We will also assume that $W_\alpha(D) = k_\alpha$, $W_\vartheta(D) = k_\vartheta$, $F(D)L(D) = k_\delta$, that the rocket radio receiver is acted upon not only by signals simulating the operation of the radar station and the motion of the rocket, but by radio interference as well, and that the equations for the rocket, kinematic link and automatic pilot for /607 the horizontal guidance plane are of the same form as for the vertical plane and differ only in the absence of signals similar to A_0, δ_0 and the subscript "1" on the coefficients, functions and independent variables.

In order to be able to select a model diagram, it is necessary to replace the real equations of the rocket, kinematic link and automatic pilot by computer equations and model the radio beam of the control system. First, we will consider the equations describing the process of rocket guidance in a vertical plane.

It follows from figure 10.12, with $\theta_c = \theta_t = 0$, that

$$\varepsilon_r = -\frac{h_t}{r_r},$$
$$\dot{h}_t = -v\theta,$$
$$\dot{\theta} = \frac{1}{T_v}(\alpha - A_0),$$
$$\ddot{\alpha} + 2d\omega_0\dot{\alpha} + \omega_0^2\alpha = a_\delta(\delta_r + \delta_0),$$
$$\delta_r = k_\delta u'_y + k_\alpha\alpha + k_\vartheta\vartheta,$$
$$\vartheta = \theta + \alpha,$$

where u'_y is the voltage acting at the output of the rocket radio equipment for the vertical control plane, taking into account the effect of interference.

As already mentioned, when real apparatus is included in the model, the investigation of processes must be at the true time scale, and therefore the preparation of the written equations will involve only a replacement of ε_r, h_t, θ, α, δ_r and ϑ by the corresponding voltages.

We will assume that

$$\varepsilon_r = \frac{u_\varepsilon}{M_\varepsilon},\quad h_t = \frac{u_h}{M_h},\quad \theta = \frac{u_\theta}{M_\theta},\quad \alpha = \frac{u_\alpha}{M_\alpha},\quad \delta_r = \frac{u_\delta}{M_\delta} \text{ and } \vartheta = \frac{u_\vartheta}{M_\vartheta}.$$

where u_ε, u_h, u_θ, u_α, u_δ and u_ϑ are voltages characterizing the parameters ε_r, h_t, θ, α, δ_r and ϑ, and M_ε, M_h, M_θ, M_α, M_δ and M_ϑ are the scale factors. Then the reduced system of equations is transformed to the following form

$$\left.\begin{aligned} u_\varepsilon &= k_4 u_h, \\ \dot{u}_h &= k_3 u_\theta, \\ \dot{u}_\theta &= k_2 u_\alpha - u_a, \\ \ddot{u}_\alpha + 2d\omega_0 \dot{u}_\alpha + \omega_0^2 u_\alpha &= k_1 u_\delta + u_0, \\ u_\delta &= k_7 u'_y + k_8 u_\alpha + k_9 u_\vartheta, \\ u_\vartheta &= k_5 u_\alpha + k_6 u_\theta. \end{aligned}\right\} \qquad (11.8.5)$$

Here

/608

$$k_1 = a_\delta \frac{M_\alpha}{M_\delta}; \quad k_2 = \frac{1}{T_v}\frac{M_\theta}{M_\alpha}; \quad k_3 = -\frac{M_\theta}{M_h}; \quad k_4 = -\frac{1}{r_r}\frac{M_\varepsilon}{M_h};$$
$$k_5 = \frac{M_\vartheta}{M_\alpha}; \quad k_6 = \frac{M_\vartheta}{M_\theta}; \quad k_7 = k_\delta M_\delta; \quad k_8 = k_\alpha \frac{M_\delta}{M_\alpha};$$
$$k_9 = k_\vartheta \frac{M_\delta}{M_\vartheta}; \quad u_0 = \frac{a_\delta}{M_\delta} M_\alpha u_{\delta 0}; \quad u_0 = a_\delta \delta_0 M_\alpha; \quad u_a = \frac{M_\theta}{T_v} A_0.$$

Similarly we find the following computer equations determining the rocket guidance in a horizontal plane

$$\left.\begin{aligned} u_{\varepsilon.1} &= k_{4.1} u_{h.1}, \\ \dot{u}_{h.1} &= k_{3.1} u_{\theta.1}, \\ \dot{u}_{\theta.1} &= k_{2.1} u_{\alpha.1}, \\ \ddot{u}_{\alpha.1} + 2d_1\omega_{0.1}\dot{u}_{\alpha.1} + \omega_{0.1}^2 u_{\alpha.1} &= k_{1.1} u_{\delta.1}, \\ u_{\delta.1} &= k_{7.1} u'_{y.1} + k_{8.1} u_{\alpha.1} + k_{9.1} u_{\vartheta.1}, \\ u_{\vartheta.1} &= k_{5.1} u_{\alpha.1} + k_{6.1} u_{\theta.1}. \end{aligned}\right\} \qquad (11.8.6)$$

In this system

$u_{\varepsilon.1}$, $u_{h.1}$, $u_{\theta.1}$, $u_{\alpha.1}$, $u_{\delta.1}$ and $u_{\vartheta.1}$ are voltages corresponding to the signals $\varepsilon_{r.1}$, $h_{t.1}$, θ_1, α_1, δ_1 and ϑ_1;

$u'_{y.1}$ is a voltage produced by the rocket radio apparatus for the horizontal control plane with the effect of interference taken into account;

$\varepsilon_{r.1}$ and $h_{t.1}$ are the angular and linear deflections of the center of mass of the rocket relative to the equisignal direction;

θ_1. α_1 and ϑ_1 are the angles of inclination of the velocity vector of the rocket (in the horizontal plane, slip and yawing);

$\delta_{r.1}$ is the angle of deflection of the control surface (rudder);

$$k_{1.1}=a_{\delta.1}\frac{M_{\alpha.1}}{M_{\delta.1}};\quad k_{2.1}=\frac{1}{T_{v.1}}\frac{M_{\theta.1}}{M_{\alpha.1}};\quad k_{3.1}=-v_1\frac{M_{\theta.1}}{M_{h.1}};$$

$$k_{4.1}=-\frac{1}{r_{r.1}}\frac{M_{\varepsilon.1}}{M_{h.1}};\quad k_{5.1}=\frac{M_{\delta.1}}{M_{\alpha.1}};\quad k_{6.1}=\frac{M_{\vartheta.1}}{M_{\theta.1}};$$

$$k_{7.1}=k_{\delta.1}M_{\delta.1};\quad k_{8.1}=k_{\alpha.1}\frac{M_{\delta.1}}{M_{\alpha.1}};\quad k_{9.1}=k_{\vartheta.1}\frac{M_{\delta.1}}{M_{\vartheta.1}};$$

$a_{\delta.1}$, $T_{v.1}$ are the coefficient of efficiency of the control surface (rudder) and the time constant of the rocket for the horizontal plane;

$r_{r.1}$ is the distance from the control point to the rocket in the horizontal plane;

$k_{\delta.1}$, $k_{\alpha.1}$ and $k_{\vartheta.1}$ are the transfer constants of the automatic pilot /609 relative to the signals $u'_{y.1}$, α_1 and ϑ_1;

$M_{\varepsilon.1}$, $M_{h.1}$, $M_{\theta.1}$, $M_{\alpha.1}$, $M_{\delta.1}$ and $M_{\vartheta.1}$ are the scale factors for $\varepsilon_{r.1}$, $h_{t.1}$, θ_1, α_1, $\delta_{r.1}$ and ϑ_1;

$2d_1\omega_{0.1}$ is the attenuation factor and natural frequency of oscillations of the angle of slip α_1.

Since in most cases the course and pitching control channels are identical or have parameters quite close to one another, it is feasible to assume that $M_{\varepsilon.1}=M_{\varepsilon}$, $M_{h.1}=M_h$, $M_{\theta.1}=M_{\theta}$, $M_{\delta.1}=M_{\delta}$ and $M_{\vartheta.1}=M_{\vartheta}$.

In accordance with the principle of design of a beam-riding control system, at the input of the rocket radio receiver there should be radio pulses which are amplitude-modulated by a harmonic voltage. The intensity of modulation and the phase of the modulating voltage determine the value of the angle and the direction of deflection of the rocket from the radio beam. A model of the radio beam is needed for creating such radio pulses. In addition, the input of the rocket radio receiver should receive reference voltage signals.

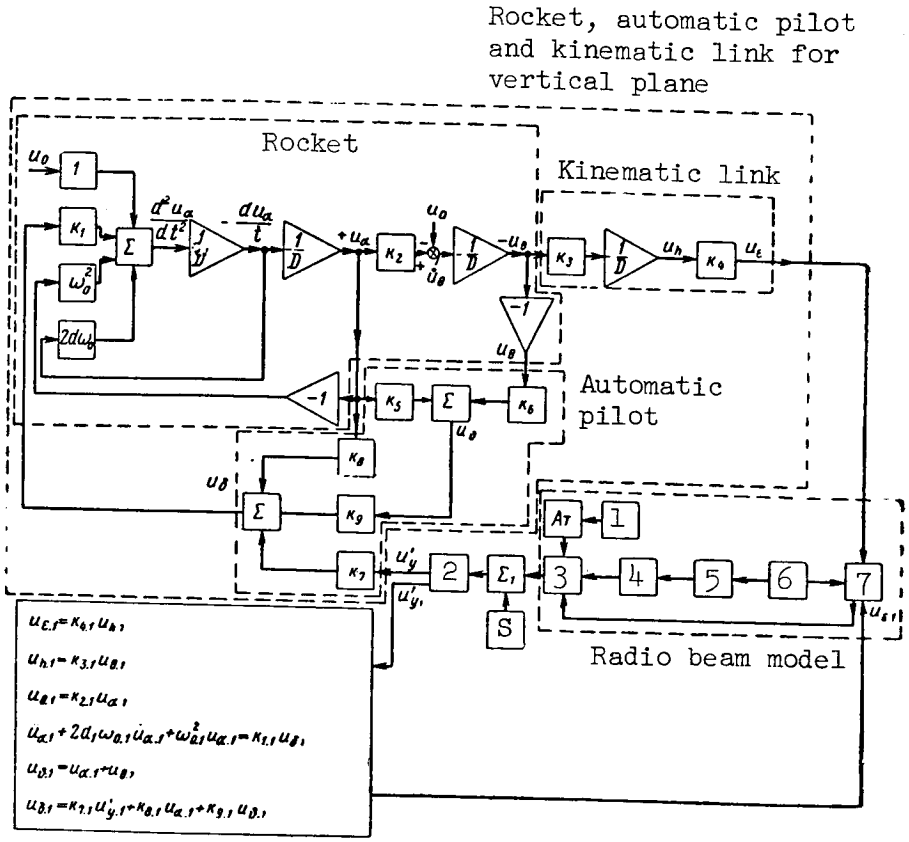

Figure 11.11

Then, using equations (11.8.5) and (11.8.6), and also a model of the radio beam, the rocket radio apparatus RRA, a radio interference source S and a summer Σ_1, it is possible to obtain the functional diagram of the modeling apparatus shown in figure 11.11. In figure 11.11, the equations of the rocket, kinematic link and automatic pilot for the vertical guidance plane are represented in the form of a diagram where the elements with the coefficients k_1, ω_0^2 and $2d\omega_0$ denote amplifiers which do not change the polarity of the input signals and the symbols Σ denote summers.

The radio beam model is created with a coupling unit CU, a generator of sinusoidal oscillations SOG, a pulse generator PG, a radio-frequency signal generator RFSG, a modulator Mod, an attenuator At and a programming mechanism PM.

The following voltage is fed from a coupling unit

$$u_c = c|\varepsilon_1|\sin(\Omega t + \varphi),$$

where c is a proportionality factor and $|\varepsilon_1| = \sqrt{\varepsilon_r^2 + \varepsilon_{r.1}^2}$.

This voltage is formed from feeding of the signals u_ε and $u_{\varepsilon.1}$, and also sinusoidal oscillations fed from the output of the SOG, which forms the voltage u_{so} with the frequency Ω equal to the frequency of scanning of a real radar set. The SOG signals also are fed to the generator PG where pulses are formed having the same repetition rate as in real radio apparatus, and a reference voltage is formed. This is done by repetition-rate modulation of the PG pulses by the voltage u_{so} and the corresponding code groups are formed.

The PG pulses control the radio-frequency signal generator RFSG, /610 whose output signals, together with the voltage u_c, are fed to the modulator Mod.

By appropriate selection of the parameters of the modulator Mod and the amplitude $c|\varepsilon_1|$ of the voltage u_c, the actually forming mismatch angle ε_1 will correspond to the necessary changes of the envelope of the received radio pulses. In order to take into account the change of strength of signals fed to the input of the rocket receiver, the modeling apparatus includes an attenuator At which is driven into motion by the programming mechanism PM.

The summer Σ_1 is used in mixing the radio interference and the signals characterizing the radio beam.

Using the modeling apparatus shown in figure 11.11, it is possible to investigate the influence of dephasing and unbalancing in the rocket radio apparatus RRA and also the effect of interference on the accuracy of rocket guidance if the voltages u_h and $u_{h.1}$ are written in some way. In addition, other parameters of the radio control system can be analyzed.

The coupling unit CU, as indicated by its name, acts as a converter /611 of the mismatch signals received at the output of the model in a rectangular coordinate system, converting them into a mismatch signal in a polar coordinate system. The functional diagram of one of the possible variants of a CU is shown in figure 11.12.

A voltage u_ε, corresponding to the angular mismatch ε_r, is fed to the armature of the relay Rel_1, and a voltage $u_{\varepsilon.1}$, proportional to the angle ε_{r1},

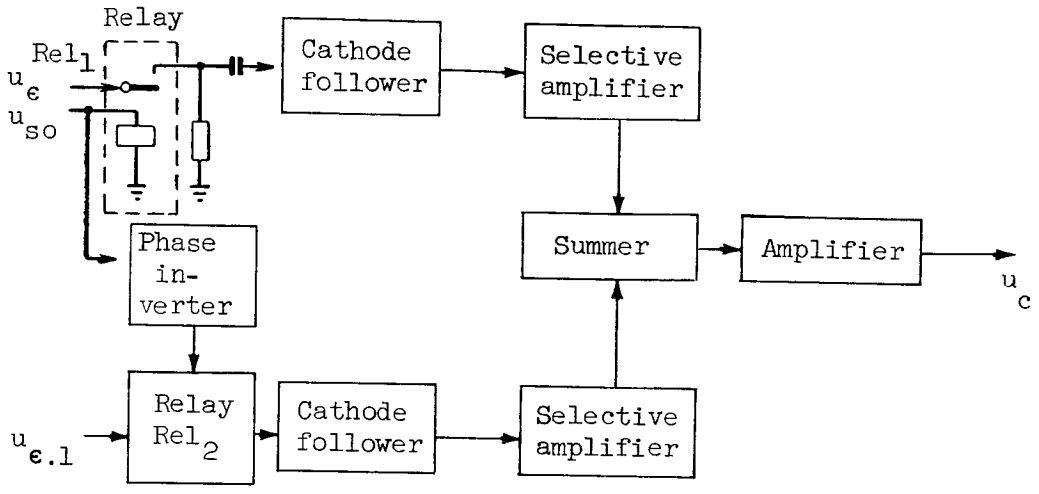

Figure 11.12

is fed to the armature of the relay Rel_2. The windings of both relays are cut into the generator SOG (fig. 11.11); the voltage u_{so} across the relay Rel_2 is fed with a 90^o shift by use of a phase inverter.

Square pulses whose repetition rate is Ω are fed from the contacts of the relays Rel_1 and Rel_2; their amplitude and polarity are dependent on the value and sign of the voltages u_ϵ and $u_{\epsilon.1}$.

The produced pulses are fed through cathode followers to selective amplifiers which form harmonic voltages proportional to $\epsilon_r \sin \Omega t$ and $\epsilon_{r.1} \cos \Omega t$. These voltages then are summed and amplified, creating the necessary voltage u_c.

If in modeling guidance processes it is necessary to take into account the characteristics of a real automatic pilot and the radar set errors, the diagram shown in figure 11.11 must be modified accordingly. For example, in order to take into account the random errors of the radar set, the appropriate random components must be added to the voltages u_ϵ and $u_{\epsilon.1}$.

Of course, the method of mixed modeling considered here is not universal. However, it can be used in solution of the problem of modeling of other types of radio control systems.

11.9. General Characteristics of Methods for Increasing the Noise Immunity of Radio Control Systems

In most cases, modern electronic apparatus has a great excess of /612 transmissivity with respect to the information necessary for rocket control. This can be attributed to the fact that the frequency spectrum of the input action stipulated by the motion of the target does not exceed several cps. At the same time, the passband of the radio receiving apparatus is determined to a considerable degree by the form of modulation of the carrier, the frequency instability of the radio transmitter generator and the heterodyne of the radio receiver, and falls in the range from several tens of kc/s to several Mc/s.

For example, in the case of an instability of $2\text{-}4\cdot10^{-4}$ and a carrier frequency of 50 Mc/s, it is necessary to have a passband equal to 10-20 kc/s.

The resulting reserve of carrying capacity can be used for increasing the noise immunity of radio control systems. An increase of the noise immunity of the radio control systems is attained by the use of measures directed to an increase of the secretiveness of transmission of control signals and of the noise immunity of the radio receiving apparatus and the guidance circuit as a whole.

An increase of secretiveness is based on the use of frequency, spatial, amplitude and temporal methods.

Among the frequency methods is change of the working waves with transition from one guidance method to another and in the control process of the same rocket, and also masking of the operation of the radio apparatus. The latter involves the creation of additional radiations hindering the reliable determination of the carrier frequency of the transmitted communications (measured coordinates of the target, control commands, etc.). For masking purposes, it is necessary to use N_{tr} rather than one transmitter; these should operate at different carrier frequencies and be modulated by the same signals, whereas the rocket receives signals from only one transmitter. Under these conditions, when interference is organized at one frequency, the probability p_o that the operation of such a control system apparatus will be discovered and that interference will be created can be evaluated approximately by use of the following formula

$$p_o = \frac{1}{N_{tr}}.$$

The masking of the parameters of the transmitted signals is attained also by use of the so-called method of transmission using quasi-random signals (ref. 111). The essence of this method, as applied to pulse command control radio links, for example, is that pulses which are chaotically following for the enemy are added to the sequence of pulses reflecting the transmitted command.

These additional signals, sometimes called a mask, are known for the receiving apparatus itself, and as a result they do not hinder detection of the transmitted communications. /613

The spatial secretiveness is determined by the width of the directional diagram of the antenna systems used. It is the greater the narrower is the beam used in the transmission and reception of the radio signals.

Amplitude methods for increasing the secretiveness essentially involve a decrease of the radiated power so that, at the input of the reconnaissance receiver, it will be less than its sensitivity. At the same time, it must be remembered that such a method for increasing secretiveness usually leads to a worsening of noise immunity.

Temporal methods for increasing secretiveness include a decrease of the duration and repetition rate of discrete signal transmission, change of the coding parameters, irregular transmission of communications, etc.

For example, if communications are transmitted discretely and aperiodically, when the carrier frequency is determined using a reconnaissance receiver with successive scanning of the stipulated frequency range, that is, a receiver of the panorama type, the secretiveness of the transmission, characterized by the probability p_o, can be evaluated in the following way.

We will assume that the duration of a single transmission of a signal of the reconnoitered radio apparatus is negligibly small in comparison with the period T_r of operation of the radio receiver and that during the time T_r a signal is transmitted not more than once.

Then the process of detection of the operation of the radio apparatus and the creation of the radio interference to affect it can be considered as a random event and the probability $p_{o.1}$ of determination of a single signal transmission will be equal to

$$p_{o.1} \approx \frac{\Delta f_{rec}}{f_r},$$

where Δf_{rec} and f_r are the width of the passband of the intermediate frequency amplifier of the reconnaissance receiver and the range of frequencies scanned by this receiver, respectively.

The detection of different signal transmissions is accomplished independently. Therefore, in the transmission of N_s signals during the time of rocket guidance for the probability p_o of detection of at least one signal, which is

equivalent to detection of the operation of the reconnoitered radio apparatus, we will have

$$p_o = 1 - \left(1 - \frac{\Delta f_{rec}}{f_r}\right)^{N_s}.$$

Hence, when $p_{o.1} \ll 1$, which usually is the case, we find

$$p_o \approx N_s \frac{\Delta f_{rec}}{f_r}.$$

The derived expression shows that when the condition $\frac{\Delta f_{rec}}{f_r} \ll 1$, the /614 probability of timely creation of interference of the suppressed radio apparatus can be insignificant if N_s is small. The value p_o becomes still smaller when the reconnaissance receiver is used for making a search in direction as well as frequency.

An increase of the secretiveness of transmission of signals in radio control systems is attained also by the integrated use of the methods described above.

An increase of the noise immunity of radio control systems is ensured by the adoption of measures facilitating the undistorted transmission of signals through the receiver when there is interference. In a general case, all possible measures are divided into two groups:

(1) measures ensuring an increase of the signal-to-noise ratio at the inputs of the receivers;

(2) measures facilitating the transmission of a signal and making difficult the transmission of interference through different elements of the receiver and the control system as a whole.

For practical purposes, an increase of the signal-to-noise ratio is related to an increase of the power of the transmitter and the coefficient of directional effect of the antennas and also to a decrease of the reflecting surface of the rocket, etc.

The second group of measures provides for the selection of the most modern methods of modulation, use of different selection methods and decrease of the quantity of information transmitted by radio due to the use of additional non-electronic pickups.

At the same time, it must be remembered that the modulation methods also should be selected taking into account the functions which are performed by the considered radio link.

For example, one of the rational methods for transmission of a reference signal in beam-riding control systems is the use of pulse-frequency modulation. Pulse-amplitude modulation is unsuitable for this purpose.

The selection of the modulation method is influenced considerably also by the conditions of tactical use of the rocket, the most probable type of artificial interference, etc.

Since it is impossible to avoid completely the effect of effective artificial interference, the modulation should be such that the influence of interference does not cause a sharp deterioration of the quality of the guidance process and a disruption of the operation of the control system, which, as already mentioned, can be manifested in the improper setting of the control surfaces of the rocket.

The passage of interference into the output stages of the receivers is made difficult by the use of selection of high-frequency signals, usually /615 called primary selection. Frequency, time, amplitude and other types of primary selection are known. Such selection is based on the use of various differences, known in advance, between the parameters of the effective high-frequency signals and the interference.

Continuous interference and the signal can differ from one another in mean intensity, width and the makeup of the spectrum of oscillations, time of presence at the input of the radio receiver, polarization of radio waves, etc. In the case of a pulse regime of operation, there are additional criteria--duration and shape of the pulses and also the repetition rate.

Usually, primary selection does not require a special change of the makeup of the modulated signal, and is ensured by the appropriate selection of the circuitry and the parameters of the radio receiver.

Frequency primary selection is obtained as a result of the maximum possible narrowing of the passband of the radio receiver input, and is an extremely effective measure for overcoming wide-band and especially noise interference. The effect of frequency selection essentially involves a decrease of the intensity of the interference passing through to the output of the radio receiver. In actual practice, the possibilities of frequency selection are limited by the frequency instability of the radio transmitter generator and the receiver heterodyne.

Time primary selection is based on the fact that the durations and times of appearance of the received pulse signals are known. The use of duration selectors ensures the transmission of signals, the duration of whose effect falls in limits stipulated in advance. At the same time, this method has a shortcoming, namely, that some of the useful signals do not pass through due to

change by interference of their duration in inadmissible limits. A knowledge of the times of appearance of the received pulses makes it possible to cut off the radio receiver at the time of a pause, which can lead to an appreciable decrease of the number of spurious signals forming at the radio receiver output.

Separation of the useful and interfering signals, based on control of the difference of their amplitudes, usually is called primary amplitude selection. The filtering out of interference pulses of a small amplitude is accomplished most easily. A "bottom" limiter is sufficient for this purpose. The response threshold of such a limiter can be either constant or variable. The necessary change of the limitation threshold usually is ensured by automatic volume control systems.

Selectors also are known which ensure exclusion of transmission of interference pulses with an amplitude exceeding the amplitude of the useful signal.

In addition to primary selection, secondary selection also is used: the latter is based on control of the parameters additionally imposed on the transmitted signal during its coding at the transmitting end. The application of the principles of secondary selection is impossible without an increase of /616 the energy of the radiated signals. There is a very great number of secondary selection methods. However, the most widely used methods are code selection and repetition of transmission of communications, the principle of signal accumulation, a knowledge of the frequency spectrum of the received signals and correction codes.

The code selection method, used widely in different electronic apparatus, makes it possible to decrease considerably the number of interference pulses passing to the output of the actuating circuits of the receiver. We recall that in code selection, communications are transmitted by use of timing codes consisting of several pulses with intervals between them which are known in advance.

Duplication (repetition) of signals is of a time, frequency or code type. The essence of the time type is that the same transmitted signal is repeated several times. Frequently, it is desirable to have repetition with acknowledgement, in which the repetition continues until the receiver gives a signal (acknowledgement) confirming the receipt of the transmitted communication. Time repetition should be used in those cases when it is necessary to increase the probability of transmission of the transmitted information (for example, a single command) and to decrease the distortion of the output signal of the receiver by averaging of all the received communications.

The probability of the transmission p_{tr} of a communication in the case of N_∂-multiple repetition can be determined on the basis of the following expression

$$p_{tr} = 1 - (1 - p_{is})^{N_\partial}, \qquad (11.9.1)$$

where p_{is} is the probability of the transmission of an individual signal in the absence of repetition.

Formula (11.9.1) is derived easily if it is remembered that $(1 - p_{is})^{N_\partial}$ is the probability that the transmitted signal will not be transmitted in the case of N_∂- multiple repetition. Since $p_{is} < 1$, with an increase of N_∂, the value p_{tr} increases.

It should be noted that the problem of increasing the probability of transmission of a single command by the repetition method is solved without any additional complication of the receiver. The only thing which is required in this case is an appropriate tuning of the apparatus producing the signal for the actuating mechanism.

The principle of accumulation essentially involves the design of an apparatus by means of which interference is stored by energy and useful signals by voltage. This method for increasing noise immunity is particularly suitable for radar sets.

In the case of frequency and code duplication, the same communication is transmitted simultaneously at several frequencies or by use of several timing codes.

By knowing the spectral composition of the signals produced by the radio transmitter, it is possible to create an optimal filter ensuring a maximum signal-to-noise ratio at its output. Such a filter usually is extremely effective for overcoming fluctuation noise. /617

For example, if periodically repeated pulses are used, their reproduction, with insignificant distortions, does not require use of a filter with a passband equal to approximately $\Delta F_f = \frac{1\text{-}3}{\tau_p}$, where τ_p is the duration of the arriving pulses. These pulses will be reproduced by means of a series of n_f narrow-band filters which transmit only components with the frequencies F_i, $2F_i$, ..., $n_f F_i$, where F_i is the pulse repetition rate. In this case, the number n_f should be selected on the basis of the following relation

$$n_f = \frac{1 - 3}{F_i \tau_p} = \frac{\Delta F_f}{F_i}. \qquad (11.9.2)$$

Such a series of n_f filters is called a comb filter. The use of a comb filter makes it possible to decrease the intensity of interference at the output because some of the components of the interference, having frequencies outside the band ΔF_i of each of the filters, are not transmitted. It can be shown easily that the ratio of the intensity of the fluctuation interference p_{nc} at the output of a comb filter to the intensity of this same interference p_{no} at the output of an ordinary filter with the transmission band ΔF_f is equal to

$$\frac{p_{nc}}{p_{no}} = \frac{n\Delta F_i}{\Delta F_f}.$$

Taking expression (11.9.2) into account, we obtain

$$\frac{p_{nc}}{p_{no}} = \frac{\Delta F_i}{F_i}.$$

It therefore follows that a decrease of the intensity of interference by use of a comb filter is determined by the ratio of the passband ΔF_i of a single filter of the series n_f to the pulse repetition rate F_i. For example, if F_i = 1000 cps and the transmission bands for all the components of the comb filter are identical and equal to 100 cps, $p_{nc}/p_{no} = 10$.

The use of comb filters also is possible when there are modulated pulse control signals. However, in this case the gain in noise immunity is decreased somewhat.

In apparatus based on use of pulse-code modulation, noise immunity can be increased by use of correction codes. As is well known, these can be divided into detecting and correcting codes. Detecting codes make it possible to /618 detect errors in the received communications and correcting codes have the property not only of detecting errors, but also their correction.

An increase of the noise immunity of the control system to a considerable degree can be facilitated by combination of electronic and nonelectronic devices. The fact is that a number of parameters (such as the range between the rocket and the control point) can be produced with a sufficiently high degree of accuracy by the programming mechanism. As a result, an electronic range finder, connected to such a time mechanism, should perform only correction of the latter. However, the correction problem can be solved successfully

by use of a servosystem with a smaller velocity transfer constant, which is equivalent to a decrease of the range finder passband.

By approximately such an interrelationship between the electronic and non-electronic instruments used in measuring different coordinates, it is possible to obtain a complex system which has greater noise immunity than an ordinary electronic apparatus.

We note, in conclusion, that when there is radio interference, the quality of rocket guidance is influenced considerably by the principle of operation of the radio apparatus used and satisfaction of those requirements which were mentioned in the discussion of coordinators and command control radio links.

CHAPTER 12. RADIO FUSES

12.1. Principles of Design and Principal Types of Radio Fuses

The probability of a direct hit of radio-controlled rockets intended /619
for the damage of small targets, especially when the latter are moving at a high velocity, is for all practical purposes close to zero. As a result, it is necessary to automatically detonate the warhead of the rocket when it enters the zone of effective damage of the target. In some cases, the solution of this problem is based on use of radio fuses which are radio robot systems which produce an individual command for excitation of processes of ignition of the explosive.

The principles of design of radio fuses and the requirements imposed on them are based on the basic ideas and problems of control of a detonation, which in turn are determined by the character of the effect of the warhead.

As is well known, for the detonation of a warhead at the time when the maximum effect is ensured, it is most important to determine the relative position of the target and rocket, and then cause the detonation of the warhead in such a way that the maximum quantity of the damaging components will be directed to destruction of the most vulnerable parts of the target.

Under real conditions, depending on the type of warhead, the functions performed by the radio fuses to some extent can be modified. For example, if the rocket is supplied with an isotropic warhead, the radio fuse should form a command at the time when the rocket is situated at a given or minimum distance from the target. When an anisotropic warhead is used, it should be detonated when the vector of the relative velocity of propagation of the damaging components coincides with the direction of the rocket-target line. /620
This means that the apparatus of the radio fuse for detonation of the anisotropic warhead must create a detonation command taking into account not only the distance between the rocket and the target, but also the character of the relative approach of these objects.

From the point of view of the use of the circumstances under which the target is damaged with maximum probability, a radio fuse seeming continues the process of rocket guidance without exerting an influence on its control components.

It now is possible to distinguish two principal groups of radio fuses (ref. 4). The first group includes radio fuses operating on the basis of signals received from the target to be damaged. The radio fuses of the second group constitute command control systems such as are used, for example, for

transition of a winged rocket into a dive or the cutoff of the engine in a ballistic rocket. However, the coordinator of such a radio fuse usually should measure insignificant distances with very small errors. In addition, in some cases it also must determine the direction of the velocity vector of approach of the rocket to the target. The single command radio links discussed in chapter 7 can be used for transmission and reception of commands.

The most favorable conditions for the use of radio fuses of the second group are those cases when the warheads are isotropic or close to isotropic. This can be attributed to the considerable technical difficulties of sufficiently precise determination of the character of motion of the rocket and target when there are small distances between them, which usually must be done when an anisotropic warhead is used.

The principle of operation of radio fuses of the first group can be understood easily if the principles of design of electronic homing systems are recalled. The difference between radio fuses of the first group and homing systems in essence involves only the purpose of the produced commands. At the same time it should be noted that the radio fuses used for detonation of a warhead of the isotropic type do not determine the angular coordinates of the target in relation to the velocity vector of the longitudinal axis of the rocket.

Like homing systems, radio fuses of the first group can be passive, semiactive and active. An active radio fuse contains a radio transmitter scanning the target to be damaged and a receiver reacting to the reflected signals. In semiactive radio fuses, there is no transmitter and the target is scanned by an outside source situated away from the rocket. The operation of a passive fuse is based on the reception of radio signals produced by apparatus which is situated on the target to be damaged. The use of passive radio fuses is limited by the necessity for preliminary reconnaissance of the parameters of the radio apparatus of the target and the possibility of deactivation of these /621 radio sources during the guidance of the rocket. The principal shortcoming of semiactive radio fuses is in coping with the maneuvering of a rocket-carrying aircraft or vessel during rocket guidance from a moving point and the need for continuous tracking of the target to the time of its annihilation. For the mentioned reasons only active radio fuses are in common use.

Since anisotropic warheads in many cases are more desirable than isotropic warheads, the problem of matching the region of damaging of the target and the region of triggering of the radio fuse is extremely important in the design of radio fuses.

12.2. General Information on the Matching of the Region of Damaging of the Target and the Region of Triggering of the Radio Fuse

The problem of optimal matching of the regions of damaging of the target and the triggering of the radio fuse is complex and is poorly discussed in the literature. For this reason, in this section we will discuss only an approximate approach to the solution of this problem. The matching of the region of damage of the target by an anisotropic warhead and the conditions for

triggering of an active radio fuse essentially involve determination of the direction of the maximum of radiation and reception of the radio fuse antenna and computation of the width of its directional diagram. In addition, it is necessary to take into account the range of triggering of the radio fuse, using as a point of departure the radius of effect of the damaging components of the warhead.

On the basis of quite simple concepts, it can be concluded that the maximum of radiation and reception of the radio fuse should coincide with the direction of the vector of the relative velocity of motion of the maximum quantity of damaging components of the warhead and target, and the configuration of the directional diagram should correspond to the configuration of the region of damage of the target. The latter can be attributed to the fact that the triggering of the radio fuse at great and small ranges to the target, when the maximum and minimum of the damaging components are directed to it, leads to a virtually identical effectiveness of the warhead.

Figure 12.1 is given for familiarization with the approximate method for matching the regions of damaging of the target and triggering of the radio fuse. In this figure, o_r and the $o_r x_1$ axis determine the position of the center of mass of the rocket and its longitudinal axis at some time t, and the angle φ_{de} is the direction of the maximum damaging effect of an anisotropic warhead. We will assume that the zone of damage is a volume obtained by rotating part of the plane bounded by the curve 1 (fig. 12.1a) about the $o_r x_1$ axis. Then the direction β_0 (fig. 12.1b) of the reception maximum of the radio fuse antenna can be found in the following way. In the case of detonation of /622 the warhead of a rocket moving with the relative velocity

$$v_0 = v - v_t, \tag{12.2.1}$$

assume the damaging components begin to move relative to the rocket with the velocity v_{de}. Then the velocity v_{app} of approach to the target will be

$$v_{app} = v_{de} + v_0. \tag{12.2.2}$$

We note that here and in the text which follows, it is assumed that the vector v coincides with the $o_r x_1$ axis. If the vectors v_{de} and v_0 are projected onto the $o_r x_1$ axis and onto the normal to it, we find that

$$\tan \beta_0 = \frac{v_{de} \sin \varphi_{de} + v_0 \sin \alpha_0}{v_{de} \cos \varphi_{de} + v_0 \cos \alpha_0},$$

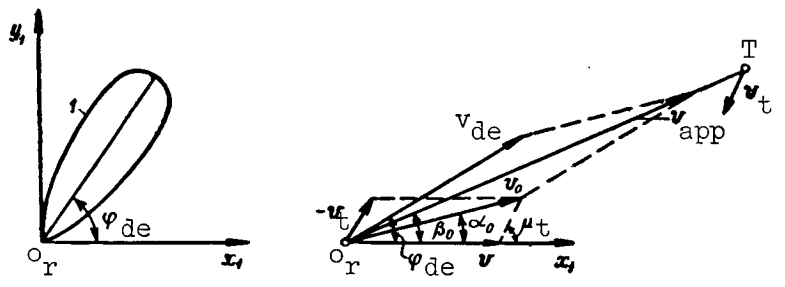

a b

Figure 12.1

where the angles φ_{de} and α_0 are read counterclockwise from the $o_r x_1$ axis.

However, it follows from figure 12.1b that

$$v_0 \cos \alpha_0 = v + v_t \cos \mu_t$$

and

$$v_0 \sin \alpha_0 = v_t \sin \mu_t,$$

where μ_t is the slope of the velocity vector v_t to the $o_r x_1$ axis.

Then we will have

$$\tan \beta_0 = \frac{v_{de} \sin \varphi_{de} + v_t \sin \mu_t}{v_{de} \cos \varphi_{de} + v + v_t \cos \mu_t}. \qquad (12.2.3)$$

Expression (12.2.3) makes it possible to compute the angle β_0 characterizing the direction of the relative motion of the maximum of the damaging effect of the warhead for given values v, v_t and v_{de}. However, under real conditions, the value μ_t can vary in broad limits, whereas the value v_t is approximately known because a particular controlled rocket is intended for damaging targets only of a certain class. If the range of change of μ_t is /623

limited by tactical or some other conditions of rocket use, the possible values of the angle μ_t also can be estimated approximately. Under these conditions, it is easy to determine the maximum and minimum values of the angle β_0, and as a result it is easy to establish the mean value β_0.

In practice, it is found that the variations of β_0 are not great even with a change of μ_t in a very broad range if the velocities v_{de} and v considerably exceed v_t. For example, when $\varphi_{de} = \frac{\pi}{2}$, $v_{de} = 4v_t$ and $v = 2v_t$

$$\tan \beta_0 = \frac{4 + \sin \mu_t}{2 + \cos \mu_t}$$

and for $0 \leq \mu_t \leq 360^\circ$, the angle β_0 changes only from 50.4 to 76.5°. When μ_t falls in the range 150-210°, which corresponds to the case of the launching of a rocket in an overtaking trajectory, the value β_0 changes by only 4.5°.

On the basis of the above, the conclusion can be drawn that the angle of inclination of the maximum of radiation and reception must be selected as the mean arithmetical value of the sum of the maximum and minimum of the values β_0, determined using formula (12.2.3). At the same time, it obviously is necessary to require the creation of a corresponding zone of the damaging effect of the warhead and the width of the directional diagram of the radio fuse antenna.

The problem of the matching of the regions of damage by the warheads and the triggering of the radio fuses of the rockets for damage of surface, water and underwater targets is simplified somewhat in comparison with the effect of the rockets against air targets. This is because it is possible to neglect the velocities of motion of targets situated on the land, on the water and underwater.

The analysis made here is not exhaustive because no allowance was made for many factors exerting an influence on the effectiveness of control of the detonation. Among these factors are the following oscillations of the rocket around its center of mass, changes of the state of the external medium surrounding the target and the rocket, fluctuations of the velocities of the damaging components, etc.

All presently known methods, including pulse methods, theoretically are suitable for determination of the range of the detonation, which in dependence on the type of warhead, can characterize the stipulated or minimum distance between the rocket and the target, and also the value r, dependent on the relative position of the rocket and target. However, the use of pulse methods requires apparatus of rather large size and weight. In addition, in pulse operation, the minimum effective range of the radio fuse is limited by the dead zone. Radio fuses with continuous radiation, therefore, have come into the widest use.

The detonation of a warhead at a stipulated range is accomplished /624 most easily by use of the so-called amplitude method. It is known that the

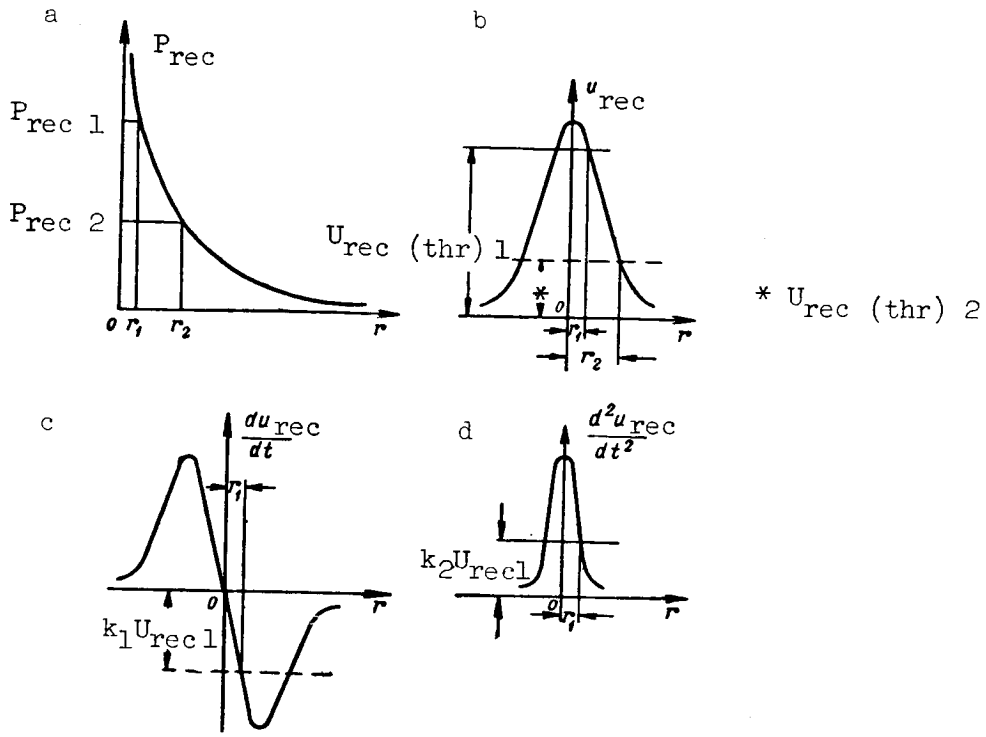

Figure 12.2

power P_{rec} which will reach the input of the receiver of an active radio fuse changes according to the law (fig. 12.2a)

$$P_{rec} = \frac{k}{r^4},$$

where k is the proportionality factor.

The value P_{rec} increases most sharply in the case of small values of distance r between the rocket and the target. This makes it possible to fix, with a high degree of accuracy, the stipulated range of the detonation if the output stage of the radio fuse gives the necessary triggering threshold. At the same time, it must be remembered that the range of the detonation will be dependent on the effective reflecting surface of the target.

The voltage u_{rec} forming at the output of the receiver of a radio fuse with an omnidirectional antenna, depending on the distance r, changes as shown in figure 12.2b, where the negative values r characterize the distance of the rocket from the target. /625

For example, if the radio fuse should form a detonation command when $r = r_1$, when the power $P_{rec\ 1}$ is fed to the input (fig. 12.2a) and a voltage $U_{rec\ 1}$ at the output of the radio receiver is formed, it is necessary to use an amplitude selector with the response threshold $U_{rec\ (thr)\ 1}$. If it is required that the warhead be detonated at the distance $r = r_2$, the response threshold should be set at the level $U_{rec\ (thr)\ 2}$. It should be noted here that, when a radio fuse which is triggered at a given distance is carried aboard the rocket, it is impossible for the rocket to make a direct hit on the target.

The problem of triggering a radio fuse at a stipulated distance from a target can be solved also on the basis of an analysis of the derivative $\frac{du_{rec}}{dt}$ of the output voltage $u_{rec}(t)$ of the receiver of the radio fuse for the time t (r, distance, is a function of the latter). The character of the dependence of $\frac{du_{rec}}{dt}$ is shown in figure 12.2c. This figure shows that by placing at the output of the receiver of the radio fuse a device which is triggered when $\frac{du_{rec\ 1}}{dt} = k_1 U_{rec\ 1}$, where k_1 is a proportionality factor, it is possible to ensure the stipulated distance r_1 of detonation of the warhead.

If we do not take into account the fluctuations of the received signal and radio noise, determination of the detonation range using the signal $\frac{du_{rec}}{dt}$ is accomplished more precisely than on the basis of the voltage u_{rec}. This can be attributed to the considerable steepness of the signal $\frac{du_{rec}}{dt}$ for values r close to zero.

The distance of triggering can be fixed more precisely by using the second time derivative of the voltage u_{rec} (fig. 12.2d).

The detonation command at the required range also can be formed using apparatus similar to radio navigation altimeters with frequency modulation. The principle of change of range in such radio fuses is based on the detection of the difference frequency of direct and reflected frequency-modulated signals. It is found that the mean value of the difference frequency is related unambiguously to the value r.

Determination of the minimum range between the rocket and target is accomplished quite simply using Doppler velocity measuring instruments. It is well known that the Doppler frequency F_D of a signal forming at the output of the

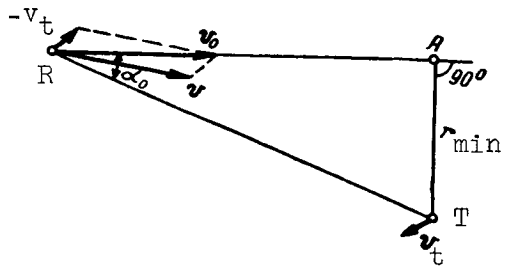

Figure 12.3

receiver of a radio fuse changes directly proportional to the radial velocity v_r of approach of the rocket to the target. This means that in the case of guidance of a rocket R (fig. 12.3), moving with the velocity v, to a target T, moving with the velocity v_t, /626

$$F_D = f_0 \frac{2v_0 \cos \alpha_0}{c} \qquad (12.2.4)$$

where f_0 is the carrier frequency of the radio fuse, v_0 is the value of the relative velocity of approach of the rocket to the target, and c is the speed of light.

In the region of meeting of the rocket with the target, their motion with a sufficiently high accuracy can be considered linear and uniform. Then $v_0 \approx$ const and the frequency F_D is dependent only on the angle α_0. The value α_0 increases with approach of the rocket to the target; at point A, situated at the minimum distance r_{min} from the target, it attains the value $\frac{\pi}{2}$, and then becomes greater than $\frac{\pi}{2}$. As a result, at the output of the radio fuse receiver, when a frequency detector is present, it is possible to obtain a voltage $u_D = k_D F_D$, where k_D is a proportionality factor.

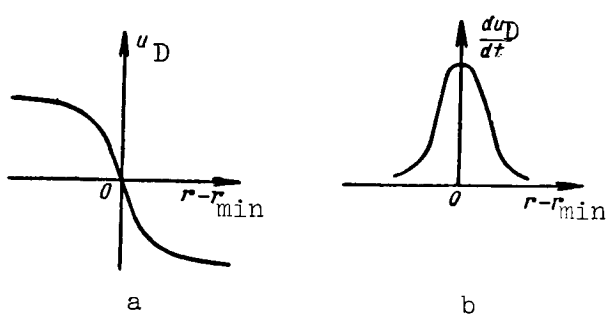

a b

Figure 12.4

The dependence of u_D on $r - r_{min}$ has the form shown in figure 12.4a.

Figure 12.4a shows that the detonation of the warhead at the minimum distance r_{min}, also including the value $r_{min} = 0$, occurs in this case when an output signal with $u_D = 0$ is formed at the output of the radio fuse.

It is easy to see that such a radio fuse must be supplied with an antenna whose reception maximum should be directed along the normal to the trajectory of motion of the rocket. This radio fuse can be applicable when using either isotropic or anisotropic warheads. The charge of anisotropic type should /627 be such that the vector of relative velocity of motion of its damaging elements is approximately perpendicular to the vector v.

A distinguishing feature of the function $u_D = f(r - r_{min})$, shown in figure 12.4a is the relatively slow change of u_D in the case of a considerable value r and the instability of the zero due to the influence of various kinds of fluctuations. The limits of the distances r close to r_{min} are defined more clearly using the derivative $\frac{du_D}{dt}$, shown in figure 12.4b. In this case, the output device of the radio fuse should be triggered at the level of the signal maximum $\frac{du_D}{dt}$. The minimum distance between the rocket and the target also can be determined on the basis of an analysis of the signals $\frac{du_{rec}}{dt}$ and $\frac{d^2u_{rec}}{dt^2}$ (fig. 12.2c, d), since the zero value of the derivative $\frac{du_{rec}}{dt}$ and the maximum value $\frac{d^2u_{rec}}{dt^2}$ will occur not only when $r = 0$, but also when $r = r_{min}$, where $r_{min} \neq 0$.

12.3. Diagrams of Active Radio Fuses

In accordance with the problems to be solved, the general functional diagram of an active radio fuse can be represented as shown in figure 12.5.

The oscillations radiated by the transmitter Tr reach the target to be damaged and are reflected from it. The reflected signals are received by the receiver Rec, linked to the analyzer A. In addition, the analyzer A receives the voltage of the radio transmitter. Comparison of the parameters of the direct and reflected signals in the analyzer makes possible target selection and the forming of a voltage characterizing distance r.

In order for the radio fuse to react with a high reliability to signals of only a single target (target selection), the analyzer includes a filter which transmits a definite range of Doppler frequencies (refs. 4 and 112).

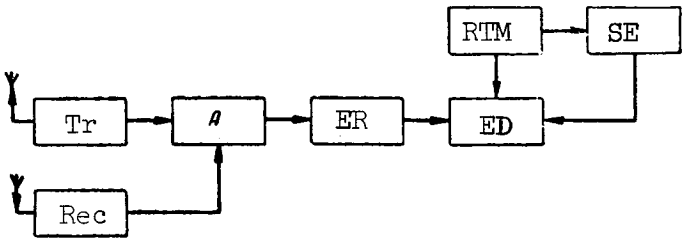

Figure 12.5

The output signal of the analyzer acts on an electronic relay ER having a stipulated response threshold U_{thr}. The value U_{thr}, as already /628

noted, is selected in accordance with the stipulated distance r_{st} of detonation of the warhead.

In a case when the voltage at the output reaches the computed value the electronic relay is triggered and activates the electrical primer of the detonator ED, provided the range triggering mechanism RTM is in a working position. The RTM is a sort of safety fuse which forestalls spontaneous detonation of the radio fuse when it is being prepared for use and in the initial segment of rocket flight.

After the rocket has covered the stipulated distance from the time of launching, the RTM, in response to the programming mechanism which it includes, brings the circuit of the electrical detonator into a working state.

The safety exploder SE, connected to the RTM, is used for detonation of the rocket in the event of an inadmissibly large miss.

Depending on the specific methods for determination of distance r and the angular position of the vector v_0, and also the method of target selection,

there will be in the circuits of radio fuses different antenna and analyzer characteristics and different methods for coupling the receiver to the transmitter. For example, when determining distance to the target from the value of the voltage u_{rec} (fig. 12.2b) forming at the output of the receiver and

target selection on the basis of an analysis of Doppler frequencies, we obtain the functional diagram of the radio fuse shown in figure 12.6.

This fuse, sometimes called a Doppler fuse, includes: a transmitter Tr, operating in a regime of nonattenuating oscillations at the frequency f_0, a

receiver Rec, at whose input arrives the signal reflected from the target upon its entry into the limits of the angle of aperture of the directional diagram of the receiving antenna and an actuating mechanism. The actuating mechanism includes: a mixer Mix, a selective amplifier SA, a detector (rectifier) D,

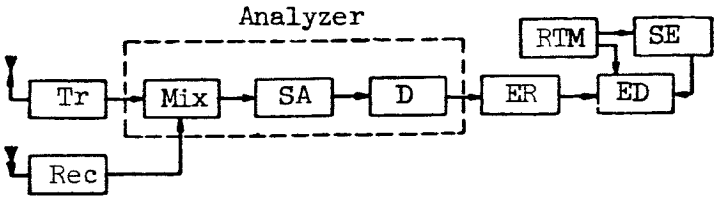

Figure 12.6

an electronic relay ER, an electrical detonator ED, a range triggering mechanism RTM and a safety exploder SE.

At the output of the mixer Mix a voltage is formed which has the frequency F_D and an amplitude which increases with approach of the rocket to the target. The selective amplifier, containing a selective filter, is used for filter- /629 ing out all components of the frequencies which do not characterize the radial velocity of approach of the rocket to the target.

In selecting the passband ΔF_a of the selective amplifier, it is necessary to use as a point of departure the maximum and minimum values of the Doppler frequencies $F_{D\ max}$ and $F_{D\ min}$, which can be formed with different possible aspects of approach of the rocket to the target.

It follows from expression (12.2.4) that

$$F_{D\ max} = 2\frac{v_{0\ max}(\cos\alpha_0)_{max}}{c} f_0,$$

$$F_{D\ min} = 2\frac{v_{0\ min}(\cos\alpha_0)_{min}}{c} f_0.$$

Here $v_{0\ max}$ and $v_{0\ min}$ are the maximum and minimum possible values of the velocities of approach of the rocket to the target; $(\cos\alpha_0)_{max}$ and $(\cos\alpha_0)_{min}$ are the maximum and minimum possible values $\cos\alpha$, dependent on the angles between the vector of relative velocity of approach v_0 and the rocket-target line.

The voltage appearing at the output of the SA has a variable frequency and an increasing amplitude. This voltage is fed to the detector, performing the function of a rectifier.

It should be noted that a detector is not a vital element of the radio fuse because the relay also is capable of correct triggering when it is fed a voltage of variable current. However, in some cases, a detector is used

because the possibility exists of additional filtration of parasitic components, which can lead to erroneous triggering of the radio fuse.

In the considered diagram of a radio fuse, the analyzer includes a mixer, selective amplifier and detector.

If it is necessary that the radio fuse be triggered at a minimum distance from a target, as already mentioned, it is necessary to record the time when the Doppler frequency F_D becomes equal to zero. For this reason, the analyzer includes a frequency detector rather than an amplitude detector. As the frequency detector it is possible for example, to use the frequency bridge mentioned in chapter 5. In addition, a radio fuse of such a type also can be constructed using a frequency detector with a differentiator at its output.

In the study of all the types of radio fuses mentioned here it was assumed that there were a radio transmitter, radio receiver and mixer as separate components. However, for the purpose of weight economy and smaller size, all these can be combined into a single stage. Then, with respect to the functional diagram shown in figure 12.6, under the condition that there is no detector D, it is possible to design the simplified diagram shown in figure 12.7 (ref. 111), where the electrical detonator, range triggering mechanism and safety exploder are not shown. /630

In this fuse, the antenna A transmits and receives radio signals. The generator Gen_1 is based on the Hartley oscillator principle. The signals reflected from the target, received by the antenna A, are mixed in the nonlinear stage Gen_1 with the generated voltage, and as a result a voltage of the add and subtract (Doppler) frequencies f_{add} and F_D is formed, which is fed to the Gen_2 amplifier. The grid circuit has a filter R_1C_1 delaying the components with the frequency f_{add}. The amplified oscillations of Doppler frequency act on the electronic relay.

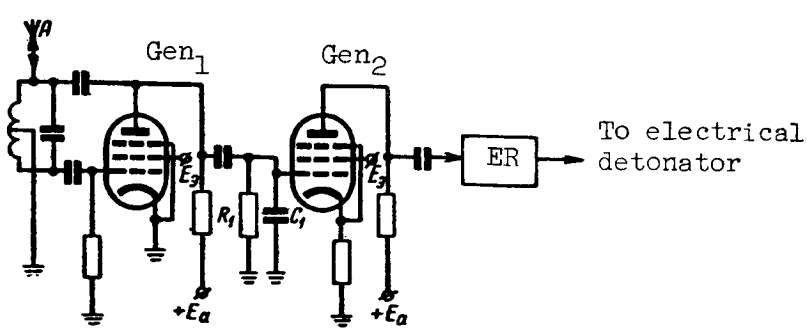

Figure 12.7

Note: $E_э$ not identified in text.

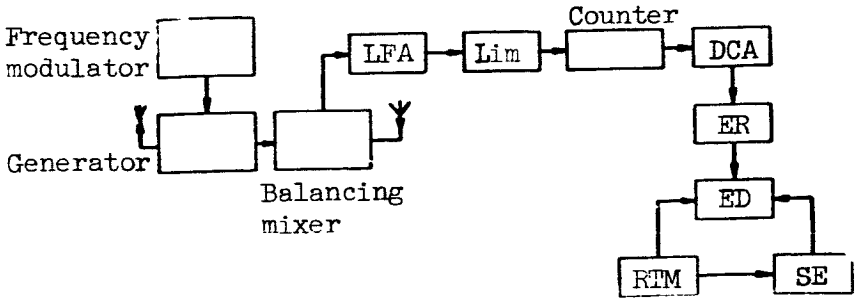

Figure 12.8

It can be seen from the diagram in figure 12.7 that the basic ideas of design of radio fuses reacting to the intensity of the arriving signals and selecting the target on the basis of the velocity of approach can be realized using quite simple technical means.

In the case of determination of the distance between the rocket and target by use of frequency-modulated oscillations, the functional diagram of the radio fuse has the form shown in figure 12.8.

We note that figure 12.8, if the electronic relay is not taken into account, represents a radio navigation range finder (altimeter) with frequency modulation. A detailed analysis of such a range finder is given in most instructional manuals on radio navigation apparatus and especially in the book listed as reference 11. Therefore, here we will present only a qualitative discussion of the transpiring processes. The generator, controlled by a frequency modulator, produces oscillations whose frequency changes periodically on the sawtooth principle. The signals reflected from the target, after some time from the moment of radiation, arrive at the receiving antenna coupled to a balancing mixer, to which is also fed a voltage from the amplifier /631 output.

At the output of the balancing mixer, a voltage is created which represents the beats between the direct and reflected signals. As already mentioned, the mean value of the frequency of these beats is proportional, with a sufficient degree of accuracy, to the delay of the reflected signal and therefore to the distance to the target.

The low-frequency amplifier LFA and the limiter Lim are used for amplification of the low-frequency beats and forming from them pulses of a rigorously determined amplitude. The counter forms a dc voltage whose value changes proportional to the repetition frequency of the input pulses. The signal formed at the output of the counter passes through a dc amplifier DCA and then is fed to an electronic relay ER. When the value of the DCA voltage reaches the response threshold of the relay, the latter feeds a command for detonation of the warhead.

12.4. Characteristics of the Operation of Radio Fuses and General Requirements Imposed on Them

One of the principal characteristics of any radio fuse is the maximum efficiency of its operation, obtained when there is optimal matching of the regions of damage of the target and triggering of the radio fuse. For this reason, great attention must be devoted to matching problems during the designing of radio fuses. In addition, it is necessary to take into account the characteristics of the operation of radio fuses and all the principal requirements imposed on rocket equipment (small weight, size, minimum power consumption, etc.). Also very important is the requirement of a high noise immunity of the radio fuses and the reliability of their operation.

In Doppler radio fuses, the frequency F_D varies in extremely wide limits; its minimum value $F_{D\,min}$ can be close to zero. Under these conditions, at the output of the selective filter, there can be parasitic components of voltage caused by vibrations of the rocket, the microphone effect of the electron tubes, etc. It therefore becomes necessary to make an appropriate selection of the parameters of the radio fuse so that it will not be triggered prematurely. /632

One of the methods for eliminating the influence of low-frequency fluctuations is an increase of the carrier frequency f_0 of the radio fuse and the limitation at the bottom of the minimum value of the frequency F_D transmitted by the selective amplifier. As follows from expression (12.2.4), an increase of f_0 leads to an increase of F_D. At the same time, it must be remembered that the cutoff of components with small values F_D requires detonation of the warhead at a distance exceeding r_{min}.

Another important characteristic of the radio fuse is its separation from the remaining equipment of the rocket by a compartment with a warhead. The placement of the radio fuse in the nosecone of the rocket leads to need for developing autonomous sources of electrical energy. This can be done either with batteries or turbogenerators, brought into motion by the oncoming air flow. In order for the battery sources of current to be stored in warehouses for a long period, the electrolyte usually is placed in a separate cylinder which is connected automatically to electrodes only after launching of the rocket.

In order to decrease the size of the radio fuse, it is of considerable importance to use one receiving-transmitting antenna and small electronic instruments and radio parts.

As an illustration of the comments made here concerning the construction of radio fuses, figure 12.9 shows the design of the British V-T radio fuse. A characteristic of this fuse is that the radio transmitter begins to radiate

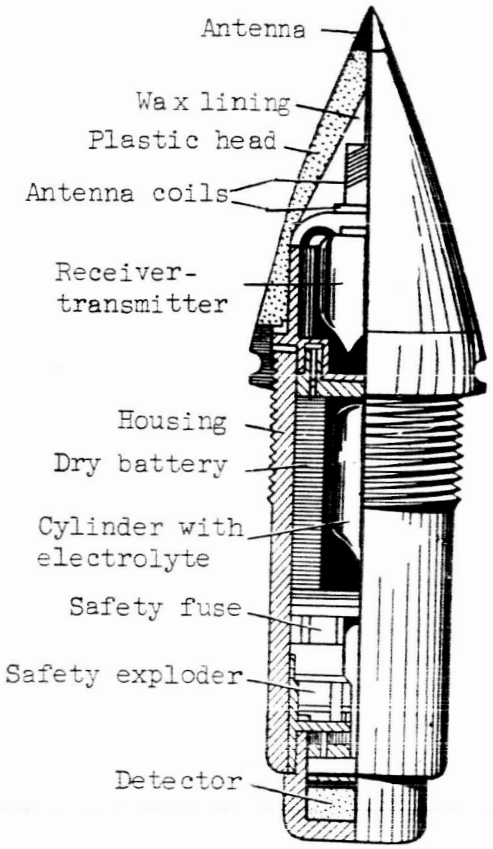

Figure 12.9

only some time after the launching of the rocket, when the battery and the elements of the radio apparatus are ready for operation.

It is necessary to ensure a high noise immunity of radio fuses because the radio interference created by the operating electronic apparatus used for other purposes and created by the enemy can lead to a premature detonation of the warhead and, thereby, make the launching of controlled rockets ineffective. The use of measures directed toward ensuring the continued operability, when there is both passive and active artificial interference, meets with a number of difficulties associated with the rigorous requirements on small size and weight of radio fuses. However, despite this, by the use of elements solving a complex of problems, it is possible to attain considerable results with respect to the creation of noiseproof devices for the detonation of warheads. /633

For example, by the selection of a carrier frequency and the parameters of the filter in the selective amplifier of a Doppler radio fuse, it is possible to attain an appreciable decrease of the influence of passive interference. At the same time, an appropriate selection of the time of transition of the range resetting mechanism into a working state ensures a decrease in the

possibility of false formation of a detonation command under the influence of both passive and active radio interference. The same purpose is served by the cutting in of the radio transmitter only when the rocket is in the immediate vicinity of the point where the radio fuse is to be triggered.

In addition, for increasing the noise immunity of the radio fuse, it is possible to use a number of those measures which are used in the design of electronic apparatus for other purposes. It should be emphasized here that more rigorous requirements are imposed on the noise immunity of radio fuses than on other apparatus used in guidance of a rocket. This is because the interference causing premature explosion of the warhead means an end to the very purpose for which the rocket was launched, and at the same time the influence of interference on the radio control system in some cases only causes some worsening of its characteristics.

For example, the influence of interference on a radio control system over a short period of time may exert an insignificant influence on the accuracy of rocket guidance. The effect of the same interference on a radio fuse with the range resetting mechanism in a ready state can cause the destruction of the rocket.

The need for ensuring a high reliability of the operation of radio fuses is completely obvious and requires no further explanation. It is important to use a minimum number of reliably operating parts in meeting this requirement. In addition, in many cases, it is desirable to apply the principle of duplication (stand-by system) (ref. 8), which in application to the device under discussion means the use of several fuses of the same or different types.

Duplication in parallel or in series, or a mixed type of duplication /634 is possible. In the case of duplication in parallel, the detonation occurs at the time of triggering of at least one fuse. If duplication in series is used, annihilation of the target is possible only with the triggering of all the fuses.

In mixed duplication one part of the fuses is connected in parallel and the other in series.

For clarification of the most desirable method of duplication we will consider the problem of the probabilities of normal, late and early detonations of the warhead, and also the probability of nondetonation as a result of nontriggering of the fuses. The case when three identical fuses are used will be considered first. We will assume here that normal, early and late detonations characterize normal, early and late triggering of fuses, proceeding on the requirement that the target be damaged.

Assume that the probabilities of normal, early and late detonations and also the probability of nondetonation for each of the fuses is identical and equal to p_1, p_2, p_3, and p_4, respectively. Then, taking into account the nondependence of triggering of individual fuses, it can be found (ref. 8) that in the case of duplication in parallel

$$p_n > 1 - 3p_2 - p_4^3 - p_3^3 - 3p_3^2 p_4 - 3p_3 p_4^2,$$
$$p_e < 3p_2,$$
$$p_1 = p_3^3\left(1 + \frac{3p_4}{p_3} + \frac{3p_4^2}{p_3^2}\right)$$
$$p_{nd} = p_4^3.$$

Here p_n is the probability of normal triggering of at least one of the three fuses, p_e and p_1 are the probabilities of early and late detonations of the warhead, and p_{nd} is the probability of nondetonation of the warhead.

Analysis of these expressions shows that duplication in parallel leads to a decrease of the probability of nondetonations, a decrease of the probability of late detonations and an increase of the number of premature detonations. At the same time, the probability p_n, in dependence on the values p_2, p_3 and p_4, can be decreased or increased in comparison with p_1, and also remain equal to p_1.

In the case of duplication in series, we will have

$$p_n > 1 - p_2^3 - 3p_4 - 3p_3,$$
$$p_e = p_2^3,$$
$$p_1 < 3p_3,$$
$$p_{nd} < 3p_4.$$

In this case, there is a decrease of the number of premature detonations, /635 but there is an increase of the number of nondetonating rockets, late detonations and normal detonations.

As a result of mixed duplication

$$p_n > 1 - 3p_2^2 - 3p_4^2 - 3p_3^2 - 6p_3 p_4,$$
$$p_e < 3p_2^2,$$
$$p_1 < 3p_3^2 + 6p_3 p_4,$$
$$p_{nd} < 3p_4^2.$$

It follows from these relations that mixed duplication can give better results than duplication in parallel or in series.

Proceeding in the same way in an analysis of the effect of duplication by four, five or more fuses, it is possible to draw the following general conclusions:

(1) it is better to use an odd number of fuses than an even number;

(2) mixed duplication ensures the maximum probability of damage of a target;

(3) mixed duplication should be organized in such a way that there will be approximately an identical number of connections in series and in parallel.

The consideration of the problem of increasing the reliability of the duplication method made here has not touched upon the accuracy of adherence to the detonation distance, size of the warhead, etc. Under real conditions, when developing radio fuses, it is necessary to take into account all the problems involved in the effectiveness of damaging of the target.

We note in conclusion that in the selection and computation of a number of parameters of radio fuses, it is necessary to bear in mind the principal characteristics of the system used in guiding the rocket to the target.

REFERENCES

1. Gutkin, L. S. Principles of Radio Control of Pilotless Objects (Printsipy radioupravleniya bespilotnymi ob"yektami). Izd-vo "Sovetskoye Radio", 1959.

2. Tipugin, V. N. and Veytsel', V. A. Radio Control (Radioupravleniye). Izd-vo "Sovetskoye Radio", 1962.

3. Lokk, A. S. Control of Shells (Upravleniye snaryadami). State Technical and Theoretical Press (Gostekhizdat), 1957.

4. Myuller, F. Telemetric Control (Teleupravleniye), Foreign Literature Press (I. L.), 1957.

5. Fridlender, G. O. and Kozlov, M. S. Aviation Gyroscopic Instruments (Aviatsionnyye giroskopicheskiye pribory). State Publishing House of the Defense Industry (Oborongiz), 1961.

6. Seleznev, V. P. Navigation Apparatus (Navigatsionnyye ustroystva). Oborongiz, 1961.

7. Bodner, V. A. and Kozlov, M. S. Stabilization of Aircraft and Automatic Pilots (Stabilizatsiya letatel'nykh apparatov i avtopiloty). Oborongiz, 1961.

8. Merill, G., Goldberg, G. and Helmholtz, R. Investigation of Operations. Warheads. Missile Launching (Issledovaniye operatsiy. Boyevyye chasti. Pusk snaryadov). I. L., 1959.

9. Besserer, K. U. Engineering Handbook on Guided Missiles (Inzhenernyy spravochnik po upravlyayemym snaryadam). Military Publishing House (Voyenizdat), 1962.

10. Feodos'yev, V. I. and Sinyarev, G. B. Introduction to Rocket Technology (Vvedeniye v raketnuyu tekhniku). Second edition. Oborongiz, 1960.

11. Astaf'yev, G. P., Shebshayevich, V. S. and Yurkov, Yu. A. Radioelectronic Navigation for Aircraft (Radiotekhnicheskiye sredstva navigatsii letatel'nykh apparatov). Izd-vo "Sovetskoye Radio", 1962.

12. Kel'zon, A. S. Dynamic Problems of Cybernetics (Dinamicheskiye zadachi kibernetiki). State All-Union Publishing House of the Shipbuilding Industry (Sudpromgiz), 1959.

13. Marisov, V. I. and Kucherov, I. K. Controlled Missiles (Upravlyayemyye snaryady). Voyenizdat, 1959.

14. Krysenko, G. D. Control of Jet Missiles (Upravleniye reaktivnymi snaryadami). Voyenizdat, 1960.

15. Peresada, S. A. Anti-Aircraft Guided Missiles (Zenitnyye upravlyayemyye rakety). Voyenizdat, 1961.

16. Barsukov, F. I. Radiotelemechanics (Radiotelemekhanika). State Power Engineering Publishing House (Gosenergoizdat), 1962.

17. Missile Armament of the Capitalist Countries. Review 1960-1962. ("Raketnoye oruzhiye kapitalisticheskikh stran". Obzor 1960-1962). Voyenizdat, 1962.

18. Bert, Ye. Theoretical Principles of Missile Control Systems (Teoreticheskiye printsipy sistem upravleniya snaryadov). Voprosy Raketnoy Tekhniki (V. R. T.), No. 3, 1960.

19. Tzyan, G., Adamson, T. and Knut, Ye. Automatic Long-Range Rocket Control (Avtomaticheskoye upravleniye raketami dal'nego deystviya). V. R. T., No. 13, 1953.

20. Manovtsev, A. P. and Ravin, G. I. Principles of Teleguidance and Telecontrol (Osnovy teleupravleniya i telekontrolya). Gosenergoizdat, 1959.

21. Radio Control of Spaceships (Radioupravleniye kosmicheskimi korablyami). Zarubezhnaya Radioelektronika (Z. R.), No. 12, 1959.

22. Guided Missiles (Upravlyayemyye snaryady). Translated from English, edited by I. Ye. Petrov. I. L., 1960.

23. Nikolayev, M. N. Missile against Missile (Snaryad protiv snaryada). Voyenizdat, 1960.

24. Guidance of Missiles by Radar Stations (Upravleniye snaryadami pri pomoshchi radiolokatsionnykh stantsiy). V. R. T., No. 4, 1956.

25. Modern Techniques of Control of Jet-Propelled Missiles (Sovremennaya tekhnika upravleniya reaktivnymi snaryadami). V. R. T., No. 5, 1955.

26. Gibson. Some Principles of Systems of Control of Jet-Propelled Missiles (Nekotoryye printsipy sistem upravleniya reaktivnymi snaryadami). V. R. T., No. 6, 1956.

27. Romik and Ran'ye. Problems in Developing Systems for Guidance of Guided Missiles (Problemy razrabotki sistem navedeniya upravlyayemykh snaryadov). V. R. T., No. 5, 1955.

28. Ril. Requirements Imposed on Missile Control Systems. Stabilization and Guidance (Trebovaniya k sistemam upravleniya snaryadami. Stabilizatsiya i navedeniye). V. R. T., No. 4, 1958.

29. Gardner. Guidance of Jet-Propelled Weapons and Related Problems (Upravleniye reaktivnym oruzhiyem i smezhnyye voprosy). V. R. T., No. 3, 1957.

30. Krasovskiy, A. A. and Pospelov, G. S. Principles of Automation and Technical Cybernetics (Osnovy avtomatiki i tekhnicheskoy kibernetiki). Gosenergoizdat, 1962.

31. Solodovnikov, V. V. Statistical Dynamics of Linear Automatic Control Systems (Statisticheskaya dinamika lineynykh sistem avtomaticheskogo upravleniya). State Publishing House for Physical and Mathematical Literature (Fizmatgiz), 1960.

32. Pugachev, V. S. Theory of Random Functions and Its Application to Automatic Control Problems (Teoriya sluchaynykh funktsiy i yeye primeneniye k zadacham avtomaticheskogo upravleniya). Third edition. Fizmatgiz, 1962.

33. Levin, B. R. Theory of Random Processes and Its Application in Radioengineering (Teoriya sluchaynykh protsessov i yeye primeneniye v radiotekhnike). Second edition. Izd-vo "Sovetskoye Radio", 1960.

34. Bunimovich, V. I. Fluctuating Processes in Radio Receivers (Flyuktuatsionnyye protsessy v radio priyemnykh ustroystvakh). Izd-vo "Sovetskoye Radio", 1951.

35. Fel'dbaum, A. A. Automatic Control Electrical Systems (Elektricheskiye sistemy avtomaticheskogo regulirovaniya). Oborongiz, 1954.

36. Krivitskiy, B. Kh. Automatic Systems of Radioengineering Apparatus (Avtomaticheskiye sistemy radiotekhnicheskikh ustroystv). Gosenergoizdat, 1962.

37. Lening, J. K. and Bettin, R. G. Random Processes in Automatic Control Problems (Sluchaynyye protsessy v zadachakh avtomaticheskogo upravleniya). I. L., 1958.

38. Chien Hsüeh-sen. Technical Cybernetics (Tekhnicheskaya kibernetika). I. L., 1956

39. Bellman, R., Gliksberg, I. and Gross, O. Some Problems in the Mathematical Theory of Control Processes (Nekotoryye voprosy matematicheskoy teorii protsessov upravleniya). I. L., 1962.

40. Venttsel', Ye. S. Theory of Probabilities (Teoriya veroyatnostey). Second edition. Fizmatgiz, 1962.

41. Rods, D. R. Introduction to Monopulse Radar (Vvedeniye v monoimpul'snuyu radiolokatsiyu). Izd-vo "Sovetskoye Radio", 1960.

42. Khelgren, Problems in the Theory of Monopulse Radar (Vorposy teori monoimpul'snoy radiolokatsii). Z. R., No. 12, 1962; No. 1, 1963.

43. Batler, I. L. A Centimeter-Wave Antenna with Conical Beam Oscillation Using a Three-Vibrator Exciter (Antenna santimetrovykh voln s koniches-kim kachaniyem lucha, ispol'zuyushchaya trekhvibratornyy obluchatel'). Z. R., No. 12, 1959.

44. Shnitkin, Kh. Antennas with Electrical Beam Control (Antenny s elektricheskim upravleniyem luchom). Z. R., No. 2, 1962.

45. Sivers, A. P. Radar Receivers (Radiolokatsionnyye priyemniki). Izd-vo "Sovetskoye Radio", 1953.

46. Bardzhes, I. S. Future of Radar (Budushcheye radiolokatsii). Z. R., No. 12, 1961.

47. Krasovskiy, A. A. On the Theory of Two-Channel Tracking Systems with a Relay Element in the ac Current Circuit (K teorii dvukhkanal'nykh sledyashchikh sistem s releynym elementom v tsepi peremennogo toka). Avtomatika i Telemekhanika, Vol. 21, No. 9, 1960.

48. N'yuton, Dzh. K. et al. Theory of Linear Tracking Systems (Teoriya lineynykh sledyashchikh sistem). Fizmatgiz, 1961.

49. Sausvort, J. E. Principles and Application of Waveguide Transmission (Printsipy i primeneniya volnovodnoy peredachi). Izd-vo "Sovetskoye Radio", 1955.

50. Vinitskiy, A. S. Outlines of the Principles of Radar with Continuous Radiation of Radio Waves (Ocherk osnov radiolokatsii pri nepreryvnom izluchenii radiovoln). Izd-vo "Sovetskoye Radio", 1961.

51. Zhilesin, I. F. et al. Development and Use of Coherent Radar Systems (Razvitiye i primeneniye kogerentnykh radiolokatsionnykh sistem). Z. R., No. 3, 1962.

52. Ageyev, D. V. and Rodionov, Ya. G. Frequency-Modulated Radio Reception with Tracking Adjustment (Chastotno-modulirovannyy radiopriyem so sledyashchey nastroykoy). Gosenergoizdat, 1958.

53. Sommer, G. An Improved Radar Station Operating by the Simultaneous Phase Comparison Method (Usovershenstvovannaya radiolokatsionnaya stantsiya, rabotayushchaya po metodu odnovremennogo sravneniya faz). V. R. T., No. 1 (37), 1957.

54. Krasovskiy, A. A. On Two-Channel Automatic Control Systems with Antisymmetrical Couplings (O dvukhkanal'nykh sistemakh avtomaticheskogo

regulirovaniya s antisimmetrichnymi svyazyami). Avtomatika i Telemekhanika, Vol. 18, No. 2, 1957.

55. Principles of Automatic Control (Osnovy avtomaticheskogo regulirovaniya). Vols. 1 and 2. Edited by V. V. Solodovnikov. State Scientific and Technical Publishing House of Literature on Machinery (Mashgiz), 1954.

56. Theory of Tracking Systems (Teoriya sledyashchikh sistem). Translated from English. Edited by Ya. Z. Tsypkin. I. L., 1951.

57. Fal'kovich, S. Ye. Reception of Radar Signals on a Background of Fluctuating Noise (Priyem radiolokatsionnykh signalov na fone flyuktuatsionnykh pomekh). Izd-vo "Sovetskoye Radio", 1961.

58. Krasovkiy, A. A. Two-Channel Tracking Systems with Antisymmetrical Couplings Used under the Influence of Random Effects (Dvukhkanal'nyye sledyashchiye sistemy s antisimmetrichnymi svyazyami pri nalichii sluchaynykh vozdeystviy). Avtomatika i Telemekhanika, Vol. 22, No. 2, 1961.

59. Shchukin, A. N. Dynamic and Fluctuating Errors of Guided Objects (Dinamicheskiye i flyuktuatsionnyye oshibki upravlyayemykh ob"yektov). Izd-vo "Sovetskoye Radio", 1961.

60. Shapiro, I. I Computation of the Trajectories of Ballistic Missiles Using Radar Station Data (Raschet trayektoriy ballisticheskikh snaryadov po dannym radiolokatsionnykh stantsiy). I. L., 1961.

61. Perov, V. P. Statistical Synthesis of Pulses Systems (Statisticheskiy sintez impul'snykh sistem). Izd-vo "Sovetskoye Radio", 1959.

62. --- Design of Radar Tracking Systems with Allowance for Random Effects (Raschet radiolokatsionnykh sledyashchikh sistem s uchetom sluchaynykh vozdeystviy). Sudpromgiz, 1961.

63. Gitis, E. I. Information Converters for Electronic Digital Computers (Preobrazovateli informatsii dlya elektronnykh tsifrovykh vychislitel'nykh ustroystv). Gosenergoizdat, 1961.

64. Kogan, B. Ya. Analog Computers and Their Use for Study of Automatic Control Systems (Elektronnyye modeliruyushchiye ustroystva i ikh primeneniye dlya issledovaniya sistem avtomaticheskogo regulirovaniya). Fizmatgiz, 1959.

65. Kitov, A. I. Electronic Digital Computers (Elektronnyye tsifrovyye mashiny). Izd-vo "Sovetskoye Radio", 1956.

66. Kotel'nikov, V. A. Theory of Potential Noise Immunity (Teoriya potentsial'noy pomekhoustoychivosti). Gosenergoizdat, 1956.

67. Kharkevich, A. A. Outlines of the General Theory of Communications (Ocherki obshchey teorii svyazi). Goztekhizdat, 1955.

68. Nichols, M. K. and Raukh, L. L. Radiotelemetry (Radiotelemetriya). I. L., 1958.

69. Remote Control and Measurement (Upravleniye i izmereniye na rasstoyanii). I. L., 1957.

70. Methods of Transmission of Measurements by Radio from Rockets and Missiles (Tekhnika peredachi izmereniy po radio s raket i snaryadov). Collection of translations. Edited by V. K. Morozov, V. G. Polya and T. A. Shmakov. Voyenizdat, 1959.

71. Barsukov, F. I. and Maksimov, M. V. Radiotelemetry (Radiotelemetriya). Voyenizdat, 1962.

72. Tepper, M. Radiotelemetry (Radiotelemetriya). Translated from English. Edited by M. V. Maksimov. Voyenizdat, 1961.

73. Smirnov, G. D. and Gorbachev, V. P. Radar Systems with Active Response (Radiolokatsionnyye sistemy s aktivnym otvetom). Voyenizdat, 1962.

74. Sytina, N. V. Autonomous Doppler Radio Navigation Instruments (Avtonomnyye dopplerovskiye radionavigatsionnyye pribory). Izd-vo "Sovetskoye Radio", 1957.

75. Korostelev, A. A. Automatic Coordinate Measurement (Avtomaticheskoye izmereniye koordinat). Voyenizdat, 1961.

76. Pozin, I. V. Noise Immunity of Pulse-Width and Pulse-Time Telemetric Measurement during Strong Fluctuating Interference (Pomekhoustoychivost' shirotno-impul'snogo i vremya-impul'snogo teleizmereniya pri sil'nykh flyuktuatsionnykh pomekhakh). Avtomatika i Telemekhanika, Vol. 20, No. 2, 1959.

77. --- Determination of Noise Immunity of Pulse-Width and Pulse-Time Telemetric Measurement (K opredeleniyu pomekhoustoychivosti shirotno-impul'snogo i vremya-impul'snogo teleizmereniya). Avtomatika i Telemekhanika, Vol. 21, No. 2, 1960.

78. Vasil'yev, A. M. Effect of a Random Voltage on a Delay Relay with Two Stable States of Equilibrium (Vozdeystviye sluchaynogo napryazheniya na zhdushcheye rele s dvumya ustoychivymi sostoyaniyami ravnovesiya). Radiotekhnika, No. 1, 1958.

79. Shastova, G. A. Noise Immunity of the Hemming Code (O pomekhoustoychivosti koda Khemming). Radiotekhnika i Elektronika, No. 1, 1958.

80. Maksimov, M. V. Mathematical Expectation of a Voltage and the Mean Number of Pulses Per Unit Time at the Output of a Coincidence Stage (Matematicheskoye ozhidaniye napryazheniya i sredneye chislo impul'sov v yedinitsu vremeni na vykhode kaskada sovpadeniy). Radiotekhnika, No. 4, 1961.

81. --- Spectral Density of Voltage at the Output of a Coincidence Stage (Spektral'naya plotnost' napryazheniya na vykhode kaskada sovpadeniy). Radiotekhnika, No. 3, 1962.

82. Livshits, A. R. Probability of n-Coincidences (O veroyatnosti n-sovpadeniy). Radiotekhnika i Elektronika, Vol. 2, No. 8, 1957.

83. Tikhonov, V. I. Effect of Large Fluctuations on an Electronic Relay (Vozdeystviye bol'shikh flyuktuatsiy na elektronnoye rele). Radiotekhnika i Elektronika, Vol. 1, No. 2, 1956.

84. Kazakov, I. Ye. Approximate Probabilistic Analysis of the Accuracy of Essentially Nonlinear Automatic Systems (Priblizhennyy veroyatnostnyy analiz tochnosti raboty sushchestvenno nelineynykh avtomaticheskikh sistem). Avtomatika i Telemekhnanika, No. 5, 1956.

85. Pupkov, K. A. Method of Investigation of the Accuracy of Essentially Nonlinear Systems of Automatic Control Using an Equivalent Transfer Function (Metod issledovaniya tochnosti sushchestvenno nelineynykh sistem avtomaticheskogo upravleniya pri pomoshchi ekvivalentnoy peredatochnoy funktsii). Avtomatika i Telemekhanika, No. 2, 1960.

86. Radio Relay Communication Lines (Radioreleynyye linii svyazi). Collection of translations. Edited by V. A. Smirnov. I. L., 1956.

87. Volzhin, A. N. and Yanovich, V. A. Anti-Radar (Protivoradiolokatsiya). Voyenizdat, 1960.

88. Vasil'yev, R. R. and Shastov, G. A. Transmission of Telemechanical Information (Peredacha telemekhanicheskoy informatsii). Gosenergoizdat, 1960.

89. Problems of Artificial Earth Satellites (Problemy iskusstvennykh sputnikov Zemli). Collection of Translations. Edited by A. A. Orlov and E. E. Shpil'rayn. I. L., 1959.

90. Leantovskiy, V. I. By Rocket to the Moon (Raketoy k Lune). Fizmatgiz, 1960.

91. Aleksandrov, S. G. and Fedorov, R. Ye. Soviet Satellites and the Space Rocket (Sovetskiye sputniki i kosmicheskaya raketa). Izd-vo AN SSSR, 1959.

92. Astashenkov, P. T. Radioelectronics in the Control of Missiles (Radioelektronika v upravlenii snaryadami). Voyenizdat, 1960.

93. Vermishev, Yu. A. Rocket Control (Upravleniye raketami). Voyenizdat, 1961.

94. Genri, I. Effective Range and Accuracy of Impact of Long-Range Ballistic Rockets (Dal'nost' deystviya i tochnost' popadaniya ballisticheskikh raket dal'nego deystviya). V. R. T., No. 3, 1960.

95. Lobanov, A. and Lyubchenko, V. Radar Interference and Overcoming It (Information from Foreign Publications) (Radiolokatsionnyye pomekhi i bor'ba s nimi (po dannym inostrannoy pechati)). Vestnik Vozdushnogo Flota, No. 8, 1954.

96. Paliy, A. I. Radio War (Radiovoyna). Voyenizdat, 1963.

97. Svetlova, G. S. and Tsukannikov, G. A. Influence of the Inaccuracy of Tuning of a Phase Discriminator on the Stability of a Two-Coordinate Automatic System (Vliyaniye netochnosti nastroyki fazovogo diskriminatora na ustoychivost' dvukhkoordinatnoy avtomaticheskoy sistemy). Optiko-Mekhanicheskaya Promyshlennost', No. 5, 1959.

98. Tartakovskiy, G. P. Radio Range Finder under the Influence of Interference and Fluctuations of a Reflected Signal (Radiodal'nomer pod vozdeystviyem pomekh i flyuktuatsiy otrazhennogo signala). Inzhenerno-Fizicheskiy Zhurnal, Vol. 1, No. 6, 1958.

99. Berger, F. Planning of Aircraft Systems for Measuring Velocity Using the Doppler Effect (Proyektirovaniye samoletnykh sistem izmereniya skorosti, ispol'zuyushchikh effekt Dopplera). V. R. T., No. 4 (46), 1958.

100. Mak-Makhon, F. The AN/APN-81 Doppler Navigation System (Dopplerovskaya navigatsionnaya sistema AN/APN-81). V. R. T., No. 5 (47), 1958.

101. Dynkin, Ye. B. On One Problem from the Theory of Probabilities (Ob odnoy zadache iz teorii veroyatnostey). Uspekhi Matematicheskikh Nauk, Vol. 4, No. 5, 1949.

102. Rubtsov, V. A. On the Problem of the Equivalence of Systems of Continuous and Discontinuous Control (K vorposu ob ekvivalentnosti sistem preryvistogo i nepreryvnogo regulirovaniya). Avtomatika i Telemekhanika, No. 10, 1958.

103. Kaliguri, J. F. Navigation Apparatus of Submarines Equipped with Polaris Rockets (Navigatsionnaya apparatura podvodnykh lodok, osnashchennykh raketami "Polaris"). Z. R., No. 3, 1961.

104. Stretton, A. Combination of Inertial Navigation and Radio Apparatus (Sochetaniye inertsial'noy navigatsii i radiosredstv). IN: Problems of Inertial Navigation (Problemy Inertsial'noy Navigatsii). Edited by N. I. Borisov. I. L., 1961.

105. Maksimov, M. V. Effect of Fluctuating Interference on a Pulse Group Selector (Deystviye flyuktuatsionnykh pomekh na selektor gruppy impul'sov). Radiotekhnika i Elektronika, Vol. 2, No. 8, 1957.

106. Design of Guided Missiles (Konstruirovaniye upravlyayemykh snaryadov). Edited by A. Ye. Paket and S. Ramo. Voyenizdat, 1963.

107. Kriksunov, L. Z. and Usol'tsev, I. F. Infrared Apparatus for the Homing of Guided Missiles (Infrakrasnyye ustroystva samonavedeniya upravlyayemykh snaryadov). Izd-vo "Sovetskoye Radio", 1963.

108. Dunn, J. H. and Howard D. D. Precision Tracking with Monopulse Radar. Electronics, Vol. 33, No. 17, 1960.

109. Hanford, P. W. Radar Testing for a War Environment. IRE National Convention Record, Vol. 7, p. 5, 1959.

110. The Construction of Missile Guidance Code Resistant to Random Interference. Bell Systems Tech. J., Vol. 39, No. 4, 1960.

111. Lowrich, R. A Secure Digital Command Link. IRE Transaction, Vol. SET-6, No. 3-4, September-December, 1960.

112. Radio Fuses (Fernzünder). Flugkörper, No. 3, 1961.

Translated for the National Aeronautics and Space Administration by John F. Holman Co. Inc.